UAB
Universitat Autònoma de Barcelona

Enhancing the scientific and heritage value of heat-altered stones in prehistoric archaeology through a molecular approach

MARGHERITA CANTELLI

ADVERTIMENT. L'accés als continguts d'aquesta tesi queda condicionat a l'acceptació de les condicions d'ús establertes per la següent llicència Creative Commons:  https://creativecommons.org/licenses/?lang=ca

ADVERTENCIA. El acceso a los contenidos de esta tesis queda condicionado a la aceptación de las condiciones de uso establecidas por la siguiente licencia Creative Commons:  https://creativecommons.org/licenses/?lang=es

WARNING. The access to the contents of this doctoral thesis it is limited to the acceptance of the use conditions set by the following Creative Commons license:  https://creativecommons.org/licenses/?lang=en

Enhancing the scientific and heritage value of heat-altered stones in prehistoric archaeology through a molecular approach

MARGHERITA CANTELLI

Under the supervision of:

André Carlo Colonese (ICTA-UAB, Departamento de Prehistoria)

Martine Regert (Université Côte d'Azur, CNRS, CEPAM)

Xavier Terradas (Institución Milá y Fontanals, CSIC)

Didier Binder (Université Côte d'Azur, CNRS, CEPAM)

2026

PhD in Prehistoric Archaeology

Departament de Prehistoria,
Universitat Autònoma de Barcelona

CEPAM, CNRS,
Université Côte d'Azur

Abstract

Heat-altered stones (HAS) offer significant yet underexplored potential for preserving molecular and stable carbon isotopic evidence of prehistoric culinary and technological activities. Despite their ubiquity, HAS have received far less analytical attention than ceramics, which have traditionally provided key insights into food processing and resource use during the Neolithic. At sites where pottery is absent or poorly preserved, opportunities to reconstruct past practices remain limited, prompting the need to evaluate alternative archives capable of retaining organic residues.

This research aims to address that gap by investigating whether HAS can serve as viable proxies for organic residue analysis. Assemblages from the Neolithic sites of La Draga (Spain) and Pendimoun (France) were examined using an integrated approach combining macroscopic morphological analysis, lipid and protein residue profiling, and stable carbon isotope measurements. Morphological observations reveal features indicative of repeated thermal exposure, including cracking, fracturing, discoloration, and sooting, reflecting both intensity and function of use. At La Draga, the diversity of stone shapes suggests a wide range of activities, encompassing plant processing, cooking, and technological tasks such as resin preparation. At Pendimoun, contrasts between Fireplace and Cooking place contexts confirm feature-specific pattern use.

Lipid analyses confirm the preservation of plant and animal residues, highlighting complex food preparation strategies and multifunctional stone use. Stable carbon isotopic data further indicate mixtures of plant and animal fats, while comparisons with contemporary ceramics reveal complementary patterns of resource exploitation. Methodological considerations emphasise the importance of rigorous sampling, sedimentary analysis, and tailored extraction procedures to distinguish authentic anthropogenic residues from environmental or post-depositional inputs.

Taken together, the findings demonstrate that HAS constitute a reliable and informative archaeological archive, capable of providing activity-specific molecular signatures and insights into subsistence, technology, and domestic organisation. Establishing analytical frameworks for their study broadens the scope of molecular archaeology to include contexts that predate ceramics or lack ceramic assemblages, thereby opening new opportunities for investigating prehistoric lifeways that would otherwise remain inaccessible.

Resum

Les roques termoalterades (HAS) representen un recurs arqueològic amb un gran potencial, encara poc explorat, per a preservar evidències moleculars i isotòpiques sobre activitats culinàries i tecnològiques prehistòriques. Tot i la seva presència freqüent als jaciments, han rebut menys atenció que la ceràmica, que tradicionalment ha permès reconstruir la transformació d'aliments i l'ús de recursos durant el Neolític. En contextos on la ceràmica és absent o mal conservada, cal recórrer a arxius alternatius capaços de retenir residus orgànics.

Amb aquest objectiu, s'han analitzat conjunts de HAS dels jaciments neolítics de La Draga (Espanya) i Pendimoun (França), mitjançant un enfocament integrat que combina observacions morfològiques, anàlisi de residus lipídics i proteomics, i mesures d'isòtops estables del carboni. Les característiques morfològiques com fissures, fracturacions, decoloracions i ennegriments, evidencien exposicions tèrmiques reiterades i permeten inferir la intensitat i la funció d'ús. A La Draga, la diversitat de formes litiques suggereix activitats variades, des del processament vegetal i la cocció fins a tasques tecnològiques com la preparació de resines. A Pendimoun, les diferències entre els contextos de Fireplace i Cooking Place confirmen patrons d'ús específics.

Les anàlisis lipídiques mostren la preservació de residus vegetals i animals, revelant estratègies complexes de preparació d'aliments i un ús multifuncional de les roques. Les dades isotòpiques indiquen mescles de greixos vegetals i animals, i la comparació amb ceràmiques contemporànies mostra patrons complementaris d'explotació de recursos. Les consideracions metodològiques subratllen la importància d'un mostreig rigorós, de l'anàlisi de sediments i de protocols d'extracció adaptats per distingir residus antropogènics d'aportacions ambientals o postdeposicionals.

En conjunt, els resultats demostren que les HAS constitueixen un arxiu arqueològic fiable i molt informatiu, capaç de proporcionar signatures moleculars específiques d'activitat i d'ampliar el coneixement sobre subsistència, tecnologia i organització domèstica en societats prehistòriques. L'establiment de marcs analítics per al seu estudi amplia l'abast de l'arqueologia molecular a contextos anteriors o aliens a l'ús de la ceràmica, obrint noves vies per investigar formes de vida que, d'una altra manera, restarien inaccessible.

Resumen

Las rocas termoalteradas (HAS) representan un recurso arqueológico con un notable, aunque todavía poco explorado, potencial para preservar evidencias moleculares y de isótopos estables de carbono relacionadas con actividades culinarias y tecnológicas prehistóricas. A pesar de su presencia frecuente en los yacimientos, han recibido menos atención analítica que la cerámica, tradicionalmente empleada para reconstruir la transformación de alimentos y el uso de recursos durante el Neolítico. En contextos donde la cerámica está ausente o mal conservada, se hace necesario recurrir a archivos alternativos capaces de retener residuos orgánicos.

Con este objetivo, se analizaron conjuntos de HAS procedentes de los yacimientos neolíticos de La Draga (España) y Pendimoun (Francia), mediante un enfoque integrado que combina observaciones morfológicas macroscópicas, análisis de residuos lipídicos y proteicos, y mediciones de isótopos estables de carbono. Las características morfológicas muestran rasgos indicativos de exposiciones térmicas reiteradas como fisuras, fracturas, decoloración y ennegrecimiento, que reflejan tanto la intensidad como la función de uso. En La Draga, la diversidad de formas líticas sugiere actividades variadas, desde el procesamiento de plantas, la cocción y tareas tecnológicas como la preparación de resinas. En Pendimoun, las diferencias entre los contextos de Fireplace y Cooking Place confirman patrones de uso específicos para cada estructura.

Los análisis lipídicos confirman la preservación de residuos vegetales y animales, reflejando estrategias complejas de preparación de alimentos y un uso multifuncional de las piedras. Los datos isotópicos de carbono indican además mezclas de grasas vegetales y animales, mientras que las comparaciones con cerámicas contemporáneas muestran patrones complementarios de explotación de recursos. Desde una perspectiva metodológica, el estudio destaca la importancia de un muestreo riguroso, el análisis de sedimentos y procedimientos de extracción adaptados para distinguir los residuos antropogénicos de los aportes ambientales o postdeposicionales.

Los resultados demuestran que las HAS constituyen un archivo arqueológico fiable y altamente informativo, capaz de proporcionar firmas moleculares específicas de actividades y de ampliar el conocimiento sobre subsistencia, tecnología y organización doméstica en sociedades prehistóricas. El establecimiento de marcos analíticos para su estudio amplía el alcance de la arqueología molecular a contextos anteriores o ajenos al uso de cerámica, abriendo nuevas oportunidades para investigar formas de vida prehistóricas que, de otro modo, permanecerán inaccesibles.

Résumé

Les roches thermo-altérées (HAS) offrent un potentiel significatif, encore peu exploré, pour la conservation de traces moléculaires et isotopiques liées aux activités culinaires et technologiques préhistoriques. Bien qu'elles soient couramment présentes sur les sites, ces roches ont reçu beaucoup moins d'attention que la céramique, traditionnellement utilisée pour reconstituer la transformation des aliments et l'exploitation des ressources pendant le Néolithique. Dans les contextes où la céramique est absente ou mal conservée, il devient nécessaire de recourir à des archives alternatives capables de préserver des résidus organiques.

Dans ce cadre, des assemblages de HAS provenant des sites néolithiques de La Draga (Espagne) et de Pendimoun (France) ont été analysés selon une approche intégrée combinant observations morphologiques macroscopiques, analyses des résidus lipidiques et protéiques, et mesures d'isotopes stables du carbone. Les caractéristiques morphologiques, comme fissures, fractures, décolorations et noircissements, témoignent d'expositions thermiques répétées et permettent d'inférer l'intensité et la fonction d'utilisation. À La Draga, la diversité des formes lithiques suggère une large gamme d'activités, allant du traitement des végétaux et de la cuisson à des tâches technologiques telles que la préparation de résines. À Pendimoun, les contrastes entre les contextes « Fireplace » et « Cooking Place » révèlent des schémas d'utilisation spécifiques.

Les analyses lipidiques confirment la conservation de résidus végétaux et animaux, révélant des stratégies complexes de préparation alimentaire et un usage multifonctionnel des roches thermo-altérées. Les données isotopiques indiquent des mélanges de graisses végétales et animales, et la comparaison avec la céramique contemporaine met en évidence des schémas complémentaires d'exploitation des ressources. Les considérations méthodologiques soulignent l'importance d'un échantillonnage rigoureux, de l'analyse des sédiments et de protocoles d'extraction adaptés pour distinguer les résidus anthropiques des apports environnementaux ou post-dépositionnels.

Dans l'ensemble, les HAS constituent une archive archéologique fiable et très informative, capable de fournir des signatures moléculaires spécifiques aux activités et d'enrichir la compréhension de la subsistance, de la technologie et de l'organisation domestique dans les sociétés préhistoriques. L'élaboration de cadres analytiques pour leur étude étend le champ de l'archéologie moléculaire à des contextes antérieurs à la céramique ou dépourvus d'assemblages céramiques, ouvrant ainsi de nouvelles perspectives pour l'étude des modes de vie préhistoriques autrement inaccessibles.

"History at its best, in my view, is the most subversive discipline,
inasmuch as it can tell us how things that we are likely to take for granted came to be."
James C. Scott
Against the Grain: A Deep History of the Earliest States (2017)

Dedicated to Mattia and Marta,
with the wish that you achieve all your dreams in life.

Acknowledgements

This thesis would not have been possible without the support, guidance, and encouragement of many people and institutions.

First and foremost, I would like to express my gratitude to my supervisors, André Carlo Colonese, Martine Regert, Xavier Terradas and Didier Binder, for their guidance, encouragement, and invaluable advice throughout this research. Your expertise and support have been essential in shaping this work. I am especially grateful to André and Martine for their constant mentorship, insightful discussions, and careful feedback, which greatly strengthened both the design and interpretation of this study. I am also deeply grateful to Xavier and Didier, not only for their guidance throughout the project, but also for their key role in the fieldwork, collecting and safeguarding the stone assemblage, which made this study possible. Beyond the academic guidance, I sincerely appreciate the empathy and support all the supervisors have shown during difficult personal moments.

I am sincerely grateful to the members of the ICTA-UAB and CEPAM, whose discussions, technical advice, and good humour created an inspiring and collaborative environment. Special thanks are due to Nuria Moraleda-Cibrián, Joan Villanueva, Krista McGrath, Arnaud Mazuy and Léa Drieu for their assistance with laboratory work, analytical procedures, and for always being willing to troubleshoot at crucial moments.

This project benefited greatly from the institutions and archaeological teams who made material accessible. I am particularly grateful to the La Draga team, with whom I had the opportunity to participate in the excavation campaign, an experience that was both inspiring and invaluable for this research. I would also like to thank Raquel Piqué Horta and Alain Carré for allowing me to sample the sediments, which was essential for this study. I also thank Igor Bogdanovic for his guidance and supervision during the 3D analysis at the OpenLabs-UAB, which greatly enhanced my technical skills.

Finally, I acknowledge the financial support provided by the European Union's Horizon 2020 research and innovation programme, which made this research, as well as the associated travel and laboratory analyses, possible.

To the ESRs of ChemArch and everyone in the wider ChemArch network, I hope our paths will cross again in the future. During the workshops and conferences we shared, I was warmly welcomed into the group even though I joined a few months later, and I am truly grateful for that. Among them, I would like to give special thanks to Alice Di Muro, Ingrid, and Jakob, with whom I shared both the challenges of UAB and many memorable moments over beers and tapas in Barcelona. I also wish to thank Alice Cao, a kind and generous colleague, who shared with me the often challenging topic of working with stones and made that learning process much more rewarding.

I would also like to thank some very special friends who made my time in Barcelona unforgettable. Alice, a passionate *romana de Roma*, welcomed me and offered her help even before I got to know her, instantly making me feel part of the group. Anna, a kind and caring soul, is someone you can always rely on. Thank you both for always being there, you were a breath of fresh air during the most challenging moments. We know what it means to pack everything up and set off in pursuit of a dream, and sharing that experience with you has been truly special.

I would also like to thank all my friends from Italy, who have known me for a long time and are well accustomed to my constant moving around. Despite the distance and my many travels, you have always remained present, offering support, encouragement, and friendship. Your steadiness and care mean more to me than words can express.

A special thanks to my family, with whom I have shared a challenging period over the past few years, yet always close, building a bond that is very dear to me. Thank you to my sister, who has always been by my side, no matter what. Thank you to my mom, who has tried to understand my need to explore different places and experiences. And thank you to my dad, a man of few words, who taught me so much with his simple "*stato ben ti*?"… well, Dad, I'm more than fine.

And at last, Sandro, thank you for always believing in me, often even more than I believe in myself, for completely understanding my needs and goals in life, and for constantly encouraging me to aim high.

Funding

This work was funded by the European Union's Horizon 2020 research and innovation programme under grant agreement ChemArch No 956351. This work contributes to EarlyFoods, which has received funding from the Agència de Gestió d'Ajuts Universitaris i de Recerca de Catalunya (2021 SGR 00527 and 2021 SGR 00501). This work contributes to the "ICTA-UAB María de Maeztu" Programme for Units of Excellence of the Spanish Ministry of Science and Innovation (CEX2024-001506-M).

List of figures

Figure 1. Condensed and simplified map of the spread of farming in western Eurasia (9600 - 4000 BCE) from Gronenborn and Horejs (Gronenborn and Horejs, 2023). ……..9

Figure 2. Distribution maps of early Neolithic sites in the Western Mediterranean. Reproduced from Perrin et al. (Perrin and Manen, 2021). ……13

Figure 3. Set of ceramic vessels from the Early Neolithic (Cardial and Epicardial). Reproduced from Binder *et al.* (Binder et al., 2010a). Drawings by J.Coularou. ……..16

Figure 4. Geographical location of the case studies (the world map was created using the OpenStreetMap package: (Fellows and Stotz, 2023)). ……20

Figure 5. Schematic profile illustration examples of stone structures: (a) burnt mound, (b) scattered stones, (c) pit, (d) heart. ……..20

Figure 6. Sankey plot showing the relationship between methodologies applied and archaeological questions about HAS. ……21

Figure 7. Methodological approaches over the 20th and early 21st centuries. ……22

Figure 8. Illustration example of generic cooking techniques: (A) platform hearth, (B) stone boiling technique, (C) earth oven. ……...26

Figure 9. Structure of some of the naturally occurring lipids. (A) palmitic acid, saturated FA; (B) palmitoleic acid, unsaturated FA; (C) cholesterol; (D) β-sitosterol; (E) triglyceride; (F) abietic acid, diterpenoid; (G) triacontanyl palmitate, wax ester. ……..36

Figure 10. Structures of selected biomarkers relevant to archaeological residue analysis. (A) Tricosylresorcinol, AR 23:0; (B)16-hentriacontanone, ketone; (C) C18 ω-(o-alkylphenyl)alkanoic acid, APAA; (D) azelaic acid, dicarboxylic acid. ……..39

Figure 11. Schematic representation of a gas chromatograph and its main components. Adapted from (Stauffer, Dolan and Newman, 2008). ……..44

Figure 12. Biogeographical Regions in Europe. Map produced by the European Environment Agency, reflecting the status of biogeographical regions based on 2016 data. Originally published in June 2017 and last modified in September 2024 (European Environment Agency, 2017). ……49

Figure 13. Graphical overview of the modern reference dataset used in this study, showing 68% confidence ellipses (Dudd, 1999; Spangenberg and Ogrinc, 2001; Spangenberg, Jacomet and Schibler, 2006; Spangenberg et al., 2010; Craig et al., 2011, 2012; Debono-Spiteri, 2012; March, 2013; Cramp and Evershed, 2014; Colonese et al., 2015; Carrer et al., 2016; Lucquin, Gibbs and Uchiyama, 2016; Jambrina-Enríquez et al., 2019; Tarifa Mateo, 2019; Pääkkönen, Evershed and Asplund, 2020; Courel et al., 2021; Bondetti et al., 2021b; Drieu et al., 2021; Dolbunova et al., 2023; Tarifa-Mateo et al., 2023). ……..……51

Figure 14. Preservation of organic residues in prehistoric and protohistoric ceramics across different European regions (A: Northern Europe, B: Central Europe, C: Southern Europe), shown in relation to soil pH levels. Reproduced from Drieu (Drieu, 2017). ……..……53

Figure 15. Main lipid products from Neolithic sites in Southern Europe, based on published references compiled from the AROLD database (Debono-Spiteri, 2012; Salque et al., 2012; Roffet-Salque et al., 2015; Debono Spiteri et al., 2016; Fanti et al., 2018; Lucejko et al., 2018; McClure et al., 2018; Tarifa Mateo, 2019; Tarifa-Mateo et al., 2019, 2021; Breu et al., 2021, 2023a; Drieu et al., 2021; Evershed et al., 2022; Maggi et al., 2023; Fanti, Drieu and Regert, 2024). The map visualizes the presence (not proportion) of product categories such as ruminant fats, non-ruminant fats, dairy products, beeswax, plant oils, and other plant-based substances, across different areas. Basemap data sourced from Natural Earth (Massicotte and South, 2023). For the AROLD database see Prévost *et al* (Prévost et al., 2023) and https://www.cepam.cnrs.fr/datas/ArOLD.php. …….....…...54
Figure 16. Schematic representation of methodological steps for lipid analysis on lithic artefacts based on the records cited in this chapter. ……..56
Figure 17. General structure of the 20 amino acids and their R groups found in proteins. Adapted from Brown and Brown (Brown and Brown, 2011). ……61
Figure 18. La Draga archaeological site in northeastern Iberian Peninsula and general plan of the excavated sectors from Andreaki at al. (Andreaki et al., 2022). ……67
Figure 19. Stratigraphic correlation of all three excavated sectors in La Draga from Andreaki at al. (Andreaki et al., 2022). ……...67
Figure 20. Pottery fragments from the Early Neolithic site of La Draga documented by Bertin at al. (Bertin et al., 2024). ……....70
Figure 21. Combustion structure E249 (2010) and E266 (2023), both of which incorporate heat-altered stones (HAS) (Piqué et al., 2023). Photographs courtesy of the La Draga team. ……71
Figure 22. (A) Reconstruction of Neolithic structures at the Neolithic Park of La Draga, showcasing various architectural elements from the prehistoric period. (B) Excavations conducted in Zone B of La Draga, 2023 field season, revealing significant archaeological findings. ……..71
Figure 23. Location of Pendimoun rock-shelter (A) and surrounding landscape (B). View from the west; arrows indicate the shelter's position at the point of intersection. Map (A) generated using geographic data sourced from the rnaturalearth package (Massicotte and South, 2023) and adapted from (Bok1982., 2009). Image (B) from Binder *et al.* (Binder et al., 2020; Delhon et al., 2020; Drieu et al., 2021), (© J.V. Pradeau). ……..….73
Figure 24. Pendimoun rock-shelter excavations: (A) map of successive operations, from Binder *et al.* (Binder et al., 2014), and (B) stratigraphic profile of northern sector, from Binder *et al.* (Binder et al., 2020; Delhon et al., 2020; Drieu et al., 2021). ……...73
Figure 25. Representative pottery forms from Pendimoun rock-shelter. (A) Impressa phase; (B) Cardial phase. Reconstructions based on 3D scan. Adapted from Drieu *et al*. (Drieu et al., 2021). ……76
Figure 26. Partial digital map of Pendimoun sector North during Phase 3 (5100-4790 BCE) showing the location of firing structures 14549 (cooking place; L20) and 14647 (fireplace; L21). ……..….77
Figure 27. Examples of HAS from La Draga. ……80
Figure 28. Grid of sectors B/D at La Draga showing the location of HAS and associated sediment sampling points. ……80
Figure 29. Examples of HAS from Pendimoun, already sectioned into smaller fragments for petrographic analysis. ……...…….83

Figure 30. Partial map of Pendimoun sector North during Phase 3 (5100-4790 BCE) showing the location of structure FP-14549 (L20) and CP-14647 (L21). Ashes (including burned manure) are shown in blue, while burned stones are in grey. ……..…….84
Figure 31. Workflow for the creation of 3D models of selected HAS at OpenLab UAB. (A) Laser scanning equipment used for high-resolution surface capture; (B) Model processing using VXelements software; (C) Photogrammetry setup for image acquisition; (D) Photogrammetric modelling and reconstruction in Agisoft Metashape software. ……..88
Figure 32. Drilling of a heat-altered stone (HAS) using a hand-held drill with carbide/diamond bit for sample collection. ……..89
Figure 33. Schematic representation of HAS showing the sampling spots: external (e), taken from the outermost surface, and internal (i), collected a few millimetres beneath the same location to assess lipid penetration. …..90
Figure 34. Schematic workflow of the methodology applied for lipid analysis on HAS and sediment samples conducted at ICTA-UAB (Barcelona, Spain) and CEPAM-UniCA (Nice, France). ……95
Figure 35. Representative examples of heat-alteration patterns observed on HAS: (A) fracture on sample LD12-4007, (B) sooting on sample LD23-35300, (C) discoloration and superficial adhesion on sample LD12-4035, and (D) discoloration, sooting and superficial adhesion on sample LD11-2156. ……..100
Figure 36. Spherical HAS specimens showing variation in surface and composition: (A) LD10-883 and (B) LD11-1540 with smooth, rounded surfaces and localized discoloration; (C) LD23-25396 with a vesicular (scoria) surface, one polished side, and evidence of sooting. ……..…….101
Figure 37. Tabular HAS specimens showing evidence of heat alteration and potential use-wear: (A) LD10-663 with a concave, levigated surface and linear striations; (B) LD23-25300 with localised sooting along one edge; (C) LD12-4035 exhibiting surface discoloration, cracking, and possible superficial deposits; (D) LD12-3791 exhibiting deep surface cracking; (E) LD23-25430 with a flat, levigated surface, sooting and discoloration; (F) LD12-4007 showing sooting and a fracture. ……...102
Figure 38. Large tabular HAS specimen LD12-3951 showing minimal sooting, reddening, and exfoliation on one side, and pronounced soothing on the opposite side. ……...103
Figure 39. Pot-lid fracture specimens (A) LD11-1547 and (B) LD11-1987, showing convex exterior and concave fracture surfaces. ……...…...103
Figure 40. Prismatic HAS specimens illustrating variation in shape and surface alteration: (A) LD10-500 with a sub-rounded and contrasting angular form; (B) LD10-518 showing cracking, sooting, and discoloration; (C) LD11-2156 with a triangular prism-like shape, sooting, surface discoloration, and possible superficial deposits. ……..104
Figure 41. Partial total ion chromatograms (TIC) of acid/methanol extract of sediment sample LD-JC78-VIa showing saturated fatty acids ($C_{XX:0}$), branched ($C_{XX:0}$ Br), unsaturated fatty acids ($C_{XX:1}$), diacids (DC_{XX}), hydroxy fatty acids (^), sterols and derivatives, tetracyclic and pentacyclic triterpenes, contaminants (*), and *n*-alkanes internal standards (IS $_{ALKXX}$). ……..108
Figure 42. Partial total ion chromatograms (TIC) of solvent extract of sediment sample LD-JC78-VIa showing saturated fatty acids ($C_{XX:0}$), linear alcohols (CxxOH), *n*-alkanes (ALKxx), hydroxy fatty acids (^), sterols and derivatives, tetracyclic and pentacyclic triterpenes, alkylresorcinol (ARxx), wax esters (Wxx), contaminants (*), and *n*-alkanes internal standards (IS $_{ALKXX}$). ……109

Figure 43. Partial total ion chromatograms (TIC) of acid/methanol of sediment sample LD-JA79-VIa g showing saturated fatty acids ($C_{XX:0}$), branched fatty acids ($C_{XX:0}$ Br), isoprenoid acids (4,8,12-trimethyltridecanoic acid, pristanic and phytanic acid), with a *m/z* 101 ion chromatogram showing the ratio of phytanic acid diastereomers (SRR and RRR). …….109
Figure 44. Bar plot of lipid yields of La Draga samples, categorised by deposit, external and internal aliquotes. The solid line represents the threshold of 5 µg g^{-1}. …….110
Figure 45. Boxplot of lipid yields for La Draga samples, categorised by deposit (n = 3), external (n = 15), and internal (n = 10) aliquotes. Grey points represent individual data values. ……..111
Figure 46. Boxplot of lipid yields for La Draga samples, categorised by lithological categories, carbonate rocks (marl, limestone) (n = 7), igneous rocks (volcanic) (n = 4), and siliciclastic rocks (sandstone) (n = 14). Grey points represent individual data values. ……..112
Figure 47. Partial total ion chromatograms (TIC) of acid/methanol extract of HAS sample LD11-1540e showing saturated fatty acids ($C_{XX:0}$), diacids (DC_{XX}), branched ($C_{XX:0}$ Br), unsaturated fatty acids ($C_{XX:1}$), contaminants (*), and *n*-alkanes internal standards (IS $_{ALKXX}$). …….114
Figure 48. Partial total ion chromatograms (TIC) of acid/methanol extract of HAS sample LD11-25300e showing saturated fatty acids ($C_{XX:0}$), branched ($C_{XX:0}$ Br), unsaturated fatty acids ($C_{XX:1}$), *n*-alkanes (ALK xx), sterols and derivatives, contaminants (*), and *n*-alkanes internal standards (IS $_{ALKXX}$). ……..….115
Figure 49. Partial total ion chromatograms (TIC) of acid/methanol extract of HAS sample LD10-518i showing saturated fatty acids ($C_{XX:0}$), branched ($C_{XX:0}$ Br), unsaturated fatty acids ($C_{XX:1}$), benzene polycarboxylic acid (BPCA), diterpenoids, contaminants (*), and *n*-alkanes internal standards (IS $_{ALKXX}$). ……..115
Figure 50. Partial total ion chromatograms (TIC) of solvent extract of HAS sample LD10-833e showing linear alcohols (CxxOH), *n*-alkanes (ALKxx), sterols and derivatives, contaminants (*), and *n*-alkanes internal standards (IS $_{ALKXX}$). ……116
Figure 51. Partial total ion chromatograms (TIC) of solvent extract of HAS sample LD23-5396i showing saturated fatty acids ($C_{XX:0}$), linear alcohols (CxxOH), monoacylglycerols (MAGs), sterols and derivatives, alkylresorcinol (ARxx), contaminants (*), and *n*-alkanes internal standards (IS $_{ALKXX}$). ……..…116
Figure 52. Plots of $\delta^{13}C$ values of palmitic ($C_{16:0}$) and stearic acid ($C_{18:0}$) for HAS and sediment samples at La Draga. Coloured symbols indicate different aliquot types, while shaded ellipses represent reference ranges for modern reference, showing 68% confidence ellipses (see Figure 13, chapter 3.1.2; Annex 3). Abbreviations: D = dairy products, R = ruminant adipose fat, NR = non ruminant adipose fat, P = plant products. Mixing curves are as described in Annex 5. The mixing curves have been calculated to illustrate the $\delta^{13}C$ values which would result from the mixing of C_3 plant products (C3), domestic porcine adipose fat (DP), and wild non ruminant adipose fat (WNR). ……..……..119
Figure 53. Plots of $\delta^{13}C$ values of palmitic ($C_{16:0}$) and stearic acid ($C_{18:0}$), and $\Delta^{13}C$ (the difference between the $\delta^{13}C$ values of the $C_{16:0}$ and $C_{18:0}$ fatty acids) versus $\delta^{13}C_{16:0}$, for HAS samples at La Draga. Point size is proportional to total lipid concentration, and colours indicate different aliquot types. Grey shaded ellipses show 68% confidence intervals for modern reference ranges see Figure 13, chapter 3.1.2; Annex 3). Abbreviations: D = dairy products, R = ruminant adipose fat, NR = non ruminant adipose fat, P = plant products. Mixing curves are as described in Annex 5. The mixing curves have been calculated to illustrate the $\delta^{13}C$ values which would

result from the mixing of C_3 plant products (C3), domestic porcine adipose fat (DP), and wild non ruminant adipose fat (WNR). ……120
Figure 54. Plots of $\delta^{13}C$ values of palmitic ($C_{16:0}$) and stearic acid ($C_{18:0}$) for samples at La Draga. The presence (filled points) and absence (open points) of cholesterol (A), plant sterols (B), alkylresorcinol (C) and diterpenoids (D) are indicated. Colours correspond to different aliquot types, and grey shaded ellipses show 68% confidence intervals for modern reference ranges (see Figure 13, chapter 3.1.2; Annex 3). Mixing curves are as described in Annex 5. The mixing curves have been calculated to illustrate the $\delta^{13}C$ values which would result from the mixing of C_3 plant products (C3), domestic porcine adipose fat (DP), and wild non ruminant adipose fat (WNR). ……...……...121
Figure 55. Plots of $\delta^{13}C$ values of palmitic ($C_{16:0}$) and stearic acid ($C_{18:0}$) for samples at La Draga, subdivided between the oldest occupation (A) and more recent Neolithic occupation (B) phase. Colours correspond to different aliquot types, and grey shaded ellipses show 68% confidence intervals for modern reference ranges (see Figure 13, chapter 3.1.2; Annex 3). Mixing curves are as described in Annex 5. The mixing curves have been calculated to illustrate the $\delta^{13}C$ values which would result from the mixing of C_3 plant products (C3), domestic porcine adipose fat (DP), and wild non ruminant adipose fat (WNR). ……..……122
Figure 56. (A) Plot of $\delta^{13}C$ values of palmitic ($C_{16:0}$) and stearic acid ($C_{18:0}$) and (B) $\Delta^{13}C$ (the difference between the $\delta^{13}C$ values of the $C_{16:0}$ and $C_{18:0}$ fatty acids) versus %SRR diastereomer, for samples at La Draga. The presence (filled points) and absence (open points) of aquatic biomarkers (4,8,12-TMTD, pristanic and phytanic acids) are indicated. Colours correspond to different aliquot types, and grey shaded ellipses show 68% confidence intervals for modern reference ranges (see Figure 13, chapter 3.1.2; Annex 3). ……..…..123
Figure 57. Representative examples of heat-alteration patterns observed on HAS: (A) discoloration on sample PDM-N04-15297 (Detrital carbonate rock), (B) discoloration, sooting, and superficial adhesion on sample PDM-N04-15197, (C) reddening on sample PDM-N04-15419, and (D) cracking on sample PDM-N04-15348. ……..133
Figure 58. Selected HAS fragments recovered from firing structure 14549 (Fireplace). ……..133
Figure 59. Selected HAS fragments recovered from firing structure 14647 (Cooking place). ……..134
Figure 60. Partial total ion chromatograms (TIC) of acid/methanol extract of sediment sample PDM-S15367 showing saturated fatty acids ($C_{XX:0}$), branched ($C_{XX:0}$ Br), unsaturated fatty acids ($C_{XX:1}$), diacids (DC_{XX}), hydroxy fatty acids (^), sterols and derivatives, pentacyclic triterpenes, contaminants (*), and *n*-alkanes internal standards (IS $_{ALKXX}$). ……137
Figure 61. Partial total ion chromatograms (TIC) of solvent extract of sediment sample PDM-S15367 showing saturated fatty acids ($C_{XX:0}$), linear alcohols (CxxOH), *n*-alkanes (ALKxx), hydroxy fatty acids (^), sterols and derivatives, wax esters (Wxx), contaminants (*), and *n*-alkanes internal standards (IS $_{ALKXX}$). …….138
Figure 62. Partial total ion chromatograms (TIC) of acid/methanol of sediment sample XX showing saturated fatty acids ($C_{XX:0}$), branched fatty acids ($C_{XX:0}$ Br), isoprenoid acids (4,8,12-trimethyltridecanoic acid, pristanic and phytanic acid), with a *m/z* 101 ion chromatogram showing the ratio of phytanic acid diastereomers (SRR and RRR). ……...……138
Figure 63. Bar plot of lipid yields for Pendimoun samples, categorised by internal, external and deposit aliquots. The solid line represents the threshold of 5 µg g^{-1}. ……..139

Figure 64. Boxplot of lipid yields for Pendimoun samples, categorised by deposit (n = 2), external (n = 18) and internal (n = 14) aliquots. Grey points represent individual data values. ……...140
Figure 65. Boxplot of lipid yields for Pendimoun samples, categorised by firing structures, including Cooking place-14647 (n = 20) and Fireplace-14549 (n = 14). Grey points represent individual data values. …….141
Figure 66. Boxplot of lipid yields for Pendimoun samples, showing deposit (n = 1), external (n = 10) and internal (n = 9) aliquots of HAS from the Cooking place, along with deposit (n = 1), external (n = 8) and internal (n = 5) aliquots of HAS from theFireplace. Grey points represent individual data values. ……142
Figure 67. Partial total ion chromatograms (TIC) of acid/methanol extract of HAS sample PMD-N04-15199e showing saturated fatty acids ($C_{XX:0}$), branched fatty acids ($C_{XX:0\ Br}$), unsaturated fatty acids ($C_{XX:1}$), diacids (DC_{XX}), *n*-alkanes (ALK xx), cholesterol, contaminants (*), and *n*-alkanes internal standards (IS_{ALKXX}). ……145
Figure 68. Partial total ion chromatograms (TIC) of acid/methanol extract of HAS sample PMD-N04-15348e showing saturated fatty acids ($C_{XX:0}$), unsaturated fatty acids ($C_{XX:1}$), diacids (DC_{XX}), sterols and derivatives, contaminants (*), and *n*-alkanes internal standards (IS_{ALKXX}). ……...145
Figure 69. Partial total ion chromatograms (TIC) of solvent extract of HAS sample PDM-N04-15203e showing linear alcohols (CxxOH), monoacylglycerols (MAG), *n*-alkanes (ALK xx), contaminants (*), and *n*-alkanes internal standards (IS_{ALKXX}). ……...146
Figure 70. Partial total ion chromatograms (TIC) of acid/methanol extract of HAS sample PMD-N04-15201e showing saturated fatty acids ($C_{XX:0}$), unsaturated fatty acids ($C_{XX:1}$), diacids (DC_{XX}), ketones (Kxx), contaminants (*), and *n*-alkanes internal standards (IS_{ALKXX}). ……..146
Figure 71. Plots of $\delta^{13}C$ values of palmitic ($C_{16:0}$) and stearic acid ($C_{18:0}$), and $\Delta^{13}C$ (difference between the $\delta^{13}C$ values of the $C_{16:0}$ and $C_{18:0}$ fatty acids) versus $\delta^{13}C_{16:0}$, of HAS and sediment samples from Fireplace (FP-14549) and Cooking place (CP-14647) at Pendimoun. Coloured symbols indicate different aliquot types, while shaded ellipses represent reference ranges for modern reference, showing 68% confidence ellipses (see Figure 13, chapter 3.1.2; Annex 3). Abbreviations: D = dairy products, R = ruminant adipose fat, NR = non ruminant adipose fat, P = plant products. ……...148
Figure 72. Plots of $\delta^{13}C$ values of palmitic ($C_{16:0}$) and stearic acid ($C_{18:0}$), and $\Delta^{13}C$ (the difference between the $\delta^{13}C$ values of the $C_{16:0}$ and $C_{18:0}$ fatty acids) versus $\delta^{13}C_{16:0}$, for HAS samples from Fireplace (FP-14549) and Cooking place (CP-14647) at Pendimoun. Point size is proportional to total lipid concentration, and colours indicate different aliquot types. Grey shaded ellipses show 68% confidence intervals for modern reference ranges (see Figure 13, chapter 3.1.2; Annex 3). Abbreviations: D = dairy products, R = ruminant adipose fat, NR = non ruminant adipose fat, P = plant products. ……150
Figure 73. Plots of $\delta^{13}C$ values of palmitic ($C_{16:0}$) and stearic acid ($C_{18:0}$) for samples from Cooking place (CP-14647) at Pendimoun. The presence (filled points) and absence (open points) of cholesterol (A) and dicarboxylic acids (B) are indicated. Colours correspond to different aliquot types, and grey shaded ellipses show 68% confidence intervals for modern reference ranges (see Figure 13, chapter 3.1.2; Annex 3). ……..151
Figure 74. (A) Plot of $\delta^{13}C$ values of palmitic ($C_{16:0}$) and stearic acid ($C_{18:0}$) and (B) $\Delta^{13}C$ (the difference between the $\delta^{13}C$ values of the $C_{16:0}$ and $C_{18:0}$ fatty acids) versus %SRR diastereomer, for samples from Cooking place (CP-14647) at Pendimoun. The presence (filled points) and absence (open points) of aquatic biomarkers (4,8,12-TMTD, pristanic and phytanic acids) are indicated. Colours correspond to different aliquot types, and

grey shaded ellipses show 68% confidence intervals for modern reference ranges (see Figure 13, chapter 3.1.2; Annex 3). …….152
Figure 75. Boxplot of lipid yields for La Draga HAS (n = 28; e, i and d) and ceramic vessels (n = 27) (Tarifa Mateo, 2019). Grey points represent individual data values. ……..179
Figure 76. Plots of $\delta^{13}C$ values of palmitic ($C_{16:0}$) and stearic acid ($C_{18:0}$), and $\Delta^{13}C$ (difference between the $\delta^{13}C$ values of the $C_{16:0}$ and $C_{18:0}$ fatty acids) versus $\delta^{13}C_{16:0}$, of HAS, sediments and ceramic samples from La Draga. Coloured symbols indicate different aliquot types, while shaded ellipses represent reference ranges for modern reference, showing 68% confidence ellipses (see Figure 13, chapter 3.1.2). Abbreviations: D = dairy products, R = ruminant adipose fat, NR = non ruminant adipose fat, P = plant products. Mixing curves are as described in Annex 5. The mixing curves have been calculated to illustrate the $\delta^{13}C$ values which would result from the mixing of C_3 plant products (C3), domestic porcine adipose fat (DP), and wild non ruminant adipose fat (WNR). …….180
Figure 77. Boxplot of lipid yields for Pendimoun HAS (n = 34; e, i and d) and ceramic vessels (n = 53) (Drieu et al., 2021). Grey points represent individual data values. ……..……182
Figure 78. Plots of $\delta^{13}C$ values of palmitic ($C_{16:0}$) and stearic acid ($C_{18:0}$), and $\Delta^{13}C$ (difference between the $\delta^{13}C$ values of the $C_{16:0}$ and $C_{18:0}$ fatty acids) versus $\delta^{13}C_{16:0}$, of HAS from Cooking place and ceramic samples from Pendimoun. Coloured symbols indicate different aliquot types, while shaded ellipses represent reference ranges for modern reference, showing 68% confidence ellipses (see Figure 13, chapter 3.1.2). Abbreviations: D = dairy products, R = ruminant adipose fat, NR = non ruminant adipose fat, P = plant products. …….183
Figure 79. Overview of materials suitable for organic residue analysis. Heat-Altered Stones (HAS) are now included alongside established materials, illustrating their emerging role in reconstructing prehistoric subsistence and technology. ……189

List of tables

Table 1. Heat/fire alteration patterns of HAS according to Neubauer (Neubauer, 2018). ……24

Table 2. HAS features related to culinary practices. ...…….27

Table 3. Lipid analysis methodology of various studies categorised by lithic tools. ……59

Table 4. List of HAS and sediment samples from La Draga selected for this study. ……...82

Table 5. List of HAS and sediment samples from Pendimoun selected for this study. ……85

Table 6. Contextual and morphological information of heat-altered stones (HAS) from La Draga. Variables include excavation year, sector, stratigraphic context, feature, grid position, occupation phase, mineral composition, dimensions, weight, and associated thermal alteration patterns. ……...105

Table 7. Summary of lipid analyses results on sediments from La Draga. Lipid yields are presented alongside the principal and diagnostic compounds detected through combined extractions (AE, SE), with associated stable carbon isotope data. Compounds include saturated fatty acids (SFA), branched fatty acids (BrFA), unsaturated fatty acids (UFA), hydroxy FA (Hy), dicarboxylic fatty acids (DC), n-alkanes (ALK), alcohols (OH), ketones (K), terpenoids (terp), isoprenoids (4,8,12-TMTD: 4,8,12-trimethyl-tridecanoic acid, pri: pristanic acid; phy: phytanic acid), sterols (ster), monoacylglycerols (MAGs), wax esters (WE), alkyresorcinol (AR), and additional biomarkers (B3CA: benzene tricarboxylic acid). Compounds in red were found in both HAS and sediments. Stable carbon isotope ($\delta^{13}C$) values are present as $\delta^{13}C_{16:0}$ (‰), $\delta^{13}C_{18:0}$ (‰), together with the isotopic offset $\Delta^{13}C$ (‰), calculated as $\delta^{13}C_{18:0}$ - $\delta^{13}C_{16:0}$. ……...125

Table 8. Summary of lipid analyses results on HAS from La Draga. Lipid yields are presented alongside the principal and diagnostic compounds detected through combined extractions (AE, SE), with associated stable carbon isotope data. Compounds include saturated fatty acids (SFA), branched fatty acids (BrFA), unsaturated fatty acids (UFA), hydroxy FA (Hy), dicarboxylic fatty acids (DC), n-alkanes (ALK), alcohols (OH), ketones (K), terpenoids (terp), isoprenoids (4,8,12-TMTD: 4,8,12-trimethyl-tridecanoic acid, pri: pristanic acid; phy: phytanic acid), sterols (ster), monoacylglycerols (MAGs), alkyresorcinol (AR), and additional biomarkers (B3CA: benzene tricarboxylic acid). Compounds in red were found in both HAS and sediments. Stable carbon isotope ($\delta^{13}C$) values are present as $\delta^{13}C_{16:0}$ (‰), $\delta^{13}C_{18:0}$ (‰), together with the isotopic offset $\Delta^{13}C$ (‰), calculated as $\delta^{13}C_{18:0}$ - $\delta^{13}C_{16:0}$. ……..…127

Table 9. Mascot protein matches for residue samples from La Draga (LD-1540, LD-2156, LD-3951, LD-4035) and their likely contaminant source. Note: Taxa listed are the most likely species as the majority are highly conserved sequences across taxa (ie. keratins). Contaminant source: LR = laboratory reagent; LC = Laboratory contaminant; H/SC = handling/surface contaminant; S/SC = soil/surface contaminant. Those in red text would normally be disregarded due to only having a single peptide match, however they have been included to show that essentially all identifiable proteins were contaminants. ……..……...130

Table 10. Contextual and morphological information of heat-altered stones (HAS) from Pendimoun. Variables include excavation year, stratigraphic context, feature, grid position, occupation phase, mineral composition, weight, and associated thermal alteration patterns. ……135

Table 11. Summary of lipid analyses results on sediments from Pendimoun. Lipid yields are presented alongside the principal and diagnostic compounds detected through combined extractions (AE, SE), with associated stable carbon isotope data. Compounds include saturated fatty acids (SFA), branched fatty acids (BrFA), unsaturated fatty acids (UFA), hydroxy FA (Hy), dicarboxylic fatty acids (DC), *n*-alkanes (ALK), alcohols (OH), ketones (K), terpenoids (terp), isoprenoids (4,8,12-TMTD: 4,8,12-trimethyl-tridecanoic acid, pri: pristanic acid; phy: phytanic acid), sterols (ster), monoacylglycerols (MAGs), wax esters (WE), and additional biomarkers (B3CA: benzene tricarboxylic acid). Compounds in red were found in both HAS and sediments. Stable carbon isotope ($\delta^{13}C$) values are present as $\delta^{13}C_{16:0}$ (‰), $\delta^{13}C_{18:0}$ (‰), together with the isotopic offset $\Delta^{13}C$ (‰), calculated as $\delta^{13}C_{18:0}$ - $\delta^{13}C_{16:0}$. ……..154

Table 12. Summary of lipid analyses results on HAS from Pendimoun. Lipid yields are presented alongside the principal and diagnostic compounds detected through combined extractions (AE, SE), with associated stable carbon isotope data. Compounds include saturated fatty acids (SFA), branched fatty acids (BrFA), unsaturated fatty acids (UFA), hydroxy FA (Hy), dicarboxylic fatty acids (DC), *n*-alkanes (ALK), alcohols (OH), ketones (K), terpenoids (terp), isoprenoids (4,8,12-TMTD: 4,8,12-trimethyl-tridecanoic acid, pri: pristanic acid; phy: phytanic acid), sterols (ster), monoacylglycerols (MAGs), and additional biomarkers (B3CA: benzene tricarboxylic acid). Compounds in red were found in both HAS and sediments. Stable carbon isotope ($\delta^{13}C$) values are present as $\delta^{13}C_{16:0}$ (‰), $\delta^{13}C_{18:0}$ (‰), together with the isotopic offset $\Delta^{13}C$ (‰), calculated as $\delta^{13}C_{18:0}$ - $\delta^{13}C_{16:0}$. ……..156

Table 13. Mascot protein matches for residue samples Pendimoun (PDM-N04-15250, PDM-N04-15431, PDM-N04-15433) and their likely contaminant source. Note: Taxa listed are the most likely species as the majority are highly conserved sequences across taxa (ie. keratins). Contaminant source: LR = laboratory reagent; LC = Laboratory contaminant; H/SC = handling/surface contaminant; S/SC = soil/surface contaminant. Those in red text would normally be disregarded due to only having a single peptide match, however they have been included to show that essentially all identifiable proteins were contaminants. ……..160

Table 14. Overview of analysed HAS from La Draga, showing thermal alteration patterns, morphological characteristics, molecular signatures, and inferred functional interpretation. …….171

Table 15. Overview of analysed HAS at Pendimoun organised by Cooking Place (CP-14647) and the Fireplace (FP-14549), showing thermal alteration patterns, morphological characteristics, molecular signatures, and inferred functional interpretation. ……..……174

Table of contents

Abstract **I**
Resum **II**
Resumen **III**
Résumé **IV**
Acknowledgements **VI**
Funding **VIII**
List of figures **IX**
List of tables **XVI**
Table of contents **XVIII**
1. Introduction **1**
1.1. Filling research gaps in Neolithic foodways 1
1.2. Aims and objectives: HAS as a window on Neolithic food practices 2
1.3. Thesis outline 5
1.4. Research background 6
1.4.1. The Neolithic: adaptation and transformation of foodways in Europe 7
1.4.2. Neolithic dietary practices and food exploitation in the North-Western Mediterranean 11
2. Heat-altered stone analysis: a state-of-the-art review **18**
2.1. Geographic and chronological distributions of HAS 22
2.2. Identification and characterisation of HAS 23
2.3. Functional interpretation of HAS 25
2.4. Social implication 30
2.5. Synthesis and considerations 31
3. An overview of lipid and protein residue analysis in the investigation of past cuisine **33**
3.1. Lipid residue analysis in archaeology 33
3.1.1. Analytical Approaches for Lipid Residue Identification in Archaeological Materials 41
3.1.2. Stable carbon isotopes analysis of fatty acids 46
3.1.3. Lipid preservation in the Neolithic Mediterranean 51
3.1.4. Lipid residue analysis on stone artefacts 54
3.2. Protein residue analysis in archaeology 60
3.2.1. Proteomic approaches for Archaeological Materials 62
3.2.2. Protein analysis on lithic artefacts 64
4. Archaeological case studies **65**
4.1. La Draga 65
4.2. Pendimoun 72
5. Methodology **78**
5.1. Archaeological sample selection criteria 78
5.1.1. La Draga 79
5.1.2. Pendimoun 82
5.2. Visual inspection 85
5.3. 3D model acquisition 86

5.4. Lipid residue analysis 88
5.4.1. Statistical analysis of total lipid extract 93
5.4.2. Stable carbon isotope analysis 93
5.5. Protein analysis 95
6. Heat-altered stones as archaeological indicators: morphological and molecular evidence from La Draga and Pendimoun 98
6.1. La Draga 99
6.1.1. Visual inspection 99
6.1.2. 3D model acquisition 106
6.1.3. Lipid residue analysis 106
6.1.3.1. Stable carbon isotope analysis 117
6.1.4. Protein analysis 130
6.2. Pendimoun 132
6.2.1. Visual inspection 132
6.2.2. 3D model acquisition 136
6.2.3. Lipid residue analysis 136
6.2.3.1. Stable carbon isotope analysis 146
6.2.4. Protein analysis 160
7. Discussion 162
7.1. Distribution of HAS across distinct chronological, geographical and cultural contexts in prehistoric archaeology 162
7.2. Morphological alteration patterns in HAS: Insights from La Draga and Pendimoun 164
7.3. The Potential of HAS for Reconstructing Culinary Practices 166
7.3.1. La Draga 167
7.3.2. Pendimoun 172
7.3.3. Common considerations 175
7.4. The Molecular Variability of HAS Across Sites and Materials 175
7.4.1. Linking Ceramic and HAS Residue Evidence 177
7.5. Limitations, Methodological Considerations, and Recommendations 184
7.6. Overall Discussion: Towards a Methodological Framework for the Study of HAS 186
8. Conclusion 190
Bibliography 193
Annex 1 224
Annex 2 254
Annex 3 259
Annex 4 279
Annex 5 396
Annex 6 420

1. Introduction

1.1. Filling research gaps in Neolithic foodways[1]

Food, as a social phenomenon and as subsistence, is characterised by intricate operational chains encompassing the acquisition, distribution, transformation, storage and consumption of natural resources, including medicinal and symbolic considerations. The ways in which food is prepared and consumed provide profound insights into the collective identity of communities, serving as a vehicle of power, rules, communication, traditions and social dynamics (Morrison, 2012; Hastorf, 2016; Graff, 2020). Culinary practices are closely connected to the labour and life of the individuals involved in the gathering, handling, storage, processing, cooking, and consumption of the food (Morrison, 2012; Twiss, 2012; Graff, 2018). Such complexity between food and culture has roots that reach back to prehistoric times, where the role of food was pivotal in subsistence, human evolution and social organisation (Twiss, 2012; Graff, 2020). Foodways have been a focal point in archaeological research for several decades, as evidence of cooking and food preparation can unveil crucial insights into the life of past human groups (Graff, 2020). Profound changes in food production and preparation techniques have been documented in prehistoric times and in some cases they have helped to define key cultural changes, such as the adoption of agriculture and storage technology (Griffin, 1967; Fuller and Gonzalez Carretero, 2018). Along with the control of fire, one of the most significant evolutionary changes in prehistoric food preparation techniques was the adoption of ceramic artefacts and containers of other nature for manipulating, boiling, storing, and fermenting a variety of foodstuffs and other substances (Craig, 2021). Pottery use in prehistoric households is thought to have improved palatability and digestibility of food items, thus expanding diet and creating more complex and varied meals that laid the foundation of culinary traditions in the past (Fuller and Gonzalez Carretero, 2018). In fact, the consumption of food was not limited to raw ingredients found in nature but involved the transformation of natural resources into cultural products through alternative techniques of food processing and cooking, such as grinding, roasting, baking, boiling, fermenting, and mixing. These techniques enhanced the edibility, nutritional value, and storability of food, as well as influenced their sensory qualities and taste (Kubiak-Martens, 2002; Carmody and Wrangham, 2009; Morrison, 2012). Functional properties of edible foods are crucial to comprehend the connections between dietary composition and the technological decisions made by past human groups (Wollstonecroft, 2011; Morrison, 2012).

[1] Some contents of this subchapter are drawn from "*Diamonds in the rough - reconsidering the scientific and heritage value of heat-altered stones in prehistoric archaeology through a systematic literature review*", published in Open Research Europe (Cantelli et al., 2024). The article was authored by the candidate and represents original research conducted as part of this doctoral project.

Prehistoric cooking technology evolved through time and space in different ways, adopting a certain diversity according to the environment and the availability of resources. The Neolithic period in Western Europe saw significant transformations in food production and preparation, coinciding with the advent of agriculture and sedentary lifestyles. This period was marked by the westward migration of farming from the near east starting 8,500 years ago, representing one of the most significant historical and evolutionary events in human history on the continent (Larson et al., 2014). However, our understanding of Neolithic cooking practices remains limited. Organic food residues are rarely preserved in the archaeological record, and reconstructions are often based on a handful of archaeological artefacts including primarily ceramics (Cramp and Evershed, 2014; Spiteri, Muntoni and Craig, 2017; Hendy et al., 2018; Fanti et al., 2018) and grinding stones (Hamon, 2021). Other long-lasting cooking solutions have only received cursory attention, as is the case of boiling and roasting food with the aid of stones (exposed to high temperatures, (Kipfer, 2023)), of which evidence is alluded to by the presence of **Heat-Altered Stones** (HAS) in prehistoric sites. While ceramics played a crucial role in cooking practices, HAS offer an alternative perspective on heat-based culinary techniques. They have been recorded in disparate archaeological records, at least since the Upper Palaeolithic (Sorensen and Scherjon, 2018; Cantelli et al., 2024), in close association with household contexts, combustion structures and cooking activities (Kelley and Campbell, 1943; Petraglia, 2002; Frère-Sautot, 2003; Gerritsen, Özbal and Thissen, 2013; Petersson, 2013; Graesch et al., 2014; Custer, 2017; Fernández Ruiz et al., 2018; Neubauer, 2018; Stuart and Walker, 2018; Gaugler, 2019; Hart, 2023; Monforte-Barberán et al., 2023). In Neolithic contexts, these stones are believed to have been used as heating elements in various cooking methods, possessing the physical properties to capture, retain, and dissipate heat. Nevertheless, **the presence and function of HAS in Neolithic contexts have been largely overlooked, as well as their untapped potential for molecular analysis**. Important questions remain about the capacity of HAS to retain and preserve organic compounds resulting from human activities related to food preparation and resource processing, even though these processes are recent in geological terms. Unlike ceramic artefacts, HAS not anthropogenically manufactured, which raises the challenge of distinguishing molecules resulting from their natural geological history, including dispersal across distinct environmental contexts over geological timescales, from those potentially introduced through more recent, human-induced activities.

1.2. Aims and objectives: HAS as a window on Neolithic food practices

Our knowledge of Neolithic culinary practices in Western Europe is derived from a combination of zooarchaeological, botanical, artefact typology, and molecular studies on biological materials and artefacts (Manning et al., 2013; Rowley-Conwy et al., 2013; Fontanals Coll, 2015; Cubas,

Peyroteo-Stjerna and Fontanals-Coll, 2019; Hamon, 2021; Halstead, 2024). Among these, organic residue analysis extracted from cooking utensils has proven to be one of the most effective and innovative methods for studying the function of culinary artefacts and the cultural values associated with foodstuffs (Evershed, 1993; Cramp and Evershed, 2014; Debono Spiteri et al., 2016; Spiteri, Muntoni and Craig, 2017; Hendy et al., 2018; Breu et al., 2021; Drieu et al., 2021; Tarifa-Mateo et al., 2023). For example, lipid analysis of ceramic vessels has revealed that early farming groups in the Near East were processing dairy products as early as the 7th millennium BCE (Evershed et al., 2008a). This technique has also helped trace the spread of dairy exploitation into Europe, where distinct regional patterns emerged during the Neolithic period (Evershed et al., 2008a; Salque et al., 2013; Debono Spiteri et al., 2016). In the Mediterranean, lipid analysis indicates that ceramic vessels were primarily used to process animal fats and possibly plants (Copley et al., 2003; Debono Spiteri et al., 2016; Cubas et al., 2020; Drieu et al., 2021). Molecular and stable isotope analysis of lipids preserved in ceramic containers has also been instrumental in demonstrating the persistence of foraging practices despite the introduction of farming in some of these regions (Craig et al., 2011). While Neolithic ceramic technologies have been extensively studied through the analysis of pottery artefacts, other utensils and tools potentially used in food preparation have been overlooked. This is particularly true for Heat-Altered Stones (HAS), which are widely reported at prehistoric sites but remain poorly understood. Neglecting the role of such artefacts possibly involved in food processing risks a skewed understanding of prehistoric diets, culinary practices and their impact on past economies and subsistence strategies.

The overarching aim of this research is to add HAS to the toolkit of Neolithic studies by exploring their untapped potential as archives of food molecules derived from culinary practices and subsistence strategies, thereby enhancing our understanding of Neolithic food processing and consumption in Western Europe. These aims are pursued in this thesis through the following specific objectives:

1. **Document the distribution of HAS across distinct chronological, geographic, and cultural contexts in prehistoric archaeology.**

A systematic literature review was conducted using journal articles, book chapters and books published in English, sourced from Scopus and Web of Science. Information on HAS was collected from 73 records, published between 1943 and 2023, covering their geographic distribution, chronology, composition, technological aspects and subsistence contexts. The aim was to assess the challenges and opportunities of analysing HAS while highlighting that this class of artefacts remains largely an untapped source of information on prehistoric human activities.

2. **Identify and characterise morphological alteration patterns on stones associated with heat exposure, such as cracks, fractures, discoloration, and depositional remains from key Neolithic contexts in southwestern Europe: La Draga (Spain) and Pendimoun (France).**

Selected stones were examined for macroscopic evidence of thermal exposure. Visual inspection focused on identifying potential heat/fire-induced alteration, including cracking, thermal fractures, discoloration, and depositional remains indicative of combustion processes. To complement visual assessments, 3D scanning and photogrammetry were employed to generate high-resolution digital models of each artefact, preserving their original shape and texture prior to any destructive analysis. A digital library was created to facilitate public dissemination, enhanced heritage awareness, and support conservation efforts. This resource serves as a valuable reference for future research, enabling comparative analysis and broader discussion on HAS use in Neolithic contexts.

3. **Assess the potential of HAS for recovering information on past culinary practices using molecular (lipids, proteins) and carbon stable isotope analysis of lipid residues.**

To evaluate the suitability of HAS for reconstructing past culinary practices, molecular and carbon stable isotope analyses were conducted on lipid residues extracted from selected samples. Lipid biomarkers were identified using gas chromatography-mass spectrometry (GC-MS), enabling the detection of food-derived molecules preserved in the artefacts. Carbon stable isotope analysis provided further evidence of the origins and processing methods of organic residues, helping to distinguish plant- and animal-derived contributions. These results were then compared with lipid residue extracted from associated sediment samples to assess potential overlaps, differences and site-specific patterns in food processing and environmental influences. Although protein analysis was initially attempted on a few potential deposits, it did not yield meaningful results. Despite this, these analytical techniques aimed to determine the extent to which HAS can serve as a reliable archive of ancient dietary practices, broadening our understanding of food preparation and consumption in prehistoric communities.

4. **Compare molecular fingerprints of HAS between sites and with existing molecular analysis of associated ceramic vessels.**

To assess the origin of organic molecules in HAS and their variability across different Neolithic contexts, lipid residues extracted from HAS at La Draga and Pendimoun were compared both within and between sites. The aim was to determine whether molecular compositions differed due to regional dietary practices, resources availability, or post-depositional processes. The molecular profile of HAS were also compared to both previously published lipid residue analyses from associated ceramic vessels.

Differences and similarities in lipid distribution, degradation patterns, and stable isotope values were analysed to explore potential correlation between vessel and stone use in food processing. The results generated from this study will be deposited in open-access digital repositories to facilitate further analysis and encourage reuse by the broader research community.

1.3. Thesis outline

This thesis is structured into eight main chapters, each contributing to the overall objective of uncovering the unexplored potential of HAS as molecular archives, offering new insights into Neolithic food processing and consumption in Western Europe.

Chapter 1 introduces the research topic, highlighting the importance of studying HAS within the context of Neolithic foodways. It outlines existing research gaps, along with the aims and objectives of the study. Additionally, it provides historical background on the spread of farming in Western Europe and an overview of Neolithic food consumption in the North-Western Mediterranean, setting the stage for the study's focus.

Chapter 2 presents a systematic literature review of existing research on HAS in prehistory on a global scale. Based on a publication drafted by the candidate, this chapter constitutes original research within the doctoral project. It examines geographic and chronological distribution of HAS, methods of identification and characterisation, and their functional interpretation in archaeological contexts. It also explores the social implications of HAS and synthesises key insights from previous studies, advocating for interdisciplinary approaches to further investigate HAS function, significance, and heritage value in archaeology.

Beyond HAS, **chapter 3** discusses lipid and protein residue analysis as a complementary method for reconstructing prehistoric foodways. It begins by defining lipids and their role in archaeological research before reviewing the application of lipid residue analysis, with a particular interest in stone artefacts. The chapter also addresses challenges related to lipid preservation, particularly in the Mediterranean environment, and their implications for archaeological interpretation.

Chapter 4 introduces the archaeological sites selected for this study: La Draga (Spain) and Pendimoun (France). It provides an overview of their historical and archaeological significance, excavation history, and the materials collected for analysis. These sites were selected for their relevance as key representations of Neolithic societies in the North-Western Mediterranean, and due to the presence of evidence related to food processing activities.

The methodology chapter, **chapter 5**, outlines the research design and analytical techniques employed in this study. It details the criteria for selecting archaeological samples from both sites, the procedures for visual inspection, and the use of 3D model acquisition to create a digital database. Furthermore, it describes the lipid residue and protein analysis methods used to investigate organic traces of food processing.

Chapter 6 presents the results, organised by archaeological site, while **chapter 7** interprets their significance within the broader context of Neolithic foodways. This discussion integrates and summarises the findings acquired throughout the course of this research project, emphasising their relevance to the two distinct archaeological contexts. It also critically addresses the research questions, providing comprehensive answers based on the data obtained.

Finally, **chapter 8** concludes the thesis by summarizing key findings and outlining potential directions for future research. It reflects on the value of a multidisciplinary approach in advancing our understanding of Neolithic culinary practices and highlights the contribution of HAS analysis to archaeological studies.

Following the main chapters, the thesis includes a comprehensive bibliography documenting all sources consulted, along with annexes providing supplementary data and methodological details.

1.4. Research background

This section provides a synthesis of archaeological research on the spread of Neolithic farming in Europe, with a particular focus on the Western Mediterranean and the associated food exploitation strategies. The transition from hunting and gathering to agriculture was a complex and regionally diverse process, influenced by environmental factors, cultural interactions, and technological advancements. It not only transformed subsistence strategies but also influenced dietary choices, food procurement, and consumption practices. By examining how early agricultural communities in Europe adopted and adapted new food resources, this section explores the interplay between local environments, cultural traditions, and economic innovations. Special attention is given to the North-Western Mediterranean, where the introduction of domesticated plants and animals interacted with existing subsistence patterns, shaping distinctive regional food economies. However, this review does not aim to provide an exhaustive account of all currently available data but rather to offer a contextual framework for the study.

1.4.1. The Neolithic: adaptation and transformation of foodways in Europe

The Neolithic period marks a significant transformation in human history, characterised by substantial changes in subsistence strategies, technology, and social organisation. While the Neolithic has traditionally been defined by technological and economic shifts (Childe, 1925), ongoing archaeological research continues to refine our understanding of this transformation, highlighting its complexity and regional variability (Stock and Pinhasi, 2011; Salazar-García and García-Puchol, 2017; Perrin et al., 2018; Bouby et al., 2020; Hamon and Manen, 2021). Originally, the phenomenon was referred to as the **Neolithic Revolution** by V. Gordon Childe (Childe, 1925). It originated in the Levantine Middle East and Southeast Anatolia at around 10,000 BCE, spreading across the Mediterranean through a complex process of land and sea routes (Figure 1) (Guilaine, 2017; Salazar-García and García-Puchol, 2017). The main revolutionary factors consisted in the cultivation of cereal crops and the domestication of animals, providing unprecedented control over food resources. By managing their own food supply, early communities were less dependent on the constraints of naturally available resources. However, this transition was not linear or without complications. The shift to farming brought about significant social and environmental changes, including increased population densities, the emergence of new diseases linked to dietary changes and close contact with domesticated animals, and growing pressures on land and labor. Within this context, past societies began to actively select, plant, and cultivate edible plants, along with the breeding of certain animal species (Vigne, 2008; Antolín, 2015).

In this frame, Greece emerged as a land-bridge between Asia and Europe, acting as a crucial area where the Aegean Neolithic transitioned into the Impressed Ware culture, which subsequently spread to both sides of the Adriatic and the Western Mediterranean (Childe, 1925; Hofmanová et al., 2016). The neolithisation of **Europe** followed two main routes: the maritime and coastal route, following the northern coastline of the Mediterranean during the sixth millennium BCE, and the inland route, spreading across the Central Balkans during the late seventh millennium and into the Danubian corridor and main river valleys and fertile plains during the sixth and beginning of the fifth millennia, and further toward the Atlantic Ocean (Zilhão, 1993; Tresset and Vigne, 2007; Hamon and Manen, 2021). These differing routes influenced how Neolithic practices spread, with scholars debating whether this process was primarily driven by **cultural diffusion**, where cereal and farming methods spread without the migration of people, or **demic diffusion**, involving the movement of the farmers themselves into new territories (Zvelebil, 2001; Pinhasi, Fort and Ammerman, 2005; Fort, 2022). At first, V. Gordon Childe (Childe, 1925) asserted that the introduction of the first domesticated plants and animals in Europe occurred through the migration or the colonisation of farming and herding communities from the Near East. This view was elaborated by Ammerman and Cavalli-Sforza in their **"wave of advance"**

model (Ammerman and Cavalli-Sforza, 1984), where the spread of the Neolithic practices was driven by population expansion. As agricultural communities expanded, they moved into new territories, progressively displacing or assimilating local hunter-gatherer groups. Contrarily, Zvelebil (Zvelebil, 2001) favoured an integrationist position that combines limited colonisation, frontier mobility, and cultural contact. While these models have provided important conceptual frameworks for understanding the spread of Neolithic practices, recent advances in paleogenetic research have largely resolved the debate in favour of demic diffusion. The spread of agriculture into Europe was accompanied by significant gene flow from Anatolian and Aegean farming populations, confirming that migration played a central role in the neolithisation process (Hofmanová et al., 2016). However, this process was not uniform. In the Western Mediterranean, particularly in southern France and Iberia, archaeological and genetic evidence indicate more complex interaction dynamics, including prolonged contact, admixture, and cultural exchange between incoming farming communities and local forager groups. Such patterns appear to be less commonly observed in more continental regions, where the transition appears to have been more abrupt (Rivollat et al., 2020; Arzelier et al., 2022)

Although some Mesolithic communities across Europe appear to have been relatively stable and semi-sedentary, this pattern can not be generalised to the continent as a whole. Zvelebil (Zvelebil, 2001) argued that, in such contexts, the transition to an agricultural way of life was often gradual, involving the incorporation of Neolithic practices into existing social and economic structures. However, in regions such as southern France and northern Italy, evidence for Mesolithic subsistence strategies remains limited and fragmentary (Binder, 2000). While some sites suggest contact or coexistence between foragers and farmers, the evidence is too uneven to determine whether the transition involved replacement, acculturation, or both. Thus, it is more appropriate to consider this as a Neolithic transition rather than a Neolithic revolution (Ammerman, 2020). Moreover, contemporary studies suggest that the diffusion of the Neolithic economy across Europe followed an **arrhythmic**, irregular and gradual pattern (Guilaine, 2001). The process is no longer perceived as a simple demographic expansion but as a complex interplay of factors, involving different forms of interaction, including cultural exchange, intermarriage, and potential conflict, between Neolithic farmers and indigenous hunter-gatherer populations (Zeder, 2008; Guilaine, 2017; Perrin et al., 2018; Ammerman, 2020; Bouby et al., 2020; Perrin and Manen, 2021; Cortell-Nicolau et al., 2025). This **dynamic** process resulted in a diverse range of Neolithic cultures marked by various strategies and economic situations responding to environmental conditions. This is highlighted by recent research which demonstrated that a specific pottery-making technique, known as the Spiralled patchwork technology, characterises impresso-cardial pottery west of the Apennines, breaking with the Aegean-Balkan Neolithic technical traditions also shared by sites on the Adriatic periphery (Gomart et al., 2017, 2022).

Moreover, the Neolithic spread exhibited significant differences between maritime and inland regions, with coastal spread occurring at a markedly faster rate. This pattern suggests that coastal spread was primarily driven by demic diffusion, with migrating farming populations directly introducing agriculture. In contrast, inland expansion proceeds more slowly involving cultural exchanges (Fort, 2022).

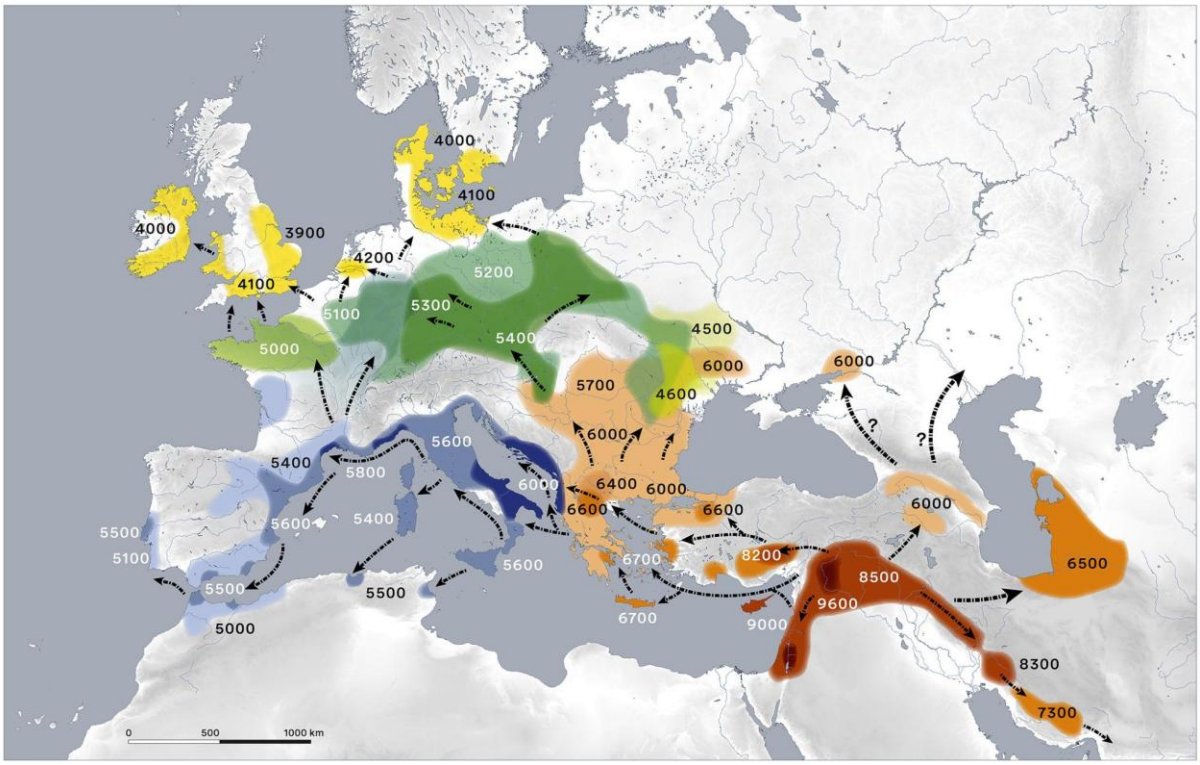


Figure 1. Condensed and simplified map of the spread of farming in western Eurasia (9600 - 4000 BCE) from Gronenborn and Horejs (Gronenborn and Horejs, 2023).

Prior to the Neolithic period, all humans relied on **hunting and gathering**, a subsistence strategy that necessitated minimal intervention in natural ecosystems. Hunter-gatherer societies traditionally operate in small, mobile groups, relocating their camps periodically to exploit seasonal resources. Therefore, they maintain a lifestyle mainly aligned with the immediate environmental conditions and resource cycles (Ammerman and Cavalli-Sforza, 1984). Cultural. technical and economic **exchanges between Neolithic and Mesolithic communities** played a crucial role in the transmission of knowledge, skills and practices. These networks enabled the diffusion of farming techniques, animal husbandry, and new forms of craftsmanship, highlighting Neolithisation as a gradual complex process of integration and exchange rather than a sudden transformation (Richter et al., 2011). Additionally, environmental factors significantly influenced the spread of agriculture, shaping the pace and extent of its adoption across different regions. Variations in climate, soil fertility and resources availability created diverse pathways for the transition to farming. While fertile soils and temperate

climates facilitated rapid agricultural adoption across Europe, harsher conditions slowed the transition, allowing hunter-gatherer lifestyles to persist longer.

The **domestication of plants and animals,** involving the genetic manipulation of species, led to the creation of new cultivars and breeds. This transition is accompanied, generally, by the so-called **Neolithic package** which, besides evidence of a subsistence based on domesticated plants and animals with taxonomy varying according to the geographical frame, includes a whole series of technical innovations in daily life such as the production of pottery and polished stone tools. These advancements had a profound impact on various aspects of past life, including nutrition, health, settlement patterns, technological development, domestic organisation and social structures (Cauvin, 1997, 2002; Renfrew, 2009; Salazar-García and García-Puchol, 2017; Vierra and Carvalho, 2019). This shift to agriculture was marked by the gradual evolution towards a **sedentary lifestyle** in some regions, resulting in residential villages (e.g. Catalhoyuk), though varied across the region, as a common feature (Fuller, Willcox and Allaby, 2011; Hamon and Manen, 2021). They typically comprise domestic areas with shared elements like houses, shared workspaces, storage facilities, burial sites, hearths, and ovens, suggesting a more permanent occupation of the village (Salazar-García and García-Puchol, 2017). Among these, **storage** methods, widely documented in Neolithic and later sites, reflect diverse strategies employed by early communities to ensure long-term security and economic stability. For instance, evidence of indoor storage suggests that households engaged in crop production, while dehusking remains found at open-air sites indicate that food processing also occurred locally within the household (Bogaard and Halstead, 2015). Additionally, the use of negative storage structures, such as silos and pits, played a crucial role in preserving surplus food and managing resources (O'Brien and Bentley, 2015; Antolín et al., 2018; Prats, Antolín and Alonso, 2020). Moreover, the development of **pottery technology** further enhanced the ability to store food and other resources, reinforcing human control over subsistence and social organisation (Childe, 1925, 1955; Guilaine, 2017; Salazar-García and García-Puchol, 2017; Hamon and Manen, 2021).

The stable and concentrated food resources provided by domesticated plants and animals facilitated long-term settlement, fostering population growth and resource accumulation. However, it is now widely recognised that sedentism often preceded domestication in many regions (Cauvin, 1997, 2002). Permanent or semi-permanent occupation allowed for the close management of local species, which in turn supported the development of more complex communities (Scott, 2017). Even though the transition from foraging to farming marked a fundamental shift in human subsistence strategies, it was neither a linear progression nor universally beneficial (Scott, 2017). While agriculture provided a more stable and energy-rich food supply, contributing to sustained population growth (Wells and Stock, 2007), it also introduced significant health challenges. The shift to a diet based predominantly on complex carbohydrates, increased the **risk of nutritional deficiencies** and associated health issues

(Cohen, 2009; Stock and Pinhasi, 2011). Beyond dietary challenges, the emergence of permanent settlements brought new environmental pressures. Close contact with domesticated animals exposed humans to novel infectious **diseases**, some of which crossed the species barrier (Wells and Stock, 2007; Cohen, 2009; Stock and Pinhasi, 2011; Scott, 2017). Despite these challenges, the domestication of plants and animals fundamentally reshaped human societies, enabling an unprecedented concentration of both food resources and human populations.

1.4.2. Neolithic dietary practices and food exploitation in the North-Western Mediterranean

The Neolithic expansion in the **Western Mediterranean** followed a distinctive pattern characterised by rapid coastal spread through multiple entry points, supporting a model of maritime pioneer colonisation over land-based expansion (Zilhão, 2001), where small groups of seafaring farmers established agricultural settlements serving as hubs for spreading farming practices. This relatively rapid spread of farming along the coasts of the Western Mediterranean has been defined by the **leapfrog colonisation**, characterised by the establishment of farming communities in new territories while bypassing intermediate areas (Rowley-Conwy et al., 2013; Bernabeu Aubán and Martí Oliver, 2014; Isern et al., 2017). Population growth during this period was influenced by **interactions** with indigenous **Mesolithic** groups, encompassing cross-mating, acculturation, and mutualism (Isern et al., 2017; Perrin and Manen, 2021; Shennan, 2018). However, some areas present a stratigraphy reflecting **hiatuses** immediately before the Neolithic phase missing the late Mesolithic occupations (Halstead, 2012; Rowley-Conwy et al., 2013; Antolín, 2016; Juan-Cabanilles and Martí Oliver, 2017; Perrin et al., 2018; Vierra and Carvalho, 2019; Piqué et al., 2021).

During the final Mesolithic in the western Mediterranean, subsistence strategies were primarily based on a combination of hunting and plant gathering, supported by an advanced flint tool production. Hunters primarily targeted terrestrial mammals, including red deer (*Cervus elaphus*), wild boar (*Sus scrofa*), roe deer (*Capreolus capreolus*), which were prevalent in the inland environments, while smaller game such as rabbit and hare (Fam. *Leporidae*) also contributed to the diet. In mountainous areas, ibex (*Capra pyrenaica*) and chamois (*Rupicapra sp.*) were key prey species. Furthermore, coastal communities gradually incorporated marine resources, exploiting molluscs, fish and marine mammals (Guilaine, 2015; Salazar-García et al., 2018). Alongside hunting, plant gathering played a crucial role in mesolithic subsistence, with evidence pointing to the collection and consumption of blackberries (*Rubus spp.*), sloes (*Prunus spinosa*) and a wide range of nuts (Vaquer et al., 1986; Zvelebil, 1994; Aura et al., 2005; Guilaine, 2015). As this period progressed, a gradual transition from food procurement to food production began, leading to a dual-mode economy where hunting and gathering coexisted with early agriculture and domestication. The cultivation of cereals and pulses, along with the

domestication of animals and the utilisation of their secondary products, became central to Neolithic subsistence strategies. However, wild resources continued to supplement diets, reflecting the persistence of foraging, hunting, and fishing in some areas (Binder, 1991; Binder and Senepart, 2004; Piqué et al., 2015). This underscored the gradual and regionally variable nature of this transition rather than a sudden, uniform adoption of agriculture (Salazar-García et al., 2018; Vierra and Carvalho, 2019).

In this framework, ceramic technology occurred leading to the development of food cooking, storage and management practices that became increasingly central to the evolving subsistence strategies (Spiteri, Muntoni and Craig, 2017; Fuller and Gonzalez Carretero, 2018; Craig, 2021). Pottery emerged not only as a practical innovation but also as a defining material marker of cultural identity, included in the so-called Neolithic package. Distinctive forms and styles of pottery became increasingly associated with specific regional groups, reflecting both the technological advancements and the social differentiation of early Neolithic communities in the Western Mediterranean. The **Impressa Ware cultures**, originating around 6000 cal BCE in the Adriatic, played a pivotal role in the Neolithic expansion into Southern France and Spain, reaching these regions by approximately 5800 and 5600 cal BCE, respectively (Binder et al., 2017, 2022a), being to date scarcely represented in the NE of Iberian Peninsula (Oms et al., 2020). The emergence of agro-pastoral societies along the French Mediterranean coast at the beginning of the 6th millennium BCE can be attributed to a colonisation model involving small groups from the Impressa complex of the Italian peninsula (Guilaine and Manen, 2002; Rowley-Conwy et al., 2013; Vierra and Carvalho, 2019; Bouby et al., 2020; Manen et al., 2021). This initial Impressa phase was followed by a more significant expansion of the **Cardial culture**, also called Franco-Iberian Cardial phase, around 5500 and 5400 cal BCE in the South of France and in Spain, which lasted several centuries. Interpretations of this transition vary: while some scholars suggest that it involved cultural discontinuities and changes in social and economic organisation (Hamon and Manen, 2021), others emphasise elements of continuity within certain regions, such as the Liguro-Provençal arc (Binder and Maggi, 2001; Binder et al., 2022a). Although the precise causes of these transformations remain unclear, it is apparent that the Cardial culture emerged as a distinct social and economic entity, potentially driven by a combination of factors, including demographic pressures, environmental changes, and cultural innovation. Recent research (Binder et al., 2022b) demonstrates that Impressa Ware networks, traditionally considered limited to coastal zones, in fact extended inland and participated in long-distance exchange systems, which challenges earlier interpretations that portrayed such network development and inland expansion as a novel feature of the Cardial expansion (Guilaine, 2018). The latter followed major fluvial routes, including Rhône, Ebro and Genil river, reaching the Pyrenees in Andorra and Aragon, as well as the Sierra Nevada in Spain. Concurrently, dense settlements emerged in regions such as Provence, Catalonia, Valencia, Andalusia, extending as far as central Portugal (Guilaine, 2015).

Diverse settlements were established adapting to the environments, ranging from open-air wetland sites with multiple dwellings to cave and rock-shelter sites (Figure 2) (Martí Oliver, 2002; Binder et al., 2017; Hamon and Manen, 2021; Manen et al., 2021). Early Neolithic settlements in **southern France** included both caves and open-air sites, with caves likely serving as seasonal hunting camps and open sites as permanent domestic settlements (Binder, 1991). Notably, some sites represent the earliest evidence of Neolithic practices in the region, including Pont de Roque Haute and Peiro Signado at Portiragne (Herault), and the lower layer of the Pendimoun shelter at Castellar (Alpes-Maritimes) (Guilaine, 2015; Shennan, 2018; Binder et al., 2020). Similarly, in **Mediterranean Iberia**, early Neolithic settlements encompassed both cave and open-air sites, reflecting a range of subsistence and settlement strategies. Key sites that provide early evidence of Neolithic lifeways include Can Sadurní and La Draga (Catalonia), Cova de les Cendres and Mas d'Is (Valencia), and Cueva de Nerja (Andalusia) (Cruz Berrocal, 2012; Bernabeu Aubán et al., 2014; Peña-Chocarro, Pérez-Jordà and Morales, 2018; Shennan, 2018; Pardo-Gordó et al., 2020).

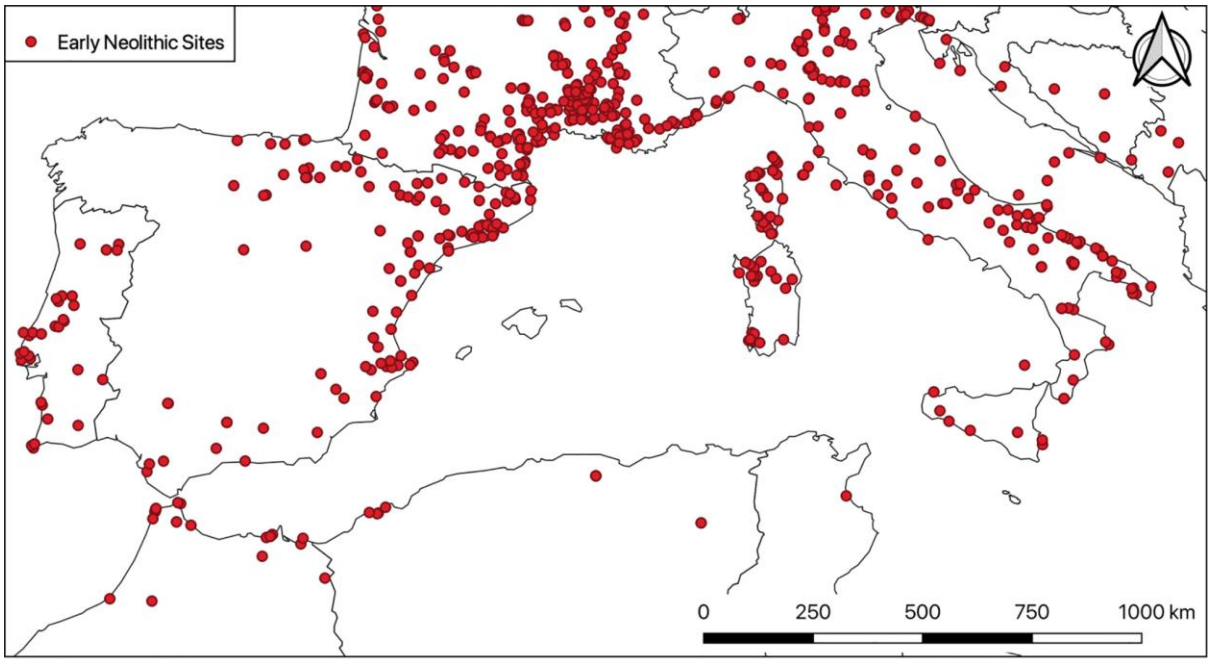


Figure 2. Distribution maps of early Neolithic sites in the Western Mediterranean. Reproduced from Perrin et al. (Perrin and Manen, 2021).

Throughout the Western Mediterranean area, a wide variety of crops were cultivated during the Neolithic with some probable regional peculiarities. Along **southern France** evidences revealed the presence of hulled wheats, such as emmer (*Triticum dicoccum*) and einkorn (*Triticum monococcum*) as predominant **cereals**, along with naked wheat (*Triticum aestivum*), barley (*Hordeum vulgare*), and pulses (Bouby et al., 2018, 2019; Binder et al., 2020; Goude et al., 2020). Later on, with the spreading of Cardial/Epicardial culture, the agriculture was mostly based on naked wheat and barley, but also

characterised by a higher presence of pea (*Pisum sativum*), poppy (*Papaver somniferum*) and wild fruits like acorn (*Quercus sp*) and hazelnuts (*Corylus avellana*), even if of secondary importance (Bouby et al., 2018, 2019; de Vareilles et al., 2020; Binder et al., 2020). Almost the same spread occurred in the **Iberian coastal** frame, where naked wheat and barley prevailed among cereals especially during the second half of the 6th millennium BCE (Antolín and Buxó, 2012; Antolín, 2015; de Vareilles et al., 2020; Araus et al., 2024). Legumes, like lentil (*Lens culinaris*) are present from the beginning stage of agricultural diffusion, while pea and board bean (*Vicia faba*) appeared to have a larger diffusion thereafter (Antolín and Buxó, 2012; Antolín, 2015). Other crops like poppy, grass (*Lathyrus sativa*), red pea (*Lathyrus cicera*), bitter vetch (*Vicia ervilia*), common vetch (*Vicia sativa*) and flax (*Linum usitatissimum*) were also part of the agricultural assortment of domestic species in the Iberian Peninsula (Zapata et al., 2004; Peña-Chocarro, Pérez-Jordà and Morales, 2018; Jesus et al., 2023). Additionally, wild fruits like acorn, hazelnut, lentisk (*Pistacia lentiscus*) and wild grape (*Vitis vinifera subsp. sylvestris*) were present mostly during the Early and Middle Neolithic (Antolín, 2015). The presence/absence of carbonised shells suggested the roasting practice of wild fruits as a particular process especially in mountain sites (Antolín, 2015).

Stable isotope evidence of the Neolithic human diet in southern Europe indicate a substantial contribution of **animal** protein to the diet during the 6th millennium BCE, suggesting a possible increase of animal processing practices (Bogaard and Halstead, 2015; Binder et al., 2020; Goude et al., 2020). Zooarchaeological studies confirm the predominance of domesticated animals over wild species, advancing the use of a mixed-economy during the Neolithic (Saña, 2013; Antolín et al., 2014; Salazar-García et al., 2018). Ovicaprid species (*Ovis aries* and *Capra hircus*) were the primary livestock, though cattle (*Bos taurus*) and suids (*Sus sp.*) were also present (Zapata et al., 2004; Navarrete et al., 2017; Binder et al., 2020; Saña et al., 2020). The concept of "secondary product revolution", introduced by Sherratt (Sherratt, 1983) proposed that domesticated animals were initially exploited for meat, while secondary products like milk, but also fibres and force of labour (riding and traction), became significant only toward the end of the Neolithic. Subsequent research has revised this view, suggesting that the exploitation of secondary products began earlier and followed species- and region-specific trajectories (Vigne and Helmer, 2007; Greenfield and Arnold, 2015). Although the exploitation of secondary products was not yet intensively and likely served as a supplementary resource to meat consumption, milk procurement represents a significant innovation linked to animal domestication. It marked a transition from the exploitation of wild animals by hunter-gathers to the deliberate and controlled use of domesticated species (Vigne and Helmer, 2007; Halstead, 2012). Recent studies provide compelling evidence of **dairying** practices in the northwestern Mediterranean region, suggesting that early Neolithic communities actively exploited animals for dairy production and consumption (Antolín, 2015; Debono Spiteri et al., 2016; Spiteri, Muntoni and Craig, 2017; Antolín et al., 2018). Moreover, **hunting** diminished in importance as a subsistence strategy, though it persisted into the Neolithic period

concerning wild boar, roe deer, deer (Halstead, 2012; Piqué et al., 2015; Spiteri, Muntoni and Craig, 2017; Salazar-García et al., 2018; Vierra and Carvalho, 2019). Likewise, **fishing** experienced a significant decline, as evidenced by the limited presence of fish bone remains, suggesting a preference for land-based activities over marine exploitation (Herrscher and Le Bras-Goude, 2010; Spiteri, Muntoni and Craig, 2017).

The transition to agriculture and pastoralism brought about a technological shift, marked by the introduction of **new tools**. These tools became essential to the daily routines and labour practices of Neolithic societies, reflecting the deep integration of technological innovations into the organisation of domestic activities and the development of subsistence strategies (Zapata et al., 2004; Bernabeu Aubán and Martí Oliver, 2014). The lithic industry experienced a notable shift in the production of tools. The flint knapping process produced a significant number of blades and bladelets serving as laminar supports for a variety of implements, including knives, sickles, drills and perforators, primarily used in agricultural tasks (Martí Oliver, 2002; Defranould, 2021). Additionally, stone polishing techniques yielded a wide range of axes and adzes, which were predominantly associated with wood processing (Martí Oliver, 2002; Shennan et al., 2017). Grinding stones also played an important role in this scenario, emphasising the intensification of agricultural practices and advancements in food preparation techniques. Their widespread presence at Neolithic sites underscores their essential function as utilitarian implements for processing large quantities of cereals into flour (Hamon, 2021). Equally significant was the innovation in grain storage, which involved the use of pits, vessels and basketry containers, representing a critical advancement in the management and preservation of agricultural surpluses (Antolín and Buxó, 2012; Antolín, 2015).

Pottery production appears closely tied to the development of new food consumption practices, though it may have also served other functions, such as symbolic, ritual or craft-related uses. As vessels were employed for storing, cooking and serving food, they facilitated the adoption of novel culinary techniques. The introduction of ceramics enabled the processing and consumption of a wider variety of foodstuffs, particularly cereals, and allowed for more complex food preparations (Spiteri, Muntoni and Craig, 2017; Vierra and Carvalho, 2019). As previously outlined, Impressa/Cardial wares are among the earliest ceramic forms to emerge in the Mediterranean region (Figure 3). Their characteristic decorative style consists of impressions made through fingers, sharp instruments and/or shells (Guilaine, 2018). The disparate **morphologies** of ceramic vessels, encompassing a diversity of shapes and dimensions, can be indicative of varied **functions**, reflecting different necessities linked to food production and consumption. This relationship has been the focus of extensive research, particularly concerning the pottery production, exploring the chaîne opératoire, as well as the analysis of decorative patterns and other technical aspects (Bernabeu Aubán, 1989; Binder et al., 2010a, 2010b; Bernabeu Aubán et al., 2011; Drieu, 2017). Within this framework, vessel morphology has been recognised as a

critical indicator of functionality, enabling the differentiation between ceramic used for storage, processing, cooking, and consumption (Martí Oliver, 2002). For instance, big vessels are commonly interpreted as suitable for storage and transportation of goods, while smaller vessels and flat containers are often associated with food preparation and serving (Breu, 2019; Tarifa-Mateo et al., 2024). Such functional distinction not only provides insight into subsistence practices but also contributes to broader understanding of the social, economic and cultural dimension of pottery use in past communities (Breu et al., 2021). Additional analyses on pottery, such as **organic residue** and **isotopic analysis**, have significantly contributed to the study of Neolithic food production and consumption in the North-Western Mediterranean (Spiteri, Muntoni and Craig, 2017; Cubas, Peyroteo-Stjerna and Fontanals-Coll, 2019; Drieu et al., 2019, 2021; Breu et al., 2023b). These methods allow researchers to extract and identify organic compounds absorbed and preserved in ceramic vessels. The results reveal evidence of the processing of animal fats alongside plant products (see Chapter 3 for more details), suggesting a diversified diet and a refined use of resources.

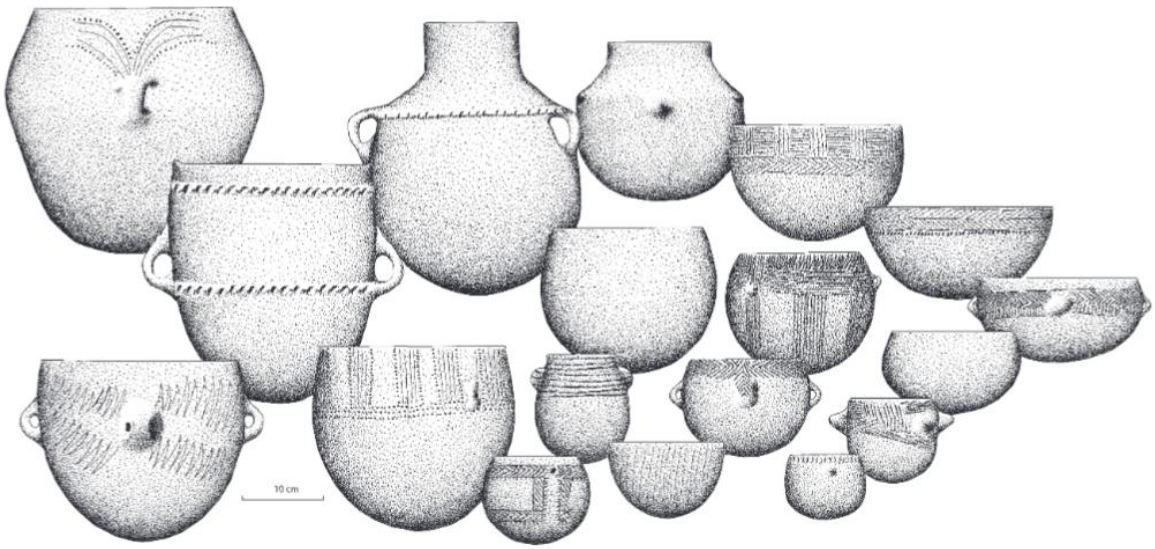


Figure 3. Set of ceramic vessels from the Early Neolithic (Cardial and Epicardial). Reproduced from Binder *et al.* (Binder et al., 2010a). Drawings by J.Coularou.

Unlike ceramics, which represent a clear technological innovation of the Neolithic period, fireplaces and combustion structures composed of **HAS** are not unique to this framework. However, the role of HAS in Neolithic food preparation and daily life remains equally important. Hearths and fire pits commonly located in domestic contexts, serve as areas for fire-making, fulfilling essential tasks such as cooking, heating, technical procedures, and social activities. In many cases, HAS were not merely by-products of repeated exposure to fire, but were actively integrated into hearth construction, functioning as thermal agents in cooking processing (Binder, 1991; Frère-Sautot, 2003; Binder and Senepart, 2004; Fernández Ruiz et al., 2018; Monforte-Barberán et al., 2023; Hart, 2024). These stones

were either used to line the hearth or heated and directly applied in specific cooking methods, such as stone boiling or roasting. Beyond their structured use in hearths, HAS are also frequently found scattered across occupation surfaces or concentrated in discard zones, suggesting habitual reuse. The analytical potential of HAS lies in their ability to reveal subtle aspects of prehistoric culinary behaviour. Yet despite this, their presence and function in Neolithic contexts have often been overlooked in favour of other materials, like ceramics. This gap impinges upon our understanding of prehistoric culinary practices, the evolution of cuisine, and its impact on the overall diet and economies in the past (Cantelli et al., 2024).

2. Heat-altered stone analysis: a state-of-the-art review[2]

Over the last decades, HAS have been documented by archaeologists without initially being a central research focus. This trend started to shift during the 1970s and 1980s, with growing attention on understanding fire-related activities. In Europe, for instance, modern research on how prehistoric spaces were structured was heavily influenced by the school of A. Leroi-Gourhan (Leroi-Gourhan and Brézillon, 1966, 1972), which gave birth to the new field of comparative technology using analytical methods for comparing technical aspects. Consequently, the research started to move beyond simply describing hearths to investigating their role and use in prehistoric life. Similarly, Binford's research (Binford, 1978) provided a framework for understanding the various ways fire can be used, offering new insights into fire-related archaeological evidence. Within this context HAS were not studied alone, but as part of the bigger picture of fire structures use and the organisation of space around them. They have typically been presented in monographs, conference proceedings and excavation reports as components of various structures (Binder, 1991; Frère-Sautot, 2003; Olive and Taborin, 1989), indicating they were not given comprehensive consideration. As a result, finding detailed studies on HAS in published records is challenging.

Heat-altered stones are commonly reported in prehistoric sites across several continents, yet they continue to be generally overlooked and systematic studies on them are scarce. Considerable uncertainty still remains about their geographic, chronological and cultural distribution, as well as their relation to particular resources and other food processing techniques (Graesch et al., 2014; Petraglia, 2002). To address some of these gaps we conducted a review of the global literature reporting on archaeological HAS. Systematic literature reviews are essential parts of academic research (Nightingale, 2009; Okoli, 2015; Xiao and Watson, 2019; Linnenluecke, Marrone and Singh, 2020), through which a starting point for larger research can be provided. We examined 73 scientific articles, book chapters and books from 1942 to 2023, and compiled information to derive a comprehensive perspective on the geographic distribution, chronology, technological, subsistence and culinary contexts of HAS across different regions and time. We assessed some of the analytical advances and main challenges of studying HAS over the last decades.

We performed a systematic literature review in April 2024, which consisted of searching journal articles, book chapters and books published in English, in Scopus and Web of Science. In both

[2] This subchapter is drawn from "*Diamonds in the rough - reconsidering the scientific and heritage value of heat-altered stones in prehistoric archaeology through a systematic literature review*", published in Open Research Europe (Cantelli et al., 2024). The article was authored by the candidate and represents original research conducted as part of this doctoral project.

databases ALL FIELDS were searched using specific keywords relevant to the scope of this work: “Stone cooking” AND “Archaeology”, OR “Fire-cracked stones” AND “Archaeology”, OR “Heat altered stones” AND “Archaeology”, OR “Boiling stones” AND “Archaeology”. A total of 46 publications (items) were obtained from Scopus and 82 from the Web of Science. Duplicates were then removed, resulting in 123 items. These items were then analysed as follows, to take into account possible subject bias. Firstly, the abstract of each item was read independently by the first and the last authors to evaluate the relevance based on the inclusion criteria “stone/rock(s)” related to cooking/culinary activities. The first and last authors then discussed their independent assessments, which resulted in the exclusion of 84 items, reducing the dataset to 39 items. Secondly, the items were fully read by the two authors to ascertain the relevance of the entire research and a total of 5 items were excluded due to their focus on groundstones, ceramics and flake production, which were deemed off-topic. The final number of eligible items was 34. The systematic literature review, however, failed to capture several research outputs that were cited in the selected items. This prompted us to consider a snowball sampling method (Wohlin et al., 2022) to increase the overall record, which increased the number of items to 73. Grey literature (such as master's dissertations, PhD theses, and local excavation reports) was excluded from our search due to the unpredictability of mapping these resources on a global scale. Although this type of literature can provide valuable information, conducting research on global grey literature would be infeasible.

The 73 items were distinguished between experimental study (including modelling) and/or archaeological reports, and catalogued in an Excel file, with columns containing information about a set of systematically collected variables (available at https://doi.org/10.5281/zenodo.14005823). Descriptive and binary variables related to contextual information included region, site, cultural attribution (e.g. Neolithic, Middle Woodland, etc.), chronology (as reported in the original publications), subsistence system (foraging, farming, foraging/farming), presence of ceramics (Y/N), if stones were found as part of a structure(s) (hearth, stone piles, stone pits), etc. These were followed by the terminology employed to describe the stones, mineral composition and type of analysis. In addition, we classified the items according to the main content of the study: 1) identification and characterisation of heat altered stones, 2) interpretation of stone use (cooking, heating facilities), 3) theoretical propositions on the evolving nature of these stones and relative social implications.

From the 73 items recovered, 59 reported HAS in archaeological contexts, while 35 presented experimental studies mainly focused on the replication of cooking processes. Of the 59 items reporting archaeological contexts, the majority represented archaeological sites in North America (53%) and Europe (36%), followed by few studies in Africa, Oceania, Asia and South America (Figure 4). Of these, 78% could be assigned to archaeological cultures of the Holocene and the remaining 22% to the Pleistocene. Overall, 39 studies (66%) reported HAS associated to foraging groups, while 10 (17%)

reported them among farming societies, and the remaining to a combination of foraging and farming groups due to reports combining multiple sites, chronologies and/or occupations. In addition, only 16 studies (27%) reported HAS in archaeological contexts with ceramic artefacts, while the remaining 43 (73%) either lacked ceramic remains or did not mention their presence. The majority (80%) of HAS documented in the 59 records are associated with some structures, such as burnt mounds, pits, and hearths (Figure 5).



Figure 4. Geographical location of the case studies (the world map was created using the OpenStreetMap package: (Fellows and Stotz, 2023)).

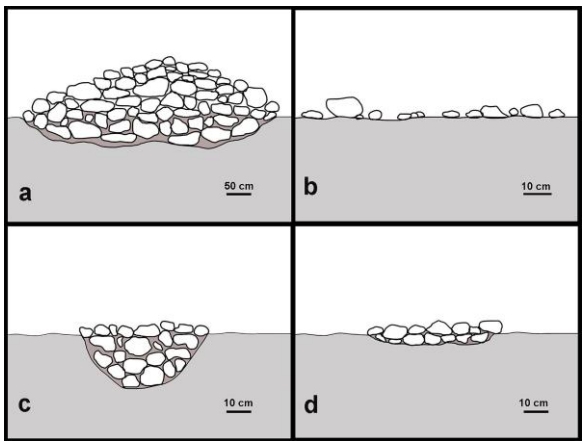


Figure 5. Schematic profile illustration examples of stone structures: (a) burnt mound, (b) scattered stones, (c) pit, (d) heart.

Notably, we found up to 32 distinct terminologies used to report HAS, which imposes considerable challenges in comparative analysis and attempts to establish common criteria for the identification of this class of artefacts (Neubauer, 2018). Moreover, our results indicate a prevalence of a few lithologies as HAS in archaeological records. Specifically, sandstone and quartzite emerge as the predominant group, followed by limestone, granite and quartz. This pattern may suggest deliberate selection of rocks with specific physical and chemical properties, as demonstrated by experimental studies (see below). Furthermore, the results show that the identification and characterisation of HAS rely mostly on experimental approaches and physico-chemical analyses, while the functional interpretation of HAS rely primarily on their spatial distribution and contexts (Figure 6) (Movius, 1966; Frison, 1983; Petraglia, 2002; Hawkes, 2018; Schaefer-Di Maida, 2022), including the presence of well-defined structures (cooking pits, burnt mound, earth ovens, stone boiling pits, etc).

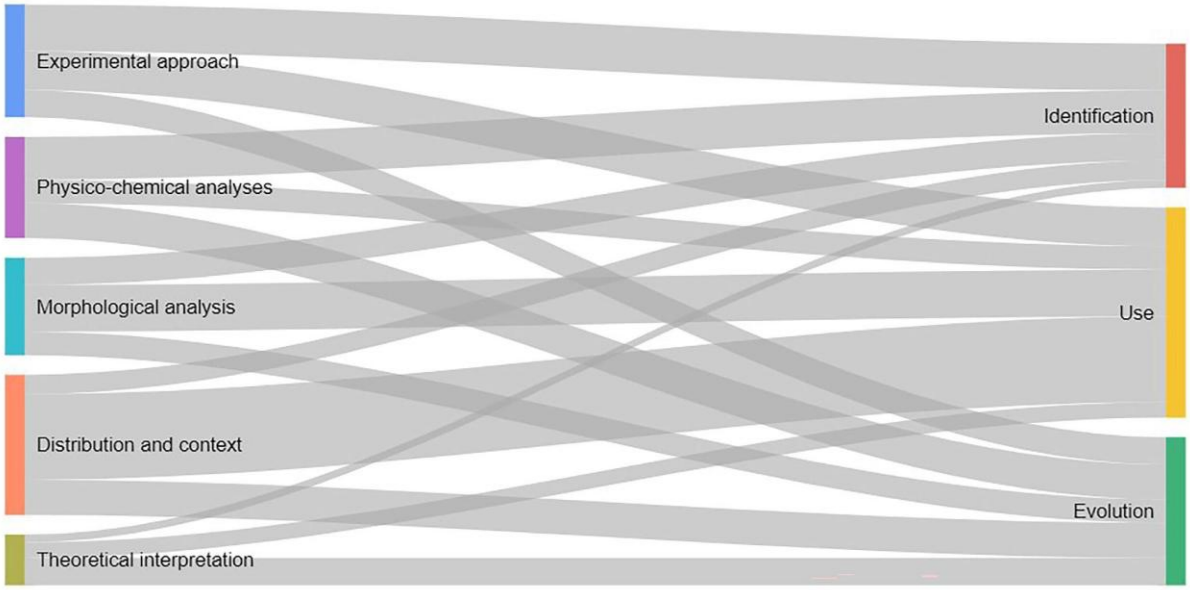


Figure 6. Sankey plot showing the relationship between methodologies applied and archaeological questions about HAS.

Our analysis revealed a significant shift in the methodological landscape of HAS research over time (Figure 7). It was not until the 1980s that chemical and physical approaches were applied, along with a marked increase in the frequency of experimental studies. Furthermore, the past two decades have seen an exponential growth in HAS research, combining also different methods. Moreover, identifications through chemical and physical analyses (e.g., digital images, dating technique, magnetic susceptibility), along with morphological observations, and experimental studies have increased in recent years.

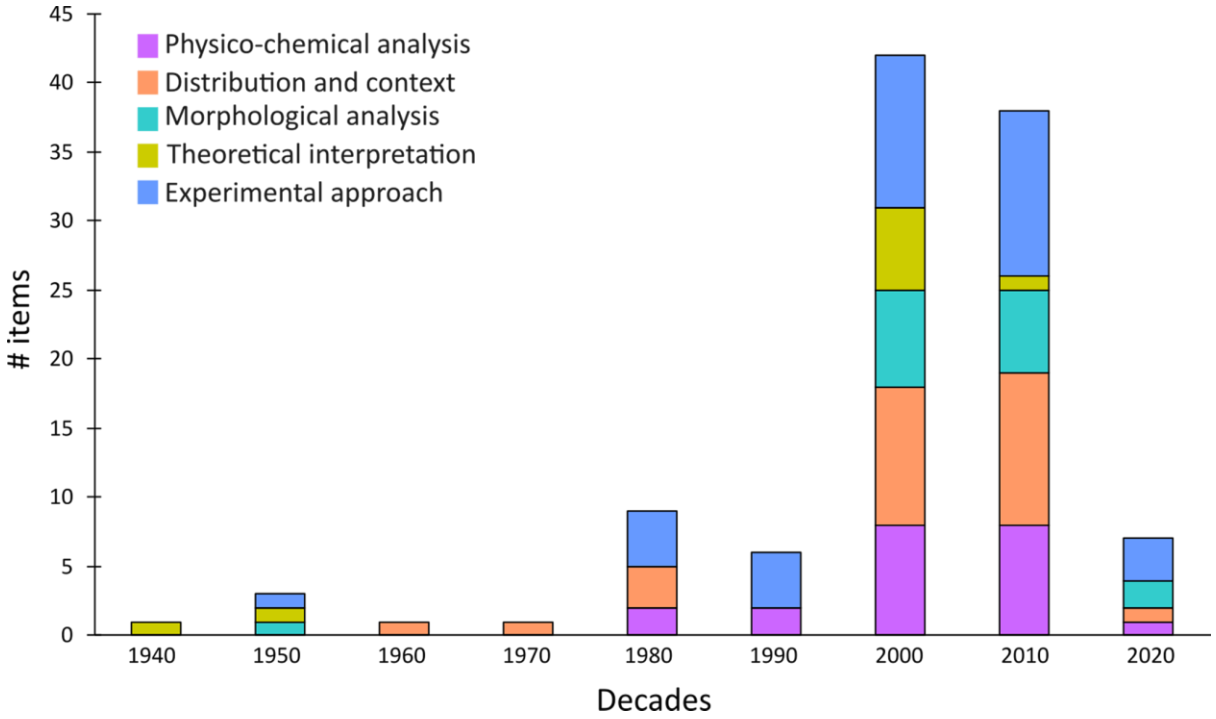


Figure 7. Methodological approaches over the 20th and early 21st centuries.

2.1. Geographic and chronological distributions of HAS

Our assessment on HAS revealed a strong research bias towards evidence from North America and Europe, as recently reported by Neubauer (Neubauer, 2024). HAS are documented since the Pleistocene from these regions, attesting that culinary and non-culinary activities using heating stones emerged among foraging groups subsisting on hunting, fishing and gathering (Petraglia, 2002; Thoms, 2009). We observed considerable gaps in knowledge on HAS for Africa, Oceania, Asia, and South America, which are key geographic areas for assessing the role of heating stones in human evolution, geographic dispersal, early cuisine and diet, and cultural transmission across the globe. We consider these regions as priority areas for future research on prehistoric HAS.

The high frequency of HAS during the middle and late Holocene testifies to the endurance of some practices over long time periods, amid the emergence of new food systems and the introduction of new resources and technologies, such as domesticated plants and animals, and ceramic containers. In North America, HAS have been predominantly reported among “Archaic” groups with foraging subsistence systems (Griffin, 1967; Sutton, 2015). A few referred to the middle Woodland period (Pagoulatos, 1992; Skibo, Malainey and Drake, 2009; Custer, 2017) and to the Basketmaker II period (Ellwood et al., 2013), which exhibits evidence of agricultural practices. In Europe, HAS were reported in few Palaeolithic and Mesolithic sites (Movius, 1966; Nakazawa et al., 2009; Little, 2014; Bang-Andersen, 2015; Pop et al., 2021), although structures containing HAS were extensively documented among farming societies of north Europe from the Neolithic to the Iron Age (O’Kelly, 1954; Barfield

and Hodder, 1987; Ó Drisceoil, 1988; Anthony et al., 2001; Eskola, Okkonen and Jungner, 2003; Petersson, 2013; Viberg, Berntsson and Lidén, 2013; Lindgaard, 2015; Swedberg, Östlund and Jacobsson, 2017; Hawkes, 2018; Schaefer-Di Maida, 2022). These structures have been documented as *fulacht fiadh* in archaeological sites in Ireland and as burnt mounds in Britain (Barfield and Hodder, 1987; Ó Drisceoil, 1988; Anthony et al., 2001; Hawkes, 2018). Their use encompasses culinary practices, as well as burial, domestic and ritual activities (e.g. sweat lodge, feasts) involving large groups of people (Hawkes, 2018; Petersson, 2013; Ó Drisceoil, 1988; Barfield and Hodder, 1987; Custer, 2017), indicating that HAS may result from cooking and non-cooking activities. Comparable structures were defined as cooking stone pits in the German and Scandinavian literature (Schaefer-Di Maida, 2022; Fretheim, 2009), suggesting their use predominantly for cooking activities but without certain evidence (Swedberg, Östlund and Jacobsson, 2017).

2.2. Identification and characterisation of HAS

One of the most significant challenges in the field of archaeology is the continued uncertainty surrounding the fundamental definitions of these artefacts and the key diagnostic elements for their identification. We also observed a generalised lack of consistency in how HAS are documented and reported, as previously observed by others (Graesch et al., 2014; Pop et al., 2021), which highlight some of the challenges of studying HAS. For example, Fire-Cracked Rocks (FCR), which describes stones that have been fragmented and shattered by fire in cooking activities, was the most commonly reported term, occurring in 61% of the items (Sullivan et al., 2001; Custer, 2017; Neubauer, 2018; Stuart and Walker, 2018; Gao et al., 2014; Cutts et al., 2019; Black and Thoms, 2015; Thoms, 2009). This was followed by the terms “heated” and “hot stones” (Nelson, 2010; Schaefer-Di Maida, 2022; Ellwood et al., 2013; Pop et al., 2021; Thoms, 2008b), along with “burned stones” (Bock, Neubeck and Pasda, 2017; Buonasera, 2005; Asfora et al., 2014; Black and Thoms, 2015). In addition, the terms “cooking” and “boiling stones” were widely used, implying specific functions in culinary activities (Buonasera, 2005; Short et al., 2015; Shantry, 2020) and in boiling liquids (Short et al., 2015; Shantry, 2020; Pop et al., 2021; Thoms, 2008a). Also reported were: “firebroken rocks” (FBR), denoting rocks that exhibit characteristics of thermally induced fractures due to heating and subsequent cooling in water (Brink and Dawe, 2003); “fire-modified rocks” (FMR), used to indicate rocks that have undergone some anthropogenic modification to improve mechanical features (Carney et al., 2022; Oestmo, 2013); “thermally altered” and “thermally modified rocks” (TMR), used to indicate stones that present physical transformations, such as fractures, cracking, crazing and discoloration, as a result of exposure to heating and cooling process (Graesch et al., 2014; Bentsen and Wurz, 2019; Nakazawa et al., 2009; Petraglia, 2002; Homsey, 2009); “culturally-heated rock” (CHR), representing rocks exposed to heat as a result of different cooking methods (Shantry, 2020), among others. In an attempt to systematise the

terminology we recommend the use of HAS when reporting this class of artefact in the absence of information on the artefact-specific functions.

Along with the terminology employed to describe the stones under investigation, we encountered a multitude of wording used in literature to define rock alterations caused by heat and/or fire. This observation has been previously acknowledged by Neubauer (Neubauer, 2018) who proposed a standardised terminology to help researchers with their description. A list of twelve distinctive patterns related to use alteration of HAS was provided along with three different types of fractures based on size and morphology (Table 1).

Table 1. Heat/fire alteration patterns of HAS according to Neubauer (Neubauer, 2018).

Use alteration patterns	**Fracture types**
1. Heat fracture 2. Differential luster 3. Fine crazing 4. Deep surface cracking 5. Exfoliation 6. Pit-lid negative/scar fracture 7. Discoloration 8. Reddening 9. Sooting 10. Oxidised patch 11. Irony oxidation 12. Adhesion	• spall/pseudo flake fragment, small and the size of a flake. • blocky/pseudo core fragment, when the stone is broken along its core. • Pot-lid "flake" fracture, which results from differential expansion causing the detachment of a fragment that appears flat on the dorsal side and convex on the ventral side, with its major thickness in the central part.

Changes in colour represents one of the more intuitive indicators for identifying thermally altered rocks, being a consequence of direct and indirect fire exposure (Pagoulatos, 2005). These changes are normally associated with a reddening of the exposed rock surface due to thermal alteration of the iron oxides. In some cases, experimental studies involved the evaluation of colour changes after heating processes between experimental and prehistoric stones. The changes are usually evaluated through visual observation, Munsell colour notations and their relative conversion into numerical values, and digital imaging (Bentsen and Wurz, 2019; Schaefer et al., 2014; Oestmo, 2013). Digital imaging techniques favoured the differentiation between unburned and experimentally burned stones based on their physical appearance (Oestmo, 2013). Given that visual observation is a subjective criterion that could be affected by the colour perception of the observer, it is crucial not to rely exclusively on colour evaluation, but to complement it with additional techniques, for example petrographic analysis, that could detect microscopic features associated with heat alteration (Homsey, 2009). Therefore, some researchers advanced the interpretation of archaeological stones throughout experimentation, considering not only discoloration, but other key factors such as fracture rate, fragment

type, crazing, pocking, spalling and shapes (e.g. prismatic or platy) (Custer, 2017; Graesch et al., 2014; Pagoulatos, 1992, 2005; Nickels et al., 2001). Moreover, experimental simulations suggested that thermal alterations were less present in stones exposed to short-term re-use, while whitening, cracking and spalling were more common on long-term re-use (Pagoulatos, 2005). A prolonged exposure to heat might cause cracking in the form of thin crack lines and spalling (the fragmentation of the stones), while sudden heating led to pot lids, crater-like surface depressions (Pagoulatos, 2005; Cutts et al., 2019). Neubauer (Neubauer, 2018) also proposed four attributes to determine the reuse of HAS. The absence of cortex along with a high percentage of fracturing pattern could indicate multiple episodes of heating and cooling, while small size and low weight could suggest that the stone has been repeatedly used.

The identification of heated or non-heated stones has also been tested through the use of physical methods. Archaeomagnetic techniques, based on magnetic susceptibility which is greater in burned stones, has proven useful in identifying stones that were heated to at least 200°C (Gose, 2000; Barbetti et al., 1980; Bischoff, Ikeya and Budinger, 1984; Nickels et al., 2001). This is an important approach for distinguishing in-situ oven and griddle stones from those heated in one place and cooled in another (Viberg, Berntsson and Lidén, 2013; Nickels et al., 2001), as would be the case for stones used in stone boiling or some types of pit steaming and baking (Gose, 2000; Swedberg, Östlund and Jacobsson, 2017; Abbott and Frederick, 1990). Alternative methods employed to test whether the stones were subjected to heating rely on radiometric and luminescence dating methods. Radiometric dating, specifically the 40Ar-39Ar technique, involves analysing potassium-bearing minerals from stones to determine if the lithic was heated to a temperature above 500ºC for at least 30 minutes (Gillespie, Budinger and Abbott, 1989). Among the luminescence-based approaches, optically stimulated luminescence (OSL) was demonstrated to be more suitable compared to thermoluminescence (TL) (Asfora et al., 2014), including post-infrared infrared (pIRIR) feldspar luminescence (Pop et al., 2021), due to its reduced material requirement and faster processing time (Rapp, Balescu and Lamothe, 1999).

2.3. Functional interpretation of HAS

Our literature investigation documented a range of cooking techniques that may have involved heating stones, including platform hearth, stone boiling and earth ovens (Figure 8). These techniques are reported throughout distinct geographic and temporal scales in North America and Europe. Platform hearth, also called rock griddle or roasting pit, is considered an open-air cooking technique consisting of a single layer of rocks upon which a fire is lit. Food can be cooked/dried directly on the rock surface or in a vessel in contact with the flames (Thoms, 2008b; Custer, 2017; Neubauer, 2018; Brink and Dawe, 2003; Thoms, 2007). Stone boiling technique involves the heating of a liquid that usually is the cooking medium. Stones previously heated in a nearby fire are placed into a container with the cooking liquid, and the stones heat heat the liquid in which the food will be processed (Brink and Dawe, 2003;

Thoms, 2008b; Short et al., 2015; Neubauer, 2018; Nelson, 2010; Speth, 2015; Thoms, 2007). This practice is also called cooking by convection (Graesch et al., 2014) and can also be used in grease rendering (Nakazawa et al., 2009; Oetelaar and Beaudoin, 2016) and the preparation of an animal carcass for skinning and removing hair (Custer, 2017). Earth ovens permit baking food thanks to the moist heat produced in an oxygen-reduced environment, even for a long period of time. They are typically formed by a pit filled with stones heated by a fire and covered with plants and food topped with an additional layer of plant materials and hot rocks, all covered by a layer of earth (Short et al., 2015; Custer, 2017; Neubauer, 2018; Carney et al., 2022; Leach, Bousman and Nickels, 2005; Hawkes, 2018; Homsey, 2009; Black and Thoms, 2015; Nickels et al., 2001). A variant of the same structure, termed a steaming pit, is characterised by a small hole in the earthen lid allowing the release of the steam or the addition of water (Thoms, 2008b; Custer, 2017; Hawkes, 2018; Thoms, 2007; Driver and Massey, 1957).

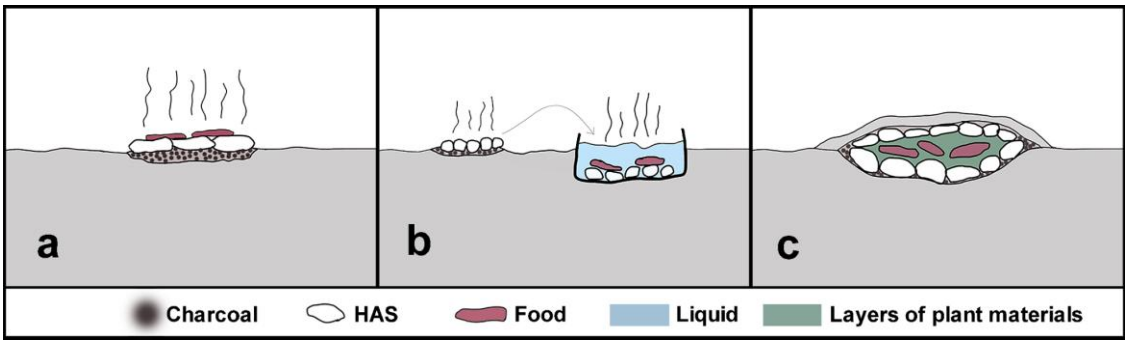


Figure 8. Illustration example of generic cooking techniques: (A) platform hearth, (B) stone boiling technique, (C) earth oven.

In addition, an attempt was made to distinguish HAS used in ritual activities from those used for culinary practices (Lindgaard, 2015). The abundance of HAS in the proximity of a water source, combined with the absence of settlement evidence and food remains, suggested that HAS were likely used for heat and steam production related to potential sweat lodge rituals rather than domestic culinary activities (Barfield and Hodder, 1987). Moreover, some investigations have assumed that stones used in rituals were subjected to prolonged and intense heat, resulting in a lower density compared to those used for cooking (Clark and Custer, 2003; Custer, 2017). Although not conclusive, this suggests that density may serve as a proxy for determining the function of HAS.

Cooking practices using heated stones were also likely affected by environmental factors, as some techniques are more or less effective under different climatic and ecological conditions. For example, although stone boiling was widespread among Indigenous groups in North America, its use was limited in areas with scarce fuel material (wood) such as the Arctic and subarctic regions (Driver and Massey, 1957). Subsequent studies have proposed that stone boiling requires large amounts of fuel

and heat conservation capacity to increase the stone temperature for its efficient use (Nelson, 2010), making it less efficient and more labour intensive in cold regions.

A large body of the assessed literature focused on establishing visual and chemical diagnostic features in order to accurately identify and assess the function of HAS in prehistoric contexts (Table 2). These approaches typically use both archaeological observations (Leach, Bousman and Nickels, 2005; Little, 2014; Schaefer-Di Maida, 2022; Bang-Andersen, 2015; Shiner and Shiner, 1977) and experimental studies (Thoms, 2008b; Brink and Dawe, 2003; Gao et al., 2014; Backhouse and Johnson, 2007; Homsey, 2009; Wilson and DeLyria, 1999).

Table 2. HAS features related to culinary practices.

Cooking technique	**Stones features**	**Key references**
Stone Boiling	River cobbles, crenulated fractures, crazing, reddening	(Brink and Dawe, 2003)
	Contraction fractures, crazing, jaggies	(Carney et al., 2022)
	Small to medium-sized rocks, lack of carbon staining	(Thoms, 2008b)
	Breakage	(Gao et al., 2014)
	Crenulated fractures, angular fragments	(Oetelaar and Beaudoin, 2016)
	Irregular crenulated fractures on the breakage faces and ridges on the inside (wet-cooling contraction)	(Neubauer, 2018)
	Angular profile, low weight	(Petraglia, 2002)
	Core type fragments	(Custer, 2017)
Roasting pit/ Griddle	Flat slabs, red oxidation stain on the upper surface, scorching, discoloration, spalling, separation along bedding planes	(Brink and Dawe, 2003)
	Spalling, smooth contours and fairly sharp edges	(Oetelaar and Beaudoin, 2016)
	Boulder to cobble-size stones, spalling	(Carney et al., 2022)
Earth oven/ Steaming pit	Flat, convex/concave breakage faces	(Carney et al., 2022)
	Carbon staining, medium to large flat rocks, cracking, oxidation	(Thoms, 2008b)
	Flat, convex, or concave breakage faces (dry-cooled expansion fracturing)	(Neubauer, 2018)
	Numerous fractures	(Gao et al., 2014)

Expansion and contraction were defined as two main agents of fractures by Neubauer (Neubauer, 2018) and were related to specific cooking technologies. Expansion breakages occur in stones heated and cooled in hearths. Since the external part is subjected to more heat and expands faster than the inner part, stones that underwent this dry-cooled process (open-air hearths) display flat, convex, or concave breakage faces that are smooth. On the other hand, contraction develops mostly in heated rocks used for stone boiling. During a rapid cooling in water the external part contracts and undergoes a thermal shock, causing irregular fractures on the breakage faces and some ridges on the inside of the stone. While the presence of both features may indicate reuse, another potential sign is the refitting of discarded HAS fragments (Leesch et al., 2010). Moreover, it is crucial to note that the final location of HAS fragments at the site may not accurately reflect the position of the fire structure where they were last used.

By conducting a series of experimental fire procedures and replicating specific technologies, such as platform hearths, stone boiling, earth ovens and sweat lodges, various studies have established some correlations between the temperature to which the rocks were exposed, the duration of exposure and the number of cracked gravels generated from stones (Custer, 2017; Graesch et al., 2014; Ellwood et al., 2013; Backhouse and Johnson, 2007; Mercieca, 2000). Hypothetically, an increase in temperature reflects an increase in the number of fractures and with each successive firing, the heated rocks gradually weaken, resulting in a greater quantity of smaller fractured rock. According to that, some authors assumed the use and reuse of rocks based on the dimension of stones, evaluating a pebble to cobble ratio. Larger stones may have been primarily used in food preparation features, while smaller fractured rocks are indicative of prolonged or more intense cooking stone usage (Carney et al., 2022). Specifically, the stone boiling process required the removal of the stones and their subsequent re-heating, which may lead to a progressive fragmentation due to thermal shock (Shantry, 2020; Graesch et al., 2014). In his studies Thoms (Thoms, 2008b) developed several experimental works on the creation and use of stone-cooking facilities. The outcome was that rocks used for simulating earth-oven cooking showed more evidence of cracking, oxidation and increased porosity, than rocks used to simulate the boiling technique.

Our research suggests that mineral composition and physical properties may similarly have played a functional role in heat stone facilities for culinary and non-culinary purposes. Some rocks (and their derived stones) may have been particularly desirable for certain culinary functions, such as quartzite and limestone exhibiting fracture resistance that allows them to break into small and reusable pieces without disintegrating, unlike granite (Frison, 1983). For example, a common characteristic among many of the recorded lithologies is the prevalence of quartz. This mineral possesses a high refractory property and a unique ability to withstand extremely high temperatures. Its low coefficient

of thermal expansion allows it to be repeatedly heated with minimal risk of breakage due to thermal shock. Experimental studies have been instrumental in testing such functional hypotheses. In some studies, the effectiveness of different rock types was investigated in relation to different cooking methods by means of controlled experiments and observations. In contrast with the extensive use of sandstones in different archaeological sites, the experimental study of Bring and Dawe(Brink and Dawe, 2003) showed that this rock type is particularly fragile, and tends to fracture more readily than fine-grained rocks when reheated. Sandstones also release substantial amounts of sand that may be undesirable during cooking activities (Brink and Dawe, 2003). Moreover, an experimental study by Ellwood (Ellwood et al., 2013) demonstrated that limestones are effective for cooking maize using hot-stones (stone-boiling), creating an alkaline cooking environment which improves the availability of important maize proteins. Limestones, however, were considered as not appropriate for boiling liquid substances because of the formation of flakes and powder during repeated heating and immersion in water (Gao et al., 2014). A similar issue was observed recently for coarse-grained basalts used for the hot stone cooking method. Placing heated coarse-grained basalt stones directly inside a vessel containing water led to the contamination of the liquid with ash and soil, compromising the palatability and edibility of the food (Langley et al., 2023). On the other hand, coarse-grained rocks (andesite, basalt, diorite, granite, gabbro) appeared to be more resistant to breakage after multiple heating episodes compared to fine-grained stones (schist, quartzite, siltstone, basalt, basaltic andesite). Basalt was the most resistant type, while on the other hand quartzite fragmented into several pieces after a few heatings (Shantry, 2020; Wilson and DeLyria, 1999).

Organic residues absorbed by or adhered to HAS present valuable information for identifying their culinary function and providing valuable information on subsistence resources. Raman spectroscopy studies, such as those conducted by Short et al. (Short et al., 2015), have observed traces of carbohydrates on archaeological stones, indicating their potential use in plant processing. Additionally, research has demonstrated the feasibility of lipid extraction from archaeological stones, representing a largely untapped source of information into past cuisines (Buonasera, 2005; Skibo, Malainey and Drake, 2009; Quigg et al., 2001). For example, the presence of lipid residues on HAS, likely absorbed into the fractures created by heating, along with the detection of cholesterol in some samples suggested that HAS were used during the processing of animal products (Skibo, Malainey and Drake, 2009). Nevertheless, challenges, including contamination, warrant further research efforts in this direction.

Ethnographic reports of North American Indigenous groups (Driver and Massey, 1957) attested the use of HAS in earth ovens primarily for processing plant commodities, including roots, bulbs and tubers, along with a frequent use of stone boiling techniques among mobile groups who employed perishable materials such as woven and bark baskets, dugout wood, and animal tissues as containers.

Additionally, some structures, such as burned rock middens, are not results of random HAS accumulations but are indicative of recurrently used earth ovens, the size of which is directly correlated with their use frequency and duration (Mitchell, 2008).

2.4. Social implication

Studies show that HAS carry significant cultural information on regional and local economies, group and population size, and site formation processes (Langley et al., 2023; Hawkes, 2018; Petraglia, 2002). The presence, frequency and size of structures containing HAS can offer clues about social dynamics. These include technological advances (Speth, 2015), such as the evolution of stone boiling to animal bone grease rendering (Oetelaar and Beaudoin, 2016; Nakazawa et al., 2009), as well as social organisation, since the increased effort required to build and maintain some structures, along with intensification of food procurement and processing (Thoms, 2008a, 2009), suggests possible cooperation between different groups of people (Hawkes, 2018; Fretheim, 2009). Additionally, these archaeological features offer evidence of domestic and ceremonial/ritual activities, including festive occasions involving large groups of people participating in cooking activities (Petersson, 2013; Swedberg, Östlund and Jacobsson, 2017; Hawkes, 2018; Mitchell, 2008) along with different uses beyond culinary applications (Hawkes, 2018; Ó Drisceoil, 1988), hinting at the versatility of HAS in ancient societies. In some cases, the appearance of HAS within specific structures (e.g. earth ovens, burnt mounds) corresponds with settlement changes, particularly in terms of assessing residential mobility (Mitchell, 2008) and site occupation patterns (O'Kelly, 1954; Petraglia, 2002). Social activities such as feasting may have influenced interactions between people, raising the sense of community, along with modifications in long-term production organisation into a more organised management of goods (Mitchell, 2008; Fretheim, 2009).

Experimental cooking simulations, including the reconstruction of hearths and the replication of stone boiling, have demonstrated the effort and resources required to use and manage fire structures. In some cases, the amount and size of HAS can provide insight into the intensity and duration of human activity at a site, along with the duration of the site occupation (Jensen, Jensen and Clegg, 1999; O'Kelly, 1954). By comparing experimental results and archaeological features, researchers suggested that some structures were likely used for a short period of time (Petraglia, 2002; Nickels et al., 2001). Furthermore, the rapid breakage of HAS with repeated use implies the reduction of their efficiency as boiling stones, thus their discard (Jensen, Jensen and Clegg, 1999). For example, Sorensen and Scherjon (Sorensen and Scherjon, 2018) developed a computer-based model simulating how various factors influence the abundance of HAS found in archaeological sites, demonstrating that the abundance of HAS can be affected by the size and frequency of fires. On the other hand, the lack of burned HAS in

an accumulation of stones could suggest minimal human use of these objects (Bock, Neubeck and Pasda, 2017).

The reuse of HAS within the settlement represents an important indicator of human resource management. These lithics can undergo multiple cycles within fire structures before becoming functionally ineffective and subsequently discarded. Burned rock middens serve as an example of structures composed of several discarded HAS (Black and Thoms, 2015; Kelley and Campbell, 1943). Archaeomagnetic techniques hold promise for distinguishing whether HAS were heated in-situ or elsewhere. This could lead to better understanding the arrangements and the construction processes of fireplaces in a settlement, along with revealing the duration of heating and the maximum temperature reached (Gose, 2000; Nickels et al., 2001). These analyses may reveal that HAS were previously part of the cover of a fireplace, being subsequently removed and placed upside down after final cooling.

Finally, dating techniques are powerful tools for placing artefacts and settlements in a specific timeframe. In the context of our research, HAS have been analysed through different dating methods such as TL, OSL and phototransferred thermoluminescence (PTTL) to assess a timespan in which the stones were heated and presumably used in fire-related activities (Anthony et al., 2001; Eskola, Okkonen and Jungner, 2003; Rhodes et al., 2009; Okkonen, 2010).

2.5. Synthesis and considerations

This review reveals significant research gaps concerning the study of HAS found in prehistoric archaeological sites. Despite decades of research, it is surprising that they continue to be generally overlooked and systematic studies on them are scarce given their potential to provide insights into various aspects of past human behaviour, including culinary practices, domestic activities, and rituals. Thus a more in-depth consideration of these artefacts is warranted. HAS are associated with a range of heating facilities, for culinary and non-culinary purposes. They have an extensive geographical and chronological distribution in North America and Europe, but notable gaps exist in our knowledge for other regions preventing us from understanding their role in human prehistory, including global dispersal and adaptation to distinct climates and ecological contexts. Identification and characterisation of HAS remain a major challenge in archaeology, and should be addressed through multidisciplinary approaches that describe and quantify a range of features, including stone composition (mineral identification), physical properties (size, shape, structure, texture, mechanical and thermal characteristics) and alterations (fragmentation, fractures, discoloration, sooting, reddening), chemical characterisation of adhered and absorbed residues along with the spatial distribution, and in-situ contextual information (presence of archaeological features). Moreover, the field faces additional persistent challenges, including a lack of standardised terminology for describing HAS and their relative

heat alteration, along with the need for a more systematic approach for documenting, and the difficulty in distinguishing between culinary and non-culinary uses.

We acknowledge that our literature review has some inherent limitations, particularly concerning the volume of work not considered here, represented by non-English and grey literature. It is our opinion that integrating these other literatures is more feasible in regional literature reviews or when dealing with specific chrono-cultural phases. Nevertheless, the study emphasises the potential of HAS research to provide insights into prehistoric culinary practices, cultural transmission, and social dynamics. It calls for more comprehensive and interdisciplinary approaches for advancing our understanding of heat-altered stones, their function and significance in prehistoric practices, leveraging their heritage values and highlighting their untapped potential to the wider archaeological community.

3. An overview of lipid and protein residue analysis in the investigation of past cuisine

Past human lifeways can be reconstructed at multiple scales, but biomolecular archaeology provides a powerful means of accessing dietary practices, subsistence strategies, and technological behaviours through the recovery of preserved organic molecules. Lipids and, to a lesser extent, proteins, owing to their relative stability over archaeological timescales, are particularly informative classes of organic compounds for investigating human interactions with food and the environment (Malainey, 2011). While research has largely focused on bones, teeth, and ceramic materials, the potential of stone artefacts as repositories of organic residues remains comparatively underexplored. The recovery and identification of lipid and protein residues on these artefacts provides an opportunity to infer food processing activities, thereby yielding critical insights into past cuisine and cultural identity. Integrating stone residue studies into the wider framework of biomolecular archaeology thus expands our capacity to reconstruct the complex interplay between subsistence practices and cultural traditions.

3.1. Lipid residue analysis in archaeology

Between biomolecules, lipids are less prone to structural modification and degradation than others, thanks to their hydrophobic nature (Evershed, 1993, 2008b; Brown and Brown, 2011; Dunne, 2017; Richards and Britton, 2020; Whelton et al., 2021). Lipid residue analysis relies on these compounds for the identification of archaeological residues, and their chemical analysis can shed light on the organic products used and processed in ancient times, like resins, oils, fats from plants and animals (Evershed, 1993; Evershed et al., 1999a; Malainey, 2011). Both surface and matrix of archaeological artefacts can retain lipids in the form of superficial visible residues or absorbed (invisible) residues since lipids can be trapped within a porous matrix (Evershed et al., 1992). This phenomenon can occur during cooking, storage or processing of foodstuffs, as well as during non-culinary practices (e.g. sealing of ceramics) (Whelton et al., 2021; Irto et al., 2022). Due to its porous nature, ceramic pottery is the most extensively analysed artefact for lipid residue analysis, offering critical insight into past culinary practices. Numerous studies have successfully identified animal fats, plant oils, and dairy residues within ceramic matrices, shedding lights on ancient food preparation and consumption practices (Spiteri, Muntoni and Craig, 2017; Cubas, Peyroteo-Stjerna and Fontanals-Coll, 2019; Drieu et al., 2019, 2021; Breu et al., 2023b). In contrast, stone tools have been the focus of relatively few lipid studies, despite their importance in food preparation and processing. Lipid preservation in archaeological contexts, however, is strongly influenced by environmental conditions, with the Mediterranean region posing specific challenges. Nevertheless, research has provided valuable

insights into ancient Mediterranean culinary traditions (Spiteri, Muntoni and Craig, 2017), although preservation biases in the region may lead to an underrepresentation of certain resources.

Lipids constitute a group of naturally occurring organic molecules composed of carbon, hydrogen and oxygen, existing in linear, branched or cyclic configurations that may include different types of functional groups that contribute to their hydrophobic or amphipathic properties. Therefore, they result to be poorly soluble in aqueous media but highly soluble in organic solvents (Bruice, 2017; Smith, 2020). Lipids of particular relevance to archaeological investigations derive from fats, oils, waxes and resins, encompassing compounds such as fatty acids (FAs), wax esters, sterols, mono- (MAGs), di- (DAGs), and triacylglycerols (TAGs) and terpenes (Figure 9) (Evershed, 1993; Brown and Brown, 2011; Dunne, 2017; Richards and Britton, 2020; Cramp et al., 2023).

Fatty acids are the most frequently encountered compounds when undertaking lipid residue analysis. They are carboxylic acids with hydrocarbon chains, with the carboxylic acid group (-COOH) at one end, which is polar, and a methyl group ($-CH_3$) at the other nonpolar end. The carbon chain length and the degree of unsaturation determine their variation (Bruice, 2017; Smith, 2020). Saturated FAs, which lack C-C double bonds, are characteristic of animal-derived products such as meat, milk, butter and lard. Between unsaturated FAs, monounsaturated FAs present a single C-C double bond and are prevalent in nuts, olive oil, sesame oil and sunflower oil, while polyunsaturated FAs, with two or more C-C double bonds, are associated with soybean oil, corn oil, nuts and fish (Brown and Brown, 2011; Dunne, 2017). FAs are key components of natural products but are rarely found in their free form. Instead, they are typically bound to other molecules, forming larger compounds such as triacylglycerols and wax esters.

TAGs consist of a glycerol molecule bound to three fatty acid chains, while MAGs and DAGs are composed of one and two fatty acid chains, respectively. They are among the most common lipids in foods such as meats, fish, dairy products, seeds, nuts and plants (Evershed, 1993; Brown and Brown, 2011; Dunne, 2017). TAGs that are solids or semi solids at room temperature are called fats, generally obtained from animals, and are composed of FAs that either are saturated or have only one double bond. Differently, liquid triglycerides are called oils, coming from plant products, and are composed of unsaturated FAs (Pollard and Heron, 2016; Bruice, 2017; Smith, 2020).

Natural **waxes**, produced by both plants and insects, consist of a mixture of long-chain nonpolar lipids (Smith, 2020). In plants, waxes are major components of cutin, a protective biopolymer in the cuticle that coats leaves and fruits, providing a hydrophobic barrier against water loss and environmental stress. Waxes are also found in animals, including in honeybee wax, insect cuticular lipids, spermaceti from sperm whales, and the surface lipids of mammalian skin. Structurally, waxes are esters formed

from long-chain carboxylic acids and long-chain alcohols, where the alcohol is not glycerol. FAs in wax esters derived from plants typically range from C_{12} to C_{24}, while the alcohols in plant waxes are generally much longer, ranging from C_{24} to C_{30} (Evershed, 1993; Smith, 2020).

The general structure of a **sterol** is characterised by four hydrocarbon rings fused together (gonane) and a hydroxyl group. They can be divided into zoosterols and phytosterols, respectively derived from animal and plant sources. Cholesterol is the most common sterol of animal origin, whereas phytosterols such as β-sitosterol, stigmasterol, and campesterol predominate in plants, with only trace amounts of cholesterol. Ergosterol, a sterol of fungal origin, is primarily found in yeasts and fungi (Evershed, 1993; Dunne, 2017).

In addition to lipids used for dietary purposes, some derive from natural products not directly consumed as food, but potentially stored or processed in culinary tools such as vessels. These often originate from resins, tars and bitumen. **Terpenes** are composed of isoprene units (C_5H_8) arranged in various configurations (Brown and Brown, 2011). They represent a major component of natural resins produced by plants, and are central to the composition of tree and plant secretions. Chemically altered plant resins and other wood products are often present in archaeological contexts as tars and pitches, resulting from the pyrolysis of resins and wood (Evershed, 1993; Dunne, 2017).

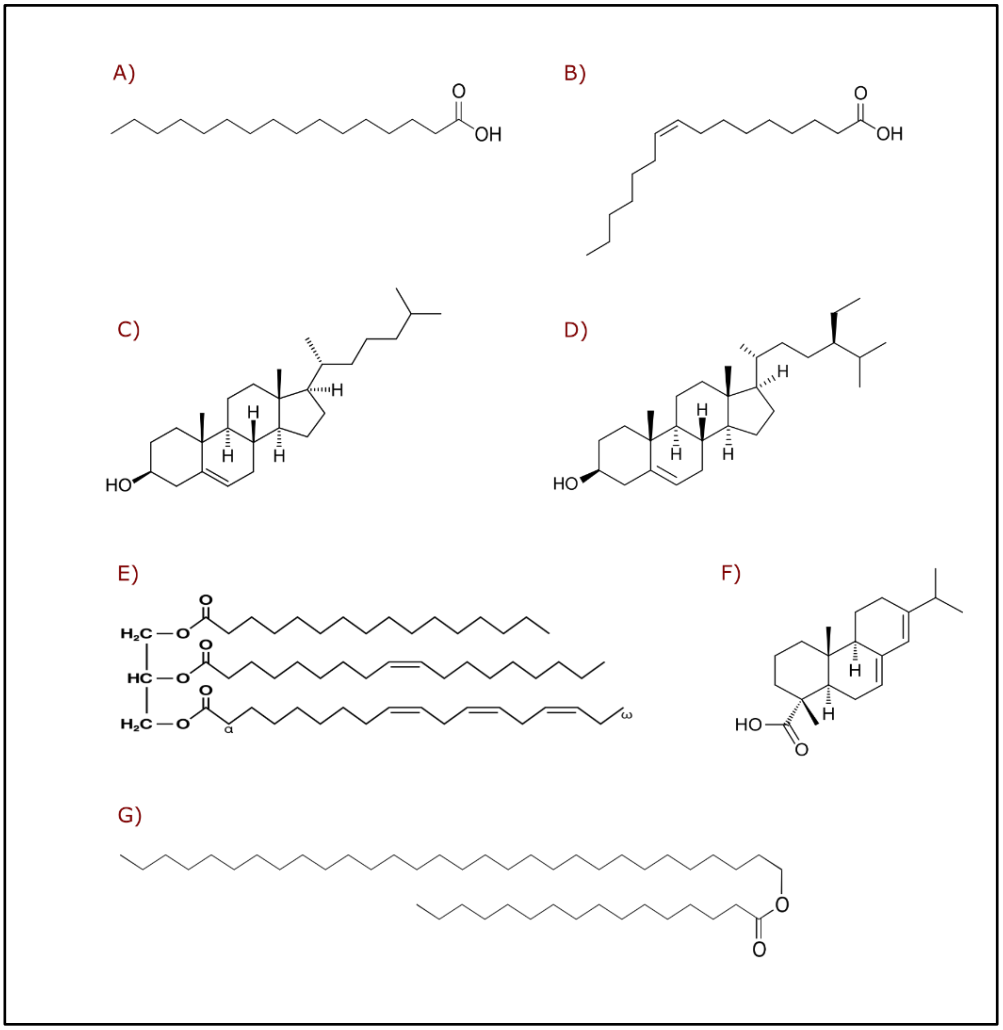


Figure 9. Structure of some of the naturally occurring lipids. (A) palmitic acid, saturated FA; (B) palmitoleic acid, unsaturated FA; (C) cholesterol; (D) β-sitosterol; (E) triglyceride; (F) abietic acid, diterpenoid; (G) triacontanyl palmitate, wax ester.

In archaeological contexts, lipid residues recovered from artefacts provide critical insights into past human behaviour, particularly in relation to subsistence practices and the use of organic materials. Lipids have been commonly extracted from materials over very long archaeological timescales, including ceramic vessels (Cubas, Peyroteo-Stjerna and Fontanals-Coll, 2019; Drieu et al., 2019, 2021; Breu et al., 2023b), soil, sediment and floor samples (van Bergen et al., 1997; Choy et al., 2016; Pecci et al., 2018), faunal and human remains (Evershed et al., 1995b; Colonese et al., 2015), and occasionally stone artefacts (Buonasera, 2005, 2007; Vázquez et al., 2008).

Lipids, although relatively resistant to decomposition compared to other biomolecules, are nonetheless susceptible to degradation. This susceptibility arises from unfavourable burial environments along with the specific use of tools prior to deposition, resulting in significant modifications and structural alteration of lipid compounds (Evershed et al., 1992; Heron and Evershed,

1993; Regert, 2011). The residues altered through such processes are commonly referred to as **archaeological biomarkers**. Greater attention has been given to refining the definition of biomarkers. In geochemistry, biomarkers are organic compounds preserved within the geological record that have typically undergone natural degradation over time, leading to the loss or alteration of their original functional groups. In contrast, archaeological contexts involved considerably shorter timeframes, and it is not uncommon for the original, or native, molecular constituents to be partially or fully preserved. Thus, it is appropriate to redefine biomarkers in archaeology as encompassing a spectrum that includes: native constituents (e.g., intact or slightly modified fatty acids, sterols, waxes), anthropogenic transformation markers (e.g., products resulting from heating), and natural degradation markers (e.g., compounds formed through microbial or environmental degradation processes during burial) (Regert, 2011).

While native lipids can provide direct evidence of the original substance, transformation and degradation markers offer insights into past processing practices and post-depositional histories. Among the various factors contributing to lipid alteration, chemical and microbial attacks target functional groups and linkages, leading to molecular changes (Evershed et al., 1992; Evershed, 1993). These changes are particularly evident in tools subjected to repeated exposure to high temperatures while processing animal or plant products, experiencing degradation through processes like oxidation, decarboxylation, dehydration, and aromatisation (Regert et al., 1998; Craig et al., 2004; Evershed, 2008b).

Alkylresorcinols (ARs) are classified as native constituents and represent a promising group of cereal-specific biomarkers in archaeological residue analysis (Colonese et al., 2017; Hammann and Cramp, 2018; Hammann et al., 2022; Doliente et al., 2024). Structurally, ARs are a class of phenolic lipids composed of a resorcinol ring substituted with an odd-numbered alkyl chain, typically ranging from C_{15} and C_{27} (Figure 10, A). They occur in high concentrations in the bran layers of rye and wheat, with lesser amounts reported in barley, millet, and maize (Ross et al., 2003; Chen et al., 2004). The relative abundance of specific homologues, such as AR 17:0 to AR 21:0 ratio, has proven effective in discriminating between species, with rye exhibiting relatively higher levels of AR 17:0 compared to wheat (Chen et al., 2004; Ross, 2012). Moreover, this ratio has been shown to provide an additional taxonomic resolution within wheat varieties based on ploidy level (Pedrazzani et al., 2021; Doliente et al., 2024). These molecular patterns are not significantly altered by cooking or processing, reinforcing the diagnostic value of ARs in archaeological residue analysis. Although ARs can also be produced by certain bacteria (Kozubek, Pietr and Czerwonka, 1996; Zabolotneva et al., 2022) and have been identified in sedges (Avsejs et al., 2002) and in sediments (Scherer et al., 2025), their chain-length distribution and contextual association with cereal remains in controlled archaeological settings strongly support their attribution to plant-derived origin.

One of the most widely recognised classes of anthropogenic transformation markers is the ω-(o-alkylphenyl)alkanoic acids (**APAAs**) (Figure 10, B), formed through the prolonged heating of unsaturated fatty acids (Hansel et al., 2004; Evershed et al., 2008b). Structurally, APAAs consist of a benzene ring with an alkyl group attached to one end and a carboxylic acid group to the other end. Two main formation pathways have been proposed for APAAs: alkali isomerisation, enhanced by the alkaline environment of ceramic matrices, and oxidative degradation via allylic radical intermediates (Bondetti et al., 2021a). These compounds are increasingly recognised as valuable biomarkers of sustained heating of lipids in archaeological ceramic vessels and serves as strong evidence for the processing of aquatic resources, as they derive from long-chain unsaturated fatty acids predominantly found in marine and freshwater organisms (Cramp and Evershed, 2014; Bondetti et al., 2021a). APAA-C_{20}, are mostly formed from heating aquatic organisms at high temperatures, and to a lesser extent, terrestrial plants and ruminants (Hansel et al., 2004; Evershed et al., 2008b). The ratio APAA-C_{20}:C_{18} has been used to distinguish between terrestrial and aquatic products, with an APAA-$C_{20}/C_{18} > 0.06$ indicative of aquatic resources (Bondetti, 2021). By contrast, the relative distribution of APAA-C_{18} isomers, specifically E/H isomer ratio, provides a valuable proxy enabling differentiation between plant-derived residues (e.g., cereals, fruits, non-leafy vegetables) from those originating in animal fats or leafy greens (Bondetti et al., 2021a). However, E/H is also influenced by temperature, mixing, and degradation, and therefore cannot be considered diagnostic on its own, and is better interpreted in combination with other molecular proxies (e.g. APAAs C_{20}/C_{18}) and fatty acid $\delta^{13}C$ values.

Another important class of anthropogenic transformation markers is mid-chain **ketones** (Figure 10, C). These compounds form through the condensation and subsequent decarboxylation of saturated fatty acids embedded in the ceramic matrix temperature exceeding 300ºC (Evershed et al., 1995a; Raven et al., 1997). This reaction results in a specific range and distribution of ketones, including hentriacontanone (31K), tritriacontanone (33K), and pentatriacontanone (35K). These are characterised by the presence of a carbonyl group bonded to two long alkyl chains, reflecting the original positions of saturated fatty acid precursors. Mid-chain ketones are considered useful indicators of intense heat exposure associated with cooking or technological processes (Drieu, Lepère and Regert, 2020). In addition, **dicarboxylic acids** (Figure 10, D) may be produced through the heating or prolonged exposure to oxygen of organic materials (e.g. plant oils) within ceramic vessels (Regert et al., 1998; Dunne et al., 2012). Their formation arises through oxidative degradation of the carbon-carbon double bonds of unsaturated fatty acids (Regert et al., 1998).

Natural degradation markers result from a range of diagenetic processes that occur post-deposition, including microbial metabolism, oxidation, and hydrolysis. Notable examples include short-chain dicarboxylic acids, typically formed through the oxidative cleavage of unsaturated fatty acids,

and hydroxy acids, which may arise from the microbial hydration of double bonds (Regert et al. 1998; Copley et al. 2005). These compounds play a critical role in differentiating between original use-related residues and altered or introduced during burial, thereby enhancing the interpretation of lipid profiles in archaeological context.

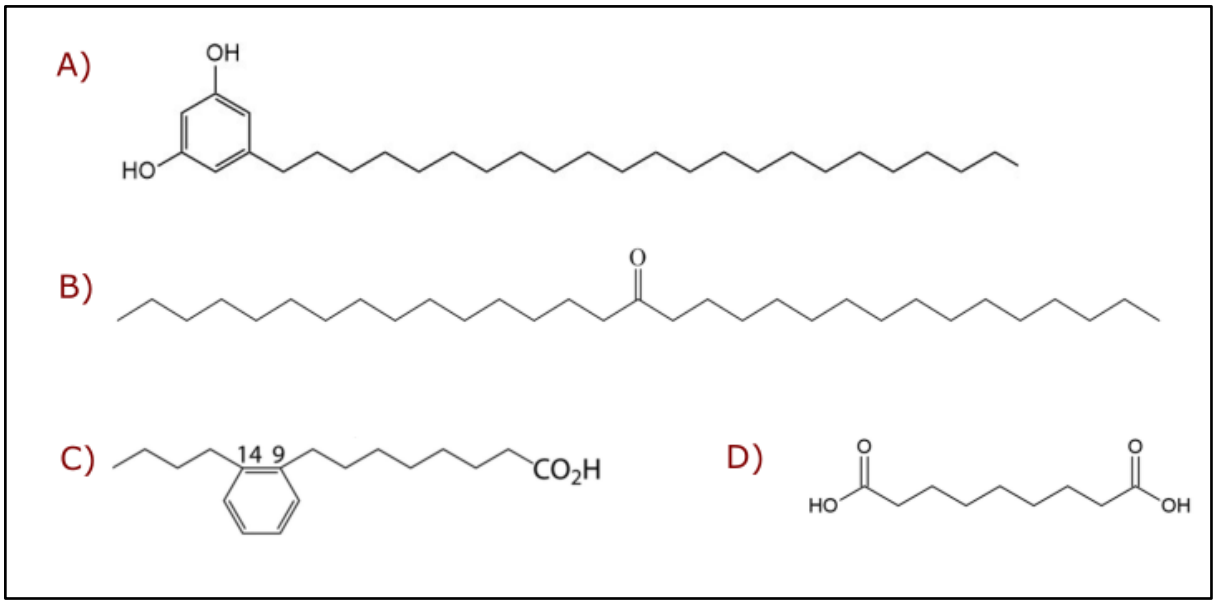


Figure 10. Structures of selected biomarkers relevant to archaeological residue analysis. (A) Tricosylresorcinol, AR 23:0; (B)16-hentriacontanone, ketone; (C) C18 ω-(o-alkylphenyl)alkanoic acid, APAA; (D) azelaic acid, dicarboxylic acid.

Understanding these pathways is essential for distinguishing "native" lipid components from anthropogenic and natural degradation products, enabling more accurate reconstructions of past human activities and burial conditions. Thus, the main approach for tracing the source of lipids in archaeological artefacts involves a comparative analysis of biomarkers with some reference materials related to compounds present in modern-day plant and animal-derived products, which were supposedly used in the past. However, molecular biomarkers from degraded archaeological residues are usually different from those found in modern reference samples. To overcome this, researchers have conducted validation studies, degradation experiments, and ethnographic research to better determine the significance of lipids preserved in ancient artefacts (Evershed, Charters and Quye, 1995; Dudd, 1999; Regert et al., 2001; Evershed et al., 2008b; Drieu, 2017).

Ceramics, in particular, are the most frequently analysed artefact type in lipid residue studies due to their widespread use, porous nature, common use in culinary activities and good preservation of absorbed organic compounds. These residues typically occur in two primary forms as visible surface residues and absorbed lipids (Evershed et al., 1992; Heron and Evershed, 1993; Regert, 2011). Visible residues, commonly referred to as deposits or encrustations, are observed on both the interior and

exterior surfaces of pottery. Exterior deposits such as soot or carbonised material, are often indicative of fire or smoke exposure and are commonly associated with activities like cooking or heating, while internal residues, including burnt or charred remains, may reflect the intentional processing or accidental burning of foodstuffs and other organic materials. In addition, resinous coatings, applied during manufacture or as sealing agent on porous materials like ceramics, are also frequently identified among culinary residues. In contrast, absorbed lipids are those that have penetrated the porous matrix of artefacts, most notably unglazed ceramics. These lipids become embedded within the matrix during the use of the artefact, through activities such as cooking or the prolonged storage of organic substances. However, not all organic residues are necessarily related to culinary activities; a variety of non-culinary practices can also result in the deposition of organic materials on ceramic surfaces, underscoring the importance of contextual interpretation in residue analysis.

In addition to ceramics, **sediments** represent an important but more complex reservoir for organic molecules. Lipid extraction from sediments can provide insights into site formation processes, environmental conditions, and the presence of anthropogenic activity such as food processing or disposal areas (van Bergen et al., 1997; Kedrowski et al., 2009; Kanthilatha et al., 2014; Choy et al., 2016; Leierer et al., 2019; Tomé et al., 2022). Sedimentary matrices can retain organic compounds derived from both natural and cultural sources, including plant waxes, animal fats, microbial lipids, and combustion by-products, thereby providing a chemically informative record of past environmental and human interactions. When contextualised within stratigraphic and spatial frameworks, sedimentary lipid profiles can aid in reconstructing activity areas, such as hearths, midden zones, occupational surfaces, and thus offer a complementary perspective to artefact-based analyses. While Heron and colleagues (Heron, Evershed and Goad, 1991) demonstrated that soil lipids are unlikely to affect the composition or isotopic values of ceramic residues, this study shows that soil lipids may contribute to the molecular profiles of certain materials, such as HAS, which appear more susceptible to environmental lipid absorption. Despite challenges related to contamination and diagenesis, lipid analysis of sediments thus provides valuable complementary evidence for interpreting site use and past human activity (Mallol et al., 2025).

Some specific biomarkers can discriminate between plant oil and animal fats, resin derivatives, aquatic fats, cereals, and natural waxes (Evershed, 1993; Regert et al., 2001; Evershed et al., 2008b; Malainey, 2011; Regert, 2011; Dunne, 2017; Whelton et al., 2021; Cramp et al., 2023). Moreover, biomarkers are also helpful for the identification of burial and post-excavation contamination, which may originate from biological sources, such as the handling of artefacts and the burial environment (i.e. soil), as well as from industrial plasticisers introduced by modern storage materials (i.e. plastic bags/film) (Evershed, 1993; Malainey, 2011).

Over the years, accurate analytical investigations have been carried out to authenticate the reliability of the established biomarkers regularly employed in lipid residue analysis (Evershed, 1993; Evershed et al., 2008b; Malainey, 2011; Regert, 2011; Dunne, 2017; Whelton et al., 2021). In response to the growing volume of archaeological research employing lipid residue analysis, a new online database (AROLD, (Pasqualini et al., 2022)) has been recently developed to support the systematic search, retrieval, and comparison of published data in this field (Prévost et al., 2023). Designed as a centralised bibliographic resource, it intends to facilitate access to international research outputs and enable comparative analysis across studies, thereby supporting more robust interpretations and synthesis of results. Moreover, the platform promotes the integration of newly acquired data into ongoing research. By serving as both a comprehensive data inventory and an advanced query tool, it fosters greater transparency, collaboration, and methodological consistency within the scientific community.

3.1.1. Analytical Approaches for Lipid Residue Identification in Archaeological Materials

This subchapter provides a focused overview of selected analytical techniques employed in the identification and characterisation of lipid residues in archaeological materials. Although the discussion is limited to a subset of methods most pertinent to the aims of this thesis, it is important to acknowledge the broader methodological landscape. Over the past several decades, a wide array of extraction and derivatisation protocols has been developed, refined, and applied across multiple scientific disciplines, including but not limited to pharmaceutical sciences, food chemistry, and chemical engineering (Christie and Han, 2012). These protocols form the foundation for lipid residue analysis, enabling researchers to isolate, modify, and detect a wide range of lipid compounds from complex matrices. The evolution of these techniques, both within and beyond the domain of archaeological science, has significantly advanced the methodological precision, sensitivity, and reliability of current analytical practices. By integrating developments from these adjacent fields, archaeological research has progressively expanded its capacity to investigate past human behaviours, dietary practices, and environmental interactions through the molecular remains preserved in artefacts.

The following discussion focuses specifically on the analytical techniques and procedures employed within archaeological science for the study of lipid residues, with particular emphasis on those applied in the present thesis. While a wide range of approaches exists, the methods outlined here represent established and widely adopted practices within the field. Lipid analysis in archaeological contexts relies on a range of **analytical techniques** that enable the identification and characterisation of preserved organic compounds. Among the most commonly employed are gas chromatography (GC), gas chromatography coupled with mass spectroscopy (GC-MS) and stable carbon ($\delta^{13}C$) isotopes

analysis. Prior to the application of these techniques, lipids must be extracted from the archaeological matrix and chemically modified, typically through derivatisation, to enhance their volatility, stability, and detectability. To minimise exogenous contamination, it is essential to thoroughly clean the surface of the artefact prior to extraction, either by scraping with a sterile scalpel or mechanically abrading with an electronic hand drill.

The **extraction procedure** yields a Total Lipid Extract (TLE), that commonly undergoes chemical derivatisation to produce methylated (ME) or trimethylsilylated (TMS) derivatives, better suited for chromatographic separation. These treatments enable the identification of molecular markers, isotopic signatures, and structural details (Regert, 2011; Cramp et al., 2023). Since lipid samples must be volatile for GC analysis, the extracts are typically prepared in an organic solvent. The most common protocols reported in the specialised literature involve extraction using a non-polar and polar solvent solution, such as dichloromethane/methanol (DCM/MeOH) or, less commonly observed, chloroform/methanol mixtures (Evershed, Heron and John Goad, 1990; Evershed et al., 1992; Charters et al., 1995). Lipids extracted in a standard volume ratio, for example 2:1 of DCM/MeOH, typically through multiple cycles of ultrasonication, ensure an efficient recovery of compounds with varying polarity. The samples are then centrifuged to separate the solid from the liquid phase, and the resulting supernatant, containing the lipids, is collected. This extract is then evaporated under a gentle stream of nitrogen to remove the solvent, and the dried residue is redissolved in a smaller volume of solvent mixture to yield the TLE.

Before gas chromatographic analysis, the TLE undergoes **chemical derivatisation** to enhance the volatility and thermal stability of the lipid compounds. In archaeological science, this is most commonly achieved using a silylating agent such as *N,O*-bis(trimethylsilyl)trifluoroacetamide (BSTFA), which is widely adopted within the field for its effectiveness in modifying a broad range of functional groups. The derivatisation reaction is typically carried out under controlled heating conditions to ensure complete transformation of reactive functional groups. This step modifies hydrophilic and reactive functional groups, enhancing the volatility and thermal stability of the compounds, and reduces intra- or intermolecular reactions during chromatographic separation. Among various derivatisation reagents, BSTFA is widely used due to its high efficiency in replacing these groups with TMS moieties. Once the reaction is complete, any remaining derivatisation reagent is typically removed under a stream of inert gas, and the derivatised sample is redissolved in a non-polar solvent to facilitate injection into the gas chromatograph. This method has proven particularly effective for identifying a wide range of lipid biomarkers, including fatty acids, sterols, TAGs, DAGs, MAGs, alkylresorcinols, and wax esters (Evershed, Heron and John Goad, 1990; Regert et al., 1998, 2001; Regert, 2011; Hammann and Cramp, 2018).

While the DCM/MeOH extraction coupled with derivatisation remains a foundational approach, **acidified methanol extraction** (H_2SO_4/MeOH) has emerged as a widely adopted alternative approach, providing an efficient protocol for the direct transesterification of lipids from archaeological residues. This method is particularly effective for recovering fatty acid methyl esters (FAMEs) from complex or highly degraded organic matrices (Craig et al., 2013; Correa-Ascencio and Evershed, 2014). In addition to facilitating the identification of lipid compounds, FAMEs also provide a convenient and widely used format for compound-specific carbon isotope ($\delta^{13}C$) analysis, which is crucial for determining the origin and processing of organic residues in archaeological contexts. In this method, a mixture of methanol and concentrated sulfuric acid is added to the powdered sample, catalysing both esterification and transesterification of free and bound fatty acids into their methyl ester derivatives during controlled heating. Following the thermal reaction, the mixture is centrifuged to separate the phases, and the lipid-containing supernatant is carefully extracted. A non-polar solvent is then used to extract the lipid fraction, and the solution is purified by filtration to remove residual moisture and any remaining acidic components. These extraction and purification steps are typically repeated to maximise lipid recovery. The extract is evaporated under a gentle stream of nitrogen to remove the solvent, and the resulting residue is redissolved in a non-polar solvent to facilitate injection into the gas chromatograph. Furthermore the FAMEs produced are suitable for compound-specific isotope analysis (Dudd, Evershed and Gibson, 1999; Mottram et al., 1999; Regert, 2011).

Each extraction method has inherent strengths and limitations. Conventional solvent extraction typically yields lower amounts of lipids, particularly from complex matrices, but it preserves the original molecular structure of compounds with ester linkages, such as triacylglycerols (TAGs), diacylglycerols (DAGs), monoacylglycerols (MAGs), and wax esters. On the other end, direct acid methanolysis enhances extraction efficiency by releasing bound lipids. However, it compromises structural integrity by hydrolysing ester bonds during processing, resulting in the loss of detailed structural information on lipid molecules.

GC serves as an initial screening step, used to separate and identify different lipid compounds (Sparkman, 2011; Christie and Han, 2012). The system (Figure 11) employs an inert gaseous mobile phase (commonly referred to as the carrier gas) and a liquid stationary phase contained within a capillary column. Samples are introduced into the system via an injection port, also known as the injector. The carrier gas, which does not chemically interact with the analytes, transports the vaporised sample onto the chromatographic column, which is housed within a temperature-controlled oven. As the sample mixture travels through the column, individual components are separated based on their chemical properties. Upon elution from the column, these components are directed to a detector, which converts their presence into an electronic signal proportional to their concentration. A commonly used detector in GC is the flame ionisation detector (FID). In an FID, the eluting compounds are combusted in a

hydrogen-air flame, resulting in the formation of ions, which are collected between two electrodes across which a potential difference is applied. The generated measurable current is directly related to the quantity of ionised species, providing sensitive and quantitative detection of organic compounds. This allows for precise quantification of various lipid classes, such as fatty acids and triacylglycerols, in archaeological samples. Identification of compounds is achieved by comparing retention times with known standards (Evershed, 1993; Regert, 2011; Pollard and Heron, 2016; Cramp et al., 2023).

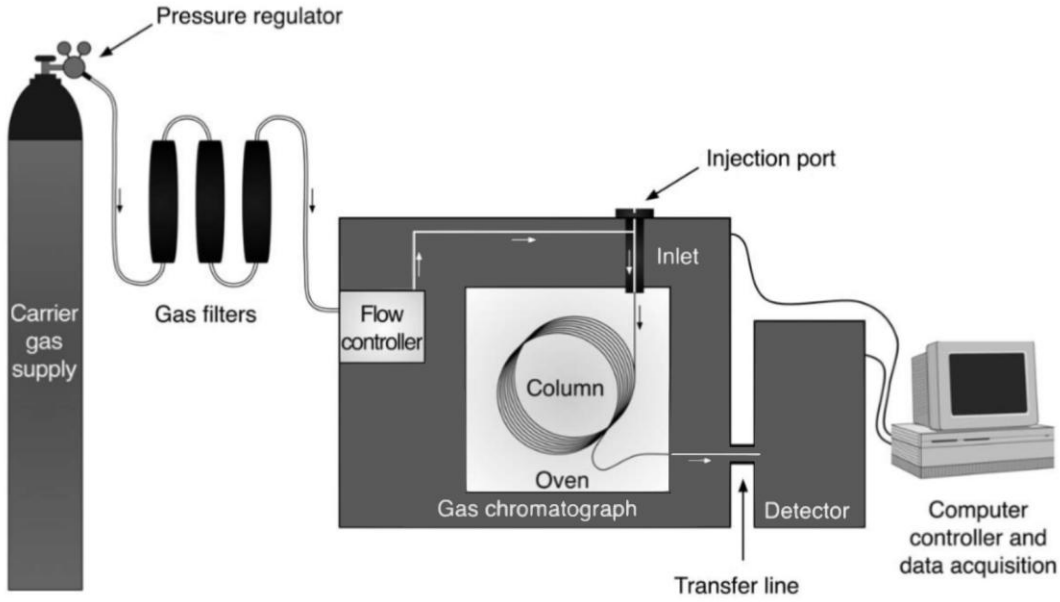


Figure 11. Schematic representation of a gas chromatograph and its main components. Adapted from (Stauffer, Dolan and Newman, 2008).

In the early 1990s, **MS** was introduced in research to obtain structural information on individual molecules and to identify separated components in complex samples (Evershed, Heron and John Goad, 1990; Evershed et al., 1992; Charters et al., 1993; Evershed, 1993). Although it is capable of quantitative analysis, MS is primarily employed for qualitative investigations (Sparkman, 2011; Christie and Han, 2012). In this process, chemical compounds are introduced into the mass spectrometer, where they undergo ionisation and fragmentation into multiple ions. Following separation, they are directed into a mass analyser typically operating under magnetic or electric fields, which separates them according to their mass-to-charge ratios (m/z). Among the various MS configurations, the quadrupole mass analyser is the most commonly used in this context. It uses an electromagnetic field that selectively filters ions, allowing only those with specific m/z values to reach the detector that provides a relative measure of their abundance. As most lipids are naturally uncharged, they become ionised through the loss of an electron when exposed to the energy beam, forming a molecular ion M^+. Given that this ion typically carries a single positive charge, its m/z ratio is directly proportional to its molecular weight. The

resulting data are presented as a mass spectrum, a graphical output in which the x-axis represents the m/z values, and the y-axis indicates the corresponding ion intensities.

When coupled with GC, the MS system receives a continuous flow of sample directly from the chromatographic column via a heated interface, ensuring seamless integration between separation and detection stages. This configuration enables the mass spectrometer to record the Total Ion Content (TIC), which represents the summed intensity of all ions generated from each eluting compound, plotted as a chromatogram of ion abundance versus retention time. The GC-MS methodology appears highly versatile, with numerous adaptations and modifications developed to extend its capabilities beyond the basic configurations. By employing selected ion monitoring (SIM) mode, the sensitivity of GC-MS can be significantly enhanced. SIM is a targeted data acquisition technique in which only preselected m/z values are monitored. This approach enables the detection of specific compounds such as cereal biomarkers (alkylresorcinols) (Colonese et al., 2017) and marine biomarkers (Evershed et al., 2008b; Cramp and Evershed, 2014).

Building on these capabilities, more recent advancements in analytical technology have introduced ultra-high-performance liquid chromatography-quadrupole coupled with Orbitrap mass spectrometry (UHPLC-Q-Orbitrap MS) as an even more sensitive approach for detecting alkylresorcinols (ARs), particularly in low concentrations samples (Doliente et al., 2024). Furthermore, pyrolysis is frequently employed as a preparatory step prior to GC or GC-MS analysis, particularly when working with complex, high-molecular-weight, or insoluble fraction of lipid extracts that are not suitable for direct chromatographic separation. In this technique, the sample undergoes thermal decomposition in an inert atmosphere resulting in the breakdown of macromolecular structures into smaller, volatile fragments. This process facilitates the release and the subsequent analysis of bound fatty acids, lipids, polysaccharides, and polyphenols (Oudemans and Boon, 1991; Regert, 2011; Cramp et al., 2023).

Pyrolysis-GC-MS (**Py-GC-MS**) thus enables the thermal decomposition of complex organic compounds into volatile fragments that can be effectively separated and identified by mass spectrometric detection (Oudemans and Boon, 1991; Kaal et al., 2014; Sanjurjo-Sánchez, Kaal and Fenollós, 2018). Additionally, tandem mass spectrometry (MS/MS) incorporates two or more mass analysers arranged in series, enabling multiple stages of MS analysis to be performed sequentially. Each successive stage typically involves further fragmentation of selected ions, thereby providing increasingly detailed structural information about the original molecule (Evershed and Bethell, 1996; Regert, 2011).

3.1.2. Stable carbon isotopes analysis of fatty acids

In addition to structural analysis, lipid studies have expanded to include **stable carbon isotopes analysis** of fatty acids, providing complementary information for the identification of lipid sources and the reconstruction of complex mixtures of organic residues preserved in archaeological samples (Evershed et al., 1994, 2002, 2008a; Quigg et al., 2001; Regert, 2011; Chasan, Spiteri and Rosenberg, 2022; Admiraal et al., 2023). The analytical method typically employed for compound-specific isotope analysis involves the serial coupling of a GC with a combustion interface and a MS equipped with a magnetic sector, linked to an elemental analyser-isotope ratio mass spectrometry (EA-IRMS). Accurate and reproducible $\delta^{13}C$ measurements are achieved through duplicate or triplicate injections of each sample (Mottram et al., 1999; Regert, 2011).

Isotopes are chemical forms of the same element that possess identical numbers of protons but differ in their numbers of neutrons. The most abundant isotopes of carbon in the biosphere and the main constituent of organic matter are the stable forms ^{13}C and ^{12}C. Carbon isotope composition ($\delta^{13}C$) refers to the relative abundance of ^{13}C in a substance or products, compared to a reference material. Given carbon's central role in virtually all biological processes, $\delta^{13}C$ values serve as sensitive indicators of physiological processes and environmental conditions during the synthesis of organic matter. Fatty acids such as palmitic acid ($C_{16:0}$) and stearic acid ($C_{18:0}$) are the most abundant in nature, among the most commonly preserved fatty acids in archaeological lipid residues, and are readily extractable from a wide range of archaeological materials, including ceramics and sediments. Importantly, these compounds are relatively resistant to diagenetic alteration during burial, making them reliable biomarkers for palaeodietary and residue analysis (Spangenberg, Jacomet and Schibler, 2006; Evershed, 2008a).

The $\delta^{13}C$ of plants and their consumers is fundamentally linked to the process of atmospheric CO_2 fixation during photosynthesis. Plants fix atmospheric CO_2 through three primary photosynthetic pathways, C_3, C_4, Crassulacean Acid Metabolism (CAM), each characterised by distinct patterns of carbon isotope fractionation (Spangenberg and Ogrinc, 2001). C_3 plants, including most temperate crops, trees and therefore fruit and nuts, preferentially fix ^{12}C over ^{13}C, resulting in low $\delta^{13}C$ values typically ranging between –34‰ and –22‰. In contrast, C_4 plants discriminate less against ^{13}C, producing higher $\delta^{13}C$ values ranging from –16‰ to –9‰, typical of plants such as maize, sorghum, and sugarcane. CAM plants, such as succulents and cacti, exhibit a broader and more variable range approximately between –33‰ and –11‰. These plant-based isotopic signatures form the basis for interpreting carbon isotope ratios in animal tissues, including fats, which ultimately reflect the animals' diets (DeNiro and Epstein, 1978). Ruminant and non-ruminant animals, as well as aquatic species, process and incorporate dietary lipids differently, resulting in characteristic $\delta^{13}C$ signatures in their

adipose and dairy fats (Dudd, Evershed and Gibson, 1999; Dudd, 1999; Evershed et al., 2002; Craig et al., 2004, 2012; Copley et al., 2005b; Evershed, 2008a). For instance, ruminant animals (e.g., cattle, sheep, goats) process dietary lipids in the rumen, where microbial biohydrogenation leads to characteristic isotopic signatures in their adipose and dairy fats. Therefore, the isotopic offset between $C_{16:0}$ and $C_{18:0}$ fatty acids, expressed as $\Delta^{13}C$ ($\delta^{13}C_{16:0} - \delta^{13}C_{18:0}$), is used to distinguish between ruminant adipose fats, dairy fats, and non-ruminant fats, each falling into different $\Delta^{13}C$ ranges (Copley et al., 2005b). By analysing the $\Delta^{13}C$ values of fatty acid residues preserved in archaeological materials, it becomes possible to infer not only the species of origin but also the type of fat, adipose versus dairy, thereby providing nuanced insights into past animal husbandry, food consumption, and culinary traditions. These differ from non-ruminant (monogastric) animals (e.g., pigs), whose digestive systems do not extensively alter dietary lipids. Notably, ruminant dairy fats exhibited a greater depletion in the $\delta^{13}C$ values of $C_{18:0}$ fatty acid compared with adipose fats. Marine organisms typically show higher $\delta^{13}C$ values than terrestrial C_3-based systems because the dominant source of carbon is dissolved carbonate which is ^{13}C-enriched compared to atmospheric carbon. Freshwater resources exhibit more variable and sometimes overlapping signatures with terrestrial resources because the main source of carbon is terrestrial detritus (plants) but may vary according to local environmental conditions (e.g. lake size and depth).

Reference datasets derived from modern animal tissues, encompassing both terrestrial and aquatic species, are essential for establishing characteristic $\delta^{13}C$ and $\Delta^{13}C$ value ranges; however, stable carbon isotope values cannot, on their own, resolve the specific taxon of origin. The earliest of these datasets, developed in the UK in the late 1990s, focused on differentiating fats from major domesticated species, thereby allowing the distinction between ruminants and non-ruminants fats, as well as dairy products (Evershed et al., 1994, 1997, 2002; Dudd, 1999; Copley et al., 2003). However, taxonomic differentiation among goat, sheep, and cattle fats remains challenging. Moreover, the validity of using this UK-dataset as a universal reference collection has been questioned (Gregg, 2009; Debono-Spiteri, 2012). Isotopic signatures of ruminant fats and dairy products from the Mediterranean and Near East differ significantly from those observed in British contexts possibly due to the effect of differing atmospheric conditions on plants and their carbon discrimination (Kohn, 2010), underscoring the need for region-specific reference frameworks (Gregg, 2009; Gregg et al., 2009; Debono-Spiteri, 2012; Drieu, 2017; Tarifa Mateo, 2019). In the absence of such tailored datasets, early studies often relied on the British reference values, occasionally adjusting for climatic factors such as aridity, however risking to introduce interpretative bias. In response, several studies have attempted to expand the existing reference dataset by incorporating animals raised in southern regions like the Mediterranean, Near East, and Africa (Pearson et al., 2007; Gregg, 2009; Debono-Spiteri, 2012; Dunne et al., 2012).

To ensure accurate comparisons between modern reference materials and archaeological samples, it is essential to apply isotopic corrections that account for the temporal changes in atmospheric carbon dioxide (CO_2) composition. Since the onset of industrialization, the $\delta^{13}C$ value of atmospheric CO_2 has significantly declined due to fossil fuel emissions, a phenomenon known as the Suess effect (Graven, Keeling and Rogelj, 2020). Consequently, this alteration has led to affect the isotopic composition of all organisms. To align with preindustrial conditions, modern reference fats are typically adjusted by a correction factor ranging between +1.14‰ and over +2.0‰, depending on the year of sample collection and the calibration approach employed (Friedli et al., 1986; Spangenberg, Jacomet and Schibler, 2006; Hellevang and Aagaard, 2015). The application of such corrections is therefore a necessary step in the development of reliable and temporally consistent reference datasets for archaeological interpretation.

Given that this study focuses on two Neolithic sites located in the Mediterranean region, the evaluation of stable carbon isotope values from modern samples has been undertaken to assess potential regional differences between the Mediterranean and Northern European areas. Previous studies have shown that C_3 plants exhibit higher $\delta^{13}C$ values in arid regions and lower values in more humid environments (Kohn, 2010). This variation is primarily due to physiological responses to water availability, which affect carbon isotope discrimination during photosynthesis. These differences in $\delta^{13}C$ values in plants directly influence the isotopic composition of animal fats, as animals incorporate plant-derived carbon into their tissues through their diet. Understanding these regional isotopic patterns in modern reference fats is essential because it allows for more accurate differentiation between Mediterranean and Northern European isotopic values in archaeological contexts. Therefore, it is important to determine whether a Mediterranean-specific isotopic reference dataset is warranted for archaeological interpretation. To define which isotopic values should be attributed to the Mediterranean region, the European biogeographical regions map was consulted to distinguish among different zones (Figure 12). These biogeographical regions are characterised by distinct ecological conditions, primarily determined by precipitation and temperature regimes, which influence plant physiology and the relative abundance of C_3 and C_4 vegetation. Such vegetation differences directly affect the $\delta^{13}C$ values within local food webs and, consequently, in animal tissue. Subsequently, statistical analyses were conducted to test whether modern $\delta^{13}C$ values differ significantly between these regions, particularly between Mediterranean and Atlantic/Continental areas.

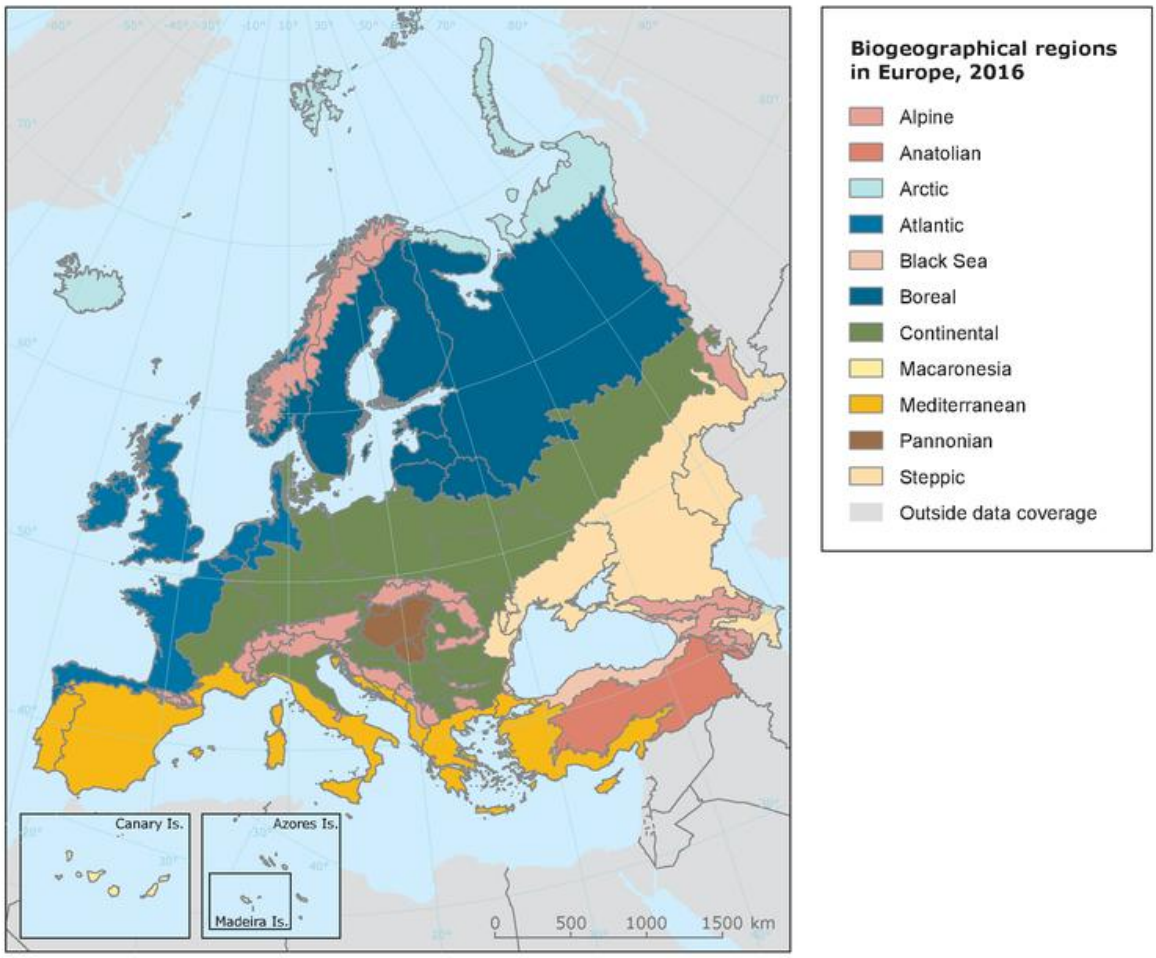


Figure 12. Biogeographical Regions in Europe. Map produced by the European Environment Agency, reflecting the status of biogeographical regions based on 2016 data. Originally published in June 2017 and last modified in September 2024 (European Environment Agency, 2017).

The full list of reference samples considered in this evaluation is provided in Annex 1. To evaluate biogeographical variation in isotopic signatures across terrestrial categories, distribution of $\delta^{13}C_{16:0}$, $\delta^{13}C_{18:0}$, and the offset $\Delta^{13}C$, were compared using pairwise Wilcoxon rank-sum tests, with *p*-values adjusted for multiple comparisons using the Holm method. This non-parametric test compares the distributions of two independent groups to determine whether their central tendencies (typically medians) differ significantly, without assuming a normal distribution of the data. For the purposes of this evaluation, only comparisons between the Mediterranean region and other biogeographical areas are considered, as it forms the reference region of archaeological interest.

The results revealed statistically significant differences in several categories (Annex 2). The Dairy category displayed the greatest degree of regional divergence. Dairy in the Mediterranean region have more ^{13}C-enriched $C_{16:0}$ and $C_{18:0}$ than in the Alps, the Atlantic and Boreal regions. However, no significant differences were observed in $\Delta^{13}C$ values, except in the Atlantic region ($p = 0.0083$). A

similar pattern was observed for the Domestic Porcine category, where adipose tissues in the Mediterranean were significantly more ^{13}C-enriched than those in the Atlantic and Boreal regions, while no significant differences were observed in $\Delta^{13}C$ values. Furthermore, the $\delta^{13}C$ values of $C_{16:0}$ and $C_{18:0}$ in the Mediterranean region were higher among Domestic ruminants when compared to the Atlantic region, and among Wild non-ruminant relative to the Boreal region. No significant differences were detected in $\delta^{13}C$ values for C_3 plant-based resources and Wild ruminant between the Mediterranean region and the other regions. Overall, the observed isotopic patterns highlight consistently higher $\delta^{13}C$ values in Mediterranean samples across multiple animal categories. These differences likely reflect regional environmental and ecological conditions, including warmer temperatures, higher aridity, and different vegetation regime (Van Klinken, van der Plicht and Hedges, 1994; Pearson et al., 2007), which collectively influence the baseline carbon isotope signatures in animal tissues.

Given the statistically significant regional differences observed across most categories, this study adopts only the Mediterranean modern reference values for subsequent isotopic interpretation. Although Annex 1 provides the full compilation of modern reference values sourced from the literature, only the Mediterranean subset is used for interpretative purposes presented in this study. Exceptions are made for the Freshwater category, for which no Mediterranean-specific data are available, and for Wild ruminant category, where data are particularly limited. In these cases, all relevant references listed in Annex 1 are considered. The full list of the selected reference samples is provided in Annex 3. This approach ensures that the comparative framework reflects the ecological and climatic conditions most relevant to the archaeological sites under investigation. To complement the statistical analysis, Figure 13 provides a graphical overview of the modern reference dataset used in this study, displaying 68% confidence ellipses for all relevant categories. This visualization serves as a summary of the isotopic variability within each group and illustrates the reference framework employed for interpreting archaeological samples from La Draga and Pendimoun.

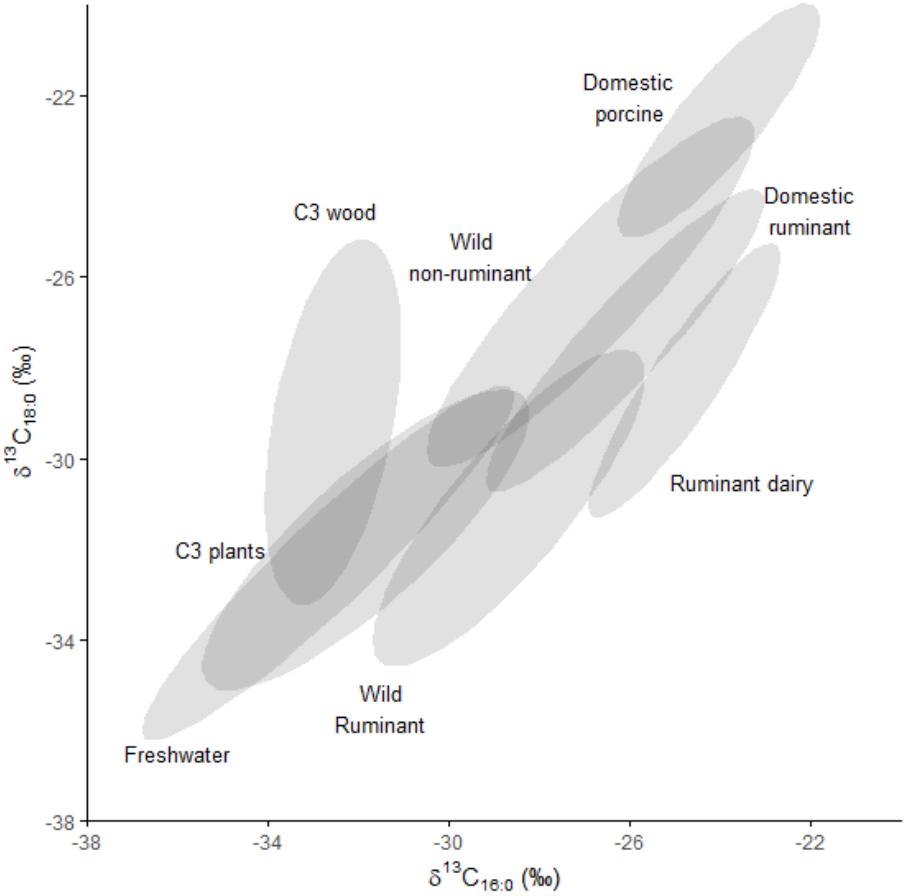


Figure 13. Graphical overview of the modern reference dataset used in this study, showing 68% confidence ellipses (Dudd, 1999; Spangenberg and Ogrinc, 2001; Spangenberg, Jacomet and Schibler, 2006; Spangenberg et al., 2010; Craig et al., 2011, 2012; Debono-Spiteri, 2012; March, 2013; Cramp and Evershed, 2014; Colonese et al., 2015; Carrer et al., 2016; Lucquin, Gibbs and Uchiyama, 2016; Jambrina-Enríquez et al., 2019; Tarifa Mateo, 2019; Pääkkönen, Evershed and Asplund, 2020; Courel et al., 2021; Bondetti et al., 2021b; Drieu et al., 2021; Dolbunova et al., 2023; Tarifa-Mateo et al., 2023).

3.1.3. Lipid preservation in the Neolithic Mediterranean

The reliability of lipid analyses is contingent upon the preservation of organic residues, which is itself influenced by a complex interplay of environmental and post-depositional factors. In the context of the Mediterranean basin, known for its environmental heterogeneity and long history of human occupation, lipid preservation presents particular challenges and opportunities that merit focused investigation. The rationale for focusing this discussion on the Neolithic sites in the Mediterranean lies in the specific case studies selected for this thesis: the archaeological sites of La Draga (Catalonia, Spain) and Pendimoun (Alpes-Maritimes, France). Both sites embody distinct environmental and archaeological settings that typify broader preservation challenges in the region (see Chapter 4 for detailed information about the sites).

Lipid analysis in the Mediterranean has provided interesting insights into past culinary practices, particularly through the study of ceramic vessels, which offer a more stable matrix for lipid retention. However, when compared to other regions of Europe, the **preservation of organic material** in Mediterranean archaeological sites appears to be notably less significant, which can limit the scope of such analyses (Drieu, 2017). This relatively poor preservation can be partly attributed to the characteristics of the Mediterranean soils, which are generally low in acidity due to their calcareous nature at many sites (Figure 14). Such conditions promote microbial and chemical activity, favouring the degradation of lipids (Moucawi et al., 1981; Drieu, 2017; Spiteri, Muntoni and Craig, 2017). Furthermore, the Mediterranean climate, marked by seasonal fluctuations alternating between hot dry periods and intense rainfall, exacerbates these preservation challenges. Such environmental conditions are less conducive to the survival of organic residues, which are more likely to be preserved in waterlogged or desiccated environments, where limited oxygen availability and inhibited microbial activity slow down degradation processes (Regert et al., 1998; Copley et al., 2005a). The low lipid recovery frequently observed in lipid residue analysis of ceramic vessels from Mediterranean contexts highlights an important methodological consideration. Rather than reflecting a limitation of the technique itself, this reduced recovery rate likely results from a combination of environmental and post-depositional factors that negatively impact organic preservation. Thus, emerging evidence suggests that climate alone does not fully account for patterns of lipid preservation in archaeological ceramics.

Notably, several Mediterranean sites exhibit excellent lipid preservation despite similar environmental conditions (Spiteri, Muntoni and Craig, 2017; Drieu et al., 2018), indicating that favourable lipid preservation is possible within the Mediterranean climatic regime and thus challenge the assumption that poor lipid recovery is necessarily linked to regional climate. This suggests that site-specific taphonomic factors, including soil pH, microbial activity, burial context, ceramic fabric, or the intensity and nature of vessel use, may have played a more significant role in lipid degradation and preservation than previously assumed. In a recent study Drieu (Drieu, Binder and Regert, 2022) outlined several good practices for lipid residue analysis in Mediterranean Neolithic contexts. Regarding environmental factors, lipid preservation appears to be more favourable in regions with acidic soils such as Corsica, northeastern Sardinia, the Tuscan archipelago, southern Calabria, and central Croatia. Cave sites also offer optimal preservation conditions due to their stable microclimates, which mitigate seasonal variations in temperature and humidity. With respect to analytical protocols, acidified methanol extraction is particularly recommended for open-air sites with neutral or slightly basic soils, while DCM/MeOH extraction can then be employed as a complementary method to enhance the interpretative potential of the data. Furthermore, wherever possible, contextual sediment samples should be collected alongside ceramic materials to assess potential contamination and improve the reliability of lipid identifications. Collectively, these considerations underscore the importance of adapting residue

analysis protocols to local taphonomic conditions in order to maximise the recovery and interpretive value of lipid residues.

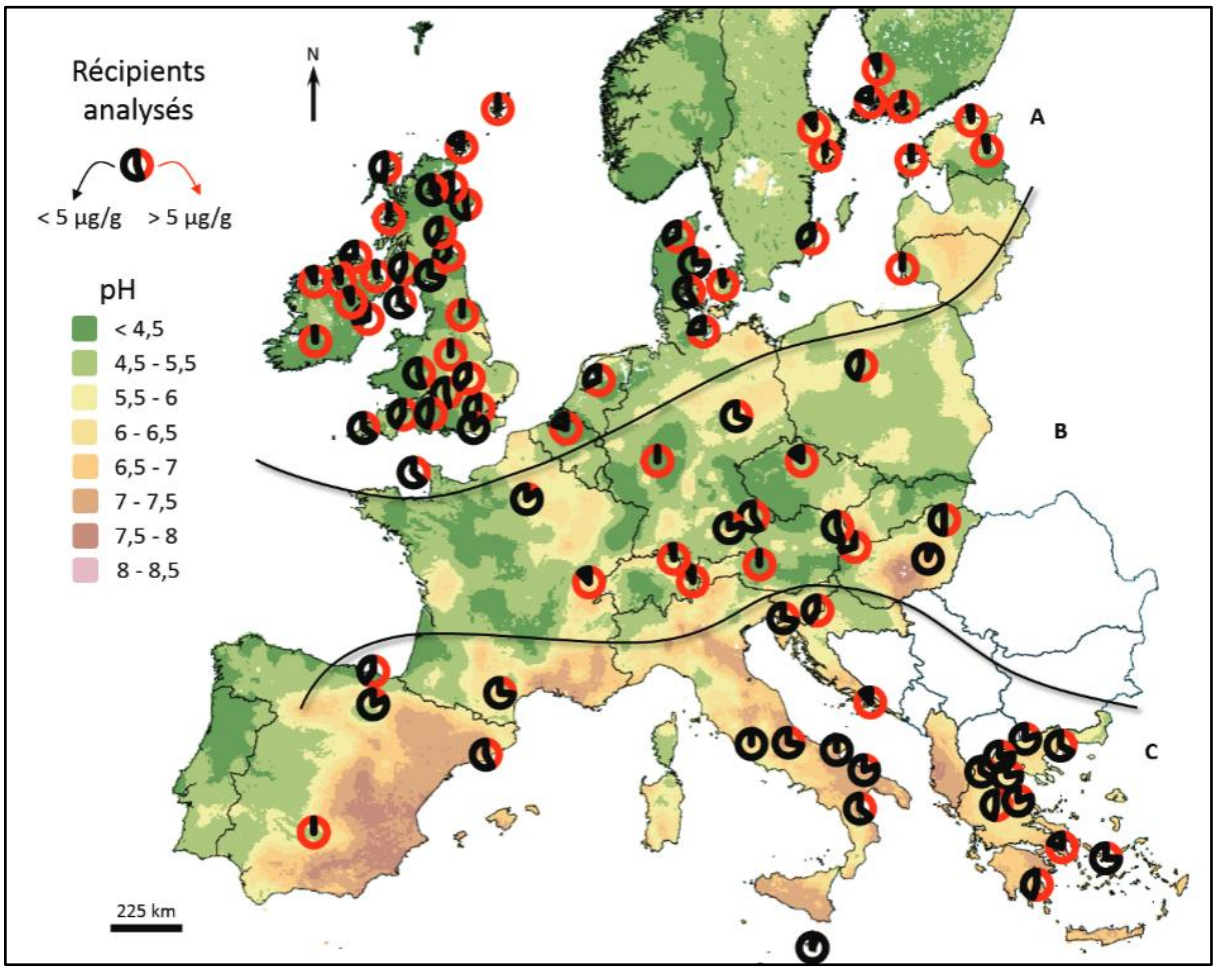


Figure 14. Preservation of organic residues in prehistoric and protohistoric ceramics across different European regions (A: Northern Europe, B: Central Europe, C: Southern Europe), shown in relation to soil pH levels. Reproduced from Drieu (Drieu, 2017).

Despite these preservation issues, lipid residue analysis has nonetheless revealed significant aspects of ancient food traditions in the region (Figure 15). Using distinct lipid extraction methods and analytical techniques (GC, HT-GC, GC-MS, GC-C-IRMS), researchers have successfully extracted and characterised lipid compounds from ceramic artefacts across Neolithic sites in southern Europe. Evidence suggests that Neolithic Mediterranean societies primarily relied on terrestrial food sources, including both ruminant and non-ruminant animals (Spiteri, Muntoni and Craig, 2017; Tarifa-Mateo et al., 2019, 2023; Breu et al., 2021; Drieu et al., 2021), alongside dairy products (Debono Spiteri et al., 2016; Spiteri, Muntoni and Craig, 2017; Breu et al., 2021). Evidence of plant residues, as well as mixtures of plant and animal products within the same vessels, points to diverse culinary practices such as combined cooking or reuse of the pottery (Spiteri, Muntoni and Craig, 2017; Fanti et al., 2018). Interestingly, marine and aquatic products are largely absent in the molecular record, despite their

environmental availability and zooarchaeological representation. This likely reflects a combination of distinct culinary techniques, preservation biases that contribute to the underrepresentation of marine food sources, and a dietary preference for terrestrial resources (Spiteri, Muntoni and Craig, 2017; Fanti et al., 2018; Drieu et al., 2021).

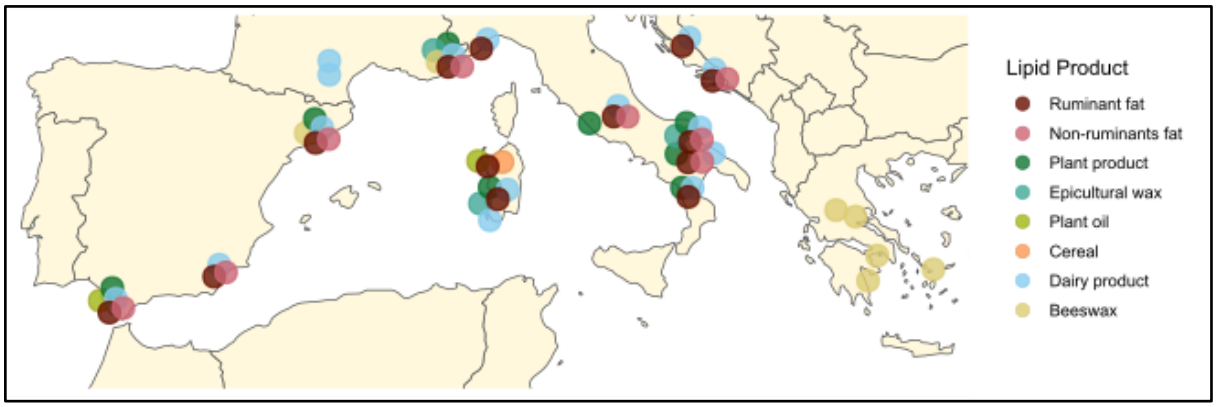


Figure 15. Main lipid products from Neolithic sites in Southern Europe, based on published references compiled from the AROLD database (Debono-Spiteri, 2012; Salque et al., 2012; Roffet-Salque et al., 2015; Debono Spiteri et al., 2016; Fanti et al., 2018; Lucejko et al., 2018; McClure et al., 2018; Tarifa Mateo, 2019; Tarifa-Mateo et al., 2019, 2021; Breu et al., 2021, 2023a; Drieu et al., 2021; Evershed et al., 2022; Maggi et al., 2023; Fanti, Drieu and Regert, 2024). The map visualizes the presence (not proportion) of product categories such as ruminant fats, non-ruminant fats, dairy products, beeswax, plant oils, and other plant-based substances, across different areas. Basemap data sourced from Natural Earth (Massicotte and South, 2023). For the AROLD database see Prévost *et al* (Prévost et al., 2023) and https://www.cepam.cnrs.fr/datas/ArOLD.php.

3.1.4. Lipid residue analysis on stone artefacts[3]

Stone artefacts represent an important witness of prehistoric societies worldwide. Examining these artefacts offers valuable insights into early human communities' technology, lifestyle, and cultural practices. They played a fundamental role in the process of adapting to different environments, facilitating essential activities such as hunting, gathering, food processing and preparation, and the construction of shelter and other survival necessities. Therefore, lithic artefacts were utilised in various aspects of daily life, including hunting, material processing (e.g. cutting, collecting, crafting), cooking and storage, and exhibit a diverse range of forms (Kooyman, 2000; Rowan and Ebeling, 2016; Kipfer, 2023). Flaked stones were commonly used for working wood, bone, and meat, as well as for harvesting and processing plants (Shea, 2007; Hurcombe, 2014). Ground stone tools have long been recognised as an essential component of domestic toolkits, particularly with the onset of agricultural activities, where

[3] This subchapter was conceptualised and co-written with Alice Cao, PhD student at the University of York and University of Copenhagen. The article was authored by the candidate and constitutes original research conducted as part of the doctoral project. The section was jointly idealised and revised as part of a detailed examination of bioarchaeological methods applied to stone tool analysis within the framework of our research. Both the candidate and Alice Cao are affiliated with the funded Chemarch project (Grant No. 956351).

they were primarily used for cereal processing. Additionally, artefacts like stone bowls, vessels and griddle stones served multiple purposes expanding beyond food preparation including tasks such as pigments processing and food storage (Rowan and Ebeling, 2016; Admiraal et al., 2018). Specifically, regarding the primary material discussed in this thesis, HAS can be considered a distinct category of lithic findings and classified within the broader context of combustion features, including cooking structures and fireplaces. These stones are generally interpreted as having been used as heating elements in various cooking techniques (Graesch et al., 2014; Custer, 2017; Neubauer, 2018). However, it is important to acknowledge that HAS may also form passively through unintentional exposure to heat, without direct use as heating devices.

Archaeological research on **lipids analysis on lithic assemblages** have mostly focused on surface-attached residues, like specifically adhering organic remains (Admiraal et al., 2018; Croft et al., 2018; Degano et al., 2019). However, limited studies have directly explored lipid residue within archaeological stone artefacts. A summary of these studies is presented here (Table 3), although it does not pretend to be exhaustive of all currently available data. Various lithic artefacts were considered, such as burned rocks, grinding and milling tools (e.g. manos, abraders, pestles), artefacts with crafted percussion signs, and stone vessels. Remarkably, a standardised protocol for lipid extraction from lithic is lacking, with existing methodologies largely relying on well-established methods used to investigate organic residues on ceramic artefacts (pottery). As schematically shown in Figure 16, lipid analysis on lithic tools typically involves several steps, including sampling, extraction, and derivatisation. To minimise possible contamination from soil or modern lipids, the superficial layer of the lithic artefact (usually 1-3 mm) is removed prior to collect the sample (Quigg et al., 2000; Buonasera, 2005, 2007; Bamyacı, 2019; Chasan, Spiteri and Rosenberg, 2022). The sampling procedure usually required the use of a hand-held drill fitted with a solvent-cleaned carbide/diamond steel bit or disc obtaining a powdered sample. To homogenise it, when needed, a solvent clean mortar and pestle may be used. For storage, powders are generally wrapped in aluminium foil and placed in plastic bags (Buonasera, 2013) or sealed in plastic test tubes (Dietrich et al., 2020). A different strategy is employed when performing extraction by immersion, wherein the entire stone, or part of it, is submerged multiple times in a proper solution (Buonasera, 2005; Beausoleil et al., 2007; Ropiot, Machado and Pepe, 2015; Luong et al., 2017, 2018, 2019). The extraction process primarily involved solvent-based extraction, where samples undergo ultrasonication in a solvent mixture, followed by centrifugation. The resulting extract is then dried under nitrogen to obtain the total lipid extract. Some studies have employed alternative methods, such as Soxhlet extraction, which enables lipid recovery through repeated solvent washing (Marchbanks and Quigg, 1990), microwave-assisted extraction with the use of a microwave accelerated reaction system (Buonasera, 2013). Finally, aliquots are then derivatised mostly through silylation and methylation. Molecular identification techniques have changed over time, with an initial analysis of samples through GC by assessing FAs area and relative percentage in comparison with modern plants

and animals samples, as well external standards (Marchbanks and Quigg, 1990; Quigg et al., 2000, 2001; Buonasera, 2005). Research later expanded to include GC-MS for more precise identification of the separated components, relying mostly on biomarkers, external standards, compounds database, experimental samples and control samples (March and Lucquin, 2006; Buonasera, 2007, 2013, 2016; Lucquin, 2007; Namdar, Stacey and Simpson, 2009; Skibo, Malainey and Drake, 2009; Heron et al., 2010; Dubesset et al., 2014; Ropiot, Machado and Pepe, 2015; García-Piquer et al., 2018; Bamyacı, 2019; Dietrich et al., 2020; Chasan, Spiteri and Rosenberg, 2022; Chasan et al., 2022). Some studies have further employed GC-MS/MS for the analysis of non-volatile low molecular weight lipids, enabling a more selective approach for target compound monitoring and increased sensitivity for the quantitative analysis (Luong et al., 2017, 2018, 2019). Moreover, stable carbon ($\delta^{13}C$) isotopes analysis of fatty acids ($C_{16:0}$ and $C_{18:0}$) has been performed through GC-c-IRMS to provide complementary information on lipid sources and possible mixtures (García-Piquer et al., 2018; Chasan et al., 2022; Langley, 2024).

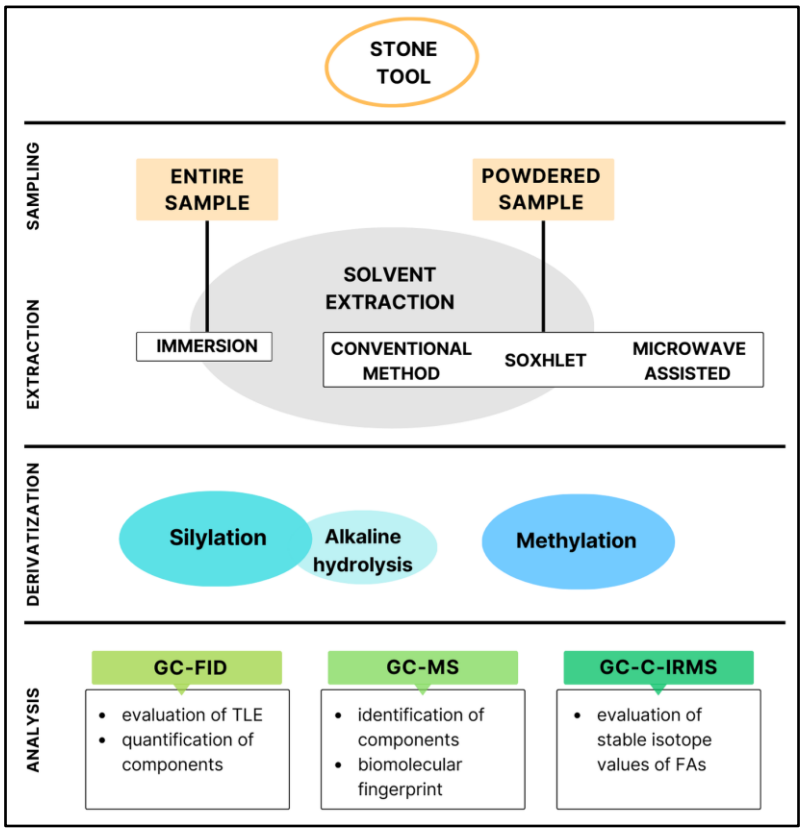


Figure 16. Schematic representation of methodological steps for lipid analysis on lithic artefacts based on the records cited in this chapter.

Lipid analysis of stone artefacts essentially serves a twofold purpose. First, it aims to evaluate the feasibility and effectiveness of lipid extraction techniques when applied to lithic materials, which present unique challenges compared to ceramics or soils. Second, it attempts to enhance our

understanding about past subsistence strategies by identifying organic residues preserved on these artefacts, thereby providing insight into the type of resources processed and the potential functions of the tools and utensils themselves. The methodological variations reported in the literature underscore the need for tailored analytical approaches. Differences in sampling techniques, extraction protocols, and derivatisation strategies reflect the challenges posed by the specific properties of lithics. As such, it is important to select methods that align with both the specific research questions and the material characteristics of the artefacts under investigation. Over the years, molecular identification of extracted lipids has yielded promising results, distinguishing between residues of plant and animal origin (Marchbanks and Quigg, 1990; Quigg et al., 2000, 2001; Namdar, Stacey and Simpson, 2009; Skibo, Malainey and Drake, 2009). Some studies have demonstrated the technique's potential in offering valuable clues about the functional roles of the artefacts, as well as determining whether the lipids were introduced through cooking activities (Dubesset et al., 2014; Ropiot, Machado and Pepe, 2015; Buonasera, 2016; Dietrich et al., 2020). However, there remains a need for further refinement of methods employed, particularly in developing a more comprehensive database of lipid compounds. This ongoing effort is driven by experimental research aimed at enhancing both the accuracy of lipid identification and the scope of the reference database (Buonasera, 2005, 2007, 2013).

Based on the selected records, stable carbon ($\delta^{13}C$) isotopes analysis was performed in a few cases, to further refine the interpretation of residue origin. A stone vessel exhibited an isotopic signature consistent with ruminant adipose fats, supporting its use in food preparation activities, particularly the processing of animal-derived fats (Chasan et al., 2022). In addition, burned stones revealed isotopic profiles and molecular markers consistent with their use within combustion structures for marine food processing (García-Piquer et al., 2018), as well as thermal activity in cooking pits and hearths associated with the processing of ruminant fats and marine oils (Langley, 2024). These findings demonstrate that stone artefacts can preserve distinct molecular and isotopic signatures reflective of diverse culinary practices. Overall, the results underscore the value of combining molecular and isotopic approaches in organic residue analysis and highlight the potential of stone artefacts as meaningful sources of organic data in archaeological contexts.

Overall, lipid analysis on stone artefacts offers a valuable avenue for reconstructing human-environment interactions and dietary practices in archaeological contexts. However, ongoing refinement of extraction and analytical methodologies is essential to improve the interpretative framework. Further research, including the integration of complementary techniques such as compound-specific isotope analysis and proteomics, may expand the scope of lipid analysis and contribute to more nuanced reconstructions of past subsistence economies.

Table 3. Lipid analysis methodology of various studies categorised by lithic tools.

Lithic tools	Sampling	Extraction Methods	Derivatisation	Analysis	Objectives	References
Burned rocks	Entire sample	Immersion	Methylation	GC GC-MS	Successful lipids extraction; Tools function; Resources identification; Subsistence practices	(Marchbanks and Quigg, 1990; Buonasera, 2005; Beausoleil et al., 2007; Ropiot, Machado and Pepe, 2015)
	Powdered sample	Soxhlet	Methylation	GC	Tools function; Subsistence practices	(Marchbanks and Quigg, 1990)
		Conventional	Methylation Silylation Neutral	GC GC-MS GC-c-IRMS	Successful lipids extraction; Tools function; Resources identification; Subsistence practices	(Quigg et al., 2000, 2001; Buonasera, 2005; March and Lucquin, 2006; Lucquin, 2007; Skibo, Malainey and Drake, 2009; Heron et al., 2010; Dubesset et al., 2014; García-Piquer et al., 2018; Langley, 2024)
Bedrock features	Powdered sample	Conventional	Methylation	GC-MS	Resources identification	(Buonasera, 2016)
Grinding tools	Powdered sample	Conventional	Methylation	GC GC-MS	Successful lipids extraction; Resources identification; Subsistence practices	(Quigg et al., 2000, 2001; Buonasera, 2007; Bamyacı, 2019)
		Microwave assisted	Methylation	GC-MS	Successful feasibility of the experimental method	(Buonasera, 2013)
Lithic artefacts	Powdered sample	Conventional	Methylation	GC	Tools function; Subsistence practices	(Marchbanks and Quigg, 1990)
	Entire sample	Immersion	Silylation	GC-MS/MS	Tools function; Resources identification	(Luong et al., 2017, 2018, 2019)
Stone vessels	Powdered sample	Conventional	Methylation Silylation Alkaline hydrolysis	GC-MS GC-c-IRMS	Successful lipids extraction; Tools function; Resources identification	(Namdar, Stacey and Simpson, 2009; Dietrich et al., 2020; Chasan, Spiteri and Rosenberg, 2022; Chasan et al., 2022)

3.2. Protein residue analysis in archaeology

The study of ancient proteins, which began in the 1930s, has gradually shaped the field of biomolecular archaeology, though proteins have only assumed a central role in recent decades (Dallongeville et al., 2016; Hendy, 2021). This specialised branch of archaeology focuses on identifying and interpreting preserved proteins from archaeological materials such as bones, teeth, hair, and artefacts, providing insights into diet, health, and artefact use. Traditionally, protein identification relied on determining amino acid composition or sequences, and immunological (antibody-based) methods became widely applied due to their relative ease and accessibility. However, while immunological assays remain a valuable approach for studying proteins on artefacts, their reliability can be limited, particularly when applied to lithics where preservation is often poor (Richards and Britton, 2020; Hendy, 2021). On the other hand, mass spectrometry-based proteomics is an alternative approach that avoids immunological methods and is specifically suited for the identification of small amounts of single proteins in complex mixtures.

Proteins are linear polymers of amino acids, composed of 20 chemically distinct subunits, which form polypeptides capable of performing a wide range of structural, catalytic, and functional roles in biological systems. Each amino acid shares a common structure (Figure 17), consisting of a central α-carbon bonded to four groups: a hydrogen atom, a carboxyl ($-COO^-$) group, an amino ($-NH_3^+$) group, and a variable side chain (R group) that distinguishes each amino acid (Brown and Brown, 2011; Richards and Britton, 2020; Smith, 2020).

Amino acids differ widely in the structure and complexity of their side chains (R groups), ranging from the simple hydrogen of glycine to the aromatic rings of tyrosine, phenylalanine, and tryptophan. These variations confer distinct chemical properties: some R groups are polar (e.g., serine, threonine) and hydrophilic, others are nonpolar (e.g., alanine, valine, leucine), while a few carry negative (aspartic acid, glutamic acid) or positive (lysine, arginine, histidine) charges. Consequently, proteins exhibit diverse chemical and biological behaviours determined by the type and sequence of constituent amino acids. With the exception of glycine, amino acids occur as two optical isomers, known as the D (*dextro*) and L (*laevo*) forms, a property referred to as chirality. **Polypeptides** form when amino acids are linked by peptide bonds, generated through condensation reactions between the carboxyl and amino groups. The resulting chain has chemically distinct termini: an N terminus with a free amino group and a C terminus with a free carboxyl group, giving the polypeptide a directional orientation from N to C.

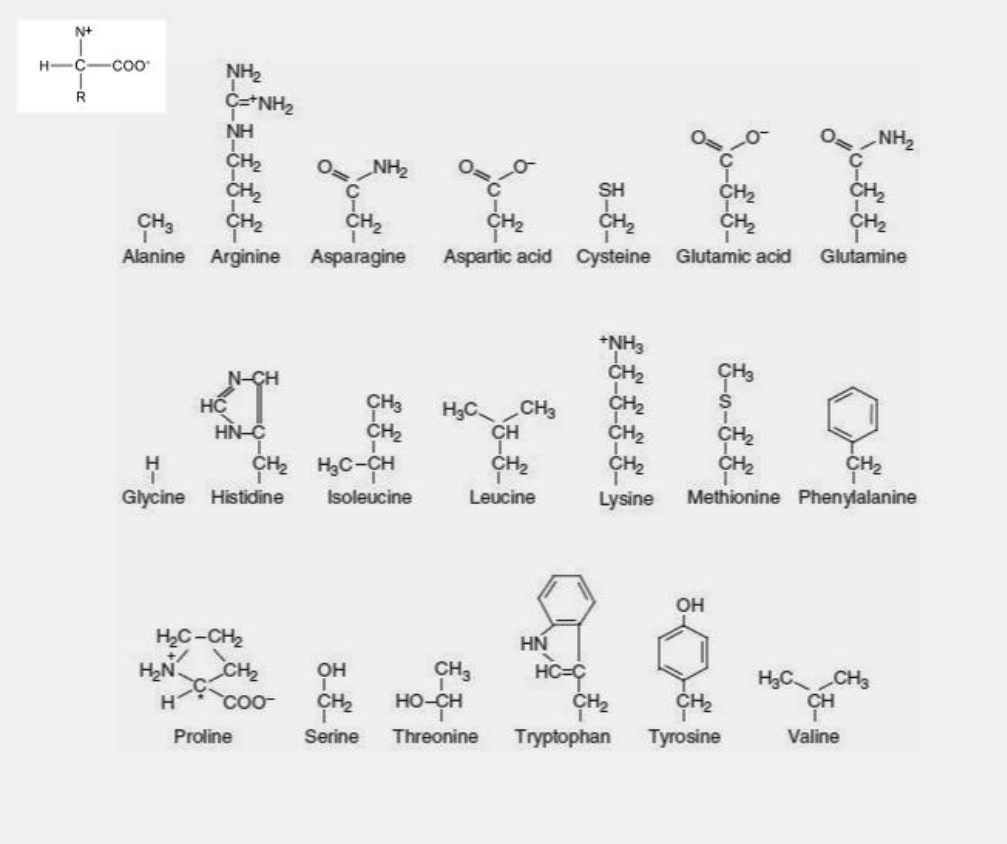


Figure 17. General structure of the 20 amino acids and their R groups found in proteins. Adapted from Brown and Brown (Brown and Brown, 2011).

Proteins exhibit four hierarchical levels of structure (Brown and Brown, 2011; Richards and Britton, 2020; Smith, 2020). The primary structure is the linear sequence of amino acids. Secondary structure arises from local folding patterns, primarily α-helices and β-sheets, stabilised by hydrogen bonding. The tertiary structure describes the three-dimensional arrangement of a single polypeptide, stabilised by hydrogen bonds, electrostatic interactions, hydrophobic effects, and sometimes disulfide bridges. Quaternary structure arises when two or more polypeptides associate to form a multisubunit protein, which can be held together by covalent bonds or weaker interactions.

In archaeological contexts, proteins are more resistant to degradation than DNA but less stable than lipids, with their higher hydrophilicity promoting leaching and contributing to their moderate diagenetic stability. They are subject to specific **structural modifications** that influence their preservation (Bada, 1991), including hydrolysis, which cleaves peptide bonds into smaller peptides and amino acids, reducing molecular size and often leading to the loss of sequence information; racemisation, which converts amino acids from the L-form to the D-form over time and can serve as both a marker of diagenetic alteration and a relative dating tool; deamidation, which alters asparagine and glutamine residues into aspartic and glutamic acids, affecting protein conformation; and biological degradation by enzymes or microbes, further breaking down proteins and collectively determining their

survival and interpretability in archaeological materials. Warm aerobic environments accelerate biomolecular degradation by increasing the rate of chemical reactions and supporting microbial activity, while extremely cold or anaerobic conditions markedly slow decomposition and enhance survival. In addition, ancient proteins are typically associated with a mineral matrix, either biomineralised, as in bones, teeth, and dental calculus, or inorganic, as in ceramics, which can further protect them from degradation.

3.2.1. Proteomic approaches for Archaeological Materials

This subchapter outlines the specific analytical techniques employed in this thesis for the extraction and identification of proteins from archaeological materials. The discussion focuses on the methods most relevant to this study, while recognising that a wider range of approaches exists within the field.

Given the scope of this thesis and the absence of an established proteomic protocol specifically tailored for lithic artifacts, the evaluation of protein preservation has been approached through comparison with ceramic residues. Ceramic vessels are known to retain organic material associated with the processing of foodstuffs, providing a possible analogue for HAS. The study of proteins in ceramics began in the 1990s, shortly after researchers had successfully identified lipid residues preserved in pottery. Early work focused on extracting proteinaceous material from ceramics by hydrolysing the proteins into amino acids, and determining their composition using ion exchange chromatography with fluorescent detection (Evershed and Tuross, 1996). Although potsherds contained lower amounts of amino acids than surrounding soil, their distinct amino acid profiles indicated that the proteins originated from sources other than environmental contamination. This work therefore demonstrated both the feasibility of detecting ancient proteins in ceramics and the importance of amino acid profiles in distinguishing authentic residues from environmental background. Over time, research on proteins in archaeological ceramics has increasingly focused on their identification and characterisation. Initially, immunological methods were employed to detect specific proteins or protein families (Craig and Collins, 2002; Craig et al., 2005; Matheson, Hall and Viel, 2009), while more recently the field has shifted towards the application of mass spectrometry, which allows for highly sensitive and precise identification of individual proteins and peptides, reconstruction of protein sequences, and even taxonomic assignment of the source material (Solazzo et al., 2008; Barker et al., 2012; Hendy et al., 2018).

Recent studies demonstrate that protein preservation in food residues is highly selective, strongly influenced by cooking, ingredient composition, and post-depositional degradation, and that the recovered proteome may not accurately reflect the original meal (Evans et al., 2024; Dekker et al.,

2025). Lithic artefacts, like ceramics, can come into contact with organic materials during use, potentially forming residues that are highly degraded and present in low concentrations. Given these challenges, applying a sensitive and robust methodology such as **Single-Pot Solid-Phase-enhanced Sample Preparation (SP3) extraction combined with Liquid Chromatography - Tandem Mass Spectrometry** (**LC-MS/MS)** may be advantageous. The SP3 protocol can enhance protein recovery from complex mineral matrices, while LC-MS/MS allows high-resolution identification of proteins, including both plant- and animal-derived sequences. Its application to lithic artefacts is exploratory, reflecting the expectation that mineral matrices in lithics may present similar challenges to ceramics, but without prior demonstration of its effectiveness in this context.

In the context of this study, proteins are extracted from lithic matrices using the **SP3 protocol** optimised specifically for foodcrust from archaeological cooking vessels (Harvey and Hendy, 2025) (See Chapter 5). SP3 employs paramagnetic beads to bind proteins in a single-pot workflow, allowing efficient removal of detergents, salts, and other inhibitors that could interfere with downstream analysis. This method is particularly well-suited to archaeological ceramics, where protein concentrations are low and matrix effects from silica and mineral residues pose significant challenges. This protocol was selected for the lithic artefacts analysed here since their mineral matrices are expected to present similar challenges to those of ceramics, likely providing a reliable means of recovering proteins from complex mineralised matrices. Following extraction, proteins are analysed using **LC-MS/MS**, a high-resolution analytical technique capable of identifying proteins from complex mixtures with taxonomic specificity. LC, unlike GC discussed in the previous subchapter, separates compounds in a liquid mobile phase rather than a gaseous one. In the context of proteomics, LC is employed to separate peptide mixtures generated by enzymatic digestion of proteins prior to mass spectrometric analysis. Separation occurs within a chromatographic column containing a stationary phase, where peptides are differentially retained and eluted according to their chemical properties. This separation reduces the complexity of the sample entering the mass spectrometer, improving sensitivity and enabling the detection of low-abundance peptides that might otherwise be obscured in complex mixtures. By combining LC with tandem MS, it becomes possible to sequence peptide fragments and obtain detailed taxonomic and functional information. In the first stage (MS1), intact peptides are detected and selected as precursor ions, that are then fragmented in the second stage (MS2), producing spectra from which the amino acid sequence can be reconstructed.

3.2.2. Protein analysis on lithic artefacts[4]

Proteomic investigation of lithic artefacts began to gain traction in the 1980s and 1990s as researchers sought direct evidence of hunting and butchery activities on artefacts such as flaked stones, scrapers, bifaces, and projectile points (Newman and Julig, 1989; Kooyman, Newman and Ceri, 1992; Loy and Hardy, 1992). Subsequent studies extended this research to include milling stones associated with animal processing (Yohe, Newman and Schneider, 1991), rock art (Williamson, 2000), and lithics connected to ritual practices (Äikäs, Bergmann and Salmi, 2012). Early studies primarily focused on proteins found in blood cells, including haemoglobin, albumin, and immunoglobulin IgG, which exhibit species-specific variations. To achieve this goal, a range of analytical approaches has been developed, spanning colorimetric assays (Loy, 1983; Custer, Ilgenfritz" and Domsa, 1988; Loy and Wood, 1989; Hyland et al., 1990; Loy and Hardy, 1992; Downs and Lowenstein, 1994; Manning, 1994; Loy and Dixon, 1998; Williamson, 2000; Matheson and Veall, 2014), immunological techniques (Loy and Wood, 1989; Hyland et al., 1990; Loy and Hardy, 1992; Downs and Lowenstein, 1994; Loy and Dixon, 1998), electrophoretic methods (Newman and Julig, 1989; Yohe, Newman and Schneider, 1991; Kooyman, Newman and Ceri, 1992; Downs and Lowenstein, 1994; Allen, Newman and Riford, 1995; Gerlach et al., 1996; Petraglia et al., 1996; Shanks, Kornfeld and Hawk, 1999; Kooyman et al., 2001; Seeman et al., 2008; Högberg, Puseman and Yost, 2009; Yohe and Bamforth, 2013), and mass spectrometry (Heaton et al., 2009; Äikäs, Bergmann and Salmi, 2012).

Although these investigations initially suggested that protein analysis could offer valuable insights into past activities, methodological inconsistencies and questions regarding the reliability of protein detection and species attribution led to intense scientific debate. The limitations of various approaches for analysing blood proteins on lithic artefacts have been discussed extensively in the literature (Cattaneo et al., 1993; Downs and Lowenstein, 1994; Fiedel, 1996; Newman et al., 1997). More recently, advances in highly sensitive mass spectroscopy, alongside improved contamination controls and the standardisation of protocols, have significantly enhanced the detection and identification of trace proteins in archaeological context (Hendy, 2021). Despite these advances, proteomic investigations of lithic artefacts remain at an exploratory stage compared to other material types such as ceramics. Further research is needed to evaluate the extent of protein preservation within lithic matrices and to refine analytical protocols tailored to such substrates. To date, no studies have specifically examined HAS for the detection of superficial deposits potentially derived from culinary

[4] This subchapter was conceptualised and co-written with Alice Cao, PhD student at the University of York and University of Copenhagen. The article was authored by the candidate and constitutes original research conducted as part of the doctoral project. The section was jointly idealised and revised as part of a detailed examination of bioarchaeological methods applied to stone tool analysis within the framework of our research. Both the candidate and Alice Cao are affiliated with the funded Chemarch project (Grant No. 956351).

activities, nor has the SP3 method coupled with LC-MS/MS been applied to lithic tools, marking a novel contribution of the present investigation.

4. Archaeological case studies

The archaeological sites of La Draga and Pendimoun were selected for this study due to their complementary potential in addressing questions related to the preservation and interpretation of heat-altered stones (HAS) within contrasting environmental and cultural contexts. Although these sites differ significantly in geographical location, environmental conditions, and cultural affiliation, their comparison offers a unique opportunity to investigate how taphonomic factors influence the preservation of organic residues associated with combustion structures. La Draga, located in northeastern Spain, is the only known Early Neolithic lakeshore settlement in the Iberian Peninsula and one of the few such sites documented in the Mediterranean region south of the Alps dating to the 6th millennium BCE. Its exceptional waterlogged preservation conditions have yielded some of the most detailed evidence for early Neolithic lifeways in the area. In contrast, the Pendimoun rock-shelter in southeastern France represents a terrestrial context with a stratigraphically rich sequence spanning from the Impressa to the Bell beakers period, providing one of the few continuous records of the Impresso-cardial transition in the western Mediterranean. The juxtaposition of these two sites enables a multi-scalar and comparative analysis of organic preservation in HAS. The markedly different excavation timelines, sampling strategies, and storage protocols implemented at La Draga and Pendimoun further enrich the comparative framework, allowing for an assessment of how such methodological variations influence the detection and interpretation of organic compounds. Beyond their contextual differences, both sites reflect a growing archaeological interest in the systematic recovery and analysis of HAS, driven by the potential of these materials to yield insights into subsistence activities. As HAS are increasingly recognised as valuable archives for reconstructing human-environment interactions, their systematic collection for archaeometric analysis reflects an emerging disciplinary consensus on their interpretive significance and underscores the need for standardised recovery and analytical protocols to maximise their research potential.

4.1. La Draga

La Draga is a Neolithic lakeshore site situated on the eastern side of Lake Banyoles in Catalunya, Spain, discovered in 1990 and represents the first prehistoric lakeside settlement found in the Iberian Peninsula (Palomo et al., 2014; Terradas, Palomo and Piqué, 2020). The site, located 170 metres above sea level, 50 kilometres from the Pyrenees, and 35 kilometres from the current Mediterranean Sea, has been extensively studied through collaborative efforts involving institutions such as the Museu Arqueologic Comarcal de Banyoles (MACB), the Centre d'Arqueologia Subaquàtica

de Catalunya (CASC), Consejo Superior de Investigaciones Científicas (CSIC-IMF), the Universitat Autònoma de Barcelona (UAB), and the Museu d'Arqueologia de Catalunya (MAC). Representing an open-air settlement dating back to the late 6th millennium cal BC, La Draga is characterised by the remarkable preservation of archaeological organic remains due to persistent waterlogged conditions (Terradas, Palomo and Piqué, 2020; Andreaki et al., 2022). The site extension is estimated to be about 15,000 square metres, with distinct sectors defined on the relationship between archaeological levels and water table (Figure 18). Although the settlement was undoubtedly situated above the lake's water table during prehistoric times, both Sector A and Sector B/D are currently located inland (Figure 19). **Sector A**, positioned at the highest point of the site, is the driest sector, with archaeological layers well above the water table. Therefore, organic remains have not been preserved, except for the tips of wooden piles situated beneath the archaeological layer. **Sector B/D** contains the earliest archaeological deposits, which lie below the waterline and remain in permanently wet or even submerged conditions. These conditions have favoured the preservation of organic materials. Additionally, **Sector C** is located underwater near the present-day shoreline. This sector has also contributed to the good conservation of organic remains (Palomo, Piqué and Terradas, 2018; Andreaki et al., 2022; López-Bultó et al., 2025). Excavations in Sector B/D have revealed **two distinct archaeological horizons**, each corresponding to a different occupation phase. These phases are separated by a paved surface made of travertine slabs, laid over an older layer of timber logs, acting as a chronological marker between the phases (Andreaki et al., 2022; López-Bultó et al., 2025). The older phase (5.315-5.200 BCE) represents the earliest occupation of the site and is distinguished by exceptional organic preservation due to waterlogged conditions. Numerous wooden remains were recovered, including hundreds of piles and beams used for constructing dwellings, as well as wooden tools related to daily life. This phase coincided with a dry climatic period, likely resulting in a lower lake level, which provided stable ground for construction near the shore, reflecting adaptive construction strategies in response to the environment. Dendrochronological analyses have allowed for greater precision in relation to the time of construction of the huts and their repairs (Andreaki et al., 2020; López-Bultó et al., 2025). The later phase (5.100-4.800 BCE) marks a shift towards stone-based construction, with the extensive use of travertine slabs to create solid occupation floors, replacing the older wooden structures. During this phase, huts were built directly on the ground atop these paved surfaces, rather than elevated on log and plank platforms as in the previous phase. Several structures were identified on top of the pavement, though no evidence of timber buildings were directly associated with it (Andreaki et al., 2022; López-Bultó et al., 2025). The lack of organic preservation is likely due to the absence of waterlogged conditions, with organic remains surviving only in carbonised form. This transition from wooden platforms to stone-based structures reflects a fundamental change in settlement organisation and construction methods, possibly driven by technological advancements, environmental adaptation, and social changes.

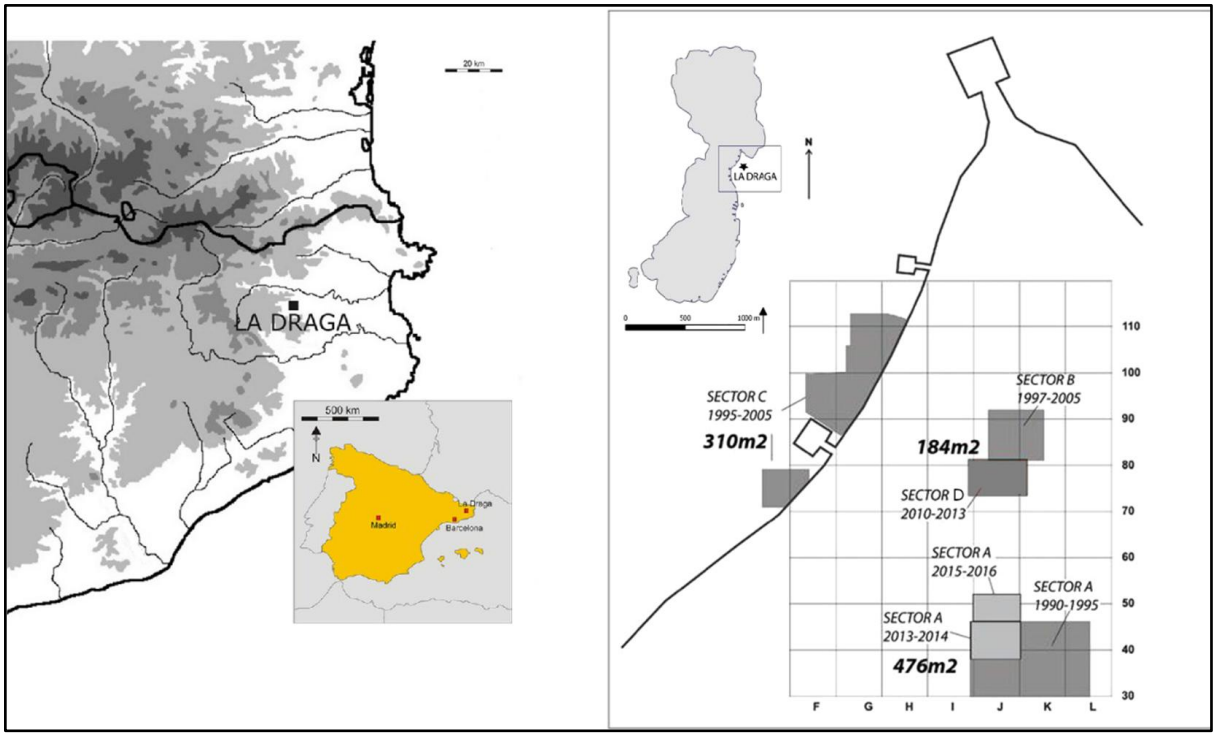


Figure 18. La Draga archaeological site in northeastern Iberian Peninsula and general plan of the excavated sectors from Andreaki at al. (Andreaki et al., 2022).

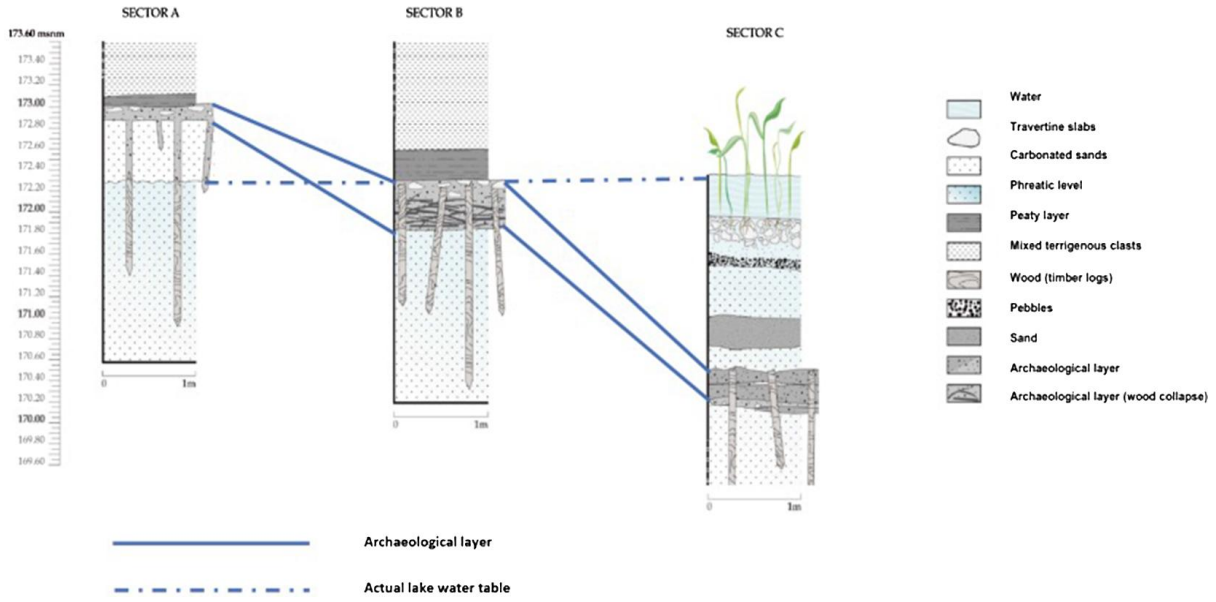


Figure 19. Stratigraphic correlation of all three excavated sectors in La Draga from Andreaki at al. (Andreaki et al., 2022).

Subsistence at la Draga was based on a mixed economy that combined livestock husbandry with agricultural production. Among the **domesticated animals**, the most commonly processed and consumed species at the site were cattle (*Bos taurus*), pigs (*Sus domesticus*), sheep (*Ovis aries*) and goats (*Capra hircus*). These animals were mostly exploited for their meat, although secondary products

such as dairy and labour, in the case of ruminants, also contributed significantly to their economic value (Saña, 2011; Terradas et al., 2012; Antolín et al., 2014; Palomo, Piqué and Terradas, 2018). In addition, dogs (*Canis familiaris*) were also domesticated, possibly for purposes related to labour or other utilitarian roles. While subordinate to animal husbandry, hunting nonetheless played a complementary role within the broader subsistence strategy (Piqué et al., 2015). Wild fauna, including red deer (*Cervus elaphus*), wild boar (*Sus scrofa*), roe deer (*Capreolus capreolus*), as well as various small mammals and birds, were also procured from nearby forest and lake environments (Saña, 2011; Palomo, Piqué and Terradas, 2018). Aquatic resources were also actively exploited. Freshwater fish, such as catfish (*Silurus glanis*) and eels (*Anguilla anguilla*), alongside marine molluscs, reflect the enduring role of fishing in the diet and point to a broad-spectrum subsistence economy that included both inland and possibly coastal species (Saña, 2011; Palomo, Piqué and Terradas, 2018; Verdún-Castelló et al., 2019). **Cereal-based agriculture** constituted a significant part of the production economy. Among cereals, naked wheat (*Triticum aestivum*) was particularly prominent, indicating a preference for free-threshing varieties. Barley (*Hordeum vulgare*) was also present, albeit to a lesser extent. In addition, hulled wheats, such as einkorn (*Triticum monococcum*) and emmer (*Triticum dicoccum*) were identified, further demonstrating the diversity of cereal exploitation (Antolín et al., 2014; Antolín, 2016; Palomo, Piqué and Terradas, 2018; Araus et al., 2024). The plant economy was not limited to cereals; other crops, notably legumes, and oil- or drug-producing species like poppy (*Papaver somniferum*), were also cultivated, suggesting a broader subsistence strategy that included protein-rich and pharmacologically useful plants. Complementing the agricultural economy was the exploitation of wild plant resources, which underscores the continued importance of foraging. A wide range of wild fruits were collected, including acorns (*Quercus sp.*), hazelnuts (*Corylus avellana*), wild grape (*Vitis vinifera subsp. sylvestris*), and sloe (*Prunus spinosa*). Aromatic herbs such as water mint (*Mentha aquatica*) and oregano (*Origanum vulgare*) were also gathered, likely for culinary or medicinal purposes (Caruso Ferme and Piqué i Huerta, 2014; Palomo, Piqué and Terradas, 2018).

Additionally, the nearby lake environment provided abundant forest and vegetation resources exploited for timber and fuel (Caruso Ferme and Piqué i Huerta, 2014; López-Bultó and Piqué Huerta, 2018), alongside clay and lithic materials used in the construction of stone structures and the production of artefacts (Terradas et al., 2012). During the initial occupation phase, oak (*Quercus sp.*) was the primary species used in construction, particularly for the posts supporting dwelling platforms. Oak and laurel (*Laurus nobilis*) were also the predominant taxa selected for combustion purposes. As the settlement evolved, there was a marked increase in the use of boxwood (*Buxus sempervirens*) between the first and second occupational phases, suggesting an adaptive response to changing resource availability or functional needs (Terradas et al., 2017; Terradas, Palomo and Piqué, 2020). The exceptional preservation of organic materials at the site has enabled the recovery of an extraordinary assemblage of wooden artefacts and others made from plant fibers, such as basketry or ropes, making

the site unique in the Iberian Peninsula. These include a wide range of everyday tools such as sickles, digging sticks, bows, arrow shafts, adzes, combs, spatulas, containers, and other utilitarian objects, reflecting various aspects of domestic and productive life. These artefacts were crafted from a range of distinct wood types, selected not arbitrarily but for their specific properties suited to particular functions (Bosch, Chinchilla and Tarrús, 2006; Palomo et al., 2011; Piqué et al., 2015; Terradas et al., 2017; Palomo, Piqué and Terradas, 2018). In addition to wooden implements, a substantial number of artefacts were manufactured from animal bones, including tools likely associated with activities such as weaving, leatherworking, and food processing (Palomo, Piqué and Terradas, 2018; Hansen, 2024). Shells were also employed in the production of personal ornaments, reflecting symbolic expression and aesthetic practices within the community (Palomo, Piqué and Terradas, 2018; Poveda, 2015).

The **ceramic assemblage** at La Draga (Figure 20) is primarily hand-modelled using locally sourced clay, which contains inclusions of quartz and mica. The vessels are generally shaped through the coiling technique, followed by smoothing and polishing before decoration (Tarrús, 2008; Bertin et al., 2024). The pottery displays a relative monotony in form, with predominantly globular profiles and rounded bases, suggesting a utilitarian focus rather than a concern for uniformity or refinement in production (Tarifa Mateo, 2019). Decoration is dominated by the Cardial ware tradition, characterised by shell impressions and dragging techniques using the edge of Cardium shells to create jagged lines or incised stripes. Relief decoration is also present, most commonly in the form of plain applied cordons, which could have had a decorative function. Overall, the decorative programme remains simple and repetitive, with motifs typically limited to horizontal bands encircling the vessel, occasionally accompanied by simple pendent elements (Palomo, Piqué and Terradas, 2018). Ceramic vessels were primarily used for cooking functions, as indicated by their shapes and archaeological context. Their forms, mainly bowls and pots, are particularly well suited for food preparation and processing, suggesting these as their main functions, while also allowing occasional use in storage and transport. The spatial distribution of ceramics, often found near hearths and domestic areas, further supports their role in cooking activities, highlighting their importance in daily subsistence and food preparation practices at the site (Bertin et al., 2024).



Figure 20. Pottery fragments from the Early Neolithic site of La Draga documented by Bertin at al. (Bertin et al., 2024).

A broad and diverse assemblage of rocks and minerals was recovered, reflecting a deliberate selection strategy aimed at producing a functional and technologically varied **lithic toolkit**. The evidence includes artefacts knapped with allochthonous flint and local quartz, as well as tools bearing polished bevels (adzes), indicative of advanced shaping techniques. Additionally, larger stone implements were identified, primarily manufactured from basalt, porphyritic rocks, and granite, and interpreted as being used for grinding activities. Other materials, such as sandstone slabs, appear to have been employed for polishing operations, while limestone pebbles exhibit traces of use related to burnishing and hide processing (Palomo, Piqué and Terradas, 2018; Terradas, Palomo and Piqué, 2020). The hearth structures have a flat section, sometimes concave when building a small basin. They appear composed of travertine blocks, sandstone slabs, and heat-altered stones, along with charcoal residues resulting from the combustion of plant-based fuel. The presence of HAS, both in combustion structures (Figure 21) and scattered throughout the site, serves as a strong indicator of sustained thermal activity, likely linked to domestic practices such as cooking, heating, or small-scale craft production. Their deliberate selection, transport to the site, and use suggests a sophisticated understanding of thermal properties, contributing to broader discussion on technological behaviour, resource exploitation, and spatial organisation within the occupation sequence.



Figure 21. Combustion structure E249 (2010) and E266 (2023), both of which incorporate heat-altered stones (HAS) (Piqué et al., 2023). Photographs courtesy of the La Draga team.

The exceptional archaeological discoveries at La Draga, along with its significant scientific and heritage value, have inspired the creation of the Neolithic Park of La Draga (Figure 22, A). It serves as an educational and cultural facility that brings the prehistoric past to life through reconstructions of Neolithic dwellings, hands-on activities, and demonstrations of ancient technologies such as flint knapping, pottery, weaving, and food processing. Notably, archaeological excavations at La Draga are ongoing (Figure 22, B), with annual field campaigns continually enriching both the academic discourse and the interpretive materials presented to the public. In this way, the park serves as a dynamic interface between research, education, and community engagement, highlighting the role of archaeology in fostering cultural continuity and enhancing public awareness of one of the Iberian Peninsula's most important prehistoric sites.

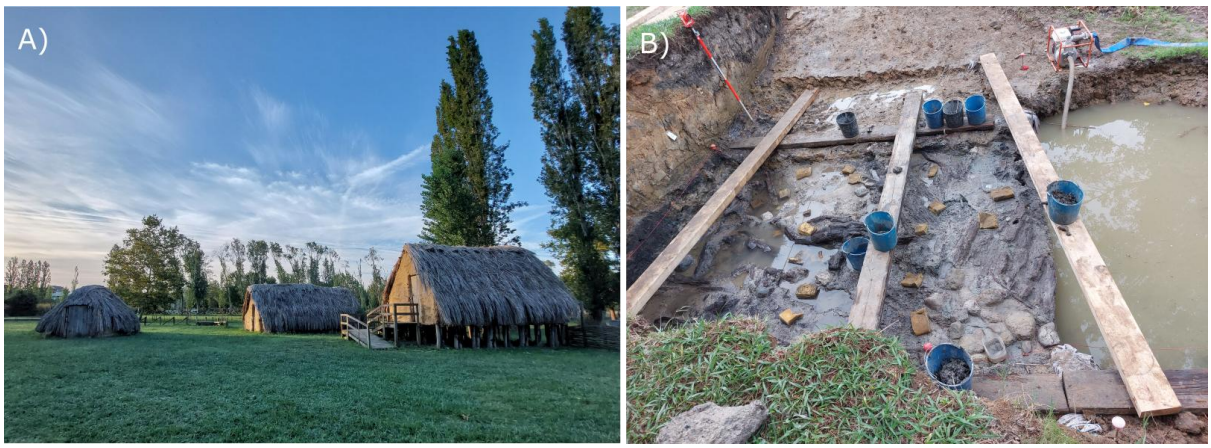


Figure 22. (A) Reconstruction of Neolithic structures at the Neolithic Park of La Draga, showcasing various architectural elements from the prehistoric period. (B) Excavations conducted in Zone B of La Draga, 2023 field season, revealing significant archaeological findings.

4.2. Pendimoun

Pendimoun is a rock-shelter located in Castellar, Alpes Maritimes, France, approximately 1 kilometre from the Italian border and less than 4 kilometres from the seaside, at an altitude of about 690 metres, facing west in the foothills of the Orméa cliff (Figure 23) (Battentier et al., 2015; Binder et al., 2020). It was first surveyed in the 1950's by L. Barral and the Museum of Prehistoric Anthropology of Monaco, and subsequently excavated by D. Binder from 1985 to 1992 (Binder et al., 1993) and from 1997 to 2006 (Battentier et al., 2015; Binder et al., 2020; Drieu et al., 2021). The site represents one of the few archaeological contexts preserving a well-stratified and chronologically secure sequence from the earliest western Mediterranean Neolithic. Its stratigraphic integrity, coupled with the richness of both environmental and cultural data, renders the site crucial for reconstructing long-term human occupation and adaptation in this region. The extensive stratigraphic sequence revealed a discontinuous but recurrent occupation, from the Mesolithic and continuing throughout the entirety of the Neolithic, ultimately extending into protohistoric and historical periods (Binder et al., 2020). The stratified deposits at Pendimoun have yielded a remarkably diverse assemblage of material culture that reflects the complex cultural dynamics of the region throughout prehistory. Notably, the earliest phases of the site had produced ceramics attributed to several distinct traditions: finger-nail impressions characteristic of southern Italian style (phases PND 1A-1B, (Manen et al., 2022)), geometric Cardial pattern referring to Central Tyrrhenian (end of phase PND 1B) and Cardium impressed ware corresponding to the Franco-Iberian Cardial tradition (phase PND2). These stylistic variants highlight the site's integration within wider interaction spheres spanning the whole Tyrrhenian area during the early 6th millennium BCE. Additionally, the stratigraphy includes human occupation associated with the Initial SMP and Prechassey Cultures (phase PND 3), Early and Late Southern Chassey, and later phases such as Bell Beakers, the Final Bronze Age, the Iron Age, and Gallo-Roman occupations (Binder et al., 2020). The stratigraphic sequence at Pendimoun was formed through a combination of natural limestone debris and anthropogenic deposits, including hearth remains, craft and domestic refuse, and dung. While some vertical disturbance occurred due to bioturbation and pit-related activity, preservation is generally good, particularly in the northern sector (Figure 24). Archaeologists identified a variety of features such as hearths, pits, postholes, and burials, alongside diffuse waste concentrations from brief occupations.

For the purpose of this study, attention is directed specifically towards the Neolithic occupation of Pendimoun, over the course of the 6th and the beginning of the 5th millennium BC. The analysis of ceramic assemblages has significantly refined the site's chronological framework thanks to a large series of ^{14}C dates on short-lived samples and Bayesian modelling: the Impressa phase (5730-5430 BCE), the Cardial phase (5550-5150 BCE), and the Initial stage of the Square Mouthed Pottery (SMP) (5150-4780 AEC) (Binder et al., 2017, 2022a).

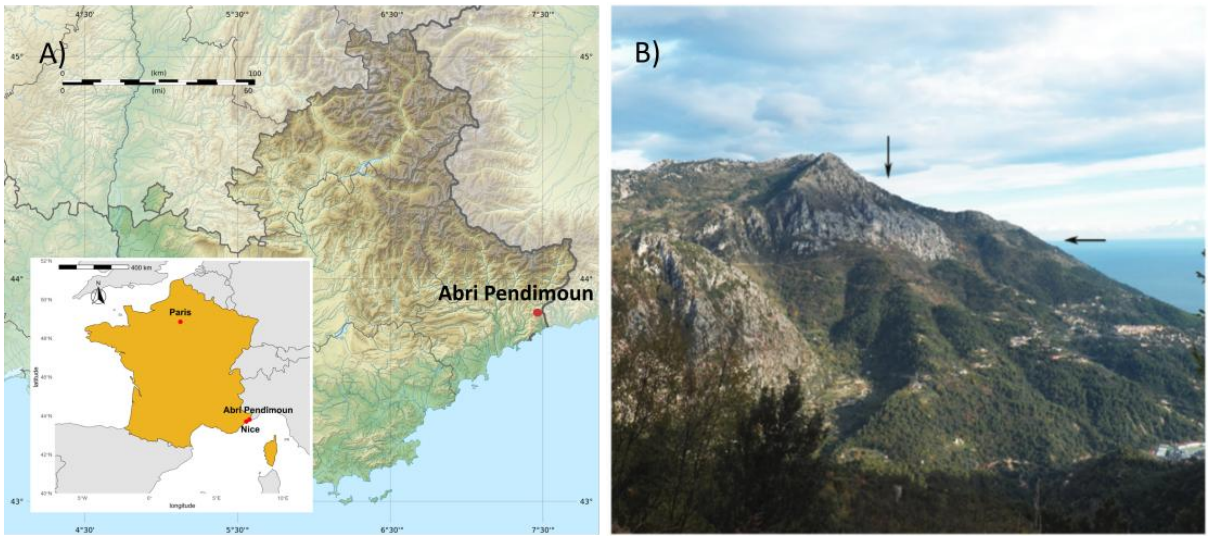


Figure 23. Location of Pendimoun rock-shelter (A) and surrounding landscape (B). View from the west; arrows indicate the shelter's position at the point of intersection. Map (A) generated using geographic data sourced from the rnaturalearth package (Massicotte and South, 2023) and adapted from (Bok1982., 2009). Image (B) from Binder *et al.* (Binder et al., 2020; Delhon et al., 2020; Drieu et al., 2021), (© J.V. Pradeau).

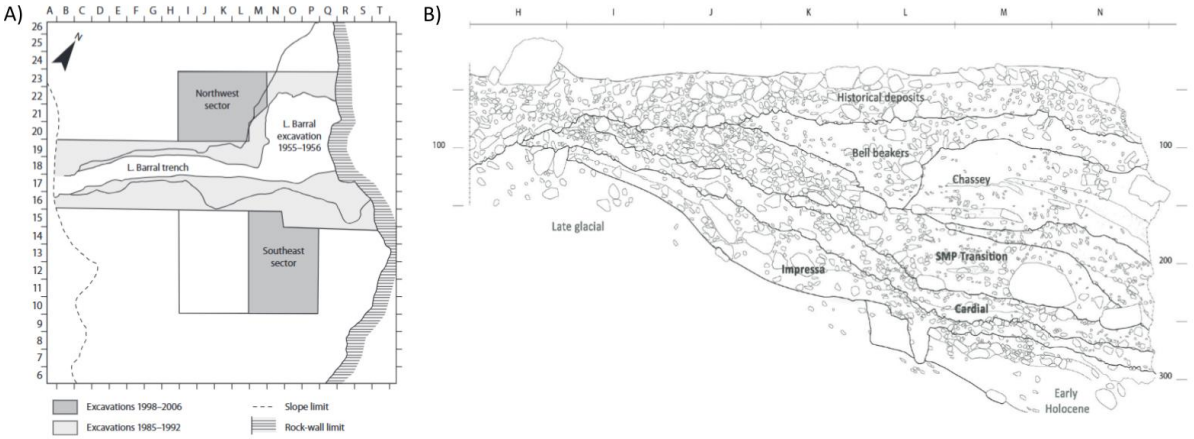


Figure 24. Pendimoun rock-shelter excavations: (A) map of successive operations, from Binder *et al.* (Binder et al., 2014), and (B) stratigraphic profile of northern sector, from Binder *et al.* (Binder et al., 2020; Delhon et al., 2020; Drieu et al., 2021).

The subsistence at Pendimoun was based on small-scale livestock and agricultural production. Despite the scarcity of remains, analysis of the **faunal assemblage** across the Impressa and Cardial phases reveals a clear predominance of domestic species, with caprines constituting the primary component of the local economy. Sheep (*Ovis aries*) were more prevalent than goats (*Capra hircus*), and their exploitation were likely on a seasonal basis, reinforcing the site's function within a mobile or semi-sedentary herding framework (Binder et al., 2020; Delhon et al., 2020; Drieu et al., 2021). While direct evidence of dairy exploitation is absent in the Impressa or early Cardial layers, the presence of goats implies potential secondary product use, particularly milk, which become increasingly plausible

as herd management strategies diversified during the early SMP phase (Rowley-Conwy et al., 2013). This shift is reflected in slaughter patterns indicating a primary focus on meat production, alongside the retention of older individuals likely associated with emerging strategies for milk and fleece exploitation (Binder et al., 2020). In addition to caprines, cattle (*Bos taurus*) and suids (*Sus sp.*) were also present, although the distinction between wild and domestic species remains ambiguous, rendering their specific role within the subsistence system uncertain (Rowley-Conwy et al., 2013; Binder et al., 2020). Hunting activities played a minor role, primarily targeting wild ruminants such as deer, alongside small mammals, including wild cats, hare, foxes (Binder et al., 1993; Rowley-Conwy et al., 2013). Complementing this terrestrial exploitation, marine resources were integrated into the Impressa and Cardial subsistence model, as evidenced by the procurement of shellfish, indicating an adaptive coastal resource exploitation strategy (Binder et al., 1993; Rowley-Conwy et al., 2013).

Agricultural production at the site was primarily based on a diversified assemblage of cereal crops. The principal cultivated species included naked barley (*Hordeum vulgare var. nudum*), emmer (*Triticum dicoccum*), and einkorn (*Triticum monococcum*), with hulled wheat present in smaller proportions. This crop composition aligns broadly with the typical spectra associated with Neolithic Impressa cultural groups in the western Mediterranean (Binder et al., 1993, 2020). Notably, the presence of hulled wheat chaff, alongside a substantial concentration of husk phytoliths, provides compelling archaeobotanical evidence for the local processing of glume wheats. These indicators point to on-site dehusking activities, reflecting a structured post-harvest processing sequence. This practice appears particularly characteristic of the Impressa phase, with a marked decline observed in the subsequent phases (Delhon et al., 2020). While evidence for cultivated plants beyond cereals remains limited, with only a few pulse remains recovered, numerous seeds from wild herbaceous plants were identified in both Impressa and Cardial layers (Binder et al., 2020). Among these, wild Poaceae species were particularly abundant, highlighting their ecological significance within the local environment as important forage resources for animals rather than as a direct target of human exploitation (Delhon et al., 2020). Wild fruits are also well represented in the assemblage and appear to have constituted a notable component of plant-based subsistence strategies. Hazelnuts (*Corylus avellana*), likely gathered for consumption, are more frequently encountered in Cardial contexts than in the earlier phases. Particularly noteworthy is the presence of carbonised acorns, which may indicate sustained or even specialised processing activities like gathering, drying, and roasting, associated with acorn consumption (Binder et al., 2020; Delhon et al., 2020). Combined with these observations, isotopic and modelling data indicate that acorns likely contributed substantially to the local diet (Gavériaux et al., 2022). Local vegetation zones provided the primary source of firewood, dominated by deciduous oaks (*Quercus sp.*), which were likely collected in a non-selective manner. Complementing these were species characteristic of open and transitional habitats, which also contributed to the fuel assemblage, reflecting a

comprehensive exploitation of the diverse wood resources available within the surrounding environment (Battentier et al., 2015).

The **ceramic assemblage** at the site of Pendimoun exhibits considerable variability in shape, volume, and decorative techniques, reflecting a functional diversity and a clear distinction among Impressa, Cardial, and SMP traditions. Impressa ceramics were produced using a variety of clay pastes, including local glauconitic clays and granitic clays from distant locations, implying the existence of long-distance material procurement networks (Basso et al., 2006; Gabriele et al., 2022; Lardeaux et al., 2022). While Impressa vessels display a wide range of morphological and dimensional variability, they are generally characterised by open forms such as spheroid, cylindrical, and open conical shapes (Figure 25, A). Of particular interest is the uniformity in construction technique across the assemblage. All vessels, regardless of size, form, or clay type, are characterised by the spiral patchwork manufacturing method, specific to the Tyrrhenian area. This technique involves the formation of circular patches from spiral-wound clay coils, which were then juxtaposed and fused to construct the vessel walls (Drieu et al., 2021; Gomart et al., 2017, 2022). Functionally, the assemblage includes vessels likely used for drawing or pouring liquids, alongside larger jars with straight walls intended for storage (Binder and Sénépart, 2010). Decorative motifs are particularly frequent on flat-based vessels and were applied using small tools, including fingernails and marine shells, through impression, incision, and pinching. These are typically organised in horizontal bands and, in some cases, arranged in the form of decorative panels (Binder et al., 1993; Binder and Sénépart, 2010; Cassard et al., 2020; Cassard, 2020). In contrast, Cardial ceramics encompass a variety of vessel forms, including bowls, pots, cooking vessels, and jars. These typically featured rounded bases and straight or slightly inward-sloping walls, with neck morphology varying across examples (Figure 25, B) (Binder and Sénépart, 2010; Cassard, 2020). Decoration is predominantly executed through impressions made with *Cardium* shells, generally applied in their natural orientation. The decorative repertoire is characterised by horizontal band constructions featuring cords and panels of short parallel bands (Binder and Sénépart, 2010). Quadrilobed rims, particularly evident on cooking pots and bowls, are a hallmark of the initial phase of the SMP culture. This morphological trait marks a clear formal innovation and serves as a diagnostic indicator of the emergence and regional development of the SMP horizon (Binder and Sénépart, 2010). Recent lipid analysis on Impressa and Cardial ceramic vessels have provided critical insight into their functional roles, revealing a marked correlation between vessel capacity and lipid yield that suggests differentiated usage patterns (Drieu et al., 2021). Small-capacity vessels consistently exhibit high lipid concentrations, indicative of their use in cooking or processing lipid-rich substances, whereas larger vessels display significantly lower lipid residues, supporting their proposed functions in storage or serving. The variability in vessel shape and volume further underscores the functional diversity of the assemblage, reflecting a broad spectrum of culinary and storage practices.

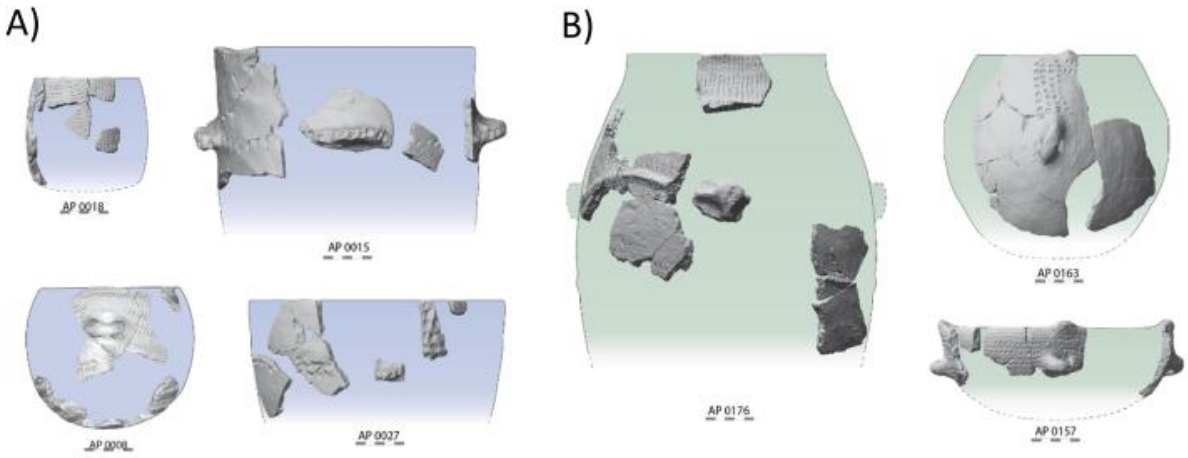


Figure 25. Representative pottery forms from Pendimoun rock-shelter. (A) Impressa phase; (B) Cardial phase. Reconstructions based on 3D scan. Adapted from Drieu *et al*. (Drieu et al., 2021).

The limited availability of local flint necessitated the importation of lithic raw blanks which were then transformed into **tools** on-site (Binder et al., 2022b). During the Impressa period, the majority of the knapped tools were used for plant processing, though only a few were associated with cereal harvesting. Lithic production and use patterns indicate a clear preference for blades and bladelets, particularly for the manufacture of awls used on wood and hide, as well as for sickle elements. Many of these implements were later recycled, retouched, and adapted for secondary functions, reflecting both technological versatility and adaptive tool curation. This pattern also suggests a careful management of resources and the possible use of alternative harvesting methods such as hand collection or uprooting (De Stefanis, 2018; Binder et al., 2020). In contrast, the Cardial period assemblage shows a marked decrease in the production of blades and bladelets, accompanied by a higher frequency of sickle elements and no evidence of post-use recycling, likely reflecting both a more systematic approach to harvesting and increased access to locally suitable flint for flake production (De Stefanis, 2018; Binder et al., 2020). Additionally, the presence of a limited number of grinding tools reveal the practice of plant processing, albeit suggesting the handling of only small quantities of grain (Binder et al., 2020). Other lithic materials, notably heat-altered stones (HAS), were identified within firing structures all along the Neolithic sequence and notably within the formative stage of the SMP culture (Figure 26). In this context, a couple of structures are of special interest, due to the great differences in their building. The "fireplace structure" (14647) provided clear evidence of in situ combustion, with stones exhibiting fire-induced fragmentation but remaining largely in place. In contrast, the "cooking place" (14549) consisted of a shallow pit filled with stones that had been heated prior to deposition. Archaeomagnetic analysis of the fireplace revealed uneven heat distribution, with the most intensely heated stones at the centre, and minimal evidence of post-combustion displacement, suggesting limited reuse (Genevey - unpublished report). Petrographic examination of HAS from the fireplace further documented thermal

shock features, including fractures, which were absent in the HAS recovered from the cooking place (Cardelli, 2013).

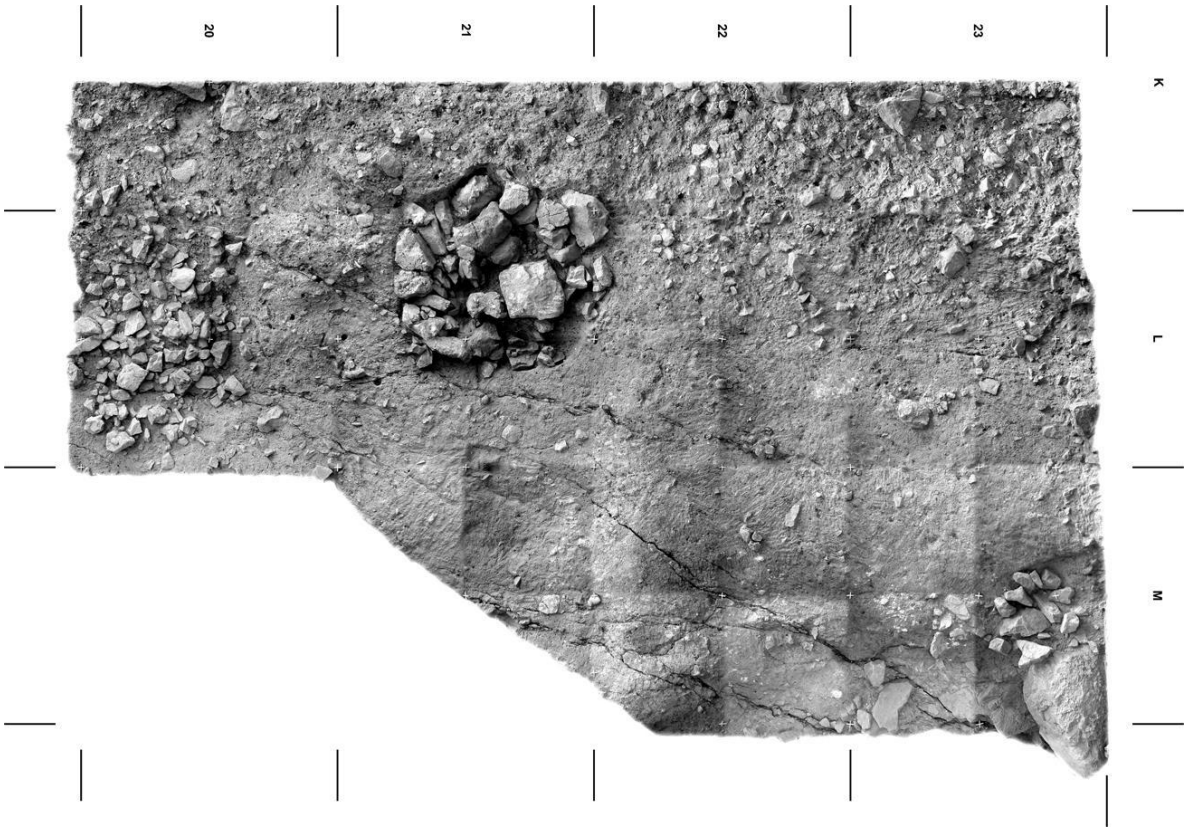


Figure 26. Partial digital map of Pendimoun sector North during Phase 3 (5100-4790 BCE) showing the location of firing structures 14549 (cooking place; L20) and 14647 (fireplace; L21).

5. Methodology

This chapter outlines the multidisciplinary methodological framework designed to address the central research aims concerning heated-altered stones (HAS) in prehistoric contexts. The study focuses on four primary objectives: documenting the distribution of HAS across diverse chronological, geographic, and cultural settings in prehistoric archaeology; identifying and characterising thermal alteration patterns on HAS from key Neolithic sites in southwestern Europe; assessing the potential of HAS to preserve molecular evidence of past culinary practices; and comparing the molecular fingerprints of HAS with those of associated ceramic vessels to explore possible correlations in food processing activities. To achieve these objectives, the research design integrates multiple complementary approaches. A systematic literature review was conducted to establish a broad contextual understanding of HAS and their archaeological significance (see Chapter 2). In parallel, macroscopic and digital analyses were carried out on selected artefacts from the Neolithic sites of La Draga (Spain) and Pendimoun (France) to identify evidence of heat exposure. Visual inspection was complemented by 3D scanning and photogrammetry, allowing for detailed documentation and the creation of a digital reference archive to support future research and heritage initiatives. To further investigate the potential of HAS as archives of ancient culinary practices, molecular and isotopic analyses were carried out on lipid residues extracted from selected HAS. Gas chromatography-mass spectrometry (GC-MS) was used to identify food-derived lipid biomarkers, while carbon stable isotope analysis provided insight into the origins and processing of organic materials. These results were interpreted alongside lipid profiles obtained from associated sediment samples to explore environmental and contextual influences. While protein analysis was attempted, it did not yield significant results and was not pursued further. Finally, molecular analysis compared lipid residues from HAS across sites and with those from associated ceramics to explore dietary patterns, resource use, and the potential role of HAS in food preparation. Collectively, these methodological approaches form an integrated strategy that connects physical, chemical, and contextual evidence to address the research questions. The following sections describe each method in detail, outlining procedures and the analytical tools applied throughout the investigation.

5.1. Archaeological sample selection criteria

Lithic samples were collected from both sites, but sampling strategies differed considerably due to variations in sample availability, site-specific conditions, and prior research. For instance, while HAS from La Draga had not been previously analysed, those from Pendimoun had undergone prior investigations, including petrographic and archaeomagnetic analyses. These HAS were sectioned for thin-section preparation, a process that may have altered their surface characteristics but yielded valuable insights into their mineralogical composition. Additionally, post-excavation handling practices

differed between the two sites. La Draga HAS recovered during the 2010–2011 excavations exhibited limitations in data quality, including missing contextual information on associated structures and sediment samples, which complicates the reconstruction of their original depositional environment. Sample storage methods also varied slightly: at both sites, HAS were stored in plastic bags, potentially exposing surfaces to plasticisers. However, at La Draga, some samples were additionally wrapped in aluminium foil due to the possible presence of combustion residues observed during fieldwork, a practice that may have helped mitigate contamination. These differences underscore the importance of standardised post-excavation protocols to minimise alterations that could affect analytical outcomes. Variations in storage conditions, coupled with inconsistencies in documentation and handling, may introduce biases that compromise the reliability of comparative studies. Acknowledging these disparities in sampling and handling strategies is crucial for ensuring dataset comparability, not only within lithic assemblages, but also in relation to other lines of evidence, such as lipid residue analyses on ceramics or studies of plant and faunal remains.

5.1.1. La Draga

The lithic selection for this study was made from a substantial assemblage accumulated over multiple excavation campaigns at the Neolithic site of La Draga. This collection comprises thousands of artifacts recovered from various stratigraphic contexts and currently stored at the *Institución Milà i Fontanals* (IMF-CSIC) in Barcelona, Spain. These lithics initially attracted attention during fieldwork due to its anthropogenic presence in the site, their spatial association with combustion structures or the presence of macroscopic features indicative of thermal alteration or other peculiar surface characteristics, such as potential organic residues. Following recovery, all artefacts were stored at room temperature in plastic bags, with some wrapped in aluminium foil to preserve potential organic residues observed during excavation (Figure 27). This preservation strategy was employed to minimise contamination and protect surface features pending further analysis. From the broader assemblage, a total of fifteen HAS were selected for this study (Table 4). These comprised 9 sandstones, 2 limestones, 2 marl and 2 volcanic stones (Annex 4). The selection criteria were based on macroscopic features that could indicate exposure to heat and potential involvement in culinary or combustion-related activities. Key indicators included thermal alterations, such as cracking, fractures and surface discoloration, along with surface deposits that could suggest organic accumulation. The selected HAS derived from distinct depositional contexts, including combustion structures (E266, E269) and scattered deposits. Some HAS were found within clearly defined hearth features, indicating direct association with fire-related activities, while others were recovered across distinct stratigraphic layers, potentially reflecting secondary deposition or post-depositional movement within the site.

In parallel, nine sediment samples were collected as contextual samples to assess potential environmental contamination and to serve as a reference for identifying endogenous and exogenous organic residues (Figure 28; Table 4). These sediment samples were strategically chosen from those taken regularly per square metre and preserved in cold storage from areas adjacent to the HAS to account for potential variations in organic residue deposition. Following collection, all sediment samples were stored under refrigeration (4 °C) in plastic bags within the Prehistoric laboratory repository (UAB) in Barcelona, until analysis.

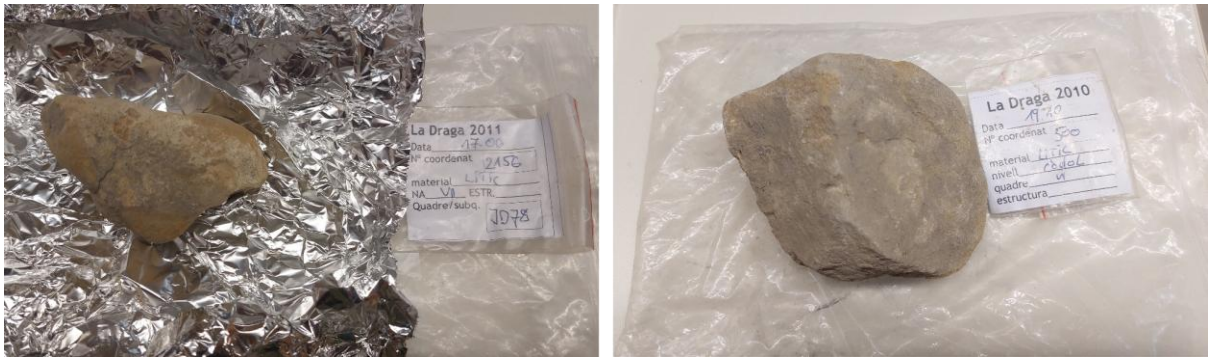


Figure 27. Examples of HAS from La Draga.

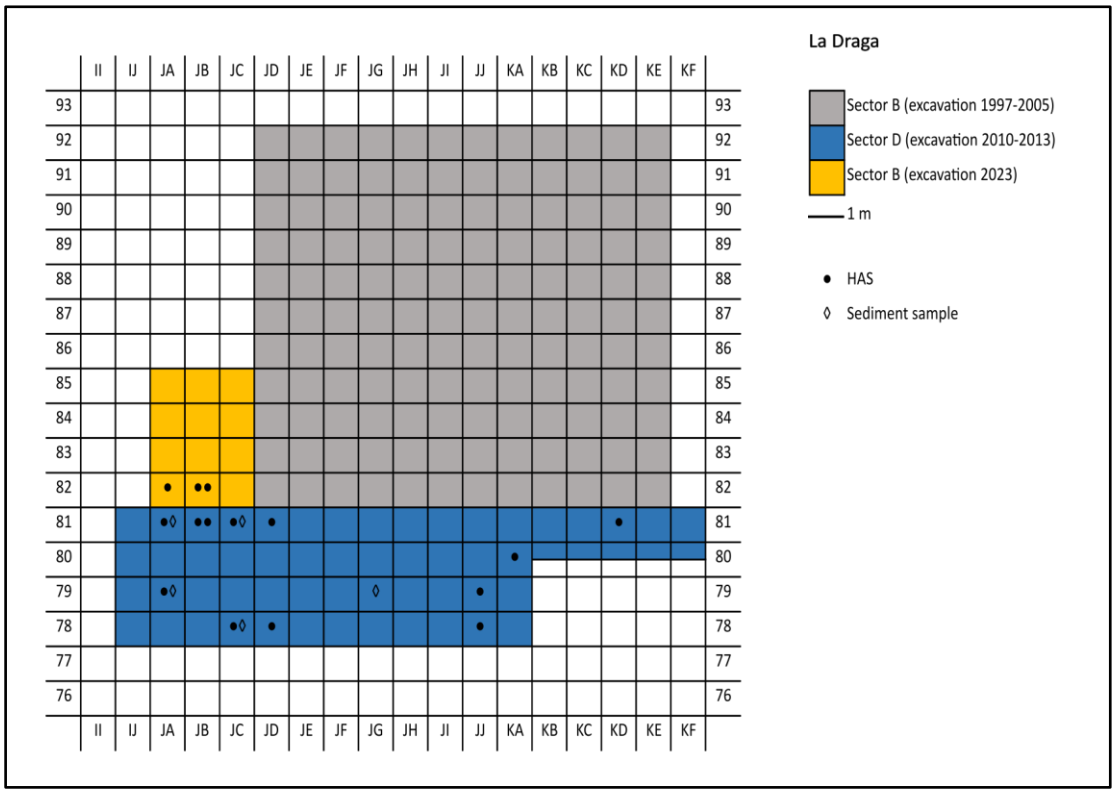


Figure 28. Grid of sectors B/D at La Draga showing the location of HAS and associated sediment sampling points.

To ensure proper handling and minimise contamination risks, nitrile gloves were worn at all times during selection, packaging, and transportation of the samples. This prevented direct contact with

the stones and sediments, reducing the possibility of introducing modern organic residues such as skin lipids, sweat, and other contaminants that could interfere with subsequent molecular analyses. After selection, all the samples were carefully rewrapped in new aluminium foil to provide cross-contamination and environmental exposure. Once wrapped, the samples were placed in labelled plastic bags and prepared for transport. Additionally, the samples were transferred to the UAB for further analysis.

To better contextualise HAS and sediments samples in Sectors D and B, additional stratigraphic information is provided. Excavation of Sector D at La Draga revealed a sequence of stratigraphic levels (0-IX) (Palomo et al., 2014), with the samples analysed in this study originating from Level VI and VII. Level VI is a compact, clay-rich deposit containing occasional small stones and fragmented organic material. Within this layer, travertine blocks are deliberately arranged to form a paved surface extending across the excavated area, interpreted as a constructed floor associated with human activity. This level belongs to the more recent occupation phase which is characterised by the use of travertine blocks for paving. In contrast, Level VII comprises timber from the collapse of wooden structures, distributed across almost the entire excavated area, and represents the oldest occupation phase at the site. Similarly, excavation of Sector B revealed multiple stratigraphic levels (Piqué et al., 2023), including Level VII-0, a partially excavated portion of Level VII. This level is interpreted as reflecting the abandonment phase of the wooden structures in the 1st occupation phase.

Table 4. List of HAS and sediment samples from La Draga selected for this study.

Sample	*Excavation Year*	*Sample ID*	*Sector*	*Stratigraphic context*	*Feature*	*Grid*	*Occupation*
HAS	2010	500	D	Level VI		KA80	more recent
HAS	2010	518	D	Level VI		KD81	more recent
HAS	2010	663	D	Level VII		JJ78	oldest
HAS	2010	833	D	Level VII		JJ79	oldest
HAS	2011	1540	D	Level VI		JD81	more recent
HAS	2011	1547	D	Level VIa		JB81	oldest
HAS	2011	1987	D	Level VIa		JB81	more recent
HAS	2011	2156	D	Level VII		JD78	oldest
HAS	2012	3791	D	Level VII		JC81	oldest
HAS	2012	3951	D	Level VIa		JA81	more recent
HAS	2012	4007	D	Level VIa		JA79	more recent
HAS	2012	4035	D	Level VIa		JC78	more recent
HAS	2023	25300	B		Structure E266	JA82	oldest
HAS	2023	25396	B	Level VII-0	Structure E269	JB82	oldest
HAS	2023	25430	B	Level VII-0	Structure E269	JB82	oldest
Sediment	2012	JC78-VIa	D	Level VIa		JC78	more recent
Sediment	2012	JA81-VIa b	D	Level VIa		JA81	more recent
Sediment	2012	JA81-VIa g	D	Level VIa		JA81	more recent
Sediment	2012	JA81-VIa n	D	Level VIa		JA81	more recent
Sediment	2012	JA79-VIa b	D	Level VIa		JA79	more recent
Sediment	2012	JA79-VIa g	D	Level VIa		JA79	more recent
Sediment	2012	JA79-VIa n	D	Level VIa		JA79	more recent
Sediment	2012	JC81-VII	D	Level VII		JC81	oldest
Sediment	2012	JG79-VII	D	Level VII		JG79	oldest

5.1.2. Pendimoun

At Pendimoun, HAS were systematically sampled from 1997 to 2006 within structures and scattering of remains. The present study is focusing on two distinct structures identified within the initial Square Mouthed Pottery deposits: a fireplace (structure 14549) and a cooking place (structure 14647). The fireplace structure exhibited evidence of *in-situ* combustion, with lithics fragmented by the action of fire but not displaced, while the cooking place consisted of a basin filled with previously heated stones, suggesting a different functional use. Archaeomagnetic analysis conducted on the fireplace structure revealed an uneven heat distribution, with the most intensely heated stones at the centre, and minimal evidence of post-combustion displacement, indicating limited reuse of the feature (Genevey - unpublished report). Petrographic analysis further supported these findings, identifying thermal shock

indicators such as fractures in the HAS from the fireplace, while such features were notably absent in samples from the cooking place (Cardelli, 2013). Following petrographic examinations, all lithics were stored at room temperature in plastic bags within the CEPAM laboratory repository (UniCA) in Nice, France. From the broader assemblage, a total of nineteen HAS were selected for this study, including 8 from the fireplace (FP-14549) and 11 from the cooking place (CP-14647) (Table 5). These comprised 18 limestones and 1 detrital carbonate rock (Annex 4). As a result of prior petrographic analysis these specimens were already sectioned into smaller fragments to obtain thin-sections (Figure 29). The selection criteria for this study were based on macroscopic features suggestive of exposure to heat and potential involvement in culinary or combustion activities. Key diagnostic traits included thermal alterations, such as cracking, fractures and surface discoloration, along with deposits that could indicate organic accumulation.

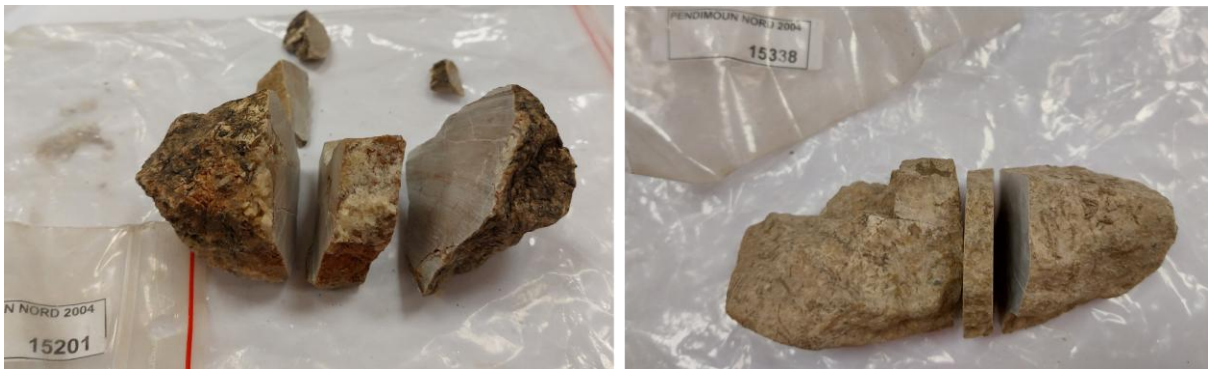


Figure 29. Examples of HAS from Pendimoun, already sectioned into smaller fragments for petrographic analysis.

In parallel, six sediment samples were collected as contextual samples to assess potential environmental contamination and to serve as a reference for identifying endogenous and exogenous organic residues (Table 5). These sediments were strategically taken from the filling of each structure and from adjacent stratigraphic units to account for potential variations in organic residue deposition. The collected sediments differ in origin between the two structures: in CP, the samples come from deposits that formed slightly after the use of the feature, whereas in FP, originates from plant and wood combustion and is directly related to the functioning of the structure. In total, one sediment sample was taken from ashes in section M21, three were collected from the cooking place area in section L20, and two from the fireplace area in L21 (Figure 30). Following collection, all sediment samples were stored in plastic bags at room temperature within the CEPAM laboratory repository (UniCA) in Nice, until analysis.

To ensure proper handling and minimise contamination risks, nitrile gloves were worn at all times during selection, packaging, and transportation of the samples. This prevented direct contact with the stones and sediments, reducing the possibility of introducing more modern organic residues such as

skin lipids, sweat, and other contaminants that could interfere with subsequent molecular analyses. After selection, all the samples were carefully rewrapped in new aluminium foil to provide cross-contamination and environmental exposure. Once wrapped, the samples were placed in labelled plastic bags and prepared for transport. Additionally, the samples were transferred to the UAB for further analysis.

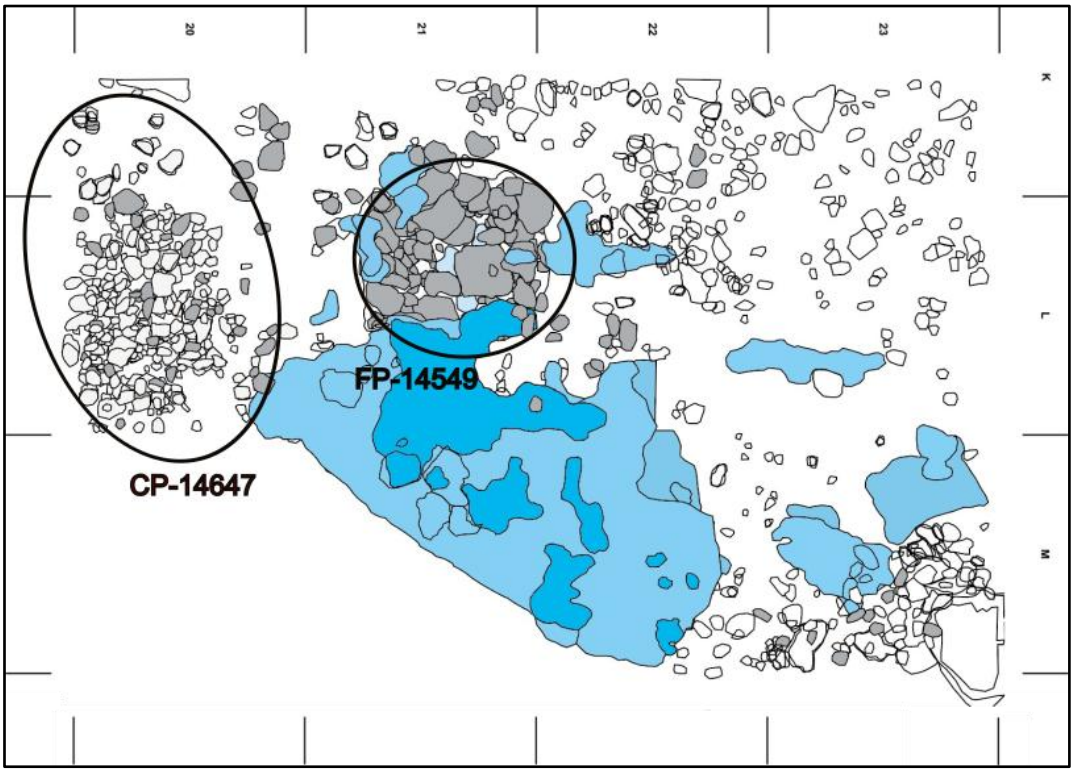


Figure 30. Partial map of Pendimoun sector North during Phase 3 (5100-4790 BCE) showing the location of structure FP-14549 (L20) and CP-14647 (L21). Ashes (including burned manure) are shown in blue, while burned stones are in grey.

Table 5. List of HAS and sediment samples from Pendimoun selected for this study.

Sample	*Excavation year*	*Sample ID*	*Stratigraphic context*	*Feature*	*Grid*	*Occupation*
HAS	2004	15250	US 14647	Cooking place	L20	Phase 3
HAS	2004	15252	US 14647	Cooking place	L20	Phase 3
HAS	2004	15329	US 14647	Cooking place	L20	Phase 3
HAS	2004	15337	US 14647	Cooking place	L20	Phase 3
HAS	2004	15338	US 14647	Cooking place	L20	Phase 3
HAS	2004	15348	US 14647	Cooking place	L20	Phase 3
HAS	2004	15355	US 14647	Cooking place	L20	Phase 3
HAS	2004	15413	US 14647	Cooking place	L20	Phase 3
HAS	2004	15419	US 14647	Cooking place	L20	Phase 3
HAS	2004	15431	US 14647	Cooking place	L20	Phase 3
HAS	2004	15433	US 14647	Cooking place	L20	Phase 3
HAS	2004	15197	US 14549	Fireplace	L21	Phase 3
HAS	2004	15199	US 14549	Fireplace	L21	Phase 3
HAS	2004	15201	US 14549	Fireplace	L21	Phase 3
HAS	2004	15203	US 14549	Fireplace	L21	Phase 3
HAS	2004	15219	US 14549	Fireplace	L21	Phase 3
HAS	2004	15225	US 14549	Fireplace	L21	Phase 3
HAS	2004	15297	US 14549	Fireplace	L21	Phase 3
HAS	2004	15398	US 14549	Fireplace	L21	Phase 3
Sediment	2004	S14466	US 14438	White ashes	M21	Phase 3
Sediment	2004	S15367	US 14647	Cooking place	L20	Phase 3
Sediment	2004	S15373	US 14647	Cooking place	L20	Phase 3
Sediment	2004	S15442	US 14647	Cooking place	L20	Phase 3
Sediment	2004	S14865	US 14549	Fireplace	L21	Phase 3
Sediment	2004	S15396	US 14549	Fireplace	L21	Phase 3

5.2. Visual inspection

As an initial screening step, a morphological analysis was conducted to identify potential heat-induced alterations on selected HAS and to assess their relevance to Neolithic combustion or cooking contexts. This phase focused on macroscopic examination, aiming to record and document key surface features that may be associated with thermal exposure or interaction with organic materials.

By systematically examining the physical characteristics of each lithic sample, this study sought to establish diagnostic criteria for recognising HAS in archaeological contexts. Key attributes such as cracks, fractures, discoloration, sooting, and superficial deposits were carefully noted, as these are commonly recognised markers of heat exposure and interaction with combusted materials. In particular,

cracks and fractures can result from thermal stress causing expansion and contraction of the stone material, while discoloration and sooting typically reflect exposure to fire or smoke (Pagoulatos, 2005; Homsey, 2009; Bentsen and Wurz, 2019). Discoloration appears as subtle changes in the stone's natural colour, often reddish, greyish, or yellowish, due to heat-induced mineral alteration, whereas sooting forms a dark coating from deposited carbon particles (Neubauer, 2018). Surface deposits were also recorded given their potential links to food preparation, processing, or other functional uses of the stones (Thoms et al., 2015). To complement the qualitative observations, precise metric measurements were taken for each sample, including length, width, thickness, and weight. These quantitative data provide additional parameters to characterise the stones and facilitate comparison across samples and sites. This morphological approach was grounded in a framework developed from previous studies that have identified reliable visual and textural criteria for detecting thermal alterations on lithic artefacts (Custer, 2017; Neubauer, 2018, 2024).

All observations and measurements were systematically recorded in a comprehensive database, which integrated morphological data with contextual information derived from excavation records, including stratigraphic provenance, site location, and associated artefact assemblages. This integrated dataset served as the foundation for guiding subsequent analytical stages, ensuring a multidisciplinary approach and a contextualised interpretation of HAS. Furthermore, the database supports ongoing comparative research by providing a structured repository of detailed morphological characteristics linked to well-documented archaeological contexts.

5.3. 3D model acquisition

To preserve the original shape and surface characteristics of each HAS before implementing any invasive techniques, high-resolution 3D models were generated for all the selected samples. This approach was essential to ensure that detailed morphological and textural information was retained, allowing for further analysis and comparison even after the lithics had been altered through sectioning or sampling. The generation of 3D models serves multiple purposes within the research framework. Firstly, it provides an accurate digital replica of each artefact, capturing surface features such as cracking, sooting, or residue patterns that are relevant for interpreting thermal exposure and use-wear. Secondly, it supports long-term conservation and data accessibility by enabling digital archiving of the collection. These models allow researchers to revisit, measure, and reassess the artefacts remotely, reducing the need for repeated physical handling and thereby minimising the risk of damage to the original materials. The 3D documentation process was conducted in collaboration with OpenLab UAB, which provided both access to specialised equipment and technical training in 3D scanning methodologies. The training covered all stages of the digitisation workflow, including data acquisition using structured light scanning systems, post-processing of raw scan data, and optimisation of digital

models for accuracy, resolution, and file management. This digital archive not only enhances the reproducibility and transparency of the study but also contributes to broader heritage dissemination initiatives. By making selected models available for future research and educational purposes, the project supports open-access archaeological data sharing and promotes the integration of digital tools in archaeological analysis and conservation.

Two distinct 3D scanners were utilised based on the dimensions of the samples, both employing high precision 3D scanning technology, white light (LED) and achieving a measurement rate of 550,000 measurements per second. The CREAFORM GO!SCAN 20 proved suitable for objects ranging from 0.05 to 0.5 metres. This scanner exhibited a resolution of 0.100 mm, an accuracy of up to 0.100 mm, and a volumetric accuracy of 0.300 mm/m. In contrast, the CREAFORM GO!SCAN 50 is designed for objects ranging from 0.3 to 3.0 metres. This scanner featured a resolution of 0.500 mm, an accuracy of up to 0.100 mm, and a volumetric accuracy of 0.300 mm/m. The models were then processed and acquired in ASCII STL and Wavefront formats through VXelements software (Figure 31-A,B).

Photogrammetry technology was employed to capture detailed surface features of samples exhibiting specific characteristics such as fractures, cracks, discoloration, or blackening, all of which could be indicative of heat alteration or fire exposure. The photogrammetry equipment utilised comprised a Canon 77D-24,2MP camera equipped with a macro lens (35mm) and a zoom lens (15-85mm). To perform the imaging process, additional accessories such as a light table, a revolving platform, and a portable studio were employed. Subsequently, the acquired images were processed and converted into Wavefront format using Agisoft Metashape software (Figure 31-C,D).

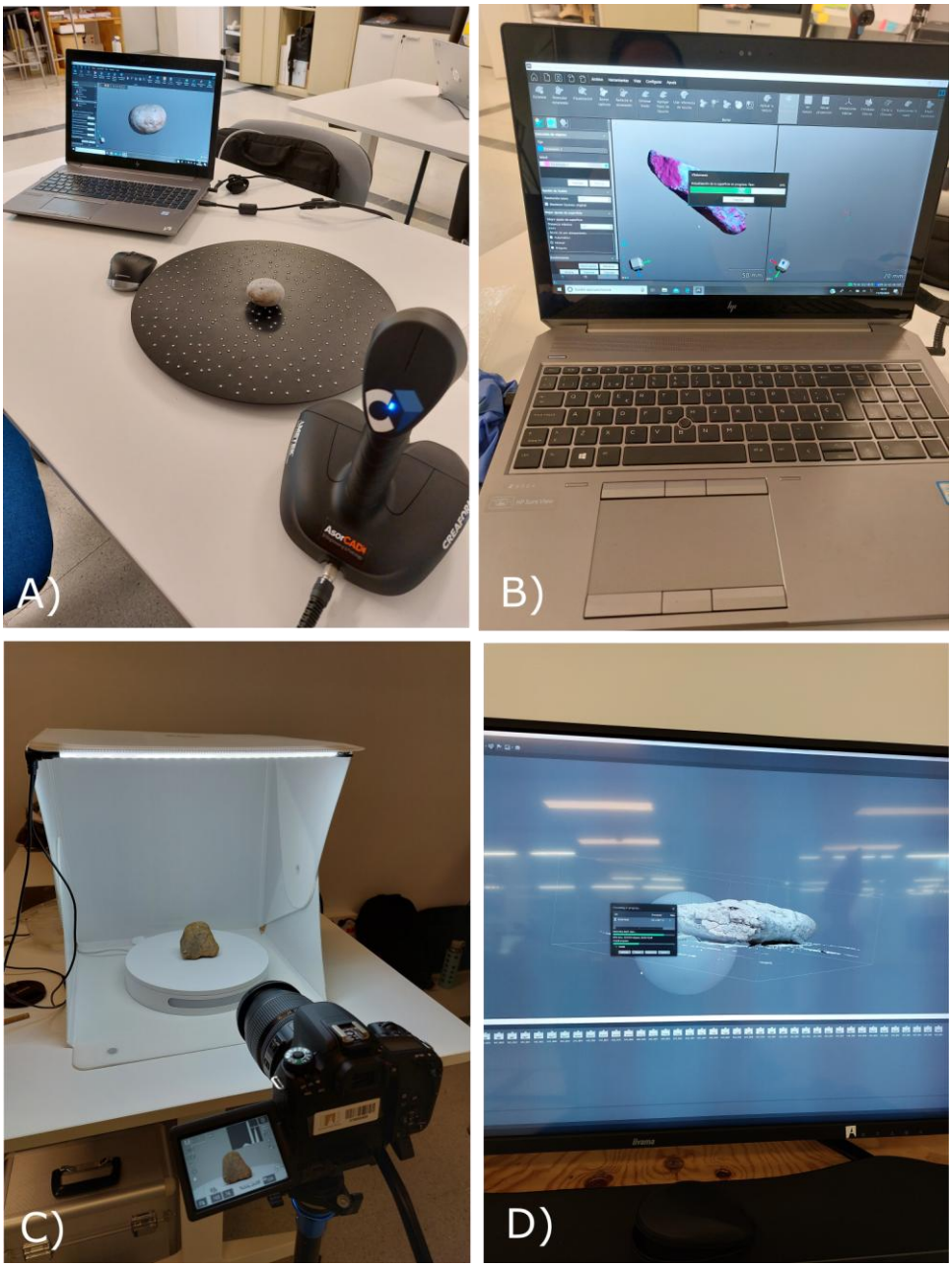


Figure 31. Workflow for the creation of 3D models of selected HAS at OpenLab UAB. (A) Laser scanning equipment used for high-resolution surface capture; (B) Model processing using VXelements software; (C) Photogrammetry setup for image acquisition; (D) Photogrammetric modelling and reconstruction in Agisoft Metashape software.

5.4. Lipid residue analysis

Given the absence of a standardised procedure for sampling and extracting residue from lithics, this study adapted well-established protocols traditionally employed for lipid analysis of ceramic vessels (Correa-Ascencio and Evershed, 2014; Drieu et al., 2021; Lundy et al., 2023). These protocols, widely validated in archaeological science, provided a reliable and reproducible framework for the

extraction of lipid biomarkers. By applying these techniques to HAS, the study aimed to assess their potential as alternative substrates for reconstructing past culinary practices and food-related activities. In accordance with the mentioned approaches, approximately 1 g of stone powder was collected from each sample using a hand-held drill with carbide/diamond bits, at the time of each extraction (Figure 32). Since two distinct extraction methods were to be performed at different times (see details below), samples were collected independently for each method. To assess the extent of lipid absorption and retention on stones, we conducted analyses on two sequential layers from the same area. Unlike standard ceramic sampling protocols, we collected the outermost layer of the stone (external; e) without discarding any superficial material. From the same location, we then collected a second sample a few millimetres beneath the surface (internal; i), to evaluate lipid penetration (Figure 33). In addition, any observed amorphous deposits adhering to the surface (deposit; d) were collected for analysis. For comparison, approximately 1g of dry contextual sediment from each of the sedimentary samples was also collected and analysed for lipid composition.



Figure 32. Drilling of a heat-altered stone (HAS) using a hand-held drill with carbide/diamond bit for sample collection.

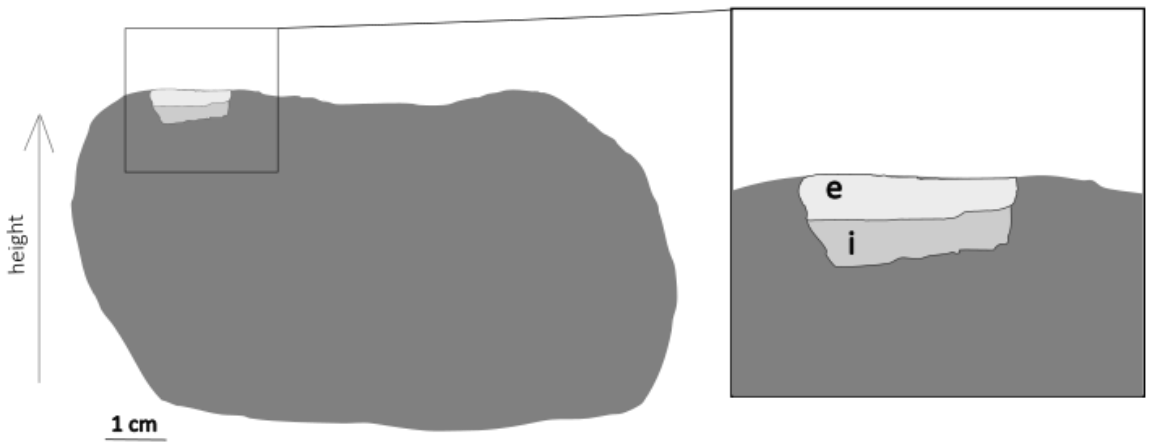


Figure 33. Schematic representation of HAS showing the sampling spots: external (e), taken from the outermost surface, and internal (i), collected a few millimetres beneath the same location to assess lipid penetration.

To ensure the reliability of molecular residue analysis and prevent modern contamination, strict handling and cleaning protocols were followed. Nitrile gloves were worn at all times during handling, drilling and lipid extraction processes. Before use, each drill bit was rinsed with ethanol to remove any residual contamination. After drilling, bits were cleaned in an ultrasonic bath containing a mixture of dichloromethane (DCM) and methanol (MeOH) (2:1, v/v) for at least 15 minutes to dissolve any organic residues. Once cleaned, the bits were wrapped in aluminium foil to prevent exposure to contaminants. Additionally, fresh drill bits were used for each sample to ensure no cross-contamination. After drilling, the resulting powdered samples were carefully transferred to pre-cleaned glass Hach tubes for weighing and further processing. All glassware used at ICTA-UAB was cleaned with specific-grade cleaners or solvents and/or heated in a muffle kiln at 450°C to ensure complete sterilisation.

To achieve a comprehensive molecular characterization of the lipid residues, two complementary extraction methods were applied to all samples (see Chapter 3.1.1). In the first one, an **acidified methanol extraction (AE)** method was applied to all samples. In brief, a mixture of methanol (4 ml) and sulfuric acid (800 µl) was added to one gram of sample, along with an internal standard (10 µl of *n*-alkane C_{34}), and heated at 70°C for 4 hours. Given that some samples originate from carbonatic-rich matrices, the pH was checked to ensure it was maintained in the acidic range before proceeding with centrifugation, as these materials can neutralise the acid during extraction. After centrifugation, the resulting supernatant was carefully extracted and transferred to a labelled glass tube. A 2 ml of *n*-hexane was added, and the supernatant removed and passed through a filter pipette with potassium carbonate (K_2CO_3). This process was repeated three times. Subsequently, the samples were dried under a gentle stream of nitrogen, resuspended in *n*-hexane, and transferred to an auto-sampling vial equipped with a micro insert. A second internal standard (10 µl of *n*-alkane C_{36}) was added before analysis by

GC techniques. An aliquot of this solution was kept for GC-C-IRMS analyses, after the removal of sulphur using activated copper. In this procedure, small copper bars were first cleaned (activated) with hydrochloric acid (HCl) and subsequently rinsed with appropriate organic solvents. These were then added to the lipid extract and allowed to react for 48 hours, during which the copper binds and removes elemental sulphur from the sample.

As the second extraction method, dichloromethane/methanol (DCM/MeOH) extraction **(SE)** was performed on all samples (1g) to check for the presence of mono-, di-, tri-acylglycerols (MAGs, DAGs, TAGs), wax esters and alkylresorcinols, compounds that are generally not efficiently released by acidified methanol extraction. Consequently, SE complemented AE ensuring a more complete and representative lipid profile. After drilling, and the addition of an internal standard (10 μg of *n*-alkane C_{34}), the samples were extracted in 10 mL of a DCM/MeOH solution (2:1, v/v) with ultrasonication (15 min). The samples were centrifuged (10 min at 3000 rpm) and the supernatants were collected. These operations were repeated twice. The combined lipid extracts were evaporated under nitrogen flow and dissolved in 500 μL of DCM/MeOH. Additionally, an aliquot of 100 μL was dried under a gentle stream of nitrogen after the addition of a second internal standard (10 μg of *n*-alkane C_{36}). The lipid extracts were derivatised with BSTFA at 70°C for 1 hour. Before the analysis on GC-FID and GC-MS, the samples were evaporated and redissolved in cyclohexane. For both AE and SE, a blank sample was added to each batch to monitor in-laboratory contamination.

A screening process was conducted using **GC** equipped with a flame ionisation detector **(FID)** for quantification and general screening of preservation using an Agilent 7820A Series gas chromatograph fitted with a DB-5MS column (15 m x 250 μm x 0.1 μm) at ICTA-UAB, in Barcelona. One microliter of the extract was injected via a splitless injector. The temperature of the column was kept at 50°C for 2 min and then increased by 6°C every minute until a final temperature of 340°C was reached and held for 19 min. Nitrogen was used as the carrier gas at a constant flow rate of 2 ml min^{-1}. The detector was kept at 340°C with hydrogen flow of 40 ml min^{-1}. This preliminary GC-FID screening enabled the evaluation of both compound identification and relative abundance prior to further analytical procedures. Identification was carried out by comparing retention times of peaks observed in the sample chromatograms with those of an analysed standard solution containing reference compounds (FAs $C_{16:0}$ and $C_{18:0}$). The lipid yield of each sample was achieved by integrating the total area of all detected compounds and normalising it against the known concentration of the *n*-alkane C_{34} internal standard. By comparing the chromatographic response of both *n*-alkane standards, the extent of lipid loss occurring throughout the extraction procedure was quantitatively assessed.

To identify molecular profiles, all acid extracts were analysed through **GC-MS**, using the GC component Agilent 7890A series attached to an MS Agilent 5975C Inert MSD detector with a quadrupole mass analyser, at ICTA-UAB, in Barcelona. The separation was performed through a DB-5MS (5%-phenyl)-methylpolysiloxane column (30 m × 0.250 mm × 0.25 μm) after the injection of one microlitre of sample via a splitless injector. The temperature of the column was kept at 50°C for 2 min and then increased by 6°C every minute until a final temperature of 320°C was reached and held for 19 min. Helium was used as the carrier gas at a constant flow rate of 2 ml min^{-1}. The spectra were obtained by scanning between m/z 50 and 550. This analytical procedure enabled the structural characterisation and identification of lipid compounds based on their mass spectral signatures and chromatographic retention times. Compounds were identified by their characteristic fragmentation patterns and specific m/z values, which serve as molecular fingerprints. Identification was further validated through comparison of established spectral libraries.

Additionally, all acid extracts were also analysed on a **DB-23** (50%-Cyanopropyl)-methylpolysiloxane column (60 m × 0.250 mm × 0.25 μm), at ICTA-UAB, to identify aquatic markers, such as isoprenoid fatty acids and ω-(o-alkylphenyl) alkanoic acids (APAAs) (Cramp and Evershed, 2014; Lucquin et al., 2016). The temperature of the oven was set at 50°C for 2 min, then increase to 100°C at 10°C min^{-1}, increase to 140°C at 4°C min^{-1}, increase to 160°C at 0.5°C min^{-1}, increase to 250°C at 20°C min^{-1} and held for 10 min. The SIM mode was set to detect 4,8,12-trimethyl- tridecanoic acid (4,8,12-TMTD) fragmentation (ions m/ z 64, 74, 87, 213, 256, 270), pristanic acid (ions m/ z 64, 74, 87, 88, 101, 256, 284, 312), phytanic acid (ions m/ z 64, 74, 87, 101, 171, 256, 326), and C_{16}-C_{22} APAAs (ions m/ z 64, 74, 87, 105, 256, 262, 290, 318, 346). Helium was used as carrier gas at a constant flow rate of 1.5 mL min^{-1}. The percentage of phytanic acid diastereoisomer SRR was obtained using the area of the ion *m/z* 101.

Analyses of the **solvent extracts** (DCM/MeOH) were conducted using an Agilent 8890 GC coupled with an MSD 5977B, fitted with a DB-5ht column (15 m x 320 μm x 0.1 μm) at CEPAM-CNRS, in Nice. The temperature of the column was kept at 50°C for 1 min and then increased by 15°C every minute until a final temperature of 370°C was reached and held for 12 min. Nitrogen was used as the carrier gas at a constant flow rate of 4 ml min^{-1}. The detector was kept at 370°C with hydrogen flow of 35 ml min^{-1}. The spectra were obtained by scanning between *m/z* 50 and 900.

The results obtained with these methods were used for quantification of the lipid concentration and for identification of the main molecular components. Data acquisition was performed using Agilent ChemStation and the Masshunter Workstation software (v10, www.agilent.com). Quantification, compound identification, data processing and graphic representation were carried out using the

Qualitative Analysis Module of the Masshunter Workstation. Mass spectral interpretation was based on mass spectra, retention time and comparison with the NIST/EPA/NIH Mass Spectral Library (version 2014, www.nist.gov/srd).

5.4.1. Statistical analysis of total lipid extract

The statistical analyses were conducted in R (version 4.2.2), a widely used open-source statistical computing environment suitable for managing complex data. The primary objective of the statistical component was to evaluate differences in lipid yields across distinct sampling locations on the HAS (external, internal, deposits), as well as across distinct lithological categories, including carbonate rocks (marl, limestone, and detrital carbonate), igneous rocks (volcanic), and siliciclastic rocks (sandstone). This evaluation was essential to understand whether lipid concentrations varied significantly depending on where residues were preserved or embedded within the lithic. Likewise, evaluating variation across lithology groups was crucial to examining whether the mineralogical composition of different stones influenced lipid absorption and preservation. In addition, statistical tests were employed to assess potential differences in stable carbon isotope ($\delta^{13}C$) values between external and internal samples, in order to evaluate whether isotopic signatures varied according to the sampled layers. Prior to conducting group comparisons, data were assessed for normality using the Shapiro-Wilk test. Since the data did not meet the assumption of normality, a non-parametric Kruskal-Wallis test was used to evaluate statistical differences in lipid yields across the groups. It was applied separately to both the sampling spot categories and the mineral group categories to provide an overall indication of variation within each classification. In cases where only two groups were compared, the Kruskal–Wallis test is mathematically equivalent to the Wilcoxon rank sum test (also known as Mann–Whitney U test). Following any significant results from the Kruskal-Wallis test, pairwise comparisons were conducted using Wilcoxon rank sum test to assess differences between individual groups. These post hoc tests allowed for a more detailed examination of the differences between individual sampling locations and between lithological categories. To control for multiple comparisons, Holm's correction was applied to adjust the p-values. An initial significance threshold of $\alpha = 0.05$ was applied to all statistical tests, and Holm's correction for pairwise comparisons adjusted the threshold to $\alpha = 0.025$.

5.4.2. Stable carbon isotope analysis

Stable carbon isotope analysis was conducted to further characterise the origin and processing of lipid residues recovered from HAS and sediments. Stable carbon isotope ($\delta^{13}C$) values of the predominant saturated fatty acids, palmitic ($C_{16:0}$) and stearic ($C_{18:0}$) acids, were determined by Gas chromatography-combustion-isotope ratio mass spectrometry (GC-c-IRMS) at ICTA-UAB, in Barcelona. Samples were injected in splitless mode on a DB5-MS UI fused silica column (60 m x 320 µm x 0.25 µm, J&W Scientific, Folsom, CA, USA). The $\delta^{13}C$ values of individual fatty acids were determined using a Delta V Advantage mass spectrometer (Thermo Fisher, Bremen) linked to a ConFlo

IV interface. During the initial 10 minutes, the effluent from the GC was diverted away from the combustion reactor (backflush mode). During the solvent–divert period, CO_2 reference gas was automatically introduced into the IRMS in a series of pulses and its $^{13}C/^{12}C$ measured. After the solvent-divert period, the effluent from the GC was allowed to enter the combustion reactor and IRMS. The IRMS automatically measured the ion intensities of m/z 44, 45, and 46 in its three Faraday cups corresponding to $^{12}C^{16}O_2$, $^{13}C^{16}O_2$, and $^{12}C^{16}O^{18}O$ respectively. The Isodat 3.0 software automatically computed the $^{13}C/^{12}C$ and of each sample peak, referenced to the standard CO_2 gas and its known $^{13}C/^{12}C$ content. The results were presented in per mil (‰) relative to the VPDB standard. To ensure data comparability, the instrument was calibrated using the Indiana University F8 standard. This standard contains a mixture of 8 methylated and ethylated fatty acids of known isotopic compositions. Additionally, quality control standards were intercalated every 5-6 injections to control the stability of the isotopic measurements over time. Instrumental precision and accuracy were better than ± 0.5‰. All lipid extracts were analysed in duplicate to ensure reproducibility and accuracy. Values were also corrected using mass balance to account for the methylation of the carboxyl group that occurs during acid extraction. Corrections were based on comparisons with a standard mixture of $C_{16:0}$ and $C_{18:0}$ fatty acids of known isotopic composition processed in each batch as a sample.

A schematic representation of the lipid analysis methodology applied to HAS and sediment samples is provided in Figure 34.

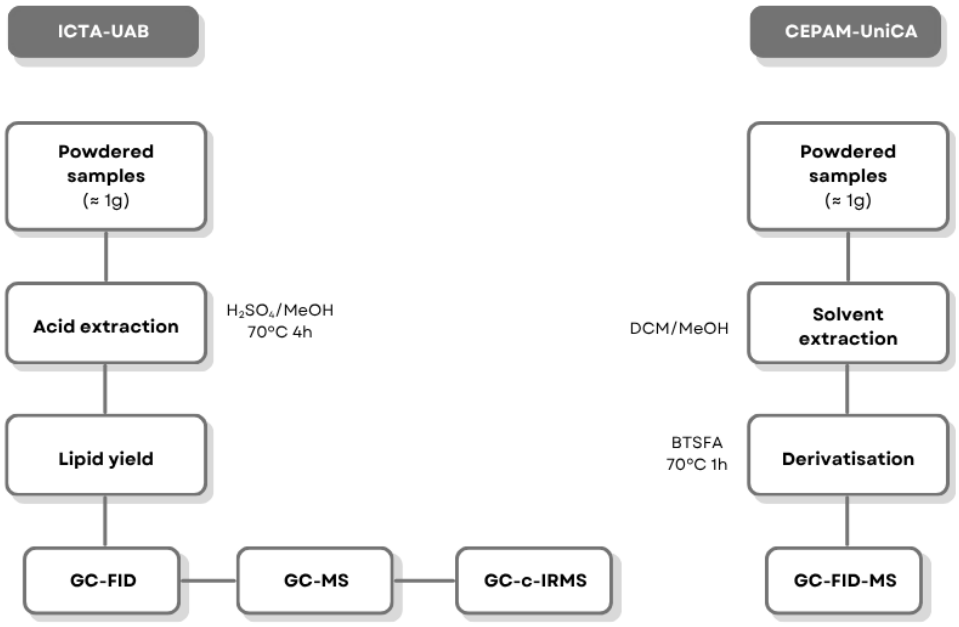


Figure 34. Schematic workflow of the methodology applied for lipid analysis on HAS and sediment samples conducted at ICTA-UAB (Barcelona, Spain) and CEPAM-UniCA (Nice, France).

5.5. Protein analysis

A selection of 7 samples was analysed by proteomics to supplement lipid-based organic residue analysis and provide further insight into processed foodstuffs. The sample selection was guided by the presence of surface residues on some HAS, suggesting potential contact with organic materials during use. The decision to include proteomic analysis was also informed by the analytical capabilities available at ICTA-UAB, which allowed the application of advanced protein extraction and identification techniques. Given the anticipated challenges of protein preservation in such contexts, only a limited number of samples were selected for this exploratory phase. Previous experimental research has shown that the number of identifiable proteins decreases markedly with repeated cooking events, reflecting the progressive degradation of proteins under prolonged heating conditions (Dekker et al., 2025). Consequently, the likelihood of protein survival in the archaeological material was expected to be low, and the analysis aimed primarily to assess the feasibility of detecting preserved proteins in lithic residues.

The samples were analysed following a modified version of the single-pot, solid-phase-enhanced sample-preparation (SP3) extraction protocol (Cleland, 2018) specifically adapted to food crust analysis (Harvey and Hendy, 2025; Dekker et al., 2025). Protein extractions were performed on approximately 100 mg of powdered potential foodcrust, with sample weights ranging from 24 to 206 mg. Each sample was treated with 150 µL of 6M guanidine hydrochloride (GuHCl), homogenised, centrifuged and incubated at 65ºC for one hour. Following incubation, the samples were centrifuged again, the supernatant was then transferred to a new tube for each sample and the resulting pellets were discarded. To each supernatant, 15 µL of 100 mM Tris(2-carboxyethyl)phosphine (TCEP) and 2-Chloroacetamide (CAA) solution was added, followed by homogenisation, centrifugation, and incubation at 99ºC for 10 minutes. The samples were then allowed to cool at room temperature for 5 minutes. 500 µg of magnetic hydrophilic and hydrophobic beads (Sera-Mag™ SpeedBeads carboxylate-modified particles, Cytiva) was added to each sample and gently mixed to ensure homogenization, then 175 µL of 100% (v/v) ethanol was added. The mixtures were incubated at 24°C with shaking at 1000 RPM for five minutes. Protein filtration was performed by placing the samples on a magnetic rack, allowing the beads to migrate for two minutes, and discarding the supernatant. The samples were then washed three times with 200 µL of 80% ethanol, gently resuspending the beads in the solution during each wash then placing it back on the magnetic rack and allowing the beads to migrate before discarding the ethanol. After the final rinse, the beads were resuspended in 100 µL 50 mM ammonium bicarbonate (AmBic) and incubated at 37°C with 750 RPM for three minutes. In-solution digestion was performed by adding 1 µL of a 0.2 µg/µL trypsin solution to the samples, followed by incubation at 37°C, 750 RPM for 18 hours. After digestion, the samples were centrifuged and placed back on the magnetic rack and the supernatant containing the digested proteins was transferred to new Eppendorf tubes, separating

them from the beads. To halt digestion, 10 µL of 5% (v/v) trifluoroacetic acid (TFA) was added to each sample. Finally, peptides were desalted using Pierce™ C18 ZipTip® pipette tips (100 µL, Thermo Scientific™). The ZipTips were primed twice with 100 µL of conditioning solution (0.1% TFA in 50:50 acetonitrile (ACN) and ultrapure water) and washed twice with 100 µL of 0.1% TFA. The sample was aspirated with the ZipTip several times to bind the peptides to the C18 filter,, and the ZipTips were washed twice more with 100 µL of 0.1% TFA, before eluting the peptides in 100 µL of conditioning solution.

The eluted peptides were analysed by liquid chromatography tandem mass spectrometry (LC-MS/MS) on an EvoSep One nanoUPLC coupled to a Bruker timsToF HT mass spectrometer with a CaptiveSpray ionisation source. at the Centre for Excellence in Mass Spectrometry at the University of York (UK). Peptides were loaded onto EvoTip Pure tips for desalting and as a disposable trap column for introduction onto an EvoSep One nanoUPLC system. A pre-set 60SPD gradient (from Evosep One HyStar Driver 2.4.125.0) was used with an 8 cm EvoSep C18 Performance column (8 cm x 150 µm, 1.5 µm) for the chromatographic separation of the peptides, which were then introduced into the timsToF HT MS. Positive PASEF-DDA, nanoESI-MS and MS2 spectra were acquired using Compass HyStar software (version 6.2, Bruker) with the following instrument source settings were: capillary voltage, 1,600 V; dry gas, 3 l/min; dry temperature; 180°C. Spectra were acquired between the mass range *m/z* 100-1,700. TIMS settings were: 1/K0 0.6 - 1.60 V.s/cm^2; Ramp time, 100 ms; Ramp rate 9.42 Hz. Data dependent acquisition was performed with 10 PASEF ramps and a total cycle time of 1.17 s. An intensity threshold of 2,500 and a target intensity of 20,000 were set with active exclusion applied for 0.4 minutes post precursor selection. Collision energy was interpolated between 20 eV at 0.6 V.s/cm^2 to 59 eV at 1.6 V.s/cm^2. Blank machine washes were run between each sample injection to examine and reduce carry-over between samples.

MS/MS ion data analysis was performed with Mascot (Matrix Science), searching against SwissProt (release 2025/10) and cRAP (release 2025/10) databases to identify the potential range of proteins preserved within the HAS residues. Search parameters were set for semi-tryptic enzymatic cleavage (considering likely sample degradation) allowing for 2 missed cleavages, with 10 ppm peptide mass tolerance and 0.5 Da fragment mass tolerance. Carbamidomethylation (C) was set as a fixed modification, with variable modifications allowed for acetylation (protein N-term), deamidation (NQ), and oxidation (M). Peptide mass tolerance was set at 10ppm and fragment. From the resultant data, all protein families matching to known or likely contaminants (including those listed specifically for archaeological materials (Evans et al., 2023)) were excluded, and only those proteins with a minimum of two distinct peptides were considered for further analysis.

6. Heat-altered stones as archaeological indicators: morphological and molecular evidence from La Draga and Pendimoun

This chapter presents the results of the multi-analytical approach undertaken to investigate heat-altered stones (HAS) from two key Neolithic sites in southwestern Europe: La Draga (Spain) and Pendimoun (France). The research was guided by two principal objectives: (i) to identify and characterise physical and morphological alteration patterns on stones associated with heat exposure, and (ii) to evaluate the potential of HAS for yielding molecular and isotopic information related to past culinary practices.

To align with the archaeological context and facilitate site-specific interpretation, the results are presented in two main sections, each dedicated to one site. Within each site-based section, the results are further subdivided according to the analytical techniques employed and described in Chapter 5: macroscopic visual inspection, 3D model acquisition, and molecular analysis of organic residues (lipid and protein). Visual inspection focused on the selection and typological classification of the sampled lithic materials, along with the identification of visual heat-alteration patterns. These qualitative observations were complemented by high-resolution 3D scanning and photogrammetry to digitally preserve each artefact's morphology and surface characteristics prior to any sampling. This process not only safeguarded the artefacts' structural integrity but also contributed to the creation of a digital archive aimed at supporting heritage awareness, conservation strategies, and future research. Molecular analyses were conducted to evaluate whether HAS could preserve organic signatures of prehistoric food processing. Lipid residues extracted from selected artefacts were analysed via gas chromatography-mass spectrometry (GC-MS), and their carbon stable isotope ratios were measured via GC-C-IRMS to distinguish plant- and animal-derived sources and infer potential culinary practices. Comparisons with lipid profiles from contextual sediment samples were undertaken to explore site-specific biochemical signatures and to assess potential environmental contamination. Attempts to analyse proteins were also made on selected samples; however, these did not yield any endogenous proteins attributable to food residues or other use-related materials.

By structuring the results by site and method, this chapter aims to provide a coherent narrative of how each line of evidence contributes to a broader understanding of the use, significance, and value of HAS in Neolithic contexts.

6.1. La Draga

6.1.1. Visual inspection

The visual inspection of the fifteen selected HAS from Sector B/D at La Draga confirmed the presence of various macroscopic features indicative of thermal alteration and use in combustion-related activities. The sample set included nine sandstones, two limestones, two marls, and two volcanic stones. In terms of shape, seven stones were classified as tabular, three as prismatic, three as spherical, and two exhibited a pot-lid shape, in line with classification schemes described by Custer (Custer, 2017). Table 6 summarises the morphological features of each HAS.

In terms of thermal alterations, approximately half of the samples (n = 7) exhibited cracking, with one stone showing fractures that divided it into two distinct fragments, suggesting exposure to considerable thermal stress. These cracks provide evidence of high-temperature exposure, potentially linked to fire-related activities (Neubauer, 2018, 2024). Additionally, seven stones displayed signs of sooting on their surfaces, a common indicator of interaction with combustion processes, with six displaying varying degrees of discoloration, further supporting the hypothesis of significant heat exposure (Neubauer, 2018, 2024). Three samples exhibited possible superficial adhesion, which may indicate contact with combustion residues or organic material, reinforcing the interpretation that these artefacts were subjected to heat and possibly interacted with organic matter during or after heating (Pagoulatos, 2005; Neubauer, 2018). Representative examples of these heat-alteration patterns are shown in Figure 35, including a fracture (sample LD12-4007, A), sooting (sample LD23-35300, B), discoloration with superficial adhesion (sample LD12-4035, C), and a combination of discoloration, sooting, and superficial adhesion (sample LD11-2156, D).

Given the diverse range of HAS investigated, which vary widely in morphology and alteration patterns, it is useful to establish the potential functions of specific subsets within the assemblage. By examining variations in shape, surface texture, and thermal properties, it is possible to infer the potential functions of each HAS, and establish criteria applicable to the wider collection. In some cases, however, specific morphologies suggest that certain stones may have served other functions prior to their involvement in heating events, meaning that particular surface features or organic residues could reflect a combination of these earlier activities rather than the heating process itself.



Figure 35. Representative examples of heat-alteration patterns observed on HAS: (A) fracture on sample LD12-4007, (B) sooting on sample LD23-35300, (C) discoloration and superficial adhesion on sample LD12-4035, and (D) discoloration, sooting and superficial adhesion on sample LD11-2156.

Specimens with **spherical morphology** (LD10-883, LD11-1540 and LD23-25396; Figure 36) share certain alteration properties but vary in mineral compositions and surface characteristics. Rounded stones typically retain heat longer than flat slabs of equivalent density due to their lower surface area-to-mass ratios, which results in slower cooling rates (Pierce, 1988; Black and Thoms, 2015). LD10-833 and LD11-1540 present smooth and levigated surfaces, typical of pebbles, along with localised discoloration. These features likely indicate natural origin rather than anthropogenic modification. At La Draga, depending on the type of macroscopic use wear preserved on the surfaces and their arrangement, analogous artefacts were recognised and classified as *mano de molino* (grinding stones) or *percutor/pulidor* (hammer or polisher) (Palomo, Piqué and Terradas, 2018). In contrast, LD23-25396 exhibits a more irregular and vesicular surface, consistent with its volcanic origin, specifically scoria. Scoria is a dark-coloured, vesicular volcanic rock formed from lava, containing abundant rounded to irregular cavities (vesicles) created by gas bubbles escaping during eruption. Notably, one side of LD23-25396 is polished, which may suggest intentional levigation, possibly indicating its use as a grinder. A similar artefact was identified and interpreted at La Draga as grinding stone (Palomo, Piqué and Terradas, 2018). Additionally, this specimen also shows evidence of sooting on the same surface, supporting a possible use within combustion context, particularly as it was recovered from Structure E269, a combustion feature. If both assumptions are valid, this would suggest that this specific HAS was not found in its original functional context as a grinding tool, but rather reflects a secondary use related to heating activities.



Figure 36. Spherical HAS specimens showing variation in surface and composition: (A) LD10-883 and (B) LD11-1540 with smooth, rounded surfaces and localized discoloration; (C) LD23-25396 with a vesicular (scoria) surface, one polished side, and evidence of sooting.

Another small volcanic specimen (LD23-25430), also recovered from Structure E269, presents a **tabular morphology**, with a flat levigated surface marked by sooting and discoloration, likely resulting from prolonged exposure to heat or direct contact with fire. The edges are jagged and irregular, suggesting that the fragment was broken off from a larger piece, possibly during use or post-depositional processes. Stones with tabular morphology, typically flat with one dimension smaller than the others, often exhibit planar, smooth or levigated surfaces, which may result from natural fracture patterns or anthropogenic modification (Custer, 2017). Among them, LD23-25300 exhibits cracking and a localised sooting along one edge, likely resulting from direct exposure to heat or contact with combustion residue. It was part of Structure E266, interpreted as a hearth, evidenced by a thin charcoal layer overlain by a whitish ash layer (Piqué et al., 2023). LD12-4035 displays cracking, surface discoloration and possible superficial deposits on one side, consistent with heat alteration. In contrast, specimen LD10-663 features a slightly concave, levigated surface with linear striations, possibly indicative of use-wear. This morphology may indicate that the stone functioned as the stationary base of a grinding implement, where repetitive mechanical action gradually produces the polished and concave surface (Neubauer, 2024; Hamon, 2008). A comparable object was identified at La Draga as a *plaqueta* (slab) (Palomo, Piqué and Terradas, 2018). Specimen LD12-4007 presents sooting and exfoliation on one side, indicative of exposure to high temperatures. A prominent fracture divides the stone in two sections, consistent with a heat/fire fracture, a type of breakage that originates internally within the stone as a result of thermal stress. The morphology aligns with what Neubauer (Neubauer, 2018) describes as blocky or pseudo-core fragments, characterised by fracturing along the core of the stone. Additionally, LD12-3791, displays a unique pattern of surface alteration characterised by deep surface cracking (Neubauer, 2024). It features deep crevices that split the surface, likely resulting from the repeated stretching and expansion of fine-crazed outer layers. These cracks appear to deepen progressively with increasing cycles of thermal shock. Representative examples of these tabular HAS specimens are shown in Figure 37.

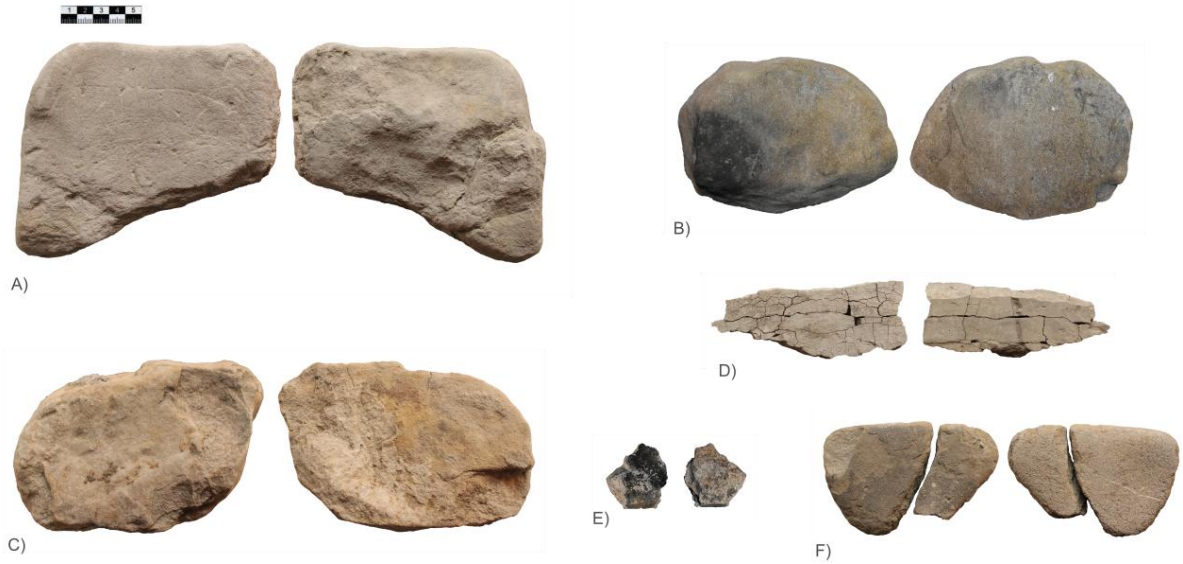


Figure 37. Tabular HAS specimens showing evidence of heat alteration and potential use-wear: (A) LD10-663 with a concave, levigated surface and linear striations; (B) LD23-25300 with localised sooting along one edge; (C) LD12-4035 exhibiting surface discoloration, cracking, and possible superficial deposits; (D) LD12-3791 exhibiting deep surface cracking; (E) LD23-25430 with a flat, levigated surface, sooting and discoloration; (F) LD12-4007 showing sooting and a fracture.

The larger and heavier specimen, LD12-3951 (Figure 38), also exhibits a tabular morphology. One side shows pronounced sooting, which may represent charred residues resulting from direct contact with fire, possibly in conjunction with wood used as fuel. In contrast, the opposite side shows minimal sooting and discoloration, specifically reddening, but instead displays evidence of exfoliation. This is a weathering process wherein repeated exposure to fluctuating temperature leads to the detachment of surface layers (Neubauer, 2018). In this case, exfoliation is evident through the absence of sheets across multiple layers. Owing to these features, the specimen can be identified as a **slab**, a flat and broad stone commonly associated with surface-based activities such as cooking or heating. The dimension of the stone and the nature of its thermal modifications suggest a functional interpretation as a potential cooking platform or griddle (Thoms, 2008b; Brink and Dawe, 2003), sufficiently large to support food preparation or cooking activities directly over an open flame.



Figure 38. Large tabular HAS specimen LD12-3951 showing minimal sooting, reddening, and exfoliation on one side, and pronounced soothing on the opposite side.

Two specimens (LD11-1547 and LD11-1987, Figure 39) correspond to **pot-lid fractures**, small, typically circular flakes, resembling the shape of a pot lid, detached from the surface of a stone. It is a diagnostic feature of thermal stress and occurs predominantly as a result of a sudden, direct exposure to fire. These specimens exhibit a convex outer surface, corresponding to the original exterior of the entire stone and a concave interior face marking the fracture surface. These features are consistent with high-temperature stress-induced breakage, typically associated with direct combustion events (Neubauer, 2018).

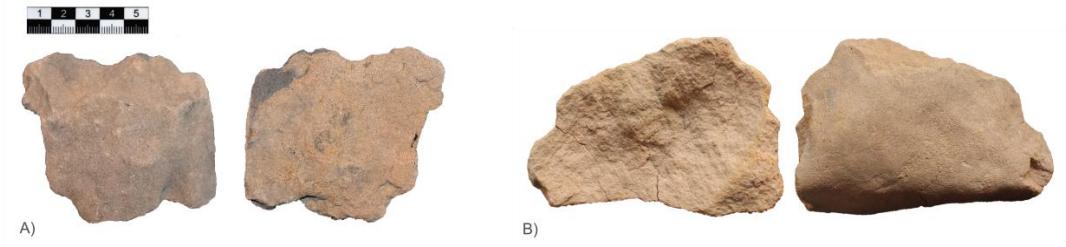


Figure 39. Pot-lid fracture specimens (A) LD11-1547 and (B) LD11-1987, showing convex exterior and concave fracture surfaces.

The specimens exhibiting a **prismatic morphology** (Figure 40) display notable variation in shape and surface characteristic. LD10-500 presents a sub-rounded form on one side, contrasting with a more angular and irregular shape on the other, suggesting either differential wear or fracturing. LD11-2156 presents a more defined triangular prism-like shape, with visible evidence of sooting concentrated on one side, alongside surface discoloration and possible superficial deposits on the other faces. LD10-

518 shows cracking, sooting and discoloration. The peculiar shape, which fits comfortably in the hand, suggests it may have functioned as a handstone (hand-held tool) (Hamon, 2008).



Figure 40. Prismatic HAS specimens illustrating variation in shape and surface alteration: (A) LD10-500 with a sub-rounded and contrasting angular form; (B) LD10-518 showing cracking, sooting, and discoloration; (C) LD11-2156 with a triangular prism-like shape, sooting, surface discoloration, and possible superficial deposits.

Table 6. Contextual and morphological information of heat-altered stones (HAS) from La Draga. Variables include excavation year, sector, stratigraphic context, feature, grid position, occupation phase, mineral composition, dimensions, weight, and associated thermal alteration patterns.

Sites	*Excav. Year*	*Sample ID*	*Sector*	*Strat. context*	*Feature*	*Grid*	*Occupation*	*Mineral*	*Length (mm)*	*Width (mm)*	*Thickness (mm)*	*Weight (g)*	*Cracks*	*Sooting*	*Discol.*	*Sup. deposit*	*Morphology*
La Draga	2010	500	D	VI		KA80	more recent	Sandstone	97	91	79	489					prismatic
La Draga	2010	518	D	VI		KD81	more recent	Sandstone	79	77	62	230	x	x	x		prismatic
La Draga	2010	663	D	VII		JJ78	oldest	Limestone	174	140	48	890					tabular
La Draga	2010	833	D	VII		JJ79	oldest	Limestone	72	60	47	163			x		spherical
La Draga	2011	1540	D	VI		JD81	more recent	Sandstone	55	48	39	98			x		spherical
La Draga	2011	1547	D	VIa		JB81	oldest	Sandstone	94	87	29	90					pot-lid
La Draga	2011	1987	D	VIa		JB81	more recent	Sandstone	105	70	30	202	x				pot-lid
La Draga	2011	2156	D	VII		JD78	oldest	Sandstone	87	54	53	205		x	x	x	prismatic
La Draga	2012	3791	D	VII		JC81	oldest	Marl	114	41	40	254	x				tabular
La Draga	2012	3951	D	VIa		JA81	more recent	Marl	255	170	35	1,685	x	x	x	x	tabular
La Draga	2012	4007	D	VIa		JA79	more recent	Sandstone	105	70	15	158	fracture	x			tabular
La Draga	2012	4035	D	VIa		JC78	more recent	Sandstone	155	95	30	786	x		x	x	tabular
La Draga	2023	25300	B		Structure E266	JA82	oldest	Sandstone	130	94	55	532	x	x			tabular
La Draga	2023	25396	B	VII-0	Structure E269	JB82	oldest	Volcanic (Scoria)	88	73	67	219		x			spherical
La Draga	2023	25430	B	VII-0	Structure E269	JB82	oldest	Volcanic	40	50	29	30		x			tabular

6.1.2. 3D model acquisition

High-resolution 3D models were successfully produced for all analysed HAS using a combination of photogrammetry and laser scanning techniques. These digital reconstructions preserve the original morphology and surface texture of each artefact and are housed in a dedicated digital library hosted by OpenLab UAB on Sketchfab [https://skfb.ly/puzEx]. This repository represents a significant research outcome, serving as an open-access resource for educational purposes and future research. Through this platform, the models can be explored in detail, reducing the need for physical handling, while offering a unique opportunity for researchers and the public to engage with these artefacts virtually.

6.1.3. Lipid residue analysis

This section presents the results of the lipid residue analyses conducted to characterise the molecular composition of HAS and sediments. A total of 33 samples (e = 15, i = 15, d = 3) from the 15 selected HAS, along with nine sediment samples from the same sector, were analysed. Acid extraction (AE) was performed on all samples, including both HAS and sediments, as this step was necessary for subsequent stable carbon isotope analysis. Solvent extraction (SE), intended primarily to identify plant-derived lipid profiles, was applied to a smaller subset of samples. Among the sediments, only two samples (LD-JC78-VIa and LD-JA81-VIa g) underwent solvent extraction, since the remaining sediments displayed comparable molecular profiles.

Although previous research has suggested that contamination of absorbed residues by surrounding sediments in ceramics is generally limited (Heron, Evershed and Goad, 1991; Aillaud, 2001), **the inclusion of sediment analysis in this study provides a basis for examining this assumption and contributes to a more robust molecular interpretation of the HAS assemblage.** As sediment lipid analyses are rarely incorporated into ceramic residue studies (Heron et al., 2010; Drieu, Binder and Regert, 2022), these data offer a useful comparative framework for interpreting HAS lipid profiles. Accordingly, the results of the sediments are presented first, followed by those of HAS, which are interpreted in relation to these contextual findings and discussed further in Chapter 7.

Before molecular identification, preliminary chemical screening revealed the presence of sulphur in nearly all the samples, likely originating from the sulphur-bearing bedrock. This was removed using activated copper bars prior to further analysis, which helped to prevent potential damage to the GC column and significantly improved the cleanliness and interpretability of the chromatograms by eliminating interfering peaks.

Lipids composition in sediments

Lipids were successfully extracted from all **sediment samples** from La Draga (Table 7 and Annex 4), yielding concentrations ranging from 134.5 to 2,658.14 μg g^{-1}. These high yields indicate good preservation of organic residues, likely favoured by the waterlogged and relatively stable conditions of the lakeshore sediments. The lipid profiles across all samples were consistent with lipids found in "natural", anthropogenic and archaeological sediments (Mallol et al., 2025; Moucawi et al., 1981; Jansen and Wiesenberg, 2017; Scherer et al., 2025). Overall, these were dominated by **saturated fatty acids (SFA)**, spanning chain lengths from $C_{8:0}$ to $C_{32:0}$, with **palmitic ($C_{16:0}$), stearic ($C_{18:0}$) and lignoceric ($C_{24:0}$) acids** being the most abundant (Figure 41). The palmitic:stearic ratio (P/S) varied between 1.83 and 3.75, reflecting a consistent predominance of plant signals. This, along with relatively elevated levels of oleic acid ($C_{18:1}$) compared to stearic acid ($C_{16:0}/C_{18:0} > 2$ and $2.5 > C_{18:1}/C_{18:0} > 0.2$) is indicative of plant-derived oil. **Monomethyl-branched fatty acids** ($C_{13:0Br}$, $C_{15:0Br}$ and $C_{17:0Br}$) were detected in all samples and are commonly associated with bacterial activity, potentially arising from soil microbial processes (Evershed, 1993; Regert, 2011). **Monounsaturated fatty acids (MUFA)**, primarily palmitoleic acid ($C_{16:1}$), oleic acid ($C_{18:1}$), gondoic acid ($C_{20:1}$) and erucic acid ($C_{22:1}$), were also identified across the analysed samples.

In addition to fatty acids, a wide range of plant-derived biomarkers were identified, including **phytosterols** such as β-sitosterol, stigmasterol and their derivatives (e.g. stigmastanol), **pentacyclic triterpenes** such as β-amyrin, α-amyrin, β-amyrone, erythrodiol, oleandione, lupeol, betulin and betulinaldehyde, as well as the **tetracyclic triterpene** friedelan-3-one (Figures 41 and 42). The marked predominance of even-numbered ***n*-alkanols** (C_{18} to C_{32}) detected as their TMS derivatives, together with the occurrence of odd-numbered long-chain ***n*-alkanes** (C_{27} to C_{31}) and trace amounts of even carbon numbered long-chain **wax esters** (W_{42} to W_{48}), further supports their attribution to vascular plant leaf waxes (Figure 42) (Eglinton and Hamilton, 1967; Gülz, 1994; Charters et al., 1995; Ribechini et al., 2008). The presence of oxidation products of unsaturated fatty acids, such as **hydroxylated FAs** (C_{16} to C_{26}) and **dicarboxylic acids** (C_8 to C_{30}) is likewise consistent with post-depositional processes associated with burial conditions (Regert et al., 1998; Eerkens, 2005).

Traces of **benzene tricarboxylic acid**, a by-product of charred organic matter, were detected in four samples. Among **isoprenoid acids**, 4,8,12-TMTD, pristanic and phytanic acid were also identified (Figure 43), with SRR isomers ranging between 58% and 75%. The co-occurrence of these compounds provides strong evidence for aquatic organisms including plants and animals (Cramp and Evershed, 2014; Lucquin et al., 2016), however this interpretation should be approached with some caution, given the fact that only %SRR values exceeding 75 are generally indicative of aquatic oils (Lucquin et al., 2016; Dolbunova et al., 2023). As a degradation product of phytol, these acids may

originate from both aquatic and terrestrial plant sources, or alternatively reflect low-level microbial transformation processes during burial.

Notably, three homologues of **alkylresorcinol** (AR21:0, AR23:0 and AR25:0) were identified in two samples. Although these compounds have previously been reported in ceramic artefacts as a proxy for cereal process (Colonese et al., 2017; Hammann and Cramp, 2018; Hammann et al., 2022; Doliente et al., 2024), they can also occur in sediments (Scherer et al., 2025).

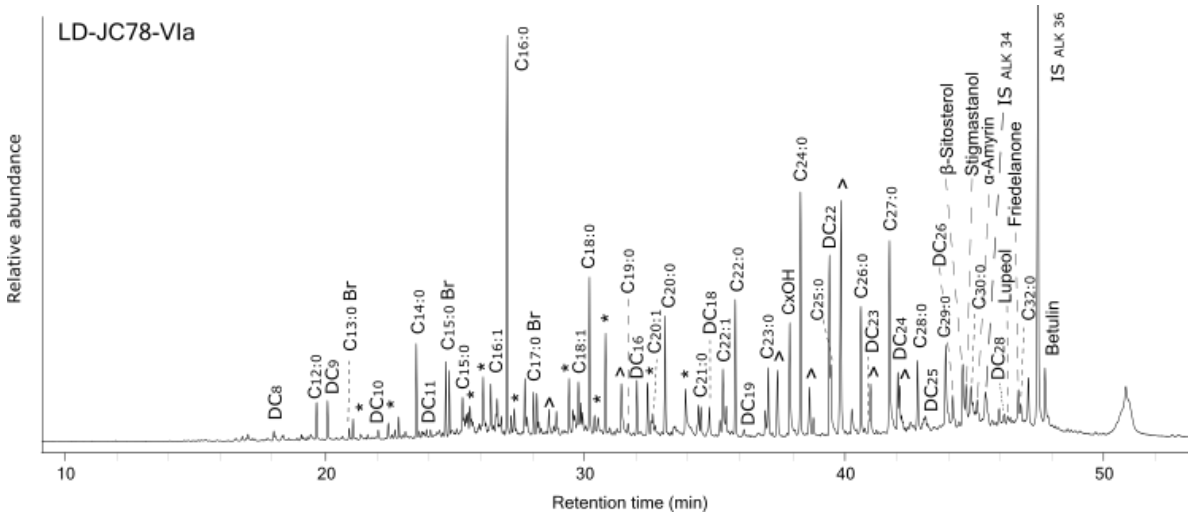


Figure 41. Partial total ion chromatograms (TIC) of acid/methanol extract of sediment sample LD-JC78-VIa showing saturated fatty acids ($C_{XX:0}$), branched ($C_{XX:0}$ Br), unsaturated fatty acids ($C_{XX:1}$), diacids (DC_{XX}), hydroxy fatty acids (^), sterols and derivatives, tetracyclic and pentacyclic triterpenes, contaminants (*), and *n*-alkanes internal standards (IS $_{ALKXX}$).

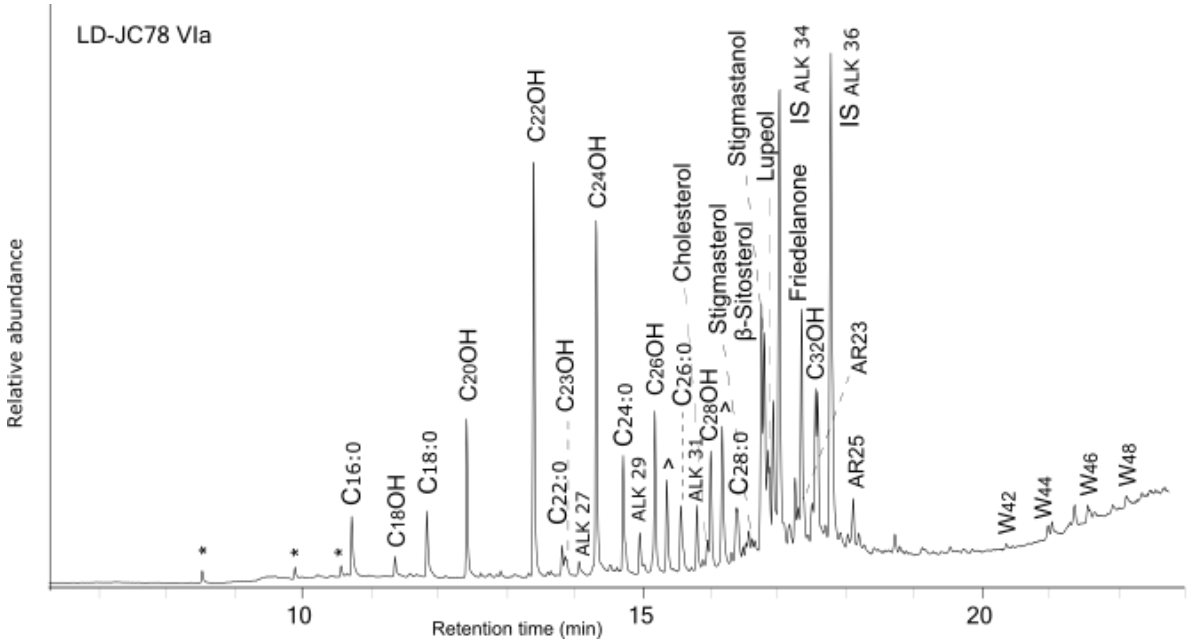


Figure 42. Partial total ion chromatograms (TIC) of solvent extract of sediment sample LD-JC78-VIa showing saturated fatty acids ($C_{XX:0}$), linear alcohols (CxxOH), *n*-alkanes (ALKxx), hydroxy fatty acids (^), sterols and derivatives, tetracyclic and pentacyclic triterpenes, alkylresorcinol (ARxx), wax esters (Wxx), contaminants (*), and *n*-alkanes internal standards (IS $_{ALKXX}$).

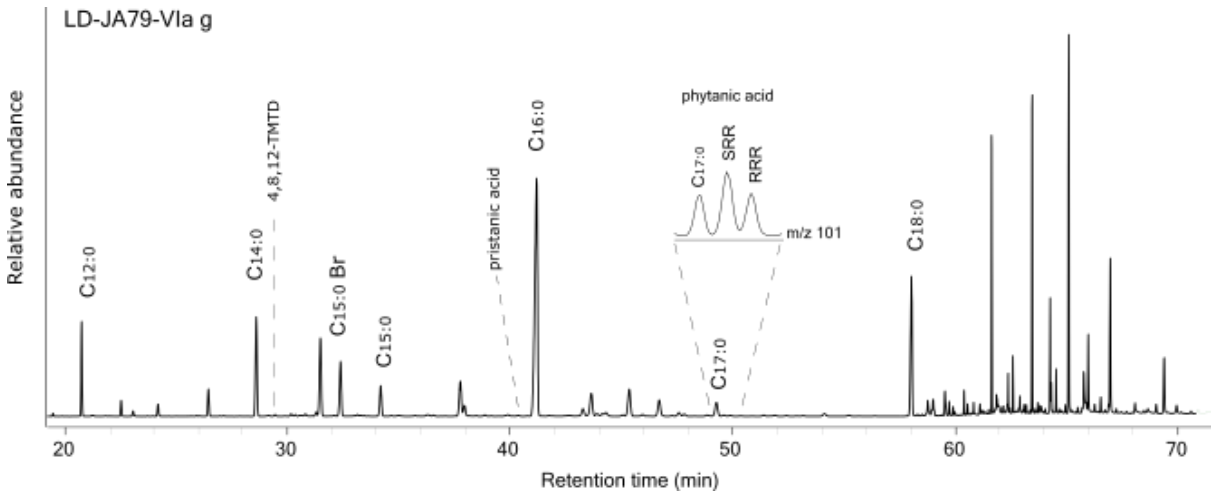


Figure 43. Partial total ion chromatograms (TIC) of acid/methanol of sediment sample LD-JA79-VIa g showing saturated fatty acids ($C_{XX:0}$), branched fatty acids ($C_{XX:0}$ Br), isoprenoid acids (4,8,12-trimethyltridecanoic acid, pristanic and phytanic acid), with a *m/z* 101 ion chromatogram showing the ratio of phytanic acid diastereomers (SRR and RRR).

Lipids composition in HAS

Lipids were extracted from the internal, external and deposit samples from all HAS, with concentrations ranging from 0.23 to 407.00 µg g^{-1} (Figure 44). These values are lower than those observed in the sediments, reflecting a potential reduced capacity of stones to retain organic residues.

From these, appreciable amounts of lipids (> 5 µg g^{-1} (Evershed et al., 2008b; Craig et al., 2013)) were obtained from 67% of internal (n = 10) and 100% external (n = 15) samples, along with 100% of deposits (n = 3). For the following analyses, only lipid yields exceeding this threshold were considered.

Figure 45 provides a visual summary of the lipid yield concentrations across the three aliquots, showing slightly greater variability in the external samples, which exhibit a wider range of values compared to the others. A Kruskal-Wallis rank sum test, however, indicated no statistically significant differences across the three aliquot groups (external, internal, and deposits; $\chi^2 = 1.42$, df = 2, $p = 0.401$). A post-hoc pairwise comparison using Dunn's test with Holm correction confirmed that no individual pair of aliquots differs significantly in lipid yields.

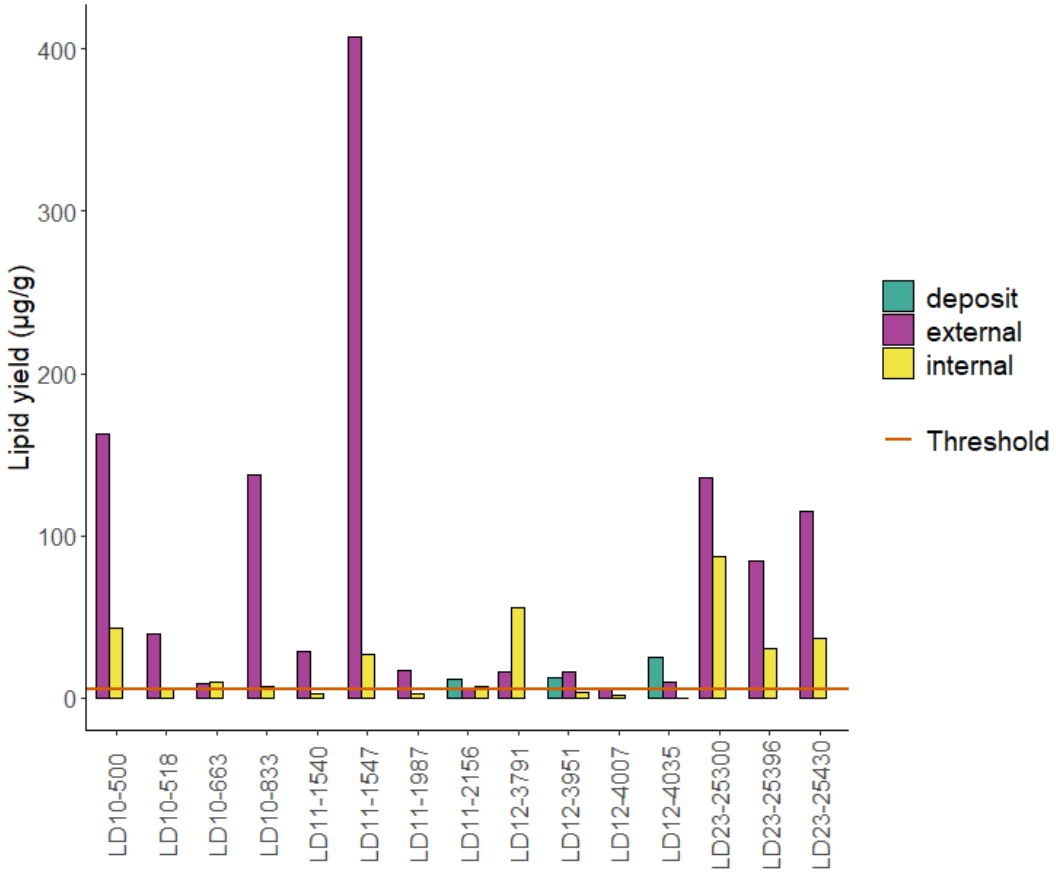


Figure 44. Bar plot of lipid yields of La Draga samples, categorised by deposit, external and internal aliquots. The solid line represents the threshold of 5 µg g^{-1}.

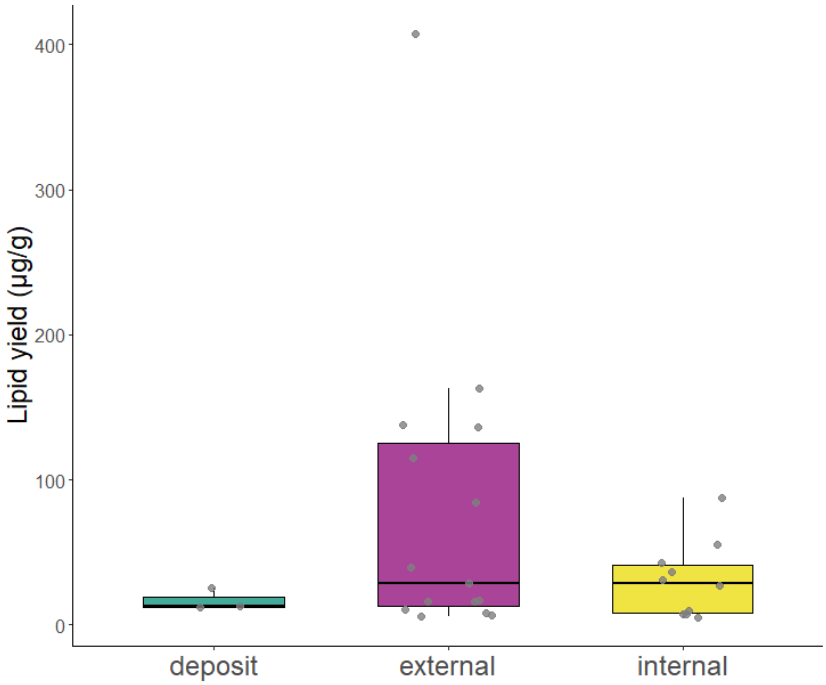


Figure 45. Boxplot of lipid yields for La Draga samples, categorised by deposit (n = 3), external (n = 15), and internal (n = 10) aliquots. Grey points represent individual data values.

To evaluate whether the mineralogical composition of stones influenced lipid preservation, HAS were grouped according to their lithological type. Specifically, they were classified into three categories, such as carbonate rocks (including marl, limestone, and detrital carbonate), igneous rocks (volcanic), and siliciclastic rocks (sandstone), and lipid yield were examined across groups. A visual summary is provided in Figure 46. The Kruskal-Wallis rank sum test indicated no statistically significant variation in lipid yields across the three lithological groups ($\chi^2 = 1.80$, df = 2, $p = 0.406$). Consequently, no post-hoc pairwise comparisons were performed.

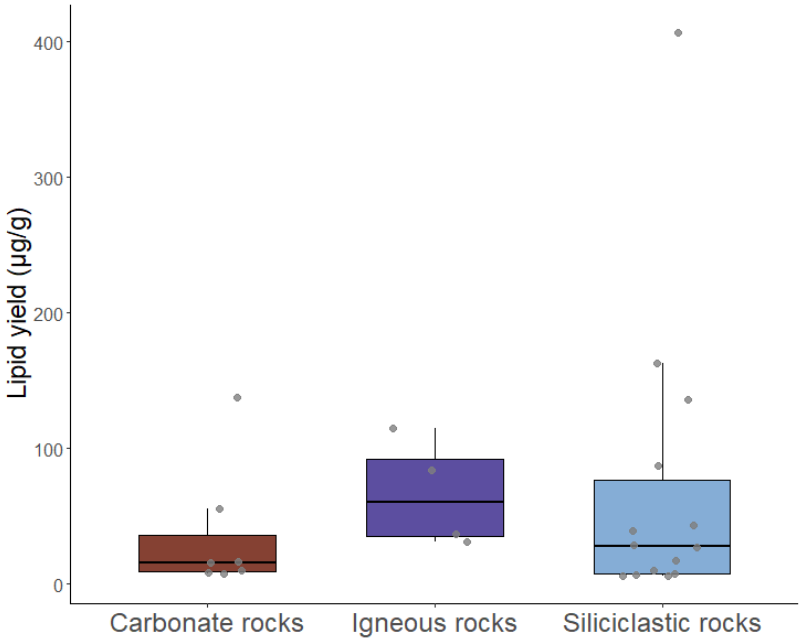


Figure 46. Boxplot of lipid yields for La Draga samples, categorised by lithological categories, carbonate rocks (marl, limestone) (n = 7), igneous rocks (volcanic) (n = 4), and siliciclastic rocks (sandstone) (n = 14). Grey points represent individual data values.

Lipid extracts from HAS revealed a chemically diverse range of compounds (Table 8 and Annex 4). Although the lipid composition and abundance differed from those of the sediments, they exhibit several important similarities. Across all samples (including internal, external and deposits), the lipid profile was dominated by short- to long-chain **saturated fatty acids (SFA)**, which mainly spanned between $C_{8:0}$ to $C_{30:0}$, dominated by **palmitic ($C_{16:0}$)** and **stearic ($C_{18:0}$) acids** (Figure 47), with a palmitic:stearic ratio (P/S) ranging from 0.82 to 2.20. The distribution of SFAs broadly resembles that observed in the sediments, even though similar P/S ratios have been also found among aquatic organisms (Craig et al., 2007; Papakosta et al., 2015), as well as in monogastric animals such as pig (Regert, 2011). Post-depositional degradation, especially under anaerobic conditions such as at La Draga, may have affected fatty acid profiles (Evershed et al., 1992; Rosiak, Kałużna-Czaplińska and Gątarek, 2020), and thus the ratios should be interpreted with caution.

Likewise, **monomethyl-branched fatty acids** ($C_{15:0Br}$ and $C_{17:0Br}$) were detected in 86% (n = 24) and 79% (n = 22) of the samples, respectively, and were also present in the sediments. While these compounds are found naturally in the adipose and dairy fats of ruminant animals (Evershed, 1993; Regert, 2011), they are also commonly associated with soil bacterial activity (Dudd, Regert and Evershed, 1998; Kühn, Schweitzer and Ruess, 2019). As such their soil microbial origin remains plausible, especially in degraded or low-lipid samples. Traces of **cholesterol** and some of its derivatives (e.g. cholestan-3-ol, cholesterol methyl ether, 7-keto-cholesterol) were identified in 25% (n = 7) of the

samples, with three also containing lanost-8en-3-ol. These compounds are commonly associated with ruminant fats (Regert, 2011; Hammann et al., 2018; Whelton et al., 2021), but again were found in natural and archaeological sediments (Wen-Yen and Meinschein, 1976; Mallol et al., 2025). Notably, four of these cholesterol-containing samples also exhibited **plant sterols**, such as γ/β-sitosterol, campesterol, stigmasterol, along with their derivatives (e.g. stigmastan-3,5-diene, stigmastanol, stigmast-5-ene,3β-methoxy) (Figure 48). While the combined presence of monomethyl-branched fatty acids and cholesterol could tentatively be linked to the presence of ruminant fats, the co-occurrence of plant sterols and their common presence in the sediments suggests they may have also derived from soil organic matter.

Many other compounds detected in the sediments were also identified in the HAS. These include **monounsaturated fatty acids (MUFA)** ($C_{16:1}$; 36%, n = 10; $C_{18:1}$; 68%, n = 19; $C_{22:1}$; 57%, n = 16) (Figure 47), ***n*-alkanes** present in small amounts (57%, n = 16) (Figure 48), traces of **benzene tricarboxylic acid** (21%; n = 6) (Figure 49), and long-chain linear alcohols (C_{18} to C_{32}; 18%, n = 5) (Figure 50). **Alkylresorcinols** (AR23 and AR25) were detected in both the internal and external aliquots of a single HAS (LD23-25396; Figure 51). Among **isoprenoid acids**, 4,8,12-TMTD (18%; n = 5), pristanic acid (93%; n = 26) and phytanic acid (61%; n = 17) were also present, although with generally low SRR percentage (with only one exceeding 75%). Notably, 4,8,12-TMTD was detected solely in four external and one deposit aliquots of some HAS. Its presence in the contextual sediment samples, combined with the absence of APAAs, suggest that these compounds most likely derive from environmental lipids (e.g. lakeshore environment) rather than from the original use of the stones.

Oxidation products such as **hydroxy fatty acids** (C_{20} to C_{28}; 11%, n = 3), and **dicarboxylic acids** (C_9 to C_{28}; 54%, n = 15) were also present. Their occurrence in particular, may reflect not only prolonged environmental degradation but also exposure to heat, possibly linked to artefact use involving repeated heating during cooking practices (Regert et al., 1998; Eerkens, 2005). Nevertheless, among these oxidation products, tridecanedioic acid (brassylic acid, C_{13}) emerged as the most frequently detected diacid in HAS samples, albeit in low amounts, and was absent in the sediments. This compound is likely formed through the oxidative degradation of erucic acid ($C_{22:1}$) (Fuessl, Yamamoto and Schneller, 2012; Copley et al., 2005a), a monounsaturated fatty acid particularly abundant in certain seed oils. The presence of such diacids may, therefore, point to the processing of plant materials potentially under heating conditions that accelerated lipid oxidation. In addition to the compounds shared with the sediments, other lipids were detected exclusively in the HAS samples.

This is the case of **diterpenoid** compounds (19-Norabieta-8,11,13-triene, 10,18-Bisnorabieta-8,11,13-triene, Isopimaric acid, Abietatriene, Dehydroabietal, Methyl dehydroabietate), which are indicative of coniferous resin use and were identified in a limited subset of HAS samples, specifically

in 13% of external (n = 2) and 10% of internal samples (n = 1) (Figure 49). Among these, dehydroabietic acid, the most abundant compound of pitch from *Pinus* species, is typically formed through the oxidative degradation of abietic acid under conditions of heat exposure (Dimitrakoudi et al., 2011). The simultaneous presence of biomarkers such as methyl dehydroabietate, dehydroabietal, norabietatrienes, and isopimaric acid point towards pyrolysis of pine wood. These compounds are well-documented thermal transformation products of conifer resins and are widely used as diagnostic indicators of heated pine-based materials in archaeological contexts (Rageot et al., 2021; Dimitrakoudi et al., 2011).

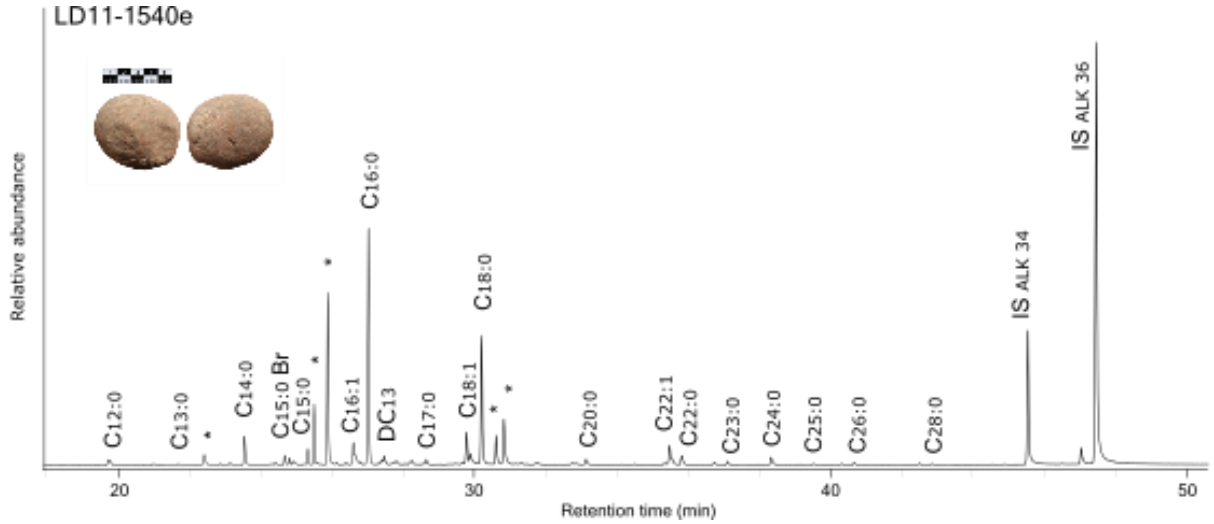


Figure 47. Partial total ion chromatograms (TIC) of acid/methanol extract of HAS sample LD11-1540e showing saturated fatty acids ($C_{XX:0}$), diacids (DC_{XX}), branched ($C_{XX:0}$ Br), unsaturated fatty acids ($C_{XX:1}$), contaminants (*), and *n*-alkanes internal standards (IS $_{ALKXX}$).

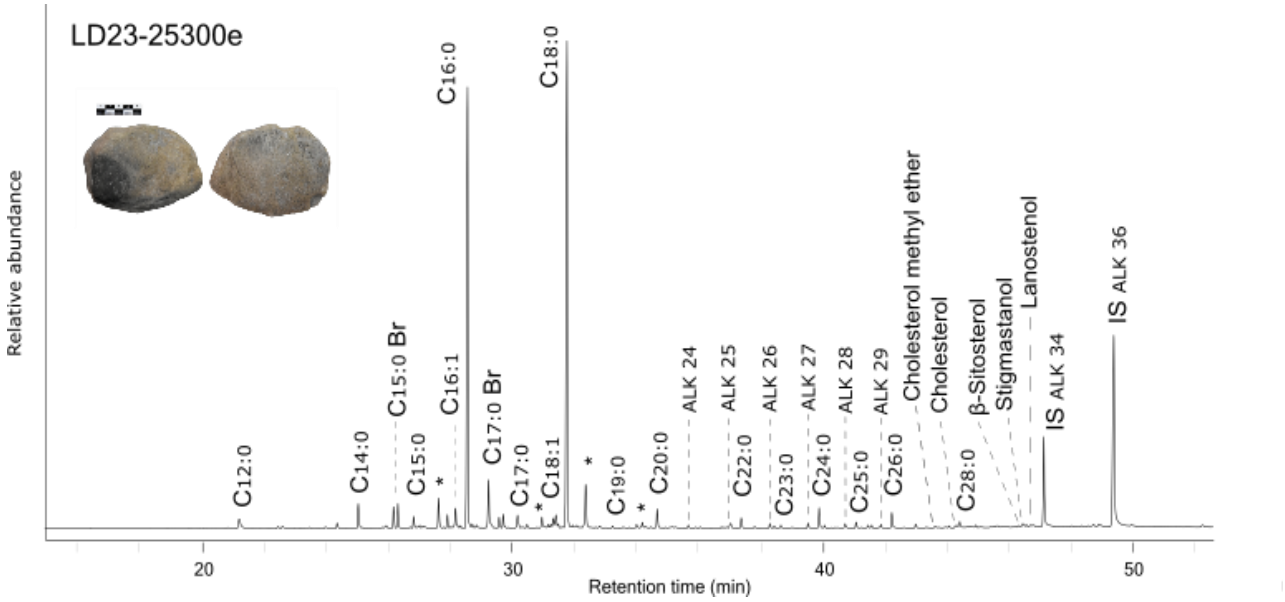


Figure 48. Partial total ion chromatograms (TIC) of acid/methanol extract of HAS sample LD11-25300e showing saturated fatty acids ($C_{XX:0}$), branched ($C_{XX:0}$ Br), unsaturated fatty acids ($C_{XX:1}$), *n*-alkanes (ALK xx), sterols and derivatives, contaminants (*), and *n*-alkanes internal standards (IS $_{ALKXX}$).

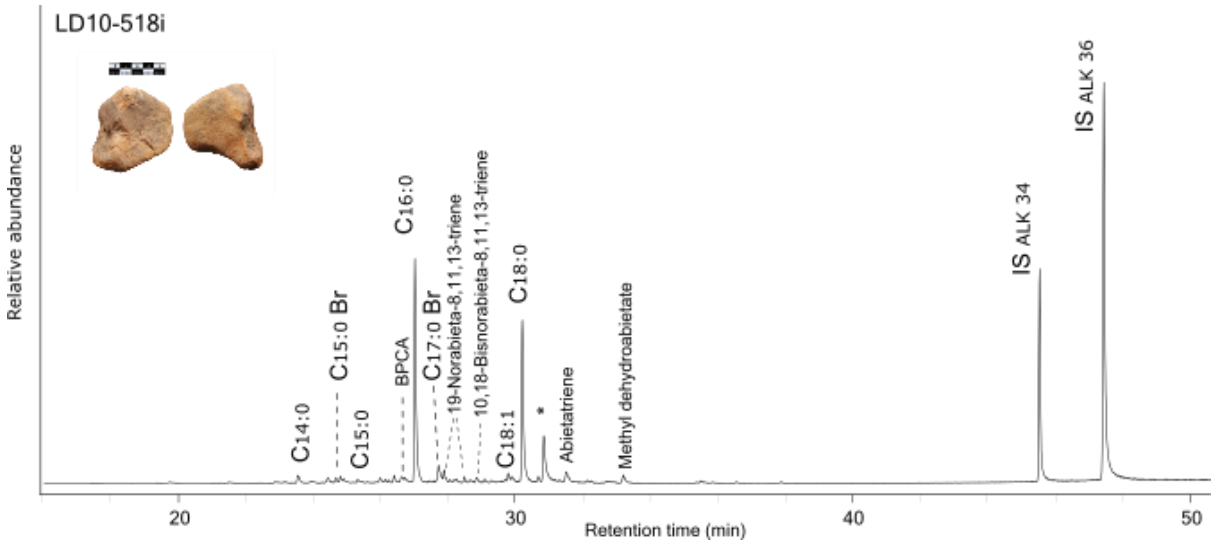


Figure 49. Partial total ion chromatograms (TIC) of acid/methanol extract of HAS sample LD10-518i showing saturated fatty acids ($C_{XX:0}$), branched ($C_{XX:0}$ Br), unsaturated fatty acids ($C_{XX:1}$), benzene polycarboxylic acid (BPCA), diterpenoids, contaminants (*), and *n*-alkanes internal standards (IS $_{ALKXX}$).

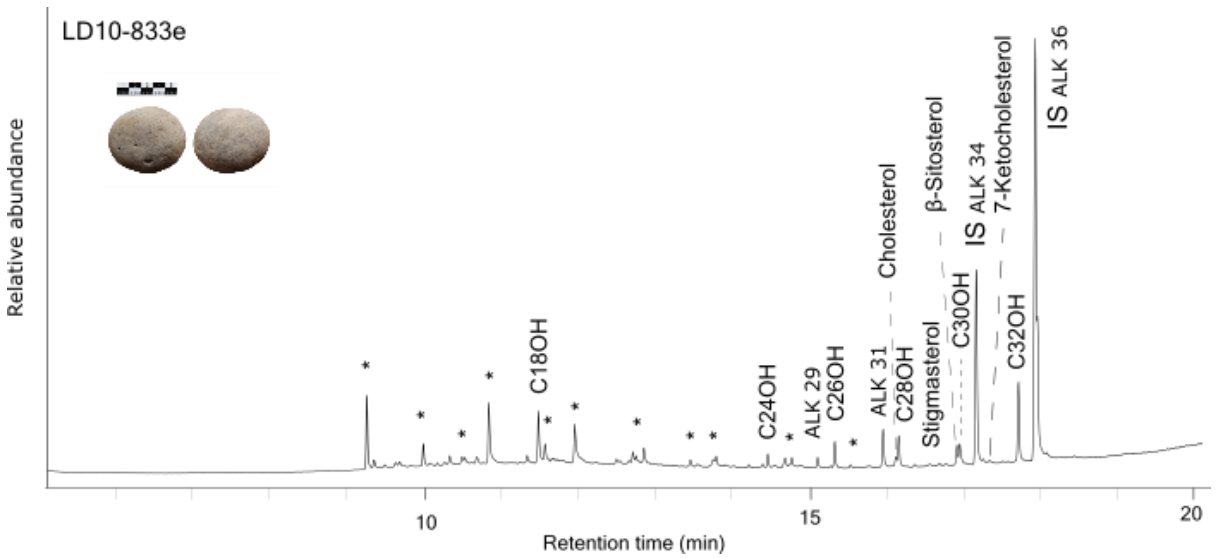


Figure 50. Partial total ion chromatograms (TIC) of solvent extract of HAS sample LD10-833e showing linear alcohols (CxxOH), *n*-alkanes (ALKxx), sterols and derivatives, contaminants (*), and *n*-alkanes internal standards (IS $_{ALKXX}$).

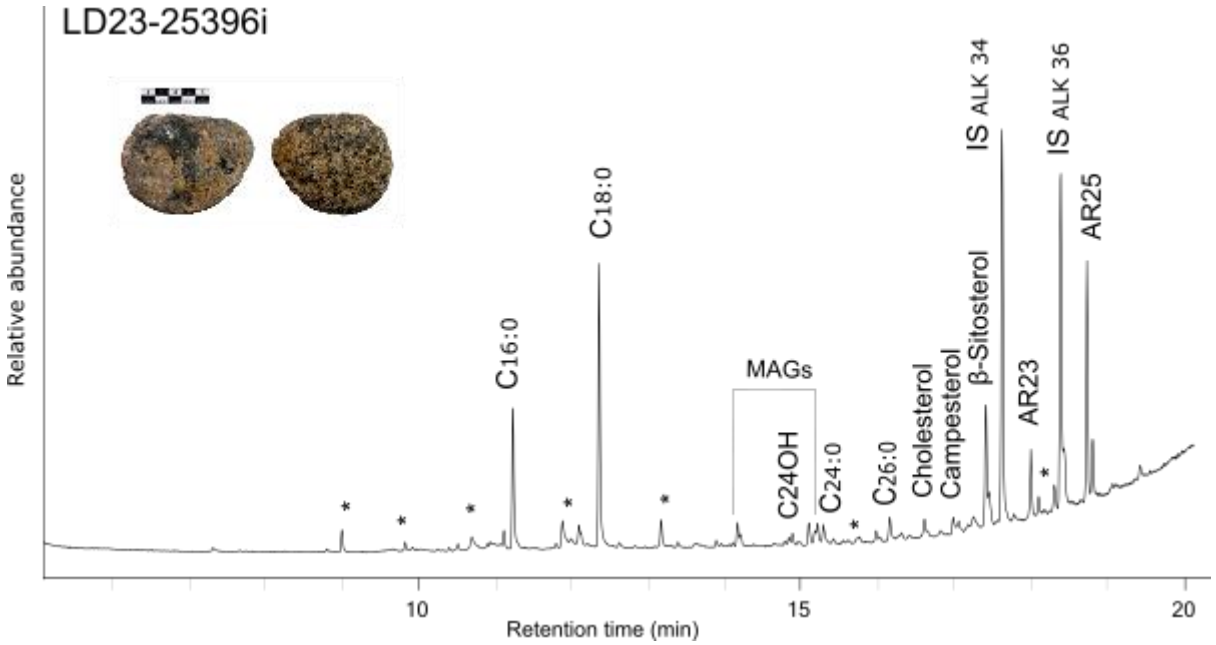


Figure 51. Partial total ion chromatograms (TIC) of solvent extract of HAS sample LD23-5396i showing saturated fatty acids ($C_{XX:0}$), linear alcohols (CxxOH), monoacylglycerols (MAGs), sterols and derivatives, alkylresorcinol (ARxx), contaminants (*), and *n*-alkanes internal standards (IS $_{ALKXX}$).

It is worth noting that compounds typically associated with the prolonged heating of terrestrial and aquatic oils in ceramics matrix, such as *ω*-(o-alkylphenyl) octadecanoic acids (Hansel et al., 2004; Bondetti et al., 2021a) and long-chain ketones (Evershed et al., 1995a), were not detected in any of the analysed HAS, including those showing visible evidence of thermal alteration. Their absence suggests that the thermal modification of these stones may not have been directly linked to the cooking or processing of plant or animal products and could instead reflect alternative uses, such as exposure to fire for technological, ritual, or domestic purposes. However, the absence of APAAs in stones is not necessarily unusual. Laboratory experiments have shown that APAAs formation can be influenced by factors such as the type of stone or ceramic, heating conditions, and the chemical composition of the material (Evershed et al., 2008b; Bondetti et al., 2021a; Langley, 2024). Low APAAs distributions have been observed even under controlled conditions, suggesting that their absence in archaeological stones may fall within the natural variability of biomarker formation rather than indicating the complete lack of animal or plant lipids.

To gain further insight into the origin of the lipid compounds, their distinction from the surrounding sediments, and to explore the functional significance of HAS at La Draga, stable isotope analysis of main fatty acids was undertaken.

6.1.3.1. Stable carbon isotope analysis

To further assess the origin and potential processing of lipid residues recovered from the sediments and HAS, stable carbon isotope ($\delta^{13}C$) analyses were conducted on the predominant saturated fatty acids, palmitic ($C_{16:0}$) and stearic ($C_{18:0}$). For each sample, an aliquot of the acidified extract was retained for GC-C-IRMS analysis, following the removal of sulphur using activated copper. The resulting isotopic data are presented and discussed below.

The $\delta^{13}C$ values of palmitic ($C_{16:0}$) and stearic ($C_{18:0}$) acids were obtained from 44% (n = 4) of sediment samples, ranging from -32‰ to -30‰ and from -35‰ to -31‰, respectively (Table 7, Figure 52). Most samples plotted within the C_3 plant range, with a single sample (LD-JA81-VIa b) overlapping the wild-ruminant cluster. This sample suggests that the isotopic composition of the sediments may record anthropogenic inputs from on-site human activities, such as the processing of animal products, which would be corroborated by faunal remains recovered from the reference square JA81 (Antolín et al., 2014). Interestingly, another sediment sample from the same square (LD-JA81-VIa g) did not show a similar isotopic signal.

In contrast, $\delta^{13}C$ values of palmitic ($C_{16:0}$) and stearic ($C_{18:0}$) acids obtained from HAS samples display a broad distribution, ranging approximately from -36‰ to -28‰ for $\delta^{13}C_{16:0}$, and -32‰ and -28‰ for $\delta^{13}C_{18:0}$ (Table 8, Figure 52). Most HAS samples cluster within the isotopic ranges associated with C_3 plant or freshwater lipid sources, with fewer aligning with the wild non-ruminant and domestic ruminant reference values. Notably, most HAS values fall within the isotope distribution of the sediment samples. These comparable signatures, together with a similar lipid profile, may indicate an environment (prior to their use) or sedimentary (post-deposition at the site) origin of lipids. A few samples plot within the C_3 wood range, potentially reflecting lipids derived from burnt wood used as fuel in combustion structures. In addition, some samples fall outside the defined reference ellipses and the distribution of sediment samples.

To evaluate the potential contribution of different food sources to the isotopic signatures observed in the samples, a calculation was undertaken based on the theoretical mixing of varying proportions of resource categories (Annex 5). This approach allows for the assessment of how combinations of different source inputs might influence the resulting isotopic values. To achieve this, theoretical mixing lines were developed using a two-source concentration equation in (Dudd, 1999) and data are presented in Annex 5. These mixing lines represent the expected isotopic values resulting from various proportional combinations of animal fats and plant-derived oils (Figure 52). Some samples plot along the mixing curves between the reference C_3 plant products and domestic porcine adipose fats, as well as between C_3 plant products and wild non-ruminant adipose fat (e.g. wild boar and rabbit (Saña,

2011)), indicating a predominance of C_3 plant-derived oils over animal fats. A few samples could not be matched with the analysed reference resources, suggesting additional sources were present but not captured in this study. These could include, for example, aquatic birds, which are also documented in the archaeological record (Garcia, 2011; Antolín et al., 2013; Piqué et al., 2015). These observations, however, comprehensively support the hypothesis of a mixture of animal adipose fats and plant oils for these specific samples.

When plotting the derived $\Delta^{13}C$ values against $\delta^{13}C_{16:0}$, 96% (n = 27) of HAS, samples are grouped between 6.3‰ and -1‰, which is a range indicative of non-ruminant adipose fats and plants (Figure 52). This pattern suggests that mixtures of animal adipose fats and plant oils should be considered, as they can produce similar isotopic signatures (Hendy et al., 2018). In contrast, the sediment samples are evenly distributed, falling within the non-ruminant/plant region and the ruminant/plant area.

Statistical comparisons of stable carbon isotope values between internal and external HAS layers at La Draga were conducted to assess whether isotopic compositions varied according to the sampled aliquots. Using Wilcoxon rank sum tests, no significant differences were observed for $\delta^{13}C_{16:0}$ ($W = 91.5$, $p = 0.375$) or $\delta^{13}C_{18:0}$ ($W = 85.5$, $p = 0.579$) between internal and external layers. These results suggest that isotopic values are broadly consistent across HAS layers providing coherent isotopic information.

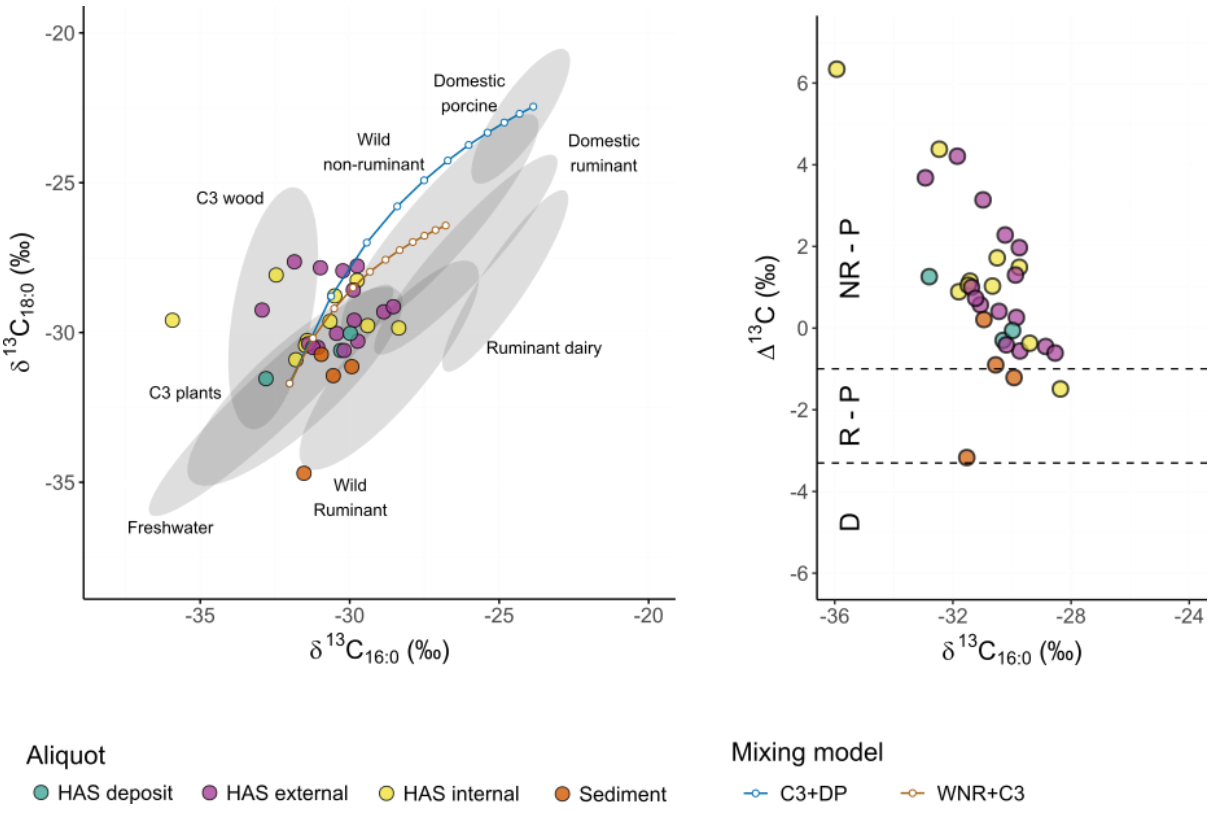


Figure 52. Plots of $\delta^{13}C$ values of palmitic ($C_{16:0}$) and stearic acid ($C_{18:0}$) for HAS and sediment samples at La Draga. Coloured symbols indicate different aliquot types, while shaded ellipses represent reference ranges for modern reference, showing 68% confidence ellipses (see Figure 13, chapter 3.1.2; Annex 3). Abbreviations: D = dairy products, R = ruminant adipose fat, NR = non ruminant adipose fat, P = plant products. Mixing curves are as described in Annex 5. The mixing curves have been calculated to illustrate the $\delta^{13}C$ values which would result from the mixing of C_3 plant products (C3), domestic porcine adipose fat (DP), and wild non ruminant adipose fat (WNR).

Considering the isotopic distributions as a function of lipid concentration, many of the high-yield HAS samples plotted outside the established reference ellipses, along the animal-plant mixing lines (Figure 53), and contained animal lipids (cholesterol) together with plant-related compounds (sterols) together with isotopic values distinct from the sediments (Figure 54A-B). Furthermore, HAS samples containing alkylresorcinols exhibited isotopic profiles that differed from those of sediment samples also containing AR (Figure 54C). By contrast, samples containing diterpenoids show a different isotopic pattern, mostly falling within the reference range for C_3 plants and sediments (Figure 54D), although diterpenoids were not detected in the sediments, suggesting their occurrence in the HAS reflect a distinct source.

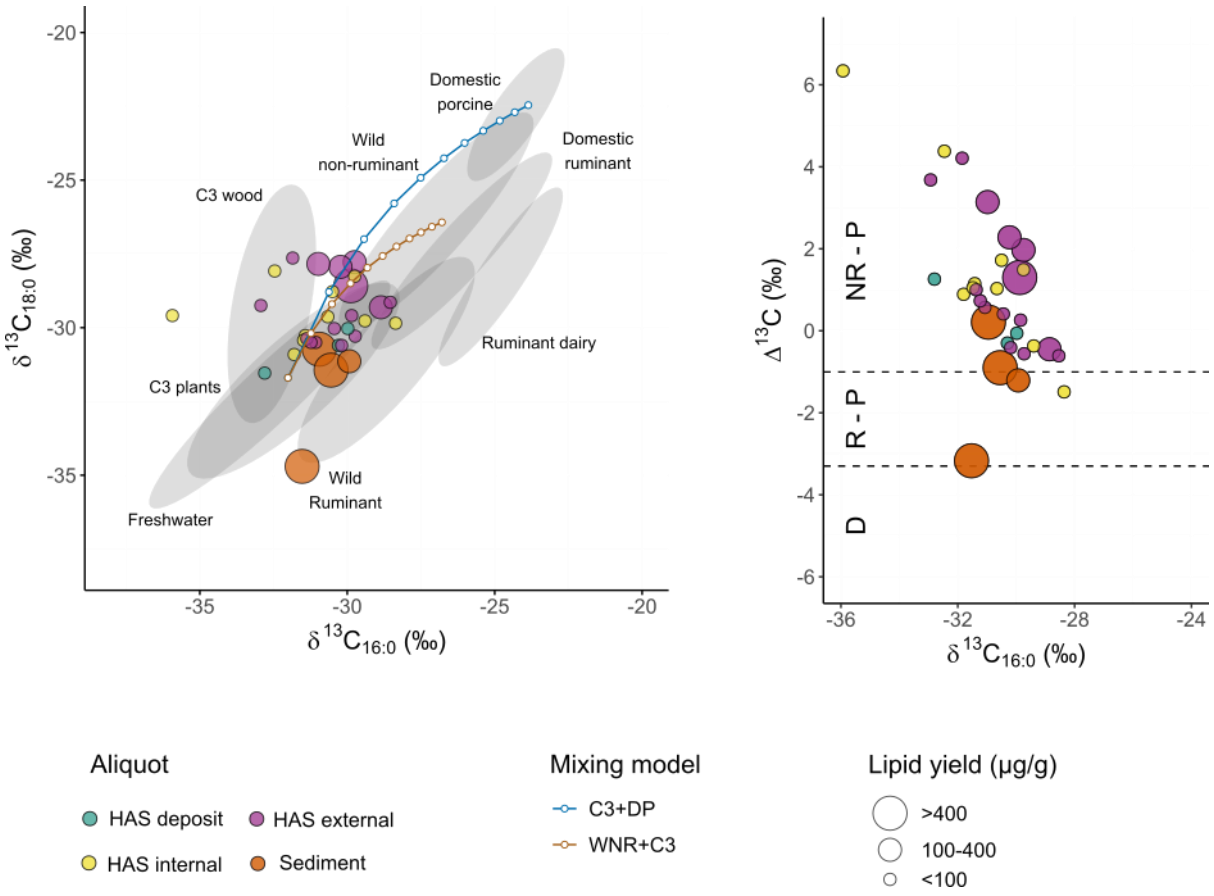


Figure 53. Plots of $\delta^{13}C$ values of palmitic ($C_{16:0}$) and stearic acid ($C_{18:0}$), and $\Delta^{13}C$ (the difference between the $\delta^{13}C$ values of the $C_{16:0}$ and $C_{18:0}$ fatty acids) versus $\delta^{13}C_{16:0}$, for HAS samples at La Draga. Point size is proportional to total lipid concentration, and colours indicate different aliquot types. Grey shaded ellipses show 68% confidence intervals for modern reference ranges see Figure 13, chapter 3.1.2; Annex 3). Abbreviations: D = dairy products, R = ruminant adipose fat, NR = non ruminant adipose fat, P = plant products. Mixing curves are as described in Annex 5. The mixing curves have been calculated to illustrate the $\delta^{13}C$ values which would result from the mixing of C_3 plant products (C3), domestic porcine adipose fat (DP), and wild non ruminant adipose fat (WNR).

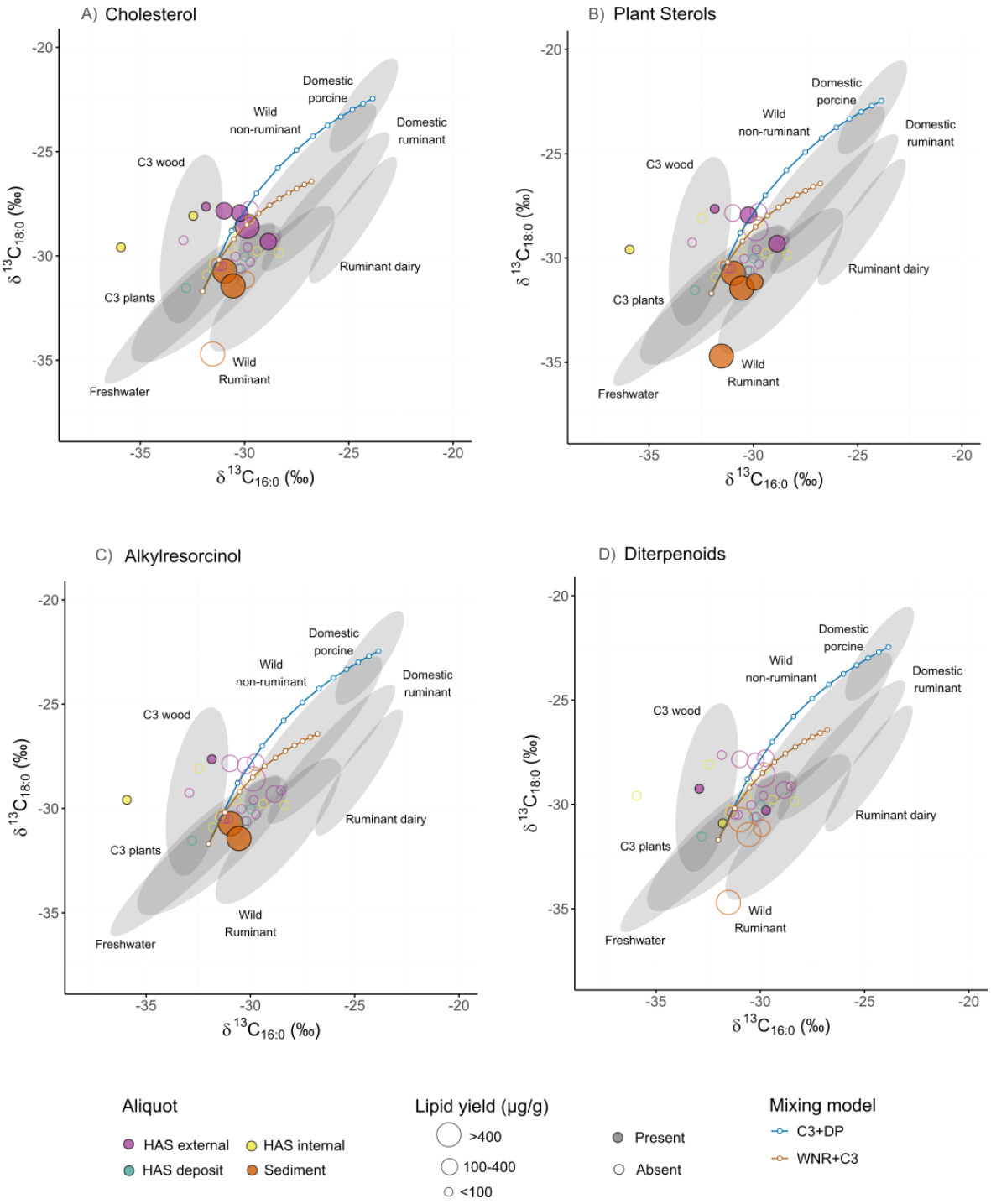


Figure 54. Plots of $\delta^{13}C$ values of palmitic ($C_{16:0}$) and stearic acid ($C_{18:0}$) for samples at La Draga. The presence (filled points) and absence (open points) of cholesterol (A), plant sterols (B), alkylresorcinol (C) and diterpenoids (D) are indicated. Colours correspond to different aliquot types, and grey shaded ellipses show 68% confidence intervals for modern reference ranges (see Figure 13, chapter 3.1.2; Annex 3). Mixing curves are as described in Annex 5. The mixing curves have been calculated to illustrate the $\delta^{13}C$ values which would result from the mixing of C_3 plant products (C3), domestic porcine adipose fat (DP), and wild non ruminant adipose fat (WNR).

Some interesting considerations can be made regarding the two different occupation phases of the site based on lipid composition and isotopic signatures. HAS samples from the oldest phase, characterised by wooden structures, contain relatively high concentrations of lipids, including cholesterol, plant sterols, and alkylresorcinols, whereas the corresponding sediment sample contains only plant sterols. This suggests that some compounds preserved on the lithics may reflect human activities, rather than solely environmental inputs. Furthermore, the isotopic signatures of some HAS align with C_3 wood, and several other samples are associated with combustion structures (Figure 55A), which is consistent with the use of wood as fuel. By contrast, HAS samples from the most recent Neolithic occupation phase, characterised by the construction of travertine block pavement and structures, exhibit lower lipid yields (Figure 55B), suggesting either reduced accumulation of organic residues or different lithic use compared with the earlier phase. Some samples contain diterpenoids, indicative of the processing or use of conifer products during this occupation. By contrast, the corresponding sediments contain AR, which are absent from the HAS, highlighting differences between environmental inputs and residues preserved on the lithics.

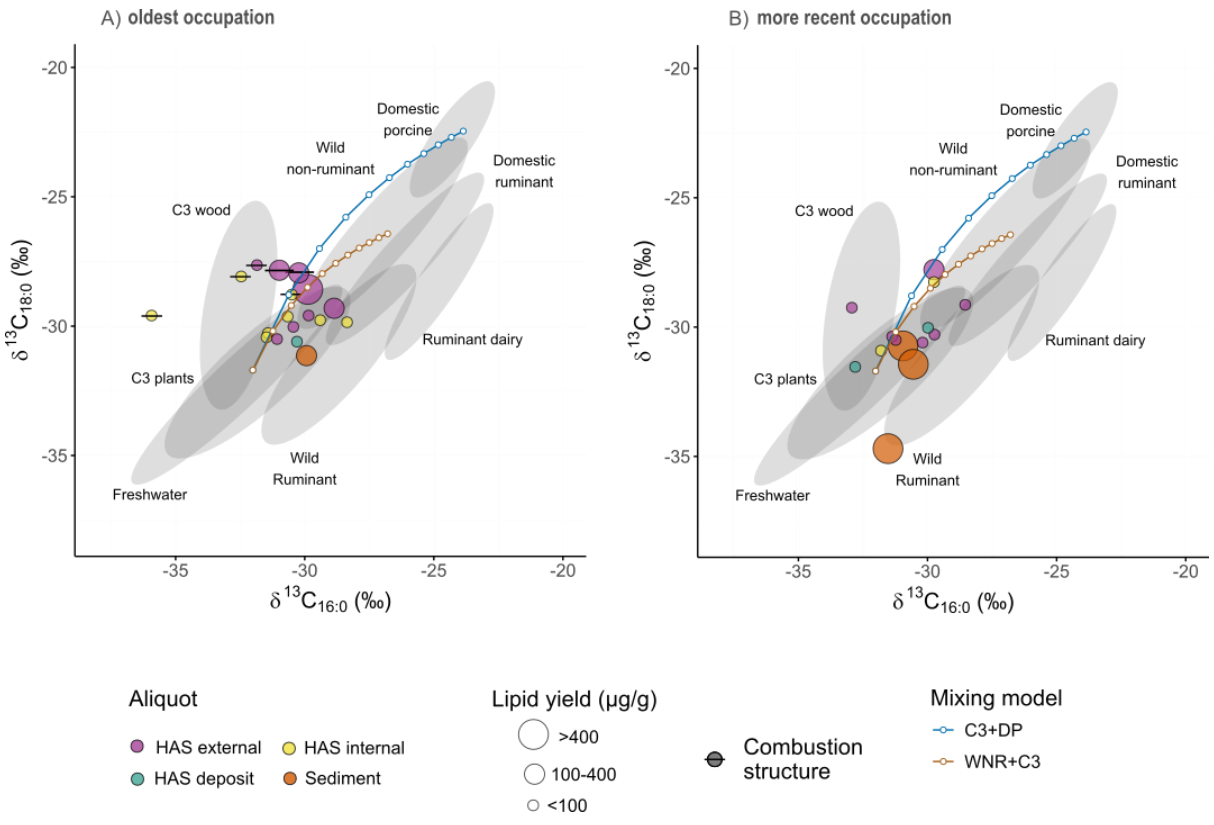


Figure 55. Plots of $\delta^{13}C$ values of palmitic ($C_{16:0}$) and stearic acid ($C_{18:0}$) for samples at La Draga, subdivided between the oldest occupation (A) and more recent Neolithic occupation (B) phase. Colours correspond to different aliquot types, and grey shaded ellipses show 68% confidence intervals for modern reference ranges (see Figure 13, chapter 3.1.2; Annex 3). Mixing curves are as described in Annex 5. The mixing curves have been

calculated to illustrate the $\delta^{13}C$ values which would result from the mixing of C_3 plant products (C3), domestic porcine adipose fat (DP), and wild non ruminant adipose fat (WNR).

Considering the co-occurrence of aquatic biomarkers (4,8,12-TMTD, pristanic and phytanic acids) in both sediments and HAS samples, the isotopic signatures suggest a potential exploitation of freshwater resources (Figure 56), consistent with the lakeshore settings of the site. However, the relatively low %SRR of phytanic acid, combined with the evaluation of $\Delta^{13}C$ against %SRR, does not provide a definitive distinction between aquatic and terrestrial inputs as observed in other studies (Lucquin et al., 2016; Shoda et al., 2020). Therefore, while aquatic inputs cannot be ruled out, the evidence is more consistent with a combination of environmental deposition and minor contributions from aquatic organisms, rather than clear indications of targeted exploitation.

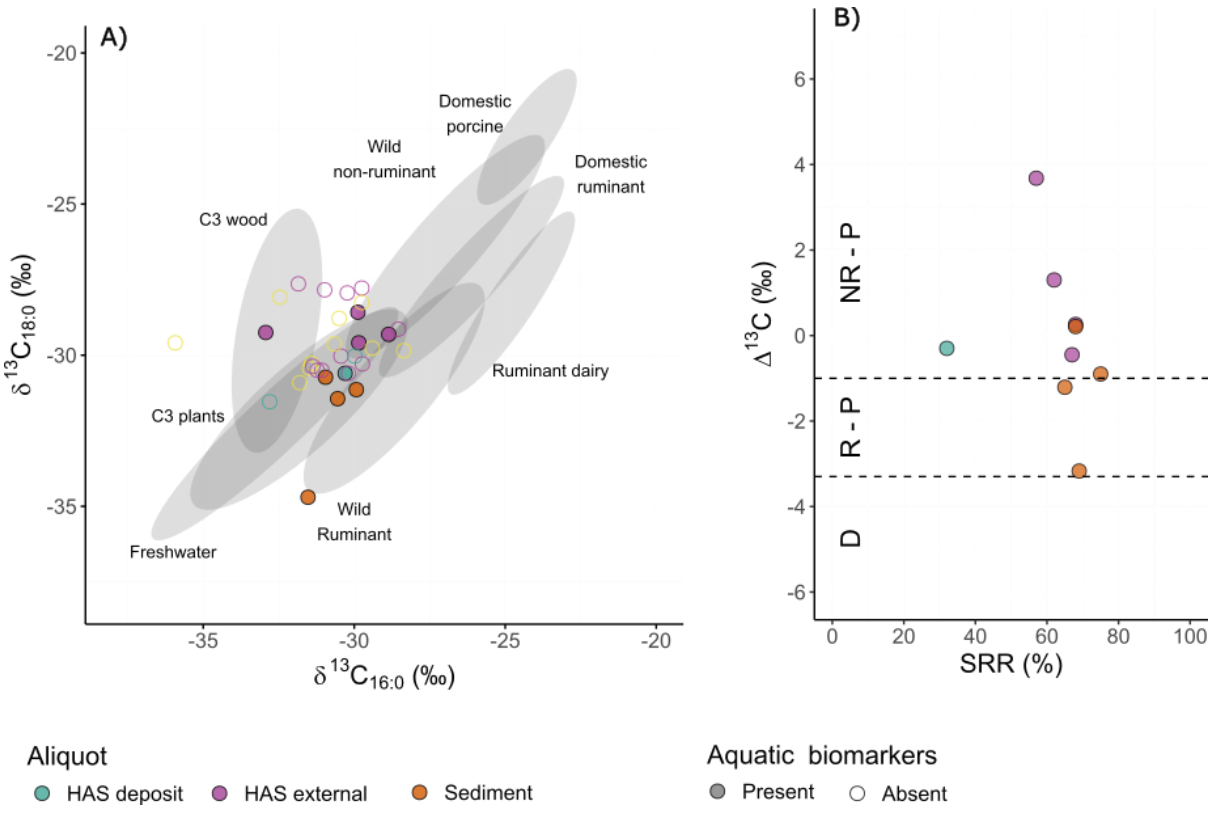


Figure 56. (A) Plot of $\delta^{13}C$ values of palmitic ($C_{16:0}$) and stearic acid ($C_{18:0}$) and (B) $\Delta^{13}C$ (the difference between the $\delta^{13}C$ values of the $C_{16:0}$ and $C_{18:0}$ fatty acids) versus %SRR diastereomer, for samples at La Draga. The presence (filled points) and absence (open points) of aquatic biomarkers (4,8,12-TMTD, pristanic and phytanic acids) are indicated. Colours correspond to different aliquot types, and grey shaded ellipses show 68% confidence intervals for modern reference ranges (see Figure 13, chapter 3.1.2; Annex 3).

Synthetic conclusion on the site of La Draga

Taken together, the results from La Draga indicate that some HAS preserve a range of molecular and isotopic compositions, with some dominated by soil organic matter, and others reflecting a mixture of environmental inputs and anthropogenic activity, including the processing of plant and animal products. It should be emphasised that the sediments themselves may not solely reflect environmental lipids. Given that they were collected from areas associated with archaeological evidence of human activity, they could also carry anthropogenic signatures, consistent with other studies (Heron et al., 2010; Sistiaga et al., 2014; Kanthilatha et al., 2014; Choy et al., 2016). Moreover, the two occupation phases at the site are associated with distinct residue patterns, with the oldest phase reflecting more intensive use of organic resources, including plant and animal materials and wood as fuel, and the more recent phase indicating lower residue accumulation and evidence for the use of conifer products. Overall, these patterns highlight how residue preservation reflects both environmental inputs and changes in site use and human activities over time.

Table 7. Summary of lipid analyses results on sediments from La Draga. Lipid yields are presented alongside the principal and diagnostic compounds detected through combined extractions (AE, SE), with associated stable carbon isotope data. Compounds include saturated fatty acids (SFA), branched fatty acids (BrFA), unsaturated fatty acids (UFA), hydroxy FA (Hy), dicarboxylic fatty acids (DC), n-alkanes (ALK), alcohols (OH), ketones (K), terpenoids (terp), isoprenoids (4,8,12-TMTD: 4,8,12-trimethyl-tridecanoic acid, pri: pristanic acid; phy: phytanic acid), sterols (ster), monoacylglycerols (MAGs), wax esters (WE), alkyresorcinol (AR), and additional biomarkers (B3CA: benzene tricarboxylic acid). Compounds in red were found in both HAS and sediments. Stable carbon isotope ($\delta^{13}C$) values are present as $\delta^{13}C_{16:0}$ (‰), $\delta^{13}C_{18:0}$ (‰), together with the isotopic offset $\Delta^{13}C$ (‰), calculated as $\delta^{13}C_{18:0}$ - $\delta^{13}C_{16:0}$.

Material	*Sample*	*Lipid yield (µg/g)*	*$C_{16:0}/C_{18:0}$*	*$C_{18:1}/C_{18:0}$*	*Major and diagnostic compounds detected*	*$\delta^{13}C_{16:0}$ (‰)*	*$\delta^{13}C_{18:0}$ (‰)*	*$\Delta^{13}C$ (‰) ($\delta^{13}C_{18:0}$ - $\delta^{13}C_{16:0}$)*
Sediment	JC78-VIa	1742.27	2.59	1.47	SFA (C12, C14-28, C29, C30, C32), BrFA (C13, C15, C17), UFA (C16:1, C18:1, C20:1, C22:1), Hy (C16, C22, C23, C24, C25, C26), DC (C8, C9-11, C16, C18, C19, C22, C23, C24-26, C28), ALK (C27, C29, C31), OH (C18, C20, C22, C23, C24, C26, C28, C32), terp (Amyrin, Friedelen-3-one, Betulin, Lupeol, Lupeol der), 4,8,12-TMTD, pri, phy (68% SRR), ster (Cholesterol, Stigmasterol, β-Sitosterol, Stigmastanol), WE (C42, 44, 46, 48), AR (AR23, 25)	-30.95	-30.73	0.22
Sediment	JA81-VIa b	1750.49	2.19	2.26	SFA (C12, C14-28, C29, C30), BrFA (C13, C15, C17), UFA (C16:1, C18:1, C20:1, C22:1), Hy (C16, C22, C23, C24, C25, C26), DC (C8, C9, C16, C18, C24-26, C28), terp (Amyrin, Friedelen-3-one, Betulin), 4,8,12-TMTD, pri, phy (69% SRR), ster (β-Sitosterol, Stigmastanol)	-31.53	-34.70	-3.17
Sediment	JA81-VIa g	1070.80	2.17	2.12	SFA (C12-28, C29, C30), BrFA (C13, C15, C17), UFA (C16:1, C18:1, C20:1, C22:1), Hy (C16, C22, C23, C24, C25, C26), DC (C9, C11, C13, C16, C18, C24-26, C28), ALK (C27, C29, C31), OH (C18, C20, C22, C23, C24, C26, C28, C32), terp (Amyrin, Friedelen-3-one, Betulin, Lupeol der), 4,8,12-TMTD, pri, phy (75% SRR), ster (Cholesterol, Stigmasterol, β-Sitosterol, Stigmastanol), MAGs, WE (C46, 48), AR (AR21, 25), B3CA	-30.55	-31.44	-0.89
Sediment	JA81-VIa n	399.97	2.79	1.63	SFA (C9-28, C29, C30), BrFA (C13, C15, C17), UFA (C16:1, C18:1, C20:1, C22:1), Hy (C16, C21, C22, C23, C24, C25, C26), DC (C8, C9, C16, C18, C24-26, C28, C30), terp (Amyrin, Friedelen-3-one, Betulin), 4,8,12-TMTD, pri, phy (71% SRR), ster (β-Sitosterol, Stigmastanol)			

Material	*Sample*	*Lipid yield (µg/g)*	$C_{16:0}/C_{18:0}$	$C_{18:1}/C_{18:0}$	*Major and diagnostic compounds detected*	$\delta^{13}C_{16:0}$ (‰)	$\delta^{13}C_{18:0}$ (‰)	$\Delta^{13}C$ (‰) ($\delta^{13}C_{18:0} - \delta^{13}C_{16:0}$)
Sediment	JA79-VIa b	348.08	1.97	2.06	SFA (C9, C11-12, C14-28, C29, C30), BrFA (C13, C15, C17), UFA (C16:1, C18:1, C20:1, C22:1), Hy (C22, C23, C24, C25), DC (C9, C16, C18, C24, C26, C28), terp (Amyrin, Friedelen-3-one, Betulin), ster (β-Sitosterol, Stigmastanol), B3CA			
Sediment	JA79-VIa g	545.32	2.63	1.70	SFA (C8-28, C29, C30, C32), BrFA (C13, C15, C17), UFA (C16:1, C18:1, C20:1, C22:1), Hy (C16, C21, C22, C23, C24, C25), DC (C9, C11, C16, C18, C24-26, C28), terp (Erythrodiol, Amyrin, Friedelen-3-one, Betulin), 4,8,12-TMTD, pri, phy (62% SRR), ster (β-Sitosterol, Stigmastanol), B3CA			
Sediment	JA79-VIa n	2658.14	1.83	1.91	SFA (C10-28, C29, C30, C32), BrFA (C13, C15, C17), UFA (C16:1, C18:1, C20:1, C22:1), Hy (C16, C21, C22, C23, C24, C25, C26), DC (C9, C11, C16, C18, C24, C26, C28), terp (Erythrodiol, Amyrin, Friedelen-3-one, Betulin), 4,8,12-TMTD, pri, phy (70% SRR), ster (β-Sitosterol, Stigmastanol), B3CA			
Sediment	JC81-VII	290.60	3.75	1.20	SFA (C12, C14, C16-18, C20-28, C29), BrFA (C15, C17), UFA (C18:1), Hy (C21, C22, C23, C24, C25, C26), DC (C9, C16, C18, C22, C24, C26), terp (Amyrin, β-Amyrone, Friedelen-3-one), 4,8,12-TMTD, pri, phy (58% SRR), ster (Stigmastanol)			
Sediment	JG79-VII	134.50	2.86	1.67	SFA (C12, C14-24, C26-28, C29), BrFA (C13, C15, C17), UFA (C16:1, C18:1), Hy (C16, C21, C22, C23, C24, C25, C26), DC (C8-C10, C16, C18, C24-26), terp (Lupenone, Amyrin, Friedelen-3-one, Betulin, Betulinaldehyde, Oleandione), 4,8,12-TMTD, pri, phy (65% SRR), ster (β-Sitosterol, Stigmastanol)	-29.93	-31.14	-1.21

Table 8. Summary of lipid analyses results on HAS from La Draga. Lipid yields are presented alongside the principal and diagnostic compounds detected through combined extractions (AE, SE), with associated stable carbon isotope data. Compounds include saturated fatty acids (SFA), branched fatty acids (BrFA), unsaturated fatty acids (UFA), hydroxy FA (Hy), dicarboxylic fatty acids (DC), n-alkanes (ALK), alcohols (OH), ketones (K), terpenoids (terp), isoprenoids (4,8,12-TMTD: 4,8,12-trimethyl-tridecanoic acid, pri: pristanic acid; phy: phytanic acid), sterols (ster), monoacylglycerols (MAGs), alkyresorcinol (AR), and additional biomarkers (B3CA: benzene tricarboxylic acid). Compounds in red were found in both HAS and sediments. Stable carbon isotope ($\delta^{13}C$) values are present as $\delta^{13}C_{16:0}$ (‰), $\delta^{13}C_{18:0}$ (‰), together with the isotopic offset $\Delta^{13}C$ (‰), calculated as $\delta^{13}C_{18:0} - \delta^{13}C_{16:0}$.

Material	*Sample*	*Aliquot*	*Lipid yield (µg/g)*	*$C_{16:0}/C_{18:0}$*	*$C_{18:1}/C_{18:0}$*	*Major and diagnostic compounds detected*	*$\delta^{13}C_{16:0}$ (‰)*	*$\delta^{13}C_{18:0}$ (‰)*	*$\Delta^{13}C$ (‰) ($\delta^{13}C_{18:0} - \delta^{13}C_{16:0}$)*
HAS	LD10-500	e	162.57	0.95	24.95	SFA (C14-20, C22-24, C26, C28), BrFA (C15, C17), UFA (C16:1, C18:1, C22:1), DC (C10-11, C12, C13), ALK (C23, C24, C26, C27, C28, C29), pri, phy (28% SRR)	-29.75	-27.78	1.97
HAS	LD10-500	i	42.91	0.92		SFA (C12, C14-18, C20, C22, C24, C26), BrFA (C15, C17), UFA (C16:1, C18:1, C22:1), DC (C13), ALK (C23, C26, C27), pri (tr)	-29.75	-28.26	1.49
HAS	LD10-518	e	39.24	1.48	2.35	SFA (C12, C14-16, C18), BrFA (C15), UFA (C16:1, C18:1, C22:1), terp (19-Norabieta-8,11,13-triene, 10,18-Bisnorabieta-8,11,13-triene, Isopimaric acid, Abietatriene, Dehydroabietal, Methyl dehydroabietate), pri (tr), B3CA (tr)	-29.73	-30.29	-0.56
HAS	LD10-518	i	5.36	1.33	14.04	SFA (C14-16, C18), BrFA (C15, C17), UFA (C18:1), terp (19-Norabieta-8,11,13-triene, 10,18-Bisnorabieta-8,11,13-triene, Abietatriene, Methyl dehydroabietate), pri (tr), B3CA (tr)	-31.80	-30.91	0.89
HAS	LD10-663	e	8.47	0.96	11.89	SFA (C14-18, C20, C22, C24), BrFA (C15, C17), UFA (C16:1, C18:1, C22:1), DC (C13), pri (tr), phy (49% SRR)	-30.40	-30.00	0.40
HAS	LD10-663	i	10.01	1.28		SFA (C14-16, C18, C20), BrFA (C15, C17), UFA (C16:1)	-31.42	-30.27	1.15
HAS	LD10-833	e	137.42	1.27	6.28	SFA (C8-C27, C28, C30), BrFA (C15, C17), UFA (C18:1, C22:1), DC (C10, C12, C13, C16), ALK (C29, C31), OH (C18, C24, C26, C28, C30, C32), 4,8,12-TMTD, pri, phy (67% SRR), ster (Cholesterol, 7-keto-cholesterol, Stigmasterol, β-Sitosterol), B3CA (tr)	-28.90	-29.30	-0.40

Material	*Sample*	*Aliquot*	*Lipid yield (µg/g)*	$C_{16:0}/C_{18:0}$	$C_{18:1}/C_{18:0}$	*Major and diagnostic compounds detected*	$\delta^{13}C_{16:0}$ (‰)	$\delta^{13}C_{18:0}$ (‰)	$\Delta^{13}C$ (‰) ($\delta^{13}C_{18:0}$ - $\delta^{13}C_{16:0}$)
HAS	LD10-833	i	7.35	1.21	11.22	SFA (C14-18, C20, C22, C24), UFA (C18:1, C18:2, C22:1), pri, phy (60% SRR), B3CA (tr)	-29.40	-29.77	-0.37
HAS	LD11-1540	e	28.51	1.81	2.79	SFA (C12-18, C20, C22-26, C28), BrFA (C15), UFA (C16:1, C18:1, C22:1), DC (C13), ALK (C29, C31), pri, phy (63% SRR)	-28.54	-29.14	-0.60
HAS	LD11-1547	e	407.00	1.89	7.55	SFA (C12-18, C20, C22-26, C28, C30), BrFA (C17), UFA (C18:1, C22:1), Hy (C24), DC (C11, C12, 13), ALK (C17, C18, C25, C26, C27, C29-31), OH (C18), 4,8,12-TMTD (tr), pri, phy (62% SRR), ster (Cholesterol, β-Sitosterol), MAGs	-29.88	-28.58	1.30
HAS	LD11-1547	i	27.14	1.20		SFA (C14, C16-18, C20, C22), BrFA (C17), UFA (C22:1), ALK (C25), OH (C18), pri (tr), phy (48% SRR), MAGs	-30.66	-29.63	1.03
HAS	LD11-1987	e	16.98	2.20	7.28	SFA (C12-18, C20, C22-26, C28), BrFA (C15, C17), UFA (C16:1, C18:1, C22:1), DC (C13), ALK (C29, C31), terp (Methyl dehydroabietate), 4,8,12-TMTD, pri, phy (57% SRR)	-32.90	-29.30	3.60
HAS	LD11-2156	d	11.80	1.50	8.18	SFA (C12, C14-18, C20, C22, C24, C26, C28), BrFA (C15, C17), UFA (C16:1, C18:1, C18:2, C19:1, C22:1), DC (C13), 4,8,12-TMTD, pri, phy (32% SRR)	-30.30	-30.60	-0.30
HAS	LD11-2156	e	6.38	1.99		SFA (C12, C14-18, C20, C22, C24), BrFA (C15, C17), UFA (C18:1, C22:1), pri	-31.10	-30.50	0.60
HAS	LD11-2156	i	6.99	1.74		SFA (C12, C14-18, C20), BrFA (C15, C17), UFA (C18:1, C22:1), pri	-31.48	-30.43	1.05
HAS	LD12-3791	e	15.76	1.66		SFA (C12, C14-28, C30), UFA (C22:1), DC (C11, C12-15), ALK (C16, C18-23), 4,8,12-TMTD (tr), pri, phy (68% SRR)	-29.90	-29.60	0.30
HAS	LD12-3791	i	55.27	1.58		SFA (C12, C14, C16-20), ALK (C16, C18-23), OH (C18, C24), MAGs	-28.36	-29.85	-1.49
HAS	LD12-3951	d	12.75	1.03		SFA (C14-18, C20, C22-24, C26, C28), BrFA (C15), DC (C13), pri, phy (33% SRR)	-30.00	-30.00	0.00
HAS	LD12-3951	e	15.96	1.14		SFA (C14-18, C20, C22-26, C28), BrFA (C15, C17), DC (C13), pri	-30.20	-30.60	-0.40
HAS	LD12-4007	e	5.45	0.95		SFA (C14-18, C20, C22-26, C28), BrFA (C15, C17), ALK (C25, C27, C29, C31), pri, phy (78% SRR), B3CA (tr)	-31.40	-30.40	1.00

Material	*Sample*	*Aliquot*	*Lipid yield (µg/g)*	$C_{16:0}/C_{18:0}$	$C_{18:1}/C_{18:0}$	*Major and diagnostic compounds detected*	$\delta^{13}C_{16:0}$ (‰)	$\delta^{13}C_{18:0}$ (‰)	$\Delta^{13}C$ (‰) ($\delta^{13}C_{18:0}$ - $\delta^{13}C_{16:0}$)
HAS	LD12-4035	d	25.36	1.05	62.31	SFA (C14-28, C30), BrFA (C15, C17), UFA (C18:1, C19:1, C22:1), DC (C13), pri, phy (35% SRR), B3CA (tr)	-32.80	-31.50	1.30
HAS	LD12-4035	e	10.12	1.10		SFA (C14-18, C20, C22, C24, C26), BrFA (C15, C17), UFA (C18:1, C19:1), DC (C13), pri, phy (44% SRR)	-31.23	-30.50	0.73
HAS	LD23-25300	e	135.94	0.93		SFA (C12, C14-26, C28), BrFA (C13, C15, C17), UFA (C16:1, C18:1, 22:1), ALK (C24-26, C27, C28, C29), pri (tr), phy (41% SRR), ster (Cholesterol, β-Sitosterol, Stigmastanol, Lanostenol)	-30.23	-27.94	2.29
HAS	LD23-25300	i	87.19	0.91		SFA (C12, C14-20, C22, C24, C26, C28), BrFA (C15, C17), UFA (C18:1), ALK (C25-26, C27, C28, C29), pri (tr), ster (Lanostenol), B3CA (tr)	-32.46	-28.08	4.38
HAS	LD23-25396	e	84.08	0.92	48.14	SFA (C14-28, C30), BrFA (C15, C17), UFA (C16:1, C18:1), Hy (C20, C22, C24, C28), DC (C16, C24, C26, C28), ALK (C24-26, C27, C28, C29), OH (C24, C26), pri, phy (37% SRR), ster (Cholesterol, Cholestan-3-ol, β-Sitosterol methyl ether, γ-Sitosterol, β-Sitosterol, Stigmastanol), MAGs, AR (AR23, 25)	-31.85	-27.64	4.21
HAS	LD23-25396	i	30.72	1.39	13.33	SFA (C14-28, C30), BrFA (C15, C17), UFA (C18:1), Hy (C24, C28), DC (C24-26, C28), OH (C24), pri, phy (38% SRR), ster (Cholesterol, β-Sitosterol methyl ether, γ-Sitosterol, Lanostenol, Campesterol, β-Sitosterol, Stigmastanol), MAGs, AR (AR23, 25)	-35.93	-29.59	6.34
HAS	LD23-25430	e	114.90	0.90		SFA (C12, C14-20, C22-28, C30), BrFA (C15, C17), ALK (C22-26, C27, C28, C29, C30, C31, C32, C33), pri, ster (Cholesterol)	-30.98	-27.84	3.14
HAS	LD23-25430	i	36.36	0.82		SFA (C12, C14-18, C20, C22-26, C28, C30), BrFA (C15, C17), DC (C10), ALK (C22-26, C27, C28, C29, C30, C31, C32, C33)	-30.50	-28.78	1.72

6.1.4. Protein analysis

In the selected subset of HAS from La Draga analysed by proteomics, three samples (LD11-2156, LD12-3951, and LD12-4035) were chosen because they presented potential superficial deposits, consistent with the criteria outlined in the methodological section and suggesting potential contact with organic matter. In contrast, LD11-1540 showed no macroscopic residue yet was included owing to its localized discoloration, which was considered indicative of use-related alteration.

No proteins endogenous to the potential food residues were identified in any of the analysed samples. For all samples, the matched proteins were found to be contaminants, likely originating from the handling of the material, common laboratory contaminants, or from the burial environment (soil-dwelling bacteria). The protein profiles essentially reflected those of the two blank control samples, suggesting that little to no endogenous protein was present in the residues, or alternatively none were able to be successfully extracted (Table 9).

In the four samples analysed the main proteins were keratins (various types), trypsin, and streptavidin. Keratins are common laboratory contaminants and likely originate from handling and manipulating of the stones (in the deposit or in the laboratory) as they are key components of skin, hair and fingernails. Trypsin, the reagent used in this analysis to enzymatically cleave the proteins into smaller peptides, can undergo self-cleavage during protein digestion and thus its residues are often identified during protein analysis. Streptavidin is a common laboratory contaminant in mass spectrometry, and in this case likely originates from the magnetic separation beads used for protein extraction.

Table 9. Mascot protein matches for residue samples from La Draga (LD-1540, LD-2156, LD-3951, LD-4035) and their likely contaminant source. Note: Taxa listed are the most likely species as the majority are highly conserved sequences across taxa (e.g. keratins). Contaminant source: LR = laboratory reagent; LC = Laboratory contaminant; H/SC = handling/surface contaminant; S/SC = soil/surface contaminant. Those in red text would normally be disregarded due to only having a single peptide match, however they have been included to show that essentially all identifiable proteins were contaminants.

Sample	Protein	Taxa (most likely)	Score	# peptide matches	Cont. source
LD11-1540	Keratin, type I cytoskeletal 9	*Homo sapiens*	148	5	H/SC
	Trypsin	*Sus scrufa*	124	10	LR
	Keratin, type II cytoskeletal 2 epidermal	*Homo sapiens*	98	2	H/SC

Sample	Protein	Taxa (most likely)	Score	# peptide matches	Cont. source
	Keratin, type I cytoskeletal 10	*Homo sapiens*	86	5	H/SC
	Streptavidin	*Streptomyces avidinii*	54	1	LC
	Keratin, type II cytoskeletal 5	*Homo sapiens*	49	1	H/SC
LD11-2156	Streptavidin	*Streptomyces avidinii*	144	11	LC
	Streptavidin-V2	*Streptomyces violaceus*	39	2	LC
	Trypsin	*Sus scrufa*	114	7	LR
	60 kDa heat shock protein	*Homo sapiens*	75	1	H/SC
	Uncharacterized protein ORF257	Bacterial	27	1	S/SC
LD11-3951	Streptavidin	*Streptomyces avidinii*	115	4	LC
	Trypsin	*Sus scrufa*	94	6	LR
	Keratin, type I cytoskeletal 9	*Homo sapiens*	85	3	H/SC
	Keratin, type II cytoskeletal 1	*Homo sapiens*	44	1	H/SC
LD11-4035	Keratin, type I cytoskeletal 9	*Homo sapiens*	78	1	H/SC
	Keratin, type I cytoskeletal 10	*Homo sapiens*	78	1	H/SC
	Keratin, type II cytoskeletal 1	*Homo sapiens*	53	1	H/SC
Blank_1	Trypsin	*Sus scrufa*	121	8	LR
	Streptavidin	*Streptomyces avidinii*	41	2	LC
Blank_2	Trypsin	*Sus scrufa*	181	14	LR
	Streptavidin	*Streptomyces avidinii*	91	5	LC
	Keratin, type I cytoskeletal 9	*Homo sapiens*	70	1	H/SC
	A-kinase anchor protein 13	*Homo sapiens*	48	1	H/SC
	Keratin, type I cytoskeletal 10	*Homo sapiens*	48	1	H/SC

6.2. Pendimoun

6.2.1. Visual inspection

The visual inspection of the nineteen selected HAS from Pendimoun revealed patterns indicative of thermal exposure, consistent with their recovery from two distinct firing structures interpreted as serving different functions during the site's initial SMP occupation (fireplace FP-14549; cooking place CP-14647). The sample set consisted of 18 limestone and 1 detrital carbonate rock fragments, all previously sectioned for petrographic analysis, exhibiting irregular shapes with predominantly subangular edges, although their entire form cannot be fully assessed. Table 10 summarises the morphological features of the assemblage.

Evidence of thermal alteration was visibly identified in several specimens. Discoloration was observed in six stones, three of which (PDM-N04-15197, PDM-N04-15337, and PDM-N04-15419) exhibit distinct reddening. This alteration is typically associated with chemical changes in mineral composition (oxidation) induced by protracted exposure to high temperatures (Pagoulatos, 1992; Neubauer, 2018, 2024). Superficial adhesion, likely resulting from contact with molten residues or heat-affected organic materials, was documented in two HAS. Additionally, five specimens show evidence of sooting, possibly resulting from interaction with combustion processes (Pagoulatos, 2005; Neubauer, 2018), while two others exhibit cracking patterns consistent with thermal stress (Neubauer, 2018, 2024). These alteration patterns, often occurring in combination, point to repeated or intense exposure to fire, likely in direct contact with burning fuel or within areas subject to sustained high temperatures. Collectively, these features reinforce the interpretation of the stones as HAS, directly associated with the two circular firing structures from which they were recovered. Representative examples of these heat-alteration patterns are shown in Figure 57, including discoloration on the detrital carbonate rock (sample PDM-N04-15297, A), a combination of discoloration, sooting, and superficial adhesion (sample PDM-N04-15197, B), reddening (sample PDM-N04-15419, C) and cracking (sample PDM-N04-15348, D).

Importantly, no substantial differences in either morphology or heat-alteration patterns were observed between the HAS recovered from the two firing structures, suggesting broadly similar exposure conditions despite their functional distinction (Figure 58-59).

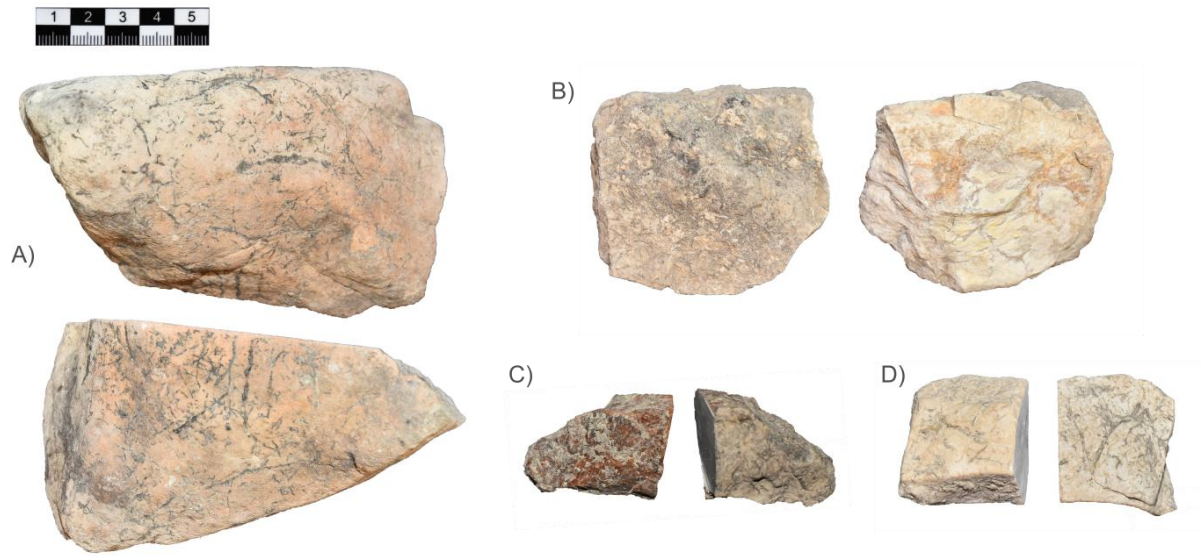


Figure 57. Representative examples of heat-alteration patterns observed on HAS: (A) discoloration on sample PDM-N04-15297 (Detrital carbonate rock), (B) discoloration, sooting, and superficial adhesion on sample PDM-N04-15197, (C) reddening on sample PDM-N04-15419, and (D) cracking on sample PDM-N04-15348.

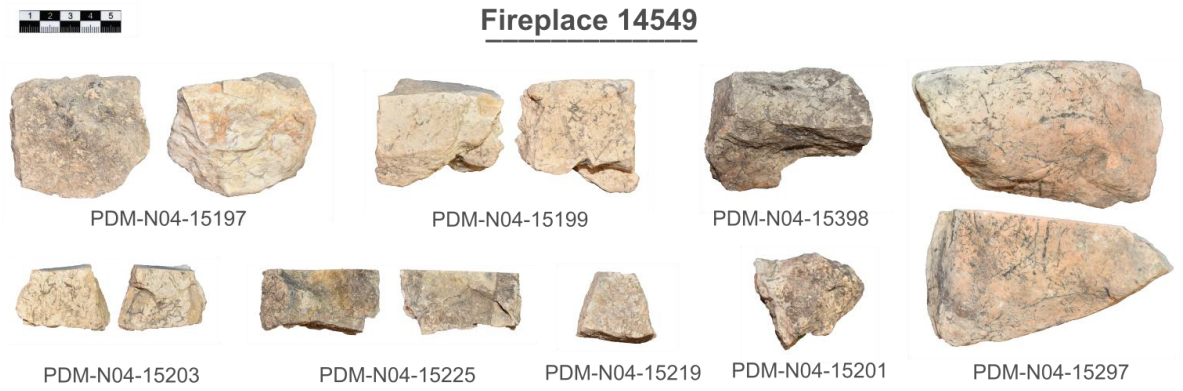


Figure 58. Selected HAS fragments recovered from firing structure 14549 (Fireplace).

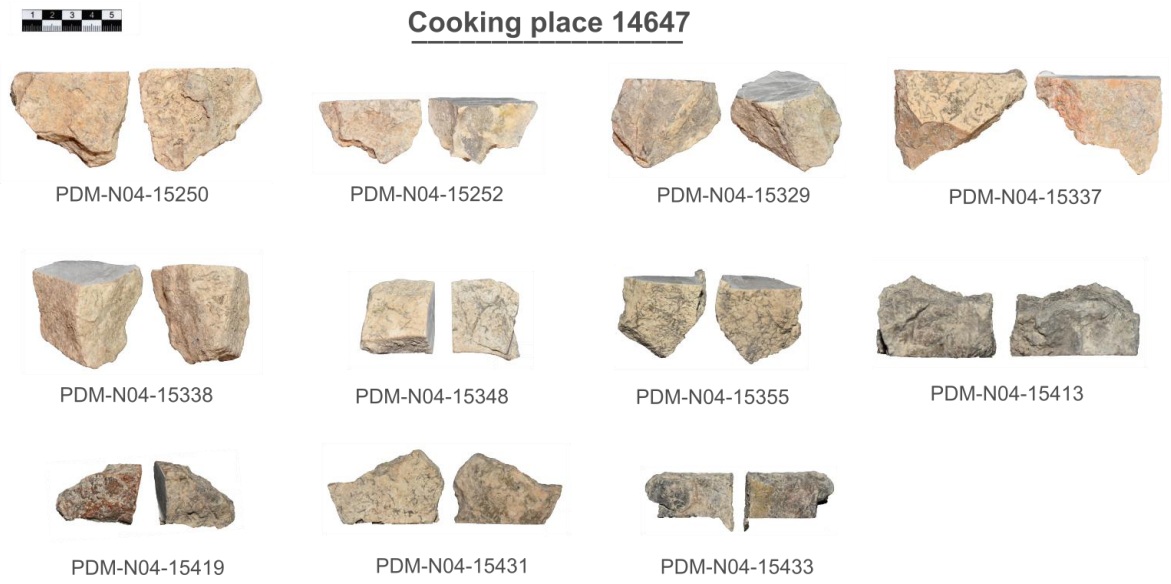


Figure 59. Selected HAS fragments recovered from firing structure 14647 (Cooking place).

Table 10. Contextual and morphological information of heat-altered stones (HAS) from Pendimoun. Variables include excavation year, stratigraphic context, feature, grid position, occupation phase, mineral composition, weight, and associated thermal alteration patterns.

Sites	*Excav. Year*	*Sample ID*	*Strat. context*	*Feature*	*Grid*	*Occupation*	*Mineral*	*Weight (g)*	*cracks*	*sooting*	*discoloration*	*sup. deposit*
Pendimoun	2004	15250	US 14647	Cooking place	L20	Phase 3	Limestone	135				x
Pendimoun	2004	15252	US 14647	Cooking place	L20	Phase 3	Limestone	38	x	x		
Pendimoun	2004	15329	US 14647	Cooking place	L20	Phase 3	Limestone	92		x		
Pendimoun	2004	15337	US 14647	Cooking place	L20	Phase 3	Limestone	100			x	
Pendimoun	2004	15338	US 14647	Cooking place	L20	Phase 3	Limestone	118				
Pendimoun	2004	15348	US 14647	Cooking place	L20	Phase 3	Limestone	42	x			
Pendimoun	2004	15355	US 14647	Cooking place	L20	Phase 3	Limestone	62				
Pendimoun	2004	15413	US 14647	Cooking place	L20	Phase 3	Limestone	174				
Pendimoun	2004	15419	US 14647	Cooking place	L20	Phase 3	Limestone	30			x	
Pendimoun	2004	15431	US 14647	Cooking place	L20	Phase 3	Limestone	64				
Pendimoun	2004	15433	US 14647	Cooking place	L20	Phase 3	Limestone	36		x		
Pendimoun	2004	15197	US 14549	Fireplace	L21	Phase 3	Limestone	154		x	x	x
Pendimoun	2004	15199	US 14549	Fireplace	L21	Phase 3	Limestone	163				
Pendimoun	2004	15201	US 14549	Fireplace	L21	Phase 3	Limestone	85			x	
Pendimoun	2004	15203	US 14549	Fireplace	L21	Phase 3	Limestone	52				
Pendimoun	2004	15219	US 14549	Fireplace	L21	Phase 3	Limestone	38				
Pendimoun	2004	15225	US 14549	Fireplace	L21	Phase 3	Limestone	90		x		
Pendimoun	2004	15297	US 14549	Fireplace	L21	Phase 3	Detrital carbonate rock	243			x	
Pendimoun	2004	15398	US 14549	Fireplace	L21	Phase 3	Limestone	197			x	

6.2.2. 3D model acquisition

High-resolution 3D models were produced for all analysed HAS using a combination of photogrammetry and laser scanning techniques. These digital reconstructions preserve the original morphology and surface texture of each artefact and are housed in a dedicated digital library hosted by OpenLab UAB on Sketchfab [https://skfb.ly/puzEA]. The repository constitutes a significant research outcome, serving as an open-access resource for educational purposes and future research. The models can be explored in detail online, reducing the need for physical handling, while offering a unique opportunity for researchers and the public to engage with these artefacts virtually.

6.2.3. Lipid residue analysis

As presented for the La Draga samples, this section presents the results of the lipid residue analyses conducted to characterise the molecular composition of HAS and sediments. A total of 39 samples (e = 19, i = 18, d = 2) from the 19 selected HAS, along with six sediment samples were analysed. Acid extraction (AE) was performed on all samples, including both HAS and sediments, as this step was necessary for subsequent stable carbon isotope analysis. Solvent extraction (SE), intended primarily to identify plant-derived lipid profiles, was applied to a smaller subset of samples. Among sediments, only two samples (PDM-S14466 and PDM-S15367) underwent solvent extraction, since the remaining sediments displayed comparable molecular profiles.

Sediment results are presented first, followed by those of the HAS, which are interpreted in relation to the contextual data and discussed further in Chapter 7. As observed for La Draga samples, preliminary chemical screening revealed the presence of sulphur in most cases, likely originating from the sulphur-bearing bedrock, and removed using the method described above.

Lipids composition in sediments

Lipids were successfully extracted from all **sediment samples** from Pendimoun (Table 11 and Annex 4), yielding concentrations ranging from 577.68 to 5,165.71 µg g^{-1}. These values are notably high and, in several cases, exceed those recorded for the sediments from La Draga. While the reasons for these elevated concentrations cannot be determined from the available data, the results indicate that the Pendimoun sediments contain substantial amounts of preserved organic material, reflecting variability that can occur between different depositional contexts. As for La Draga, the lipid profiles across all samples were dominated by **SFA**, spanning chain lengths from $C_{8:0}$ to $C_{34:0}$, with **palmitic ($C_{16:0}$), stearic ($C_{18:0}$), lignoceric ($C_{24:0}$) and cerotic ($C_{26:0}$) acids** being the most abundant (Figure 60). The palmitic:stearic ratio (P/S) varied between 1.18 and 1.54. This, along with relatively elevated levels

of oleic acid ($C_{18:1}$) compared to stearic acid ($2.5 > C_{18:1}/C_{18:0} > 0.2$) suggest that sedimentary lipids originated primarily from plant material. However, both P/S and O/S ratios are lower than those observed in LD sediments, reflecting the comparative higher concentrations of stearic and oleic acids.

Some of the compounds detected in sediments from Pendimoun are similar to those previously identified at La Draga, including the presence of **monomethyl-branched fatty acids** ($C_{13:0Br}$, $C_{15:0Br}$ and $C_{17:0Br}$), **monounsaturated fatty acids (MUFA)** ($C_{16:1}$, $C_{18:1}$, $C_{20:1}$, $C_{22:1}$), **hydroxylated FAs** (C_{22} to C_{28}) and **dicarboxylic acids** (C_8 to C_{31}), reflecting soil microbial activity and post-depositional processes associated with burial conditions. **Phytosterols** and their derivatives (β-sitosterol, stigmasterol, stigmastanol), as well as **pentacyclic triterpenes** (β/α-amyrin), indicate plant origin, whereas the presence of cholesterol derivatives points to contributions from animal sources (Figure 60). The predominance of ***n*-alkanols** (C_{18} to C_{34}, with maximum at C_{26}) together with long-chain ***n*-alkanes** (C_{15} to C_{33}, with maximum at C_{31}) and trace amounts of even-carbon long-chain **wax esters** (W_{44} to W_{52}), further supports their attribution to vascular plant leaf waxes (Figure 61) (Eglinton and Hamilton, 1967; Gülz, 1994; Charters et al., 1995; Ribechini et al., 2008). This profile is more clearly expressed in PDM sediments than in LD sediments, where pentacyclic triterpenes are the dominant compounds. In addition, traces of **benzene tricarboxylic acid**, a by-product of charred organic matter, were detected in three samples. Among **isoprenoid acids**, 4,8,12-TMTD, pristanic (traces), and phytanic acid were identified, with SRR isomer percentages of 96% in all samples (Figure 62), consistently higher than those observed in LD sediments. Notably, no homologues of AR were detected for PDM sediment samples.

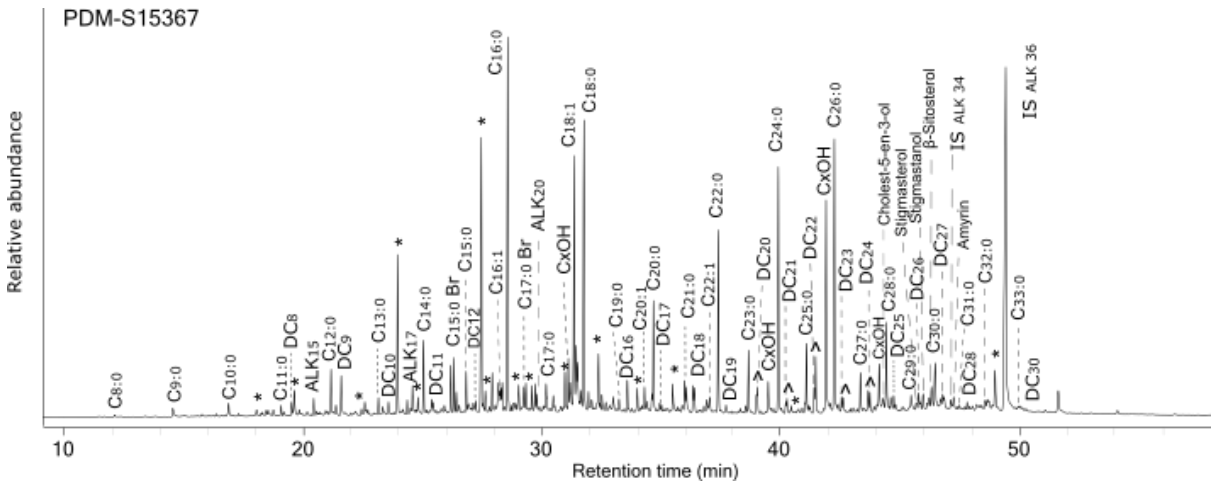


Figure 60. Partial total ion chromatograms (TIC) of acid/methanol extract of sediment sample PDM-S15367 showing saturated fatty acids ($C_{XX:0}$), branched ($C_{XX:0}$ Br), unsaturated fatty acids ($C_{XX:1}$), diacids (DC_{XX}), hydroxy fatty acids (^), sterols and derivatives, pentacyclic triterpenes, contaminants (*), and *n*-alkanes internal standards (IS $_{ALKXX}$).

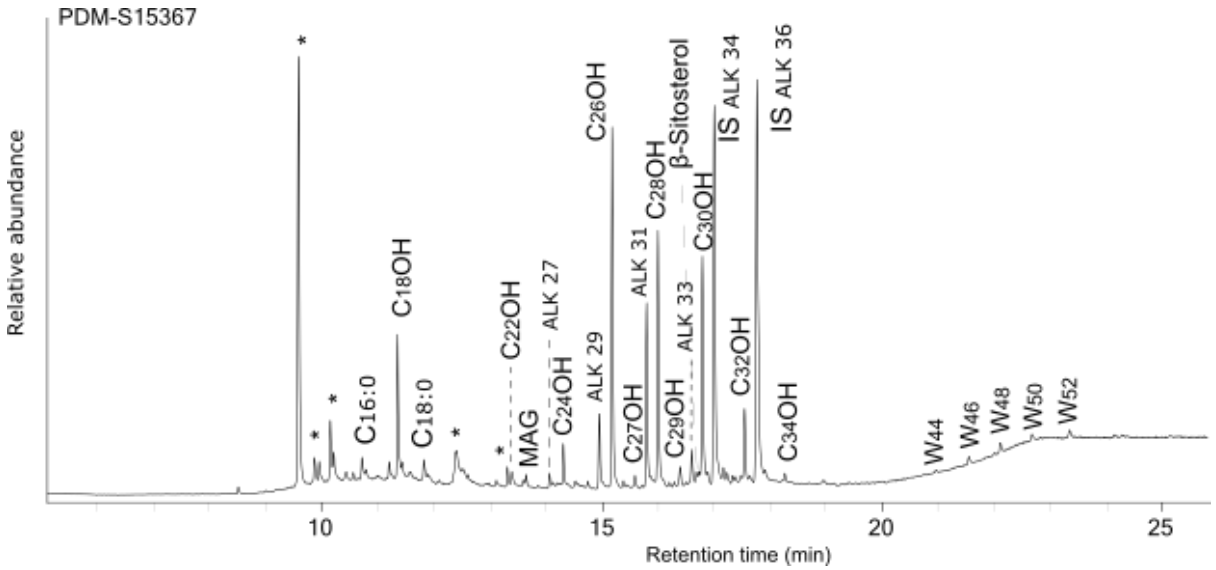


Figure 61. Partial total ion chromatograms (TIC) of solvent extract of sediment sample PDM-S15367 showing saturated fatty acids ($C_{XX:0}$), linear alcohols (CxxOH), *n*-alkanes (ALKxx), hydroxy fatty acids (^), sterols and derivatives, wax esters (Wxx), contaminants (*), and *n*-alkanes internal standards (IS $_{ALKXX}$).

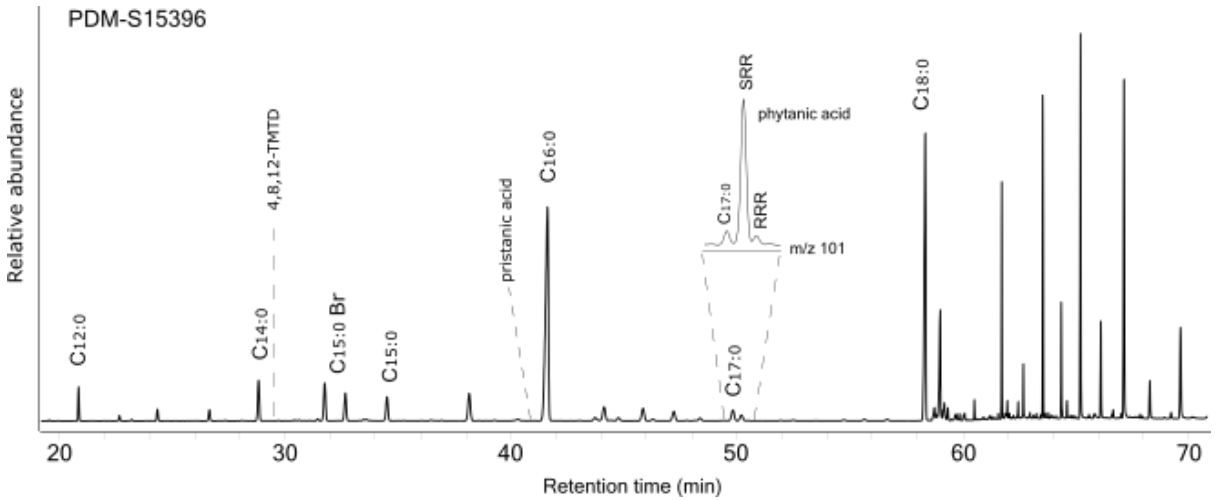


Figure 62. Partial total ion chromatograms (TIC) of acid/methanol of sediment sample XX showing saturated fatty acids ($C_{XX:0}$), branched fatty acids ($C_{XX:0}$ Br), isoprenoid acids (4,8,12-trimethyltridecanoic acid, pristanic and phytanic acid), with a *m/z* 101 ion chromatogram showing the ratio of phytanic acid diastereomers (SRR and RRR).

Lipids content in HAS

Lipids were extracted from the internal, external and deposit samples from almost all HAS, with concentrations ranging from 4.32 to 519.83 µg g^{-1} (Figure 63). Interpretable amounts of lipids (> 5 µg g^{-1} (Evershed et al., 2008b; Craig et al., 2013)) were recovered from 74% of internal (n = 14) and 100% external (n = 18) samples, along with 100% of deposits (n = 2). For the following analyses, only samples with lipid concentrations exceeding the threshold above were considered.

Figure 64 provides a visual summary of the lipid yields across the three aliquots, highlighting notable variations, particularly within the external samples, which display a wider range and higher median values compared to the others. Although variability is evident, formal statistical analysis was necessary to evaluate whether these observed differences were significant. The Kruskal-Wallis rank sum test indicated a statistically significant difference across the three aliquot groups (external, internal, and deposits; $\chi^2 = 7.65$, df = 2, $p = 0.022$). Post-hoc pairwise comparisons using Dunn's test with Holm correction identified differences between internal and external samples ($p = 0.018$), with external surfaces yielding higher lipid concentrations (median = 145.31 µg g^{-1}) compared with internal samples (median = 36.26 µg g^{-1}). This result was further supported by a Wilcoxon rank sum exact test focused on internal vs. external samples, confirming a statistically significant difference ($W = 193$, $p = 0.010$). This reinforces the observation that lipids are more concentrated on external surfaces than internal layers.

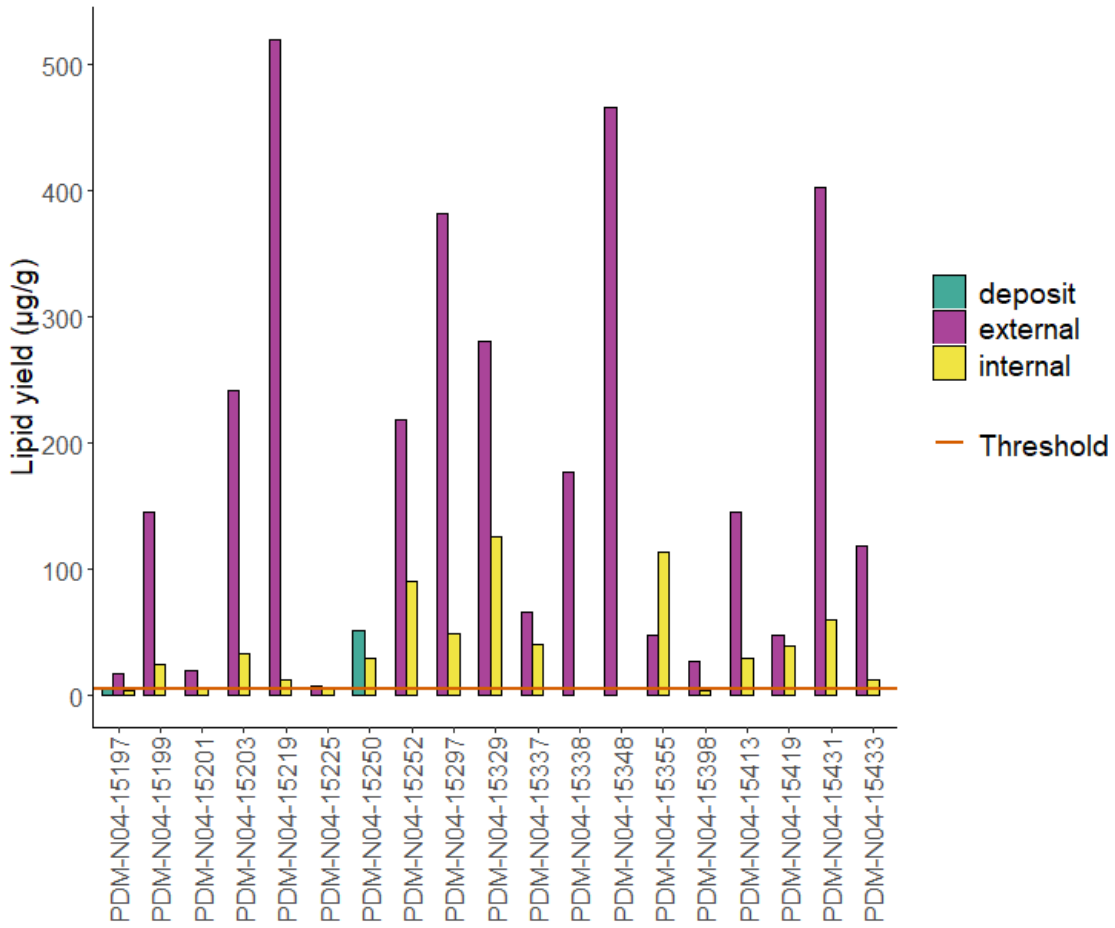


Figure 63. Bar plot of lipid yields for Pendimoun samples, categorised by internal, external and deposit aliquots. The solid line represents the threshold of 5 µg g^{-1}.

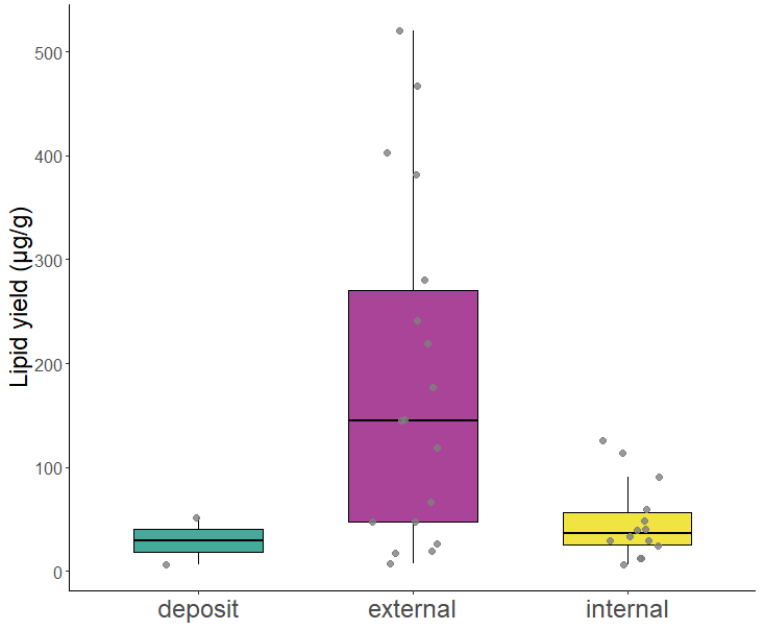


Figure 64. Boxplot of lipid yields for Pendimoun samples, categorised by deposit (n = 2), external (n = 18) and internal (n = 14) aliquots. Grey points represent individual data values.

For Pendimoun, all sampled HAS belonged to the same lithological type except one, precluding any statistical comparison between lithology groups. The samples were instead divided into two groups: those from the structure 14549 (Fireplace) and those from the structure 14647 (Cooking place). Figure 65 shows that lipid concentrations tend to be higher and more variable in the Cooking place samples, whereas the Fireplace samples are generally lower and exhibit less variation. A Kruskal–Wallis rank sum test indicates a borderline significant difference ($\chi^2 = 3.70$, df = 1, p = 0.05). Median lipid concentrations were higher in the Cooking place (CP-14647; 78.73 µg g^{-1}) than in the Fireplace (FP-14549; 25.73 µg g^{-1}). Since only two groups were compared, the Dunn post-hoc test is equivalent to a Mann–Whitney U test, which confirms the marginal difference between the structures. These results suggest that lipid yields tend to be greater in CP-14647, although the statistical support is limited, and variability within each structure is considerable.

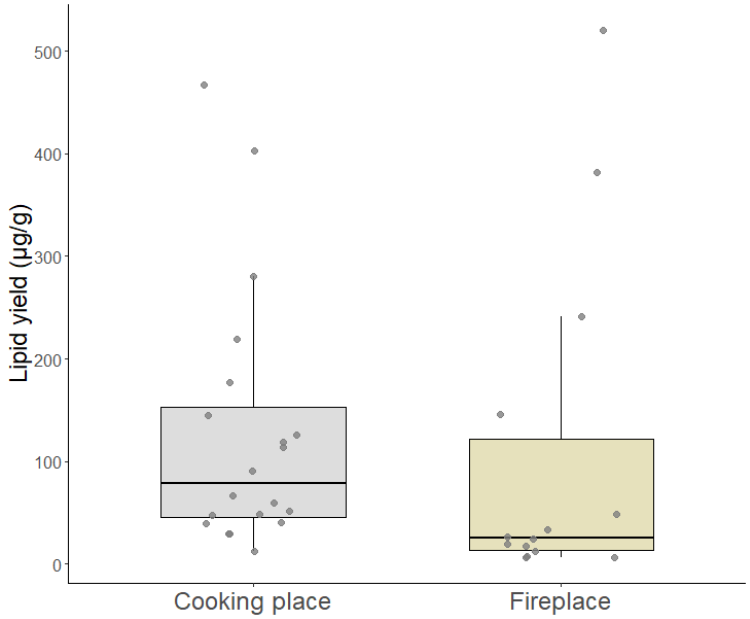


Figure 65. Boxplot of lipid yields for Pendimoun samples, categorised by firing structures, including Cooking place-14647 (n = 20) and Fireplace-14549 (n = 14). Grey points represent individual data values.

When aliquots are examined separately by structure, contrasting patterns emerge. Within the Cooking place (CP-14647), a Kruskal–Wallis rank sum test revealed significant differences in lipid concentrations among aliquot types ($\chi^2 = 7.44$, df = 2, $p = 0.024$). Post-hoc pairwise comparisons using Dunn's test with Holm correction showed that external samples contained significantly higher lipid concentrations than internal ones ($p = 0.011$), whereas deposits did not differ significantly from either group. This indicates that lipids in the HAS from Cooking place were preferentially concentrated on external surfaces of stones, while internal layers and deposits exhibited comparatively lower concentrations. In contrast, within the Fireplace (FP-14549), no significant differences were detected across aliquot types ($\chi^2 = 3.79$, df = 2, $p = 0.150$). Dunn's tests likewise confirmed that none of the pairwise comparisons were significant (all $p > 0.10$). Although external samples tended to show higher concentrations than deposits or internal samples, this trend lacked statistical support. The corresponding boxplot (Figure 66) shows the distributions across aliquots in the two structures.

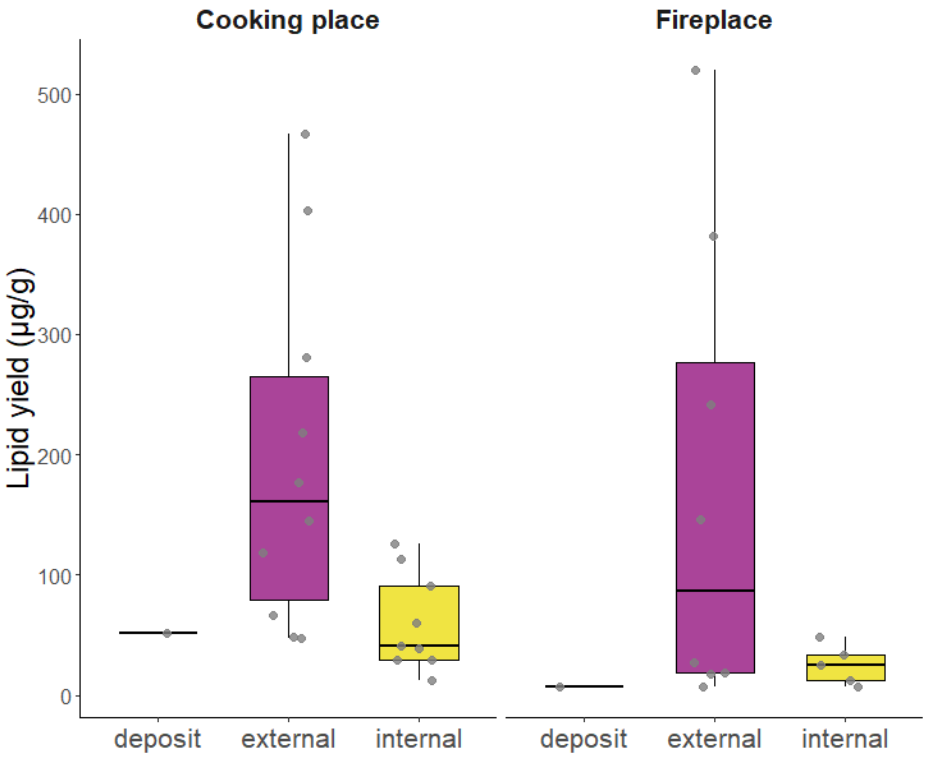


Figure 66. Boxplot of lipid yields for Pendimoun samples, showing deposit (n = 1), external (n = 10) and internal (n = 9) aliquots of HAS from the Cooking place, along with deposit (n = 1), external (n = 8) and internal (n = 5) aliquots of HAS from the Fireplace. Grey points represent individual data values.

Regarding the nature of the recovered lipids, all samples contained detectable quantities of phthalates (*m/z* 149) and benzoic acid derivatives (*m/z* 105 and 123), which could originate from modern post-excavation contamination due to long-term storage in plastic bags (Evershed, 1993). These contaminants were identified and excluded from the calculation of lipid yields to avoid skewing the quantitative results. Additionally, small amounts of squalene, one of the major lipid components of human sebum, were detected in almost all of the samples extracted through the DCM/MeOH method, revealing contamination from the handling of the stones (Evershed, 1993).

Lipid extracts from HAS revealed a chemically diverse range of compounds (Table 12 and Annex 4). Although differing in composition and abundance from the sediments, several important similarities were observed. Across all samples (including internal, external and deposits), the lipid profile was dominated by short- to long-chain **saturated fatty acids (SFA)** ($C_{9:0}$ to $C_{32:0}$), dominated by **palmitic ($C_{16:0}$)** and **stearic ($C_{18:0}$) acids** (Figure 67), with a palmitic:stearic ratio (P/S) ranging from 0.64 to 2.33. The slightly predominance of palmitic acid likely reflects aquatic organism, plants oils (Papakosta et al., 2015; Craig et al., 2007), as well as monogastric animals (Regert, 2011), although post-depositional degradation may have influenced fatty acid profiles (Evershed et al., 1992; Rosiak, Kałużna-Czaplińska and Gątarek, 2020), so the ratios should be interpreted with caution.

As observed for La Draga samples, the presence of **monomethyl-branched fatty acids** ($C_{15:0Br}$ and $C_{17:0Br}$) in a few samples (15 %, n = 5) (Figure 67) is more likely attributable to soil bacterial activity than ruminant fats (Kühn, Schweitzer and Ruess, 2019; Dudd, Regert and Evershed, 1998). (Evershed, 1993; Regert, 2011). In addition, traces of **cholesterol** and some of its derivatives (i.g. Cholestan-3,5-diene, and cholesterol methyl ether) were identified in 24% (n = 8) of the samples (Figure 68). These sterols are commonly associated with ruminant fats (Regert, 2011; Hammann et al., 2018; Whelton et al., 2021), but again were found in natural and archaeological sediments (Mallol et al., 2025; Wen-Yen and Meinschein, 1976). Only one of these samples containing cholesterol also exhibited **plant sterols** (β-sitosterol and stigmasterol). The co-occurrence of these compounds, along with their presence in the sediments, points towards a likely derivation from soil organic matter.

Many other compounds identified in the sediments were also detected in the HAS, including traces of **benzene tricarboxylic acid** (26%, n = 9), ***n*-alkanes** present in small amounts (44%, n = 15) (Figures 67, 69), trace of even-carbon long-chain **wax esters** (W_{46}) (3%, n = 1), and **long-chain linear alcohols (**C_{14}-C_{32}) (65%, n = 22) (Figure 69). These compounds, often derived from plant waxes (Eglinton and Hamilton, 1967; Gülz, 1994), may indicate contact with plant-derived material, either through intentional plant use or via post-depositional environmental contamination. **Monounsaturated fatty acids (MUFA)**, mainly oleic acid ($C_{18:1}$) and erucic acid ($C_{22:1}$), were found in almost all of the analysed samples (100%, n = 34 and 91%, n = 31, respectively), while palmitoleic acid ($C_{16:1}$) were less common (35%, n = 12). Erucic acid in particular, is closely associated with tridecanedioic acid (brassylic acid, C_{13}), the most frequently detected **diacid** in these samples (50%, n = 17) (Figures 67, 68, 70), which forms through the oxidative degradation of erucic acid under heating conditions that promote lipid oxidation (Fuessl, Yamamoto and Schneller, 2012; Copley et al., 2005a). The high co-occurrence of erucic acid and its corresponding diacid therefore suggests that erucic acid-rich lipids, likely derived from certain seed oils, underwent substantial thermal alteration, either from the artefact use (e.g. repeated heating) or due to post-depositional processes within the burial environment (Regert et al., 1998; Eerkens, 2005).

In addition, **hydroxy fatty acid** (C_{24}) was identified as a further oxidation product, though occurring in only 6% (n = 2) of the samples. Among **isoprenoid acids**, 4,8,12-TMTD (24%; n = 18), pristanic acid (91%; n = 31) and phytanic acid (56%; n = 19) were also detected, with SRR percentage ranging from 62% to 96%. As for LD samples, 4,8,12-TMTD occurred mostly in external aliquots of HAS (e = 17, d =1, i =1).

In addition to the compounds shared with the sediments, other lipids were detected exclusively in the HAS samples. A single sample (PDM-N04-15297e) exhibited the presence of **methyl**

dehydroabietate, a compound commonly associated with conifer resins. While such biomarker is widely used as an indicator of plant resin in archaeological contexts (Rageot et al., 2021; Dimitrakoudi et al., 2011), its presence alone does not necessarily indicate heated pine-based materials, as previously suggested for the La Draga samples.

It is worth noting that traces of **ketones**, specifically tritriacontan-16-one (33K) and pentatriacontane-18-one (35K) were identified in a single sample (PDM-N04-15201e) (Figure 70). Such compounds are generally considered indicative of heat exposure (Evershed et al., 1995a; Raven et al., 1997; Evershed et al., 1999b), although recent work suggest they may also form in small quantities due to heating during drilling in the sampling process (Longoni et al., 2024). As observed in LD samples, other compounds typically associated with the prolonged heating of terrestrial and aquatic resources in ceramics matrix were not detected, even in HAS associated with the Cooking place, where processing and cooking activities would be expected. Notably, recent experimental studies confirm that such compounds can be present in HAS subjected to various cooking experiments (Langley, 2024).

However, other compounds typically associated with the prolonged heating of terrestrial and aquatic oils in ceramics matrix, such as ω-(o-alkylphenyl) octadecanoic acids (Hansel et al., 2004; Bondetti et al., 2021a), were not detected in any of the analysed HAS. Their absence in the Fireplace samples is consistent with the suggested function of this structure, where stones were heated for postponed reuse and/or to provide heat or light. In the Cooking Place, the lack of these compounds does not necessarily indicate a lack of animal or plant processing, but may reflect the natural variability of biomarker formation under different conditions (Evershed et al., 2008b; Bondetti et al., 2021a; Langley, 2024) as discussed for LD.

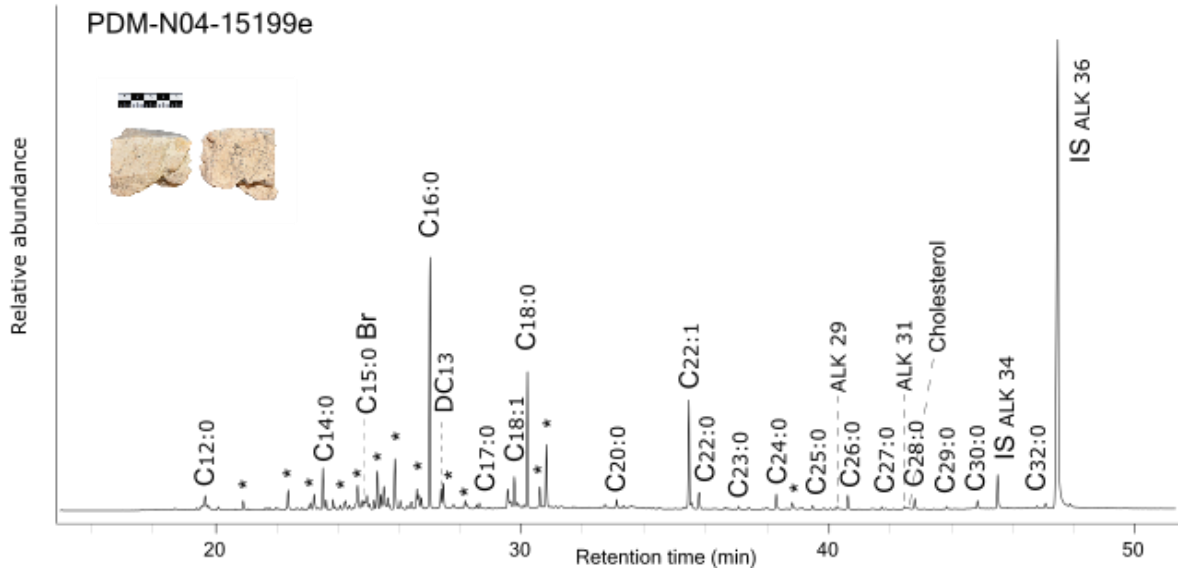


Figure 67. Partial total ion chromatograms (TIC) of acid/methanol extract of HAS sample PMD-N04-15199e showing saturated fatty acids ($C_{XX:0}$), branched fatty acids ($C_{XX:0\ Br}$), unsaturated fatty acids ($C_{XX:1}$), diacids (DC_{XX}), *n*-alkanes (ALK xx), cholesterol, contaminants (*), and *n*-alkanes internal standards ($IS_{\ ALKXX}$).

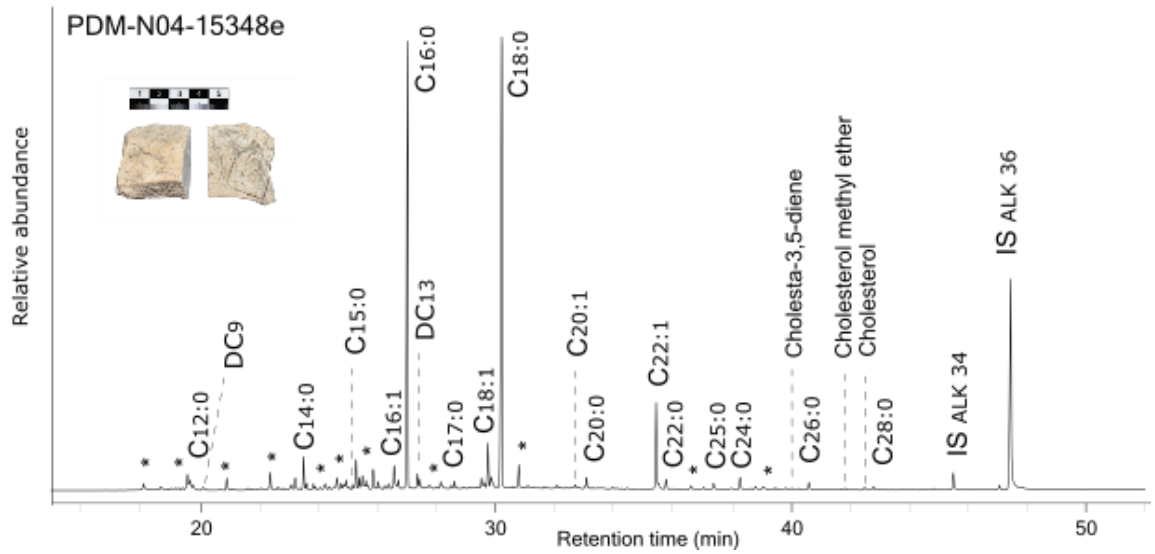


Figure 68. Partial total ion chromatograms (TIC) of acid/methanol extract of HAS sample PMD-N04-15348e showing saturated fatty acids ($C_{XX:0}$), unsaturated fatty acids ($C_{XX:1}$), diacids (DC_{XX}), sterols and derivatives, contaminants (*), and *n*-alkanes internal standards ($IS_{\ ALKXX}$).

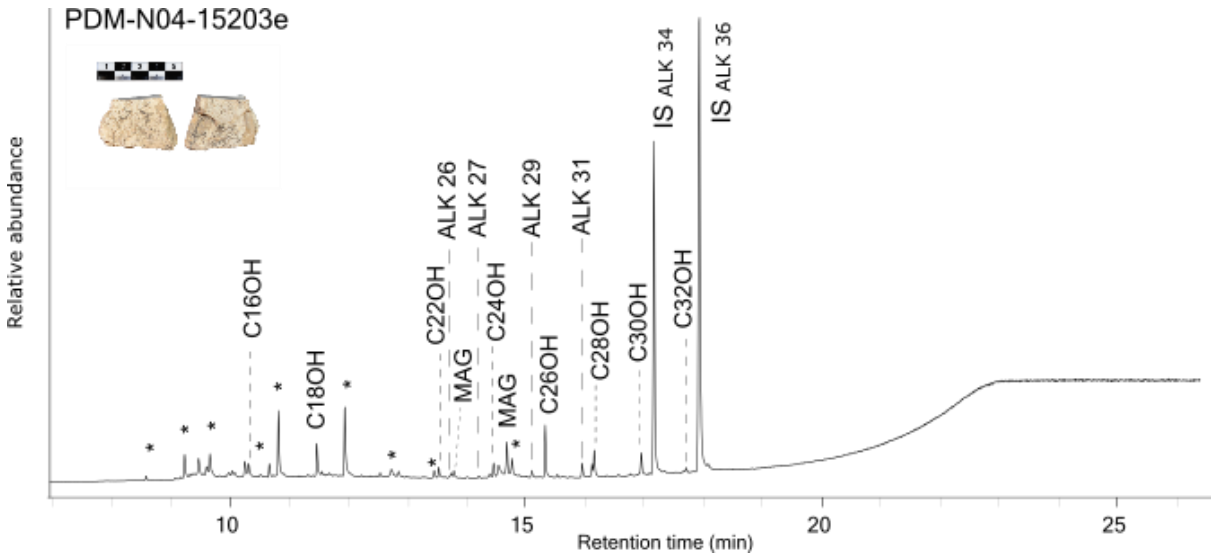


Figure 69. Partial total ion chromatograms (TIC) of solvent extract of HAS sample PDM-N04-15203e showing linear alcohols (CxxOH), monoacylglycerols (MAG), *n*-alkanes (ALK xx), contaminants (*), and *n*-alkanes internal standards (IS $_{ALKXX}$).

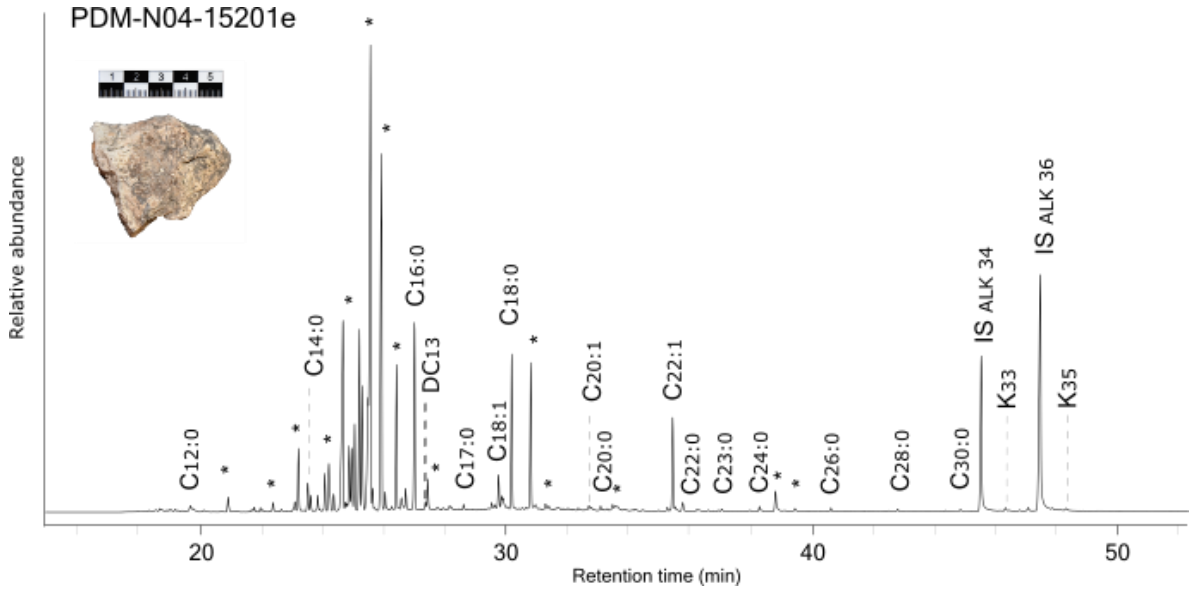


Figure 70. Partial total ion chromatograms (TIC) of acid/methanol extract of HAS sample PMD-N04-15201e showing saturated fatty acids ($C_{XX:0}$), unsaturated fatty acids ($C_{XX:1}$), diacids (DC_{XX}), ketones (Kxx), contaminants (*), and *n*-alkanes internal standards (IS $_{ALKXX}$).

6.2.3.1. Stable carbon isotope analysis

To further investigate the origin and possible processing of lipid residues recovered from HAS, stable carbon isotope ($\delta^{13}C$) measurements were undertaken on the two predominant saturated fatty acids: palmitic acid ($C_{16:0}$) and stearic acid ($C_{18:0}$). For each sample, an aliquot of the acidified extract

was retained for GC-C-IRMS analysis, following the removal of sulphur using activated copper. The resulting isotopic data are presented and discussed below, organised by structure.

The $\delta^{13}C$ values of palmitic ($C_{16:0}$) and stearic acid ($C_{18:0}$) were obtained from all of the sedimentary samples, both ranging from -31‰ to -30‰ (Table 11, Figures 71). These values exhibit a narrow isotopic range, predominantly within the C_3 plant values, irrespective of their association with Fireplace, Cooking place or ashes. The $\delta^{13}C$ values of palmitic ($C_{16:0}$) and stearic acid ($C_{18:0}$) were obtained from 79% of HAS samples (Table 11, Figures 71). Of these, 85% originated from Cooking place (e: 80%, n = 8; i: 100%, n = 9), and 71% from Fireplace (e: 88%, n = 7; i: 60%, n = 3).

The $\delta^{13}C$ values in HAS samples from the **Fireplace** (FP-14549) display a localised distribution of approximately -30‰ to -29‰ for $\delta^{13}C_{16:0}$, and -31‰ and -29‰ for $\delta^{13}C_{18:0}$. All HAS samples fall within the isotopic ranges associated with C_3 plant or freshwater lipid sources and the distribution of sediment samples (Figure 71). When plotting the derived $\Delta^{13}C$ values against $\delta^{13}C_{16:0}$, nearly all the samples cluster between 4‰ and -1‰ along with sediment samples, with one value extending into the ruminant/plant region. Overall, these values are primarily indicative of non-ruminant adipose fats and plants, suggesting that mixtures of animal adipose fats and plant oils should be considered, as they can produce similar isotopic signatures (Hendy et al., 2018).

By contrast, in the **Cooking place** (CP-14647) the corresponding $\delta^{13}C$ values of HAS display a broader distribution, ranging from approximately -31‰ to -27‰ for $\delta^{13}C_{16:0}$, and -33‰ and -28‰ for $\delta^{13}C_{18:0}$ (Figure 71). Most HAS samples lie within the isotopic ranges associated with C_3 plant or freshwater lipid sources, with fewer aligning with the domestic ruminant reference values. Additionally, some samples overlap with the isotopic ranges of wild non-ruminant (PDM-N04-15419i) and both domestic and wild ruminants (PDM-N04-15431e/i, PDM-N04-15329e/i, PDM-N04-15433i). When plotting the derived $\Delta^{13}C$ values against $\delta^{13}C_{16:0}$, most samples cluster between 4‰ and -1‰ along with sediment samples, a range indicative of non-ruminant adipose fats and plants, while three HAS samples fall within the ruminant/plant region (PDM-N04-15329e/i, PDM-N04-15433i), with a further two extending into the dairy zone (PDM-N04-15431e/i).

Statistical comparisons of stable carbon isotope values between internal and external HAS layers were conducted separately for each structure. For the Cooking place, no significant differences were observed for $\delta^{13}C_{16:0}$ ($W = 26.5$, $p = 0.386$) or $\delta^{13}C_{18:0}$ ($W = 28.5$, $p = 0.500$). Similarly, for the Fireplace, $\delta^{13}C_{16:0}$ ($W = 12$, $p = 0.820$) and $\delta^{13}C_{18:0}$ ($W = 8$, $p = 0.649$) did not differ significantly between internal and external layers, indicating that isotopic signatures are broadly consistent across HAS layers. Despite the higher lipid concentrations observed on external surfaces, both internal and external samples

remain representative of the same organic input, confirming the reliability of isotopic analyses across HAS layers.

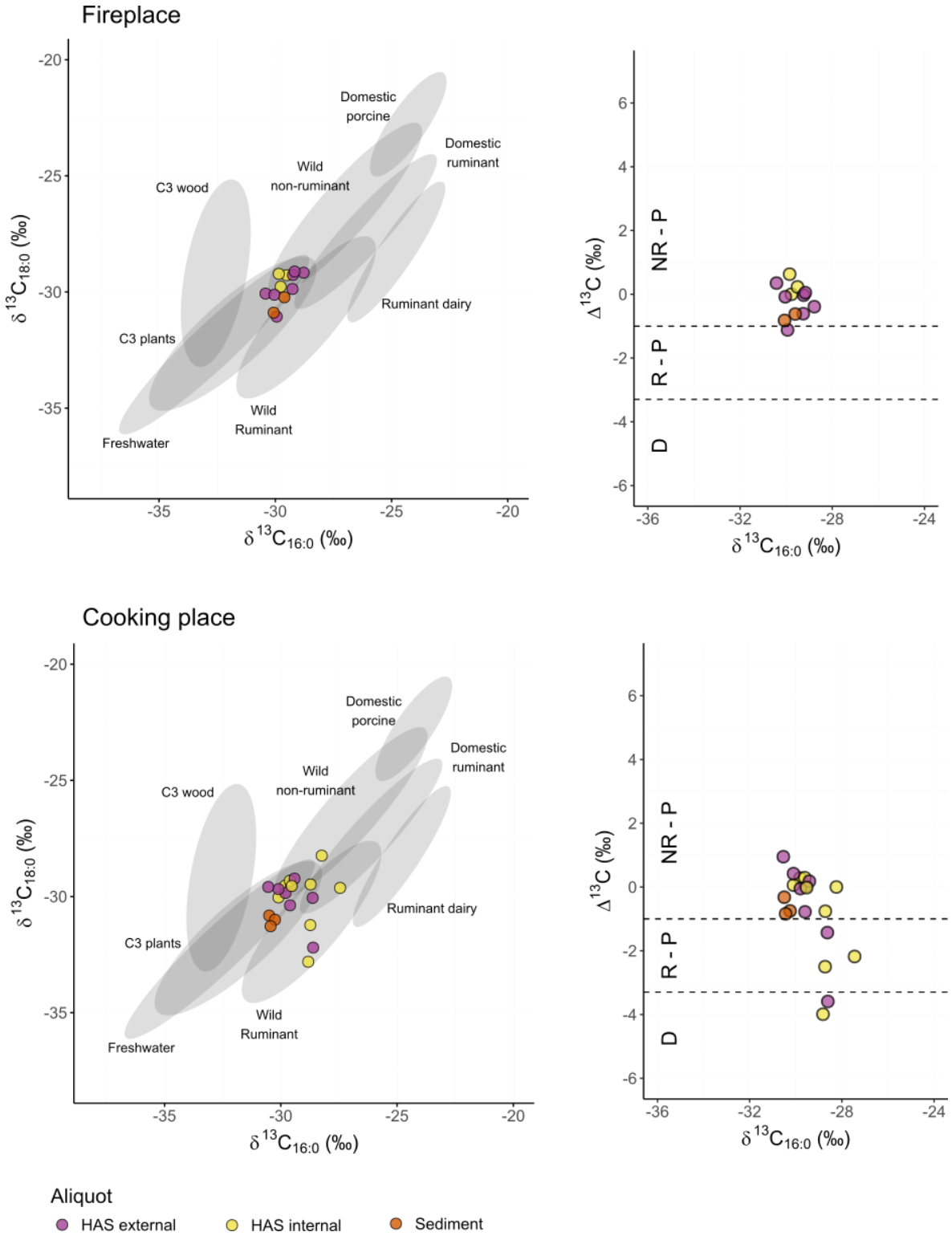


Figure 71. Plots of $\delta^{13}C$ values of palmitic ($C_{16:0}$) and stearic acid ($C_{18:0}$), and $\Delta^{13}C$ (difference between the $\delta^{13}C$ values of the $C_{16:0}$ and $C_{18:0}$ fatty acids) versus $\delta^{13}C_{16:0}$, of HAS and sediment samples from Fireplace (FP-14549)

and Cooking place (CP-14647) at Pendimoun. Coloured symbols indicate different aliquot types, while shaded ellipses represent reference ranges for modern reference, showing 68% confidence ellipses (see Figure 13, chapter 3.1.2; Annex 3). Abbreviations: D = dairy products, R = ruminant adipose fat, NR = non ruminant adipose fat, P = plant products.

Considering isotopic distributions in relation to the lipid concentration, samples with higher lipid yield are predominantly derived from external aliquots in both structures (Figure 72), consistent with previous observations. Notably, among the Cooking Place (CP-14647) samples, several of those with elevated lipid concentrations plot within the isotopic ranges characteristic of both wild and domestic ruminants.

While the molecular profiles of HAS largely point to plant-derived inputs and do not reveal major differences between the Fireplace and Cooking Place structures, the isotopic results present a more distinctive picture. Sterols and their derivatives were detected in HAS samples plotting within isotopic areas compatible with both plant and wild non-ruminant inputs (Figure 73A), suggesting the possibility of mixed resources. This overlap underscores the complexity of interpreting lipid residues from fire-related contexts, where inputs from multiple sources, such as plant foods, fuel materials, and animal products, may converge, leaving signatures that are only partially preserved in the molecular record.

Another noteworthy feature is the occurrence of dicarboxylic acids (Figure 73B), which are detected predominantly in the external samples of the HAS from the Cooking Place and in the associated sedimentary samples. The presence of these compounds likely reflects oxidative degradation of unsaturated fatty acids, driven by greater exposure to environmental factors, and highlights differential preservation processes between external and internal contexts.

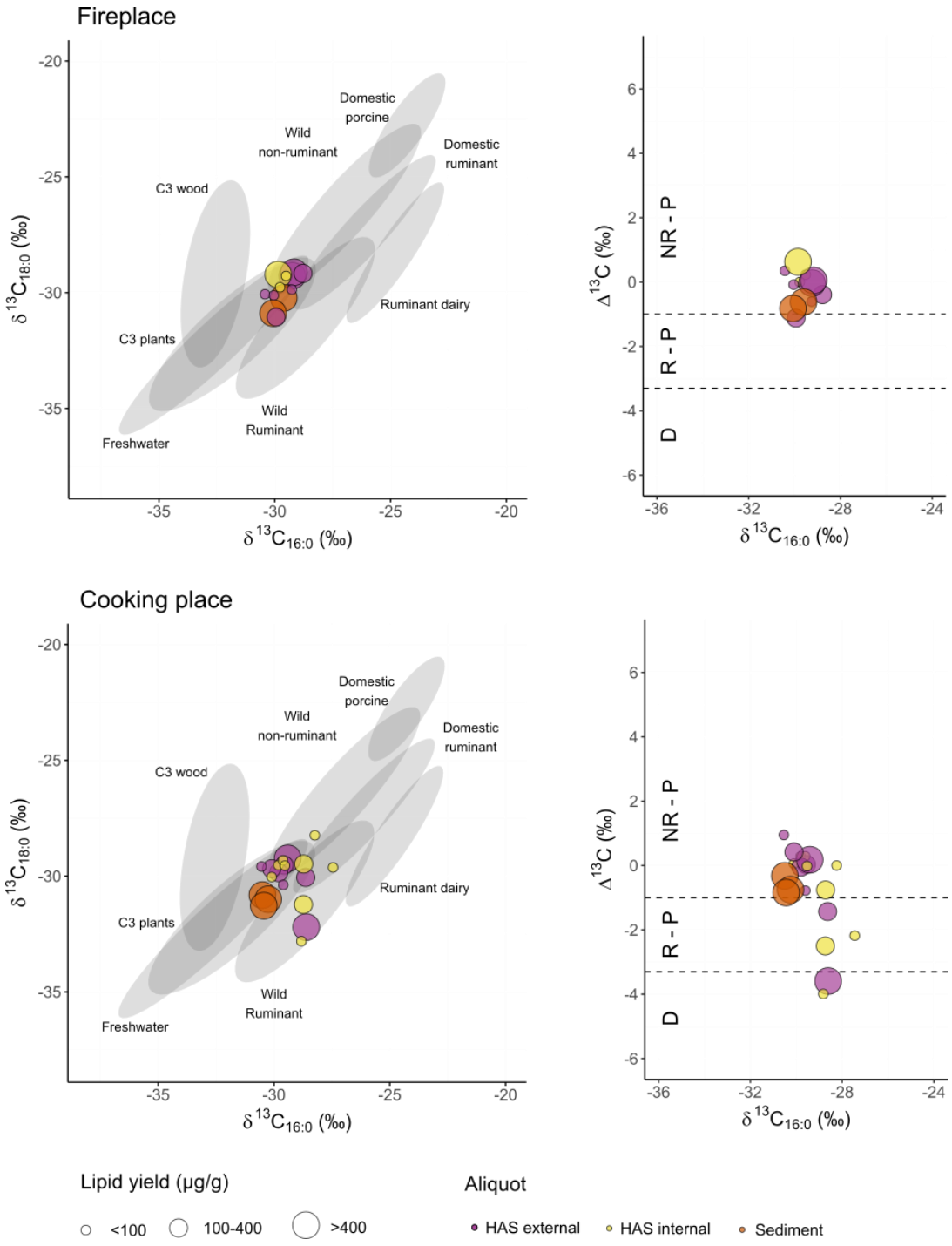


Figure 72. Plots of $\delta^{13}C$ values of palmitic ($C_{16:0}$) and stearic acid ($C_{18:0}$), and $\Delta^{13}C$ (the difference between the $\delta^{13}C$ values of the $C_{16:0}$ and $C_{18:0}$ fatty acids) versus $\delta^{13}C_{16:0}$, for HAS samples from Fireplace (FP-14549) and Cooking place (CP-14647) at Pendimoun. Point size is proportional to total lipid concentration, and colours indicate different aliquot types. Grey shaded ellipses show 68% confidence intervals for modern reference ranges (see Figure 13, chapter 3.1.2; Annex 3). Abbreviations: D = dairy products, R = ruminant adipose fat, NR = non ruminant adipose fat, P = plant products.

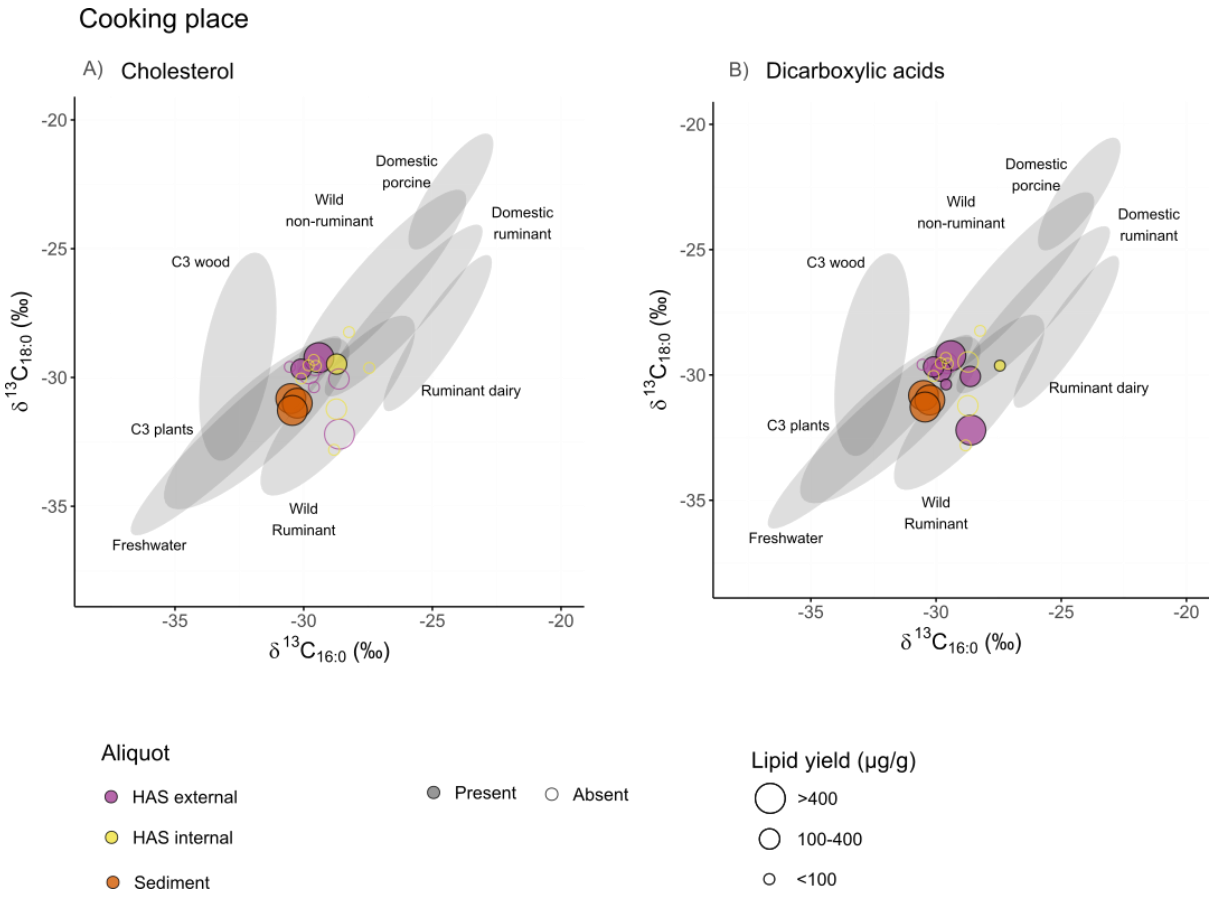


Figure 73. Plots of $\delta^{13}C$ values of palmitic ($C_{16:0}$) and stearic acid ($C_{18:0}$) for samples from Cooking place (CP-14647) at Pendimoun. The presence (filled points) and absence (open points) of cholesterol (A) and dicarboxylic acids (B) are indicated. Colours correspond to different aliquot types, and grey shaded ellipses show 68% confidence intervals for modern reference ranges (see Figure 13, chapter 3.1.2; Annex 3).

The co-occurrence of some biomarkers (4,8,12-TMTD, pristanic and phytanic acids) in both sediments and HAS samples form Pendimoun, together with the isotopic signatures, suggests possible exploitation of freshwater resources at the Fireplace. In contrast, the Cooking place presents a more complex picture, with mixed residues that cannot be clearly attributed to aquatic sources (Figure 74). Although phytanic acid exhibits relatively high %SRR values, the combined evaluation of $\Delta^{13}C$ against %SRR does not provide a definitive distinction between aquatic and terrestrial inputs (Lucquin et al., 2016; Shoda et al., 2020). Therefore, the detection of aquatic biomarkers on HAS in the rockshelter should be interpreted cautiously, as it may stem from a combination of environmental deposition and minor contributions from aquatic organisms, rather than providing clear evidence of deliberate exploitation.

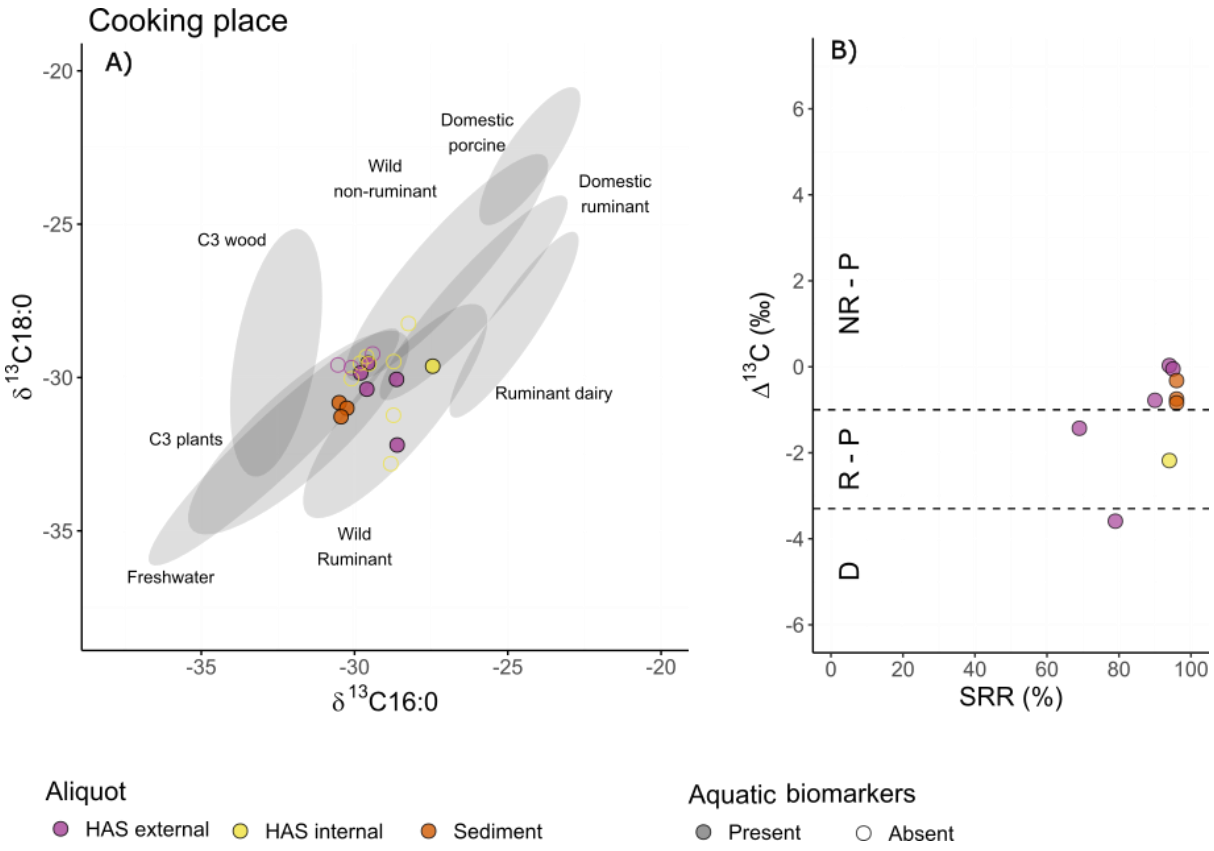


Figure 74. (A) Plot of $\delta^{13}C$ values of palmitic ($C_{16:0}$) and stearic acid ($C_{18:0}$) and (B) $\Delta^{13}C$ (the difference between the $\delta^{13}C$ values of the $C_{16:0}$ and $C_{18:0}$ fatty acids) versus %SRR diastereomer, for samples from Cooking place (CP-14647) at Pendimoun. The presence (filled points) and absence (open points) of aquatic biomarkers (4,8,12-TMTD, pristanic and phytanic acids) are indicated. Colours correspond to different aliquot types, and grey shaded ellipses show 68% confidence intervals for modern reference ranges (see Figure 13, chapter 3.1.2; Annex 3).

Synthetic conclusion on the site of Pendimoun

Taken together, the results from Pendimoun indicate that HAS preserve a variable range of molecular and isotopic signals, reflecting both natural and anthropogenic inputs. Some samples are largely dominated by soil organic matter similar to that found in sediments, whereas others reflect a combination of environmental inputs and human practices, including the processing and use of both plant and animal materials including dairy. As discussed above for La Draga, the surrounding sediments themselves may also contain anthropogenic signatures, emphasising the need to consider the broader depositional and post-depositional context when interpreting residue data.

Moreover, the two firing features identified in the site as Fireplace and Cooking place demonstrate distinct patterns of residue accumulation. The Fireplace appears to have a more restricted use, with residues indicative of a limited range of organic inputs that largely correspond with

sedimentary signatures, whereas the Cooking place exhibits a more heterogeneous residue profile. This diversity suggests a broader exploitation of organic resources at the Cooking place, including both plant and animal materials, which may reflect different functional roles, cooking practices, or repeated episodes of use. Collectively, these observations highlight not only the potential of HAS to preserve complex biochemical information but also the importance of integrating molecular, isotopic, and contextual evidence to reconstruct past human behaviour and site formation processes.

Table 11. Summary of lipid analyses results on sediments from Pendimoun. Lipid yields are presented alongside the principal and diagnostic compounds detected through combined extractions (AE, SE), with associated stable carbon isotope data. Compounds include saturated fatty acids (SFA), branched fatty acids (BrFA), unsaturated fatty acids (UFA), hydroxy FA (Hy), dicarboxylic fatty acids (DC), *n*-alkanes (ALK), alcohols (OH), ketones (K), terpenoids (terp), isoprenoids (4,8,12-TMTD: 4,8,12-trimethyl-tridecanoic acid, pri: pristanic acid; phy: phytanic acid), sterols (ster), monoacylglycerols (MAGs), wax esters (WE), and additional biomarkers (B3CA: benzene tricarboxylic acid). Compounds in red were found in both HAS and sediments. Stable carbon isotope ($\delta^{13}C$) values are present as $\delta^{13}C_{16:0}$ (‰), $\delta^{13}C_{18:0}$ (‰), together with the isotopic offset $\Delta^{13}C$ (‰), calculated as $\delta^{13}C_{18:0}$ - $\delta^{13}C_{16:0}$.

Material	*Sample*	*Structure*	*Lipid yield (µg/g)*	*$C_{16:0}/C_{18:0}$*	*$C_{18:1}/C_{18:0}$*	*Major and diagnostic compounds detected*	*$\delta^{13}C_{16:0}$ (‰)*	*$\delta^{13}C_{18:0}$ (‰)*	*$\Delta^{13}C$ (‰) ($\delta^{13}C_{18:0}$ - $\delta^{13}C_{16:0}$)*
Sediment	PDM-S14466		577.68	1.24	0.47	SFA (C12-30, C31, C32, C33, C34), BrFA (C17), UFA (C16:1, C18:1, C20:1), Hy (C24, C26), DC (C9, C10, C11, C12, C16, C18, C20, C22, C24, C26, C28, C30, C31), ALK (C16, 25, 27, 29, 31, 33), OH (C18, C22, C24, C26-30, C32, C34), terp (Amyrin), 4,8,12-TMTD, pri (tr), phy (96% SRR), ster (Stigmastanol, β-Sitosterol), MAG, WE (C46, 48, 50, 52), B3CA	-29.70	-30.14	-0.44
Sediment	PDM-S15367	CP-14647	5165.71	1.54	0.65	SFA (C8, C9, C10, C12-30, C31, C32, C33), BrFA (C15, C17), UFA (C16:1, C18:1, C20:1, C22:1), Hy (C22, C23, C24, C25, C26), DC (C8, C9, C10, C11, C12, C16-28, C30), ALK (C15, 17, 20, 27, 29, 31, 33), OH (C18, C22, C24, C26, C27, C28, C29, C30, C32, C34), terp (Amyrin), 4,8,12-TMTD, pri (tr), phy (96% SRR), ster (Cholest-5-en-3-ol, Stigmasterol, Stigmastanol, β-Sitosterol), MAG, WE (C44, 46, 48, 50, 52)	-30.50	-30.82	-0.32
Sediment	PDM-S15373	CP-14647	4875.11	1.39	0.48	SFA (C11-30, C31, C32, C33), BrFA (C17), UFA (C16:1, C18:1, C20:1, C22:1), Hy (C22, C23, C24, C25-27), DC (C8, C9, C10, C11, C12, C14, C16, C17, C18, C19-21, C22, C23, C24, C25, C26, C27, C28, C30), ALK (C15, 18, 20), OH (?), terp (Amyrin), 4,8,12-TMTD, pri (tr), phy (96% SRR), ster (Cholest-5-en-3-ol, Stigmasterol, Stigmastanol, β-Sitosterol)	-30.25	-31.00	-0.75
Sediment	PDM-S15442	CP-14647	1301.13	1.47	0.59	SFA (C12-30, C31, C32), BrFA (C13, C15, C17), UFA (C16:1, C18:1, C20:1, C22:1), Hy (C22, C23, C24, C25, C26, C27, C28), DC (C9, C10, C11, C12, C15-30), ALK (C15, 17, 18, 20), OH (?), terp (Amyrin), 4,8,12-TMTD, pri (tr), phy (96% SRR), ster	-30.44	-31.28	-0.84

Material	*Sample*	*Structure*	*Lipid yield (µg/g)*	*$C_{16:0}/C_{18:0}$*	*$C_{18:1}/C_{18:0}$*	*Major and diagnostic compounds detected*	*$\delta^{13}C_{16:0}$ (‰)*	*$\delta^{13}C_{18:0}$ (‰)*	*$\Delta^{13}C$ (‰) ($\delta^{13}C_{18:0}$ - $\delta^{13}C_{16:0}$)*
						(Cholest-5-en-3-ol, Stigmasterol, Stigmastanol, β-Sitosterol), B3CA			
Sediment	PDM-S14865	FP-14549	1506.23	1.18	0.60	SFA (C9-30, C31, C32, C33, C34), BrFA (C15, C17), UFA (C16:1, C18:1, C20:1, C22:1), Hy (C22, C23, C24, C25, C26), DC (C8, C9, C10, C11, C12, C16, C18, C19, C22-26, C28, C30), OH (?), terp (Amyrin), 4,8,12-TMTD, pri (tr), phy (96% SRR), ster (Cholest-5-en-3-ol, Stigmasterol, Stigmastanol, β-Sitosterol), B3CA	-29.61	-30.23	-0.62
Sediment	PDM-S15396	FP-14549	1047.82	1.31	0.47	SFA (C8, C9, C10, C12-30, C31, C32, C33, C34), BrFA (C13, C15, C17), UFA (C16:1, C18:1, C20:1, C22:1), Hy (C22, C23, C24, C25-27), DC (C8, C9, C10, C11, C12, C16-19, C21-28, C30), ALK (C15, 17, 18, 20), OH (?), terp (Amyrin), 4,8,12-TMTD, pri (tr), phy (96% SRR), ster (Cholest-5-en-3-ol, Stigmasterol, Stigmastanol, β-Sitosterol)	-30.07	-30.89	-0.82

Table 12. Summary of lipid analyses results on HAS from Pendimoun. Lipid yields are presented alongside the principal and diagnostic compounds detected through combined extractions (AE, SE), with associated stable carbon isotope data. Compounds include saturated fatty acids (SFA), branched fatty acids (BrFA), unsaturated fatty acids (UFA), hydroxy FA (Hy), dicarboxylic fatty acids (DC), *n*-alkanes (ALK), alcohols (OH), ketones (K), terpenoids (terp), isoprenoids (4,8,12-TMTD: 4,8,12-trimethyl-tridecanoic acid, pri: pristanic acid; phy: phytanic acid), sterols (ster), monoacylglycerols (MAGs), and additional biomarkers (B3CA: benzene tricarboxylic acid). Compounds in red were found in both HAS and sediments. Stable carbon isotope ($\delta^{13}C$) values are present as $\delta^{13}C_{16:0}$ (‰), $\delta^{13}C_{18:0}$ (‰), together with the isotopic offset $\Delta^{13}C$ (‰), calculated as $\delta^{13}C_{18:0}$ - $\delta^{13}C_{16:0}$.

Material	*Sample*	*Structure*	*Aliquot*	*Lipid yield (µg/g)*	*$C_{16:0}/C_{18:0}$*	*$C_{18:1}/C_{18:0}$*	*Major and diagnostic compounds detected*	*$\delta^{13}C_{16:0}$ (‰)*	*$\delta^{13}C_{18:0}$ (‰)*	*$\Delta^{13}C$ (‰) ($\delta^{13}C_{18:0}$ - $\delta^{13}C_{16:0}$)*
HAS	PDM-N04-15250	CP-14647	d	51.61	1.26	9.12	SFA (C16, C18, C20, C22-26, C28, C30), UFA (C18:1), ALK (C31), OH (C13, C16, C18), 4,8,12-TMTD, pri			
HAS	PDM-N04-15250	CP-14647	i	29.32	1.00	14.12	SFA (C16-18, C20-26, C28), UFA (C18:1, C22:1), OH (C18), pri, phy (89% SRR), B3CA (tr)	-29.81	-29.53	0.28
HAS	PDM-N04-15252	CP-14647	e	218.70	1.14	4.30	SFA (C16-18, C20, C22-30), UFA (C16:1, C18:1, C22:1), ALK (C31), OH (C16, C18, C26), 4,8,12-TMTD (tr), pri, phy (94% SRR)	-29.56	-29.53	0.03
HAS	PDM-N04-15252	CP-14647	i	90.93	1.30	7.53	SFA (C14-18, C20, C22, C24), UFA (C16:1, C18:1, C22:1), pri	-29.61	-29.32	0.29
HAS	PDM-N04-15329	CP-14647	e	280.53	1.69	3.28	SFA (C12-14, C16-18, C20, C22-30), UFA (C16:1, C18:1, C20:1, C22:1), DC (C13), ALK (C31), OH (C18, C26, C28, C30), 4,8,12-TMTD, pri, phy (69% SRR)	-28.63	-30.06	-1.43
HAS	PDM-N04-15329	CP-14647	i	125.46	0.64	12.10	SFA (C12, C14, C16-26, C28), UFA (C18:1, C22:1), OH (C18), pri, phy (79% SRR), B3CA (tr)	-28.73	-31.23	-2.50
HAS	PDM-N04-15337	CP-14647	e	66.53	1.63	8.99	SFA (C12, C14, C16-18, C20, C22-30, C32), UFA (C18:1, C22:1), DC (C13), ALK (C22), OH (C16, C18, C26), 4,8,12-TMTD, pri, phy (93% SRR), B3CA (tr)			

Material	*Sample*	*Structure*	*Aliquot*	*Lipid yield (µg/g)*	$C_{16:0}/C_{18:0}$	$C_{18:1}/C_{18:0}$	*Major and diagnostic compounds detected*	$\delta^{13}C_{16:0}$ (‰)	$\delta^{13}C_{18:0}$ (‰)	$\Delta^{13}C$ (‰) ($\delta^{13}C_{18:0}$ - $\delta^{13}C_{16:0}$)
HAS	PDM-N04-15337	CP-14647	i	40.69	2.03		SFA (C16, C18, C20, C22, C24, C26, C28), UFA (C18:1, C22:1), pri (tr), B3CA (tr)	-30.10	-30.04	0.06
HAS	PDM-N04-15338	CP-14647	e	177.35	1.68	1.81	SFA (C12, C14, C16-18, C20, C22-30, C32), UFA (C18:1, C20:1, C22:1), DC (C13), ALK (C29, C31), OH (C16, C17, C18, C26, C28, C30), 4,8,12-TMTD, pri, phy (95% SRR), B3CA (tr)	-29.80	-29.85	-0.05
HAS	PDM-N04-15348	CP-14647	e	466.68	1.00	7.25	SFA (C12, C14-18, C20, C22, C24-26, C28), UFA (C16:1, C18:1, C20:1, C22:1), DC (C9, 13), OH (C16, C18, C26), pri, phy (91% SRR), ster (Cholesta-3,5-diene, Cholesterol methyl ether, Cholesterol), WE (C46 tr)	-29.41	-29.23	0.18
HAS	PDM-N04-15355	CP-14647	e	48.04	1.48	1.79	SFA (C9-13, C16-18, C20, C22-30), UFA (C18:1, C22:1), Hy (C24), DC (C9, C13), ALK (C22, C23, C26, C29, C31), OH (C16, C17, C18, C26, C28, C30), 4,8,12-TMTD, pri, phy (90% SRR)	-29.60	-30.38	-0.78
HAS	PDM-N04-15355	CP-14647	i	113.59	1.24	3.90	SFA (C14-18, C20, C22-26, C28), BrFA (C17), UFA (C16:1, C18:1, C18:2, C22:1), Hy (C24), pri, ster (Cholesta-3,5-diene, Cholesterol methyl ether, Cholesterol)	-28.72	-29.48	-0.76
HAS	PDM-N04-15413	CP-14647	e	144.86	1.32	2.35	SFA (C12, C14, C16-18, C20, C22, C24-26, C28), UFA (C18:1, C22:1), DC (C10, C13), ALK (C31), OH (C16, C17, C18, C26, C28, C30, C32), pri, phy (89% SRR), ster (Cholesta-3,5-diene, Cholesterol methyl ether), B3CA (tr)	-30.10	-29.68	0.42
HAS	PDM-N04-15413	CP-14647	i	29.02	1.18	6.22	SFA (C16, C18), UFA (C18:1, C22:1), OH (C16, C18), pri (tr)	-29.53	-29.55	-0.02
HAS	PDM-N04-15419	CP-14647	e	47.77	1.29	11.95	SFA (C14, C16, C18, C20, C24-26, C28, C30), UFA (C18:1), OH (C16, C18), 4,8,12-TMTD (tr), pri (tr)	-30.54	-29.59	0.95
HAS	PDM-N04-15419	CP-14647	i	39.09	1.42		SFA (C16-18, C20, C22, C24), UFA (C18:1, C22:1), B3CA	-28.24	-28.24	0.00

Material	*Sample*	*Structure*	*Aliquot*	*Lipid yield (µg/g)*	*$C_{16:0}/C_{18:0}$*	*$C_{18:1}/C_{18:0}$*	*Major and diagnostic compounds detected*	*$\delta^{13}C_{16:0}$ (‰)*	*$\delta^{13}C_{18:0}$ (‰)*	*$\Delta^{13}C$ (‰) ($\delta^{13}C_{18:0}$ - $\delta^{13}C_{16:0}$)*
HAS	PDM-N04-15431	CP-14647	e	403.22	0.94	9.64	SFA (C12, C14-30, C32), BrFA (C17), UFA (C18:1, C22:1), DC (C9, C10, C13), ALK (C29, C31), OH (C16, C18, C26, C28), 4,8,12-TMTD, pri, phy (79% SRR)	-28.61	-32.20	-3.59
HAS	PDM-N04-15431	CP-14647	i	59.91	0.93	12.71	SFA (C14-18, C20-24, C26), BrFA (C17), UFA (C18:1, C22:1), phy (62% SRR)	-28.82	-32.81	-3.99
HAS	PDM-N04-15433	CP-14647	e	118.40	1.46	3.69	SFA (C9-13, C16-18, C20, C22-30, C32), UFA (C18:1, C22:1), DC (C13), ALK (C20, C22, C29, C30, C31), OH (C16, C18, C26, C28), phy (96% SRR)			
HAS	PDM-N04-15433	CP-14647	i	12.13	1.69		SFA (C11-13, C16-18, C20, C22-30), UFA (C18:1, C22:1), DC (C13), ALK (C20, C22, C29, C30, C31), 4,8,12-TMTD, pri, phy (94% SRR)	-27.45	-29.63	-2.18
HAS	PDM-N04-15197	FP-14549	d	6.77			SFA (C16), UFA (C18:1, C22:1), pri (tr)			
HAS	PDM-N04-15197	FP-14549	e	17.68	1.05	12.23	SFA (C16-18, C20, C24, C26, C28, C30), UFA (C18:1), ALK (C24, C26, C29, C30, C31), OH (C16, C18, C26, C28), 4,8,12-TMTD (tr), pri (tr), ster (Cholesterol, Stigmasterol, β-Sitosterol)	-30.42	-30.07	0.35
HAS	PDM-N04-15199	FP-14549	e	145.75	1.97	4.03	SFA (C12, C14, C16-18, C20, C22-30, C32), BrFA (C15), UFA (C18:1, C22:1), ALK (C26, C29, C31), DC (C13), OH (C14, C16, C18, C26, C28, C30), 4,8,12-TMTD, pri, phy (87% SRR), MAGs	-29.94	-31.06	-1.12
HAS	PDM-N04-15199	FP-14549	i	24.57	1.79	6.30	SFA (C9, C12, C14-18, C20, C22, C24, C26, C28), BrFA (C15), UFA (C18:1, C22:1), DC (C13), pri (tr), B3CA (tr)			
HAS	PDM-N04-15201	FP-14549	e	19.21	1.24	2.29	SFA (C12, C14, C16-18, C20, C22-24, C26, C28, C30), UFA (C18:1, C20:1, C22:1), DC (C13), K (C33, 35), 4,8,12-TMTD (tr), pri, phy (77% SRR)			
HAS	PDM-N04-15201	FP-14549	i	6.84	1.21		SFA (C14, C16-18, C20, C22), UFA (C18:1, C22:1), pri (tr), B3CA	-29.77	-29.77	0.00

Material	*Sample*	*Structure*	*Aliquot*	*Lipid yield (µg/g)*	*$C_{16:0}/C_{18:0}$*	*$C_{18:1}/C_{18:0}$*	*Major and diagnostic compounds detected*	*$\delta^{13}C_{16:0}$ (‰)*	*$\delta^{13}C_{18:0}$ (‰)*	*$\Delta^{13}C$ (‰) ($\delta^{13}C_{18:0}$ - $\delta^{13}C_{16:0}$)*
HAS	PDM-N04-15203	FP-14549	e	241.34	1.28	1.99	SFA (C12, C14-18, C20, C22-30), UFA (C16:1, C18:1, C20:1, C22:1), DC (C13), ALK (C26, C27, C29, C31), OH (C16, C18, C22, C24, C26, C28, C30, C32), 4,8,12-TMTD (tr), pri, phy (80% SRR), ster (Cholesterol methyl ether, Cholesterol), MAGs	-28.78	-29.17	-0.39
HAS	PDM-N04-15203	FP-14549	i	33.43	1.32		SFA (C14-18, C20, C24, C26, C28), UFA (C18:1, C18:1, C22:1), ALK (C26, C31), OH (C18, C22, C24, C26, C28, C30), MAGs	-29.51	-29.28	0.23
HAS	PDM-N04-15219	FP-14549	e	519.83	0.94	8.14	SFA (C14-18, C20, C22-24, C26, C28, C30), UFA (C16:1, C18:1, C22:1), DC (C13), 4,8,12-TMTD (tr), pri, phy (72% SRR)	-29.24	-29.27	-0.03
HAS	PDM-N04-15219	FP-14549	i	12.63			SFA (C14-18, C20, C22), UFA (C16:1, C18:1, C22:1), OH (C16, C18), pri (tr)			
HAS	PDM-N04-15225	FP-14549	e	7.04	1.69	8.78	SFA (C16-18, C20, C22, C24, C26), UFA (C18:1, C22:1), DC (C13), OH (C18, C26, C28, C30), 4,8,12-TMTD (tr), pri	-30.04	-30.12	-0.08
HAS	PDM-N04-15297	FP-14549	e	381.78	2.33	3.58	SFA (C9, C10, C12, C16-18, C20, C22, C24, C26, C28), UFA (C16:1, C18:1, C22:1), DC (C13), terp (Methyl dehydroabietate), 4,8,12-TMTD, pri, phy (77% SRR)	-29.17	-29.12	0.05
HAS	PDM-N04-15297	FP-14549	i	48.37	2.17	4.24	SFA (C9, C10, C12, C16, C18), UFA (C16:1, C18:1, C22:1), pri	-29.85	-29.22	0.63
HAS	PDM-N04-15398	FP-14549	e	26.88	1.31	2.60	SFA (C12, C14, C16-18, C20, C22-26, C28, C30), UFA (C16:1, C18:1, C22:1), DC (C13), ALK (C29, C31, C33), OH (C16, C18, C26, C28, C30, C32), 4,8,12-TMTD (tr), pri, phy (85% SRR), ster (Cholesterol)	-29.26	-29.87	-0.61

6.2.4. Protein analysis

Three HAS were selected for proteomic analysis based on macroscopic and stable carbon isotopic criteria. Sample PDM-N04-15250 was chosen due to the presence of a potential superficial deposit, suggestive of contact with organic material. Sample PDM-N04-15431 was selected because the $\delta^{13}C$ values of both external and internal aliquots fell within the isotopic ranges associated with wild ruminants and dairy products. Likewise, sample PDM-N04-15433 was included because its $\delta^{13}C$ values overlapped with the ranges of both domestic and wild ruminants, indicating potential processing of multiple types of animal resources.

As with the La Draga residues, all identified proteins in the Pendimoun samples were found to be contaminants likely originating from handling, the burial environment or laboratory contaminants, with the protein profiles again reflecting those of the blank controls (Table 13). The main proteins identified in the three samples were again trypsin, streptavidin, and keratins. Two samples (PDM-N04-15250, PDM-N04-15431) provided evidence of proteins potentially originating from the environmental context (i.e. soil-dwelling bacteria), however in both cases these were only represented by a single peptide and thus could not be authenticated.

Table 13. Mascot protein matches for residue samples Pendimoun (PDM-N04-15250, PDM-N04-15431, PDM-N04-15433) and their likely contaminant source. Note: Taxa listed are the most likely species as the majority are highly conserved sequences across taxa (ie. keratins). Contaminant source: LR = laboratory reagent; LC = Laboratory contaminant; H/SC = handling/surface contaminant; S/SC = soil/surface contaminant. Those in red text would normally be disregarded due to only having a single peptide match, however they have been included to show that essentially all identifiable proteins were contaminants.

Sample	Protein	Taxa (most likely)	Score	# peptide matches	Cont. source
PDM-N04-15250	Trypsin	*Sus scrufa*	190	15	LR
	Keratin, type I cytoskeletal 9	*Homo sapiens*	123	4	H/SC
	Probable multidrug ABC transporter permease	*Escherichia coli*	63	1	S/SC
	Cationic trypsin-3	*Rattus norvegicus*	61	1	LR
	A-kinase anchor protein 13	*Homo sapiens*	48	1	H/SC
	Streptavidin	*Streptomyces avidinii*	46	1	LC
	Streptavidin-V2	*Streptomyces violaceus*	29	2	LC
	Holliday junction branch migration complex subunit RuvA	*Parasynechococcus marenigrum*	19	1	S/SC

Sample	Protein	Taxa (most likely)	Score	# peptide matches	Cont. source
	Serine/threonine-protein kinase KSP1	*Saccharomyces cerevisiae*	15	1	LC
PDM-N04-15431	Streptavidin	*Streptomyces avidinii*	97	3	LC
	Trypsin	*Sus scrufa*	95	8	LR
	Uroporphyrinogen decarboxylase	*Mycolicibacterium gilvum*	62	1	S/SC
	S-adenosylmethionine decarboxylase proenzyme 2	*Brassica juncea*	25	1	S/SC
PDM-N04-15433	Trypsin	*Sus scrufa*	177	14	LR
	Keratin, type I cytoskeletal 9	*Homo sapiens*	79	1	H/SC
	Streptavidin	*Streptomyces avidinii*	72	4	LC
	60 kDa heat shock protein	*Homo sapiens*	48	1	H/SC
	Keratin, type II cytoskeletal 1	*Homo sapiens*	44	1	H/SC
	Streptavidin-V2	*Streptomyces violaceus*	42	1	LC
	Keratin, type II cytoskeletal 2 epidermal	*Homo sapiens*	41	1	H/SC
Blank_1	Trypsin	*Sus scrufa*	121	8	LR
	Streptavidin	*Streptomyces avidinii*	41	2	LC
Blank_2	Trypsin	*Sus scrufa*	181	14	LR
	Streptavidin	*Streptomyces avidinii*	91	5	LC
	Keratin, type I cytoskeletal 9	*Homo sapiens*	70	1	H/SC
	A-kinase anchor protein 13	*Homo sapiens*	48	1	H/SC
	Keratin, type I cytoskeletal 10	*Homo sapiens*	48	1	H/SC

7. Discussion

This thesis set out to demonstrate the value of heat-altered stones (HAS) as repositories of anthropogenic molecular and technological evidence, capable of illuminating past diets, resource exploitation, fire-related and technological practices. Rather than being treated simply as by-products of fire, HAS can preserve molecular traces that reveal what substances past societies processed and the techniques they employed. Documenting and analysing HAS as artefacts in their own right allows for a broader exploration of daily life, encompassing culinary practices, subsistence strategies, and associated social activities that are often archaeologically elusive. In this way, this study restores value to a class of material long underestimated, highlighting its potential to enrich interpretations of Neolithic foodways. The preceding chapters have addressed this aim through a series of specific objectives, each contributing to the development of a more robust framework for recognising, interpreting, and utilising HAS in archaeological research. The present chapter brings these strands together, revisiting the research questions outlined at the outset, assessing the key findings, and situating them within wider archaeological debates. It also reflects on the methodological and interpretative contributions of the study, before considering their implications for future research.

7.1. Distribution of HAS across distinct chronological, geographical and cultural contexts in prehistoric archaeology

Although HAS have been documented for decades, they have rarely been the central focus of archaeological investigation, often appearing incidentally within studies of hearths, burnt mounds, and other fire-related features, or in broader discussions of spatial organisation, which has limited the availability of detailed datasets for comparative purposes. A limitation of this study is the exclusion of grey literature, such as master's dissertations, doctoral theses, and local excavation reports. Whilst such sources may provide valuable insights at the regional scale, their incorporation into a global review is constrained by the absence of systematic archiving and consistent accessibility. Incorporating them would have reduced the overall consistency and comparability of the dataset, even though their potential value for localised case studies is acknowledged.

Over time, however, research has begun to recognise the potential of HAS to illuminate aspects of past human behaviour, including culinary practices, technological knowledge, and spatial organisation. A significant shift in the methodological landscape has been observed, with chemical and physical approaches only being applied from the 1980s onwards, coinciding with a marked increase in experimental studies. Moreover, the past two decades have seen exponential growth in research

combining multiple analytical methods. By systematically reviewing the literature, it is possible to trace the evolving methodological approaches, regional emphases, and cultural interpretations that have shaped our understanding of HAS, while also identifying persistent gaps and challenges.

The systematic review of the literature (Chapter 2) confirms that HAS are widely distributed across multiple regions and chronological periods, yet they remain under-analysed, underscoring the need for more systematic study to fully understand their archaeological significance. The majority of documented occurrences are concentrated in North America and Europe, predominantly within Holocene contexts, with a smaller proportion dating to the Pleistocene, highlighting the long-standing and cross-cultural significance of these artefacts (Cantelli et al., 2024). Importantly, HAS are found in a variety of spatial contexts, from well-defined hearths, pits, and burnt mounds to more dispersed assemblages, reflecting both their functional versatility and **the challenges of interpreting their role in past human activities**. Evidence suggests they were primarily used in cooking techniques such as platform hearths, stone boiling, and earth ovens, with the thermal history, fracture patterns, and stone size reflecting specific uses. Equally critical is **the issue of identification and characterisation**, which has long posed methodological challenges in archaeology. Inconsistent terminology, ranging from fire-cracked rocks (FCR) and heated stones to thermally modified rocks (TMR), complicates efforts to systematically document these artefacts. Beyond nomenclature, accurate recognition relies on multiple indicators, including colour changes, fracture patterns, crazing, spalling, and fragment morphology, all of which can reflect the intensity, duration, and frequency of heating events. While visual inspection and colour charts provide a starting point, complementary techniques are essential for reliably detecting thermal alteration.

In addition to these methodological considerations, **HAS provide key insights into prehistoric lifeways**, revealing technological practices, resource management strategies, and social organisation. Their presence, frequency, and characteristics can indicate occupation intensity, site use, and patterns of mobility, while also reflecting cooperative and communal activities such as feasting or complex food preparation. Analytical and experimental approaches further demonstrate the effort involved in their use, their functional lifespan, and the temporal span of fire-related activities, highlighting the broader interpretive potential of HAS for understanding cultural and behavioural patterns in past societies.

Overall, the synthesis of 73 records spanning eighty years provided a substantial understanding of the geographic, chronological, and cultural patterns of HAS, while also highlighting **persistent gaps in research, methodological inconsistencies and terminological ambiguities**. Building on this foundation, the methodology applied in the present study aimed to establish a framework for the reliable identification and characterisation of HAS. This represents the first step of the research, laying the

groundwork for addressing subsequent questions about their culinary applications, contribution to subsistence strategies, household management, and broader role in Neolithic life.

7.2. Morphological alteration patterns in HAS: Insights from La Draga and Pendimoun

The choice of **the Neolithic sites of La Draga (Spain) and Pendimoun (France)** was central to this study, as their contrasting environmental and cultural contexts provided an ideal framework for assessing the preservation and interpretation of HAS into a similar chronological and cultural period. La Draga, an Early Neolithic lakeshore settlement dated to the 6th millennium BCE and attributed to Cardial ware facies, offers exceptional waterlogged conditions that preserve organic materials rarely encountered elsewhere in the Iberian Peninsula and Mediterranean environments, making it a key reference point for understanding early farming lifeways. In contrast, Pendimoun, a rock-shelter with a long stratigraphic sequence spanning from the Impressa to the Bell Beaker periods, provides one of the few continuous records of the Impresso-Cardial transition in the western Mediterranean. Differences in excavation timing, sampling strategies, and post-excavation practices between the two sites further enrich the comparative framework, enabling a more nuanced understanding of post-depositional processes and their impact on HAS preservation. The comparison of these sites therefore provides a valuable framework for assessing how contrasting environmental conditions, excavation strategies, and post-excavation practices may affect the preservation of organic residues in HAS. Collectively, their study underscores the significance of examining HAS within diverse contexts, both to capture the **variability of Neolithic culinary and subsistence practices** and to contribute to the development of more consistent and robust methodological approaches for future research.

As the second research question seeks to identify and characterise morphological alteration patterns on HAS, **stone artefacts from La Draga (n = 15) and Pendimoun (n = 19) were examined for macroscopic evidence of thermal modification**. Although this number is relatively small compared to the abundance of ceramic artefacts, lithic tools, and faunal remains commonly studied by archaeologists, it represents a notably high sample within the still limited body of research dedicated to heat-altered stones. Focus was placed on features indicative of exposure to heat or fire, including cracking, thermal fractures, discolouration, and depositional residues resulting from combustion processes. Each artefact was also documented using 3D scanning and photogrammetry, producing high-resolution models that preserve original shape and texture and contribute to a digital database for research and heritage purposes. The 3D models are publicly accessible through a repository hosted by OpenLab UAB on Sketchfab (LD = https://skfb.ly/puzEx; PDM = https://skfb.ly/puzEA). The patterns

identified through these methods provide a robust basis for assessing the functional and contextual role of HAS within each site.

The visual inspection of HAS from Sector B/D at **La Draga** revealed diverse macroscopic features indicative of thermal alteration and use in fire-related activities. The assemblage, including diverse raw materials such as sandstones, limestones, marls, and volcanic stones, displayed a variety of morphologies (tabular, prismatic, spherical, and pot-lid) highlighting differential responses to heat and potential functional diversity. Macroscopic patterns such as cracking, sooting, discolouration, and superficial deposits, are consistent with exposure to high temperatures and interaction with combustion contexts. Taken together, **morphology and thermal features suggest functional differentiation**. Spherical stones, with smooth, levigated surfaces and evidence of sooting and discoloration, may represent grinding tools (*mano de molino*) subsequently exposed to fire, indicating potential secondary use in combustion context. Tabular stones likely served as cooking platforms or griddles. Prismatic stones appear to have undergone repeated heating cycles, pointing to their use as hand-held tools or in specific heating tasks. Finally, pot-lid fractures reflect rapid and direct thermal stress.

The HAS assemblage from **Pendimoun** provides valuable insights into the role of thermally altered stones within fire-related activities during the site's earliest SMP occupation. Although the material had been previously sectioned for petrographic analysis, the preserved fragments indicate predominantly subangular forms. This precludes the possibility of drawing firm conclusions regarding intentional shaping or selection. Nonetheless, the contextual association of all specimens with two circular firing features, a fireplace (FP-14549) and a cooking place (CP-14647), supports their interpretation as **deliberately integrated components of fire installations** rather than incidental inclusions. Macroscopic traces of thermal alteration, including reddening, sooting, cracking and superficial adhesion, indicate **repeated or prolonged exposure to high temperatures**, most likely in direct contact with burning fuel. Even though petrographic observations (Cardelli, 2013) suggested a distinction between the two firing structures, with thermal shock fractures identified in HAS from the fireplace, macroscopic analysis conducted in this study revealed no clear differences in morphology or surface alteration between the two assemblages.

Taken together, the examination of HAS from La Draga and Pendimoun highlights the value of macroscopic, visual inspection for identifying and characterising thermally altered stones. At both sites, features such as cracking, discolouration, sooting, superficial deposits, and thermal fractures provide clear evidence of exposure to fire, allowing lithic artefacts to be confidently classified as HAS. La Draga exhibited a broader range of morphologies and functional differentiation, whereas Pendimoun displayed more uniform subangular forms. In both cases, careful documentation of alteration patterns facilitated a robust assessment of fire-related activity. The comparative analysis thus demonstrates that

systematic recording of thermal alteration patterns provides a reliable basis for interpreting the use and significance of stones in prehistoric fire practices, independent of site-specific preservation conditions or prior analytical interventions.

7.3. The Potential of HAS for Reconstructing Culinary Practices

As the third research question seeks to assess the potential of HAS for recovering information on past culinary practices, **selected stones from La Draga and Pendimoun were subjected to molecular and carbon stable isotope analyses**. This question addresses the growing need to diversify our sources of information on past dietary and subsistence practices derived from organic residue analysis of archaeological artefacts, which have so far focused primarily on ceramic vessels.

Stone artefacts, including ground stone implements, flaked tools, and stone vessels, have long been understood as central to daily life, fulfilling roles in hunting, plant and animal processing, cooking, and storage. Specifically, HAS occupy a distinct position within this spectrum, often interpreted as heating elements or components of combustion-related contexts, although some may form passively through incidental exposure to fire. Archaeological studies targeting lipid residues on lithics have predominantly focused on surface-attached residues, while direct extraction from the stone matrix remains less common. Existing protocols typically adapt methods developed for ceramics, encompassing sampling, solvent-based extraction, derivatisation, and molecular analysis through GC, GC-MS, or, more recently, GC-MS/MS. Stable carbon isotope analysis ($\delta^{13}C$) of fatty acids has occasionally been employed to refine interpretations of residue origin and mixtures. Building on these methodological developments, this study is therefore pioneering in applying lipid residue analysis to HAS, and the comparatively large dataset provides an important foundation for developing methodological and interpretative frameworks in this emerging field.

The application of lipid residue analysis on HAS from the two Neolithic sites of La Draga and Pendimoun has produced noteworthy results. Lipid residues were extracted and characterised using GC-FID and GC-MS, allowing the identification of food-derived compounds preserved in the artefacts. The results were systematically compared with lipid residues from associated sediment samples to evaluate potential environmental contamination, site-specific patterns, and overlaps with HAS signatures. Several biomarkers typically identified in ceramic lipid analyses were detected in both HAS and contextual sediments, indicating that comparable molecular compounds and stable carbon isotope signatures can be preserved across different archaeological matrices. Complementary stable carbon isotope measurements provided insight into the origins and processing of these organic residues, serving

as a valuable technique that complements conventional lipid profiling. When used alongside molecular analysis, $\delta^{13}C$ measurements provide additional information on the source of lipids, for example by helping to distinguish between plant- and animal-derived inputs and identify mixed residues. This underscores the broader potential of residue analysis beyond ceramics, providing valuable insight into the preservation pathways and functional roles of materials involved in prehistoric subsistence practices.

Complementing the lipid and stable carbon isotope results, proteomic analysis of selected HAS from both sites did not detect any endogenous proteins attributable to food residues or other use-related materials. Although samples were selected based on superficial deposits, or $\delta^{13}C$ evidence suggestive of animal product processing, all identified proteins were contaminants from handling, laboratory procedures, or the burial environment, and protein profiles closely matched blank controls. The absence of detectable proteins likely reflects the combined effects of repeated heating, stone porosity, and post-depositional processes, which readily degrade proteins. In contrast to lipids, proteins appear unlikely to be preserved on HAS, limiting the applicability of proteomic analysis for reconstructing past culinary practices on these artefacts.

7.3.1. La Draga

At La Draga, the successful recovery of lipids from all HAS aliquots demonstrates that these stones are highly suitable for molecular analysis. Importantly, no significant differences were observed across lithological categories, indicating that the mineral composition of the stones did not substantially influence lipid preservation. Whereas sediment samples primarily reflect a background signal dominated by plant-derived inputs, HAS retain residues that appear more directly associated with anthropogenic activities, including culinary practices. Their lipid profiles are dominated by saturated fatty acids, primarily palmitic and stearic, consistent with patterns commonly observed in archaeological lipid assemblages. Beyond these major components, the detection of additional molecular markers provides a more refined insight into past resource use. Importantly, the **combined analysis of HAS and their associated sediments proved crucial for evaluating potential environmental contamination**.

Plant sterols, long-chain alcohols, alkylresorcinols, and oxidation products such as dicarboxylic acids were detected in some HAS, pointing to the processing of plant resources, including cereals. Although these compounds were also present in the corresponding sediments, which may partly contribute to the HAS profile, the sediments themselves could also carry evidence of human activity and not solely environmental inputs. This evidence is consistent with the carpological assemblage of the site, which includes remains of cultivated and wild plants, particularly cereals, pulses, and fruits

(Antolín and Buxó, 2011; Antolín et al., 2014). This correspondence between the molecular and archaeobotanical data strengthens the interpretation that at least **some stones were initially involved in plant-processing, possibly linked to domestic practices within the settlement such as grinding, before being re-used as HAS**. This highlights the issue of tool recycling, a practice widely attested in Neolithic contexts, where milling tools were frequently incorporated into hearths or other heating structures. Consequently, the plant-derived biomarkers preserved on these HAS may reflect residues from the original function of the stones rather than processes occurring after their incorporation into combustion structures, highlighting the importance of considering tool reuse when interpreting molecular evidence.

The presence of diterpenoid biomarkers derived from pine resin in a subset of stones is particularly noteworthy. These compounds may result from the heating of coniferous resins and therefore could reflect either the use of resinous wood as fuel or its deliberate processing for technological purposes. Archaeobotanical evidence at La Draga demonstrates that yew (*Taxus baccata*), pine (*Pinus sylvestris-nigra*), and juniper (*Juniperus* sp.) were the principal resins-producing taxa and were primarily exploited for technological purposes. These resins were predominantly used as adhesives in tool manufacture, as evidenced by their application on composite artefacts including sickles and ornaments like marble bracelets (Palomo et al., 2013; Piqué et al., 2015; Rageot et al., 2021). In contrast, oak (*Quercus* sp.), boxwood (*Buxus sempervirens*), and laurel (*Laurus nobilis*) were the principal species used for firewood at the site (Terradas et al., 2017; López-Bultó and Piqué Huerta, 2018; Terradas, Palomo and Piqué, 2020). Regional evidence further indicates that, in the north-eastern Iberian Peninsula, Pinaceae species were primarily exploited for the collection of their resins, used as adhesives, and not for firewood (Breu et al., 2023b), reinforcing the interpretation that the diterpenoid signature preserved in these specific HAS reflect activity-related residues linked to technological activities and not merely culinary practices. In this context, the use of hand-held stones to crush and heat pine resin provides a plausible explanation for the presence of diterpenoid residues. Notably, these diterpenoids were detected in HAS associated with the more recent occupation phase, characterised by the construction of travertine block pavement and structures, possibly suggesting that resin-related technological activities were more common during this phase. The absence of these compounds in sediment samples further strengthens this conclusion, demonstrating that the diterpenoid signal is specifically associated with human activity rather than environmental deposition. Importantly, these findings suggest that **the function of some HAS extended beyond culinary applications into technological activities, specifically the processing of resins**.

The molecular analysis of HAS from La Draga corroborates their interaction with fire, as previously suggested by the selection of artefacts exhibiting visible traces of heating and/or their association with combustion structures. The presence of dicarboxylic and hydroxy fatty acids, alongside

oxidation products of unsaturated fatty acids, is consistent with thermal alteration resulting from heating. These signals, when considered alongside structural transformations of resin biomarkers (e.g., dehydroabietic acid), and heat alteration patterns, demonstrate that some HAS were subjected to repeated or prolonged heating events. Notably, some HAS associated with combustion structures also exhibit isotopic signatures consistent with C_3 wood, further reinforcing the link between these stones and fire-related activities. While the specific purpose of this heating cannot be determined solely from the chemical data, the findings support the interpretation that stones identified as **HAS on the basis of heat alteration patterns were actively involved in activities requiring thermal exposure**.

Of particular note is that HAS samples exhibiting the highest lipid yields are frequently plotted outside established reference ellipses, suggesting complex, mixed isotopic signatures. These patterns are best explained by the co-occurrence of plant oils and animal fats. Theoretical mixing lines constructed from reference C_3 plant products and domestic porcine or wild animal adipose fats demonstrate that such isotopic positions correspond to mixtures of these resources in varying proportions. This suggests that **some stone artefacts absorbed residues derived from multiple food sources, reflecting the simultaneous processing of both plant and animal materials or a lengthy trajectory of use and recycling of these artefacts**. This pattern aligns with archaeobotanical and zooarchaeological evidence from La Draga, indicating a diversified subsistence economy that relied on the combined exploitation of plant and animal resources (Saña, 2011; Terradas et al., 2012; Antolín et al., 2014).

Integration of molecular and isotopic data with morphological observations of HAS reveals broader patterns of use (Table 14). Spherical stones, for instance, display molecular signatures of plant resources, suggesting their use as grinders for plant processing (LD10-833, LD11-1540), with one specimen (LD23-25396) indicating possible cereal processing prior to its re-use in combustion features. Another stone recovered from a combustion context (LD-25300) might have functioned as a culinary feature, given its mixed isotopic signature indicative of both plant and porcine fat resources. A single tabular stone (LD12-3951) exhibits morphological and heat-alteration patterns consistent with its use as a griddle or support surface, even if the molecular profile is less conclusive. Another tabular specimen (LD10-663), however, yielded plant-derived residues consistent with grinding activities. Pot-lid fractured stones (LD11-1547, LD11-1987), as well as one tabular stone exhibiting extensive cracking (LD11-3791), are best interpreted as having functioned within combustion structures, where repeated exposure to high heat caused thermal fracturing. However, specimen LD11-1547, which exhibits a mixed isotopic signature indicative of both plant and porcine fat resources, may likewise have been used as a culinary feature. Finally, one prismatic stone with a diterpenoid signature (LD10-518) most likely represents a hand-held tool employed in resin processing.

These combined results demonstrate that HAS at La Draga retain residues that not only reflect food processing and cooking activities but also extend to previous technological practices. Crucially, the molecular and isotopic evidence for plant sterols, alkylresorcinols, and mixed plant-animal lipid signatures show that HAS retained traces of diverse foodstuffs, including cereals and composite resources. **Their distinctive preservation, when compared to the surrounding sediments, underscores the value of HAS as activity-specific archives that capture residues more directly associated with human behaviour**.

Furthermore, variations in molecular and isotopic signatures across different specimens and contexts may also reflect changes in the use and function of HAS between occupation phases. These differences could reflect shifts in the types of resources processed or in the organisation of domestic and technological activities over time. Consequently, **HAS do not merely record isolated episodes of activity but can also provide insight into broader temporal patterns of resource exploitation and technological adaptation at La Draga**.

Table 14. Overview of analysed HAS from La Draga, showing thermal alteration patterns, morphological characteristics, molecular signatures, and inferred functional interpretation.

Occupation phase	*Excavation year*	*Sample ID*	*Feature*	*Cracks*	*Sooting*	*Discol.*	*Sup. deposit*	*Morphology*	*Molecular signature*	*Use interpretation*
oldest	2010	663						tabular	Plant resources	Grinder base
	2010	833				x		spherical	Plant resources	Grinder
	2011	1547						pot-lid	Mixed resources	Culinary feature
	2011	2156			x	x	x	prismatic		
	2012	3791		x				tabular		Combustion feature
	2023	25300	Structure E266	x	x			tabular	Mixed resources	Culinary feature
	2023	25396	Structure E269		x			spherical	Plant resources (cereals)	Grinder and (subsequently) combustion feature
	2023	25430	Structure E269		x			tabular	Mixed resources	Combustion feature
more recent	2010	500						prismatic	Mixed resources	Culinary feature
	2010	518		x	x	x		prismatic	Coniferous resin	Hand-held tool
	2011	1540				x		spherical	Plant resources	Grinder
	2011	1987		x				pot-lid	Coniferous resin	Combustion feature
	2012	3951		x	x	x	x	tabular		Griddle/support surface
	2012	4007		fracture	x			tabular		
	2012	4035		x		x	x	tabular		

7.3.2. Pendimoun

Also in the case of Pendimoun, the recovery of lipids from the majority of HAS aliquots was successful, demonstrating that these stones are highly suitable for molecular analysis. External surfaces consistently yield higher concentration than internal and deposit aliquots. Although all stones except one belong to a single lithology, allowing only limited comparison across stone types, differentiation emerges between the two firing features. HAS from the Cooking Place (CP-14647) generally display higher lipid concentrations than those from the Fireplace (FP-14549), with external surfaces in CP-14647 showing the most pronounced enrichment. Molecular profiles are largely similar across both contexts, reflecting a shared combustion-related background, while the elevated lipid concentration in CP-14647 likely indicates more intensive contact with lipid-bearing materials, consistent with food-processing activities.

Their lipid profiles are dominated by saturated fatty acids, primarily palmitic and stearic, consistent with patterns commonly observed in archaeological lipid assemblages. Beyond these major components, the detection of additional molecular markers points to the **processing of plant resources or the association with sedimentary samples**. Anthracological evidence concerning the SMP occupation phase point to a dominant presence of deciduous oak (*Quercus f.c*) (Battentier et al., 2015), while phytolith analysis indicates the use of young plant material for fodder, bedding, or other purposes (Delhon et al., 2020).

Monounsaturated fatty acids, notably oleic and erucic acids, often co-occur with dicarboxylic acids such as brassylic acid, indicative of thermal alteration of seed oils, possibly from Brassicaceae-type seeds (Colombini et al., 2005). Apart from sediments, plant sterols were identified only in one HAS sample from Fireplace, a pattern that may indicate more intense or prolonged heating, leading to their complete thermal degradation. Collectively, these molecular signatures provide strong evidence that many of the stones were subjected to repeated or sustained heating events, consistent with their use in prehistoric firing-related activities. While the specific purpose of this heating cannot be determined solely from the chemical data, it supports the interpretation that **HAS were actively involved in activities requiring thermal exposure**.

The fact that ketones were detected in only a single HAS sample, from Fireplace, suggests that their presence is unlikely to result from heating during drilling, as recent studies have cautioned (Longoni et al., 2024), but rather reflects genuine thermal exposure associated with the prehistoric use of the stone. Since the drilling procedure was applied uniformly across all HAS, any ketones generated by this process would be expected to occur consistently across multiple samples. Their isolated

occurrence therefore points to authentic exposure to fire, reinforcing the interpretation of these stones as having been directly involved in firing-related activities. Notably, recent experimental analyses on heated stones failed to detect long-chain ketones despite extensive extraction and fractionation procedures, highlighting the need for further research to understand their formation under such conditions (Langley, 2024).

Although the molecular profiles of HAS from the Cooking Place and the Fireplace are broadly similar and largely dominated by plant-derived compounds, the stable carbon isotope data reveal subtle but significant differences in resource use (Table 15). Some stones from the Cooking Place exhibit $\delta^{13}C$ values within the ranges associated with wild and domestic ruminants, wild non-ruminants, and, in the case of $\Delta^{13}C$ values, even dairy products. This suggests that, in addition to processing plants, **the Cooking Place was used for handling a variety of animal products that may have been partially degraded or left limited molecular traces**. Although the faunal assemblage at the site is relatively scarce, it nevertheless attests to the clear presence of ruminants (Binder et al., 2020), a pattern that is reflected in the isotopic evidence pointing to ruminant-derived fats among the animal residues. In contrast, the Fireplace shows no isotopic evidence for significant animal inputs, indicating that its use was largely restricted to a general heating feature. Taken together, the results from Pendimoun demonstrate that HAS effectively preserve residues reflecting the intensity of thermal exposure and the diversity of activities carried out within the site's firing features.

Table 15. Overview of analysed HAS at Pendimoun organised by Cooking Place (CP-14647) and the Fireplace (FP-14549), showing thermal alteration patterns, morphological characteristics, molecular signatures, and inferred functional interpretation.

Structure	*Sample ID*	*cracks*	*sooting*	*discoloration*	*sup. deposit*	*Molecular signature*	*Use interpretation*
CP-14647	15250				x		Culinary feature
	15252	x	x				
	15329		x			Ruminant resources	
	15337			x			
	15338					Plant resources	
	15348	x				Mixed resources	
	15355					Mixed resources	
	15413					Mixed resources	
	15419			x		Non-ruminant resources	
	15431					Wild ruminant resources (dairy)	
	15433		x			Ruminant resources	
FP-14549	15197		x	x	x	Plant resources	Combustion feature
	15199					Plant resources / Thermal alteration	
	15201			x		Plant resources / Thermal alteration	
	15203					Plant resources	
	15219						
	15225		x				
	15297			x		Plant resources	
	15398			x		Plant resources	

7.3.3. Common considerations

The molecular profiles of the sediments are broadly similar to those of HAS, indicating some background contribution from the depositional environment at La Draga, and, in the case of Pendimoun, primarily reflecting combustion-derived inputs rather than contamination. However, specific biomarkers and isotopic offsets suggest that the **lipid compositions of HAS reflect additional and specific inputs or processes beyond those of the surrounding sediments**. This distinction is further supported by the fact that wax esters were detected exclusively in the sediments, reinforcing the differences between the two matrices. In addition, the stable carbon isotope values of the sediments differ from those of the HAS, confirming that the isotopic signatures preserved in the stones are not entirely derived from environmental inputs. Together, these observations indicate that both the molecular and isotopic characteristics of HAS reflect their original use and exposure, rather than contamination from the surrounding soils. Nevertheless, the case of Pendimoun shows that modern contamination can occur, particularly through handling and/or storage in plastic bags, underscoring the importance of rigorous sampling and laboratory protocols.

While stable carbon isotope analysis and lipid profiling demonstrate considerable potential for interpreting the use of stone artefacts, other biomolecular approaches remain more problematic. In particular, **protein analysis has so far produced largely inconclusive results on stones**, reflecting poor preservation and methodological limitations. This likely reflects the greater sensitivity of proteins to heat and post-depositional processes, which can rapidly denature and degrade them, whereas lipids are more chemically robust and able to persist in microstructures (Evans et al., 2024). These findings indicate that, unlike ceramics, stone artefacts are not yet a reliable substrate for protein-based investigations, and protocols developed for other materials remain unsuitable. Consequently, lipid-based methods, preferably combined with isotopic analysis, currently offer the most robust analytical approach for reconstructing past culinary practices from stone tools.

7.4. The Molecular Variability of HAS Across Sites and Materials

To address the fourth research question, a comparative analysis of HAS from La Draga and Pendimoun reveals distinct **site- and feature-specific differences in lipid concentrations, molecular profiles, stable carbon isotope signatures, and morphological characteristics**. In addition, the molecular profile of HAS is considered alongside previously published lipid residue analyses from associated ceramic vessels, in order to evaluate the extent to which patterns in the lithic assemblage may be correlated with those identified in ceramic contexts. The results nonetheless provide a basis for

critical reflection on the roles of these artefacts within broader food processing strategies and their integration into wider archaeological narratives concerning subsistence, culinary practice, and technological choice.

Sediments themselves can provide valuable insights into both environmental conditions and past human activity, serving as repositories of chemical signatures that contextualise artefact use, according to its spatial position. The molecular analysis of sediment samples from the two sites reveals contrasts that are not apparent from isotopic data alone. While isotopic signatures are broadly similar, suggesting comparable general sources of organic matter, detailed lipid profiles reveal distinct patterns of input and preservation.

Sediments from the PDM site are dominated by vascular plant waxes, reflecting a predominance of terrestrial plant material, possibly derived from surrounding vegetation or from plant materials intentionally introduced during site use, aligning closely with the sedimentary profiles previously reported (Drieu, Binder and Regert, 2022). This interpretation is supported by phytolith evidence, which likewise indicates the presence of young plant material for fodder, bedding, or other uses (Delhon et al., 2020).

In contrast, LD sediments are characterised by pentacyclic triterpenes and tetraterpenes, indicative of resinous or woody tissues, alongside alkylresorcinols that signal cereal or plant-derived sources. Interestingly, both sites contain aquatic biomarkers, despite their differing environmental settings. At the lakeshore site of LD, these compounds likely reflect direct input from the adjacent water body, whereas at the PDM rockshelter, located away from standing water, their origin is less certain and may reflect the remobilisation of material from underlying layers. Collectively, these observations emphasise **the importance of contextual sediment analysis for distinguishing between natural and anthropogenic sources of lipids**, and they **provide a critical baseline for subsequent comparisons with HAS**, where environmental contamination must be carefully assessed in relation to site-specific sediment inputs.

Morphologically, HAS from La Draga display a broad range of functional types including grinders, griddles, and combustion-associated, which correspond well with their molecular and isotopic characteristics. Taken together, this combined evidence suggests that **heated stones at La Draga were multi-functional, likely used for different purposes at various stages of their use-life. They may have been employed for a range of activities including direct culinary practices (e.g., griddling, plant/cereal grinding) and technological practices (e.g., resin processing), making them a key component of the Neolithic toolkit**. Pendimoun stones, by contrast, are less morphologically diverse, yet the distinctions between stones from the Cooking Place and the Fireplace align closely with the

observed chemical and isotopic patterns, supporting interpretations of feature-specific activity. Although simpler in form, **Pendimoun HAS were nonetheless associated with prehistoric cooking and plant-processing activities**. The chemical and isotopic signatures demonstrate the specific types of use associated with each firing feature, highlighting the **functional significance of these stones within Neolithic daily life**.

At both sites, the external surfaces of HAS consistently exhibit higher lipid concentrations than internal layers, although the extent and variability of this enrichment differ between sites and features. At Pendimoun, the contrast is particularly pronounced between the Cooking Place and the Fireplace, with stones from the Cooking Place showing both higher and more variable lipid concentrations, whereas lipid yields at La Draga are comparatively more uniform across stones. Molecular compositions at both sites are dominated by saturated fatty acids, primarily palmitic and stearic acids, yet important site-specific differences are apparent. HAS from La Draga include additional markers such as plant sterols, long-chain alcohols, alkylresorcinols, and diterpenoid compounds, reflecting both cereal processing and resin-related technological activities. In contrast, Pendimoun stones preserve mostly plant-derived lipids, with sterols detected only sporadically, and their profiles vary according to the specific firing feature, highlighting differences in local use. Notably, aquatic biomarkers were detected in HAS from both sites, paralleling the sedimentary molecular profiles.

Stable carbon isotope values further distinguish the two sites. At La Draga, high-lipid samples exhibit mixed plant-animal signatures, while diterpenoid-bearing stones retain C_3 plant signals, indicative of combined culinary and technological applications. At Pendimoun, isotopic patterns reveal functional contrasts between features: the Cooking Place shows evidence of diverse animal inputs alongside plant residues, whereas the Fireplace primarily preserves plant-derived signatures.

7.4.1. Linking Ceramic and HAS Residue Evidence

The discussion of HAS is further contextualised by lipid residue analyses conducted on ceramic vessels from La Draga and Pendimoun, the latter representing earlier occupation phases, specifically Impressa and Cardial. Considered together, these materials may contribute to a more integrated perspective on food processing practices, as ceramic containers can potentially provide evidence of cooking and storage activities that may not only be contrasted with, but also reflected in, some of the results observed for HAS. A summary of lipid analysis results and interpretations for ceramic vessels from both sites is provided in Annex 6, compiling the published data from (Tarifa Mateo, 2019; Drieu, 2017; Drieu et al., 2021).

The following section summarises **published lipid residue analyses on ceramics from La Draga** (Tarifa Mateo, 2019). The primary aim of the research was to characterise lipids preserved within the ceramic matrix. Samples were taken from the lips or bases of the vessels, and the extraction was carried out using microwave-assisted solvent extraction with DCM/MeOH (2:1 v/v) (Gregg et al. 2009, Gregg and Slater 2010). In total, 27 pottery fragments from different stratigraphic levels of Sector D at La Draga, excavated in 2012, were analysed. The sample set included nine sherds from Level VIa (occupation layer), 15 from Level VII (collapse of wooden structures), and two from Level VIII (posts in chalk).

The molecular profiles of the ceramic vessels were dominated by fatty acids and exhibited a relatively high P/S ratio, although precise values were not reported. UFAs and TAGs were also detected in some samples. The analysis of TAGs distribution in ten ceramic samples enabled the discrimination of different types of animal fats, revealing evidence of dairy use in four samples, subcutaneous animal fat in one, and ambiguous results for the remainder. Stable carbon isotope analysis was possible only for three samples, two of which were consistent with dairy products and one with ruminant fats. Notably, the two samples associated with dairy products corresponded to those previously identified by TAG profiles, thereby providing additional confirmation. Interestingly, the sample with an isotopic signature suggesting ruminant adipose fats also belonged to the group of four with TAGs attributable to dairy use, highlighting the potential overlap and the complexity in distinguishing between different animal fat sources.

These published results provide a reference framework for La Draga against which the molecular profiles obtained from HAS can be compared, allowing for the identification of potential correspondences, divergences, and complementary evidence regarding the use of vessels and stones in food processing. The comparison of lipid concentrations shows that ceramic samples exhibited higher lipid concentration than HAS, when considered collectively across internal, external and deposit aliquots (Figure 75). However, this difference should be interpreted cautiously, as the two materials were extracted using different extraction methods (DCM/MeOH for ceramics and acid extraction for HAS), which target different lipid classes. Nevertheless, this difference likely may reflect variations in material properties, with lithic surfaces less porous than ceramic matrices, and therefore accumulating lower quantities of organic residues. Such disparities in lipid retention highlight the importance of considering artefact characteristics when interpreting molecular data in archaeological contexts, as differences in lipids yield may not necessarily reflect differences in intensity of use but may also result from the absorption capacity of the matrix.

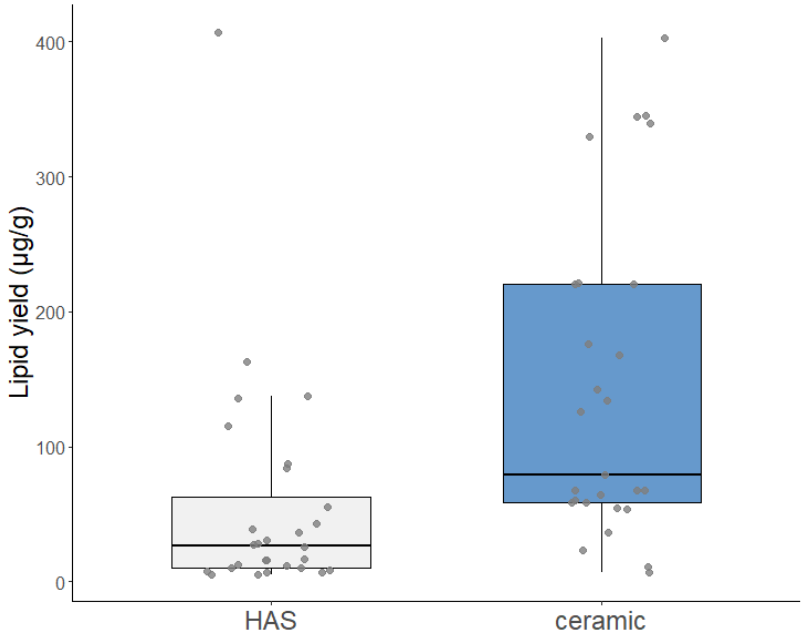


Figure 75. Boxplot of lipid yields for La Draga HAS (n = 28; e, i and d) and ceramic vessels (n = 27) (Tarifa Mateo, 2019). Grey points represent individual data values.

The molecular profile of both categories shared certain characteristics, with SFAs predominating and UFAs also present. However, a notable distinction lies in the presence of triacylglycerols (TAGs), which were detected in ceramic samples but absent in HAS. TAGs are often associated with animal fats, including dairy products, and their absence in HAS may be interpreted as evidence that these stones were not involved in the processing of dairy. However, a possible other explanation is that the higher temperature to which HAS were exposed could have degraded these compounds, preventing their preservation. These observations support the interpretation of HAS as multifunctional tools involved in the processing of a variety of plant- and animal-based substances, while underscoring the importance of considering the effects of heat on lipid preservation when comparing different artefact categories.

Further evidence for functional differentiation comes from stable carbon isotope data. The $\delta^{13}C$ values of ceramic samples differed significantly from those of HAS and sediments, indicating that the lipids preserved in ceramics derived from different sources compared to those associated with the lithic assemblage (Figure 76). It should be noted, however, that the isotopic dataset for ceramics is limited (n = 3), which limits the extent to which these observations can be considered representative of the entire ceramic assemblage. Taken together, these comparisons reinforce the interpretation that **ceramics and HAS had complementary but distinct roles**. While ceramics appear to have been engaged in the preparation and storage of lipid-rich foods, including dairy, **HAS likely served in alternative food processing and technological activities**. However, the absence of TAGs in HAS may reflect thermal

degradation rather than a complete lack of dairy-related use, highlighting the need for caution when interpreting their specific functions.

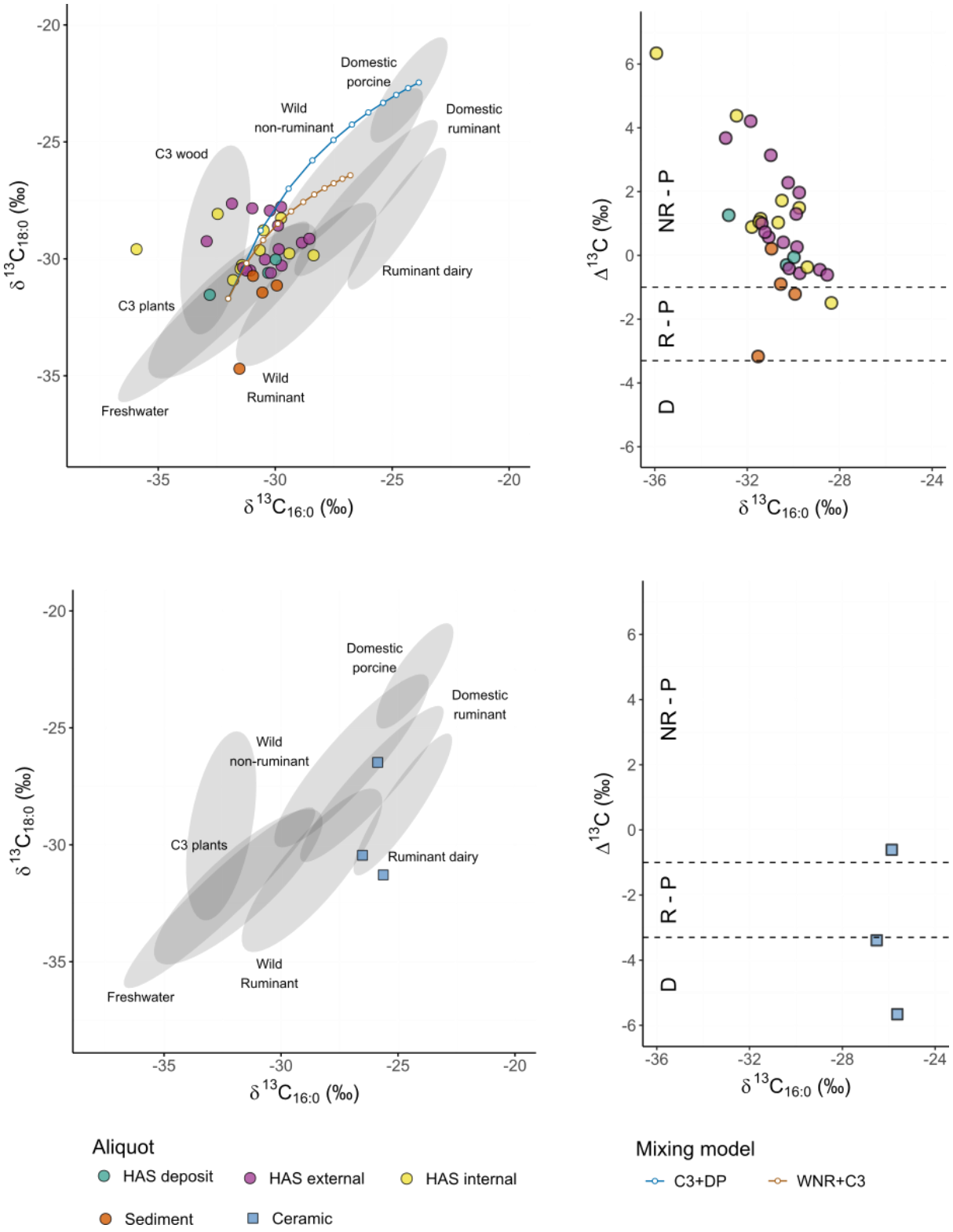


Figure 76. Plots of $\delta^{13}C$ values of palmitic ($C_{16:0}$) and stearic acid ($C_{18:0}$), and $\Delta^{13}C$ (difference between the $\delta^{13}C$ values of the $C_{16:0}$ and $C_{18:0}$ fatty acids) versus $\delta^{13}C_{16:0}$, of HAS, sediments and ceramic samples from La Draga.

Coloured symbols indicate different aliquot types, while shaded ellipses represent reference ranges for modern reference, showing 68% confidence ellipses (see Figure 13, chapter 3.1.2). Abbreviations: D = dairy products, R = ruminant adipose fat, NR = non ruminant adipose fat, P = plant products. Mixing curves are as described in Annex 5. The mixing curves have been calculated to illustrate the $\delta^{13}C$ values which would result from the mixing of C_3 plant products (C3), domestic porcine adipose fat (DP), and wild non ruminant adipose fat (WNR).

The following section summarises **published lipid residue analyses on ceramics from Pendimoun**. A first sampling of 38 potsherds and four contextual sedimentary samples was undertaken through DCM/MeOH (2:1 v/v) extraction (Drieu, 2017), followed by a second sampling of 52 potsherds with acid extraction (H_2SO_4/MeOH) (Drieu et al., 2021; Drieu, Binder and Regert, 2022). Selected extracts were further analysed for TAGs, wax esters, and alkylresorcinols by solvent extraction, while GC-MS on a DB-23 column in SIM mode was employed to identify aquatic biomarkers. Well-preserved extracts (TLE > 10 µg g^{-1}) were subsequently characterised by GC-C-IRMS (Drieu et al., 2021; Drieu, Binder and Regert, 2022). Sherds were generally taken from the upper body of vessels and represent both the Cardial and Impressa phases.

Solvent extraction yielded very low lipid concentrations for most potsherds, with only two producing interpretable results. Their molecular profiles were dominated by fatty acids ($C_{10:0}$ to $C_{18:0}$), particularly palmitic acid. One sample also contained UFAs and traces of a dihydroxy acid, suggesting a possible plant or aquatic origin (Drieu, 2017). By contrast, sediments produced higher lipid yields and distinct molecular profiles dominated by wax esters, linear alcohols, and *n*-alkanes, suggesting that contamination from sediments into the ceramics was limited (Drieu, 2017). Subsequent application of an acidified methanol extraction method proved far more effective, enabling isotopic measurements of fatty acids. The resulting molecular profiles exhibited a broader range of compounds which, combined with the $\delta^{13}C$ values of palmitic and stearic acids, allowed for more detailed interpretations (Drieu et al., 2021; Drieu, Binder and Regert, 2022). It should also be noted that these further analyses allowed for reinterpretation of the sample initially suggesting plant or aquatic origin, which was ultimately attributed to porcine adipose fat. In the following, only those results most relevant for comparison with HAS analyses are presented.

The comparison of total lipid concentrations between HAS and ceramics from Pendimoun shows generally similar lipid concentrations (Figure 77). Unlike La Draga, HAS and ceramic vessels from Pendimoun show no marked differences in lipid yields, suggesting that both matrices retained comparable amounts of lipids under the conditions present at the site. This highlights that **the capacity of artefact materials to accumulate organic residues can vary across archaeological contexts, with differences in lipid yield influenced by both site-specific preservation factors and material properties**.

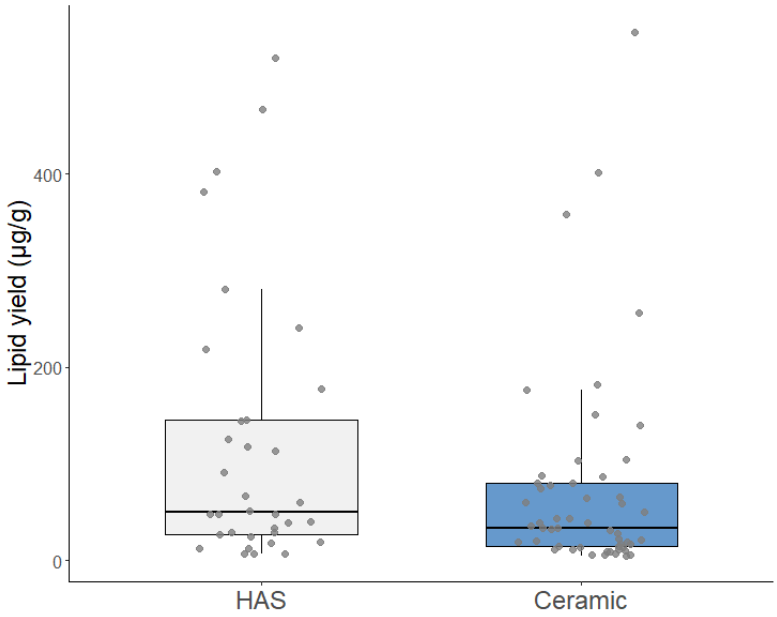


Figure 77. Boxplot of lipid yields for Pendimoun HAS (n = 34; e, i and d) and ceramic vessels (n = 53) (Drieu et al., 2021). Grey points represent individual data values.

Molecular and stable carbon isotopic analyses of Pendimoun pottery indicate a predominance of ruminant animal fats, with minor contributions from porcine fats, plant oils, leafy plants, and beeswax, reflecting diverse dietary and resource practices. The lack of clear evidence of aquatic products or significant dairy use points to a terrestrial subsistence economy centred on meat and other terrestrial resources. Lipid concentrations showed no correlation with period, location, or ceramic type. However, small vessels were lipid-rich, likely used for cooking or specialised processing, whereas very large vessels, frequently associated with plant products, had low lipid yields and were probably used for storage or communal purposes (Drieu et al., 2021).

Molecular and stable carbon isotopic profiles of HAS reveal different patterns, with HAS from the Fireplace dominated by plant-derived inputs, that may reflect environmental contamination or the use of wood/leaves as fuel. In contrast, HAS from the Cooking place presented occasional ruminant fat contributions, consistent with the interpretations from ceramic residues. Notably, only a few samples indicated the presence of dairy resources, consistent with the ceramic records, which suggests limited exploitation of dairy products and a primary focus on meat from domestic animals. However, an increase in dairy use is suspected during the subsequent SMP phase. Moreover, despite HAS being associated with SMP phase and ceramic vessels with Impressa and Cardial phases, their isotopic signatures are similar (Figure 78), suggesting a **potential continuity in food-processing practices across different prehistoric phases**.

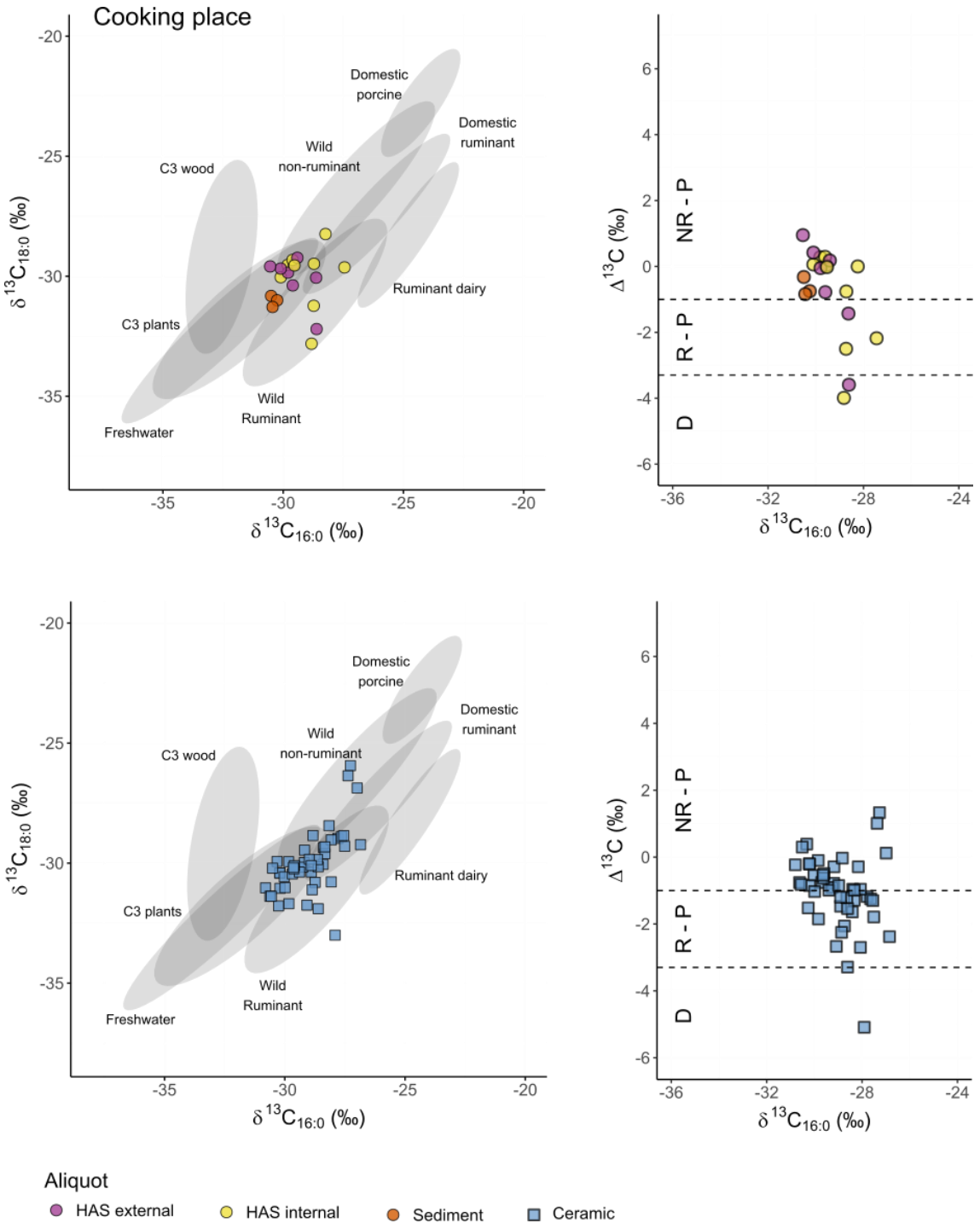


Figure 78. Plots of $\delta^{13}C$ values of palmitic ($C_{16:0}$) and stearic acid ($C_{18:0}$), and $\Delta^{13}C$ (difference between the $\delta^{13}C$ values of the $C_{16:0}$ and $C_{18:0}$ fatty acids) versus $\delta^{13}C_{16:0}$, of HAS from Cooking place and ceramic samples from Pendimoun. Coloured symbols indicate different aliquot types, while shaded ellipses represent reference ranges for modern reference, showing 68% confidence ellipses (see Figure 13, chapter 3.1.2). Abbreviations: D = dairy products, R = ruminant adipose fat, NR = non ruminant adipose fat, P = plant products.

7.5. Limitations, Methodological Considerations, and Recommendations

Despite the insights gained from lipid analysis in this study, several methodological limitations must be acknowledged. Stone artefacts present particular challenges in terms of preservation, contamination, and the absence of standardised protocols. Recognising these limitations is essential not only to ensure reproducibility and interpretive reliability but also to inform future research that aims to fully exploit the potential of lithic artefacts for reconstructing past culinary practices. The following section outlines key procedural considerations, limitations encountered, and recommendations for further work in this area.

Currently, **no accepted guideline exists for the systematic extraction and analysis of lipids from stone artefacts, including HAS**. Protocols vary considerably between studies in terms of sampling, extraction, and derivatisation strategies, limiting comparability. The development of an effective, standardised methodological framework would therefore be crucial to ensure reproducibility, improve interpretive reliability, and fully harness the potential of HAS for reconstructing past culinary practices. In this study, protocols traditionally used for ceramics (Correa-Ascencio and Evershed, 2014; Drieu et al., 2021; Lundy et al., 2023) were adapted to HAS, highlighting the need for slight but essential modifications.

The following **key observations emerged from applying ceramic protocols to stone artefacts:**

1. **Handling and cleanliness:** Proper handling should be considered as a critical first step prior to extraction, and maintaining rigorous standards is essential throughout the analytical process to minimise contamination and ensure the reliability of results. Stone implements should not be stored directly in plastic bags, as this can introduce plasticiser contamination that may interfere with molecular analyses. Instead, each sample should be wrapped in aluminium foil before being placed in bags, and stored at room temperature away from direct light sources to further reduce the risk of contamination. During sampling and extraction, nitrile gloves should always be worn to prevent the transfer of skin oils or other contaminants, and gloves should be changed regularly between samples. Drill bits used for sampling should be thoroughly rinsed with a proper solvent and cleaned ultrasonically after each use to avoid cross-contamination. Additionally, all glassware, tools and containers of sort should be rigorously cleaned and, where appropriate, heated to prevent contamination. These precautions collectively ensure that the subsequent extraction and analysis of organic residues are based on uncontaminated material, increasing the confidence and reproducibility of the results.

2. **Surface sampling:** Unlike ceramics, where the outermost millimetre is typically discarded to minimise contamination, lithics in this study were sampled without removing the superficial layer. Results indicate that contamination from handling and plasticisers can be substantial, particularly on the external surface, as observed in the Pendimoun samples. To mitigate the risk of modern contamination and improve the reliability of lipid identification, it is strongly recommended to discard a very thin outer layer (approximately 1 mm) before sampling. Furthermore, in this study, sampling limestone proved to be a time-consuming process, as the collection of approximately 1 g of material required close to one hour. It is also critical to regulate the drill speed carefully to avoid the generation of excessive heat, which may compromise or degrade lipid residues (Longoni et al., 2024). Alternative methodologies have also been explored, such as the core-sampling approach employed by (Langley, 2024); however, limited control over sampling depth may have contributed to the relatively low lipid yields reported.
3. **Carbonate-rich matrices and pH:** Stones composed of carbonate-rich matrices, such as limestone, can neutralise the acidic extraction solution, which may result in the formation of "gelatinous" residues. Such reactions can reduce the efficiency of lipid recovery and affect the quality and interpretability of results. Therefore, it is critical to monitor and maintain acidic conditions throughout the extraction process, adjusting the solution as necessary to counteract any buffering effects of carbonate-rich lithic matrices.
4. **Sulfur removal:** Elemental sulphur can interfere with GC and other analytical techniques, producing artefactual peaks and hindering accurate compound identification. To mitigate these issues, the removal of elemental sulphur prior to analysis is highly recommended. This is typically achieved by treating samples with activated copper, which binds and eliminates the sulphur from the extract. Incorporating this step ensures cleaner chromatograms and enhances the reliability and precision of molecular characterisation.
5. **Extraction methods:** To obtain a comprehensive lipid profile from lithic artefacts, it is advisable to apply complementary extraction methods that target a broad range of compounds. Acidified methanol (AE) is particularly effective for releasing free fatty acids and other polar lipids, and facilitate stable isotope analysis, while DCM/MeOH (SE) extracts a wider spectrum of non-polar compounds, including wax esters, MAGs, DAGs, and TAGs.
6. **Analytical setup:** Where laboratory facilities permit, combined GC-FID-MS analysis is preferred. This approach allows simultaneous acquisition of quantitative data via FID and structural identification via MS, optimising both time and resources while providing robust data.

While the adaptation of ceramic-based protocols has provided a valuable starting point for lipid analysis of stone artefacts, several methodological limitations persist, particularly regarding

contamination control, sampling strategies, and matrix-specific challenges. Careful handling, surface layer management, attention to drill speed, and consideration of matrix effects are essential to maximise lipid recovery and ensure reproducible results. The incorporation of steps such as sulphur removal and the use of complementary extraction and analytical methods further enhances data quality and interpretive reliability. Moving forward, the development of standardised protocols tailored to stone materials will be crucial to facilitate comparability across studies and exploit their potential for reconstructing past culinary and technological practices.

A further consideration specific to HAS is the unknown pre-use history, or "biovita", of the materials. Unlike ceramics, which are manufactured from raw materials by humans and whose formation context is well understood, HAS were naturally occurring stones before their introduction into archaeological contexts. Consequently, some stones may have already contained lipid residues prior to their deposition or further use at the site, potentially influencing analytical results. This limitation highlights the challenge of distinguishing lipids associated with human activity from those originating from the stone's earlier life. An interesting avenue for future research would be to analyse stones collected outside archaeological sites, or randomly recovered stones in contemporary fields, to characterise background lipid profiles and better contextualise residues detected in HAS.

7.6. Overall Discussion: Towards a Methodological Framework for the Study of HAS

The present study aims to evaluate the informative potential of HAS and to contribute to the development of best practices for the application of organic residue analysis (ORA) on stone artefacts, with particular emphasis on heat-altered stones (HAS). Traditionally, ORA has focused primarily on ceramics, which are widely recognised for their ability to preserve molecular residues related to vessel function and subsistence practices. However, in many archaeological contexts, particularly those preceding the advent of pottery or where ceramics are poorly preserved, stone artefacts may represent the only viable material for molecular investigations. On the other hand, in contexts where both types of artefacts are represented, various possibilities for complementary analysis arise, contributing to a better reconstruction of the subsistence and ways of life of prehistoric communities. **By systematically analysing HAS from two well-characterised Mediterranean Neolithic sites, La Draga and Pendimoun, this study provides a comparative framework for assessing the analytical potential, interpretive reliability, and contextual significance of residues preserved in thermally altered stone materials**.

The selection of La Draga and Pendimoun as case studies was guided by a combination of shared cultural characteristics and contrasting environmental contexts. Both sites are key witnesses to the Early Neolithic of western Mediterranean and provide rich archaeological datasets documenting subsistence, material culture, and domestic activities. However, their depositional and environmental settings differ markedly: La Draga is a lakeshore settlement with exceptional organic preservation, whereas Pendimoun represents a rockshelter context with more complex taphonomic conditions and more limited organic survival. The decision to study HAS from these two sites was therefore intended to test the robustness of residue preservation and detection under varying conditions, while benefiting from the extensive archaeological research already conducted at both locations. Their well-established subsistence records and attested ceramic production offered an essential comparative framework for assessing whether the molecular and stable carbon isotopic results obtained from HAS were reliable and contextually consistent with the broader archaeological evidence.

A principal objective of this research was to evaluate the interpretive reliability of lipid residues preserved in HAS, particularly in relation to other archaeological materials such as sediments and ceramics. By examining samples from two distinct environments, the study sought to determine whether the residues extracted from HAS were representative of human activities and not solely the result of environmental or post-depositional processes. The correspondence observed between the residue data and the known economic activities at both La Draga and Pendimoun supports the view that HAS can preserve meaningful chemical and isotopic information. **This finding strengthens confidence in the use of HAS as analytical materials, particularly in cases where ceramics are unavailable or poorly preserved**. Demonstrating that HAS can reliably preserve biomarkers of both plant and animal origin opens new avenues for the application of ORA to prehistoric contexts where ceramics are scarce or absent. Such circumstances include pre-Neolithic sites in Europe, as well as other world regions, such as parts of South America, where pottery emerged considerably later. In these settings, HAS could provide a critical line of evidence for reconstructing subsistence practices and technological aspects.

The increasing attention devoted to the study of HAS also reflects a growing awareness of their potential to inform on domestic and technological activities. Recent experimental research (e.g. (Langley, 2024)) has shown that controlled heating experiments can reproduce the formation, alteration, and preservation of lipid biomarkers in lithic materials. Such experiments are invaluable for defining diagnostic features, establishing preservation thresholds, and assessing the influence of temperature and combustion conditions on molecular integrity. Integrating experimental datasets with archaeological analyses, as recommended here, will be essential for refining sampling strategies and analytical protocols, as well as for distinguishing anthropogenic residues from those derived from environmental contamination or post-depositional processes.

Equally important to the methodological framework developed here is the inclusion of sediment samples as both contextual and analytical materials. Sediments provide critical background information for evaluating the authenticity of residues extracted from artefacts, enabling the identification of potential environmental inputs or diagenetic alterations. In the present study, sediment samples yielded consistent carbon stable isotopic signatures, while some HAS displayed distinct molecular and isotopic profiles that could be linked to specific resources. These results demonstrate that **the combined analysis of artefacts and sediments provides a more comprehensive understanding of residue formation and preservation processes, and should therefore become a standard component of lipid analysis**.

In conclusion, this research establishes an important step towards a methodological framework for the study of heat-altered stones through lipid residue analysis. By demonstrating the reliability of HAS as carriers of molecular information and by situating their analysis within broader archaeological and environmental contexts, the study expands the methodological toolkit available for investigating prehistoric subsistence and technology. **HAS can now be considered alongside more commonly analysed materials, such as ceramic vessels, lithic tools, faunal and human remains, phytoliths and sediments, as part of the range of artefacts suitable for lipid residue analysis** (Figure 79). As the field continues to grow, future research should aim to standardise analytical protocols, strengthen experimental reference collections, and explore a wider range of cultural and environmental settings. In doing so, HAS analysis will increasingly contribute to a more nuanced and inclusive understanding of early technological and domestic practices across diverse prehistoric contexts.

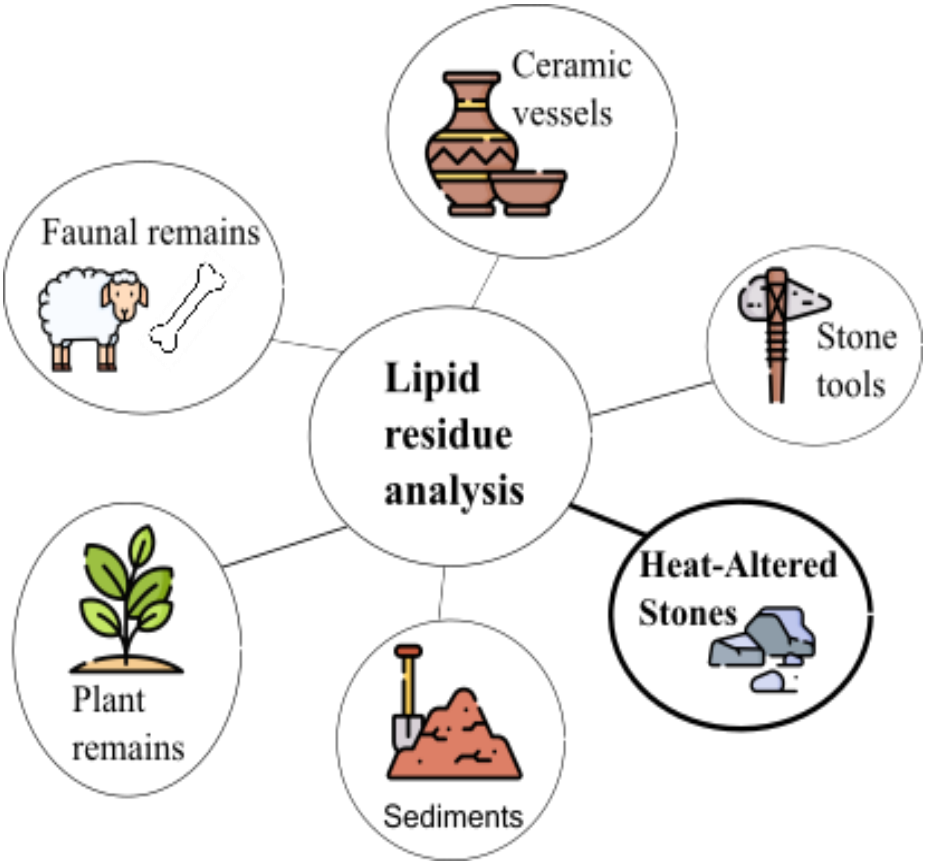


Figure 79. Overview of materials suitable for organic residue analysis. Heat-Altered Stones (HAS) are now included alongside established materials, illustrating their emerging role in reconstructing prehistoric subsistence and technology.

8. Conclusion

This study demonstrates that heat-altered stones (HAS) constitute a significant and underexplored source of information on past human activity, capable of providing insights into both culinary and technological practices. By examining assemblages from the Neolithic sites of La Draga and Pendimoun through a combination of macroscopic, molecular, and carbon stable isotopic analyses, the research shows that HAS are not merely incidental by-products of fire, but artefacts that preserve tangible traces of human behaviour. Their morphology, chemical composition, and stable carbon isotopic signatures together provide a multifaceted view of prehistoric life, complementing evidence derived from ceramics, faunal remains, and sediments.

Morphological observations reveal that HAS display features indicative of repeated or prolonged thermal exposure, including cracking, fracturing, discoloration, and sooting. At La Draga, the variety of forms, ranging from spherical, tabular and prismatic stones to pot-lid fragments, reflects a diversity of functional roles, encompassing plant processing, cooking, and technological activities such as resin processing. Pendimoun, by contrast, presents a more uniform lithic assemblage, yet differentiation between stones from a Cooking Place and a Fireplace illustrates feature-specific activities, with the former associated with more intensive culinary use. These morphological patterns, when considered alongside chemical and stable carbon isotopic evidence, reinforce the conclusion that HAS were active participants in Neolithic subsistence and domestic practices.

Lipid residue analysis confirms that HAS preserve molecular signatures of both plant and animal origin, providing a direct link to the resources processed by past communities. At La Draga, saturated and unsaturated fatty acids dominate, complemented by plant sterols, alkylresorcinols, diterpenoids, and other biomarkers that suggest the processing of cereals, other plant resources, and coniferous resins. Mixed stable carbon isotopic signatures further indicate the co-occurrence of plant and animal fats, reflecting complex food preparation strategies and multifunctional use of individual stones. At Pendimoun, lipid profiles are largely plant-dominated, though stable carbon isotopic evidence from the Cooking Place indicates contributions from ruminant and porcine fats. These results underscore the capacity of HAS to preserve residues directly associated with human activity, distinct from the background signals recorded in surrounding sediments, while also highlighting the importance of contextual sampling to distinguish anthropogenic inputs from environmental contributions.

Comparison with ceramic vessels further illustrates the unique interpretive value of HAS. While ceramics from La Draga and Pendimoun reveal evidence of lipid-rich foods, including dairy products, some HAS samples also show traces of dairy, indicating that these compounds were not entirely absent.

These observations suggest a differentiation of uses of tasks between artefact types, with ceramics serving as containers for cooking and storage of certain resources, while HAS were involved in alternative food-processing and technological activities, often including repeated exposure to heat. Such complementary patterns demonstrate that a nuanced understanding of past subsistence strategies requires the integrated study of multiple material types, each preserving different aspects of human behaviour.

The methodological component of this research underscores both the opportunities and challenges inherent in studying HAS. By adapting lipid extraction protocols developed for ceramics, the study illustrates the importance of rigorous contamination control, careful management of surface layers, attention to drill speed, and consideration of matrix-specific effects such as carbonate buffering and sulphur interference. While lipid analysis, particularly when paired with stable carbon isotope measurements, proves highly effective for reconstructing culinary and technological practices, protein analysis remains largely inconclusive on lithic substrates, highlighting the current limitations of biomolecular approaches beyond lipids. These methodological reflections provide a foundation for the development of standardised protocols, which will be essential for ensuring reproducibility and comparability in future studies.

Taken together, the findings of this thesis establish HAS as a reliable and informative archaeological archive. They reveal not only the presence of plant and animal residues but also the intensity and nature of thermal exposure, the multifunctionality of artefacts, and temporal variations in use. At La Draga, evidence for cereal processing, combined plant-animal mixtures, and resin-related technological activities paints a picture of a diversified and complex subsistence economy. At Pendimoun, distinctions between the Cooking Place and Fireplace demonstrate feature-specific use, reflecting both environmental and cultural constraints on resource processing.

Beyond these site-specific insights, this study has broader implications for archaeological research, extending even to the stage of field excavation, with the necessity to consider HAS as other artefacts and collecting, mapping and storing them following the rules of the art. HAS offer a robust alternative or complement to ceramic vessels in contexts where pottery is scarce, poorly preserved, or entirely absent. Their demonstrated capacity to retain lipid residues and stable carbon isotopic signatures opens new avenues for organic residue analysis at sites predating the advent of ceramics, as well as at settlements where no ceramic assemblages have been identified. This expands the scope of molecular archaeology, allowing researchers to investigate culinary and technological behaviours in a wider range of prehistoric contexts. Moreover, the careful analysis of sediments in conjunction with rigorously applied methodological protocols provides a reliable means of distinguishing residues that genuinely reflect human activity from those that may derive from natural environmental inputs or post-

depositional processes. By establishing this framework, it becomes possible to interpret the chemical signatures preserved in HAS with greater confidence, recognising them as evidence of past culinary and technological practices rather than as artefacts of contamination.

The findings presented here open multiple avenues for future research, both in terms of methodological development and the broader application of HAS as analytical proxies. A clear priority lies in the continued refinement and standardisation of protocols for sampling, extraction, and analysis. While the adaptation of methods developed for ceramics has proven effective, the development of procedures tailored specifically to the diverse lithologies and pre-use histories of HAS would improve reproducibility and enhance interpretive confidence. Controlled experimental studies exploring the effects of heating, duration, and substrate composition on the preservation of lipids and isotopic signatures on stone artefacts would provide crucial reference datasets, allowing a more precise calibration of archaeological results and facilitating the discrimination between anthropogenic and natural inputs.

In conclusion, this thesis establishes HAS as a key component of the prehistoric material record, capable of preserving detailed and activity-specific molecular signatures. The integrated analysis of morphology, lipid residues, and stable carbon isotopes demonstrates that these stones reflect not only culinary and technological practices but also broader patterns of resource exploitation, functional diversity, and domestic organisation. When considered alongside sediments, ceramics, faunal and botanical remains, HAS provide a complementary perspective that enhances the interpretive framework for understanding early human subsistence, technology, and daily life. As the field of organic residue analysis continues to develop, HAS are poised to play an increasingly central role in reconstructing prehistoric lifeways, offering a window into behaviours that were previously invisible within the archaeological record.

Bibliography

Abbott, J. T. and Frederick, C. (1990). Proton magnetometer investigations of burned rock middens in west-central Texas: Clues to formation processes. *Journal of archaeological science*, 17, pp.535–545. [Online]. Available at: doi:10.1016/0305-4403(90)90034-3.

Admiraal, M. et al. (2018). Investigating the function of prehistoric stone bowls and griddle stones in the Aleutian Islands by lipid residue analysis. *Quaternary Research*, 91 (3), pp.1–13. [Online]. Available at: doi:10.1017/qua.2018.31.

Admiraal, M. et al. (2023). Chemical analysis of pottery reveals the transition from a maritime to a plant-based economy in pre-colonial coastal Brazil. *Scientific reports*, 13 (1), p.16771. [Online]. Available at: doi:10.1038/s41598-023-42662-5.

Äikäs, T., Bergmann, U. and Salmi, A. K. (2012). An attempt to use blood residue analysis to identify sacrificial practices at sieidi sites. *Fennoscandia Archaeologica*, XXIX.

Aillaud, S. (2001). *Field and laboratory studies of diagenetic reactions affecting lipid residues absorbed in unglazed archaeological pottery vessels*. PhD thesis, University of Bristol.

Allen, J., Newman, M. E. and Riford, M. (1995). Blood and Plant Residues on Hawaiian Stone Tools from Two Archaeological Sites in Upland Kāne'ohe, Ko'olau Poko District, O'ahu Island. *Asian perspective*, 34 (2), pp.283–302. [Online]. Available at: https://www.jstor.org/stable/42928365.

Ammerman, A. (2020). The Neolithic transition in Europe at 50 years. *arXiv [q-bio.PE]*. *arXiv* [Online]. Available at: http://arxiv.org/abs/2012.11713.

Ammerman, A. J. and Cavalli-Sforza, L. L. (1984). *The neolithic transition and the genetics of populations in Europe*. Princeton, NJ: Princeton University Press.

Andreaki, V. et al. (2020). Un modelo bayesiano para la cronología del yacimiento neolítico de La Draga (Banyoles, Girona). Un caso de estudio con ChronoModel 2.0. In: Barceló, J. A. and Morell, B. (Eds). *Métodos cronométricos en Arqueología, Historia y Paleontología*. Dextra editorial. pp.403–418.

Andreaki, V. et al. (2022). Absolute Chronology at the Waterlogged Site of La Draga (Lake Banyoles, NE Iberia): Bayesian Chronological Models Integrating Tree-Ring Measurement, Radiocarbon Dates and Micro-Stratigraphical Data. *Radiocarbon*, 64 (5), pp.907–948. [Online]. Available at: doi:10.1017/RDC.2022.56.

Anthony, I. M. C. et al. (2001). Dating a burnt mound from Kilmartin, Argyll, Scotland. *Quaternary science reviews*, 20 (5-9), pp.921–925. [Online]. Available at: doi:10.1016/S0277-3791(00)00025-1.

Antolín, F. et al. (2013). The Application of Systematic Sampling Strategies for Bioarchaeological Studies in the Early Neolithic Lakeshore Site of La Draga. *Journal of Wetland Archaeology*, 13 (1), pp.29–49. [Online]. Available at: doi:10.1179/1473297113Z.0000000002.

Antolín, F. et al. (2014). An integrated perspective on farming in the early Neolithic lakeshore site La Draga (Banyoles, Spain). *Environmental Archaeology*, 19 (3), pp.241–255. [Online]. Available at: doi:10.1179/1749631414Y.0000000027.

Antolín, F. (2015). Entre agricultores primitivos, cultivos de rozas y pastores transhumantes. Una mirada crítica a los modelos económicos propuestos para los grupos neolíticos del noreste peninsular y una aportación desde el registro carpológico. *Revista d arqueologia de Ponent*, 25 (11-45).

Antolín, F. (2016). *Local, Intensive and Diverse?*, Advances in Archaeobotany 2. Drenthe,

Netherlands: Barkhuis. [Online]. Available at: doi:10.2307/j.ctt20p56hs.

Antolín, F. et al. (2018). Herders in the mountains and farmers in the plains? A comparative evaluation of the archaeobiological record from Neolithic sites in the eastern Iberian Pyrenees and the southern lower lands. *Quaternary international: the journal of the International Union for Quaternary Research*, 484, pp.75–93. [Online]. Available at: doi:10.1016/j.quaint.2017.05.056.

Antolín, F. and Buxó, R. (2011). L'explotació de les plantes: Contribució a la història de l'agricultura i de l'alimentació vegetal del neolític a Catalunya. In: Bosch, A., Chinchilla, J. and Tarrús, J. (Eds). *El poblat lacustre del neolític antic de La Draga: Excavacions de 2000-2005*. Generalitat de Catalunya. pp.146–174.

Antolín, F. and Buxó, R. (2012). Chasing the traces of the diffusion of agriculture during the Early Neolithic in the Western Mediterranean: open questions and future perspectives. *Rubricatum*, 5, pp.95–102. [Online]. Available at: http://edoc.unibas.ch/50239/.

Araus, J. L. et al. (2024). Isotope and morphometrical evidence reveals the technological package associated with agriculture adoption in western Europe. *Proceedings of the National Academy of Sciences of the United States of America*, 121 (32), p.e2401065121. [Online]. Available at: doi:10.1073/pnas.2401065121.

Arzelier, A. et al. (2022). Neolithic genomic data from southern France showcase intensified interactions with hunter-gatherer communities. *iScience*, 25 (11), p.105387. [Online]. Available at: doi:10.1016/j.isci.2022.105387.

Asfora, V. K. et al. (2014). Characterization of the burning conditions of archaeological pebbles using the thermal sensitization of the 110 °C TL peak of quartz. *Radiation measurements*, 71, pp.485–489. [Online]. Available at: doi:10.1016/j.radmeas.2014.04.022.

Aura, J. E. et al. (2005). Plant economy of hunter-gatherer groups at the end of the last Ice Age: plant macroremains from the cave of Santa Maira (Alacant, Spain) ca. 12000–9000 b.p. *Vegetation history and archaeobotany*, 14 (4), pp.542–550. [Online]. Available at: doi:10.1007/s00334-005-0002-1.

Avsejs, L. A. et al. (2002). 5-n-Alkylresorcinols as biomarkers of sedges in an ombrotrophic peat section. *Organic geochemistry*, 33 (7), pp.861–867. [Online]. Available at: doi:10.1016/s0146-6380(02)00046-3.

Backhouse, P. N. and Johnson, E. (2007). Where were the hearths: An experimental investigation of the archaeological signature of prehistoric fire technology in the alluvial gravels of the Southern Plains. *Journal of archaeological science*, 34 (9), pp.1367–1378. [Online]. Available at: doi:10.1016/j.jas.2006.10.027.

Bada, J. L. (1991). Amino acid cosmogeochemistry. *Philosophical transactions of the Royal Society of London. Series B, Biological sciences*, 333 (1268), pp.349–358. [Online]. Available at: doi:10.1098/rstb.1991.0084.

Bamyacı, A. O. (2019). Residue analysis of grinding stones from Chalcolithic gülpinar. *Elektronik sosyal bilimler dergisi*, 18 (69), pp.90–104. [Online]. Available at: doi:10.17755/esosder.394134.

Bang-Andersen, S. (2015). The telltale potency of a simple milligram of charcoal found in a hearth left by Mesolithic reindeer hunters in the Norwegian mountains. *Environmental Archaeology*, 20 (1), pp.82–88. [Online]. Available at: doi:10.1179/1461410314Z.00000000072.

Barbetti, M. et al. (1980). Palaeomagnetism and the search for very ancient fireplaces in Africa. *L'Anthropologie*, 18 (2/3), pp.299–304. [Online]. Available at: http://www.jstor.org/stable/44602417.

Barfield, L. and Hodder, M. (1987). Burnt mounds as saunas, and the prehistory of bathing. *Antiquity*, 61 (233), pp.370–379. [Online]. Available at: doi:10.1017/s0003598x00072926.

Barker, A. et al. (2012). An optimized approach for protein residue extraction and identification from ceramics after cooking. *Journal of archaeological method and theory*, 19 (3), pp.407–439. [Online]. Available at: doi:10.1007/s10816-011-9120-5.

Basso, E. et al. (2006). The Neolithic pottery of Abri Pendimoun (Castellar, France): A petro-archaeometric study. *Geological Society London Special Publications*, 257 (1), pp.33–48. [Online]. Available at: doi:10.1144/GSL.SP.2006.257.01.03.

Battentier et al. (2015). L'abri Pendimoun (Castellar, Alpes-Maritimes): nouvelles données sur l'évolution du couvert forestier et l'exploitation du milieu au Néolithique (5 800-2 000 ans cal BCE). *Quaternaire*, 26 (4), pp.279–292. [Online]. Available at: doi:10.4000/quaternaire.7417.

Beausoleil, J.-M. et al. (2007). Un alignement de fours à pierres chauffées du premier âge du Fer : la ligne de feux d'Eyrein (Corrèze). *Documents d'archéologie méridionale*, (29-30), pp.75–111. [Online]. Available at: doi:10.4000/dam.1572.

Bentsen, S. E. and Wurz, S. (2019). Color Me Heated? A Comparison of Potential Methods to Quantify Color Change in Thermally-Altered Rocks. *Journal of Field Archaeology*, 44 (4), pp.215–233. [Online]. Available at: doi:10.1080/00934690.2019.1591092.

van Bergen, P. F. et al. (1997). Organic geochemical studies of soils from the Rothamsted Classical Experiments—I. Total lipid extracts, solvent insoluble residues and humic acids from Broadbalk Wilderness. *Organic geochemistry*, 26 (1-2), pp.117–135. [Online]. Available at: doi:10.1016/s0146-6380(96)00134-9.

Bernabeu Aubán, J. (1989). *La tradición cultural de las cerámicas impresas en la zona oriental de la península ibérica*, 86. Diputación provincial de València.

Bernabeu Aubán, J. et al. (2011). La cerámica neolítica durante el VI milenio cal AC en el Mediterráneo central peninsular. *SAGVNTVM Extra*, 12, pp.153–178. [Online]. Available at: https://turia.uv.es/index.php/saguntumextra/article/view/1742.

Bernabeu Aubán, J. et al. (2014). AEA 2012 Conference Reading: Socioecological dynamics at the time of Neolithic transition in Iberia. *Environmental archaeology*, 19 (3), pp.214–225. [Online]. Available at: doi:10.1179/1749631414y.0000000032.

Bernabeu Aubán, J. and Martí Oliver, B. (2014). The first agricultural groups in the Iberian Peninsula. In: Manen, C., Perrin, T. and Guilaine, J. (Eds). *La transition néolithique en Méditerranée. The Neolithic transition in the Mediterranean.* Arles/Toulouse: Errance/Archives d'Ecologie Préhistorique.

Bertin, I. et al. (2024). Assessing the role of wooden vessels, basketry, and pottery at the early Neolithic site of La Draga (banyoles, Spain). *Open Archaeology*, 10 (1). [Online]. Available at: doi:10.1515/opar-2022-0360.

Binder, D. (1991). *Une économie de chasse au Néolithique ancien. La Grotte Lombard à Saint-Valier-de-Thiey (Alpes-Maritimes)*. CNRS (Ed). Monographie du C.R.A., nº 5.

Binder, D. et al. (1993). L'abri Pendimoun à Castellar (Alpes-Maritimes). Nouvelles données sur le complexe culturel de la céramique imprimée méditerranéenne dans son contexte stratigraphique. *Gallia préhistoire*, 35 (1), pp.177–251. [Online]. Available at: doi:10.3406/galip.1993.2087.

Binder, D. (2000). Mesolithic and Neolithic interaction in southern France and northern Italy: new

data and current hypotheses. In: Price, T. D. (Ed). *Europe's First Farmers*. Cambridge: Cambridge University Press. pp.117–143. [Online]. Available at: doi:10.1017/cbo9780511607851.006.

Binder, D. et al. (2010a). Les productions céramiques du Néolithique ancien entre Provence et Catalogne. In: Manen, C. et al. (Eds). *Premières sociétés paysannes de Méditerranée occidentale: Structures des productions céramiques. Séance de la Société préhistorique française (Toulouse 2007)*. 51. 2010. Mémoire de la Société Préhistorique Française. pp.115–129.

Binder, D. et al. (2010b). Les productions céramiques du Néolithique ancien : proposition d'un protocole d'analyse. In: Manen, C. et al. (Eds). *Premières sociétés paysannes de Méditerranée occidentale. Structures des productions céramiques. Séance de la Société préhistorique française (Toulouse 2007)*. 51. 2010. Mémoire de la Société préhistorique française. pp.29–42.

Binder, D. et al. (2014). First Sculpted Human Face in the Western Mediterranean Early Neolithic. *Cambridge Archaeological Journal*, 24 (1), pp.1–17. [Online]. Available at: doi:10.1017/S0959774314000043.

Binder, D. et al. (2017). Modelling the earliest north-western dispersal of Mediterranean Impressed Wares: new dates and Bayesian chronological model. *Documenta Praehistorica*, 44, pp.54–77. [Online]. Available at: doi:10.4312/dp.44.4.

Binder, D. et al. (2020). First farming in the North-Western Mediterranean: Evidence from Castellar – Pendimoun during the sixth millennium BCE. In: J.G. Kurt, L. Sorensen, and P. Rowley-Conwy (Ed). *Farmers at the frontier. A pan-european perspective on neolithisation*. Owbow Books. pp.145–160. [Online]. Available at: https://ebookcentral.proquest.com/lib/uab/detail.action?docID=6383468.

Binder, D. et al. (2022a). Le complexe de la Céramique Imprimée en Méditerranée centrale et nord-occidentale : une synthèse chronoculturelle (VII e et VI e millénaires AEC). In: *Céramiques imprimées de Méditerranée occidentale (VIe millénaire AEC) : données, approches et enjeux nouveaux. Western Mediterranean Impressed Wares (6th millennium BCE): new data, approaches and challenges*. Actes de la séance de la Société préhistorique française de Nice (mars 2019). 2022. pp.27–124. [Online]. Available at: https://hal.science/hal-04162726.

Binder, D. et al. (2022b). Matières premières, réseaux sociaux et diffusion du Néolithique en Méditerranée du nord-ouest : apports des industries lithiques taillées des horizons Impressa de Finale Ligure -Arene Candide et Castellar -Pendimoun. In: Binder, D. and Manen, C. (Eds). *Céramiques imprimées de Méditerranée occidentale (VIe millénaire AEC) : données, approches et enjeux nouveaux / Western Mediterranean Impressed Wares (6th millennium BCE): New data, approaches and challenges. Actes de la séance de la Société préhistorique française de Nice (mars 2019).* Paris: Société préhistorique française. [Online]. Available at: https://cnrs.hal.science/hal-03905995/.

Binder, D. and Maggi, R. (2001). Le Néolithique ancien de l'arc liguro-provençal. *Bulletin de la Société préhistorique française*, 98 (3), pp.411–422. [Online]. Available at: doi:10.3406/bspf.2001.12528.

Binder, D. and Senepart, I. (2004). Derniers chasseurs et premiers paysans de Vaucluse. Mésolithique et Néolithique ancien: 7000-4700 av. J.-C. In: Buisson-Catil, J. et al. (Eds). *Vaucluse prehistorique : Le territoire, les Hommes, les cultures et les sites*. Le Pontet, France: Editions A. Barthelemy. pp.131–162. [Online]. Available at: https://www.researchgate.net/publication/260087106.

Binder, D. and Sénépart, I. (2010). La séquence de l'Impresso-Cardial de l'abri Pendimoun et l'évolution des assemblages céramiques en Provence. *Mémoire LI de la Société Préhistorique française*, pp.149–167.

Binford, L. R. (1978). *Nunamiut ethnoarchaeology*. New York: Academic Press.

Bischoff, J. L., Ikeya, M. and Budinger, F. E., Jr. (1984). A TL/ESR Study of the Hearth Feature at the Calico Archaeological Site, California. *American antiquity*, 49 (4), pp.764–774. [Online]. Available at: http://www.jstor.org/stable/279741 .

Black, S. L. and Thoms, A. V. (2015). Hunter-Gatherer Earth Ovens in the Archaeological Record: Fundamental Concepts. *American antiquity*, 79 (2), pp.203–226. [Online]. Available at: doi:10.7183/0002-7316.79.2.204.

Bock, C., Neubeck, V. and Pasda, C. (2017). Non-flint from the Middle Pleistocene site of Bilzingsleben (excavation from 1971 to 2002). *Quartär – Internationales Jahrbuch zur Erforschung des Eiszeitalters und der Steinzeit*, 64, pp.7–25. [Online]. Available at: doi:10.7485/QU64_1.

Bogaard, A. and Halstead, P. (2015). Subsistence practices and social routine in Neolithic Southern Europe. In: Fowler, C., Harding, J. and Hofmann, D. (Eds). *The Oxford Handbook of Neolithic Europe*. Oxford University Press. pp.385–410. [Online]. Available at: doi:10.1093/oxfordhb/9780199545841.013.020.

Bok1982. (2009). *Provence-Alpes-Côte d'Azur region relief location map [Image]*. [Online]. Available at: https://commons.wikimedia.org/wiki/File:Provence-Alpes-Cotes_d%27Azur_region_relief_location_map.jpg.

Bondetti, M. et al. (2021a). Investigating the formation and diagnostic value of ω-(o-alkylphenyl)alkanoic acids in ancient pottery. *Archaeometry*, 63 (3), pp.594–608. [Online]. Available at: doi:10.1111/arcm.12631.

Bondetti, M. (2021). *Is there an 'aquatic' Neolithic?: New insights from organic residue analysis of early Holocene pottery from European Russia and Siberia*. University of Groningen Press. [Online]. Available at: doi:10.33612/diss.157185365.

Bondetti, M. et al. (2021b). Neolithic farmers or Neolithic foragers? Organic residue analysis of early pottery from Rakushechny Yar on the Lower Don (Russia). *Archaeological and anthropological sciences*, 13 (8), p.141. [Online]. Available at: doi:10.1007/s12520-021-01412-2.

Bosch, A., Chinchilla, J. and Tarrús, J. (2006). *Els objectes de fusta del poblat neolític de la Draga. Excavacions 1995-2005*. Monografies del Centre d'Arqueologia Subaquàtica de Catalunya 6. Girona : Museu d'Arqueologia de Catalunya-CASC.

Bouby, L. et al. (2018). Ressource végétales et économie de subsistance au Néolithique en France (6000-2000 av J.C.). In: Guilaine, J. and Garcia, D. (Eds). *La protohistoire de la France*. Hermann. pp.141–152. [Online]. Available at: doi:10.3917/herm.garci.2018.01.0142.

Bouby, L. et al. (2019). Early farming economy in Mediterranean France: fruit and seed remains from the Early to Late Neolithic levels of the site of Taï (ca 5300–3500 cal bc). *Vegetation history and archaeobotany*, 28 (1), pp.17–34. [Online]. Available at: doi:10.1007/s00334-018-0683-x.

Bouby, L. et al. (2020). Early Neolithic (ca. 5850-4500 cal BC) agricultural diffusion in the Western Mediterranean: An update of archaeobotanical data in SW France. *PloS one*, 15 (4), p.e0230731. [Online]. Available at: doi:10.1371/journal.pone.0230731.

Breu, A. (2019). *Earliest pottery use in north-eastern Iberia. Organic residue analyses on vessels from the first farmers and herders*. Ph.D. Thesis, Universitat Autònoma de Barcelona.

Breu, A. et al. (2021). Variation in pottery use across the Early Neolithic in the Barcelona plain. *Archaeological and anthropological sciences*, 13 (3). [Online]. Available at: doi:10.1007/s12520-021-01296-2.

Breu, A. et al. (2023a). Diversified pottery use across 5th and 4th millennium cal BC Neolithic coastal communities along the Strait of Gibraltar. *Archaeological and anthropological sciences*, 15 (4), p.51. [Online]. Available at: doi:10.1007/s12520-023-01751-2.

Breu, A. et al. (2023b). Resinous deposits in Early Neolithic pottery vessels from the northeast of the Iberian Peninsula. *Journal of Archaeological Science: Reports*, 47, p.103744. [Online]. Available at: doi:10.1016/j.jasrep.2022.103744.

Brink, J. W. and Dawe, B. (2003). Hot Rocks as Scarce Resources: The Use, Re-Use and Abandonment of Heating Stones at Head-Smashed-In Buffalo Jump. *Plains anthropologist*, 48 (186), pp.85–104. [Online]. Available at: doi:10.1080/2052546.2003.11949298.

Brown, T. A. and Brown, K. (2011). *Biomolecular Archaeology: An Introduction*. John Wiley & Sons. [Online]. Available at: https://play.google.com/store/books/details?id=0KHpdj_n1i4C.

Bruice, P. Y. (2017). *Organic Chemistry*. Eight edition. Harlow, Essex, England: Pearson Education Limited.

Buonasera, T. Y. (2005). Fatty acid analysis of prehistoric burned rocks: a case study from central California. *Journal of archaeological science*, 32 (6), pp.957–965. [Online]. Available at: doi:10.1016/j.jas.2005.01.012.

Buonasera, T. Y. (2007). Investigating the presence of ancient absorbed organic residues in groundstone using GC–MS and other analytical techniques: a residue study of several prehistoric milling tools from central California. *Journal of archaeological science*, 34 (9), pp.1379–1390. [Online]. Available at: doi:10.1016/j.jas.2006.10.028.

Buonasera, T. Y. (2013). Extracting new information from old experiments: GC/MS analysis of lipid residues in aged experimental grinding tools. *SAS Bulletin*, 36 (1), pp.2–7.

Buonasera, T. Y. (2016). Lipid residues preserved in sheltered bedrock features at Gila Cliff Dwellings National Monument, New Mexico. *Journal of lithic studies*, 3 (3), pp.78–101. [Online]. Available at: doi:10.2218/jls.v3i3.1304.

Cantelli, M. et al. (2024). Diamonds in the rough - reconsidering the scientific and heritage value of heat-altered stones in prehistoric archaeology through a systematic literature review. *Open research Europe*, 4, p.254. [Online]. Available at: doi:10.12688/openreseurope.18837.1.

Cardelli, R. (2013). *Étude pétroarchéologique des foyers de combustion de Pendimoun au Néolithique moyen : mise en évidence des problématiques*. Master's thesis, Université Côte d'Azur.

Carmody, R. N. and Wrangham, R. W. (2009). The energetic significance of cooking. *Journal of human evolution*, 57 (4), pp.379–391. [Online]. Available at: doi:10.1016/j.jhevol.2009.02.011.

Carney, M. et al. (2022). Bulbs and Biographies, Pine Nuts and Palimpsests: Exploring Plant Diversity and Earth Oven Reuse at a Late Period Plateau Site. *Archaeological and anthropological sciences*, 14 (7), p.130. [Online]. Available at: doi:10.1007/s12520-022-01588-1.

Carrer, F. et al. (2016). Chemical analysis of pottery demonstrates prehistoric origin for high-altitude alpine dairying. *PloS one*, 11 (4), p.e0151442. [Online]. Available at: doi:10.1371/journal.pone.0151442.

Caruso Ferme, L. and Piqué i Huerta, R. (2014). Landscape and forest exploitation at the ancient Neolithic site of La Draga (Banyoles, Spain). *The Holocene*, 24 (3), pp.266–273. [Online]. Available at: doi:10.1177/0959683613517400.

Cassard, L. et al. (2020). Chaines opératoires décoratives des poteries imprimées de Méditerranée

occidentale : apports de l'imagerie 3D surfacique. In: Binder, D. and Manen, C. (Eds). *Céramiques imprimées de Méditerranée occidentale (VIe millénaire AEC) : données, approches et enjeux nouveaux / Western Mediterranean Impressed Wares (6th millennium BCE): New data, approaches and challenges. Actes de la séance de la Société préhistorique française de Nice (mars 2019)*. Paris: Société préhistorique française. pp.349–378.

Cassard, L. (2020). *Systèmes de production céramique des premiers paysans du domaine liguro-provençal (VIème millénaire BCE) : traditions techniques des décors*. PhD thesis, Université Côte d'Azur.

Cattaneo, C. et al. (1993). Blood residues on stone tools: indoor and outdoor experiments. *World archaeology*, 25 (1), pp.29–43. [Online]. Available at: doi:10.1080/00438243.1993.9980226.

Cauvin, J. (1997). *Naissance des divinités - Naissance de l'agriculture. La révolution des symboles au Néolithique*. Paris: CNRS (Empreintes).

Cauvin, J. (2002). The symbolic foundations of the neolithic revolution in the near east. In: *Fundamental Issues in Archaeology*. Boston, MA: Springer US. pp.235–252. [Online]. Available at: doi:10.1007/0-306-47166-3_10.

Charters, S. et al. (1993). Quantification and distribution of lipid in archaeological ceramics: Implications for sampling potsherds for organic residue analysis and the classification of vessel use. *Archaeometry*, 35 (2), pp.211–223. [Online]. Available at: doi:10.1111/j.1475-4754.1993.tb01036.x.

Charters, S. et al. (1995). Evidence for the mixing of fats and waxes in archaeological ceramics. *Archaeometry*, 37 (1), pp.113–127. [Online]. Available at: doi:10.1111/j.1475-4754.1995.tb00730.x.

Chasan, R. et al. (2022). Foodways of an agro-pastoral community: Organic residue analysis of pottery and stone vessels at Middle Chalcolithic Tel Tsaf. *Journal of Archaeological Science: Reports*, 43, p.103491. [Online]. Available at: doi:10.1016/j.jasrep.2022.103491.

Chasan, R., Spiteri, C. and Rosenberg, D. (2022). Dietary continuation in the southern Levant: a Neolithic-Chalcolithic perspective through organic residue analysis. *Archaeological and anthropological sciences*, 14 (3), p.49. [Online]. Available at: doi:10.1007/s12520-022-01519-0.

Chen, Y. et al. (2004). Alkylresorcinols as markers of whole grain wheat and rye in cereal products. *Journal of agricultural and food chemistry*, 52 (26), pp.8242–8246. [Online]. Available at: doi:10.1021/jf049726v.

Childe, V. G. (1925). *The dawn of European civilization*. London, England: Kegan Paul.

Childe, V. G. (1955). *Man makes Himself*. New York, NY: The New American Library of Wolrd Literature.

Choy, K. et al. (2016). Chemical profiling of ancient hearths reveals recurrent salmon use in Ice Age Beringia. *Proceedings of the National Academy of Sciences of the United States of America*, 113 (35), pp.9757–9762. [Online]. Available at: doi:10.1073/pnas.1606219113.

Christie, W. W. and Han, X. (2012). *Lipid analysis : isolation, separation, identification and structural analysis of lipids*. 4th ed. Oxford: Woodhead Pub.

Clark, C. C., IV and Custer, J. F. (2003). Rethinking Delaware archaeology: A beginning. *North American archaeologist*, 24 (1), pp.29–81. [Online]. Available at: doi:10.2190/nvty-3kgp-gkkn-rxpq.

Cleland, T. P. (2018). Human Bone Paleoproteomics Utilizing Single-Pot, Solid-Phase-Enhanced Sample Preparation Method Maximize Detected Proteins Reduce Humics. *J. Proteome Res*, 17, pp.3976–3983. [Online]. Available at: doi:10.1021/acs.jproteome.8b00637)46.HarveyVL.

Cohen, M. N. (2009). Rethinking the origins of agriculture. Introduction. *Current anthropology*, 50 (5), pp.591–595. [Online]. Available at: doi:10.1086/603548.

Colonese, A. C. et al. (2015). Archaeological bone lipids as palaeodietary markers: Lipids as dietary markers. *Rapid communications in mass spectrometry: RCM*, 29 (7), pp.611–618. [Online]. Available at: doi:10.1002/rcm.7144.

Colonese, A. C. et al. (2017). New criteria for the molecular identification of cereal grains associated with archaeological artefacts. *Scientific reports*, 7 (1), p.6633. [Online]. Available at: doi:10.1038/s41598-017-06390-x.

Copley, M. S. et al. (2003). Direct chemical evidence for widespread dairying in prehistoric Britain. *Proceedings of the National Academy of Sciences of the United States of America*, 100 (4), pp.1524–1529. [Online]. Available at: doi:10.1073/pnas.0335955100.

Copley, M. S. et al. (2005a). Gas chromatographic, mass spectrometric and stable carbon isotopic investigations of organic residues of plant oils and animal fats employed as illuminants in archaeological lamps from Egypt. *The Analyst*, 130 (6), pp.860–871. [Online]. Available at: doi:10.1039/b500403a.

Copley, M. S. et al. (2005b). Processing of milk products in pottery vessels through British prehistory. *Antiquity*, 79 (306), pp.895–908. [Online]. Available at: doi:10.1017/s0003598x00115029.

Correa-Ascencio, M. and Evershed, R. P. (2014). High throughput screening of organic residues in archaeological potsherds using direct acidified methanol extraction. *Analytical Methods*, 6 (5), pp.1330–1340. [Online]. Available at: doi:10.1039/C3AY41678J [Accessed 13 February 2023].

Cortell-Nicolau, A. et al. (2025). Demographic interactions between the last hunter-gatherers and the first farmers. *Proceedings of the National Academy of Sciences of the United States of America*, 122 (14), p.e2416221122. [Online]. Available at: doi:10.1073/pnas.2416221122.

Courel, B. et al. (2021). The use of early pottery by hunter-gatherers of the Eastern European forest-steppe. *Quaternary science reviews*, 269 (107143), p.107143. [Online]. Available at: doi:10.1016/j.quascirev.2021.107143.

Craig, O. E. et al. (2004). Stable carbon isotopic characterisation of free and bound lipid constituents of archaeological ceramic vessels released by solvent extraction, alkaline hydrolysis and catalytic hydropyrolysis. *Journal of analytical and applied pyrolysis*, 71 (2), pp.613–634. [Online]. Available at: doi:10.1016/j.jaap.2003.09.001.

Craig, O. E. et al. (2005). The identification of prehistoric dairying activities in the Western Isles of Scotland: an integrated biomolecular approach. *Journal of archaeological science*, 32 (1), pp.91–103. [Online]. Available at: doi:10.1016/j.jas.2004.06.009.

Craig, O. E. et al. (2007). Molecular and isotopic demonstration of the processing of aquatic products in northern European prehistoric pottery. *Archaeometry*, 49 (1), pp.135–152. [Online]. Available at: doi:10.1111/j.1475-4754.2007.00292.x.

Craig, O. E. et al. (2011). Ancient lipids reveal continuity in culinary practices across the transition to agriculture in Northern Europe. *Proceedings of the National Academy of Sciences of the United States of America*, 108 (44), pp.17910–17915. [Online]. Available at: doi:10.1073/pnas.1107202108.

Craig, O. E. et al. (2012). Distinguishing wild ruminant lipids by gas chromatography/combustion/isotope ratio mass spectrometry. *Rapid communications in mass spectrometry: RCM*, 26 (19), pp.2359–2364. [Online]. Available at: doi:10.1002/rcm.6349.

Craig, O. E. et al. (2013). Earliest evidence for the use of pottery. *Nature*, 496 (7445), pp.351–354. [Online]. Available at: doi:10.1038/nature12109.

Craig, O. E. (2021). Prehistoric Fermentation, Delayed-Return Economies, and the Adoption of Pottery Technology. *Current Anthropology*, 62 (24), pp.S233–S241. [Online]. Available at: doi:https://doi.org/10.1086/716610.

Craig, O. E. and Collins, M. J. (2002). The removal of protein from mineral surfaces: Implications for residue analysis of archaeological materials. *Journal of archaeological science*, 29 (10), pp.1077–1082. [Online]. Available at: doi:10.1006/jasc.2001.0757.

Cramp, L. and Evershed, R. P. (2014). Reconstructing Aquatic Resource Exploitation in Human Prehistory Using Lipid Biomarkers and Stable Isotopes. In: Holland, H. D. and Turekian, K. K. (Eds). *Treatise on Geochemistry (Second Edition)*. Oxford: Elsevier. pp.319–339. [Online]. Available at: doi:10.1016/B978-0-08-095975-7.01225-0.

Cramp, L. J. E. et al. (2023). Lipids in archaeology. *Handbook of Archaeological Sciences*, Wiley., pp.529–556. [Online]. Available at: doi:10.1002/9781119592112.ch26.

Croft, S. et al. (2018). Pine traces at Star Carr: Evidence from residues on stone tools. *Journal of Archaeological Science: Reports*, 21, pp.21–31. [Online]. Available at: doi:10.1016/j.jasrep.2018.06.021.

Cruz Berrocal, M. (2012). The early neolithic in the Iberian peninsula and the western Mediterranean: A review of the evidence on migration. *Journal of world prehistory*, 25 (3-4), pp.123–156. [Online]. Available at: doi:10.1007/s10963-012-9059-9.

Cubas, M. et al. (2020). Latitudinal gradient in dairy production with the introduction of farming in Atlantic Europe. *Nature communications*, 11 (1), p.2036. [Online]. Available at: doi:10.1038/s41467-020-15907-4.

Cubas, M., Peyroteo-Stjerna, R. and Fontanals-Coll, M. (2019). Long-term dietary change in Atlantic and Mediterranean Iberia with the introduction of agriculture: a stable isotope perspective. *Archaeological and anthropological sciences*. [Online]. Available at: https://link.springer.com/article/10.1007/s12520-018-0752-1.

Custer, J. F. (2017). Experimental analysis of fire-cracked rocks from varied use contexts: Fracture attributes. *North American Archaeologist*, 38 (3), pp.237–291. [Online]. Available at: doi:10.1177/0197693117696533.

Custer, J. F., Ilgenfritz", J. and Domsa, K. R. (1988). A Cautionary Note on the Use of Chemstrips for Detection of Blood Residues on Prehistoric Stone Tools. *Journal of archaeological science*, 15, pp.343–345.

Cutts, R. B. et al. (2019). Thermal curved-fragments: A method for identifying anthropogenic fire in the archaeological record. *Journal of archaeological science*, 106, pp.10–22. [Online]. Available at: doi:10.1016/j.jas.2019.03.006.

Dallongeville, S. et al. (2016). Proteins in Art, Archaeology, and Paleontology: From Detection to Identification. *Chemical reviews*, 116 (1), pp.2–79. [Online]. Available at: doi:10.1021/acs.chemrev.5b00037.

Debono-Spiteri, C. (2012). *Pottery use at the transition to agriculture in the western Mediterranean. Evidence from biomolecular and isotopic characterisation of organic residues in Impressed/Cardial Ware vessels*. Ph.D. Thesis, University of York, U.K.

Debono Spiteri, C. et al. (2016). Regional asynchronicity in dairy production and processing in early farming communities of the northern Mediterranean. *Proceedings of the National Academy of Sciences of the United States of America*, 113 (48), pp.13594–13599. [Online]. Available at: doi:10.1073/pnas.1607810113.

Defranould, E. (2021). The Cardial–Epicardial Early Neolithic of lower Rhône Valley (south-eastern France): A lithic perspective. *Open Archaeology*, 7 (1), pp.939–952. [Online]. Available at: doi:10.1515/opar-2020-0182.

Degano, I. et al. (2019). Hafting of Middle Paleolithic tools in Latium (central Italy): New data from Fossellone and Sant'Agostino caves. *PloS one*, 14 (6), p.e0213473. [Online]. Available at: doi:10.1371/journal.pone.0213473.

Dekker, J. A. A. et al. (2025). An unclean slate, discrepancies between food input and recovered protein signal from experimental foodcrusts. *bioRxiv*. [Online]. Available at: doi:10.1101/2025.02.03.636240.

Delhon, C. et al. (2020). Phytoliths as a seasonality indicator? The example of the Neolithic site of Pendimoun, south-eastern France. *Vegetation history and archaeobotany*, 29 (2), pp.229–240. [Online]. Available at: doi:10.1007/s00334-019-00739-0.

DeNiro, M. J. and Epstein, S. (1978). Influence of diet on the distribution of carbon isotopes in animals. *Geochimica et cosmochimica acta*, 42 (5), pp.495–506. [Online]. Available at: doi:10.1016/0016-7037(78)90199-0.

De Stefanis, C. (2018). *Systèmes techniques des derniers chasseurs-cueilleurs et des premiers agro-pasteurs du domaine liguro-provençal (7000-5500 av. J.C) : approche fonctionnelle*. [Online]. Available at: http://www.theses.fr/2018AZUR2012.

Dietrich, L. et al. (2020). Investigating the function of Pre-Pottery Neolithic stone troughs from Göbekli Tepe – An integrated approach. *Journal of archaeological science, reports*, 34 (102618), p.102618. [Online]. Available at: doi:10.1016/j.jasrep.2020.102618.

Dimitrakoudi, E. A. et al. (2011). Characterization by gas chromatography-mass spectrometry of diterpenoid resinous materials in Roman-age amphorae from northern Greece. *European journal of mass spectrometry* , 17 (6), pp.581–591. [Online]. Available at: doi:10.1255/ejms.1155.

Dolbunova, E. et al. (2023). The transmission of pottery technology among prehistoric European hunter-gatherers. *Nature human behaviour*, 7 (2), pp.171–183. [Online]. Available at: doi:10.1038/s41562-022-01491-8.

Doliente, J. E. et al. (2024). Alkylresorcinol detection and identification in archaeological pottery using ultra-high-performance liquid chromatography-quadrupole/Orbitrap mass spectrometry. *Rapid communications in mass spectrometry: RCM*, 38 (15), p.e9771. [Online]. Available at: doi:10.1002/rcm.9771.

Downs, E. F. and Lowenstein, J. M. (1994). Identification of Archaeological Blood Proteins: a Cautionary Note. *Journal of archaeological blood proteins: a cautionary note*, 22, pp.11–16. [Online]. Available at: doi:10.1016/S0305-4403(95)80160-X.

Drieu, L. (2017). *Fabrication et usages des poteries durant le Néolithique et la Protohistoire en Europe: Les Apports de l'archéologie biomoléculaire*. Ph.D. Thesis, Université Côte d'Azur.

Drieu, L. et al. (2018). Domestic activities and pottery use in the Iron Age Corsican settlement of Cuciurpula revealed by organic residue analysis. *Journal of archaeological science, reports*, 19, pp.213–223. [Online]. Available at: doi:10.1016/j.jasrep.2018.02.032.

Drieu, L. et al. (2019). Influence of porosity on lipid preservation in the wall of archaeological pottery. *Archaeometry*, 61 (5), pp.1081–1096. [Online]. Available at: doi:10.1111/arcm.12479.

Drieu, L. et al. (2021). A Neolithic without dairy? Chemical evidence from the content of ceramics from the Pendimoun rock-shelter (Castellar, France, 5750–5150 BCE). *Journal of Archaeological Science: Reports*, 35, p.102682. [Online]. Available at: doi:10.1016/j.jasrep.2020.102682.

Drieu, L., Binder, D. and Regert, M. (2022). Studying the use of the pots from the Pendimoun rock shelter: considerations about organic residue analysis of Mediterranean Neolithic pottery. In: Binder, D. and Manen, C. (Eds). *Céramiques imprimées de Méditerranée occidentale (VIe millénaire AEC) : données, approches et enjeux nouveaux*. 18. 2022. Séances de la Société préhistorique française. pp.379–391.

Drieu, L., Lepère, C. and Regert, M. (2020). The missing step of pottery chaîne opératoire: Considering post-firing treatments on ceramic vessels using macro- and microscopic observation and molecular analysis. *Journal of archaeological method and theory*, 27 (2), pp.302–326. [Online]. Available at: doi:10.1007/s10816-019-09428-8.

Driver, H. E. and Massey, W. C. (1957). Comparative Studies of North American Indians. *Transactions of the American Philosophical Society*, 47 (2), pp.165–456. [Online]. Available at: doi:10.2307/1005714.

Dubesset, D. et al. (2014). Les foyers à pierres chauffantes du Hameau des Laurons (Les Arcs-sur-Argens, Var). *Documents d'archéologie méridionale*, (37), pp.25–50. [Online]. Available at: doi:10.4000/dam.6090.

Dudd, S. N. (1999). *Molecular and Isotopic Characterisation of Animal Fats in Archaeological Pottery*. Ph.D. Thesis, Bristol University.

Dudd, S. N., Evershed, R. P. and Gibson, A. M. (1999). Evidence for varying patterns of exploitation of animal products in different prehistoric pottery traditions based on lipids preserved in surface and absorbed residues. *Journal of archaeological science*, 26 (12), pp.1473–1482. [Online]. Available at: doi:10.1006/jasc.1998.0434.

Dudd, S. N., Regert, M. and Evershed, R. P. (1998). Assessing microbial lipid contributions during laboratory degradations of fats and oils and pure triacylglycerols absorbed in ceramic potsherds. *Organic geochemistry*, 29 (5), pp.1345–1354. [Online]. Available at: doi:10.1016/S0146-6380(98)00093-X.

Dunne, J. et al. (2012). First dairying in green Saharan Africa in the fifth millennium BC. *Nature*, 486 (7403), pp.390–394. [Online]. Available at: doi:10.1038/nature11186.

Dunne, J. (2017). *Organic Residue Analysis and Archaeology: Guidance for Good Practice*. Historic England. [Online]. Available at: doi:10.5284/1108856.

Eerkens, J. W. (2005). Gc–ms analysis and fatty acid ratios of archaeological potsherds from the western Great Basin of north America. *Archaeometry*, 47 (1), pp.83–102. [Online]. Available at: doi:10.1111/j.1475-4754.2005.00189.x.

Eglinton, G. and Hamilton, R. J. (1967). Leaf epicuticular waxes. *Science (New York, N.Y.)*, 156 (3780), pp.1322–1335. [Online]. Available at: doi:10.1126/science.156.3780.1322.

Ellwood, E. C. et al. (2013). Stone-boiling maize with limestone: experimental results and implications for nutrition among SE Utah preceramic groups. *Journal of archaeological science*, 40 (1), pp.35–44. [Online]. Available at: doi:10.1016/j.jas.2012.05.044.

Eskola, K. O., Okkonen, J. and Jungner, H. (2003). Luminescence dating of a coastal Stone Age dwelling place in Northern Finland. *Quaternary science reviews*, 22 (10), pp.1287–1290. [Online]. Available at: doi:10.1016/S0277-3791(03)00077-5.

European Environment Agency. (2017). *Biogeographical Regions in Europe*. [Online]. Available at: www.eea.europa.eu/en/analysis/maps-and-charts/biogeographical-regions-in-europe-2.

Evans, M. et al. (2023). Detection of dairy products from multiple taxa in Late Neolithic pottery from Poland: an integrated biomolecular approach. *Royal Society open science*, 10 (3), p.230124. [Online]. Available at: doi:10.1098/rsos.230124.

Evans, M. et al. (2024). The impact of cooking and burial on proteins: a characterisation of experimental foodcrusts and ceramics. *Royal Society open science*, 11 (9), p.240610. [Online]. Available at: doi:10.1098/rsos.240610.

Evershed, R. P. et al. (1992). The survival of food residues: new methods of analysis, interpretation and application. *Proceedings of the British Academy*, 77, pp.187–208.

Evershed, R. P. (1993). Biomolecular archaeology and lipids. *World archaeology*, 25 (1), pp.74–93. [Online]. Available at: doi:10.1080/00438243.1993.9980229.

Evershed, R. P. et al. (1994). Application of Isotope Ratio Monitoring Gas Chromatography-Mass Spectrometry to the Analysis of Organic Residues of Archaeological Origin. *Analyst*, 119, pp.909–914. [Online]. Available at: doi:10.1039/AN9941900909.

Evershed, R. P. et al. (1995a). Formation of long-chain ketones in ancient pottery vessels by pyrolysis of acyl lipids. *Tetrahedron letters*, 36 (48), pp.8875–8878. [Online]. Available at: doi:10.1016/0040-4039(95)01844-8.

Evershed, R. P. et al. (1995b). Preliminary results for the analysis of lipids in ancient bone. *Journal of archaeological science*, 22 (2), pp.277–290. [Online]. Available at: doi:10.1006/jasc.1995.0030.

Evershed, R. P. et al. (1997). New criteria for the identification of animal fats preserved in archaeological pottery. *The Science of Nature*, 84 (9), pp.402–406. [Online]. Available at: doi:10.1007/s001140050417.

Evershed, R. P. et al. (1999a). Lipids as carriers of anthropogenic signals from prehistory. *Phil.Trans. R. Soc. Lond. B*, 354, pp.19–31.

Evershed, R. P. et al. (1999b). Lipids as carriers of anthropogenic signals from prehistory. *Philosophical transactions of the Royal Society of London. Series B, Biological sciences*, 354 (1379), pp.19–31. [Online]. Available at: doi:10.1098/rstb.1999.0357.

Evershed, R. P. et al. (2002). Identification of animal fats via compound specific δ13C values of individual fatty acids: assessments of results for reference fats and lipid extracts of archaeological pottery vessels. *Documenta Praehistorica*, 29, pp.73–96. [Online]. Available at: doi:10.4312/dp.29.7.

Evershed, R. P. et al. (2008a). Earliest date for milk use in the Near East and southeastern Europe linked to cattle herding. *Nature*, 455 (7212), pp.528–531. [Online]. Available at: doi:10.1038/nature07180.

Evershed, R. P. (2008a). Experimental approaches to the interpretation of absorbed organic residues in archaeological ceramics. *World archaeology*, 40 (1), pp.26–47. [Online]. Available at: doi:10.1080/00438240801889373.

Evershed, R. P. et al. (2008b). Experimental Evidence for the Processing of Marine Animal Products and other Commodities Containing Polyunsaturated Fatty Acids in Pottery Vessels. *Archaeometry*, 50

(1), pp.101–113. [Online]. Available at: doi:10.1111/j.1475-4754.2007.00368.x.

Evershed, R. P. (2008b). Organic residue analysis in archaeology: The archaeological biomarker revolution. *Archaeometry*, 50 (6), pp.895–924. [Online]. Available at: doi:10.1111/j.1475-4754.2008.00446.x.

Evershed, R. P. et al. (2022). Dairying, diseases and the evolution of lactase persistence in Europe. *Nature*, 608 (7922), pp.336–345. [Online]. Available at: doi:10.1038/s41586-022-05010-7.

Evershed, R. P. and Bethell, P. H. (1996). Application of multimolecular biomarker techniques to the identification of fecal material in archaeological soils and sediments. In: *ACS Symposium Series*. ACS symposium series. American Chemical Society. Washington, DC: American Chemical Society. pp.157–172. [Online]. Available at: doi:10.1021/bk-1996-0625.ch013.

Evershed, R. P., Charters, S. and Quye, A. (1995). Interpreting lipid residues in archaeological ceramics: Preliminary results from laboratory simulations of vessel use and burial. *Materials Research Society symposia proceedings. Materials Research Society*, 352 (85). [Online]. Available at: doi:10.1557/proc-352-85.

Evershed, R. P., Heron, C. and John Goad, L. (1990). Analysis of organic residues of archaeological origin by high-temperature gas chromatography and gas chromatography-mass spectrometry. *The Analyst*, 115 (10), pp.1339–1342. [Online]. Available at: doi:10.1039/AN9901501339.

Evershed, R. and Tuross, N. (1996). Proteinaceous material from potsherds and associated soils. *Journal of archaeological science*, 23 (3), pp.429–436. [Online]. Available at: doi:10.1006/jasc.1996.0038.

Fanti, L. et al. (2018). The role of pottery in Middle Neolithic societies of western Mediterranean (Sardinia, Italy, 4500-4000 cal BC) revealed through an integrated morphometric, use-wear, biomolecular and isotopic approach. *Journal of archaeological science*, 93, pp.110–128. [Online]. Available at: doi:10.1016/j.jas.2018.03.005.

Fanti, L., Drieu, L. and Regert, M. (2024). Pottery use by the first Neolithic communities of Sardinia (Italy) : functional analysis of vessels from Su Carroppu di Sirri, Carbonia. *Rivista di scienze preistoriche*, LXXIV. [Online]. Available at: doi:10.32097/1266.

Fellows, I. and Stotz, J. P. (2023). *OpenStreetMap: Access to Open Street Map Raster Images*. [Online]. Available at: https://CRAN.R-project.org/package=OpenStreetMap.

Fernández Ruiz, J. et al. (2018). Las estructuras de combustión de grandes dimensiones de época neolítica en el nordeste de la península ibérica. Aportaciones a su conocimiento a partir del yacimiento de Reina Amalia 38 (Barcelona). *Cypsela: revista de prehistòria i protohistòria*, 21, pp.7–21. [Online]. Available at: https://raco.cat/index.php/Cypsela/article/view/348847.

Fiedel, S. (1996). Blood from Stones? Some Methodological and Interpretive Problems in Blood Residue Analysis. *Journal of archaeological science*, 23 (1), pp.139–147. [Online]. Available at: doi:10.1006/jasc.1996.0011.

Fontanals Coll, M. (2015). *Estudi dels modes de subsistència de les comunitats neolítiques del nord-est de la Península Ibèrica: reconstrucció paleodietètica a partir dels isòtops estables*. Ph.D. Thesis, Universitat Autònoma de Barcelona.

Fort, J. (2022). Dispersal distances and cultural effects in the spread of the Neolithic along the northern Mediterranean coast. *Archaeological and anthropological sciences*, 14 (8). [Online]. Available at: doi:10.1007/s12520-022-01619-x.

Frère-Sautot, M.-C. (2003). *Le feu domestique et ses structures au Néolithique et aux Âges des métaux: actes du colloque de Bourg-en-Bresse et Beaune, 7 et 8 octobre 2000*. M. Mergoil.

Fretheim, S. E. (2009). Feast in the forest: creating a common cultural identity in the interior of the Scandinavian Peninsula in the Late Mesolithic. In: McCartan, S. et al. (Eds). *Mesolithic horizons: papers presented at the Seventh International Conference on the Mesolithic in Europe*. 2009. Oxford Books. pp.378–384.

Friedli, H. et al. (1986). Ice core record of the $^{13}C/^{12}C$ ratio of atmospheric CO_2 in the past two centuries. *Nature*, 324, pp.237–238.

Frison, G. C. (1983). Stone Circles, Stone-Filled Fire Pits, Grinding Stones and High Plains Archaeology. *Plains anthropologist*, 28 (102), pp.81–92. [Online]. Available at: doi:10.1080/2052546.1983.11909175.

Fuessl, A., Yamamoto, M. and Schneller, A. (2012). Opportunities in bio-based building blocks for polycondensates and vinyl polymers. In: *Polymer Science: A Comprehensive Reference*. 5. Elsevier. pp.49–70. [Online]. Available at: doi:10.1016/b978-0-444-53349-4.00132-1.

Fuller, D. Q. and Gonzalez Carretero, L. (2018). The archaeology of Neolithic cooking traditions: Archaeobotanical approaches to baking, boiling and fermenting. *Archaeology international*, 21 (1), p.109. [Online]. Available at: doi:10.5334/ai-391.

Fuller, D. Q., Willcox, G. and Allaby, R. G. (2011). Cultivation and domestication had multiple origins: arguments against the core area hypothesis for the origins of agriculture in the Near East. *World archaeology*, 43 (4), pp.628–652. [Online]. Available at: doi:10.1080/00438243.2011.624747.

Gabriele, M. et al. (2022). An assessment of Early Farmers' pottery, pastes and raw materials transfers in the Ligurian-Provençal region (Impressa, first half of the 6th millennium BCE). In: Binder, D. and Manen, C. (Eds). *Céramiques imprimées de Méditerranée occidentale (VIe millénaire AEC) : données, approches et enjeux nouveaux / Western Mediterranean Impressed Wares (6th millennium BCE): New data, approaches and challenges. Actes de la séance de la Société préhistorique française de Nice (mars 2019)*. Paris: Société préhistorique française. pp.177–211.

Gao, X. et al. (2014). The discovery of Late Paleolithic boiling stones at SDG 12, north China. *Quaternary international: the journal of the International Union for Quaternary Research*, 347, pp.91–96. [Online]. Available at: doi:10.1016/j.quaint.2014.07.003.

Garcia, L. L. (2011). Estudi preliminar de les restes d'aus del poblat neolític de La Draga Banyoles, Pla de l'Estany. In: Bosch, A., Chinchilla, J. and Tarrús, J. (Eds). *El poblat lacustre neolític de la Draga. Excavacions de 1990 a 1998.* Girona: Centre d'Arqueologia Subaquatica de Catalunya. pp.213–221.

García-Piquer, A. et al. (2018). An experimental ethnoarchaeology and analytical approach to fire-related management strategies in a hunter–fisher–gatherer society from the southern tip of Tierra del Fuego (Argentina). *Ethnoarchaeology*, 10 (2), pp.121–140. [Online]. Available at: doi:10.1080/19442890.2018.1510609.

Gaugler, K. (2019). *Heating Stones: A Multi-Proxy Approach to the Analysis of Fire-Cracked Rock at Three Monongahela Sites in Southwestern Pennsylvania*. Master of Arts, Indiana University of Pennsylvania.

Gavériaux, F. et al. (2022). L'alimentation des premières sociétés agropastorales du Sud de la France : premières données isotopiques sur des graines et fruits carbonisés néolithiques et essais de modélisation. *Comptes rendus. Palevol*, 21 (19), pp.391–410. [Online]. Available at: doi:10.5852/cr-palevol2022v21a19.

Gerlach, S. C. et al. (1996). Blood Protein Residues on Lithic Artifacts from Two Archaeological Sites in the De Long Mountains, Northwestern Alaska. *Arctic*, 49 (1), pp.1–10. [Online]. Available at: http://www.jstor.org/stable/40511980.

Gerritsen, F. A., Özbal, R. and Thissen, L. C. (2013). The Earliest Neolithic Levels at Barcin Höyük, Northwestern Turkey. *Anatolica XXXXIX*, 39, pp.53–92. [Online]. Available at: doi:10.2143/ANA.39.0.2990784.

Gillespie, A., Budinger, F. and Abbott, E. (1989). Verification of prehistoric campfires by 40Ar39Ar analysis of fire-baked stones. *Journal of archaeological science*, 16, pp.271–291. [Online]. Available at: doi:10.1016/0305-4403(89)90006-X.

Gomart, L. et al. (2017). Spiralled patchwork in pottery manufacture and the introduction of farming to Southern Europe. *Antiquity*, 91 (360), pp.1501–1514. [Online]. Available at: doi:10.15184/aqy.2017.187.

Gomart, L. et al. (2022). Technical frontiers and social boundaries in the Impressed Ware complex: ceramic manufacture as a proxy of Neolithisation processes in the Western Mediterranean. In: et C. Manen, D. B. (Ed). *Céramiques imprimées de Méditerranée occidentale (VIe millénaire AEC) : données, approches et enjeux nouveaux / Western Mediterranean Impressed Wares (6th millennium BCE): new data, approaches and challenges, Actes de la Séance de la Société préhistorique française, Nice, 18-20 mars 2019*. Séances de la Société préhistorique française. 18. pp.125–146. [Online]. Available at: https://hal.science/hal-03908891.

Gose, W. A. (2000). Palaeomagnetic Studies of Burned Rocks. *Journal of archaeological science*, 27 (5), pp.409–421. [Online]. Available at: doi:10.1006/jasc.1999.0465.

Goude, G. et al. (2020). New insights on Neolithic food and mobility patterns in Mediterranean coastal populations. *American journal of physical anthropology*, 173 (2), pp.218–235. [Online]. Available at: doi:10.1002/ajpa.24089.

Graesch, A. P. et al. (2014). Thermally Modified Rock: The Experimental Study of 'Fire-Cracked' Byproducts of Hot Rock Cooking. *North American Archaeologist*, 35 (2), pp.167–200. [Online]. Available at: doi:10.2190/NA.35.2.c.

Graff, S. R. (2018). Archaeological Studies of Cooking and Food Preparation. *Journal of Archaeological Research*, 26 (3), pp.305–351. [Online]. Available at: http://www.jstor.org/stable/44984074.

Graff, S. R. (2020). Archaeology of cuisine and cooking. *Annual review of anthropology*, 49 (1), pp.337–354. [Online]. Available at: doi:10.1146/annurev-anthro-102317-045734.

Graven, H., Keeling, R. F. and Rogelj, J. (2020). Changes to carbon isotopes in atmospheric CO2 over the industrial era and into the future. *Global biogeochemical cycles*, 34 (11), p.e2019GB006170. [Online]. Available at: doi:10.1029/2019GB006170.

Greenfield, H. J. and Arnold, E. R. (2015). 'Go(a)t milk?' New perspectives on the zooarchaeological evidence for the earliest intensification of dairying in south eastern Europe. *World archaeology*, 47 (5), pp.792–818. [Online]. Available at: doi:10.1080/00438243.2015.1029076.

Gregg, M. W. (2009). *Organic residue analysis and the earliest uses of pottery in the ancient Middle East*. PhD thesis, University of Toronto.

Gregg, M. W. et al. (2009). Subsistence practices and pottery use in Neolithic Jordan: molecular and isotopic evidence. *Journal of archaeological science*, 36 (4), pp.937–946. [Online]. Available at: doi:10.1016/j.jas.2008.09.009.

Griffin, J. B. (1967). Eastern North American Archaeology: A Summary. *Science*, 156 (3772), pp.175–191. [Online]. Available at: doi:10.1126/science.156.3772.175.

Gronenborn, D. and Horejs, B. (2023). *Expansion of farming in western Eurasia, 9600 - 4000 cal BC (update vers. 2023.1)*. [Online]. Zenodo. Available at: doi:10.5281/ZENODO.5903164.

Guilaine, J. (2001). La diffusion de l'agriculture en Europe: une hypothèse arythmique. *Zephyrus*, (55-53), pp.267–272.

Guilaine, J. (2015). The neolithization of Mediterranean Europe. In: Fowler, C., Harding, J. and Hofmann, D. (Eds). *The Oxford Handbook of Neolithic Europe*. Oxford University Press. pp.81–98. [Online]. Available at: doi:10.1093/oxfordhb/9780199545841.013.064.

Guilaine, J. (2017). The Neolithic transition: From the Eastern to the western Mediterranean. In: *Times of Neolithic Transition along the Western Mediterranean*. Cham: Springer International Publishing. pp.15–31. [Online]. Available at: doi:10.1007/978-3-319-52939-4_2.

Guilaine, J. (2018). A personal view of the neolithisation of the Western Mediterranean. *Quaternary international: the journal of the International Union for Quaternary Research*, 470, pp.211–225. [Online]. Available at: doi:10.1016/j.quaint.2017.06.019.

Guilaine, J. and Manen, C. (2002). La ceramica impressa della Francia meridionale. In: Fugazzola Delpino, M. A., Pessina, A. and Tiné, V. (Eds). *Le ceramiche impresse nel Neolitico Antico. Italia e Mediterraneo*. Roma: Istituto poligrafico e Zecca dello Stato. pp.37–49.

Gülz, P.-G. (1994). Epicuticular leaf waxes in the evolution of the plant kingdom. *Journal of plant physiology*, 143 (4-5), pp.453–464. [Online]. Available at: doi:10.1016/s0176-1617(11)81807-9.

Halstead, P. (2012). Las transformaciones económicas del Neolítico en Europa. In: Rojo, M. A., Garrido, R. and García, I. (Eds). *El Neolítico en la península Ibérica y su contexto europeo*. Cátedra. pp.27–40.

Halstead, P. (2024). Zooarchaeological evidence for livestock management in (earlier) Neolithic Europe: Outstanding questions and some limitations of current approaches. *Quaternary international: the journal of the International Union for Quaternary Research*, 683-684, pp.42–50. [Online]. Available at: doi:10.1016/j.quaint.2023.09.013.

Hammann, S. et al. (2018). Cholesterol degradation in archaeological pottery mediated by fired clay and fatty acid pro-oxidants. *Tetrahedron letters*, 59 (50), pp.4401–4404. [Online]. Available at: doi:10.1016/j.tetlet.2018.10.071.

Hammann, S. et al. (2022). Neolithic culinary traditions revealed by cereal, milk and meat lipids in pottery from Scottish crannogs. *Nature communications*, 13 (1), p.5045. [Online]. Available at: doi:10.1038/s41467-022-32286-0.

Hammann, S. and Cramp, L. J. E. (2018). Towards the detection of dietary cereal processing through absorbed lipid biomarkers in archaeological pottery. *Journal of archaeological science*, 93, pp.74–81. [Online]. Available at: doi:10.1016/j.jas.2018.02.017.

Hamon, C. (2008). Functional analysis of stone grinding and polishing tools from the earliest Neolithic of north-western Europe. *Journal of archaeological science*, 35 (6), pp.1502–1520. [Online]. Available at: doi:10.1016/j.jas.2007.10.017.

Hamon, C. (2021). A revolution in food preparation? Grinding and pounding plants in the first farming communities of Western Europe and the Mediterranean region. *Food and History*. [Online]. Available at: doi:10.1484/j.food.5.126408.

Hamon, C. and Manen, C. (2021). The mechanisms of neolithisation of Western Europe: Beyond a south/north approach. *Open Archaeology*, 7 (1), pp.718–735. [Online]. Available at: doi:10.1515/opar-2020-0164.

Hansel, F. A. et al. (2004). Thermally produced ω-(o-alkylphenyl)alkanoic acids provide evidence for the processing of marine products in archaeological pottery vessels. *Tetrahedron letters*, 45 (14), pp.2999–3002. [Online]. Available at: doi:10.1016/j.tetlet.2004.01.111.

Hansen, J. (2024). *From ideology to economy. Unveiling the taxonomic origin of animal bone artefacts with palaeoproteomic analysis*. Ph.D. Thesis, Universitat Autònoma de Barcelona.

Hart, P. (2023). *Foyers et structures de chauffe domestiques des âges des métaux De la méthode d'analyse dynamique des structures à l'apport de l'ethnologie et au cas particulier des structures à pierres chauffées*. Dissertation, Université de Strasbourg, Université de Freiburg-im-Breisgau.

Hart, P. (2024). Structures Archéologiques à Pierres Chauffées: un Petit Air de Polynésie? Assurément, mais pas Exclusivement! In: *Le Banquet cérémoniel entre archéologie et ethnologie*. Archaeopress Publishing Ltd. pp.209–246. [Online]. Available at: doi:10.2307/jj.14736595.11.

Harvey, V. L. and Hendy, J. (2025). *SP3 protocol optimised for foodcrust protein extraction from archaeological cooking vessels v1*. [Online]. Available at: doi:10.17504/protocols.io.e6nvwb22wvmk/v1.

Hastorf, C. A. (2016). *The Practices of a Meal in Society*. Cambridge University Press., pp.55–80. [Online]. Available at: doi:10.1017/9781316597590.005.

Hawkes, A. (2018). *The Archaeology of Prehistoric Burnt Mounds in Ireland*. Archaeopress.

Heaton, K. et al. (2009). Towards the application of desorption electrospray ionisation mass spectrometry (DESI-MS) to the analysis of ancient proteins from artefacts. *Journal of archaeological science*, 36 (10), pp.2145–2154. [Online]. Available at: doi:10.1016/j.jas.2009.05.016.

Hellevang, H. and Aagaard, P. (2015). Constraints on natural global atmospheric CO2 fluxes from 1860 to 2010 using a simplified explicit forward model. *Scientific reports*, 5 (1), p.17352. [Online]. Available at: doi:10.1038/srep17352.

Hendy, J. et al. (2018). Ancient proteins from ceramic vessels at Çatalhöyük West reveal the hidden cuisine of early farmers. *Nature communications*, 9 (1), p.4064. [Online]. Available at: doi:10.1038/s41467-018-06335-6.

Hendy, J. (2021). Ancient protein analysis in archaeology. *Science advances*, 7 (3), p.eabb9314. [Online]. Available at: doi:10.1126/sciadv.abb9314.

Heron, C. et al. (2010). Application of lipid biomarker analysis to evaluate the function of 'slab-lined pits' in Arctic Norway. *Journal of archaeological science*, 37 (9), pp.2188–2197. [Online]. Available at: doi:10.1016/j.jas.2010.03.016.

Heron, C. and Evershed, R. P. (1993). The analysis of organic residues and the study of pottery use. *Archaeological method and theory*, 5, pp.247–284. [Online]. Available at: https://www.jstor.org/stable/pdf/20170233.pdf.

Heron, C., Evershed, R. P. and Goad, L. J. (1991). Effects of migration of soil lipids on organic residues associated with buried potsherds. *Journal of archaeological science*, 18 (6), pp.641–659. [Online]. Available at: doi:10.1016/0305-4403(91)90027-m.

Herrscher, E. and Le Bras-Goude, G. (2010). Southern French Neolithic populations: Isotopic evidence for regional specificities in environment and diet. *American journal of physical*

anthropology, 141 (2), pp.259–272. [Online]. Available at: https://onlinelibrary.wiley.com/doi/10.1002/ajpa.21141.

Hofmanová, Z. et al. (2016). Early farmers from across Europe directly descended from Neolithic Aegeans. *Proceedings of the National Academy of Sciences of the United States of America*, 113 (25), pp.6886–6891. [Online]. Available at: doi:10.1073/pnas.1523951113.

Högberg, A., Puseman, K. and Yost, C. (2009). Integration of use-wear with protein residue analysis – a study of tool use and function in the south Scandinavian Early Neolithic. *Journal of archaeological science*, 36 (8), pp.1725–1737. [Online]. Available at: doi:10.1016/j.jas.2009.03.030.

Homsey, L. K. (2009). The Identification and Prehistoric Selection Criteria of Fire-cracked Rock: an Example from Dust Cave, Alabama. *Southeastern Archaeology*, 28, pp.101–116. [Online]. Available at: http://www.jstor.com/stable/40713502.

Hurcombe, L. (2014). *Archaeological Artefacts as Material Culture*. Routledge.

Hyland, D. C. et al. (1990). Identification of the Species of Origin of Residual Blood on Lithic Material. *American antiquity*, 55 (1), pp.104–112. [Online]. Available at: doi:10.2307/281496.

Irto, A. et al. (2022). Lipids in Archaeological Pottery: A Review on Their Sampling and Extraction Techniques. *Molecules* , 27 (11). [Online]. Available at: doi:10.3390/molecules27113451.

Isern, N. et al. (2017). Modeling the role of voyaging in the coastal spread of the Early Neolithic in the West Mediterranean. *Proceedings of the National Academy of Sciences of the United States of America*, 114 (5), pp.897–902. [Online]. Available at: doi:10.1073/pnas.1613413114.

Jambrina-Enríquez, M. et al. (2019). n-Alkyl nitriles and compound-specific carbon isotope analysis of lipid combustion residues from Neanderthal and experimental hearths: Identifying sources of organic compounds and combustion temperatures. *Quaternary science reviews*, 222 (105899), p.105899. [Online]. Available at: doi:10.1016/j.quascirev.2019.105899.

Jansen, B. and Wiesenberg, G. L. B. (2017). Opportunities and limitations related to the application of plant-derived lipid molecular proxies in soil science. *SOIL*, 3 (4), pp.211–234. [Online]. Available at: doi:10.5194/soil-3-211-2017.

Jensen, K., Jensen, J. and Clegg, C. (1999). Inferring intensity of site use from the breakdown rate and discard patterns of fire-cracked rock at Playa View Dune. *Utah Archaeology*, 12, pp.51–64.

Jesus, A. et al. (2023). Morphometrics of waterlogged archaeological seeds give new insights into the domestication and spread of Papaver somniferum L. in Western Europe. *PloS one*, 18 (5), p.e0286190. [Online]. Available at: doi:10.1371/journal.pone.0286190.

Juan-Cabanilles, J. and Martí Oliver, B. (2017). New approaches to the neolithic transition: The last hunters and first farmers of the western Mediterranean. In: *Times of Neolithic Transition along the Western Mediterranean*. Cham: Springer International Publishing. pp.33–65. [Online]. Available at: doi:10.1007/978-3-319-52939-4_3.

Kaal, J. et al. (2014). How useful is pyrolysis-GC/MS for the assessment of molecular properties of organic matter in archaeological pottery matrix? An exploratory case study from north-west Spain. *Archaeometry*, 56 (S1), pp.187–207. [Online]. Available at: doi:10.1111/arcm.12057.

Kanthilatha, N. et al. (2014). Identification of preserved fatty acids in archaeological floor sediments from prehistoric sites at Ban Non Wat and Nong Hua Raet in northeast Thailand using gas chromatography. *Journal of archaeological science*, 46, pp.353–362. [Online]. Available at: doi:10.1016/j.jas.2014.03.033.

Kedrowski, B. L. et al. (2009). Gc/ms analysis of fatty acids from ancient hearth residues at the Swan Point archaeological site. *Archaeometry*, 51 (1), pp.110–122. [Online]. Available at: doi:10.1111/j.1475-4754.2008.00384.x.

Kelley, J. C. and Campbell, T. N. (1943). What Are the Burnt Rock Mounds of Texas? *American antiquity*, 7 (3), pp.319–322. [Online]. Available at: http://www.jstor.org/stable/275488.

Kipfer, B. A. (2023). *Archaeologist's Fieldwork Guide*. John Wiley & Sons. [Online]. Available at: https://www.perlego.com/book/3802482/archaeologists-fieldwork-guide.

Kohn, M. J. (2010). Carbon isotope compositions of terrestrial C3 plants as indicators of (paleo)ecology and (paleo)climate. *Proceedings of the National Academy of Sciences of the United States of America*, 107 (46), pp.19691–19695. [Online]. Available at: doi:10.1073/pnas.1004933107.

Kooyman, B. et al. (2001). Identification of Horse Exploitation by Clovis Hunters Based on Protein Analysis. *American antiquity*, 66 (4), pp.686–691. [Online]. Available at: doi:10.2307/2694181.

Kooyman, B., Newman, M. E. and Ceri, H. (1992). Verifying the Reliability of Blood Residue Analysis on Archaeological Tools. *Journal of archaeological science*, 19, pp.265–269.

Kooyman, B. P. (2000). *Understanding Stone Tools and Archaeological Sites*. UNM Press. [Online]. Available at: doi:10.2307/j.ctv6gqs13.

Kozubek, A., Pietr, S. and Czerwonka, A. (1996). Alkylresorcinols are abundant lipid components in different strains of Azotobacter chroococcum and Pseudomonas spp. *Journal of bacteriology*, 178 (14), pp.4027–4030. [Online]. Available at: doi:10.1128/jb.178.14.4027-4030.1996.

Kubiak-Martens, L. (2002). New evidence for the use of root foods in pre-agrarian subsistence recovered from the late Mesolithic site at Halsskov, Denmark. *Vegetation history and archaeobotany*, 11, pp.23–31. [Online]. Available at: doi:10.1007/s003340200003.

Kühn, J., Schweitzer, K. and Ruess, L. (2019). Diversity and specificity of lipid patterns in basal soil food web resources. *PloS one*, 14 (8), p.e0221102. [Online]. Available at: doi:10.1371/journal.pone.0221102.

Langley, A. et al. (2023). An experimental study of wet-cooking in organic vessels: implications for understanding the evolution of cooking technologies. *Archaeological and anthropological sciences*, 15 (9), p.142. [Online]. Available at: doi:10.1007/s12520-023-01843-z.

Langley, A. (2024). *Invisible technologies and the container revolution*. PhD thesis, University of York. [Online]. Available at: https://etheses.whiterose.ac.uk/id/eprint/36571/.

Lardeaux, J.-M. et al. (2022). From geomaterials to archaeological pastes: the example of 'granitic' pottery productions from Neolithic Castellar - Pendimoun (Alpes-Maritimes, France). In: Binder, D. and Manen, C. (Eds). *Céramiques imprimées de Méditerranée occidentale (VIe millénaire AEC) : données, approches et enjeux nouveaux / Western Mediterranean Impressed Wares (6th millennium BCE): New data, approaches and challenges. Actes de la séance de la Société préhistorique française de Nice (mars 2019)*. Paris: Société préhistorique française. pp.277–306.

Larson, G. et al. (2014). Current perspectives and the future of domestication studies. *Proceedings of the National Academy of Sciences of the United States of America*, 111 (17), pp.6139–6146. [Online]. Available at: doi:10.1073/pnas.1323964111.

Leach, J. D., Bousman, C. B. and Nickels, D. L. (2005). Assigning Context to Artifacts in Burned-Rock Middens. *Journal of Field Archaeology*, 30 (2), pp.201–203. [Online]. Available at: doi:10.1179/009346905791072332.

Leesch, D. et al. (2010). *Hearths and hearths-related activities in Magdalenian open-air sites: The case studies of Champréveyres and Monruz (Switzerland) and their relevance to an understanding of upper palaeolithic site structure*. In: Poltowicz-Bobak, M. and Bobak, D. (Eds). 2010. pp.53–69.

Leierer, L. et al. (2019). Insights into the timing, intensity and natural setting of Neanderthal occupation from the geoarchaeological study of combustion structures: A micromorphological and biomarker investigation of El Salt, unit Xb, Alcoy, Spain. *PloS one*, 14 (4), p.e0214955. [Online]. Available at: doi:10.1371/journal.pone.0214955.

Leroi-Gourhan, A. and Brézillon, M. (1972). Fouilles de Pincevent : essai d'analyse ethnographique d'un habitat magdalénien : (la section 36). *Gallia*, 7. [Online]. Available at: doi:10.1016/0047-2484(76)90061-0.

Leroi-Gourhan, A. and Brézillon, M. N. (1966). L'habitation magdalénienne n° 1 de Pincevent près Monterau (Seine-et-Marne). *Gallia préhistoire*, 9 (2), pp.263–385. [Online]. Available at: doi:10.3406/galip.1966.1264.

Lindgaard, E. (2015). Subsistence in central Norway elucidated through rock art excavation and documentation. In: Stebergløkken, H. et al. (Eds). *Subsistence in central Norway elucidated through rock art excavation and documentation*. Archaeopress. pp.99–110.

Linnenluecke, M. K., Marrone, M. and Singh, A. K. (2020). Conducting systematic literature reviews and bibliometric analyses. *Australian Journal of Management*, 45 (2), pp.175–194. [Online]. Available at: doi:10.1177/0312896219877678.

Little, A. (2014). Clonava Island revisited: a story of cooking, plants and re-occupation during the Irish Late Mesolithic. *Proceedings of the Royal Irish Academy: Archaeology, Culture, History, Literature*, 114C, pp.35–55. [Online]. Available at: doi:10.3318/priac.2014.114.09.

Longoni, M. et al. (2024). Organic residue analysis in archaeological pottery. Heating markers in non-cooking vessels from Etruscan Tarquinia (Italy): A sampling problem? *Journal of Archaeological Science: Reports*, 53, p.104365. [Online]. Available at: doi:10.1016/j.jasrep.2023.104365.

López-Bultó, O. et al. (2025). Dendrochronology and Bayesian radiocarbon modelling at the Early Neolithic site of la Draga (Banyoles, NE Spain). In: *Natural Science in Archaeology*. Cham: Springer Nature Switzerland. pp.187–204. [Online]. Available at: doi:10.1007/978-3-031-52780-7_11.

López-Bultó, O. and Piqué Huerta, R. (2018). Wood procurement at the early neolithic site of la draga (banyoles, Barcelona). *Journal of wetland archaeology*, 18 (1), pp.56–76. [Online]. Available at: doi:10.1080/14732971.2018.1466415.

Loy, T. H. (1983). Prehistoric blood residues: detection on tool surfaces and identification of species of origin. *Science*, 220 (4603), pp.1269–1271. [Online]. Available at: doi:10.1126/science.220.4603.1269.

Loy, T. H. and Dixon, E. J. (1998). Blood Residues on Fluted Points from Eastern Beringia. *American antiquity*, 63 (1), pp.21–46. [Online]. Available at: doi:10.2307/2694774 .

Loy, T. H. and Hardy, B. L. (1992). Blood residue analysis of 90,000-year-old stone tools from Tabun Cave, Israel. *Antiquity*, 66 (250), pp.24–35. [Online]. Available at: doi:10.1017/S0003598X00081011.

Loy, T. H. and Wood, A. R. (1989). Blood Residue Analysis at Çayönü Tepesi, Turkey. *Journal of Field Archaeology*, 16 (4), pp.451–460. [Online]. Available at: doi:10.1179/jfa.1989.16.4.451.

Lucejko, J. J. et al. (2018). Long-lasting ergot lipids as new biomarkers for assessing the presence of cereals and cereal products in archaeological vessels. *Scientific reports*, 8 (1), p.3935. [Online].

Available at: doi:10.1038/s41598-018-22140-z.

Lucquin, A. (2007). *Étude physico-chimique des méthodes de cuisson pré et protohistoriques*. Ph.D. Thesis, Université de Rennes 1.

Lucquin, A. et al. (2016). Utilising phytanic acid diastereomers for the characterisation of archaeological lipid residues in pottery samples. *Tetrahedron letters*, 57 (6), pp.703–707. [Online]. Available at: doi:10.1016/j.tetlet.2016.01.011.

Lucquin, A., Gibbs, K. and Uchiyama, J. (2016). Ancient lipids document continuity in the use of early hunter–gatherer pottery through 9,000 years of Japanese prehistory. *Proceedings of the*. [Online]. Available at: https://www.pnas.org/doi/abs/10.1073/pnas.1522908113.

Lundy, J. et al. (2023). Cuisine in transition? Organic residue analysis of domestic containers from 9th-14th century Sicily. *Royal Society open science*, 10 (3), p.221305. [Online]. Available at: doi:10.1098/rsos.221305.

Luong, S. et al. (2017). Development and application of a comprehensive analytical workflow for the quantification of non-volatile low molecular weight lipids on archaeological stone tools. *Analytical Methods*, 9 (30), pp.4349–4362. [Online]. Available at: doi:10.1039/C7AY01304C.

Luong, S. et al. (2018). Incorporating terpenes, monoterpenoids and alkanes into multiresidue organic biomarker analysis of archaeological stone artefacts from Liang Bua (Flores, Indonesia). *Journal of Archaeological Science: Reports*, 19, pp.189–199. [Online]. Available at: doi:10.1016/j.jasrep.2018.02.037.

Luong, S. et al. (2019). Combined organic biomarker and use-wear analyses of stone artefacts from Liang Bua, Flores, Indonesia. *Scientific reports*, 9 (1), p.17553. [Online]. Available at: doi:10.1038/s41598-019-53782-2.

Maggi, R. et al. (2023). Caverna delle Arene Candide. Scavi 1997-2012. Appunti sul Neolitico. *Rivista di Scienze Preistoriche LXXIII*, pp.419–466.

Malainey, M. E. (2011). *A Consumer's Guide to Archaeological Science*. Springer New York. [Online]. Available at: doi:10.1007/978-1-4419-5704-7.

Mallol, C. et al. (2025). Advancing archaeological sedimentary lipid biomarker analysis: A review of recent developments and methodological guidelines. *iScience*, 28 (3), p.112064. [Online]. Available at: doi:10.1016/j.isci.2025.112064.

Manen, C. et al. (2021). Territoriality and settlement in Southern France in the Early Neolithic: Diversity as a strategy? *Open Archaeology*, 7 (1), pp.923–938. [Online]. Available at: doi:10.1515/opar-2020-0179.

Manen, C. et al. (2022). Towards reinterpretation decorative Impressa styles implications establishing cultural affiliations beginning 6th millennium Western Mediterranean. In: Binder, D. and Manen, C. (Eds). *Céramiques imprimées de Méditerranée occidentale (VIe millénaire AEC) : données, approches et enjeux nouveaux / Western Mediterranean Impressed Wares (6th millennium BCE): New data, approaches and challenges. Actes de la séance de la Société préhistorique française de Nice (mars 2019)*. Paris: Société préishotique française. pp.147–175.

Manning, A. P. (1994). A Cautionary Note on the use of Hemastix and Dot-blot Assays for the Detection and Confirmation of Archaeological Blood Residues. *Journal of archaeological science*, 21 (2), pp.159–162. [Online]. Available at: doi:10.1006/jasc.1994.1018.

Manning, K. et al. (2013). The origins and spread of stock-keeping: the role of cultural and

environmental influences on early Neolithic animal exploitation in Europe. *Antiquity*, 87 (338), pp.1046–1059. [Online]. Available at: doi:10.1017/s0003598x00049851.

Marchbanks, M. L. and Quigg, J. M. (1990). Appendix G: Organic Residue and Phytolith Analysis. In: Boyd, D. K. et al. (Eds). *Phase II Investigations at Prehistoric and Rock Art Sites, Justiceburg Reservoir, Garza and Kent Counties, Texas, Volume II*. Reports of Inestigation No. 71. Prewitt and Associates. pp.496–519. [Online]. Available at: doi:10.21112/ita.1990.1.18.

March, R. J. (2013). Searching for the functions of fire structures in eynan (mallaha) and their formation processes: A geochemical approach. In: Bar-Yosef, O. and Valla, F. R. (Eds). *Natufian Foragers in the Levant. Terminal Pleistocene Social Changes in Western Asia*. 227–83. International Monographs in Prehistory. Ann Arbor, Michigan: Berghahn. pp.227–283. [Online]. Available at: doi:10.1515/9781789201574-020.

March, R. J. and Lucquin, A. (2006). About cooking and firing: Chemical analysis of fat residues from experimental and archaeological data. In: Iovino, M. R. (Ed). *Colloque The Signifiance of Experimentation for the Interpretation of the Archaeological Processes: Methods, Problems and Projects*. 2006.

Martí Oliver, B. (2002). La ceramica impressa della Penisola Iberica. In: Fugazzola Delpino, M. A., Pessina, A. and Tiné, V. (Eds). *Le ceramiche impresse nel Neolitico Antico. Italia e Mediterraneo*. Roma: Istituto poligrafico e Zecca dello Stato. pp.51–61.

Massicotte, P. and South, A. (2023). *rnaturalearth: World Map Data from Natural Earth. R package version 1.0.1*. [Online]. Available at: https://CRAN.R-project.org/package=rnaturalearth.

Matheson, C. D. and Veall, M.-A. (2014). Presumptive blood test using Hemastix® with EDTA in archaeology. *Journal of archaeological science*, 41, pp.230–241. [Online]. Available at: doi:10.1016/j.jas.2013.08.018.

Matheson, C., Hall, J. and Viel, R. (2009). Drawing first blood from Maya ceramics at Copán, Honduras. In: *Archaeological Science Under a Microscope: Studies in Residue and Ancient DNA Analysis in Honour of Thomas H. Loy*. ANU Press. [Online]. Available at: doi:10.22459/ta30.07.2009.14.

McClure, S. B. et al. (2018). Fatty acid specific δ13C values reveal earliest Mediterranean cheese production 7,200 years ago. *PloS one*, 13 (9), p.e0202807. [Online]. Available at: doi:10.1371/journal.pone.0202807.

Mercieca, A. (2000). Burnt and broken: An experimental study of heat fracturing in silcrete. *Australian Archaeology*, 51 (1), pp.40–47. [Online]. Available at: doi:10.1080/03122417.2000.11681679.

Mitchell, M. D. (2008). Making Places: Burned Rock Middens, Feasting, and Changing Land Use in the Upper Arkansas River Basin. In: *Archaeological Landscapes on The High Plains*. pp.41–70. [Online]. Available at: www.scopus.com/inward/record.uri?eid=2-s2.0-84895600574&partnerID=40&md5=83927cf927aee1d7dd4d118e636623ad.

Monforte-Barberán, A. et al. (2023). A multidisciplinary toolset to study a fifth millennium combustion structure from the northeastern coast of the Iberian Peninsula. *Journal of archaeological science, reports*, 47 (103760), p.103760. [Online]. Available at: doi:10.1016/j.jasrep.2022.103760.

Morrison, K. D. (2012). Great Transformations: On the Archaeology of Cooking. In: Graff, S. R. and Rodríguez-Alegría, E. (Eds). *The Menial Art of Cooking Archaeological Studies of Cooking and Food Preparation*. University Press of Colorado. pp.231–244.

Mottram, H. R. et al. (1999). New chromatographic, mass spectrometric and stable isotope approaches to the classification of degraded animal fats preserved in archaeological pottery. *Journal of chromatography. A*, 833 (2), pp.209–221. [Online]. Available at: doi:10.1016/s0021-9673(98)01041-3.

Moucawi, J. et al. (1981). Decomposition of lipids in soils: Free and esterified fatty acids, alcohols and ketones. *Soil biology & biochemistry*, 13 (6), pp.461–468. [Online]. Available at: doi:10.1016/0038-0717(81)90035-3.

Movius, H. L. (1966). The Hearths of the Upper Périgordian and Aurignacian Horizons at the Abri Pataud, Les Eyzies (Dordogne), and Their Possible Significance. *American anthropologist*, 68 (2), pp.296–325. [Online]. Available at: http://www.jstor.org/stable/670743.

Nakazawa, Y. et al. (2009). On stone-boiling technology in the Upper Paleolithic: behavioral implications from an Early Magdalenian hearth in El Mirón Cave, Cantabria, Spain. *Journal of archaeological science*, 36 (3), pp.684–693. [Online]. Available at: doi:10.1016/j.jas.2008.10.015.

Namdar, D., Stacey, R. J. and Simpson, S. J. (2009). First results on thermally induced porosity in chlorite cooking vessels from Merv (Turkmenistan) and implications for the formation and preservation of archaeological lipid residues. *Journal of archaeological science*, 36 (11), pp.2507–2516. [Online]. Available at: doi:10.1016/j.jas.2009.07.003.

Navarrete, V. et al. (2017). Feeding management strategies among the early neolithic pigs in the NE of the Iberian peninsula. *International journal of osteoarchaeology*, 27 (5), pp.839–852. [Online]. Available at: doi:10.1002/oa.2598.

Nelson, K. (2010). Environment, cooking strategies and containers. *Journal of Anthropological Archaeology*, 29 (2), pp.238–247. [Online]. Available at: doi:10.1016/j.jaa.2010.02.004.

Neubauer, F. (2018). Use-Alteration Analysis of Fire- Cracked Rocks. *American Antiquity*, 83 (4), pp.681–700. [Online]. Available at: doi:10.1017/aaq.2018.33.

Neubauer, F. (2024). *Fire-Cracked Rock Analysis*. Springer International Publishing. [Online]. Available at: doi:10.1007/978-3-031-64824-3.

Newman, M. E. et al. (1997). Blood'' From Stones? Probably: A Response to Fiedel. *Journal of archaeological science*, 24, pp.1023–1027. [Online]. Available at: doi:10.1006/jasc.1996.0180.

Newman, M. and Julig, P. (1989). The Identification of Protein Residues on Lithic Artifacts from a Stratified Boreal Forest Site. *Canadian Journal of Archaeology / Journal Canadien d'Archéologie*, 13, pp.119–132. [Online]. Available at: http://www.jstor.org/stable/41102826.

Nickels, D. L. et al. (2001). *Test Excavations at the Culebra Creek Site, 41BX126, Bexar County, Texas*. Index of Texas Archaeology: Open Access Gray Literature from the Lone Star State (Ed). 2001. [Online]. Available at: doi:10.21112/ita.2001.1.11 .

Nightingale, A. (2009). A guide to systematic literature reviews. *Surgery*, 27 (9), pp.381–384. [Online]. Available at: doi:10.1016/j.mpsur.2009.07.005.

O'Brien, M. J. and Bentley, R. A. (2015). The role of food storage in human niche construction: An example from Neolithic Europe. *Environmental archaeology*, 20 (4), pp.364–378.

Ó Drisceoil, D. A. (1988). Burnt mounds: cooking or bathing? *Antiquity*, 62, pp.671–680. [Online]. Available at: doi:10.1017/S0003598X00075062.

Oestmo, S. (2013). Digital imaging technology and experimental archeology: a methodological framework for the identification and interpretation of fire modified rock (FMR). *Journal of*

archaeological science, 40 (12), pp.4429–4443. [Online]. Available at: doi:10.1016/j.jas.2013.07.011.

Oetelaar, G. A. and Beaudoin, A. B. (2016). Evidence of cultural responses to the impact of the Mazama ash fall from deeply stratified archaeological sites in southern Alberta, Canada. *Quaternary international: the journal of the International Union for Quaternary Research*, 394, pp.17–36. [Online]. Available at: doi:10.1016/j.quaint.2014.08.015.

O'Kelly, M. J. (1954). Excavations and Experiments in Ancient Irish Cooking-Places. *Journal of the Royal Society of Antiquaries of Ireland. Royal Society of Antiquaries of Ireland*, 84 (2), pp.105–155. [Online]. Available at: http://www.jstor.org/stable/25509173.

Okkonen, J. (2010). Detecting social complexity among the Neolithic Hunter-Gatherers in Finland - example of Pattijoki Kastelli. In: Gheorghiu, D. (Ed). *Neolithic and Chalcolithic Archaeology in Eurasia: Building Techniques and Spatial Organisation*. BAR International Series. 2097. 2010. Int Union Prehistor Protohistor Sci. pp.85–87.

Okoli, C. (2015). A guide to conducting a standalone systematic literature review. *Communications of the Association for Information Systems*, 37. [Online]. Available at: doi:10.17705/1cais.03743.

Olive, M. and Taborin, Y. (1989). *Nature et fonction des foyers préhistoriques*. Association pour la promotion de la recherche archéologique en Île de France (Mémoires du Musée de préhistoire d'Ile de France, 2) (Ed).

Oms, F. X. et al. (2020). La (in)determinación del horizonte impressa en el NE de la península Ibérica. In: Pardo-Gordó, S. (Ed). *Contextualizando la cerámica impressa: Horizontes culturales en la península Ibérica.Bellaterra: UAB*. pp.101–112.

Oudemans, T. F. M. and Boon, J. J. (1991). Molecular archaeology: Analysis of charred (food) remains from prehistoric pottery by pyrolysis—gas chromatography/mass spectrometry. *Journal of analytical and applied pyrolysis*, 20, pp.197–227. [Online]. Available at: doi:10.1016/0165-2370(91)80073-h.

Pääkkönen, M., Evershed, R. P. and Asplund, H. (2020). Compound-specific stable carbon isotope values of fatty acids in modern aquatic and terrestrial animals from the Baltic Sea and Finland as an aid to interpretations of the origins of organic residues preserved in archaeological pottery. *Journal of Nordic Archaeological Science*, (19), pp.3–19. [Online]. Available at: https://www.archaeology.su.se/english/publications/publication- series/jonas/jonas-19.

Pagoulatos, P. (1992). The Re-Use of Thermally Altered Stone. *North American Archaeologist*, 13 (2), pp.115–129. [Online]. Available at: doi:10.2190/BUH5-3BVN-UP4K-J91G.

Pagoulatos, P. (2005). Experimental burned rock studies on the Edwards Plateau: A view from camp bullis, Texas. *North American archaeologist*, 26 (3), pp.289–329. [Online]. Available at: doi:10.2190/9j4u-1m73-1wt4-ad9n.

Palomo, A. et al. (2011). Harvesting cereals and other plants in Neolithic Iberia: the assemblage from the lake settlement at La Draga. *Antiquity*, 85 (329), pp.759–771. [Online]. Available at: doi:10.1017/s0003598x00068290.

Palomo, A. et al. (2013). Woodworking technology in the Early Neolithic site of La Draga (Banyoles, Spain). In: *Regards croisés sur les outils liés au travail des végétaux. An interdisciplinary focus on plant-working tools.* 2013. pp.383–396.

Palomo, A. et al. (2014). Prehistoric Occupation of Banyoles Lakeshore: Results of Recent Excavations at La Draga Site, Girona, Spain. *Journal of Wetland Archaeology*, 14, pp.58–73. [Online]. Available at: doi:10.1179/1473297114Z.00000000010.

Palomo, A., Piqué, R. and Terradas, X. (2018). *La Revolución neolítica : La Draga, el poblado de los prodigios*. Museo Arqueológico Regional de la Comunidad de Madrid.

Papakosta, V. et al. (2015). Extraction and derivatization of absorbed lipid residues from very small and very old samples of ceramic potsherds for molecular analysis by gas chromatography–mass spectrometry (GC–MS) and single compound stable carbon isotope analysis by gas chromatography–combustion–isotope ratio mass spectrometry (GC–C–IRMS). *Microchemical journal, devoted to the application of microtechniques in all branches of science*, 123, pp.196–200. [Online]. Available at: doi:10.1016/j.microc.2015.06.013.

Pardo-Gordó, S. et al. (2020). *Contextualizando la cerámica impressa: Horizontes culturales en la península Ibérica*. Bellaterra (Spain): Universitat Autònoma de Barcelona, Servei de Publicacions.

Pasqualini, A. et al. (2022). *WebPage : ArOLD : AROLDatabase (ARchaeological Organic residues Literature Database)*. [Online]. Available at: https://www.cepam.cnrs.fr/DATAS/Arold.php.

Pearson, J. A. et al. (2007). New light on early caprine herding strategies from isotope analysis: a case study from Neolithic Anatolia. *Journal of archaeological science*, 34 (12), pp.2170–2179. [Online]. Available at: doi:10.1016/j.jas.2007.09.001.

Pecci, A. et al. (2018). Combining residue analysis of floors and ceramics for the study of activity areas at the Garum Shop at Pompeii. *Archaeological and anthropological sciences*, 10 (2), pp.485–502. [Online]. Available at: doi:10.1007/s12520-017-0573-7.

Pedrazzani, C. et al. (2021). 5-n-alkylresorcinol profiles in different cultivars of einkorn, Emmer, spelt, common wheat, and tritordeum. *Journal of agricultural and food chemistry*, 69 (47), pp.14092–14102. [Online]. Available at: doi:10.1021/acs.jafc.1c05451.

Peña-Chocarro, L., Pérez-Jordà, G. and Morales, J. (2018). Crops of the first farming communities in the Iberian Peninsula. *Quaternary international: the journal of the International Union for Quaternary Research*, 470, pp.369–382. [Online]. Available at: doi:10.1016/j.quaint.2017.06.002.

Perrin, T. et al. (2018). Beyond the sea… The Neolithic transition in the southwest of France. *Quaternary international: the journal of the International Union for Quaternary Research*, 470, pp.318–332. [Online]. Available at: doi:10.1016/j.quaint.2017.05.027.

Perrin, T. and Manen, C. (2021). Potential interactions between Mesolithic hunter-gatherers and Neolithic farmers in the Western Mediterranean: The geochronological data revisited. *PloS one*, 16 (3), p.e0246964. [Online]. Available at: doi:10.1371/journal.pone.0246964.

Petersson, M. (2013). Hulje: Calendrical Rites Along a Small Stream. *Folklore: Electronic Journal of Folklore*, 55, pp.11–48. [Online]. Available at: doi:10.7592/FEJF2013.55.petersson.

Petraglia, M. et al. (1996). Immunological and Microwear Analysis of Chipped-Stone Artifacts from Piedmont Contexts. *American antiquity*, 61 (1), pp.127–135. [Online]. Available at: doi:10.2307/282307.

Petraglia, M. D. (2002). The heated and the broken: Thermally altered stone, human behavior, and archaeological site formation. *North American archaeologist*, 23 (3), pp.241–269. [Online]. Available at: doi:10.2190/4d7x-h9hr-1p4j-417l.

Pierce, C. D. (1988). A Functional Classification of Fire-Altered Rock Features from CA-SBr-5381. In: McGuire, K. and Hall, M. (Eds). *The Archaeology of Tiefort Basin, Fort Irwin, San Bernardino County, California*. Far Western Anthropological Research Group, Davis, Ca. pp.H1–H15. [Online]. Available at: https://www.researchgate.net/publication/275343792.

Pinhasi, R., Fort, J. and Ammerman, A. J. (2005). Tracing the origin and spread of agriculture in Europe. *PLoS biology*, 3 (12), p.e410. [Online]. Available at: doi:10.1371/journal.pbio.0030410.

Piqué, R. et al. (2015). Characterizing prehistoric archery: technical and functional analyses of the Neolithic bows from La Draga (NE Iberian Peninsula). *Journal of Archaeological Science*, 55, pp.166–173. [Online]. Available at: doi:10.1016/j.jas.2015.01.005.

Piqué, R. et al. (2021). Models of neolithisation of northeastern Iberian peninsula: New evidence of human occupations during the sixth millennium cal BC. *Open Archaeology*, 7 (1), pp.671–689. [Online]. Available at: doi:10.1515/opar-2020-0153.

Piqué, R. et al. (2023). *Informe dels treballs desenvolupats dins dels projectes quadriennals de recerca en matèria d'arqueologia i paleontologia de la Generalitat de Catalunya*.

Pollard, A. M. and Heron, C. (2016). *Archaeological Chemistry*. La Vergne, UNITED KINGDOM: Royal Society of Chemistry, The. [Online]. Available at: http://ebookcentral.proquest.com/lib/uab/detail.action?docID=1185179.

Pop, E. et al. (2021). Identifying Heated Rocks Through Feldspar Luminescence Analysis (pIRIR290) and a Critical Evaluation of Macroscopic Assessment. *Journal of Paleolithic Archaeology*, 4 (2), p.13. [Online]. Available at: doi:10.1007/s41982-021-00094-5.

Poveda, M. O. (2015). *Aprofitament i transformació de matèries primeres per a l'elaboració d'ornaments durant la prehistòria recent (5600-3400 cal. ane) al nord-est de la península Ibèrica*. Universitat Autònoma de Barcelona. [Online]. Available at: https://ddd.uab.cat/record/148961.

Prats, G., Antolín, F. and Alonso, N. (2020). Household storage, surplus and supra-household storage in prehistoric and protohistoric societies of the Western Mediterranean. *PloS one*, 15 (9), p.e0238237. [Online]. Available at: doi:10.1371/journal.pone.0238237.

Prévost, C. et al. (2023). The ARchaeological Organic residues Literature Database (AROLD): Construction of a tool for reviewing and querying published lipid data in organic residue analysis. *Archaeometry*. [Online]. Available at: doi:10.1111/arcm.12869.

Quigg, J. M. et al. (2000). *The Lino Site: A Stratified Late Archaic Campsite in a Terrace of the San Idelfonzo Creek, Webb County, Southern Texas*. Texas Department of Transportation. [Online]. Available at: doi:10.21112/ita.2000.1.11.

Quigg, J. M. et al. (2001). No Bones About It: Using Lipid Analysis of Burned Rock and Groundstone Residues to Examine Late Archaic Subsistence Practices in South Texas. *Plains anthropologist*, 46 (177), pp.283–303. [Online]. Available at: doi:10.1080/2052546.2001.11932035.

Rageot, M. et al. (2021). Management systems of adhesive materials throughout the Neolithic in the North-West Mediterranean. *Journal of archaeological science*, 126 (105309), p.105309. [Online]. Available at: doi:10.1016/j.jas.2020.105309.

Rapp, G., Balescu, S. and Lamothe, M. (1999). The Identification of Granitic Fire-Cracked Rocks Using Luminescence of Alkali Feldspars. *American antiquity*, 64 (1), pp.71–78. [Online]. Available at: doi:10.2307/2694346.

Raven, A. et al. (1997). Formation of long-chain ketones in archaeological pottery vessels by pyrolysis of acyl lipids. *Journal of Analytical and Applied Pyrolysis*, pp.267–285. [Online]. Available at: doi:10.1016/S0165-2370(97)00036-3.

Regert, M. et al. (1998). Free and bound fatty acid oxidation products in archaeological ceramic vessels. *Proceedings. Biological sciences*, 265 (1409), pp.2027–2032. [Online]. Available at:

doi:10.1098/rspb.1998.0536.

Regert, M. et al. (2001). Chemical alteration and use of beeswax through time: Accelerated ageing tests and analysis of archaeological samples from various environmental contexts. *Archaeometry*, 43 (4), pp.549–569. [Online]. Available at: doi:10.1111/1475-4754.00036.

Regert, M. (2011). Analytical strategies for discriminating archeological fatty substances from animal origin. *Mass spectrometry reviews*, 30 (2), pp.177–220. [Online]. Available at: doi:10.1002/mas.20271.

Renfrew, C. (2009). *Prehistory: The Making of the Human Mind*. New York, NY: Random House.

Rhodes, E. J. et al. (2009). Archaeological surfaces in western NSW: Stratigraphic contexts and preliminary OSL dating of hearths. In: Fairbairn, A., OConnos, S. and Marwixk, B. (Eds). *New Directions in Archaeological Science*. 2009. pp.189–200.

Ribechini, E. et al. (2008). Gas chromatographic and mass spectrometric investigations of organic residues from Roman glass unguentaria. *Journal of chromatography A*, 1183 (1-2), pp.158–169. [Online]. Available at: doi:10.1016/j.chroma.2007.12.090.

Richards, M. P. and Britton, K. (2020). *Archaeological Science: An Introduction*. Cambridge University Press. [Online]. Available at: doi:10.1017/9781139013826.

Richter, T. et al. (2011). Interaction before agriculture: Exchanging material and sharing knowledge in the final Pleistocene Levant. *Cambridge archaeological journal*, 21 (1), pp.95–114. [Online]. Available at: doi:10.1017/s0959774311000060.

Rivollat, M. et al. (2020). Ancient genome-wide DNA from France highlights the complexity of interactions between Mesolithic hunter-gatherers and Neolithic farmers. *Science advances*, 6 (22), p.eaaz5344. [Online]. Available at: doi:10.1126/sciadv.aaz5344.

Roffet-Salque, M. et al. (2015). Widespread exploitation of the honeybee by early Neolithic farmers. *Nature*, 527 (7577), pp.226–230. [Online]. Available at: doi:10.1038/nature15757.

Ropiot, V., Machado, C. and Pepe, C. (2015). Des fours à pierres chauffées du premier âge du Fer sur le site de Bastide Neuve III à Velaux (Bouches-du-Rhône). *Documents d'archéologie méridionale*, (38), pp.163–176. [Online]. Available at: doi:10.4000/dam.5913.

Rosiak, A., Kałużna-Czaplińska, J. and Gątarek, P. (2020). Analytical interpretation of organic residues from ceramics as a source of knowledge about our ancestors. *Critical reviews in analytical chemistry*, 50 (3), pp.189–195. [Online]. Available at: doi:10.1080/10408347.2019.1602821.

Ross, A. B. et al. (2003). Alkylresorcinols in cereals and cereal products. *Journal of agricultural and food chemistry*, 51 (14), pp.4111–4118. [Online]. Available at: doi:10.1021/jf0340456.

Ross, A. B. (2012). Present status and perspectives on the use of alkylresorcinols as biomarkers of wholegrain wheat and rye intake. *Journal of nutrition and metabolism*, 2012, p.462967. [Online]. Available at: doi:10.1155/2012/462967.

Rowan, Y. M. and Ebeling, J. R. (2016). *New approaches to old stones: Recent studies of ground stone artifacts*. London, England: Routledge.

Rowley-Conwy, P. et al. (2013). Early domestic animals in Italy, Istria, the Tyrrhenian Island and Southern France. In: Colledge, S. et al. (Eds). *The origins and spread of domestic animals in southwest Asia and Europe*. Walnut Creek, CA: Left Coast Press. pp.161–194.

Salazar-García, D. C. et al. (2018). 'To "seafood" or not to "seafood"?' An isotopic perspective on

dietary preferences at the Mesolithic-Neolithic transition in the Western Mediterranean. *Quaternary international: the journal of the International Union for Quaternary Research*, 470, pp.497–510. [Online]. Available at: doi:10.1016/j.quaint.2017.12.039.

Salazar-García, D. C. and García-Puchol, O. (2017). Current thoughts on the neolithisation process of the western Mediterranean. In: *Times of Neolithic Transition along the Western Mediterranean*. Cham: Springer International Publishing. pp.1–11. [Online]. Available at: doi:10.1007/978-3-319-52939-4_1.

Salque, M. et al. (2012). New insights into the Early Neolithic economy and management of animals in Southern and Central Europe revealed using lipid residue analyses of pottery vessels. *Anthropozoologica*, 47 (2), pp.45–62. [Online]. Available at: doi:10.5252/az2012n2a4.

Salque, M. et al. (2013). Earliest evidence for cheese making in the sixth millennium BC in northern Europe. *Nature*, 493 (7433), pp.522–525. [Online]. Available at: doi:10.1038/nature11698.

Saña, M. (2011). La gestó dels recursos animal. In: Bosch, A., Chinchilla, J. and Tarrús, J. (Eds). *El poblat lacustre del neolític antic de La Draga: Excavacions de 2000-2005.* Generalitat de Catalunya. pp.177–212.

Saña, M. (2013). Domestication of animals in the Iberian Peninsula. In: Colledge S, Conolly J, Dobney K, Manning K, Shennan S (Ed). *The origins and spread of domestic animals in southwest Asia and Europe*. Walnut Creek, CA: Left Coast Press. pp.195–220.

Saña, M. et al. (2020). Integrating domesticates: earliest farming experiences in the Iberian Peninsula. In: J.G. Kurt, L. Sorensen, and P. Rowley-Conwy (Ed). *Farmers at the Frontier. A Pan-European perspective on Neolithisation*. Oxbow Books. pp.161–176. [Online]. Available at: http://ebookcentral.proquest.com/lib/uab/detail.action?docID=6383468.

Sanjurjo-Sánchez, J., Kaal, J. and Fenollós, J. L. M. (2018). Organic matter from bevelled rim bowls of the Middle Euphrates: Results from molecular characterization using pyrolysis-GC–MS. *Microchemical journal, devoted to the application of microtechniques in all branches of science*, 141, pp.1–6. [Online]. Available at: doi:10.1016/j.microc.2018.05.001.

Schaefer-Di Maida, S. (2022). Current Research on Bronze Age 'Cooking Stone Pits' in Northern Germany and Southern Scandinavia. *European Journal of Archaeology*, 25 (4), pp.463–482. [Online]. Available at: doi:10.1017/eaa.2022.19.

Schaefer, J. et al. (2014). Identifying, Dating, and Explaining Fire-Affected Rock Features in the Western Colorado Desert, Alta California. *California Archaeology*, 6 (1), pp.65–94. [Online]. Available at: doi:10.1179/1947461X14Z.00000000026.

Scherer, S. et al. (2025). A method for the simultaneous extraction, concentration, and quantitation of miliacin and 5-n-alkylresorcinols from soils and sediments. *Journal of chromatography A*, 1758 (466200), p.466200. [Online]. Available at: doi:10.1016/j.chroma.2025.466200.

Scott, J. C. (2017). *Against the grain: A deep history of the earliest states*, Yale agrarian studies. New Haven, CT: Yale University Press. [Online]. Available at: doi:10.2307/j.ctv1bvnfk9.

Seeman, M. F. et al. (2008). Evaluating protein residues on Gainey phase Paleoindian stone tools. *Journal of archaeological science*, 35 (10), pp.2742–2750. [Online]. Available at: doi:10.1016/j.jas.2008.05.001.

Shanks, O. C., Kornfeld, M. and Hawk, D. D. (1999). Protein Analysis of Bugas-Holding Tools: New Trends in Immunological Studies. *Journal of archaeological science*, 26 (9), pp.1183–1191. [Online]. Available at: doi:10.1006/jasc.1998.0353.

Shantry, K. (2020). The selection of boiling stones from a heterogeneous supply. *Journal of Archaeological Science: Reports*, 29, p.102030. [Online]. Available at: doi:10.1016/j.jasrep.2019.102030.

Shea, J. J. (2007). Lithic Archaeology, or, What Stone Tools Can (and Can't) Tell Us about Early Hominin Diets. In: Ungar, P. S. (Ed). *Evolution of the human diet: The Known, the Unknown, and the Unknowable*. Oxford University Press. pp.212–232.

Shennan, S. et al. (2017). Supply and demand in prehistory? Economics of neolithic mining in NW Europe (NEOMINE). *Archaeology international*, 20 (1), pp.74–79. [Online]. Available at: doi:10.5334/ai-358.

Shennan, S. (2018). *The First Farmers of Europe: An Evolutionary Perspective*, Cambridge World Archaeology. Cambridge University Press.

Sherratt, A. (1983). The Secondary Exploitation of Animals in the Old World. *World Archaeology*, 15 (1), pp.90–104. [Online]. Available at: http://www.jstor.org/stable/124640.

Shiner, J. L. and Shiner, M. V. (1977). Structure and Organization of a Burned rock midden: the Indian Creek site, Real Conty, Texas. *Plains anthropologist*, 22 (78), pp.263–282. [Online]. Available at: http://www.jstor.org/stable/25667405.

Shoda, S. et al. (2020). Late Glacial hunter-gatherer pottery in the Russian Far East: Indications of diversity in origins and use. *Quaternary science reviews*, 229 (106124), p.106124. [Online]. Available at: doi:10.1016/j.quascirev.2019.106124.

Short, L. et al. (2015). Facile residue analysis of recent and prehistoric cook stones using handheld Raman spectrometry. *Journal of Raman spectroscopy: JRS*, 46 (1), pp.126–132. [Online]. Available at: doi:10.1002/jrs.4593.

Sistiaga, A. et al. (2014). The Neanderthal meal: a new perspective using faecal biomarkers. *PloS one*, 9 (6), p.e101045. [Online]. Available at: doi:10.1371/journal.pone.0101045.

Skibo, J., Malainey, M. E. and Drake, E. C. (2009). Stone Boiling, Fire-Cracked Rock, and Nut Oil: Exploring the Origins of Pottery Making on Grand Island. *The Winsconsis Archeologist*, 10 (1&2), pp.47–64. [Online]. Available at: https://www.researchgate.net/publication/280558226_Stone_boiling_fire-cracked_rock_and_nut_oil_Exploring_the_origins_of_pottery_making_on_Grand_Island.

Smith, M. B. (2020). *Biochemistry : An Organic Chemistry Approach*. Milton, UNITED KINGDOM: Taylor & Francis Group. [Online]. Available at: http://ebookcentral.proquest.com/lib/uab/detail.action?docID=6184727.

Solazzo, C. et al. (2008). Identification of protein remains in archaeological potsherds by proteomics. *Analytical chemistry*, 80 (12), pp.4590–4597. [Online]. Available at: doi:10.1021/ac800515v.

Sorensen, A. C. and Scherjon, F. (2018). fiReproxies: A computational model providing insight into heat-affected archaeological lithic assemblages. *PloS one*, 13 (5), p.e0196777. [Online]. Available at: doi:10.1371/journal.pone.0196777.

Spangenberg, J. E. et al. (2010). Microstructural, chemical and isotopic evidence for the origin of late neolithic leather recovered from an ice field in the Swiss Alps. *Journal of archaeological science*, 37 (8), pp.1851–1865. [Online]. Available at: doi:10.1016/j.jas.2010.02.003.

Spangenberg, J. E., Jacomet, S. and Schibler, J. (2006). Chemical analyses of organic residues in archaeological pottery from Arbon Bleiche 3, Switzerland – evidence for dairying in the late

Neolithic. *Journal of archaeological science*, 33 (1), pp.1–13. [Online]. Available at: doi:10.1016/j.jas.2005.05.013.

Spangenberg, J. E. and Ogrinc, N. (2001). Authentication of vegetable oils by bulk and molecular carbon isotope analyses with emphasis on olive oil and pumpkin seed oil. *Journal of agricultural and food chemistry*, 49 (3), pp.1534–1540. [Online]. Available at: doi:10.1021/jf001291y.

Sparkman, O. (2011). *Gas Chromatography Mass Spectrometry: Practical Guide*. Elsevier Science & Technology. [Online]. Available at: https://ebookcentral.proquest.com/lib/uab/detail.action?docID=670206.

Speth, J. D. (2015). When Did Humans Learn to Boil? *PaleoAnthropology*, pp.54–67. [Online]. Available at: doi:10.4207/PA.2015.ART96.

Spiteri, C., Muntoni, I. M. and Craig, O. E. (2017). Dietary practices at the onset of the neolithic in the western Mediterranean revealed using a combined biomarker and isotopic approach. In: *Times of Neolithic Transition along the Western Mediterranean*. Cham: Springer International Publishing. pp.253–279. [Online]. Available at: doi:10.1007/978-3-319-52939-4_10.

Stauffer, E., Dolan, J. A. and Newman, R. (2008). Gas Chromatography and Gas Chromatography—Mass Spectrometry. In: Stauffer, E., Dolan, J. A. and Newman, R. (Eds). *Fire Debris Analysis*. Burlington: Academic Press. pp.235–293. [Online]. Available at: doi:10.1016/B978-012663971-1.50012-9.

Stock, J. T. and Pinhasi, R. (2011). Introduction: Changing paradigms in our understanding of the transition to agriculture: Human bioarchaeology, behaviour and adaptaion. In: *Human Bioarchaeology of the Transition to Agriculture*. Chichester, UK: John Wiley & Sons, Ltd. pp.1–13. [Online]. Available at: doi:10.1002/9780470670170.ch1.

Stuart, G. S. L. and Walker, E. G. (2018). Pollen and charcoal studies at the Wolf Willow site, Wanuskewin Heritage Park, Saskatoon, Canada. *Vegetation history and archaeobotany*, 27 (3), pp.507–525. [Online]. Available at: doi:10.1007/s00334-017-0639-6.

Sullivan, A. P. et al. (2001). Economic and Land-Use Implications of Prehistoric Fire-Cracked-Rock Piles, Northern Arizona. *Journal of Field Archaeology*, 28 (3-4), pp.367–382. [Online]. Available at: doi:10.1179/jfa.2001.28.3-4.367.

Sutton, M. (2015). *Prehistory of North America*. Routledge. [Online]. Available at: https://play.google.com/store/books/details?id=C1RACwAAQBAJ.

Swedberg, S., Östlund, A. and Jacobsson, O. (2017). Tanum 1821—Examining cooking pits in landscape studies. In: Wessman, A. and Bergerbrant, S. (Eds). *New Perspectives on the Bronze Age: Proceedings of the 13th Nordic Bronze Age Symposium held in Gothenburg 9th to 13th June 2015*. 2017. Archaeopress. pp.219–231. [Online]. Available at: https://www.torrossa.com/gs/resourceProxy?an=4923794&publisher=FZR707#page=229.

Tarifa-Mateo, N. et al. (2019). New insights from Neolithic pottery analyses reveal subsistence practices and pottery use in early farmers from Cueva de El Toro (Málaga, Spain). *Archaeological and anthropological sciences*, 11 (10), pp.5199–5211. [Online]. Available at: doi:10.1007/s12520-019-00874-9.

Tarifa Mateo, N. (2019). *Pottery use on the Mediterranean coast of the Iberian Peninsula*. Saña, M. and Rosell, A. (Eds). Ph.D. Thesis, Universitat Autònoma de Barcelona (UAB).

Tarifa-Mateo, N. et al. (2021). Pottery use in the mining site of variscite Mines de Gavà (Barcelona, Spain) during the 4th millennium BC based on organic residue analysis. *Journal of archaeological*

science, reports, 38 (103080), p.103080. [Online]. Available at: doi:10.1016/j.jasrep.2021.103080.

Tarifa-Mateo, N. et al. (2023). Investigating livestock management in the early Neolithic archaeological site of Cabecicos Negros (Almería, Spain) from the organic residue analysis in pottery. *Scientific reports*, 13 (1), p.4797. [Online]. Available at: doi:10.1038/s41598-023-31036-6.

Tarifa-Mateo, N. et al. (2024). Milk production in pottery. Evidence for various exploited resources used by the first farmers in Central Pyrenees using the morphological, chemical and stable carbon isotopic composition of organic residues from ceramic vessels. *Archaeological and anthropological sciences*, 16 (7). [Online]. Available at: doi:10.1007/s12520-024-02001-9.

Tarrús, J. (2008). La Draga (Banyoles, Catalonia), an Early Neolithic Lakeside Village in Mediterranean Europe. *Catalan historical review*, pp.17–33. [Online]. Available at: doi:10.2436/20.1000.01.2.

Terradas, X. et al. (2012). *Áreas de aprovisionamiento, territorios de subsistencia y producciones técnicas en el Neolítico antiguo de La Draga*. In: Borrell, M. et al. (Eds). 2012. pp.441–448.

Terradas, X. et al. (2017). Farming Practices in the Early Neolithic According to Agricultural Tools: Evidence from La Draga Site (Northeastern Iberia). In: García-Puchol, O. and Salazar-García, D. (Eds). *Times of Neolithic Transition along the Western Mediterranean. Fundamental Issues in Archaeology*. Springer, Cham. [Online]. Available at: doi:10.1007/978-3-319-52939-4_8.

Terradas, X., Palomo, A. and Piqué, R. (2020). El poblado neolítico de La Draga (Banyoles, Girona). Resultados de las excavaciones recientes y nuevos retos de investigación. In: *Actualidad de la investigación arqueológica en España I (2018-2019)*. 2020. pp.251–169.

Thoms, A. V. (2007). Fire-cracked rock features on sandy landforms in the Northern Rocky Mountains: Toward establishing reliable frames of reference for assessing site integrity. *Geoarchaeology*, 22 (5), pp.477–510. [Online]. Available at: doi:10.1002/gea.20169.

Thoms, A. V. (2008a). Ancient Savannah Roots of the Carbohydrate Revolution in South-Central North America. *Plains anthropologist*, 53 (205), pp.121–136. [Online]. Available at: doi:10.1179/pan.2008.008.

Thoms, A. V. (2008b). The fire stones carry: Ethnographic records and archaeological expectations for hot-rock cookery in western North America. *Journal of Anthropological Archaeology*, 27 (4), pp.443–460. [Online]. Available at: doi:10.1016/j.jaa.2008.07.002.

Thoms, A. V. (2009). Rocks of ages: propagation of hot-rock cookery in western North America. *Journal of archaeological science*, 36 (3), pp.573–591. [Online]. Available at: doi:10.1016/j.jas.2008.11.016.

Thoms, A. V. et al. (2015). Baking Geophytes and Tracking Microfossils: Taphonomic Implications for Earth-Oven and Paleodietary Research. *Journal of Archaeological Method and Theory*, 22 (4), pp.1038–1070. [Online]. Available at: doi:10.1007/s10816-014-9216-9.

Tomé, L. et al. (2022). Fuel sources, natural vegetation and subsistence at a high-altitude aboriginal settlement in Tenerife, Canary Islands: Microcontextual geoarchaeological data from Roques de García Rockshelter. *Archaeological and anthropological sciences*, 14 (10). [Online]. Available at: doi:10.1007/s12520-022-01661-9.

Tresset, A. and Vigne, J.-D. (2007). Substitution of species, techniques and symbols at the Mesolithic-Neolithic transition in Western Europe. In: *Going Over: The Mesolithic-Neolithic Transition in North-West Europe*. British Academy. pp.188–210. [Online]. Available at: doi:10.5871/bacad/9780197264140.003.0010.

Twiss, K. (2012). The Archaeology of Food and Social Diversity. *Journal of Archaeological Research*, 20 (4), pp.357–395. [Online]. Available at: doi:10.1007/s10814-012-9058-5.

Van Klinken, G. J., van der Plicht, H. and Hedges, R. E. M. (1994). Bond$^{13}C/^{12}C$ ratios reflect (palaeo-)climatic variations. *Geophysical research letters*, 21 (6), pp.445–448. [Online]. Available at: doi:10.1029/94gl00177.

Vaquer, J. et al. (1986). Mesolithic plant exploitation at the Balma Abeurador (France). *Oxford journal of archaeology*, 5 (1), pp.1–18. [Online]. Available at: doi:10.1111/j.1468-0092.1986.tb00127.x.

de Vareilles, A. et al. (2020). One sea but many routes to Sail. The early maritime dispersal of Neolithic crops from the Aegean to the western Mediterranean. *Journal of archaeological science, reports*, 29 (102140), p.102140. [Online]. Available at: doi:10.1016/j.jasrep.2019.102140.

Vázquez, C. et al. (2008). Combining TXRF, FT-IR and GC-MS information for identification of inorganic and organic components in black pigments of rock art from Alero Hornillos 2 (Jujuy, Argentina). *Analytical and bioanalytical chemistry*, 391 (4), pp.1381–1387. [Online]. Available at: doi:10.1007/s00216-008-2038-4.

Verdún-Castelló, E. et al. (2019). The consumption of molluscs in the first farming societies: the Neolithic settlement of La Draga (northeast of the Iberian Peninsula). *Archaeological and anthropological sciences*, 11 (1), pp.69–86. [Online]. Available at: doi:10.1007/s12520-017-0532-3.

Viberg, A., Berntsson, A. and Lidén, K. (2013). Archaeological prospection of a high altitude Neolithic site in the Arctic mountain tundra region of northern Sweden. *Journal of archaeological science*, 40 (6), pp.2579–2588. [Online]. Available at: doi:10.1016/j.jas.2013.02.004.

Vierra, B. J. and Carvalho, A. F. (2019). The Mesolithic–Neolithic transition: The view from Southwest Europe and the American Southwest. *Quaternary international: the journal of the International Union for Quaternary Research*, 515, pp.208–224. [Online]. Available at: doi:10.1016/j.quaint.2017.09.018.

Vigne, J.-D. (2008). Zooarchaeological aspects of the neolithic diet transition in the near east and Europe, and their putative relationships with the neolithic demographic transition. In: *The Neolithic Demographic Transition and its Consequences*. Dordrecht: Springer Netherlands. pp.179–205. [Online]. Available at: doi:10.1007/978-1-4020-8539-0_8.

Vigne, J.-D. and Helmer, D. (2007). Was milk a "secondary product in the Old World Neolithisation process Its role in the domestication of cattle sheep and goats. *Anthropozoologica*, 42 (2), pp.9–40.

Wells, J. C. K. and Stock, J. T. (2007). The biology of the colonizing ape. *American journal of physical anthropology*, Suppl 45 (S45), pp.191–222. [Online]. Available at: doi:10.1002/ajpa.20735.

Wen-Yen, H. and Meinschein, W. G. (1976). Sterols as source indicators of organic materials in sediments. *Geochimica et cosmochimica acta*, 40 (3), pp.323–330. [Online]. Available at: doi:10.1016/0016-7037(76)90210-6.

Whelton, H. L. et al. (2021). A call for caution in the analysis of lipids and other small biomolecules from archaeological contexts. *Journal of archaeological science*, 132, p.105397. [Online]. Available at: doi:10.1016/j.jas.2021.105397.

Williamson, B. S. (2000). Direct Testing of Rock Painting Pigments for Traces of Haemoglobin at Rose Cottage Cave, South Africa. *Journal of archaeological science*, 27 (9), pp.755–762. [Online]. Available at: doi:10.1006/jasc.1999.0489.

Wilson, D. C. and DeLyria, D. V. (1999). The Experimental Reduction of Rock in a Camas Oven: Towards an Understanding of the Behavioral Significance of Fire-cracked Rock. *Archaeology in Washington*, VII, pp.81–89.

Wohlin, C. et al. (2022). Successful combination of database search and snowballing for identification of primary studies in systematic literature studies. *Information and Software Technology*, 147, p.106908. [Online]. Available at: doi:10.1016/j.infsof.2022.106908.

Wollstonecroft, M. M. (2011). Investigating the role of food processing in human evolution: a niche construction approach. *Archaeological and anthropological sciences*, 3 (1), pp.141–150. [Online]. Available at: doi:10.1007/s12520-011-0062-3.

Xiao, Y. and Watson, M. (2019). Guidance on Conducting a Systematic Literature Review. *Journal of Planning Education and Research*, 39 (1), pp.93–112. [Online]. Available at: doi:10.1177/0739456X17723971.

Yohe, R. M. and Bamforth, D. B. (2013). Late Pleistocene protein residues from the Mahaffy cache, Colorado. *Journal of archaeological science*, 40 (5), pp.2337–2343. [Online]. Available at: doi:10.1016/j.jas.2013.01.015.

Yohe, R. M., II, Newman, M. E. and Schneider, J. S. (1991). Immunological identification of small-mammal proteins on aboriginal milling equipment. *American antiquity*, 56 (4), pp.659–666. [Online]. Available at: doi:10.2307/281543.

Zabolotneva, A. A. et al. (2022). An overview of alkylresorcinols biological properties and effects. *Journal of nutrition and metabolism*, 2022, p.4667607. [Online]. Available at: doi:10.1155/2022/4667607.

Zapata, L. et al. (2004). Early neolithic agriculture in the Iberian peninsula. *Journal of world prehistory*, 18 (4), pp.283–325. [Online]. Available at: doi:10.1007/s10963-004-5621-4.

Zeder, M. A. (2008). Domestication and early agriculture in the Mediterranean Basin: Origins, diffusion, and impact. *Proceedings of the National Academy of Sciences of the United States of America*, 105 (33), pp.11597–11604. [Online]. Available at: doi:10.1073/pnas.0801317105.

Zilhão, J. (1993). The spread of Agro-pastoral economies across Mediterranean Europe: A view from the Far West. *Journal of Mediterranean archaeology*, 6 (1), pp.5–63. [Online]. Available at: doi:10.1558/jmea.v6i1.5.

Zilhão, J. (2001). Radiocarbon evidence for maritime pioneer colonization at the origins of farming in west Mediterranean Europe. *Proceedings of the National Academy of Sciences of the United States of America*, 98 (24), pp.14180–14185. [Online]. Available at: doi:10.1073/pnas.241522898.

Zvelebil, M. (1994). Plant Use in the Mesolithic and its Role in the Transition to Farming. *Proceedings of the Prehistoric Society*, 60, pp.35–74. [Online]. Available at: doi:10.1017/S0079497X00003388.

Zvelebil, M. (2001). The agricultural transition and the origins of Neolithic society in Europe. *Documenta Praehistorica*, 28, pp.1–26. [Online]. Available at: doi:10.4312/dp.28.1.

Annex 1

List of modern reference samples used to evaluate regional variation in $\delta^{13}C$ values. The table includes isotopic data for various resource categories drawn from published literature.

C3 plant

Common name	Taxa	Provenience	Biogeographical region	$\Delta^{13}C$ (‰)	$\delta^{13}C_{16:0}$ (‰)	$\delta^{13}C_{18:0}$ (‰)	Reference
Olive oil	*Olea europaea*	Slovenia	Continental	1.1	-33.0	-31.9	(Spangenberg and Ogrinc, 2001)
Olive oil	*Olea europaea*	Slovenia	Continental	0.1	-29.9	-29.8	(Spangenberg and Ogrinc, 2001)
Olive oil	*Olea europaea*	Slovenia	Continental	-0.1	-30.7	-30.8	(Spangenberg and Ogrinc, 2001)
Olive oil	*Olea europaea*	Slovenia	Continental	0.6	-31.4	-30.8	(Spangenberg and Ogrinc, 2001)
Olive oil	*Olea europaea*	Slovenia	Continental	-0.4	-31.0	-31.4	(Spangenberg and Ogrinc, 2001)
Olive oil	*Olea europaea*	Croatia	Mediterranean	0.5	-31.5	-31.0	(Spangenberg and Ogrinc, 2001)
Olive oil	*Olea europaea*	Croatia	Mediterranean	-0.2	-30.4	-30.6	(Spangenberg and Ogrinc, 2001)
Olive oil	*Olea europaea*	Croatia	Mediterranean	-0.9	-29.1	-30.0	(Spangenberg and Ogrinc, 2001)
Olive oil	*Olea europaea*	Croatia	Mediterranean	0.7	-32.0	-31.3	(Spangenberg and Ogrinc, 2001)
Olive oil	*Olea europaea*	Croatia	Mediterranean	1.3	-31.0	-29.7	(Spangenberg and Ogrinc, 2001)
Pumpkin seed oil	*Cucurbita pepo*	Slovenia	Continental	-1.5	-29.7	-31.2	(Spangenberg and Ogrinc, 2001)

Common name	Taxa	Provenience	Biogeographical region	$\Delta^{13}C$ (‰)	$\delta^{13}C_{16:0}$ (‰)	$\delta^{13}C_{18:0}$ (‰)	Reference
Pumpkin seed oil	*Cucurbita pepo*	Slovenia	Continental	2.4	-29.7	-27.3	(Spangenberg and Ogrinc, 2001)
Sunflower oil		Slovenia	Continental	0.8	-32.0	-31.2	(Spangenberg and Ogrinc, 2001)
Sunflower oil		Slovenia	Continental	1.2	-30.8	-29.6	(Spangenberg and Ogrinc, 2001)
Soybean oil		Slovenia	Continental	-0.1	-32.4	-32.5	(Spangenberg and Ogrinc, 2001)
Sesame oil		Slovenia	Continental	0.2	-28.1	-27.9	(Spangenberg and Ogrinc, 2001)
Bulrush	*Typha*	Russia (SE)	Steppic	-1.3	-31.8	-33.1	(Bondetti et al., 2021b)
Wild thyme	*Thymus*	Russia (SE)	Steppic	3.7	-38.5	-34.8	(Bondetti et al., 2021b)
Silverberry	*Elaeagnus*	Russia (SE)	Steppic	0.0	-31.9	-31.9	(Bondetti et al., 2021b)
Wild rose berry	*Rosa*	Russia (SE)	Steppic	-0.7	-29.0	-29.7	(Bondetti et al., 2021b)
Dog rose berry	*Rosa canina*	Russia (SE)	Steppic	-0.6	-32.1	-32.7	(Bondetti et al., 2021b)
Wild pear	*Pyrus*	Russia (SE)	Steppic	1.2	-33.5	-32.3	(Bondetti et al., 2021b)
Wild apple	*Malus*	Russia (SE)	Steppic	2.6	-32.7	-30.1	(Bondetti et al., 2021b)
Wheat		Italy	Mediterranean	-1.4	-29.6	-31	(Drieu et al., 2021)
Barley		Italy	Mediterranean	-0.6	-30.6	-31.2	(Drieu et al., 2021)
Einkorn		France	Mediterranean	-1.5	-31.4	-32.9	(Drieu et al., 2021)
Einkorn		France	Mediterranean	-1.0	-32	-33	(Drieu et al., 2021)

Common name	Taxa	Provenience	Biogeographical region	$\Delta^{13}C$ (‰)	$\delta^{13}C_{16:0}$ (‰)	$\delta^{13}C_{18:0}$ (‰)	Reference
Einkorn		France	Mediterranean	-1.7	-32.2	-33.9	(Drieu et al., 2021)
Barley		France	Mediterranean	0.8	-36.4	-35.6	(Drieu et al., 2021)
Cabbage	*Brassica oleracea capitata*	France	Mediterranean	2.0	-27.1	-25.2	(March, 2013)
Kohlrabi	*Brassica oleracea var. gongylodes*	France	Mediterranean	0.8	-28.6	-27.7	(March, 2013)
Spinach	*Spinacia oleracea*	France	Mediterranean	5.2	-33.2	-28.0	(March, 2013)
Flax	*Linum usitatissimum*	France	Mediterranean	0.2	-30.2	-30.0	(March, 2013)
Manioc	*Manihot esculenta*	France	Mediterranean	1.7	-37.6	-35.9	(March, 2013)
Hazelnut	*Corylus avellana*	France	Mediterranean	-2.1	-29.3	-31.4	(March, 2013)
Hazelnut	*Corylus avellana*	France	Mediterranean	-0.8	-29.9	-30.7	(March, 2013)
Nettle	*Urtica sp.*	France	Mediterranean	0.9	-34.5	-33.6	(March, 2013)
Parsnip	*Pastinaca sativa*	France	Mediterranean	2.6	-38.0	-35.4	(March, 2013)
Oat	*Avena sativa*	France	Mediterranean	0.5	-34.2	-33.7	(March, 2013)
Oat	*Avena sativa*	France	Mediterranean	-0.2	-33.7	-33.9	(March, 2013)
Wheat	*Triticum sp.*	France	Mediterranean	-1.1	-33.0	-34.1	(March, 2013)
Wild carrot	*Daucus carotta*	France	Mediterranean	1.8	-32.8	-31.0	(March, 2013)

C3 wood

Common name	Taxa	Provenience	Biogeographical region	$\Delta^{13}C$ (‰)	$\delta^{13}C_{16:0}$ (‰)	$\delta^{13}C_{18:0}$ (‰)	Reference
Celtis tree	*Celtis australis L.*	Spain	Mediterranean	0.4	-32.2	-31.8	(Jambrina-Enríquez et al., 2019)
Celtis tree	*Celtis australis L.*	Spain	Mediterranean	2.9	-31.8	-28.8	(Jambrina-Enríquez et al., 2019)
Celtis tree	*Celtis australis L.*	Spain	Mediterranean	6.0	-33.1	-27.1	(Jambrina-Enríquez et al., 2019)
Celtis tree	*Celtis australis L.*	Spain	Mediterranean	1.4	-34.4	-33.0	(Jambrina-Enríquez et al., 2019)
Celtis tree	*Celtis australis L.*	Spain	Mediterranean	5.1	-32.1	-27.0	(Jambrina-Enríquez et al., 2019)

Dairy ruminant

Common name		Provenience	Biogeographical region	$\Delta^{13}C$ (‰)	$\delta^{13}C_{16:0}$ (‰)	$\delta^{13}C_{18:0}$ (‰)	Reference
Cow milk		Malta	Mediterranean	-2.4	-24.2	-26.6	(Debono-Spiteri, 2012)
Cow milk		Malta	Mediterranean	-3.2	-23.6	-26.8	(Debono-Spiteri, 2012)
Sheep milk		Malta	Mediterranean	-4.6	-24.7	-29.3	(Debono-Spiteri, 2012)
Sheep milk		Malta	Mediterranean	-4.3	-24.5	-28.8	(Debono-Spiteri, 2012)
Goat milk		Malta	Mediterranean	-3.2	-25.2	-28.4	(Debono-Spiteri, 2012)
Goat milk		Malta	Mediterranean	-3.0	-23.7	-26.7	(Debono-Spiteri, 2012)
Goat milk		France	Mediterranean	-5.1	-26.8	-31.9	(Drieu et al., 2021)

Common name		Provenience	Biogeographical region	$\Delta^{13}C$ (‰)	$\delta^{13}C_{16:0}$ (‰)	$\delta^{13}C_{18:0}$ (‰)	Reference
Cattle milk	*Bos taurus*	Spain	Mediterranean	-6.0	-28.0	-34.0	(Tarifa Mateo, 2019)
Goat milk	*Capra hircus*	Spain	Mediterranean	-3.9	-24.4	-28.3	(Tarifa Mateo, 2019)
Cattle milk	*Bos taurus*	Spain	Mediterranean	-3.8	-26.6	-30.4	(Tarifa Mateo, 2019)
Goat cheese	*Capra hircus*	Spain	Mediterranean	-2.0	-27.0	-29.0	(Tarifa Mateo, 2019)
Goat cheese	*Capra hircus*	Spain	Mediterranean	-2.3	-23.0	-25.3	(Tarifa Mateo, 2019)
Cattle cheese	*Bos taurus*	Spain	Mediterranean	-2.5	-25.2	-27.7	(Tarifa Mateo, 2019)
Sheep cheese	*Ovis aries*	Spain	Mediterranean	-2.7	-26.6	-29.3	(Tarifa Mateo, 2019)
Cattle milk	*Bos taurus*	Spain	Mediterranean	-4.1	-22.7	-26.8	(Tarifa Mateo, 2019)
Sheep milk	*Ovis aries*	Spain	Mediterranean	-5.2	-27.2	-32.5	(Tarifa Mateo, 2019)
Sheep yogurt	*Ovis aries*	Spain	Mediterranean	-3.0	-23.3	-26.3	(Tarifa Mateo, 2019)
Sheep cheese	*Ovis aries*	Spain	Mediterranean	-3.2	-23.9	-27.1	(Tarifa Mateo, 2019)
Goat cheese	*Capra hircus*	Spain	Mediterranean	-3.2	-25.0	-28.2	(Tarifa Mateo, 2019)
Cow milk		Germany	Continental	-6.0	-24.8	-30.8	(Debono-Spiteri, 2012)
Cattle cheese		Switzerland	Alpine	-5.3	-28.2	-33.5	(Carrer et al., 2016)
Goat milk		Switzerland	Alpine	-5.9	-28.2	-34.1	(Carrer et al., 2016)
Goat cheese		Switzerland	Alpine	-4.7	-27.6	-32.3	(Carrer et al., 2016)
Cattle	*Bos taurus*	Switzerland	Alpine	-4.6	-27.3	-31.9	(Spangenberg, Jacomet and Schibler, 2006)

Common name		Provenience	Biogeographical region	$\Delta^{13}C$ (‰)	$\delta^{13}C_{16:0}$ (‰)	$\delta^{13}C_{18:0}$ (‰)	Reference
Cattle	*Bos taurus*	Switzerland	Alpine	-5.0	-28.5	-33.5	(Spangenberg, Jacomet and Schibler, 2006)
Cattle	*Bos taurus*	Switzerland	Alpine	-4.9	-28.1	-32.9	(Spangenberg, Jacomet and Schibler, 2006)
Cattle	*Bos taurus*	Switzerland	Alpine	-5.4	-27.5	-32.9	(Spangenberg, Jacomet and Schibler, 2006)
Cattle	*Bos taurus*	Switzerland	Alpine	-3.9	-27.8	-31.7	(Spangenberg, Jacomet and Schibler, 2006)
Cattle	*Bos taurus*	Switzerland	Alpine	-4.1	-26.9	-31.0	(Spangenberg, Jacomet and Schibler, 2006)
Cattle	*Bos taurus*	Switzerland	Alpine	-3.3	-27.5	-30.7	(Spangenberg, Jacomet and Schibler, 2006)
Cattle	*Bos taurus*	Switzerland	Alpine	-2.8	-27.1	-29.9	(Spangenberg, Jacomet and Schibler, 2006)
Cattle	*Bos taurus*	Switzerland	Alpine	-2.6	-28.5	-31.0	(Spangenberg, Jacomet and Schibler, 2006)
Cattle	*Bos taurus*	Switzerland	Alpine	-6.6	-25.6	-32.2	(Spangenberg, Jacomet and Schibler, 2006)
Goat	*Capra hircus*	Switzerland	Alpine	-3.9	-24.8	-28.7	(Spangenberg, Jacomet and Schibler, 2006)
Goat	*Capra hircus*	Switzerland	Alpine	-2.6	-24.9	-27.6	(Spangenberg, Jacomet and Schibler, 2006)
Goat	*Capra hircus*	Switzerland	Alpine	-7.1	-26.2	-33.3	(Spangenberg, Jacomet and Schibler, 2006)
Goat	*Capra hircus*	Switzerland	Alpine	-7.0	-25.5	-32.4	(Spangenberg, Jacomet and Schibler, 2006)
Goat	*Capra hircus*	Switzerland	Alpine	-2.9	-28.2	-31.1	(Spangenberg, Jacomet and Schibler, 2006)
Sheep	*Ovis aries*	Switzerland	Alpine	-4.9	-29.0	-33.9	(Spangenberg, Jacomet and Schibler, 2006)
Sheep	*Ovis aries*	Switzerland	Alpine	-5.4	-28.0	-33.4	(Spangenberg, Jacomet and Schibler, 2006)
Sheep	*Ovis aries*	Switzerland	Alpine	-2.3	-30.8	-33.2	(Spangenberg, Jacomet and Schibler, 2006)

Common name		Provenience	Biogeographical region	$\Delta^{13}C$ (‰)	$\delta^{13}C_{16:0}$ (‰)	$\delta^{13}C_{18:0}$ (‰)	Reference
Sheep	*Ovis aries*	Switzerland	Alpine	-5.6	-31.4	-37.0	(Spangenberg, Jacomet and Schibler, 2006)
Sheep	*Ovis aries*	Switzerland	Alpine	-6.8	-31.3	-38.0	(Spangenberg, Jacomet and Schibler, 2006)
Sheep	*Ovis aries*	Switzerland	Alpine	-7.4	-30.9	-38.3	(Spangenberg, Jacomet and Schibler, 2006)
Sheep	*Ovis aries*	Switzerland	Alpine	-7.2	-32.0	-39.2	(Spangenberg, Jacomet and Schibler, 2006)
Cow milk	*Bos taurus*	UK	Atlantic	-3.6	-30.8	-34.4	(Dudd, 1999)
Cow milk	*Bos taurus*	UK	Atlantic	-4.3	-27.8	-32.1	(Dudd, 1999)
Sheep milk	*Ovis aries*	UK	Atlantic	-4.4	-29.4	-33.8	(Dudd, 1999)
Sheep milk	*Ovis aries*	UK	Atlantic	-4.4	-29.0	-33.4	(Dudd, 1999)
Cow milk	*Bos taurus*	UK	Atlantic	-4.8	-27.4	-32.2	(Dudd, 1999)
Cow milk	*Bos taurus*	UK	Atlantic	-4.8	-28.9	-33.7	(Dudd, 1999)
Cow milk	*Bos taurus*	UK	Atlantic	-5.3	-29.6	-34.9	(Dudd, 1999)
Cow milk	*Bos taurus*	UK	Atlantic	-5.2	-27.9	-33.1	(Dudd, 1999)
Cow milk	*Bos taurus*	UK	Atlantic	-5.5	-28.6	-34.1	(Dudd, 1999)
Cow milk	*Bos taurus*	UK	Atlantic	-5.9	-28.1	-34.0	(Dudd, 1999)
		UK	Atlantic	-5.3	-28.3	-33.6	(Copley et al., 2003)
		UK	Atlantic	-4.8	-27.8	-32.6	(Copley et al., 2003)
		UK	Atlantic	-4.8	-29.3	-34.1	(Copley et al., 2003)

Common name		Provenience	Biogeographical region	$\Delta^{13}C$ (‰)	$\delta^{13}C_{16:0}$ (‰)	$\delta^{13}C_{18:0}$ (‰)	Reference
		UK	Atlantic	-4.2	-28.3	-32.4	(Copley et al., 2003)
		UK	Atlantic	-5.9	-28.5	-34.4	(Copley et al., 2003)
		UK	Atlantic	-5.3	-30.0	-35.3	(Copley et al., 2003)
		UK	Atlantic	-4.2	-29.4	-33.6	(Copley et al., 2003)
		UK	Atlantic	-4.4	-29.8	-34.2	(Copley et al., 2003)
		UK	Atlantic	-3.6	-31.2	-34.8	(Copley et al., 2003)
		UK	Atlantic	-5.5	-29.0	-34.5	(Copley et al., 2003)
Finncattle milk	*Bos taurus*	Finland	Boreal	-3.6	-27.6	-31.2	(Pääkkönen, Evershed and Asplund, 2020)
Finncattle milk	*Bos taurus*	Finland	Boreal	-3.9	-27.3	-31.2	(Pääkkönen, Evershed and Asplund, 2020)
Finncattle milk	*Bos taurus*	Finland	Boreal	-4.7	-27.3	-32.0	(Pääkkönen, Evershed and Asplund, 2020)
Finncattle milk	*Bos taurus*	Finland	Boreal	-4.6	-27.1	-31.7	(Pääkkönen, Evershed and Asplund, 2020)
Finncattle milk	*Bos taurus*	Finland	Boreal	-4.1	-28.0	-32.1	(Pääkkönen, Evershed and Asplund, 2020)
Goat milk	*Capra hircus*	Finland	Boreal	-4.2	-25.9	-30.1	(Pääkkönen, Evershed and Asplund, 2020)
Goat milk	*Capra hircus*	Finland	Boreal	-3.7	-27.7	-31.4	(Pääkkönen, Evershed and Asplund, 2020)
Goat milk	*Capra hircus*	Finland	Boreal	-5.1	-27.7	-32.8	(Pääkkönen, Evershed and Asplund, 2020)
Goat milk	*Capra hircus*	Finland	Boreal	-3.9	-28.1	-32.0	(Pääkkönen, Evershed and Asplund, 2020)

Domestic porcine

Common name	Taxa	Provenience	Biogeographical region	$\Delta^{13}C$ (‰)	$\delta^{13}C_{16:0}$ (‰)	$\delta^{13}C_{18:0}$ (‰)	Reference
Pig	*Sus domesticus*	Spain	Mediterranean	0.4	-19.3	-18.9	(Tarifa-Mateo et al., 2023)
Pig	*Sus domesticus*	Spain	Mediterranean	2.5	-22.5	-20.0	(Tarifa-Mateo et al., 2023)
Pig	*Sus domesticus*	Spain	Mediterranean	2.6	-23.0	-20.4	(Tarifa-Mateo et al., 2023)
Pig	*Sus domesticus*	Spain	Mediterranean	1.7	-22.3	-20.6	(Tarifa-Mateo et al., 2023)
Pig	*Sus domesticus*	Spain	Mediterranean	2.2	-23.2	-21.0	(Tarifa-Mateo et al., 2023)
Pig	*Sus domesticus*	Spain	Mediterranean	0.7	-25.2	-24.5	(Tarifa-Mateo et al., 2023)
Pig	*Sus domesticus*	Spain	Mediterranean	2.6	-24.0	-21.4	(Tarifa-Mateo et al., 2023)
Pig	*Sus domesticus*	Spain	Mediterranean	2.3	-25.3	-23.0	(Tarifa-Mateo et al., 2023)
Pig	*Sus domesticus*	Spain	Mediterranean	1.6	-21.6	-20.0	(Tarifa-Mateo et al., 2023)
Pig	*Sus domesticus*	Spain	Mediterranean	2.1	-24.4	-22.3	(Tarifa-Mateo et al., 2023)
Pig	*Sus domesticus*	Spain	Mediterranean	1.1	-25.6	-24.5	(Tarifa-Mateo et al., 2023)
Pig	*Sus domesticus*	Spain	Mediterranean	0.8	-23.7	-22.9	(Tarifa-Mateo et al., 2023)
Pig	*Sus domesticus*	Spain	Mediterranean	1.0	-23.9	-22.9	(Tarifa-Mateo et al., 2023)
Pig	*Sus domesticus*	Spain	Mediterranean	1.3	-24.3	-23.0	(Tarifa-Mateo et al., 2023)
Pig	*Sus domesticus*	Spain	Mediterranean	2.4	-26.1	-23.7	(Tarifa-Mateo et al., 2023)
Pig	*Sus domesticus*	Spain	Mediterranean	-0.4	-23.9	-24.3	(Tarifa-Mateo et al., 2023)

Common name	Taxa	Provenience	Biogeographical region	$\Delta^{13}C$ (‰)	$\delta^{13}C_{16:0}$ (‰)	$\delta^{13}C_{18:0}$ (‰)	Reference
Pig	*Sus domesticus*	Spain	Mediterranean	1.1	-24.5	-23.4	(Tarifa-Mateo et al., 2023)
Pig	*Sus domesticus*	Spain	Mediterranean	2.2	-26.1	-23.9	(Tarifa-Mateo et al., 2023)
Pig	*Sus domesticus*	Spain	Mediterranean	2.2	-24.7	-22.5	(Tarifa-Mateo et al., 2023)
Pig	*Sus domesticus*	Spain	Mediterranean	2.0	-23.8	-21.8	(Tarifa-Mateo et al., 2023)
Pig	*Sus domesticus*	Spain	Mediterranean	2.0	-20.9	-18.9	(Tarifa-Mateo et al., 2023)
Pig	*Sus domesticus*	Spain	Mediterranean	0.5	-24.3	-23.8	(Tarifa-Mateo et al., 2023)
Pig	*Sus domesticus*	Spain	Mediterranean	1.2	-23.8	-22.6	(Tarifa-Mateo et al., 2023)
Pig	*Sus domesticus*	Spain	Mediterranean	1.8	-25.8	-24.0	(Tarifa-Mateo et al., 2023)
Pig	*Sus domesticus*	Spain	Mediterranean	2.6	-24.3	-21.7	(Tarifa-Mateo et al., 2023)
Pig	*Sus domesticus*	Spain	Mediterranean	0.1	-19.3	-19.2	(Tarifa-Mateo et al., 2023)
Pig		Malta	Mediterranean	0.2	-24.2	-24.0	(Debono-Spiteri, 2012)
Pig		Malta	Mediterranean	0.0	-24.5	-24.5	(Debono-Spiteri, 2012)
Pig	*Sus scrofa*	France	Mediterranean	-0.3	-27.4	-27.7	(March, 2013)
Pig	*Sus scrofa domesticus*	Switzerland	Alpine	1.2	-28.7	-27.4	(Spangenberg, Jacomet and Schibler, 2006)
Pig	*Sus scrofa domesticus*	Switzerland	Alpine	-0.9	-25.6	-26.5	(Spangenberg, Jacomet and Schibler, 2006)
Pig	*Sus scrofa*	UK	Atlantic	-0.3	-28.0	-28.3	(Colonese et al., 2015)
Pig	*Sus scrofa domesticus*	UK	Atlantic	0.8	-24.8	-24.0	(Dudd, 1999)

Common name	Taxa	Provenience	Biogeographical region	$\Delta^{13}C$ (‰)	$\delta^{13}C_{16:0}$ (‰)	$\delta^{13}C_{18:0}$ (‰)	Reference
Pig	*Sus scrofa domesticus*	UK	Atlantic	1.6	-26.4	-24.8	(Dudd, 1999)
Pig	*Sus scrofa domesticus*	UK	Atlantic	1.7	-26.5	-24.8	(Dudd, 1999)
Pig	*Sus scrofa domesticus*	UK	Atlantic	1.1	-25.5	-24.4	(Dudd, 1999)
Pig	*Sus scrofa domesticus*	UK	Atlantic	1.1	-26.0	-24.9	(Dudd, 1999)
Pig	*Sus scrofa domesticus*	UK	Atlantic	1.3	-25.1	-23.8	(Dudd, 1999)
Pig	*Sus scrofa domesticus*	UK	Atlantic	1.3	-25.7	-24.4	(Dudd, 1999)
Pig	*Sus scrofa domesticus*	UK	Atlantic	1.3	-25.4	-24.1	(Dudd, 1999)
Pig	*Sus scrofa domesticus*	UK	Atlantic	-0.9	-24.4	-25.3	(Dudd, 1999)
		UK	Atlantic	1.7	-26.9	-25.2	(Copley et al., 2003)
		UK	Atlantic	1.6	-26.8	-25.2	(Copley et al., 2003)
		UK	Atlantic	1.3	-26.1	-24.8	(Copley et al., 2003)
		UK	Atlantic	1.3	-25.8	-24.5	(Copley et al., 2003)
		UK	Atlantic	1.4	-25.5	-24.2	(Copley et al., 2003)
		UK	Atlantic	1.0	-26.4	-25.4	(Copley et al., 2003)
		UK	Atlantic	1.1	-25.9	-24.8	(Copley et al., 2003)
		UK	Atlantic	0.8	-25.2	-24.4	(Copley et al., 2003)
Pig	*Sus scrofa domesticus*	Finland	Boreal	1.6	-27.6	-26.0	(Pääkkönen, Evershed and Asplund, 2020)

Common name	Taxa	Provenience	Biogeographical region	$\Delta^{13}C$ (‰)	$\delta^{13}C_{16:0}$ (‰)	$\delta^{13}C_{18:0}$ (‰)	Reference
Pig	*Sus scrofa domesticus*	Finland	Boreal	1.5	-28.4	-26.9	(Pääkkönen, Evershed and Asplund, 2020)
Pig	*Sus scrofa domesticus*	Finland	Boreal	0.6	-27.7	-27.1	(Pääkkönen, Evershed and Asplund, 2020)
Pig	*Sus scrofa domesticus*	Finland	Boreal	1.5	-27.4	-25.9	(Pääkkönen, Evershed and Asplund, 2020)

Freshwater

Common name	Taxa	Provenience	Biogeographical region	$\Delta^{13}C$ (‰)	$\delta^{13}C_{16:0}$ (‰)	$\delta^{13}C_{18:0}$ (‰)	Reference
Northern pike	*Esox lucius*	Russia (SE)	Steppic	1.0	-36.4	-35.5	(Bondetti et al., 2021b)
Roach	*Rutilus rutilus*	Russia (SE)	Steppic	1.7	-36.3	-34.7	(Bondetti et al., 2021b)
Crucian carp	*Carassius carassius*	Russia (SE)	Steppic	0.8	-35.0	-34.2	(Bondetti et al., 2021b)
European perch	*Perca fluviatilis*	Russia (SE)	Steppic	2.2	-32.1	-29.9	(Bondetti et al., 2021b)
Ide	*Leuciscus idus*	Russia (SE)	Steppic	0.3	-29.3	-29.0	(Bondetti et al., 2021b)
Cisco		Russia (SE)	Steppic	0.0	-35.5	-35.5	(Bondetti et al., 2021b)
Grayling	*Thymallus thymallus*	Russia (SE)	Steppic	0.3	-34.4	-34.1	(Bondetti et al., 2021b)
Northern pike	*Esox lucius*	Russia (SE)	Steppic	0.6	-35.0	-34.4	(Bondetti et al., 2021b)
Wels catfish	*Silurus glanis*	Russia (SE)	Steppic	-0.1	-27.7	-27.8	(Bondetti et al., 2021b)

Common name	Taxa	Provenience	Biogeographical region	$\Delta^{13}C$ (‰)	$\delta^{13}C_{16:0}$ (‰)	$\delta^{13}C_{18:0}$ (‰)	Reference
Mussel	*Unio*	Russia (SE)	Steppic	0.7	-32.6	-31.8	(Bondetti et al., 2021b)
Mussel	*Unio*	Russia (SE)	Steppic	0.8	-34.2	-33.5	(Bondetti et al., 2021b)
Mussel	*Unio*	Russia (SE)	Steppic	1.1	-34.2	-33.1	(Bondetti et al., 2021b)
Mussel	*Unio*	Russia (SE)	Steppic	0.4	-31.6	-31.2	(Bondetti et al., 2021b)
Mussel	*Unio*	Russia (SE)	Steppic	1.2	-34.2	-33.0	(Bondetti et al., 2021b)
Mussel	*Unio*	Russia (SE)	Steppic	1.1	-35.2	-34.1	(Bondetti et al., 2021b)
Mussel	*Unio*	Russia (SE)	Steppic	1.5	-33.8	-32.2	(Bondetti et al., 2021b)
Mussel	*Unio*	Russia (SE)	Steppic	2.0	-32.2	-30.2	(Bondetti et al., 2021b)
Mussel	*Unio*	Russia (SE)	Steppic	1.0	-33.8	-32.8	(Bondetti et al., 2021b)
Mussel	*Unio*	Russia (SE)	Steppic	1.9	-33.0	-31.2	(Bondetti et al., 2021b)
Snail	*Viviparus diluvianus*	Russia (SE)	Steppic	1.0	-34.3	-33.3	(Bondetti et al., 2021b)
Snail	*Viviparus diluvianus*	Russia (SE)	Steppic	0.1	-33.9	-33.9	(Bondetti et al., 2021b)
Snail	*Viviparus diluvianus*	Russia (SE)	Steppic	1.4	-34.5	-33.1	(Bondetti et al., 2021b)
Snail	*Viviparus diluvianus*	Russia (SE)	Steppic	0.8	-33.7	-32.9	(Bondetti et al., 2021b)
Snail	*Viviparus diluvianus*	Russia (SE)	Steppic	0.3	-33.4	-33.1	(Bondetti et al., 2021b)
Snail	*Viviparus diluvianus*	Russia (SE)	Steppic	-0.4	-32.8	-33.2	(Bondetti et al., 2021b)
Snail	*Viviparus diluvianus*	Russia (SE)	Steppic	1.3	-34.0	-32.7	(Bondetti et al., 2021b)

Common name	Taxa	Provenience	Biogeographical region	$\Delta^{13}C$ (‰)	$\delta^{13}C_{16:0}$ (‰)	$\delta^{13}C_{18:0}$ (‰)	Reference
Snail	*Viviparus diluvianus*	Russia (SE)	Steppic	0.3	-33.5	-33.2	(Bondetti et al., 2021b)
Snail	*Viviparus diluvianus*	Russia (SE)	Steppic	0.3	-34.0	-33.7	(Bondetti et al., 2021b)
Snail	*Viviparus diluvianus*	Russia (SE)	Steppic	0.5	-33.0	-32.5	(Bondetti et al., 2021b)
Danube sturgeon	*Acipenser gueldenstaedtii*	Russia (SE)	Steppic	-0.2	-26.0	-26.1	(Bondetti et al., 2021b)
European eel	*Anguilla anguilla*	Denmark	Continental	-0.2	-28.4	-28.6	(Craig et al., 2011)
Northern pike	*Esox lucius*	Denmark	Continental	-0.2	-35.0	-35.2	(Craig et al., 2011)
Tench	*Tinca tinca*	Denmark	Continental	-1.1	-27.9	-29.0	(Craig et al., 2011)
Tench	*Tinca tinca*	Denmark	Continental	-2.1	-24.4	-26.5	(Craig et al., 2011)
Tench	*Tinca tinca*	Denmark	Continental	0.7	-37.4	-36.7	(Craig et al., 2011)
Northern pike	*Esox lucius*	Russia (NE)	Boreal	0.6	-31.6	-31.0	(Courel et al., 2021)
European perch	*Perca fluviatilis*	Russia (NE)	Boreal	0.1	-32.4	-32.3	(Courel et al., 2021)
Cyprinid sp.	*Cyprinidae*	Russia (NE)	Boreal	-0.5	-29.2	-29.6	(Courel et al., 2021)
Cyprinid sp.	*Cyprinidae*	Russia (NE)	Boreal	1.6	-31.6	-30.1	(Courel et al., 2021)
Common bream	*Abramis brama*	Russia (NE)	Boreal	2.4	-31.0	-28.6	(Courel et al., 2021)
European whitefish	*Coregonus lavaretus*	Switzerland	Alpine	1.1	-33.0	-31.9	(Spangenberg, Jacomet and Schibler, 2006)
Tench	*Tinca tinca*	Russia (SE)	Steppic	-0.4	-24.1	-24.5	(Dolbunova et al., 2023)

Common name	Taxa	Provenience	Biogeographical region	$\Delta^{13}C$ (‰)	$\delta^{13}C_{16:0}$ (‰)	$\delta^{13}C_{18:0}$ (‰)	Reference
Crucian carp	*Carassius carassius*	Russia (SE)	Steppic	-0.2	-30.1	-30.2	(Dolbunova et al., 2023)
Perch	*Perca fluviatilis*	Russia (SE)	Steppic	-0.3	-27.4	-27.7	(Dolbunova et al., 2023)
Perch	*Perca fluviatilis*	Russia (SE)	Steppic	-0.2	-26.5	-26.6	(Dolbunova et al., 2023)
Bream	*Abramis brama*	Russia (SE)	Steppic	-0.1	-28.5	-28.6	(Dolbunova et al., 2023)
Sander	*Sander lucioperca*	Russia (SE)	Steppic	-1.4	-23.3	-24.7	(Dolbunova et al., 2023)
Crucian carp	*Carassius carassius*	Russia (SE)	Steppic	-0.7	-28.0	-28.7	(Dolbunova et al., 2023)
Rudd	*Scardinius erythrophthalmus*	Russia (SE)	Steppic	-1.2	-27.3	-28.6	(Dolbunova et al., 2023)
Rudd	*Scardinius erythrophthalmus*	Russia (SE)	Steppic	0.6	-31.3	-30.7	(Dolbunova et al., 2023)
Pike	*Esox lucius*	Russia (SE)	Steppic	-0.1	-28.1	-28.2	(Dolbunova et al., 2023)
Roach	*Rutilus rutilus*	Russia (SE)	Steppic	-1.3	-28.0	-29.2	(Dolbunova et al., 2023)
Roach	*Rutilus rutilus*	Russia (SE)	Steppic	-1.0	-25.8	-26.8	(Dolbunova et al., 2023)
Catfish		Russia (SE)	Steppic	0.1	-29.6	-29.5	(Dolbunova et al., 2023)
Sazan	*Cyprinus carpio*	Russia (SE)	Steppic	0.1	-28.0	-27.9	(Dolbunova et al., 2023)
Carp	*Carassius carassius*	UK	Atlantic	2.0	-30.3	-28.3	(Lucquin et al., 2016)
Perch	*Perca fluviatilis*	UK	Atlantic	2.6	-31.1	-28.5	(Lucquin et al., 2016)
Pike	*Esox lucius*	UK	Atlantic	2.4	-28.3	-25.9	(Lucquin et al., 2016)

Common name	Taxa	Provenience	Biogeographical region	$\Delta^{13}C$ (‰)	$\delta^{13}C_{16:0}$ (‰)	$\delta^{13}C_{18:0}$ (‰)	Reference
Salmon	*Salmonidae sp.*	UK	Atlantic	0.1	-25.0	-24.9	(Lucquin et al., 2016)
European perch	*Perca fluviatilis*	UK	Atlantic	0.6	-35.7	-35.1	(Cramp and Evershed, 2014)
European perch	*Perca fluviatilis*	UK	Atlantic	-0.6	-35.2	-35.8	(Cramp and Evershed, 2014)
European perch	*Perca fluviatilis*	UK	Atlantic	-0.1	-34.8	-34.9	(Cramp and Evershed, 2014)
European perch	*Perca fluviatilis*	UK	Atlantic	-1.0	-34.5	-35.5	(Cramp and Evershed, 2014)
European perch	*Perca fluviatilis*	UK	Atlantic	-1.0	-34.5	-35.5	(Cramp and Evershed, 2014)
European perch	*Perca fluviatilis*	UK	Atlantic	-1.3	-34.3	-35.6	(Cramp and Evershed, 2014)
European perch	*Perca fluviatilis*	UK	Atlantic	0.4	-34.0	-33.7	(Cramp and Evershed, 2014)
European perch	*Perca fluviatilis*	UK	Atlantic	-0.1	-33.6	-33.6	(Cramp and Evershed, 2014)
European perch	*Perca fluviatilis*	UK	Atlantic	0.1	-33.4	-33.2	(Cramp and Evershed, 2014)
European perch	*Perca fluviatilis*	UK	Atlantic	-0.9	-32.9	-33.9	(Cramp and Evershed, 2014)
European perch	*Perca fluviatilis*	UK	Atlantic	-1.5	-32.6	-34.1	(Cramp and Evershed, 2014)
European perch	*Perca fluviatilis*	UK	Atlantic	-0.6	-32.2	-32.8	(Cramp and Evershed, 2014)
Roach	*Rutilus rutilus*	UK	Atlantic	-0.1	-34.1	-34.3	(Cramp and Evershed, 2014)
Roach	*Rutilus rutilus*	UK	Atlantic	-1.2	-33.6	-34.8	(Cramp and Evershed, 2014)
Roach	*Rutilus rutilus*	UK	Atlantic	-1.1	-32.8	-33.9	(Cramp and Evershed, 2014)
Roach	*Rutilus rutilus*	UK	Atlantic	-1.0	-32.7	-33.7	(Cramp and Evershed, 2014)

Common name	Taxa	Provenience	Biogeographical region	$\Delta^{13}C$ (‰)	$\delta^{13}C_{16:0}$ (‰)	$\delta^{13}C_{18:0}$ (‰)	Reference
Roach	*Rutilus rutilus*	UK	Atlantic	-0.5	-32.8	-33.3	(Cramp and Evershed, 2014)
Roach	*Rutilus rutilus*	UK	Atlantic	-0.3	-32.2	-32.5	(Cramp and Evershed, 2014)
Bleak	*Alburnus alburnus*	Finland	Boreal	0.7	-27.1	-26.4	(Pääkkönen, Evershed and Asplund, 2020)
Bleak	*Alburnus alburnus*	Finland	Boreal	1.5	-34.3	-32.8	(Pääkkönen, Evershed and Asplund, 2020)
Bleak	*Alburnus alburnus*	Finland	Boreal	-0.4	-34.6	-35.0	(Pääkkönen, Evershed and Asplund, 2020)
Bleak	*Alburnus alburnus*	Finland	Boreal	0.5	-36.1	-35.6	(Pääkkönen, Evershed and Asplund, 2020)
Bleak	*Alburnus alburnus*	Finland	Boreal	1.5	-36.5	-35.0	(Pääkkönen, Evershed and Asplund, 2020)
Burbot	*Lota lota*	Finland	Boreal	2.0	-34.8	-32.8	(Pääkkönen, Evershed and Asplund, 2020)
Ide	*Leuciscus idus*	Finland	Boreal	1.6	-33.9	-32.3	(Pääkkönen, Evershed and Asplund, 2020)
Ide	*Leuciscus idus*	Finland	Boreal	1.6	-33.3	-31.7	(Pääkkönen, Evershed and Asplund, 2020)
Northern pike	*Esox lucius*	Finland	Boreal	0.3	-33.7	-33.4	(Pääkkönen, Evershed and Asplund, 2020)
Northern pike	*Esox lucius*	Finland	Boreal	1.2	-33.9	-32.7	(Pääkkönen, Evershed and Asplund, 2020)
Northern pike	*Esox lucius*	Finland	Boreal	0.4	-32.2	-31.8	(Pääkkönen, Evershed and Asplund, 2020)
European perch	*Perca fluviatilis*	Finland	Boreal	1.1	-34.8	-33.7	(Pääkkönen, Evershed and Asplund, 2020)
European perch	*Perca fluviatilis*	Finland	Boreal	0.5	-35.6	-35.1	(Pääkkönen, Evershed and Asplund, 2020)
European perch	*Perca fluviatilis*	Finland	Boreal	0.8	-33.8	-33.0	(Pääkkönen, Evershed and Asplund, 2020)
European perch	*Perca fluviatilis*	Finland	Boreal	1.6	-35.4	-33.8	(Pääkkönen, Evershed and Asplund, 2020)

Common name	Taxa	Provenience	Biogeographical region	$\Delta^{13}C$ (‰)	$\delta^{13}C_{16:0}$ (‰)	$\delta^{13}C_{18:0}$ (‰)	Reference
European perch	*Perca fluviatilis*	Finland	Boreal	0.6	-33.4	-32.8	(Pääkkönen, Evershed and Asplund, 2020)
European perch	*Perca fluviatilis*	Finland	Boreal	-0.3	-32.5	-32.8	(Pääkkönen, Evershed and Asplund, 2020)
European perch	*Perca fluviatilis*	Finland	Boreal	-0.6	-32.5	-33.1	(Pääkkönen, Evershed and Asplund, 2020)
European perch	*Perca fluviatilis*	Finland	Boreal	-1.5	-35.8	-37.3	(Pääkkönen, Evershed and Asplund, 2020)
European perch	*Perca fluviatilis*	Finland	Boreal	0.5	-35.7	-35.2	(Pääkkönen, Evershed and Asplund, 2020)
Pike-perch	*Sander lucioperca*	Finland	Boreal	0.8	-35.0	-34.2	(Pääkkönen, Evershed and Asplund, 2020)
Pike-perch	*Sander lucioperca*	Finland	Boreal	0.3	-30.7	-30.4	(Pääkkönen, Evershed and Asplund, 2020)
Roach	*Rutilus rutilus*	Finland	Boreal	-2.5	-29.9	-32.4	(Pääkkönen, Evershed and Asplund, 2020)
Roach	*Rutilus rutilus*	Finland	Boreal	1.1	-34.5	-33.4	(Pääkkönen, Evershed and Asplund, 2020)
Vendace	*Coregonus albula*	Finland	Boreal	-1.6	-28.4	-30.0	(Pääkkönen, Evershed and Asplund, 2020)
Vendace	*Coregonus albula*	Finland	Boreal	1.3	-29.6	-28.3	(Pääkkönen, Evershed and Asplund, 2020)
Vendace	*Coregonus albula*	Finland	Boreal	-1.0	-37.3	-38.3	(Pääkkönen, Evershed and Asplund, 2020)
Vendace	*Coregonus albula*	Finland	Boreal	1.4	-28.7	-27.3	(Pääkkönen, Evershed and Asplund, 2020)

Domestic ruminant

Common name	Taxa	Provenience	Biogeographical region	$\Delta^{13}C$ (‰)	$\delta^{13}C_{16:0}$ (‰)	$\delta^{13}C_{18:0}$ (‰)	Reference
Cattle	*Bos taurus*	Spain	Mediterranean	-0.8	-27.7	-28.5	(Colonese et al., 2015)
Cattle	*Bos taurus*	Spain	Mediterranean	-2.1	-29.4	-31.5	(Colonese et al., 2015)
Cow		Malta	Mediterranean	0.1	-25.4	-25.3	(Debono-Spiteri, 2012)
Cow		Malta	Mediterranean	-0.2	-25.4	-25.6	(Debono-Spiteri, 2012)
Sheep		Malta	Mediterranean	-2.5	-24.8	-27.3	(Debono-Spiteri, 2012)
Sheep		Malta	Mediterranean	-1.4	-25.4	-26.8	(Debono-Spiteri, 2012)
Goat		Malta	Mediterranean	-1.1	-25.8	-26.9	(Debono-Spiteri, 2012)
Goat		Malta	Mediterranean	-2.0	-23.8	-25.8	(Debono-Spiteri, 2012)
Goat		France	Mediterranean	-2.4	-28.7	-31.1	(Drieu et al., 2021)
Cattle	*Bos taurus*	Spain	Mediterranean	-1.4	-23.5	-24.9	(Tarifa Mateo, 2019)
Cattle	*Bos taurus*	Spain	Mediterranean	-1.8	-22.7	-24.5	(Tarifa Mateo, 2019)
Cattle	*Bos taurus*	Spain	Mediterranean	-1.1	-26.2	-27.2	(Tarifa Mateo, 2019)
Cattle	*Bos taurus*	Spain	Mediterranean	-1.9	-29.4	-31.3	(Tarifa Mateo, 2019)
Cattle	*Bos taurus*	Spain	Mediterranean	-1.6	-24.7	-26.3	(Tarifa Mateo, 2019)
Cattle	*Bos taurus*	Spain	Mediterranean	-2.5	-24.2	-26.7	(Tarifa Mateo, 2019)
Cattle	*Bos taurus*	Spain	Mediterranean	0.1	-24.2	-24.2	(Tarifa Mateo, 2019)

Common name	Taxa	Provenience	Biogeographical region	$\Delta^{13}C$ (‰)	$\delta^{13}C_{16:0}$ (‰)	$\delta^{13}C_{18:0}$ (‰)	Reference
Sheep	*Ovis aries*	Spain	Mediterranean	-1.0	-26.1	-27.1	(Tarifa Mateo, 2019)
Sheep	*Ovis aries*	Spain	Mediterranean	-0.9	-29.4	-30.4	(Tarifa Mateo, 2019)
Sheep	*Ovis aries*	Spain	Mediterranean	-0.3	-29.5	-29.8	(Tarifa Mateo, 2019)
Sheep	*Ovis aries*	Spain	Mediterranean	-2.9	-28.3	-31.2	(Tarifa Mateo, 2019)
Sheep	*Ovis aries*	Spain	Mediterranean	0.0	-26.5	-26.5	(Tarifa Mateo, 2019)
Calf	*Bos taurus*	Switzerland	Alpine	-1.0	-25.6	-26.6	(Spangenberg et al., 2010)
Cow	*Bos taurus*	Switzerland	Alpine	0.8	-26.4	-25.6	(Spangenberg et al., 2010)
Sheep	*Bos taurus*	Switzerland	Alpine	-1.1	-27.5	-28.6	(Spangenberg et al., 2010)
Cow	*Bos taurus*	Switzerland	Alpine	-0.7	-25.7	-26.4	(Spangenberg et al., 2010)
Goat	*Ovis aries*	Switzerland	Alpine	-0.7	-28.7	-29.4	(Spangenberg et al., 2010)
Sheep	*Ovis aries*	Switzerland	Alpine	-2.4	-28.9	-31.3	(Carrer et al., 2016)
Sheep	*Ovis aries*	Switzerland	Alpine	-1.4	-30.2	-31.6	(Carrer et al., 2016)
Cattle	*Bos taurus*	Switzerland	Alpine	-3.0	-29.1	-32.1	(Carrer et al., 2016)
Cattle		Switzerland	Alpine	-1.5	-27.1	-28.6	(Spangenberg, Jacomet and Schibler, 2006)
Cattle		Switzerland	Alpine	-0.5	-27.8	-28.3	(Spangenberg, Jacomet and Schibler, 2006)
Cattle		Switzerland	Alpine	0.0	-31.4	-31.3	(Spangenberg, Jacomet and Schibler, 2006)
Cattle		Switzerland	Alpine	-0.3	-30.0	-30.2	(Spangenberg, Jacomet and Schibler, 2006)

Common name	Taxa	Provenience	Biogeographical region	$\Delta^{13}C$ (‰)	$\delta^{13}C_{16:0}$ (‰)	$\delta^{13}C_{18:0}$ (‰)	Reference
Sheep		Switzerland	Alpine	1.3	-27.7	-26.4	(Spangenberg, Jacomet and Schibler, 2006)
Sheep	*Ovis aries*	UK	Atlantic	-1.8	-29.4	-31.2	(Dudd, 1999)
Sheep	*Ovis aries*	UK	Atlantic	-1.7	-28.4	-30.1	(Dudd, 1999)
Sheep	*Ovis aries*	UK	Atlantic	-1.7	-28.7	-30.4	(Dudd, 1999)
Sheep	*Ovis aries*	UK	Atlantic	-1.9	-29.2	-31.1	(Dudd, 1999)
Sheep	*Ovis aries*	UK	Atlantic	-1.8	-29.3	-31.1	(Dudd, 1999)
Sheep	*Ovis aries*	UK	Atlantic	-2.9	-28.4	-31.3	(Dudd, 1999)
Sheep	*Ovis aries*	UK	Atlantic	-1.3	-28.8	-30.1	(Dudd, 1999)
Sheep	*Ovis aries*	UK	Atlantic	-1.8	-28.2	-30.0	(Dudd, 1999)
Sheep	*Ovis aries*	UK	Atlantic	-1.8	-30.4	-32.2	(Dudd, 1999)
Sheep	*Ovis aries*	UK	Atlantic	-2.1	-30.2	-32.3	(Dudd, 1999)
Sheep	*Ovis aries*	UK	Atlantic	-2.0	-30.5	-32.5	(Dudd, 1999)
Sheep	*Ovis aries*	UK	Atlantic	-2.4	-29.4	-31.8	(Dudd, 1999)
Sheep	*Ovis aries*	UK	Atlantic	-1.4	-29.0	-30.4	(Dudd, 1999)
Cow	*Bos taurus*	UK	Atlantic	-2.9	-28.9	-31.8	(Dudd, 1999)
Cow	*Bos taurus*	UK	Atlantic	-2.5	-29.8	-32.3	(Dudd, 1999)
Cow	*Bos taurus*	UK	Atlantic	-2.8	-28.7	-31.5	(Dudd, 1999)

Common name	Taxa	Provenience	Biogeographical region	$\Delta^{13}C$ (‰)	$\delta^{13}C_{16:0}$ (‰)	$\delta^{13}C_{18:0}$ (‰)	Reference
Cow	*Bos taurus*	UK	Atlantic	-1.7	-29.9	-31.6	(Dudd, 1999)
Cattle	*Bos taurus*	Finland	Boreal	-1.4	-27.9	-29.3	(Pääkkönen, Evershed and Asplund, 2020)
Cattle	*Bos taurus*	Finland	Boreal	-2.5	-27.2	-29.7	(Pääkkönen, Evershed and Asplund, 2020)
Cattle	*Bos taurus*	Finland	Boreal	-2.0	-28.0	-30.0	(Pääkkönen, Evershed and Asplund, 2020)
Cattle	*Bos taurus*	Finland	Boreal	-1.5	-27.5	-29.0	(Pääkkönen, Evershed and Asplund, 2020)

Wild non-ruminant

Common name	Taxa	Provenience	Biogeographical region	$\Delta^{13}C$ (‰)	$\delta^{13}C_{16:0}$ (‰)	$\delta^{13}C_{18:0}$ (‰)	Reference
Wild boar	*Sus scrofa*	Spain	Mediterranean	1.8	-25.5	-23.7	(Tarifa-Mateo et al., 2023)
Wild boar	*Sus scrofa*	Spain	Mediterranean	1.7	-25.7	-24.0	(Tarifa-Mateo et al., 2023)
Wild boar	*Sus scrofa*	Spain	Mediterranean	2.0	-25.6	-23.6	(Tarifa-Mateo et al., 2023)
Wild boar	*Sus scrofa*	Spain	Mediterranean	0.8	-25.9	-25.1	(Tarifa-Mateo et al., 2023)
Wild boar	*Sus scrofa*	Spain	Mediterranean	1.2	-26.4	-25.2	(Tarifa-Mateo et al., 2023)
Wild boar	*Sus scrofa*	Spain	Mediterranean	0.8	-25.8	-25.0	(Tarifa-Mateo et al., 2023)
Wild boar	*Sus scrofa*	Spain	Mediterranean	2.2	-26.3	-24.1	(Tarifa-Mateo et al., 2023)
Wild boar	*Sus scrofa*	Spain	Mediterranean	-0.6	-30.0	-30.6	(Tarifa-Mateo et al., 2023)

Common name	Taxa	Provenience	Biogeographical region	$\Delta^{13}C$ (‰)	$\delta^{13}C_{16:0}$ (‰)	$\delta^{13}C_{18:0}$ (‰)	Reference
Wild boar	*Sus scrofa*	Spain	Mediterranean	0.4	-26.4	-26.0	(Tarifa-Mateo et al., 2023)
Wild boar	*Sus scrofa*	Spain	Mediterranean	0.2	-23.2	-23.0	(Tarifa-Mateo et al., 2023)
Wild boar	*Sus scrofa*	Spain	Mediterranean	1.4	-26.1	-24.7	(Tarifa-Mateo et al., 2023)
Wild boar	*Sus scrofa*	Spain	Mediterranean	-0.8	-28.4	-29.2	(Tarifa-Mateo et al., 2023)
Wild boar	*Sus scrofa*	Spain	Mediterranean	0.7	-27.1	-26.4	(Tarifa-Mateo et al., 2023)
Wild boar	*Sus scrofa*	Spain	Mediterranean	-0.9	-18.9	-19.8	(Tarifa-Mateo et al., 2023)
Wild boar	*Sus scrofa*	Spain	Mediterranean	0.0	-26.8	-26.8	(Tarifa-Mateo et al., 2023)
Wild boar	*Sus scrofa*	Spain	Mediterranean	-0.1	-26.9	-27.0	(Tarifa-Mateo et al., 2023)
Wild boar	*Sus scrofa*	Spain	Mediterranean	0.2	-29.0	-28.8	(Tarifa-Mateo et al., 2023)
Wild boar	*Sus scrofa*	Spain	Mediterranean	0.4	-25.7	-25.3	(Tarifa-Mateo et al., 2023)
Wild boar	*Sus scrofa*	Spain	Mediterranean	1.5	-27.1	-25.6	(Tarifa-Mateo et al., 2023)
Wild boar	*Sus scrofa*	Spain	Mediterranean	0.3	-28.4	-28.1	(Tarifa-Mateo et al., 2023)
Wild boar	*Sus scrofa*	Spain	Mediterranean	0.5	-27.1	-26.6	(Tarifa-Mateo et al., 2023)
Wild boar	*Sus scrofa*	Spain	Mediterranean	1.5	-21.9	-20.4	(Tarifa-Mateo et al., 2023)
Wild boar	*Sus scrofa*	Spain	Mediterranean	-1.9	-22.4	-24.3	(Tarifa-Mateo et al., 2023)
Wild boar	*Sus scrofa*	Spain	Mediterranean	-3.2	-27.6	-30.8	(Tarifa-Mateo et al., 2023)
Wild boar	*Sus scrofa*	Spain	Mediterranean	-2.8	-23.5	-26.3	(Tarifa-Mateo et al., 2023)

Common name	Taxa	Provenience	Biogeographical region	$\Delta^{13}C$ (‰)	$\delta^{13}C_{16:0}$ (‰)	$\delta^{13}C_{18:0}$ (‰)	Reference
Wild boar	*Sus scrofa*	Spain	Mediterranean	-0.4	-24.6	-25.0	(Tarifa-Mateo et al., 2023)
Wild boar	*Sus scrofa*	Spain	Mediterranean	-1.4	-32.4	-33.8	(Tarifa-Mateo et al., 2023)
Wild boar		Italy	Mediterranean	0.1	-28.4	-28.3	(Debono-Spiteri, 2012)
Rabbit	*Oryctolagus cuniculus*	Spain	Mediterranean	0.9	-31.0	-30.1	(Tarifa Mateo, 2019)
Rabbit	*Oryctolagus cuniculus*	Spain	Mediterranean	0.6	-31.6	-31.0	(Tarifa Mateo, 2019)
Rabbit	*Oryctolagus cuniculus*	Spain	Mediterranean	2.1	-30.6	-28.4	(Tarifa Mateo, 2019)
Rabbit	*Oryctolagus cuniculus*	Spain	Mediterranean	2.3	-30.9	-28.6	(Tarifa Mateo, 2019)
Wild boar		Switzerland	Alpine	0.0	-24.8	-24.8	(Spangenberg et al., 2010)
Marmot	*Marmota marmota*	Switzerland	Alpine	0.5	-30.4	-29.9	(Carrer et al., 2016)
Wild boar		Germany	Continental	0.3	-25.4	-25.1	(Debono-Spiteri, 2012)
Beaver	*Castor fiber*	Russia (NE)	Boreal	-0.2	-30.8	-31.0	(Bondetti et al., 2021b)
Beaver	*Castor fiber*	Russia (SE)	Steppic	2.7	-31.1	-28.5	(Bondetti et al., 2021b)
Hare	*Lepus sp.*	Russia (SE)	Steppic	0.5	-30.8	-30.3	(Courel et al., 2021)
Mink	*Mustela lutreola*	Russia (SE)	Steppic	2.4	-29.7	-27.3	(Courel et al., 2021)
Squirrel	*Sciurus vulgaris*	Russia (SE)	Steppic	0.3	-28.9	-28.6	(Courel et al., 2021)
Marten	*Martes martes*	Russia (SE)	Steppic	0.5	-25.1	-24.6	(Courel et al., 2021)
Badger	*Meles meles*	Russia (SE)	Steppic	3.2	-27.3	-24.1	(Courel et al., 2021)

Common name	Taxa	Provenience	Biogeographical region	$\Delta^{13}C$ (‰)	$\delta^{13}C_{16:0}$ (‰)	$\delta^{13}C_{18:0}$ (‰)	Reference
Marmot	*Marmota kastschenkoi*	Russia (SE)	Steppic	2.1	-31.7	-29.6	(Courel et al., 2021)
Hare	*Lepus sp.*	Russia (NE)	Boreal	-0.1	-30.0	-30.1	(Courel et al., 2021)
Wild boar	*Sus scrofa*	Russia (NE)	Boreal	2.3	-27.6	-25.3	(Courel et al., 2021)
Brown bear	*Ursus arctos*	Russia (SE)	Steppic	-0.2	-28.9	-29.1	(Courel et al., 2021)
Fox	*Vulpes vulpes*	Russia (NE)	Boreal	-0.2	-25.5	-25.7	(Courel et al., 2021)
Otter	*Lutra lutra*	Russia (SE)	Steppic	-0.7	-27.9	-28.6	(Dolbunova et al., 2023)
Fox	*Vulpes vulpes*	Russia (SE)	Steppic	-0.2	-25.1	-25.3	(Dolbunova et al., 2023)
Marten	*Martes martes*	Russia (SE)	Steppic	-0.4	-29.5	-29.9	(Dolbunova et al., 2023)
Brown Bear	*Ursus arctos*	Estonia	Atlantic	-0.7	-26.6	-27.2	(Dolbunova et al., 2023)
Fox	*Vulpes vulpes*	Russia (SE)	Steppic	-0.2	-27.8	-28.0	(Dolbunova et al., 2023)
Yellow souslik	*Spermophilus fulvus*	Russia (SE)	Steppic	0.4	-25.5	-25.1	(Dolbunova et al., 2023)
Corsac fox	*Vulpes corsac*	Russia (SE)	Steppic	-0.7	-26.4	-27.1	(Dolbunova et al., 2023)
Wolf	*Canis lupus*	Russia (SE)	Steppic	-1.8	-26.4	-28.2	(Dolbunova et al., 2023)
Wild boar	*Sus scrofa*	Russia (SE)	Steppic	0.5	-28.4	-27.9	(Dolbunova et al., 2023)
Goose		UK	Atlantic	1.4	-28.7	-27.3	(Dudd, 1999)
Goose		UK	Atlantic	0.7	-28.7	-28.0	(Dudd, 1999)

Common name	Taxa	Provenience	Biogeographical region	$\Delta^{13}C$ (‰)	$\delta^{13}C_{16:0}$ (‰)	$\delta^{13}C_{18:0}$ (‰)	Reference
Goose		UK	Atlantic	0.9	-28.7	-27.8	(Dudd, 1999)
Goose		UK	Atlantic	1.6	-29.7	-28.1	(Dudd, 1999)
Brown bear	*Ursus arctos*	Finland	Boreal	-0.2	-28.2	-28.4	(Pääkkönen, Evershed and Asplund, 2020)
Brown bear	*Ursus arctos*	Finland	Boreal	0.0	-28.7	-28.7	(Pääkkönen, Evershed and Asplund, 2020)
Brown bear	*Ursus arctos*	Finland	Boreal	0.5	-28.8	-28.3	(Pääkkönen, Evershed and Asplund, 2020)
Brown bear	*Ursus arctos*	Finland	Boreal	0.4	-29.6	-29.2	(Pääkkönen, Evershed and Asplund, 2020)
Brown bear	*Ursus arctos*	Finland	Boreal	-1.1	-26.5	-27.6	(Pääkkönen, Evershed and Asplund, 2020)
Eurasian beaver	*Castor fiber*	Finland	Boreal	-0.3	-28.7	-29.0	(Pääkkönen, Evershed and Asplund, 2020)
Eurasian beaver	*Castor fiber*	Finland	Boreal	-1.1	-30.3	-31.4	(Pääkkönen, Evershed and Asplund, 2020)
Eurasian beaver	*Castor fiber*	Finland	Boreal	-1.2	-28.1	-29.3	(Pääkkönen, Evershed and Asplund, 2020)
Eurasian lynx	*Lynx lynx*	Finland	Boreal	0.6	-30.9	-30.3	(Pääkkönen, Evershed and Asplund, 2020)
Eurasian lynx	*Lynx lynx*	Finland	Boreal	0.2	-30.4	-30.2	(Pääkkönen, Evershed and Asplund, 2020)
Eurasian lynx	*Lynx lynx*	Finland	Boreal	-0.3	-29.3	-29.6	(Pääkkönen, Evershed and Asplund, 2020)
Eurasian lynx	*Lynx lynx*	Finland	Boreal	0.0	-29.5	-29.5	(Pääkkönen, Evershed and Asplund, 2020)
Mountain hare	*Lepus timidus*	Finland	Boreal	-0.3	-32.5	-32.8	(Pääkkönen, Evershed and Asplund, 2020)
Mountain hare	*Lepus timidus*	Finland	Boreal	-0.5	-32.2	-32.7	(Pääkkönen, Evershed and Asplund, 2020)
Mountain hare	*Lepus timidus*	Finland	Boreal	-0.5	-31.2	-31.7	(Pääkkönen, Evershed and Asplund, 2020)

Common name	Taxa	Provenience	Biogeographical region	$\Delta^{13}C$ (‰)	$\delta^{13}C_{16:0}$ (‰)	$\delta^{13}C_{18:0}$ (‰)	Reference
Wild boar	*Sus scrofa ferus*	Finland	Boreal	0.9	-26.3	-25.4	(Pääkkönen, Evershed and Asplund, 2020)
Wild boar	*Sus scrofa ferus*	Finland	Boreal	0.0	-26.6	-26.6	(Pääkkönen, Evershed and Asplund, 2020)
Wolf	*Canis lupus*	Finland	Boreal	-2.5	-28.7	-31.2	(Pääkkönen, Evershed and Asplund, 2020)
Wolf	*Canis lupus*	Finland	Boreal	-2.5	-26.9	-29.4	(Pääkkönen, Evershed and Asplund, 2020)
Wolf	*Canis lupus*	Finland	Boreal	0.6	-34.0	-33.4	(Pääkkönen, Evershed and Asplund, 2020)
Wolf	*Canis lupus*	Finland	Boreal	-1.9	-26.7	-28.6	(Pääkkönen, Evershed and Asplund, 2020)

Wild ruminant

Common name	Taxa	Provenience	Biogeographical region	$\Delta^{13}C$ (‰)	$\delta^{13}C_{16:0}$ (‰)	$\delta^{13}C_{18:0}$ (‰)	Reference
Roe deer	*Capreolus capreolus*	Spain	Mediterranean	-0.1	-30.5	-30.6	(Tarifa Mateo, 2019)
Roe deer	*Capreolus capreolus*	Spain	Mediterranean	-0.5	-30.5	-31.0	(Tarifa Mateo, 2019)
Roe deer	*Capreolus capreolus*	Spain	Mediterranean	-1.4	-29.8	-31.2	(Tarifa Mateo, 2019)
Deer		Switzerland	Alpine	-0.9	-24.4	-25.3	(Spangenberg et al., 2010)
Mule Deer		Switzerland	Alpine	0.5	-25.2	-24.7	(Spangenberg et al., 2010)
Chamois		Switzerland	Alpine	-0.8	-26.7	-27.5	(Spangenberg et al., 2010)

Common name	Taxa	Provenience	Biogeographical region	$\Delta^{13}C$ (‰)	$\delta^{13}C_{16:0}$ (‰)	$\delta^{13}C_{18:0}$ (‰)	Reference
Red deer		Switzerland	Alpine	-2.5	-30.1	-32.6	(Spangenberg et al., 2010)
Red deer	*Cervus elaphus*	Switzerland	Alpine	-2.2	-31.0	-33.1	(Spangenberg, Jacomet and Schibler, 2006)
Chamois	*Rupicapra rupicapra*	Switzerland	Alpine	-0.8	-28.4	-29.2	(Carrer et al., 2016)
Ibex	*Capra ibex*	Switzerland	Alpine	-2.9	-28.1	-31.0	(Carrer et al., 2016)
Roe deer	*Capreolus capreolus*	Switzerland	Alpine	-1.1	-29.6	-30.7	(Carrer et al., 2016)
Red deer	*Cervus elaphus*	Switzerland	Alpine	-4.3	-29.7	-34.0	(Carrer et al., 2016)
Chamois	*Rupicapra rupicapra*	Switzerland	Alpine	-2.4	-27.8	-30.2	(Carrer et al., 2016)
Roe deer		Germany	Continental	-3.8	-27.3	-31.1	(Debono-Spiteri, 2012)
Red deer		Germany	Continental	-1.2	-25.2	-26.4	(Debono-Spiteri, 2012)
Saiga	*Saiga tatarica*	Russia (SE)	Steppic	-2.5	-23.9	-26.4	(Dolbunova et al., 2023)
Roe deer	*Capreolus capreolus*	Russia (SE)	Steppic	-1.3	-31.1	-32.4	(Bondetti et al., 2021b)
Deer		Russia (SE)	Steppic	-3.3	-28.7	-32.0	(Bondetti et al., 2021b)
Reindeer	*Rangifer tarandus*	Russia (NE)	Boreal	-1.1	-23.8	-24.9	(Bondetti et al., 2021b)
Elk	*Alces alces*	Russia (NE)	Boreal	-1.5	-30.5	-32.0	(Bondetti et al., 2021b)
Elk	*Alces alces*	Russia (NE)	Boreal	-1.1	-29.8	-31.0	(Bondetti et al., 2021b)
Elk	*Alces alces*	Russia (NE)	Boreal	-1.6	-33.2	-34.8	(Bondetti et al., 2021b)
Reindeer	*Rangifer tarandus*	Russia	Boreal	-4.7	-28.2	-32.9	(March, 2013)

Common name	Taxa	Provenience	Biogeographical region	$\Delta^{13}C$ (‰)	$\delta^{13}C_{16:0}$ (‰)	$\delta^{13}C_{18:0}$ (‰)	Reference
Reindeer	*Rangifer tarandus*	Russia	Boreal	-4.9	-28.1	-33.0	(March, 2013)
Red deer	*Cervus elaphus*	Poland	Continental	-3.8	-27.6	-31.4	(Craig et al., 2012)
Red deer	*Cervus elaphus*	Poland	Continental	-3.7	-27.3	-31.0	(Craig et al., 2012)
Red deer	*Cervus elaphus*	Poland	Continental	-4.2	-28.3	-32.5	(Craig et al., 2012)
Red deer	*Cervus elaphus*	Poland	Continental	-3.7	-29.9	-33.6	(Craig et al., 2012)
Red deer	*Cervus elaphus*	Poland	Continental	-3.6	-29.0	-32.6	(Craig et al., 2012)
Red deer	*Cervus elaphus*	Poland	Continental	-4.2	-28.7	-32.9	(Craig et al., 2012)
Red deer	*Cervus elaphus*	Poland	Continental	-2.6	-30.3	-32.9	(Craig et al., 2012)
Red deer	*Cervus elaphus*	Poland	Continental	-3.6	-29.4	-33.0	(Craig et al., 2012)
Red deer	*Cervus elaphus*	Poland	Continental	-3.4	-28.8	-32.2	(Craig et al., 2012)
Red deer	*Cervus elaphus*	Poland	Continental	-3.6	-29.3	-32.9	(Craig et al., 2012)
Red deer	*Cervus elaphus*	UK	Atlantic	-1.6	-32.0	-33.6	(Lucquin, Gibbs and Uchiyama, 2016)
Roe deer	*Capreolus capreolus*	Denmark	Atlantic	-0.5	-29.2	-29.7	(Colonese et al., 2015)
Red deer	*Cervus elaphus*	UK	Atlantic	-1.4	-28.3	-29.7	(Dudd, 1999)
Red deer	*Cervus elaphus*	UK	Atlantic	-1.7	-28.8	-30.5	(Dudd, 1999)
Red deer	*Cervus elaphus*	UK	Atlantic	-0.3	-29.4	-29.7	(Dudd, 1999)
Red deer	*Cervus elaphus*	UK	Atlantic	-3.3	-28.8	-32.1	(Dudd, 1999)

Common name	Taxa	Provenience	Biogeographical region	$\Delta^{13}C$ (‰)	$\delta^{13}C_{16:0}$ (‰)	$\delta^{13}C_{18:0}$ (‰)	Reference
Red deer	*Cervus elaphus*	UK	Atlantic	-5.2	-28.0	-33.2	(Dudd, 1999)
Red deer	*Cervus elaphus*	UK	Atlantic	-3.1	-30.7	-33.8	(Dudd, 1999)
Red deer	*Cervus elaphus*	UK	Atlantic	-2.8	-30.8	-33.6	(Dudd, 1999)
Eurasian elk	*Alces alces*	Finland	Boreal	-2.4	-29.8	-32.2	(Pääkkönen, Evershed and Asplund, 2020)
Eurasian elk	*Alces alces*	Finland	Boreal	-1.6	-29.0	-30.6	(Pääkkönen, Evershed and Asplund, 2020)
Eurasian elk	*Alces alces*	Finland	Boreal	-2.2	-28.8	-31.0	(Pääkkönen, Evershed and Asplund, 2020)
Eurasian elk	*Alces alces*	Finland	Boreal	-1.9	-30.5	-32.4	(Pääkkönen, Evershed and Asplund, 2020)
Reindeer	*Rangifer tarandus*	Finland	Boreal	-2.8	-23.8	-26.6	(Pääkkönen, Evershed and Asplund, 2020)
Reindeer	*Rangifer tarandus*	Finland	Boreal	-2.9	-23.7	-26.6	(Pääkkönen, Evershed and Asplund, 2020)
Wild forest reindeer	*Rangifer tarandus fennicus*	Finland	Boreal	-3.1	-24.8	-27.9	(Pääkkönen, Evershed and Asplund, 2020)
Wild forest reindeer	*Rangifer tarandus fennicus*	Finland	Boreal	-1.8	-24.5	-26.3	(Pääkkönen, Evershed and Asplund, 2020)
Wild forest reindeer	*Rangifer tarandus fennicus*	Finland	Boreal	-1.2	-25.4	-26.6	(Pääkkönen, Evershed and Asplund, 2020)

Annex 2

Summary of $\delta^{13}C_{16:0}$, $\delta^{13}C_{18:0}$ and $\Delta^{13}C$ values across dietary categories and biogeographical regions of Europe. For each category, sample size (N), mean, and standard deviation (SD) are reported. Pairwise Wilcoxon rank-sum tests were performed to assess statistical differences between each region and the Mediterranean reference group. Statistically significant differences ($p < 0.05$) are highlighted, indicating regional variation in isotopic baselines relevant to archaeological interpretation.

Category	**Biogeographical Region**	**Isotope**	**N**	**Mean**	**SD**	***P*-value (vs Mediterranean)**	**Significance**
Dairy	Mediterranean	$\delta^{13}C_{16:0}$	19	-25.0	1.6		
		$\delta^{13}C_{18:0}$	19	-28.6	2.3		
		$\Delta^{13}C$	19	-3.6	1.1		
	Alpine	$\delta^{13}C_{16:0}$	25	-28.1	2.0	0.0011	**Yes**
		$\delta^{13}C_{18:0}$	25	-33.0	2.8	$7.30e^{-05}$	**Yes**
		$\Delta^{13}C$	25	-4.9	1.6	0.1137	No
	Atlantic	$\delta^{13}C_{16:0}$	20	-29.0	1.0	$3.80e^{-06}$	**Yes**
		$\delta^{13}C_{18:0}$	20	-33.8	0.9	$1.60e^{-05}$	**Yes**

Category	Biogeographical Region	Isotope	N	Mean	SD	*P*-value (vs Mediterranean)	Significance
		$\Delta^{13}C$	20	-4.8	0.7	0.0083	**Yes**
	Boreal	$\delta^{13}C_{16:0}$	9	-27.4	0.7	0.00649	**Yes**
		$\delta^{13}C_{18:0}$	9	-31.6	0.8	0.0342	**Yes**
		$\Delta^{13}C$	9	-4.2	0.5	1	No
Domestic Porcine	Mediterranean	$\delta^{13}C_{16:0}$	29	-23.9	1.9		
		$\delta^{13}C_{18:0}$	29	-22.5	2.0		
		$\Delta^{13}C$	29	1.4	0.9		
	Alpine	$\delta^{13}C_{16:0}$	2	-27.1	2.2	0.146	No
		$\delta^{13}C_{18:0}$	2	-27.0	0.7	0.099	No
		$\Delta^{13}C$	2	0.2	1.5	1	No
	Atlantic	$\delta^{13}C_{16:0}$	18	-25.9	0.9	0.00013	**Yes**
		$\delta^{13}C_{18:0}$	18	-24.8	1.0	$2.20e^{-05}$	**Yes**
		$\Delta^{13}C$	18	1.1	0.7	1	No

Category	Biogeographical Region	Isotope	N	Mean	SD	*P*-value (vs Mediterranean)	Significance
	Boreal	$\delta^{13}C_{16:0}$	4	-27.8	0.4	0.0075	**Yes**
		$\delta^{13}C_{18:0}$	4	-26.5	0.6	0.016	**Yes**
		$\Delta^{13}C$	4	1.3	0.5	1	No
Domestic ruminant	Mediterranean	$\delta^{13}C_{16:0}$	21	-26.2	2.2		
		$\delta^{13}C_{18:0}$	21	-27.6	2.4		
		$\Delta^{13}C$	21	-1.3	0.9		
	Alpine	$\delta^{13}C_{16:0}$	13	-28.2	1.8	0.1472	No
		$\delta^{13}C_{18:0}$	13	-29.0	2.3	0.64102	No
		$\Delta^{13}C$	13	-0.8	1.2	1	No
	Atlantic	$\delta^{13}C_{16:0}$	17	-29.2	0.7	0.002	**Yes**
		$\delta^{13}C_{18:0}$	17	-31.3	0.8	0.0003	**Yes**
		$\Delta^{13}C$	17	-2.0	0.5	0.222	No
	Boreal	$\delta^{13}C_{16:0}$	4	-27.6	0.4	1	No

Category	Biogeographical Region	Isotope	N	Mean	SD	*P*-value (vs Mediterranean)	Significance
		$\delta^{13}C_{18:0}$	4	-29.5	0.4	0.88538	No
		$\Delta^{13}C$	4	-1.9	0.5	1	No
Wild non-ruminant	Mediterranean	$\delta^{13}C_{16:0}$	32	-26.9	3.0		
		$\delta^{13}C_{18:0}$	32	-26.4	3.1		
		$\Delta^{13}C$	32	0.4	1.4		
	Alpine	$\delta^{13}C_{16:0}$	2	-27.6	4.0	1	No
		$\delta^{13}C_{18:0}$	2	-27.4	3.6	1	No
		$\Delta^{13}C$	2	0.3	0.4	1	No
	Atlantic	$\delta^{13}C_{16:0}$	5	-28.5	1.1	1	No
		$\delta^{13}C_{18:0}$	5	-27.7	0.4	1	No
		$\Delta^{13}C$	5	0.8	0.9	1	No
	Boreal	$\delta^{13}C_{16:0}$	25	-29.1	2.1	0.046	**Yes**
		$\delta^{13}C_{18:0}$	25	-29.4	2.2	0.003	**Yes**

Category	Biogeographical Region	Isotope	N	Mean	SD	*P*-value (vs Mediterranean)	Significance
		$\Delta^{13}C$	25	-0.3	1.0	0.3	No
	Steppic	$\delta^{13}C_{16:0}$	16	-28.2	2.1	1	No
		$\delta^{13}C_{18:0}$	16	-27.6	1.9	1	No
		$\Delta^{13}C$	16	0.5	1.4	1	No

Annex 3

List of modern reference samples selected for isotopic interpretation. Only Mediterranean modern reference values are included, except for the Freshwater and Wild ruminant categories, which incorporate all relevant data due to limited regional availability.

C3 plant

Common name	Taxa	Provenience	Biogeographical region	$\Delta^{13}C$ (‰)	$\delta^{13}C_{16:0}$ (‰)	$\delta^{13}C_{18:0}$ (‰)	Reference
Olive oil	*Olea europaea*	Croatia	Mediterranean	0.5	-31.5	-31.0	(Spangenberg and Ogrinc, 2001)
Olive oil	*Olea europaea*	Croatia	Mediterranean	-0.2	-30.4	-30.6	(Spangenberg and Ogrinc, 2001)
Olive oil	*Olea europaea*	Croatia	Mediterranean	-0.9	-29.1	-30.0	(Spangenberg and Ogrinc, 2001)
Olive oil	*Olea europaea*	Croatia	Mediterranean	0.7	-32.0	-31.3	(Spangenberg and Ogrinc, 2001)
Olive oil	*Olea europaea*	Croatia	Mediterranean	1.3	-31.0	-29.7	(Spangenberg and Ogrinc, 2001)
Wheat		Italy	Mediterranean	-1.4	-29.6	-31	(Drieu et al., 2021)
Barley		Italy	Mediterranean	-0.6	-30.6	-31.2	(Drieu et al., 2021)
Einkorn		France	Mediterranean	-1.5	-31.4	-32.9	(Drieu et al., 2021)
Einkorn		France	Mediterranean	-1.0	-32	-33	(Drieu et al., 2021)
Einkorn		France	Mediterranean	-1.7	-32.2	-33.9	(Drieu et al., 2021)
Barley		France	Mediterranean	0.8	-36.4	-35.6	(Drieu et al., 2021)
Cabbage	*Brassica oleracea*	France	Mediterranean	2.0	-27.1	-25.2	(March, 2013)

Common name	Taxa	Provenience	Biogeographical region	$\Delta^{13}C$ (‰)	$\delta^{13}C_{16:0}$ (‰)	$\delta^{13}C_{18:0}$ (‰)	Reference
	capitata						
Kohlrabi	*Brassica oleracea var. gongylodes*	France	Mediterranean	0.8	-28.6	-27.7	(March, 2013)
Spinach	*Spinacia oleracea*	France	Mediterranean	5.2	-33.2	-28.0	(March, 2013)
Flax	*Linum usitatissimum*	France	Mediterranean	0.2	-30.2	-30.0	(March, 2013)
Manioc	*Manihot esculenta*	France	Mediterranean	1.7	-37.6	-35.9	(March, 2013)
Hazelnut	*Corylus avellana*	France	Mediterranean	-2.1	-29.3	-31.4	(March, 2013)
Hazelnut	*Corylus avellana*	France	Mediterranean	-0.8	-29.9	-30.7	(March, 2013)
Nettle	*Urtica sp.*	France	Mediterranean	0.9	-34.5	-33.6	(March, 2013)
Parsnip	*Pastinaca sativa*	France	Mediterranean	2.6	-38.0	-35.4	(March, 2013)
Oat	*Avena sativa*	France	Mediterranean	0.5	-34.2	-33.7	(March, 2013)
Oat	*Avena sativa*	France	Mediterranean	-0.2	-33.7	-33.9	(March, 2013)
Wheat	*Triticum sp.*	France	Mediterranean	-1.1	-33.0	-34.1	(March, 2013)
Wild carrot	*Daucus carotta*	France	Mediterranean	1.8	-32.8	-31.0	(March, 2013)

C3 wood

Common name	Taxa	Provenience	Biogeographical region	$\Delta^{13}C$ (‰)	$\delta^{13}C_{16:0}$ (‰)	$\delta^{13}C_{18:0}$ (‰)	Reference
Celtis tree	*Celtis australis L.*	Spain	Mediterranean	0.4	-32.2	-31.8	(Jambrina-Enríquez et al., 2019)
Celtis tree	*Celtis australis L.*	Spain	Mediterranean	2.9	-31.8	-28.8	(Jambrina-Enríquez et al., 2019)
Celtis tree	*Celtis australis L.*	Spain	Mediterranean	6.0	-33.1	-27.1	(Jambrina-Enríquez et al., 2019)
Celtis tree	*Celtis australis L.*	Spain	Mediterranean	1.4	-34.4	-33.0	(Jambrina-Enríquez et al., 2019)
Celtis tree	*Celtis australis L.*	Spain	Mediterranean	5.1	-32.1	-27.0	(Jambrina-Enríquez et al., 2019)

Dairy ruminant

Common name		Provenience	Biogeographical region	$\Delta^{13}C$ (‰)	$\delta^{13}C_{16:0}$ (‰)	$\delta^{13}C_{18:0}$ (‰)	Reference
Cow		Malta	Mediterranean	-2.4	-24.2	-26.6	(Debono-Spiteri, 2012)
Cow		Malta	Mediterranean	-3.2	-23.6	-26.8	(Debono-Spiteri, 2012)
Sheep		Malta	Mediterranean	-4.6	-24.7	-29.3	(Debono-Spiteri, 2012)
Sheep		Malta	Mediterranean	-4.3	-24.5	-28.8	(Debono-Spiteri, 2012)
Goat		Malta	Mediterranean	-3.2	-25.2	-28.4	(Debono-Spiteri, 2012)
Goat		Malta	Mediterranean	-3.0	-23.7	-26.7	(Debono-Spiteri, 2012)
Goat milk		France	Mediterranean	-5.1	-26.8	-31.9	(Drieu et al., 2021)

Common name		Provenience	Biogeographical region	$\Delta^{13}C$ (‰)	$\delta^{13}C_{16:0}$ (‰)	$\delta^{13}C_{18:0}$ (‰)	Reference
Cattle	*Bos taurus*	Spain	Mediterranean	-6.0	-28.0	-34.0	(Tarifa Mateo, 2019)
Goat	*Capra hircus*	Spain	Mediterranean	-3.9	-24.4	-28.3	(Tarifa Mateo, 2019)
Cattle	*Bos taurus*	Spain	Mediterranean	-3.8	-26.6	-30.4	(Tarifa Mateo, 2019)
Goat	*Capra hircus*	Spain	Mediterranean	-2.0	-27.0	-29.0	(Tarifa Mateo, 2019)
Goat	*Capra hircus*	Spain	Mediterranean	-2.3	-23.0	-25.3	(Tarifa Mateo, 2019)
Cattle	*Bos taurus*	Spain	Mediterranean	-2.5	-25.2	-27.7	(Tarifa Mateo, 2019)
Sheep	*Ovis aries*	Spain	Mediterranean	-2.7	-26.6	-29.3	(Tarifa Mateo, 2019)
Cattle	*Bos taurus*	Spain	Mediterranean	-4.1	-22.7	-26.8	(Tarifa Mateo, 2019)
Sheep	*Ovis aries*	Spain	Mediterranean	-5.2	-27.2	-32.5	(Tarifa Mateo, 2019)
Sheep	*Ovis aries*	Spain	Mediterranean	-3.0	-23.3	-26.3	(Tarifa Mateo, 2019)
Sheep	*Ovis aries*	Spain	Mediterranean	-3.2	-23.9	-27.1	(Tarifa Mateo, 2019)
Goat	*Capra hircus*	Spain	Mediterranean	-3.2	-25.0	-28.2	(Tarifa Mateo, 2019)

Domestic porcine

Common name	Taxa	Provenience	Biogeographical region	$\Delta^{13}C$ (‰)	$\delta^{13}C_{16:0}$ (‰)	$\delta^{13}C_{18:0}$ (‰)	Reference
Pig	*Sus domesticus*	Spain	Mediterranean	0.4	-19.3	-18.9	(Tarifa-Mateo et al., 2023)

Common name	Taxa	Provenience	Biogeographical region	$\Delta^{13}C$ (‰)	$\delta^{13}C_{16:0}$ (‰)	$\delta^{13}C_{18:0}$ (‰)	Reference
Pig	*Sus domesticus*	Spain	Mediterranean	2.5	-22.5	-20.0	(Tarifa-Mateo et al., 2023)
Pig	*Sus domesticus*	Spain	Mediterranean	2.6	-23.0	-20.4	(Tarifa-Mateo et al., 2023)
Pig	*Sus domesticus*	Spain	Mediterranean	1.7	-22.3	-20.6	(Tarifa-Mateo et al., 2023)
Pig	*Sus domesticus*	Spain	Mediterranean	2.2	-23.2	-21.0	(Tarifa-Mateo et al., 2023)
Pig	*Sus domesticus*	Spain	Mediterranean	0.7	-25.2	-24.5	(Tarifa-Mateo et al., 2023)
Pig	*Sus domesticus*	Spain	Mediterranean	2.6	-24.0	-21.4	(Tarifa-Mateo et al., 2023)
Pig	*Sus domesticus*	Spain	Mediterranean	2.3	-25.3	-23.0	(Tarifa-Mateo et al., 2023)
Pig	*Sus domesticus*	Spain	Mediterranean	1.6	-21.6	-20.0	(Tarifa-Mateo et al., 2023)
Pig	*Sus domesticus*	Spain	Mediterranean	2.1	-24.4	-22.3	(Tarifa-Mateo et al., 2023)
Pig	*Sus domesticus*	Spain	Mediterranean	1.1	-25.6	-24.5	(Tarifa-Mateo et al., 2023)
Pig	*Sus domesticus*	Spain	Mediterranean	0.8	-23.7	-22.9	(Tarifa-Mateo et al., 2023)
Pig	*Sus domesticus*	Spain	Mediterranean	1.0	-23.9	-22.9	(Tarifa-Mateo et al., 2023)
Pig	*Sus domesticus*	Spain	Mediterranean	1.3	-24.3	-23.0	(Tarifa-Mateo et al., 2023)
Pig	*Sus domesticus*	Spain	Mediterranean	2.4	-26.1	-23.7	(Tarifa-Mateo et al., 2023)
Pig	*Sus domesticus*	Spain	Mediterranean	-0.4	-23.9	-24.3	(Tarifa-Mateo et al., 2023)
Pig	*Sus domesticus*	Spain	Mediterranean	1.1	-24.5	-23.4	(Tarifa-Mateo et al., 2023)
Pig	*Sus domesticus*	Spain	Mediterranean	2.2	-26.1	-23.9	(Tarifa-Mateo et al., 2023)

Common name	Taxa	Provenience	Biogeographical region	$\Delta^{13}C$ (‰)	$\delta^{13}C_{16:0}$ (‰)	$\delta^{13}C_{18:0}$ (‰)	Reference
Pig	*Sus domesticus*	Spain	Mediterranean	2.2	-24.7	-22.5	(Tarifa-Mateo et al., 2023)
Pig	*Sus domesticus*	Spain	Mediterranean	2.0	-23.8	-21.8	(Tarifa-Mateo et al., 2023)
Pig	*Sus domesticus*	Spain	Mediterranean	2.0	-20.9	-18.9	(Tarifa-Mateo et al., 2023)
Pig	*Sus domesticus*	Spain	Mediterranean	0.5	-24.3	-23.8	(Tarifa-Mateo et al., 2023)
Pig	*Sus domesticus*	Spain	Mediterranean	1.2	-23.8	-22.6	(Tarifa-Mateo et al., 2023)
Pig	*Sus domesticus*	Spain	Mediterranean	1.8	-25.8	-24.0	(Tarifa-Mateo et al., 2023)
Pig	*Sus domesticus*	Spain	Mediterranean	2.6	-24.3	-21.7	(Tarifa-Mateo et al., 2023)
Pig	*Sus domesticus*	Spain	Mediterranean	0.1	-19.3	-19.2	(Tarifa-Mateo et al., 2023)
Pig		Malta	Mediterranean	0.2	-24.2	-24.0	(Debono-Spiteri, 2012)
Pig		Malta	Mediterranean	0.0	-24.5	-24.5	(Debono-Spiteri, 2012)
Pig	*Sus scrofa*	France	Mediterranean	-0.3	-27.4	-27.7	(March, 2013)

Freshwater

Common name	Taxa	Provenience	Biogeographical region	$\Delta^{13}C$ (‰)	$\delta^{13}C_{16:0}$ (‰)	$\delta^{13}C_{18:0}$ (‰)	Reference
Northern pike	*Esox lucius*	Russia (SE)	Steppic	1.0	-36.4	-35.5	(Bondetti et al., 2021b)
Roach	*Rutilus rutilus*	Russia (SE)	Steppic	1.7	-36.3	-34.7	(Bondetti et al., 2021b)

Common name	Taxa	Provenience	Biogeographical region	$\Delta^{13}C$ (‰)	$\delta^{13}C_{16:0}$ (‰)	$\delta^{13}C_{18:0}$ (‰)	Reference
Crucian carp	*Carassius carassius*	Russia (SE)	Steppic	0.8	-35.0	-34.2	(Bondetti et al., 2021b)
European perch	*Perca fluviatilis*	Russia (SE)	Steppic	2.2	-32.1	-29.9	(Bondetti et al., 2021b)
Ide	*Leuciscus idus*	Russia (SE)	Steppic	0.3	-29.3	-29.0	(Bondetti et al., 2021b)
Cisco		Russia (SE)	Steppic	0.0	-35.5	-35.5	(Bondetti et al., 2021b)
Grayling	*Thymallus thymallus*	Russia (SE)	Steppic	0.3	-34.4	-34.1	(Bondetti et al., 2021b)
Northern pike	*Esox lucius*	Russia (SE)	Steppic	0.6	-35.0	-34.4	(Bondetti et al., 2021b)
Wels catfish	*Silurus glanis*	Russia (SE)	Steppic	-0.1	-27.7	-27.8	(Bondetti et al., 2021b)
Mussel	*Unio*	Russia (SE)	Steppic	0.7	-32.6	-31.8	(Bondetti et al., 2021b)
Mussel	*Unio*	Russia (SE)	Steppic	0.8	-34.2	-33.5	(Bondetti et al., 2021b)
Mussel	*Unio*	Russia (SE)	Steppic	1.1	-34.2	-33.1	(Bondetti et al., 2021b)
Mussel	*Unio*	Russia (SE)	Steppic	0.4	-31.6	-31.2	(Bondetti et al., 2021b)
Mussel	*Unio*	Russia (SE)	Steppic	1.2	-34.2	-33.0	(Bondetti et al., 2021b)
Mussel	*Unio*	Russia (SE)	Steppic	1.1	-35.2	-34.1	(Bondetti et al., 2021b)
Mussel	*Unio*	Russia (SE)	Steppic	1.5	-33.8	-32.2	(Bondetti et al., 2021b)
Mussel	*Unio*	Russia (SE)	Steppic	2.0	-32.2	-30.2	(Bondetti et al., 2021b)
Mussel	*Unio*	Russia (SE)	Steppic	1.0	-33.8	-32.8	(Bondetti et al., 2021b)
Mussel	*Unio*	Russia (SE)	Steppic	1.9	-33.0	-31.2	(Bondetti et al., 2021b)

Common name	Taxa	Provenience	Biogeographical region	$\Delta^{13}C$ (‰)	$\delta^{13}C_{16:0}$ (‰)	$\delta^{13}C_{18:0}$ (‰)	Reference
Snail	*Viviparus diluvianus*	Russia (SE)	Steppic	1.0	-34.3	-33.3	(Bondetti et al., 2021b)
Snail	*Viviparus diluvianus*	Russia (SE)	Steppic	0.1	-33.9	-33.9	(Bondetti et al., 2021b)
Snail	*Viviparus diluvianus*	Russia (SE)	Steppic	1.4	-34.5	-33.1	(Bondetti et al., 2021b)
Snail	*Viviparus diluvianus*	Russia (SE)	Steppic	0.8	-33.7	-32.9	(Bondetti et al., 2021b)
Snail	*Viviparus diluvianus*	Russia (SE)	Steppic	0.3	-33.4	-33.1	(Bondetti et al., 2021b)
Snail	*Viviparus diluvianus*	Russia (SE)	Steppic	-0.4	-32.8	-33.2	(Bondetti et al., 2021b)
Snail	*Viviparus diluvianus*	Russia (SE)	Steppic	1.3	-34.0	-32.7	(Bondetti et al., 2021b)
Snail	*Viviparus diluvianus*	Russia (SE)	Steppic	0.3	-33.5	-33.2	(Bondetti et al., 2021b)
Snail	*Viviparus diluvianus*	Russia (SE)	Steppic	0.3	-34.0	-33.7	(Bondetti et al., 2021b)
Snail	*Viviparus diluvianus*	Russia (SE)	Steppic	0.5	-33.0	-32.5	(Bondetti et al., 2021b)
Danube sturgeon	*Acipenser gueldenstaedtii*	Russia (SE)	Steppic	-0.2	-26.0	-26.1	(Bondetti et al., 2021b)
European eel	*Anguilla anguilla*	Denmark	Continental	-0.2	-28.4	-28.6	(Craig et al., 2011)
Northern pike	*Esox lucius*	Denmark	Continental	-0.2	-35.0	-35.2	(Craig et al., 2011)
Tench	*Tinca tinca*	Denmark	Continental	-1.1	-27.9	-29.0	(Craig et al., 2011)
Tench	*Tinca tinca*	Denmark	Continental	-2.1	-24.4	-26.5	(Craig et al., 2011)
Tench	*Tinca tinca*	Denmark	Continental	0.7	-37.4	-36.7	(Craig et al., 2011)

Common name	Taxa	Provenience	Biogeographical region	$\Delta^{13}C$ (‰)	$\delta^{13}C_{16:0}$ (‰)	$\delta^{13}C_{18:0}$ (‰)	Reference
Northern pike	*Esox lucius*	Russia (NE)	Boreal	0.6	-31.6	-31.0	(Courel et al., 2021)
European perch	*Perca fluviatilis*	Russia (NE)	Boreal	0.1	-32.4	-32.3	(Courel et al., 2021)
Cyprinid sp.	*Cyprinidae*	Russia (NE)	Boreal	-0.5	-29.2	-29.6	(Courel et al., 2021)
Cyprinid sp.	*Cyprinidae*	Russia (NE)	Boreal	1.6	-31.6	-30.1	(Courel et al., 2021)
Common bream	*Abramis brama*	Russia (NE)	Boreal	2.4	-31.0	-28.6	(Courel et al., 2021)
European whitefish	*Coregonus lavaretus*	Switzerland	Alpine	1.1	-33.0	-31.9	(Spangenberg, Jacomet and Schibler, 2006)
Tench	*Tinca tinca*	Russia (SE)	Steppic	-0.4	-24.1	-24.5	(Dolbunova et al., 2023)
Crucian carp	*Carassius carassius*	Russia (SE)	Steppic	-0.2	-30.1	-30.2	(Dolbunova et al., 2023)
Perch	*Perca fluviatilis*	Russia (SE)	Steppic	-0.3	-27.4	-27.7	(Dolbunova et al., 2023)
Perch	*Perca fluviatilis*	Russia (SE)	Steppic	-0.2	-26.5	-26.6	(Dolbunova et al., 2023)
Bream	*Abramis brama*	Russia (SE)	Steppic	-0.1	-28.5	-28.6	(Dolbunova et al., 2023)
Sander	*Sander lucioperca*	Russia (SE)	Steppic	-1.4	-23.3	-24.7	(Dolbunova et al., 2023)
Crucian carp	*Carassius carassius*	Russia (SE)	Steppic	-0.7	-28.0	-28.7	(Dolbunova et al., 2023)
Rudd	*Scardinius erythrophthalmus*	Russia (SE)	Steppic	-1.2	-27.3	-28.6	(Dolbunova et al., 2023)
Rudd	*Scardinius erythrophthalmus*	Russia (SE)	Steppic	0.6	-31.3	-30.7	(Dolbunova et al., 2023)

Common name	Taxa	Provenience	Biogeographical region	$\Delta^{13}C$ (‰)	$\delta^{13}C_{16:0}$ (‰)	$\delta^{13}C_{18:0}$ (‰)	Reference
Pike	*Esox lucius*	Russia (SE)	Steppic	-0.1	-28.1	-28.2	(Dolbunova et al., 2023)
Roach	*Rutilus rutilus*	Russia (SE)	Steppic	-1.3	-28.0	-29.2	(Dolbunova et al., 2023)
Roach	*Rutilus rutilus*	Russia (SE)	Steppic	-1.0	-25.8	-26.8	(Dolbunova et al., 2023)
Catfish		Russia (SE)	Steppic	0.1	-29.6	-29.5	(Dolbunova et al., 2023)
Sazan	*Cyprinus carpio*	Russia (SE)	Steppic	0.1	-28.0	-27.9	(Dolbunova et al., 2023)
Carp	*Carassius carassius*	UK	Atlantic	2.0	-30.3	-28.3	(Lucquin et al., 2016)
Perch	*Perca fluviatilis*	UK	Atlantic	2.6	-31.1	-28.5	(Lucquin et al., 2016)
Pike	*Esox lucius*	UK	Atlantic	2.4	-28.3	-25.9	(Lucquin et al., 2016)
Salmon	*Salmonidae sp.*	UK	Atlantic	0.1	-25.0	-24.9	(Lucquin et al., 2016)
European perch	*Perca fluviatilis*	UK	Atlantic	0.6	-35.7	-35.1	(Cramp and Evershed, 2014)
European perch	*Perca fluviatilis*	UK	Atlantic	-0.6	-35.2	-35.8	(Cramp and Evershed, 2014)
European perch	*Perca fluviatilis*	UK	Atlantic	-0.1	-34.8	-34.9	(Cramp and Evershed, 2014)
European perch	*Perca fluviatilis*	UK	Atlantic	-1.0	-34.5	-35.5	(Cramp and Evershed, 2014)
European perch	*Perca fluviatilis*	UK	Atlantic	-1.0	-34.5	-35.5	(Cramp and Evershed, 2014)
European perch	*Perca fluviatilis*	UK	Atlantic	-1.3	-34.3	-35.6	(Cramp and Evershed, 2014)
European perch	*Perca fluviatilis*	UK	Atlantic	0.4	-34.0	-33.7	(Cramp and Evershed, 2014)
European perch	*Perca fluviatilis*	UK	Atlantic	-0.1	-33.6	-33.6	(Cramp and Evershed, 2014)

Common name	Taxa	Provenience	Biogeographical region	$\Delta^{13}C$ (‰)	$\delta^{13}C_{16:0}$ (‰)	$\delta^{13}C_{18:0}$ (‰)	Reference
European perch	*Perca fluviatilis*	UK	Atlantic	0.1	-33.4	-33.2	(Cramp and Evershed, 2014)
European perch	*Perca fluviatilis*	UK	Atlantic	-0.9	-32.9	-33.9	(Cramp and Evershed, 2014)
European perch	*Perca fluviatilis*	UK	Atlantic	-1.5	-32.6	-34.1	(Cramp and Evershed, 2014)
European perch	*Perca fluviatilis*	UK	Atlantic	-0.6	-32.2	-32.8	(Cramp and Evershed, 2014)
Roach	*Rutilus rutilus*	UK	Atlantic	-0.1	-34.1	-34.3	(Cramp and Evershed, 2014)
Roach	*Rutilus rutilus*	UK	Atlantic	-1.2	-33.6	-34.8	(Cramp and Evershed, 2014)
Roach	*Rutilus rutilus*	UK	Atlantic	-1.1	-32.8	-33.9	(Cramp and Evershed, 2014)
Roach	*Rutilus rutilus*	UK	Atlantic	-1.0	-32.7	-33.7	(Cramp and Evershed, 2014)
Roach	*Rutilus rutilus*	UK	Atlantic	-0.5	-32.8	-33.3	(Cramp and Evershed, 2014)
Roach	*Rutilus rutilus*	UK	Atlantic	-0.3	-32.2	-32.5	(Cramp and Evershed, 2014)
Bleak	*Alburnus alburnus*	Finland	Boreal	0.7	-27.1	-26.4	(Pääkkönen, Evershed and Asplund, 2020)
Bleak	*Alburnus alburnus*	Finland	Boreal	1.5	-34.3	-32.8	(Pääkkönen, Evershed and Asplund, 2020)
Bleak	*Alburnus alburnus*	Finland	Boreal	-0.4	-34.6	-35.0	(Pääkkönen, Evershed and Asplund, 2020)
Bleak	*Alburnus alburnus*	Finland	Boreal	0.5	-36.1	-35.6	(Pääkkönen, Evershed and Asplund, 2020)
Bleak	*Alburnus alburnus*	Finland	Boreal	1.5	-36.5	-35.0	(Pääkkönen, Evershed and Asplund, 2020)
Burbot	*Lota lota*	Finland	Boreal	2.0	-34.8	-32.8	(Pääkkönen, Evershed and Asplund, 2020)
Ide	*Leuciscus idus*	Finland	Boreal	1.6	-33.9	-32.3	(Pääkkönen, Evershed and Asplund, 2020)

Common name	Taxa	Provenience	Biogeographical region	$\Delta^{13}C$ (‰)	$\delta^{13}C_{16:0}$ (‰)	$\delta^{13}C_{18:0}$ (‰)	Reference
Ide	*Leuciscus idus*	Finland	Boreal	1.6	-33.3	-31.7	(Pääkkönen, Evershed and Asplund, 2020)
Northern pike	*Esox lucius*	Finland	Boreal	0.3	-33.7	-33.4	(Pääkkönen, Evershed and Asplund, 2020)
Northern pike	*Esox lucius*	Finland	Boreal	1.2	-33.9	-32.7	(Pääkkönen, Evershed and Asplund, 2020)
Northern pike	*Esox lucius*	Finland	Boreal	0.4	-32.2	-31.8	(Pääkkönen, Evershed and Asplund, 2020)
European perch	*Perca fluviatilis*	Finland	Boreal	1.1	-34.8	-33.7	(Pääkkönen, Evershed and Asplund, 2020)
European perch	*Perca fluviatilis*	Finland	Boreal	0.5	-35.6	-35.1	(Pääkkönen, Evershed and Asplund, 2020)
European perch	*Perca fluviatilis*	Finland	Boreal	0.8	-33.8	-33.0	(Pääkkönen, Evershed and Asplund, 2020)
European perch	*Perca fluviatilis*	Finland	Boreal	1.6	-35.4	-33.8	(Pääkkönen, Evershed and Asplund, 2020)
European perch	*Perca fluviatilis*	Finland	Boreal	0.6	-33.4	-32.8	(Pääkkönen, Evershed and Asplund, 2020)
European perch	*Perca fluviatilis*	Finland	Boreal	-0.3	-32.5	-32.8	(Pääkkönen, Evershed and Asplund, 2020)
European perch	*Perca fluviatilis*	Finland	Boreal	-0.6	-32.5	-33.1	(Pääkkönen, Evershed and Asplund, 2020)
European perch	*Perca fluviatilis*	Finland	Boreal	-1.5	-35.8	-37.3	(Pääkkönen, Evershed and Asplund, 2020)
European perch	*Perca fluviatilis*	Finland	Boreal	0.5	-35.7	-35.2	(Pääkkönen, Evershed and Asplund, 2020)
Pike-perch	*Sander lucioperca*	Finland	Boreal	0.8	-35.0	-34.2	(Pääkkönen, Evershed and Asplund, 2020)
Pike-perch	*Sander lucioperca*	Finland	Boreal	0.3	-30.7	-30.4	(Pääkkönen, Evershed and Asplund, 2020)
Roach	*Rutilus rutilus*	Finland	Boreal	-2.5	-29.9	-32.4	(Pääkkönen, Evershed and Asplund, 2020)
Roach	*Rutilus rutilus*	Finland	Boreal	1.1	-34.5	-33.4	(Pääkkönen, Evershed and Asplund, 2020)

Common name	Taxa	Provenience	Biogeographical region	$\Delta^{13}C$ (‰)	$\delta^{13}C_{16:0}$ (‰)	$\delta^{13}C_{18:0}$ (‰)	Reference
Vendace	*Coregonus albula*	Finland	Boreal	-1.6	-28.4	-30.0	(Pääkkönen, Evershed and Asplund, 2020)
Vendace	*Coregonus albula*	Finland	Boreal	1.3	-29.6	-28.3	(Pääkkönen, Evershed and Asplund, 2020)
Vendace	*Coregonus albula*	Finland	Boreal	-1.0	-37.3	-38.3	(Pääkkönen, Evershed and Asplund, 2020)
Vendace	*Coregonus albula*	Finland	Boreal	1.4	-28.7	-27.3	(Pääkkönen, Evershed and Asplund, 2020)

Domestic ruminant

Common name	Taxa	Provenience	Biogeographical region	$\Delta^{13}C$ (‰)	$\delta^{13}C_{16:0}$ (‰)	$\delta^{13}C_{18:0}$ (‰)	Reference
Cattle	*Bos taurus*	Spain	Mediterranean	-0.8	-27.7	-28.5	(Colonese et al., 2015)
Cattle	*Bos taurus*	Spain	Mediterranean	-2.1	-29.4	-31.5	(Colonese et al., 2015)
Cow		Malta	Mediterranean	0.1	-25.4	-25.3	(Debono-Spiteri, 2012)
Cow		Malta	Mediterranean	-0.2	-25.4	-25.6	(Debono-Spiteri, 2012)
Sheep		Malta	Mediterranean	-2.5	-24.8	-27.3	(Debono-Spiteri, 2012)
Sheep		Malta	Mediterranean	-1.4	-25.4	-26.8	(Debono-Spiteri, 2012)
Goat		Malta	Mediterranean	-1.1	-25.8	-26.9	(Debono-Spiteri, 2012)
Goat		Malta	Mediterranean	-2.0	-23.8	-25.8	(Debono-Spiteri, 2012)
Goat		France	Mediterranean	-2.4	-28.7	-31.1	(Drieu et al., 2021)

Common name	Taxa	Provenience	Biogeographical region	$\Delta^{13}C$ (‰)	$\delta^{13}C_{16:0}$ (‰)	$\delta^{13}C_{18:0}$ (‰)	Reference
Cattle	*Bos taurus*	Spain	Mediterranean	-1.4	-23.5	-24.9	(Tarifa Mateo, 2019)
Cattle	*Bos taurus*	Spain	Mediterranean	-1.8	-22.7	-24.5	(Tarifa Mateo, 2019)
Cattle	*Bos taurus*	Spain	Mediterranean	-1.1	-26.2	-27.2	(Tarifa Mateo, 2019)
Cattle	*Bos taurus*	Spain	Mediterranean	-1.9	-29.4	-31.3	(Tarifa Mateo, 2019)
Cattle	*Bos taurus*	Spain	Mediterranean	-1.6	-24.7	-26.3	(Tarifa Mateo, 2019)
Cattle	*Bos taurus*	Spain	Mediterranean	-2.5	-24.2	-26.7	(Tarifa Mateo, 2019)
Cattle	*Bos taurus*	Spain	Mediterranean	0.1	-24.2	-24.2	(Tarifa Mateo, 2019)
Sheep	*Ovis aries*	Spain	Mediterranean	-1.0	-26.1	-27.1	(Tarifa Mateo, 2019)
Sheep	*Ovis aries*	Spain	Mediterranean	-0.9	-29.4	-30.4	(Tarifa Mateo, 2019)
Sheep	*Ovis aries*	Spain	Mediterranean	-0.3	-29.5	-29.8	(Tarifa Mateo, 2019)
Sheep	*Ovis aries*	Spain	Mediterranean	-2.9	-28.3	-31.2	(Tarifa Mateo, 2019)
Sheep	*Ovis aries*	Spain	Mediterranean	0.0	-26.5	-26.5	(Tarifa Mateo, 2019)

Wild non-ruminant

Common name	Taxa	Provenience	Biogeographical region	$\Delta^{13}C$ (‰)	$\delta^{13}C_{16:0}$ (‰)	$\delta^{13}C_{18:0}$ (‰)	Reference
Wild boar	*Sus scrofa*	Spain	Mediterranean	1.8	-25.5	-23.7	(Tarifa-Mateo et al., 2023)
Wild boar	*Sus scrofa*	Spain	Mediterranean	1.7	-25.7	-24.0	(Tarifa-Mateo et al., 2023)
Wild boar	*Sus scrofa*	Spain	Mediterranean	2.0	-25.6	-23.6	(Tarifa-Mateo et al., 2023)
Wild boar	*Sus scrofa*	Spain	Mediterranean	0.8	-25.9	-25.1	(Tarifa-Mateo et al., 2023)
Wild boar	*Sus scrofa*	Spain	Mediterranean	1.2	-26.4	-25.2	(Tarifa-Mateo et al., 2023)
Wild boar	*Sus scrofa*	Spain	Mediterranean	0.8	-25.8	-25.0	(Tarifa-Mateo et al., 2023)
Wild boar	*Sus scrofa*	Spain	Mediterranean	2.2	-26.3	-24.1	(Tarifa-Mateo et al., 2023)
Wild boar	*Sus scrofa*	Spain	Mediterranean	-0.6	-30.0	-30.6	(Tarifa-Mateo et al., 2023)
Wild boar	*Sus scrofa*	Spain	Mediterranean	0.4	-26.4	-26.0	(Tarifa-Mateo et al., 2023)
Wild boar	*Sus scrofa*	Spain	Mediterranean	0.2	-23.2	-23.0	(Tarifa-Mateo et al., 2023)
Wild boar	*Sus scrofa*	Spain	Mediterranean	1.4	-26.1	-24.7	(Tarifa-Mateo et al., 2023)
Wild boar	*Sus scrofa*	Spain	Mediterranean	-0.8	-28.4	-29.2	(Tarifa-Mateo et al., 2023)
Wild boar	*Sus scrofa*	Spain	Mediterranean	0.7	-27.1	-26.4	(Tarifa-Mateo et al., 2023)
Wild boar	*Sus scrofa*	Spain	Mediterranean	-0.9	-18.9	-19.8	(Tarifa-Mateo et al., 2023)
Wild boar	*Sus scrofa*	Spain	Mediterranean	0.0	-26.8	-26.8	(Tarifa-Mateo et al., 2023)
Wild boar	*Sus scrofa*	Spain	Mediterranean	-0.1	-26.9	-27.0	(Tarifa-Mateo et al., 2023)

Common name	Taxa	Provenience	Biogeographical region	$\Delta^{13}C$ (‰)	$\delta^{13}C_{16:0}$ (‰)	$\delta^{13}C_{18:0}$ (‰)	Reference
Wild boar	*Sus scrofa*	Spain	Mediterranean	0.2	-29.0	-28.8	(Tarifa-Mateo et al., 2023)
Wild boar	*Sus scrofa*	Spain	Mediterranean	0.4	-25.7	-25.3	(Tarifa-Mateo et al., 2023)
Wild boar	*Sus scrofa*	Spain	Mediterranean	1.5	-27.1	-25.6	(Tarifa-Mateo et al., 2023)
Wild boar	*Sus scrofa*	Spain	Mediterranean	0.3	-28.4	-28.1	(Tarifa-Mateo et al., 2023)
Wild boar	*Sus scrofa*	Spain	Mediterranean	0.5	-27.1	-26.6	(Tarifa-Mateo et al., 2023)
Wild boar	*Sus scrofa*	Spain	Mediterranean	1.5	-21.9	-20.4	(Tarifa-Mateo et al., 2023)
Wild boar	*Sus scrofa*	Spain	Mediterranean	-1.9	-22.4	-24.3	(Tarifa-Mateo et al., 2023)
Wild boar	*Sus scrofa*	Spain	Mediterranean	-3.2	-27.6	-30.8	(Tarifa-Mateo et al., 2023)
Wild boar	*Sus scrofa*	Spain	Mediterranean	-2.8	-23.5	-26.3	(Tarifa-Mateo et al., 2023)
Wild boar	*Sus scrofa*	Spain	Mediterranean	-0.4	-24.6	-25.0	(Tarifa-Mateo et al., 2023)
Wild boar	*Sus scrofa*	Spain	Mediterranean	-1.4	-32.4	-33.8	(Tarifa-Mateo et al., 2023)
Wild boar		Italy	Mediterranean	0.1	-28.4	-28.3	(Debono-Spiteri, 2012)
Rabbit	*Oryctolagus cuniculus*	Spain	Mediterranean	0.9	-31.0	-30.1	(Tarifa Mateo, 2019)
Rabbit	*Oryctolagus cuniculus*	Spain	Mediterranean	0.6	-31.6	-31.0	(Tarifa Mateo, 2019)
Rabbit	*Oryctolagus cuniculus*	Spain	Mediterranean	2.1	-30.6	-28.4	(Tarifa Mateo, 2019)
Rabbit	*Oryctolagus cuniculus*	Spain	Mediterranean	2.3	-30.9	-28.6	(Tarifa Mateo, 2019)

Wild ruminant

Common name	Taxa	Provenience	Biogeographical region	$\Delta^{13}C$ (‰)	$\delta^{13}C_{16:0}$ (‰)	$\delta^{13}C_{18:0}$ (‰)	Reference
Roe deer	*Capreolus capreolus*	Spain	Mediterranean	-0.1	-30.5	-30.6	(Tarifa Mateo, 2019)
Roe deer	*Capreolus capreolus*	Spain	Mediterranean	-0.5	-30.5	-31.0	(Tarifa Mateo, 2019)
Roe deer	*Capreolus capreolus*	Spain	Mediterranean	-1.4	-29.8	-31.2	(Tarifa Mateo, 2019)
Deer		Switzerland	Alpine	-0.9	-24.4	-25.3	(Spangenberg et al., 2010)
Mule Deer		Switzerland	Alpine	0.5	-25.2	-24.7	(Spangenberg et al., 2010)
Chamois		Switzerland	Alpine	-0.8	-26.7	-27.5	(Spangenberg et al., 2010)
Red deer		Switzerland	Alpine	-2.5	-30.1	-32.6	(Spangenberg et al., 2010)
Red deer	*Cervus elaphus*	Switzerland	Alpine	-2.2	-31.0	-33.1	(Spangenberg, Jacomet and Schibler, 2006)
Chamois	*Rupicapra rupicapra*	Switzerland	Alpine	-0.8	-28.4	-29.2	(Carrer et al., 2016)
Ibex	*Capra ibex*	Switzerland	Alpine	-2.9	-28.1	-31.0	(Carrer et al., 2016)
Roe deer	*Capreolus capreolus*	Switzerland	Alpine	-1.1	-29.6	-30.7	(Carrer et al., 2016)
Red deer	*Cervus elaphus*	Switzerland	Alpine	-4.3	-29.7	-34.0	(Carrer et al., 2016)
Chamois	*Rupicapra rupicapra*	Switzerland	Alpine	-2.4	-27.8	-30.2	(Carrer et al., 2016)
Roe deer		Germany	Continental	-3.8	-27.3	-31.1	(Debono-Spiteri, 2012)
Red deer		Germany	Continental	-1.2	-25.2	-26.4	(Debono-Spiteri, 2012)
Saiga	*Saiga tatarica*	Russia (SE)	Steppic	-2.5	-23.9	-26.4	(Dolbunova et al., 2023)

Common name	Taxa	Provenience	Biogeographical region	$\Delta^{13}C$ (‰)	$\delta^{13}C_{16:0}$ (‰)	$\delta^{13}C_{18:0}$ (‰)	Reference
Roe deer	*Capreolus capreolus*	Russia (SE)	Steppic	-1.3	-31.1	-32.4	(Bondetti et al., 2021b)
Deer		Russia (SE)	Steppic	-3.3	-28.7	-32.0	(Bondetti et al., 2021b)
Reindeer	*Rangifer tarandus*	Russia (NE)	Boreal	-1.1	-23.8	-24.9	(Bondetti et al., 2021b)
Elk	*Alces alces*	Russia (NE)	Boreal	-1.5	-30.5	-32.0	(Bondetti et al., 2021b)
Elk	*Alces alces*	Russia (NE)	Boreal	-1.1	-29.8	-31.0	(Bondetti et al., 2021b)
Elk	*Alces alces*	Russia (NE)	Boreal	-1.6	-33.2	-34.8	(Bondetti et al., 2021b)
Reindeer	*Rangifer tarandus*	Russia	Boreal	-4.7	-28.2	-32.9	(March, 2013)
Reindeer	*Rangifer tarandus*	Russia	Boreal	-4.9	-28.1	-33.0	(March, 2013)
Red deer	*Cervus elaphus*	Poland	Continental	-3.8	-27.6	-31.4	(Craig et al., 2012)
Red deer	*Cervus elaphus*	Poland	Continental	-3.7	-27.3	-31.0	(Craig et al., 2012)
Red deer	*Cervus elaphus*	Poland	Continental	-4.2	-28.3	-32.5	(Craig et al., 2012)
Red deer	*Cervus elaphus*	Poland	Continental	-3.7	-29.9	-33.6	(Craig et al., 2012)
Red deer	*Cervus elaphus*	Poland	Continental	-3.6	-29.0	-32.6	(Craig et al., 2012)
Red deer	*Cervus elaphus*	Poland	Continental	-4.2	-28.7	-32.9	(Craig et al., 2012)
Red deer	*Cervus elaphus*	Poland	Continental	-2.6	-30.3	-32.9	(Craig et al., 2012)
Red deer	*Cervus elaphus*	Poland	Continental	-3.6	-29.4	-33.0	(Craig et al., 2012)
Red deer	*Cervus elaphus*	Poland	Continental	-3.4	-28.8	-32.2	(Craig et al., 2012)

Common name	Taxa	Provenience	Biogeographical region	$\Delta^{13}C$ (‰)	$\delta^{13}C_{16:0}$ (‰)	$\delta^{13}C_{18:0}$ (‰)	Reference
Red deer	*Cervus elaphus*	Poland	Continental	-3.6	-29.3	-32.9	(Craig et al., 2012)
Red deer	*Cervus elaphus*	UK	Atlantic	-1.6	-32.0	-33.6	(Lucquin, Gibbs and Uchiyama, 2016)
Roe deer	*Capreolus capreolus*	Denmark	Atlantic	-0.5	-29.2	-29.7	(Colonese et al., 2015)
Red deer	*Cervus elaphus*	UK	Atlantic	-1.4	-28.3	-29.7	(Dudd, 1999)
Red deer	*Cervus elaphus*	UK	Atlantic	-1.7	-28.8	-30.5	(Dudd, 1999)
Red deer	*Cervus elaphus*	UK	Atlantic	-0.3	-29.4	-29.7	(Dudd, 1999)
Red deer	*Cervus elaphus*	UK	Atlantic	-3.3	-28.8	-32.1	(Dudd, 1999)
Red deer	*Cervus elaphus*	UK	Atlantic	-5.2	-28.0	-33.2	(Dudd, 1999)
Red deer	*Cervus elaphus*	UK	Atlantic	-3.1	-30.7	-33.8	(Dudd, 1999)
Red deer	*Cervus elaphus*	UK	Atlantic	-2.8	-30.8	-33.6	(Dudd, 1999)
Eurasian elk	*Alces alces*	Finland	Boreal	-2.4	-29.8	-32.2	(Pääkkönen, Evershed and Asplund, 2020)
Eurasian elk	*Alces alces*	Finland	Boreal	-1.6	-29.0	-30.6	(Pääkkönen, Evershed and Asplund, 2020)
Eurasian elk	*Alces alces*	Finland	Boreal	-2.2	-28.8	-31.0	(Pääkkönen, Evershed and Asplund, 2020)
Eurasian elk	*Alces alces*	Finland	Boreal	-1.9	-30.5	-32.4	(Pääkkönen, Evershed and Asplund, 2020)
Reindeer	*Rangifer tarandus*	Finland	Boreal	-2.8	-23.8	-26.6	(Pääkkönen, Evershed and Asplund, 2020)
Reindeer	*Rangifer tarandus*	Finland	Boreal	-2.9	-23.7	-26.6	(Pääkkönen, Evershed and Asplund, 2020)
Wild forest	*Rangifer tarandus*	Finland	Boreal	-3.1	-24.8	-27.9	(Pääkkönen, Evershed and Asplund, 2020)

Common name	Taxa	Provenience	Biogeographical region	$\Delta^{13}C$ (‰)	$\delta^{13}C_{16:0}$ (‰)	$\delta^{13}C_{18:0}$ (‰)	Reference
reindeer	*fennicus*						
Wild forest reindeer	*Rangifer tarandus fennicus*	Finland	Boreal	-1.8	-24.5	-26.3	(Pääkkönen, Evershed and Asplund, 2020)
Wild forest reindeer	*Rangifer tarandus fennicus*	Finland	Boreal	-1.2	-25.4	-26.6	(Pääkkönen, Evershed and Asplund, 2020)

Annex 4

All raw chromatograms generated during the lipid and molecular analyses presented in this study are available online at the following repository organised by sites and type of extraction: (https://drive.google.com/drive/folders/12a3syfEOGfsXrY4EfzAmmZgl5LcK9FNK?usp=sharing).

These data provide the foundation for the interpretations discussed in the main text and are accessible for verification or further study. In the sections that follow, a dedicated sheet is provided for each Heat-Altered Stone (HAS) and sediment, presenting a comprehensive overview of their characteristics, organised by sites. Each sheet includes detailed information on the archaeological context of stones and sediments, the morphology of the HAS, the results of protein and lipid analyses including identified molecules and diagnostic biomarkers, and carbon stable isotope measurements with relevant interpretations. Collectively, these sheets integrate analytical, contextual, and morphological information, offering a complete picture of each HAS and sediment sample facilitating comparison across the assemblage.

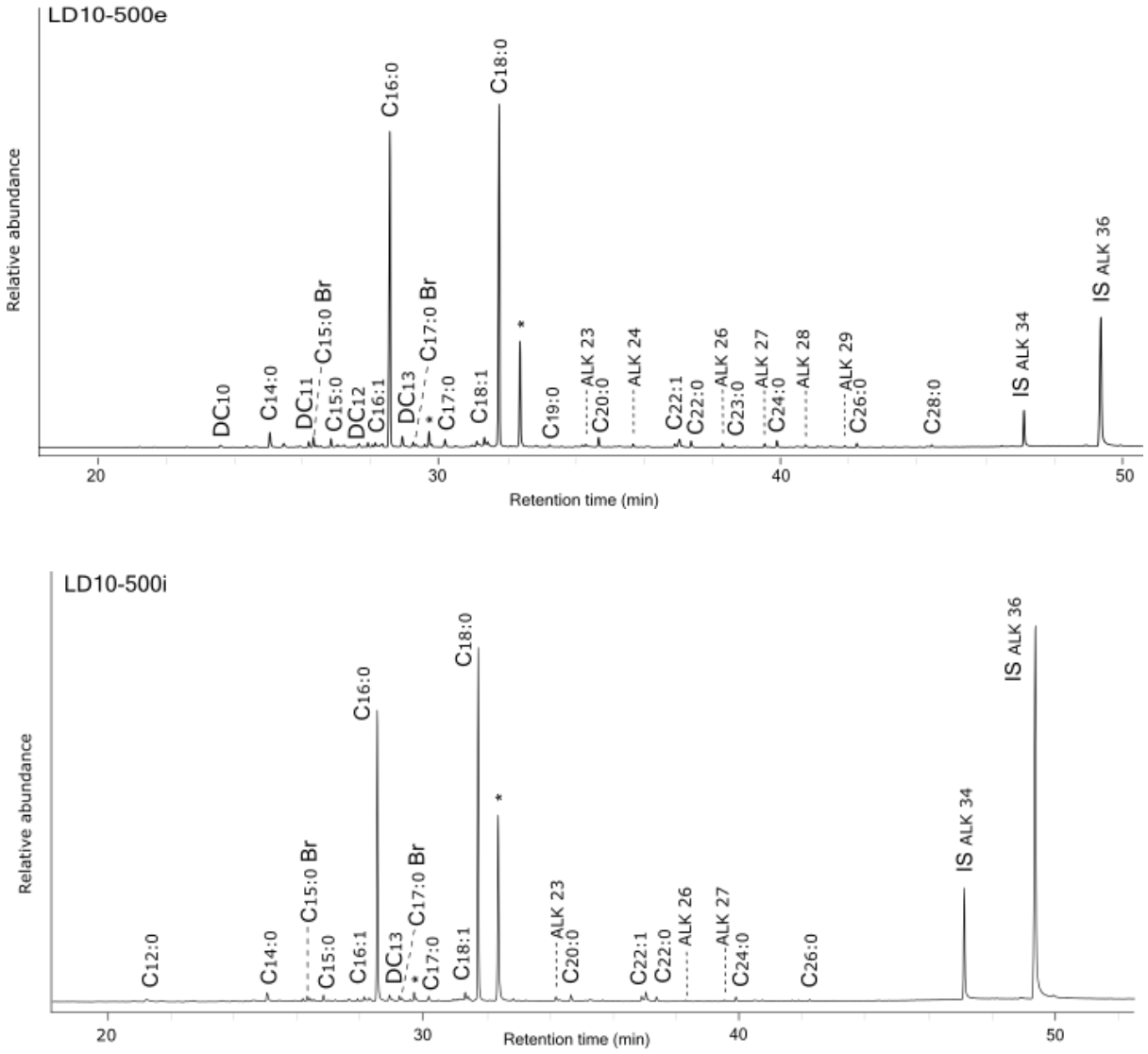
La Draga - Datasheet

		Sample id:	**LD10-500**
		info:	Sector D, level VI, grid KA80 More recent occupation
		Mineral:	Sandstone
		Dimension:	97, 91, 79 mm 489 g
Morphology:	Prismatic	3D:	https://skfb.ly/puzEx
Alteration patterns:	-		

Lipid analysis

	Lipid yield ($\mu g\ g^{-1}$)	P/S	O/S	$\delta^{13}C_{16:0}$ (‰)	$\delta^{13}C_{18:0}$ (‰)	$\Delta^{13}C$ (‰)	Lipid content
External (e)	162.57	0.95	24.95	-29.75	-27.78	1.96	SFA (C14-20, C22-24, C26, C28), BrFA (C15, C17), UFA (C16:1, C18:1, C22:1), DC (C10-11, C12, C13), ALK (C23, C24, C26, C27, C28, C29), pri, phy (28% SRR)
Internal (i)	42.91	0.92		-29.75	-28.26	1.49	SFA (C12, C14-18, C20, C22, C24, C26), BrFA (C15, C17), UFA (C16:1, C18:1, C22:1), DC (C13), ALK (C23, C26, C27), pri (tr)

Molecular signature:	Mixed resources
HAS interpretation:	Combustion feature



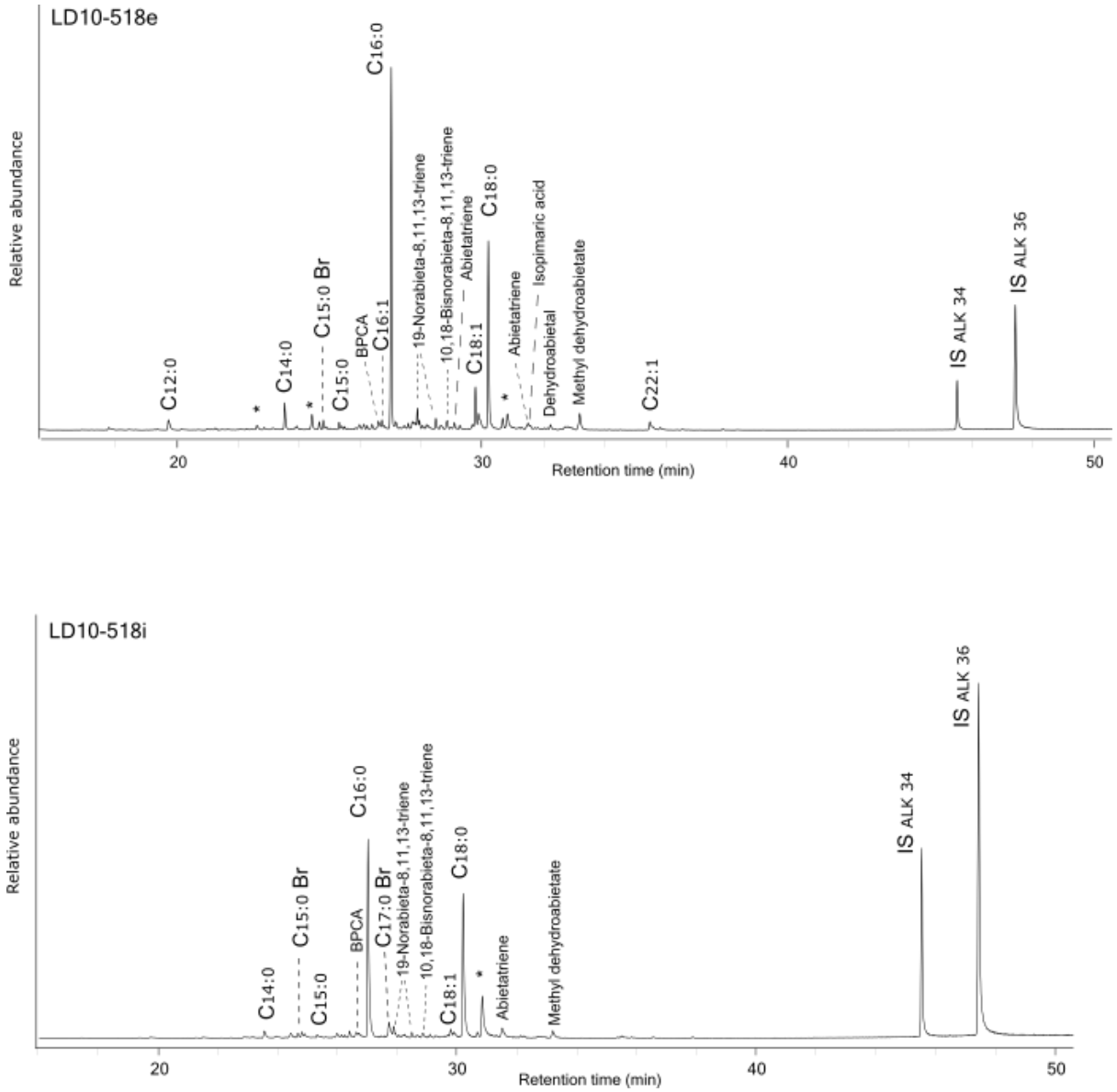
Partial total ion chromatograms (TIC) of acid/methanol extract of sample LD10-500e/i showing saturated fatty acids ($C_{XX:0}$), branched ($C_{XX:0}$ Br), unsaturated fatty acids ($C_{XX:1}$), diacids (DC_{XX}), *n*-alkanes (ALK xx), contaminants (*), and *n*-alkanes internal standards (IS_{ALKXX}).

		Sample id:	**LD10-518**
		info:	Sector D, level VI, grid KD81 More recent occupation
		Mineral:	Sandstone
		Dimension:	79, 77, 62 mm 230 g
Morphology:	Prismatic	3D:	https://skfb.ly/puzEx
Alteration patterns:	Cracks, sooting, discoloration		

Lipid analysis

	Lipid yield ($\mu g\ g^{-1}$)	P/S	O/S	$\delta^{13}C_{16:0}$ (‰)	$\delta^{13}C_{18:0}$ (‰)	$\Delta^{13}C$ (‰)	Lipid content
External (e)	39.24	1.48	2.35	-29.73	-30.29	-0.56	SFA (C12, C14-16, C18), BrFA (C15), UFA (C16:1, C18:1, C22:1), terp (19-Norabieta-8,11,13-triene, 10,18-Bisnorabieta-8,11,13-triene, Isopimaric acid, Abietatriene, Dehydroabietal, Methyl dehydroabietate), pri (tr), B3CA (tr)
Internal (i)	5.36	1.33	14.04	-31.80	-30.91	0.89	SFA (C14-16, C18), BrFA (C15, C17), UFA (C18:1), terp (19-Norabieta-8,11,13-triene, 10,18-Bisnorabieta-8,11,13-triene, Abietatriene, Methyl dehydroabietate), pri (tr), B3CA (tr)

Molecular signature:	Coniferous resin
HAS interpretation:	Hand-held tool



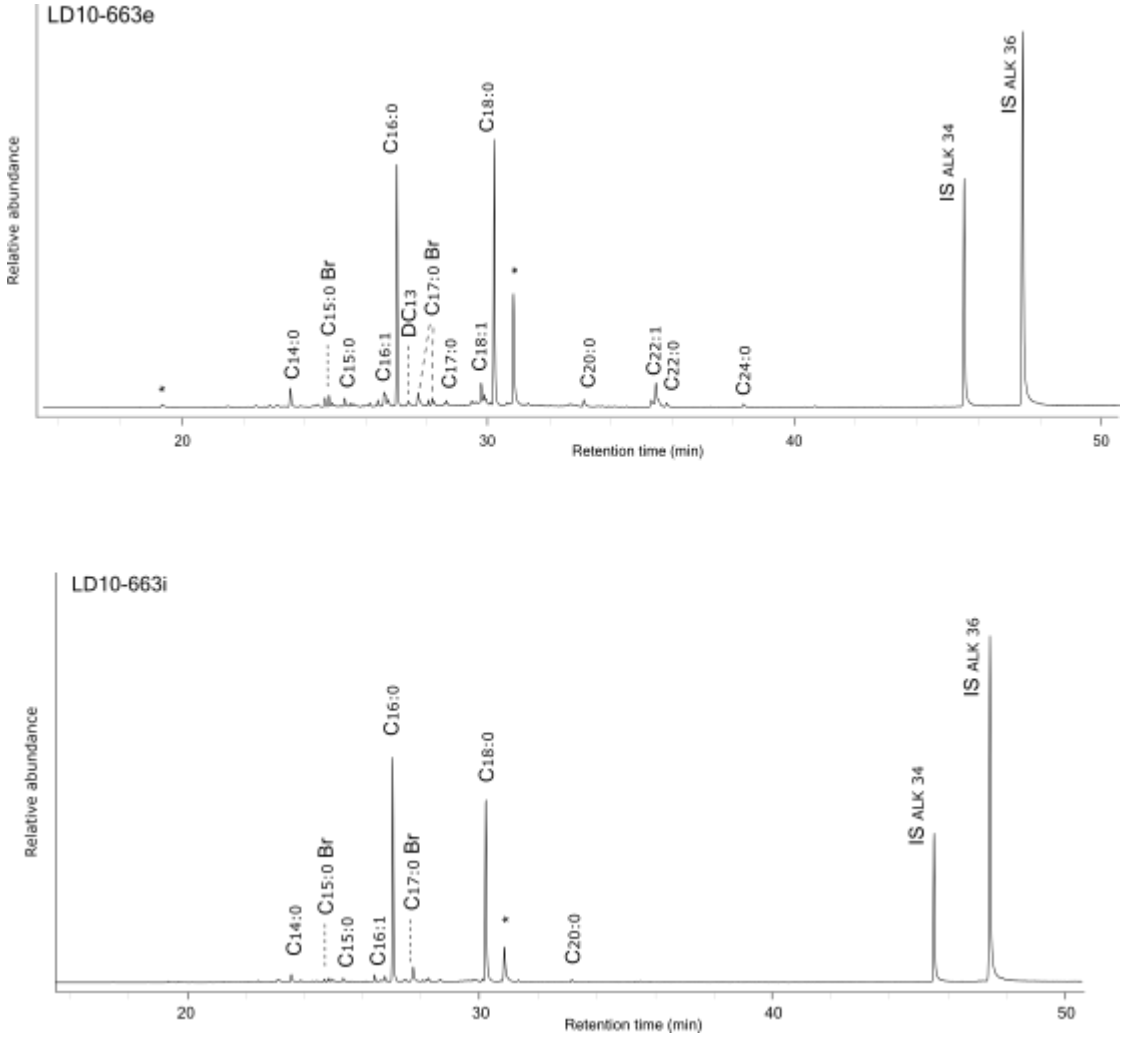
Partial total ion chromatograms (TIC) of acid/methanol extract of sample LD10-518e/i showing saturated fatty acids ($C_{XX:0}$), branched ($C_{XX:0}$ Br), unsaturated fatty acids ($C_{XX:1}$), benzene polycarboxylic acid (BPCA), terpenoids, *n*-alkanes (ALK xx), contaminants (*), and *n*-alkanes internal standards (IS $_{ALKXX}$).

		Sample id:	**LD10-663**
		info:	Sector D, level VII, grid JJ78 Oldest occupation
		Mineral:	Limestone
		Dimension:	174, 140, 48 mm 890 g
Morphology:	Tabular	3D:	https://skfb.ly/puzEx
Alteration patterns:	-		

Lipid analysis

	Lipid yield ($\mu g\ g^{-1}$)	P/S	O/S	$\delta^{13}C_{16:0}$ (‰)	$\delta^{13}C_{18:0}$ (‰)	$\Delta^{13}C$ (‰)	Lipid content
External (e)	8.47	0.96	11.89	-30.40	-30.00	0.40	SFA (C14-18, C20, C22, C24), BrFA (C15, C17), UFA (C16:1, C18:1, C22:1), DC (C13), pri (tr), phy (49% SRR)
Internal (i)	10.01	1.28		-31.42	-30.27	1.15	SFA (C14-16, C18, C20), BrFA (C15, C17), UFA (C16:1)

Molecular signature:	Plant resources
HAS interpretation:	Grinder base



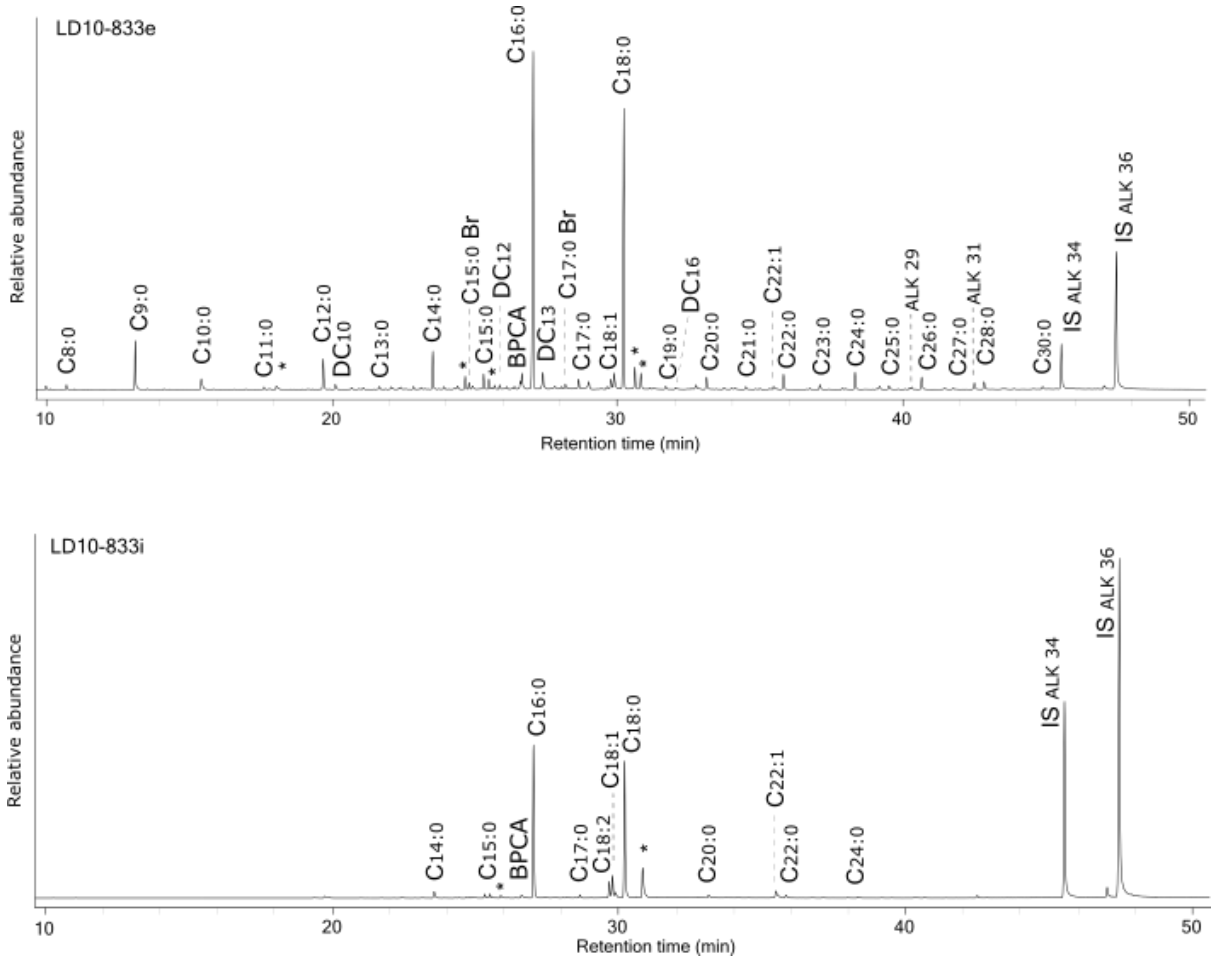
Partial total ion chromatograms (TIC) of acid/methanol extract of sample LD10-663e/i showing saturated fatty acids ($C_{XX:0}$), branched ($C_{XX:0}$ Br), unsaturated fatty acids ($C_{XX:1}$), diacids (DC_{XX}), *n*-alkanes (ALK xx), contaminants (*), and *n*-alkanes internal standards (IS $_{ALKXX}$).

		Sample id:	**LD10-833**
		info:	Sector D, level VII, grid JJ79 Oldest occupation
		Mineral:	Limestone
		Dimension:	72, 60, 47 mm 163 g
Morphology:	Spherical	3D:	https://skfb.ly/puzEx
Alteration patterns:	Discoloration		

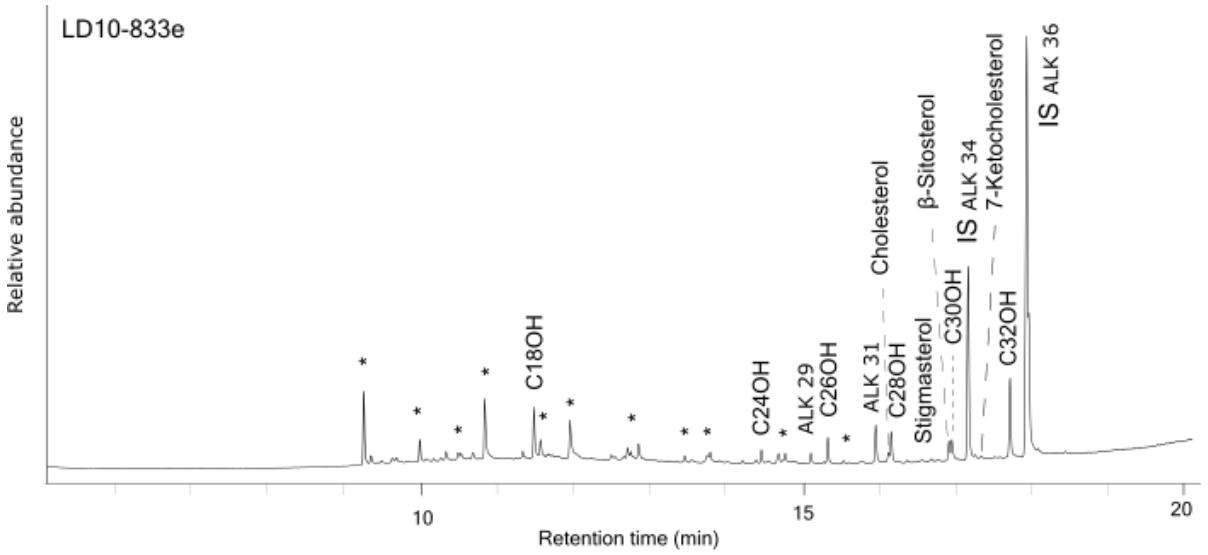
Lipid analysis

	Lipid yield ($\mu g\ g^{-1}$)	P/S	O/S	$\delta^{13}C_{16:0}$ (‰)	$\delta^{13}C_{18:0}$ (‰)	$\Delta^{13}C$ (‰)	Lipid content
External (e)	137.42	1.27	6.28	-28.90	-29.30	-0.40	SFA (C8-C27, C28, C30), BrFA (C15, C17), UFA (C18:1, C22:1), DC (C10, C12, C13, C16), ALK (C29, C31), OH (C18, C24, C26, C28, C30, C32), 4,8,12-TMTD, pri, phy (67% SRR), ster (Cholesterol, 7-keto-cholesterol, Stigmasterol, β-Sitosterol), B3CA (tr)
Internal (i)	7.35	1.21	11.22	-29.40	-29.77	-0.37	SFA (C14-18, C20, C22, C24), UFA (C18:1, C18:2, C22:1), pri, phy (60% SRR), B3CA (tr)

Molecular signature:	Plant resources
HAS interpretation:	Grinder



Partial total ion chromatograms (TIC) of acid/methanol extract of sample LD10-833e/i showing saturated fatty acids ($C_{XX:0}$), branched ($C_{XX:0}$ Br), unsaturated fatty acids ($C_{XX:1}$), benzene polycarboxylic acid (BPCA), diacids (DC_{XX}), *n*-alkanes (ALK xx), contaminants (*), and *n*-alkanes internal standards (IS_{ALKXX}).



Partial total ion chromatograms (TIC) of solvent extract of sample LD10-833e showing alcohols (CxxOH), *n*-alkanes (ALK xx), sterols and derivatives, contaminants (*), and *n*-alkanes internal standards (IS $_{ALKXX}$).

		Sample id:	**LD11-1540**
		info:	Sector D, level VI, grid JD81 More recent occupation
		Mineral:	Sandstone
		Dimension:	55, 48, 39 mm 98 g
Morphology:	Spherical	3D:	https://skfb.ly/puzEx
Alteration patterns:	Discoloration		

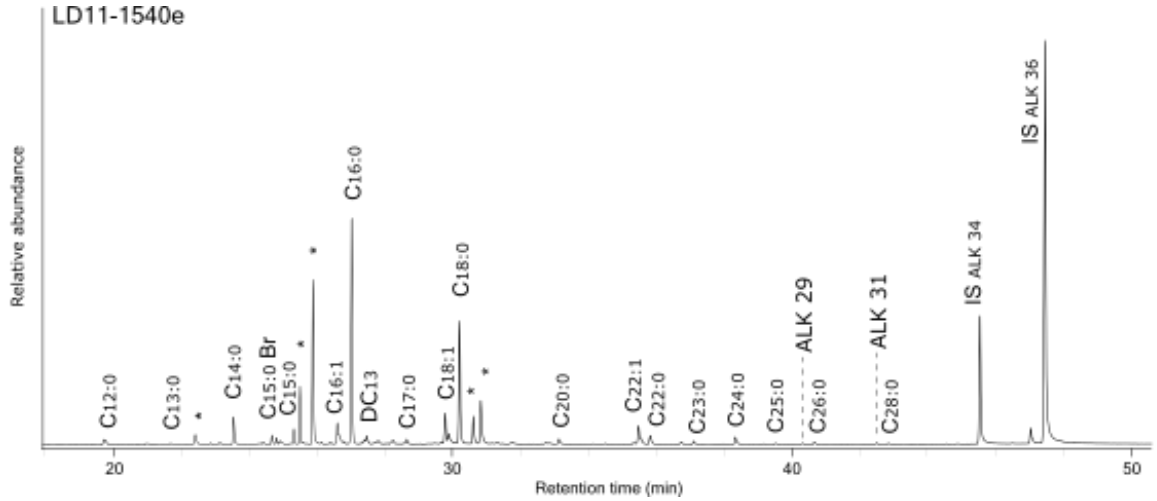
Lipid analysis

	Lipid yield ($\mu g\ g^{-1}$)	P/S	O/S	$\delta^{13}C_{16:0}$ (‰)	$\delta^{13}C_{18:0}$ (‰)	$\Delta^{13}C$ (‰)	Lipid content
External (e)	28.51	1.81	2.79	-28.54	-29.14	-0.60	SFA (C12-18, C20, C22-26, C28), BrFA (C15), UFA (C16:1, C18:1, C22:1), DC (C13), ALK (C29, C31), pri, phy (63% SRR)
Internal (i)	-	-	-	-	-	-	-

Molecular signature:	Plant resources
HAS interpretation:	Grinder

Protein analysis

Molecular signature:	-



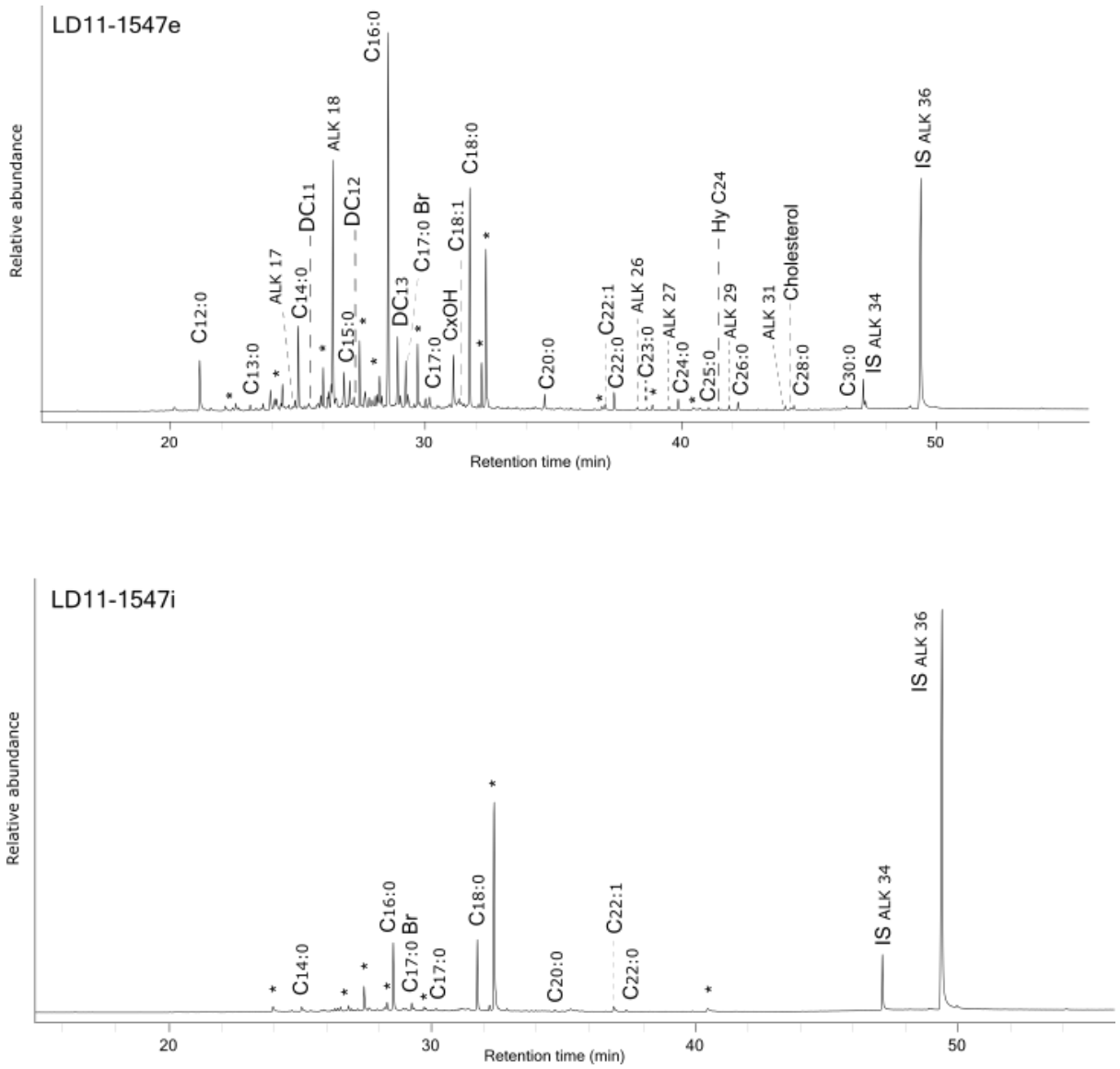
Partial total ion chromatograms (TIC) of acid/methanol extract of sample LD10-1540e showing saturated fatty acids ($C_{XX:0}$), branched ($C_{XX:0}$ Br), unsaturated fatty acids ($C_{XX:1}$), diacids (DC_{XX}), *n*-alkanes (ALK xx), contaminants (*), and *n*-alkanes internal standards (IS_{ALKXX}).

		Sample id:	**LD11-1547**
		info:	Sector D, level VIa, grid JB81 Oldest occupation
		Mineral:	Sandstone
		Dimension:	94, 87, 29 mm 90 g
Morphology:	Pot-lid	3D:	https://skfb.ly/puzEx
Alteration patterns:	-		

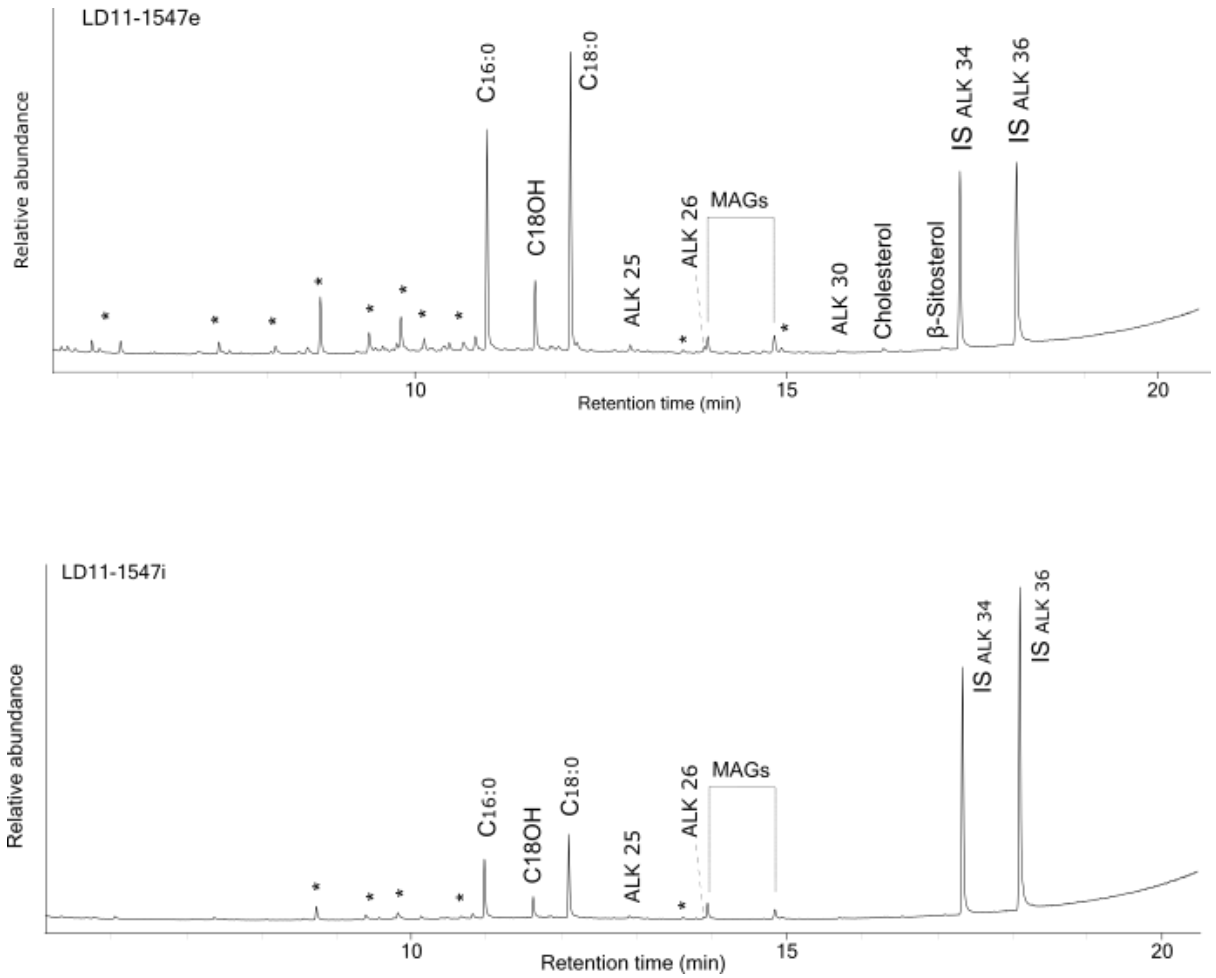
Lipid analysis

	Lipid yield ($\mu g\ g^{-1}$)	P/S	O/S	$\delta^{13}C_{16:0}$ (‰)	$\delta^{13}C_{18:0}$ (‰)	$\Delta^{13}C$ (‰)	Lipid content
External (e)	407.00	1.89	7.55	-29.88	-28.58	1.30	SFA (C12-18, C20, C22-26, C28, C30), BrFA (C17), UFA (C18:1, C22:1), Hy (C24), DC (C11, C12, 13), ALK (C17, C18, C25, C26, C27, C29-31), OH (C18), 4,8,12-TMTD (tr), pri, phy (62% SRR), ster (Cholesterol, β-Sitosterol), MAGs
Internal (i)	27.14	1.20		-30.66	-29.63	1.03	SFA (C14, C16-18, C20, C22), BrFA (C17), UFA (C22:1), ALK (C25), OH (C18), pri (tr), phy (48% SRR), MAGs

Molecular signature:	Mixed resources
HAS interpretation:	Culinary feature



Partial total ion chromatograms (TIC) of acid/methanol extract of sample LD11-1547e/i showing saturated fatty acids ($C_{XX:0}$), branched ($C_{XX:0}$ Br), unsaturated fatty acids ($C_{XX:1}$), diacids (DC_{XX}), *n*-alkanes (ALK xx), hydroxy fatty acids (Hy Cxx), contaminants (*), and *n*-alkanes internal standards (IS_{ALKXX}).



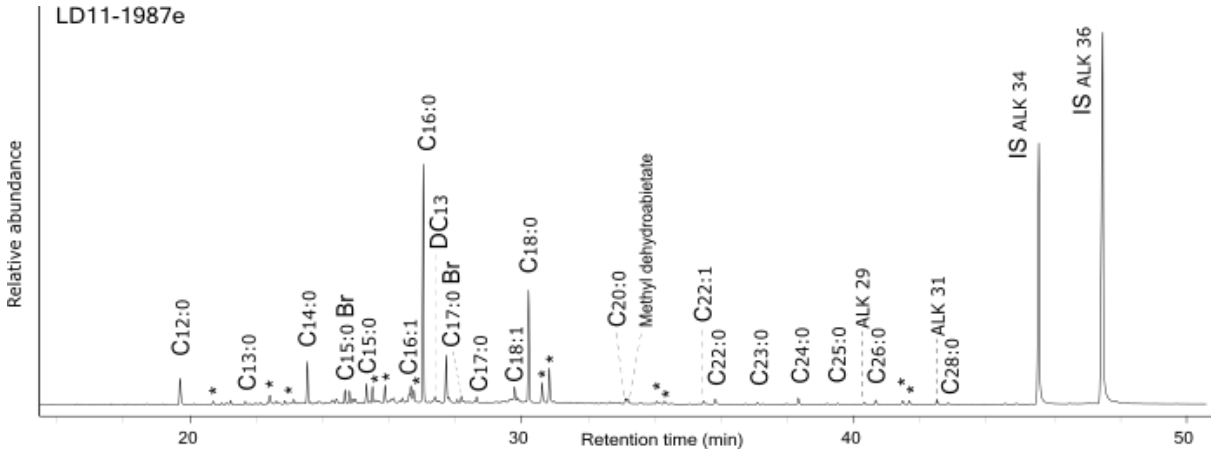
Partial total ion chromatograms (TIC) of solvent extract of sample LD11-1547e/i showing saturated fatty acids ($C_{XX:0}$), alcohols (CxxOH), *n*-alkanes (ALK xx), monoacylglycerols (MAGs), sterols and derivatives, contaminants (*), and *n*-alkanes internal standards (IS $_{ALKXX}$).

		Sample id:	**LD11-1987**
		info:	Sector D, level VIa, grid JB81 More recent occupation
		Mineral:	Sandstone
		Dimension:	105, 70, 30 mm 202 g
Morphology:	Pot-lid	3D:	https://skfb.ly/puzEx
Alteration patterns:	Cracks		

Lipid analysis

	Lipid yield ($\mu g\ g^{-1}$)	P/S	O/S	$\delta^{13}C_{16:0}$ (‰)	$\delta^{13}C_{18:0}$ (‰)	$\Delta^{13}C$ (‰)	Lipid content
External (e)	16.98	2.20	7.28	-32.90	-29.30	3.60	SFA (C12-18, C20, C22-26, C28), BrFA (C15, C17), UFA (C16:1, C18:1, C22:1), DC (C13), ALK (C29, C31), terp (Methyl dehydroabietate), 4,8,12-TMTD, pri, phy (57% SRR)
Internal (i)	-	-	-	-	-	-	-

Molecular signature:	Coniferous resin
HAS interpretation:	Combustion feature



Partial total ion chromatograms (TIC) of acid/methanol extract of sample LD11-1987e showing saturated fatty acids ($C_{XX:0}$), branched ($C_{XX:0}$ Br), unsaturated fatty acids ($C_{XX:1}$), diacids (DC_{XX}), *n*-alkanes (ALK xx), diterpenoids, contaminants (*), and *n*-alkanes internal standards (IS_{ALKXX}).

		Sample id:	**LD11-2156**
		info:	Sector D, level VII, grid JD78 Oldest occupation
		Mineral:	Sandstone
		Dimension:	87, 54, 53 mm 205 g
Morphology:	Prismatic	3D:	https://skfb.ly/puzEx
Alteration patterns:	Sooting, discoloration, superficial deposit		

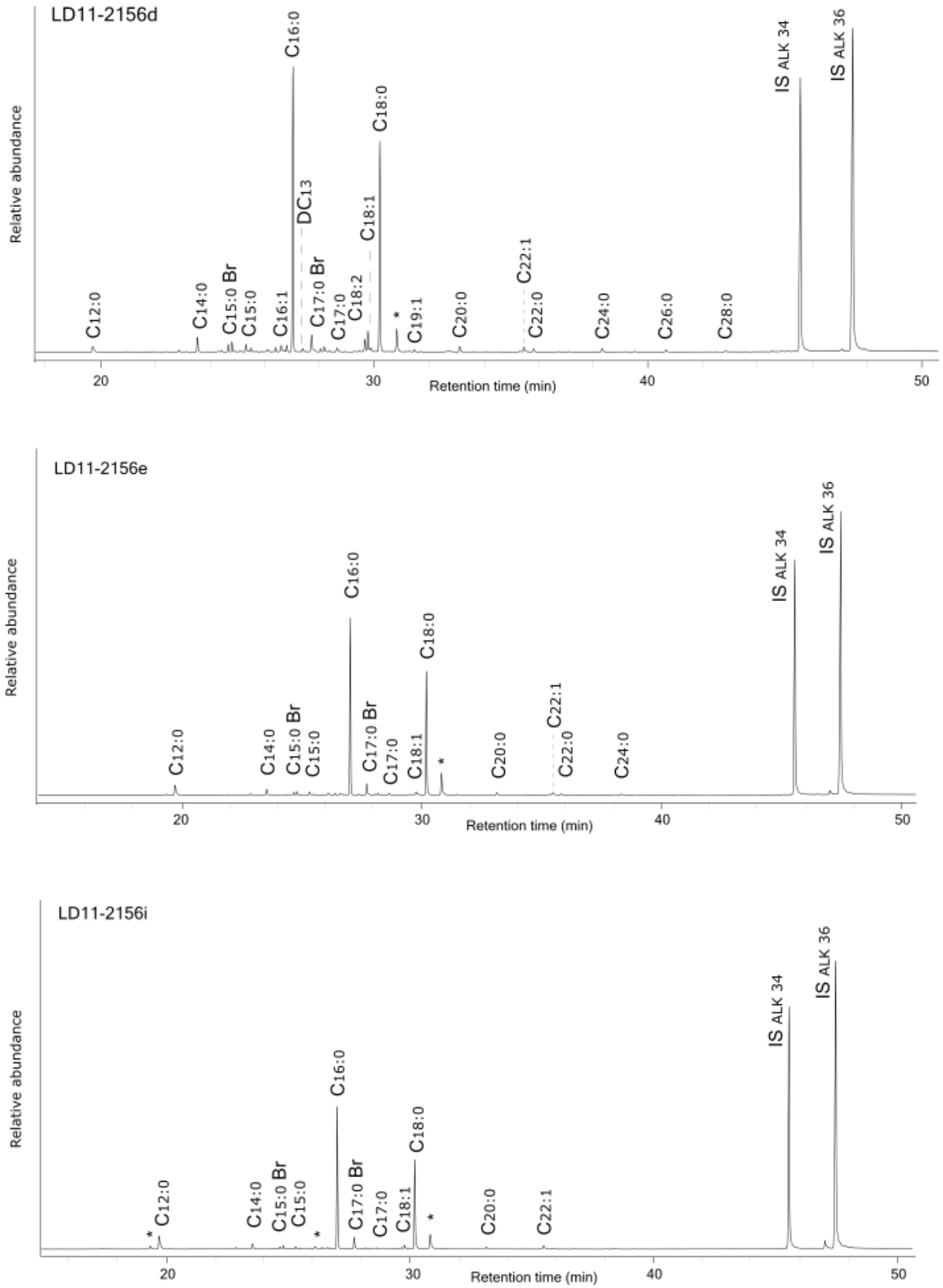
Lipid analysis

	Lipid yield ($\mu g\ g^{-1}$)	P/S	O/S	$\delta^{13}C_{16:0}$ (‰)	$\delta^{13}C_{18:0}$ (‰)	$\Delta^{13}C$ (‰)	Lipid content
Deposit (d)	11.80	1.50	8.18	-30.30	-30.60	-0.30	SFA (C12, C14-18, C20, C22, C24, C26, C28), BrFA (C15, C17), UFA (C16:1, C18:1, C18:2, C19:1, C22:1), DC (C13), 4,8,12-TMTD, pri, phy (32% SRR)
External (e)	6.38	1.99		-31.10	-30.50	0.60	SFA (C12, C14-18, C20, C22, C24), BrFA (C15, C17), UFA (C18:1, C22:1), pri
Internal (i)	6.99	1.74		-31.48	-30.43	1.05	SFA (C12, C14-18, C20), BrFA (C15, C17), UFA (C18:1, C22:1), pri

Molecular signature:	-
HAS interpretation:	-

Protein analysis

Molecular signature:	-



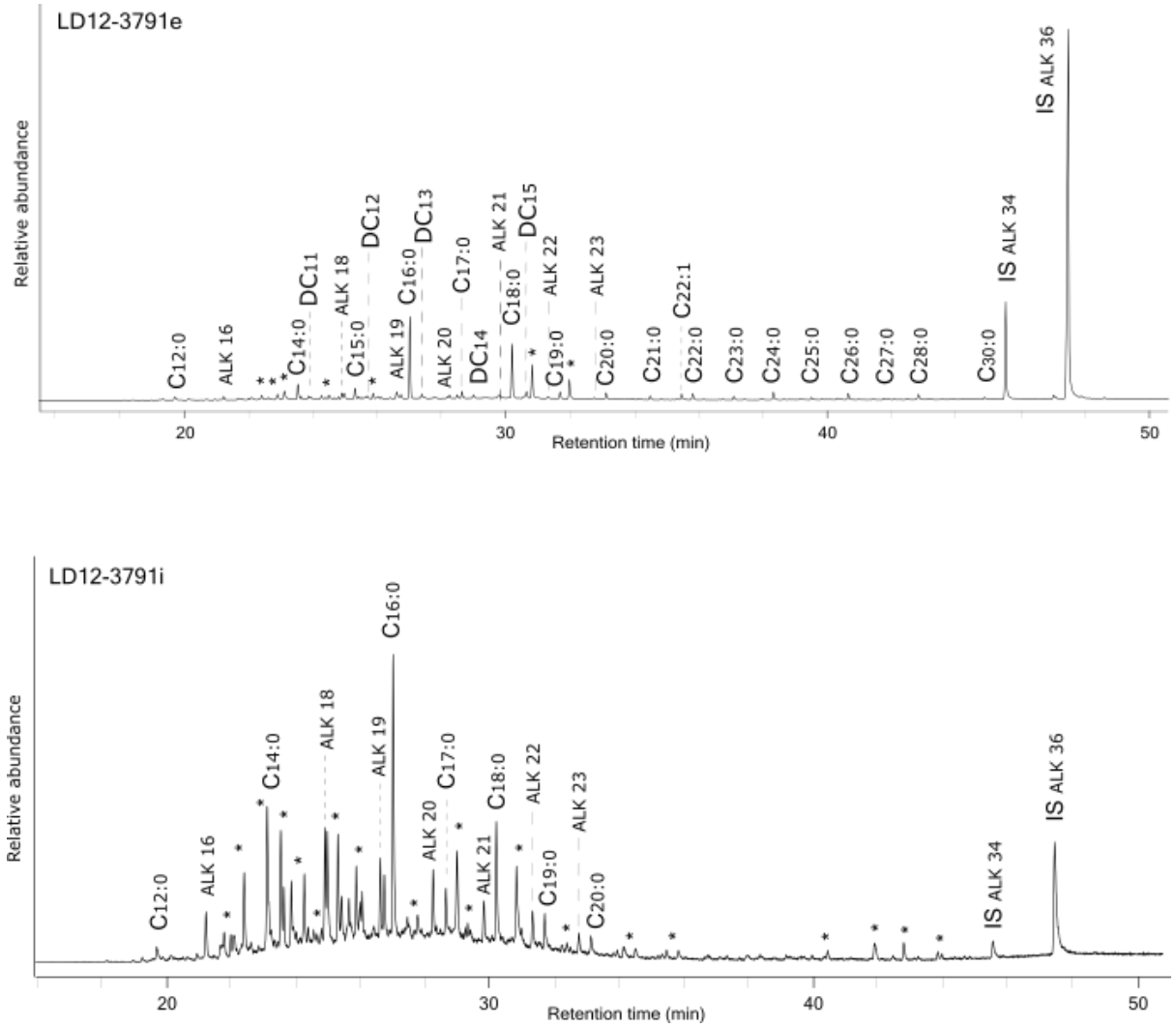
Partial total ion chromatograms (TIC) of acid/methanol extract of sample LD11-2156d/e/i showing saturated fatty acids ($C_{XX:0}$), branched fatty acids ($C_{XX:0}$ Br), unsaturated fatty acids ($C_{XX:1}$), diacids (DC_{XX}), contaminants (*), and *n*-alkanes internal standards (IS $_{ALKXX}$).

		Sample id:	**LD12-3791**
		info:	Sector D, level VII, grid JC81 Oldest occupation
		Mineral:	Marl
		Dimension:	114, 41, 40 mm 254 g
Morphology:	Tabular	3D:	https://skfb.ly/puzEx
Alteration patterns:	Cracks		

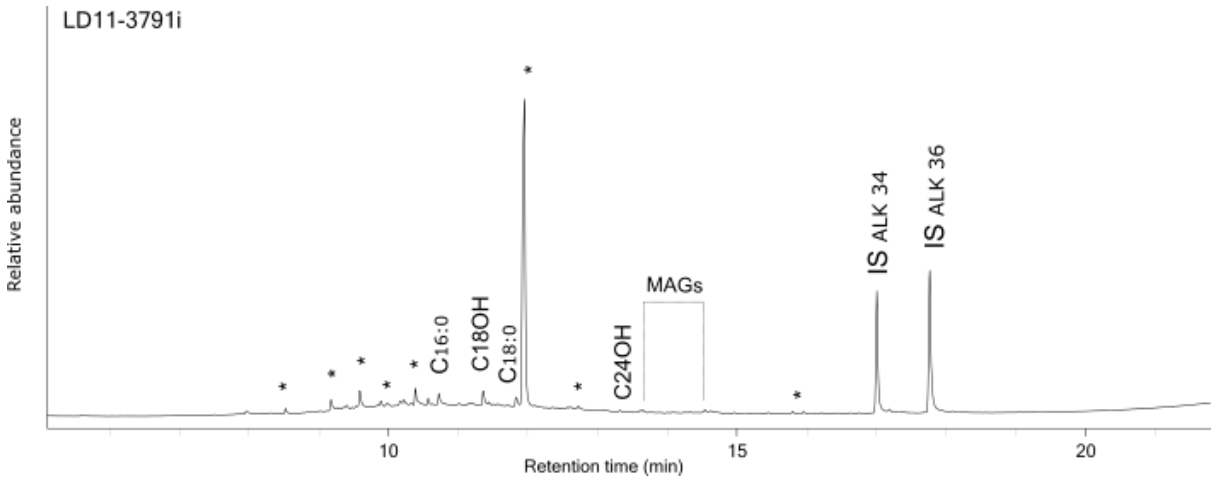
Lipid analysis

	Lipid yield ($\mu g\ g^{-1}$)	P/S	O/S	$\delta^{13}C_{16:0}$ (‰)	$\delta^{13}C_{18:0}$ (‰)	$\Delta^{13}C$ (‰)	Lipid content
External (e)	15.76	1.66		-29.90	-29.60	0.30	SFA (C12, C14-28, C30), UFA (C22:1), DC (C11, C12-15), ALK (C16, C18-23), 4,8,12-TMTD (tr), pri, phy (68% SRR)
Internal (i)	55.27	1.58		-28.36	-29.85	-1.49	SFA (C12, C14, C16-20), ALK (C16, C18-23), OH (C18, C24), MAGs

Molecular signature:	-
HAS interpretation:	Combustion feature



Partial total ion chromatograms (TIC) of acid/methanol extract of sample LD12-3791e/i showing saturated fatty acids ($C_{XX:0}$), unsaturated fatty acids ($C_{XX:1}$), diacids (DC_{XX}), *n*-alkanes (ALK xx), contaminants (*), and *n*-alkanes internal standards (IS $_{ALKXX}$).



Partial total ion chromatograms (TIC) of solvent extract of sample LD12-3791i showing saturated fatty acids ($C_{XX:0}$), alcohols (CxxOH), monoacylglycerols (MAGs), contaminants (*), and *n*-alkanes internal standards (IS $_{ALKXX}$).

		Sample id:	**LD12-3951**
		info:	Sector D, level VIa, grid JA81 More recent occupation
		Mineral:	Marl
		Dimension:	255, 170, 35 mm 1,685 g
Morphology:	Tabular	3D:	https://skfb.ly/puzEx
Alteration patterns:	Cracks, sooting, discoloration, superficial deposit		

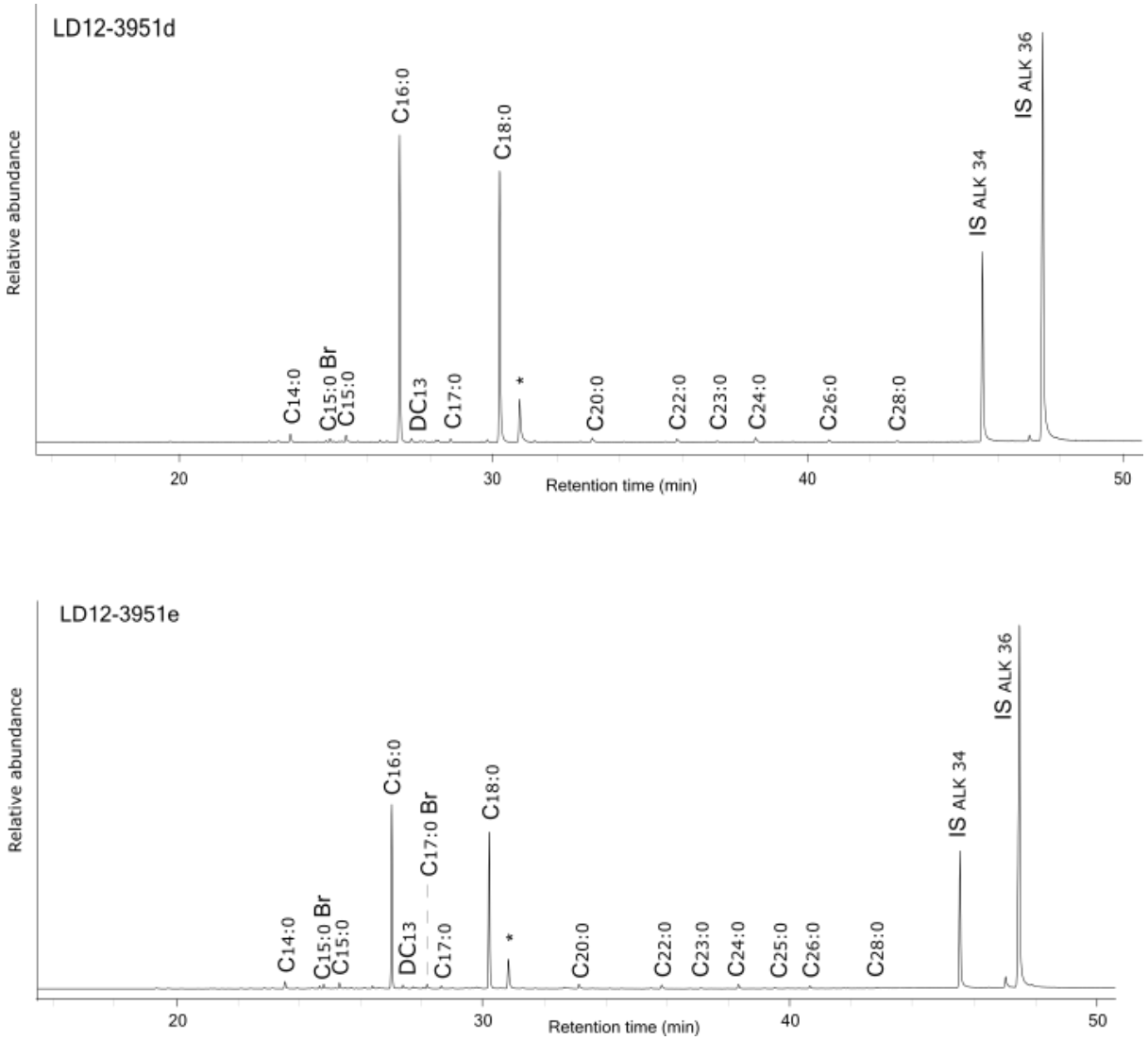
Lipid analysis

	Lipid yield ($\mu g\ g^{-1}$)	P/S	O/S	$\delta^{13}C_{16:0}$ (‰)	$\delta^{13}C_{18:0}$ (‰)	$\Delta^{13}C$ (‰)	Lipid content
Deposit (d)	12.75	1.03		-30.00	-30.00	0.00	SFA (C14-18, C20, C22-24, C26, C28), BrFA (C15), DC (C13), pri, phy (33% SRR)
External (e)	15.96	1.14		-30.20	-30.60	-0.40	SFA (C14-18, C20, C22-26, C28), BrFA (C15, C17), DC (C13), pri
Internal (i)	-	-	-	-	-	-	-

Molecular signature:	-
HAS interpretation:	Griddle/Support surface

Protein analysis

Molecular signature:	-



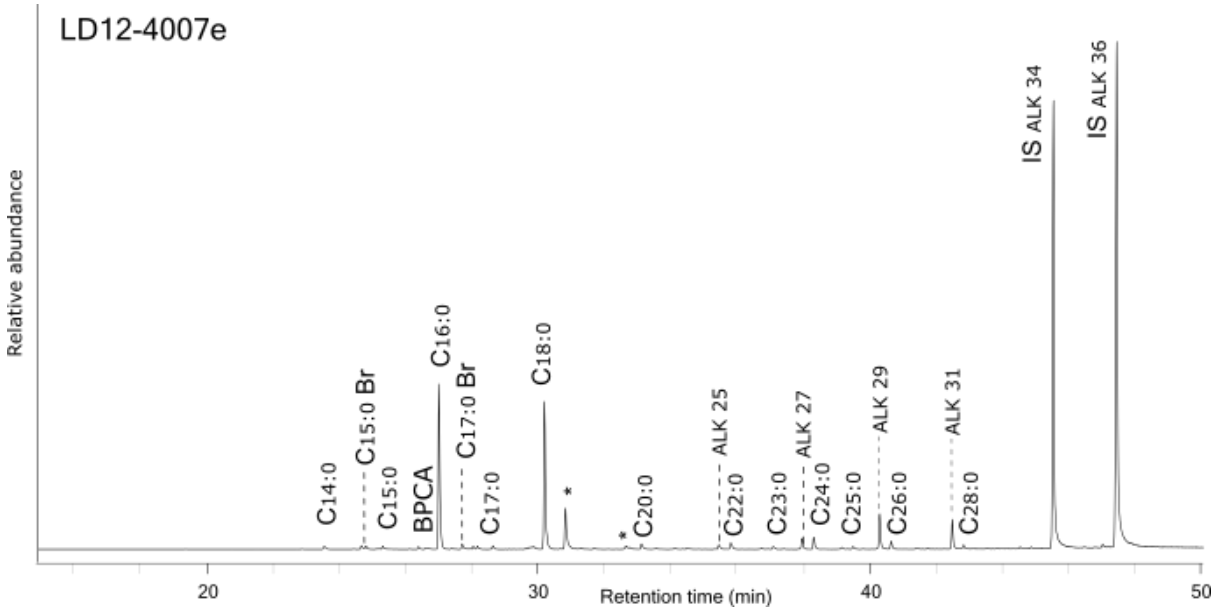
Partial total ion chromatograms (TIC) of acid/methanol extract of sample LD12-3951d/e showing saturated fatty acids ($C_{XX:0}$), branched fatty acids ($C_{XX:0}$ Br), diacids (DC_{XX}), contaminants (*), and *n*-alkanes internal standards (IS $_{ALKXX}$).

		Sample id:	**LD12-4007**
		info:	Sector D, level VIa, grid JA79 More recent occupation
		Mineral:	Sandstone
		Dimension:	105, 70, 15 mm 158 g
Morphology:	Tabular	3D:	https://skfb.ly/puzEx
Alteration patterns:	Fracture, sooting		

Lipid analysis

	Lipid yield ($\mu g\ g^{-1}$)	P/S	O/S	$\delta^{13}C_{16:0}$ (‰)	$\delta^{13}C_{18:0}$ (‰)	$\Delta^{13}C$ (‰)	Lipid content
External (e)	5.45	0.95		-31.40	-30.40	1.00	SFA (C14-18, C20, C22-26, C28), BrFA (C15, C17), ALK (C25, C27, C29, C31), pri, phy (78% SRR), B3CA (tr)
Internal (i)	-	-	-	-	-	-	-

Molecular signature:	-
HAS interpretation:	-



Partial total ion chromatogram (TIC) of acid/methanol extract of sample LD12-4007e showing saturated fatty acids ($C_{XX:0}$), branched fatty acids ($C_{XX:0}$ Br), *n*-alkanes (ALK xx), benzene polycarboxylic acid (BPCA), contaminants (*), and *n*-alkanes internal standards (IS $_{ALKXX}$).

		Sample id:	**LD12-4035**
		info:	Sector D, level VIa, grid JC78 More recent occupation
		Mineral:	Sandstone
		Dimension:	155, 95, 30 mm 786 g
Morphology:	Tabular	3D:	https://skfb.ly/puzEx
Alteration patterns:	Cracks, discoloration, superficial deposit		

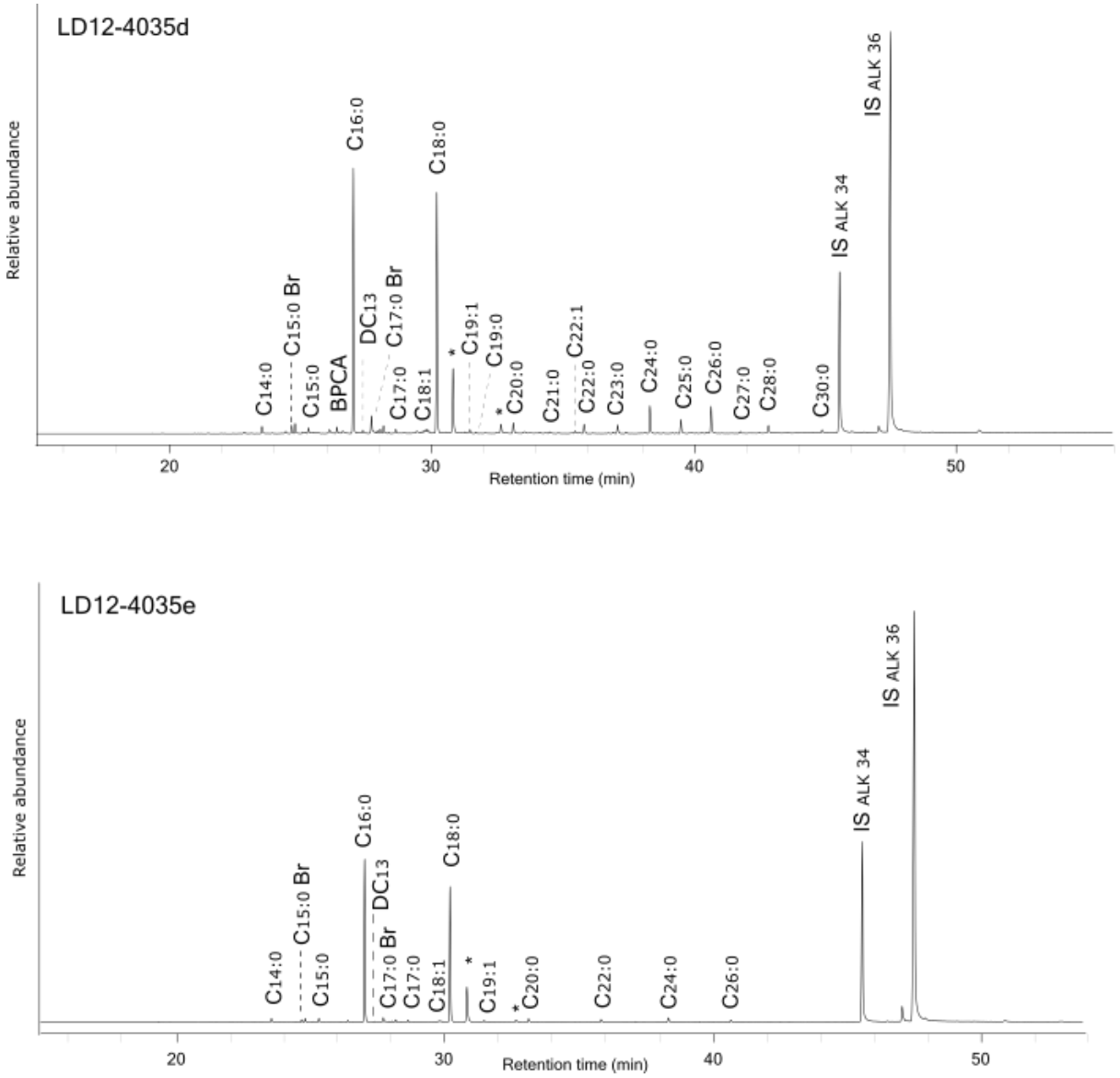
Lipid analysis

	Lipid yield ($\mu g\ g^{-1}$)	P/S	O/S	$\delta^{13}C_{16:0}$ (‰)	$\delta^{13}C_{18:0}$ (‰)	$\Delta^{13}C$ (‰)	Lipid content
Deposit (d)	25.36	1.05	62.31	-32.80	-31.50	1.30	SFA (C14-28, C30), BrFA (C15, C17), UFA (C18:1, C19:1, C22:1), DC (C13), pri, phy (35% SRR), B3CA (tr)
External (e)	10.12	1.10		-31.23	-30.50	0.73	SFA (C14-18, C20, C22, C24, C26), BrFA (C15, C17), UFA (C18:1, C19:1), DC (C13), pri, phy (44% SRR)
Internal (i)	-	-	-	-	-	-	-

Molecular signature:	-
HAS interpretation:	-

Protein analysis

Molecular signature:	-



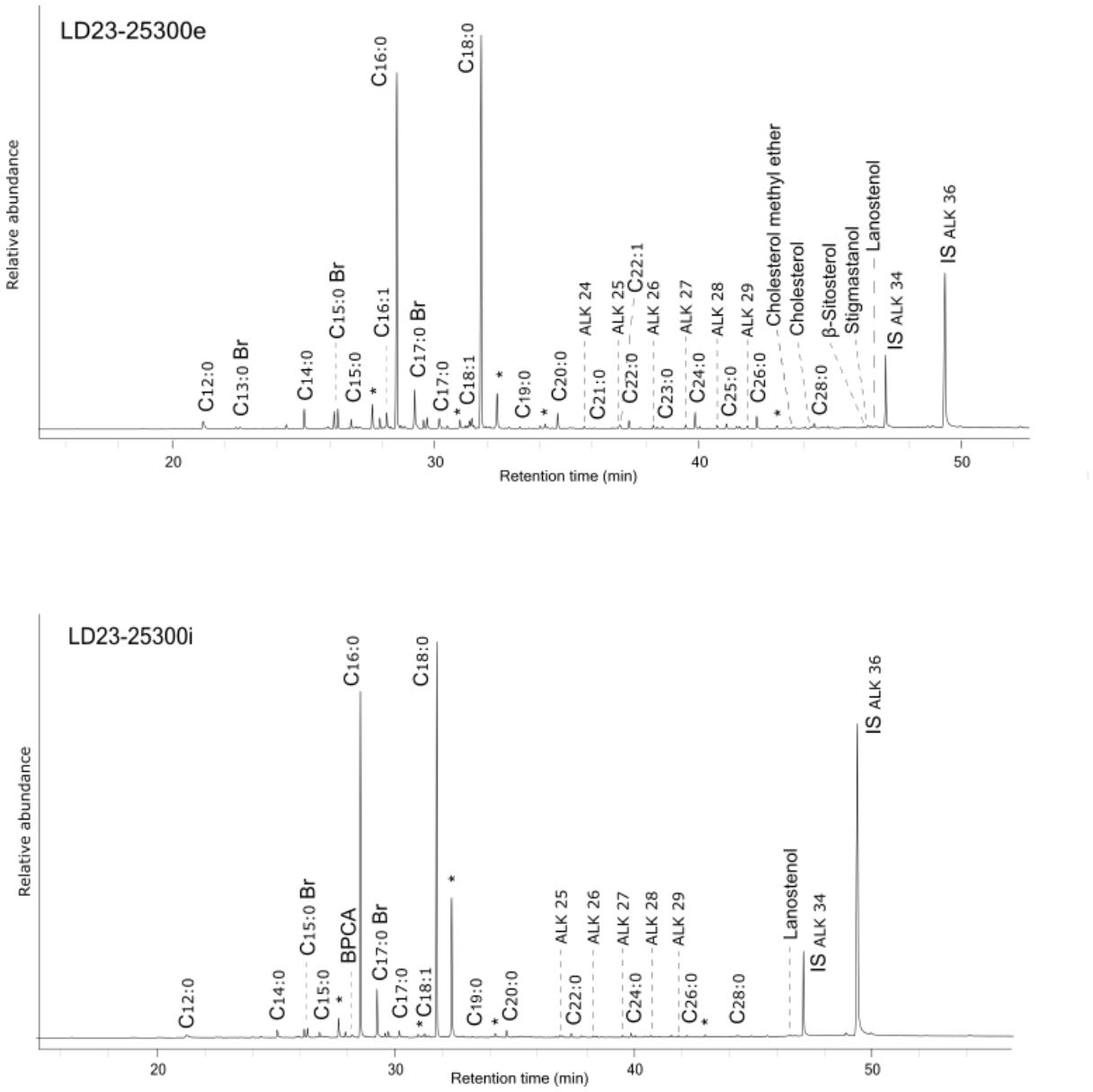
Partial total ion chromatograms (TIC) of acid/methanol extract of sample LD12-4035d/e showing saturated fatty acids ($C_{XX:0}$), branched fatty acids ($C_{XX:0}$ Br), unsaturated fatty acids ($C_{XX:1}$), diacids (DC_{XX}), benzene polycarboxylic acid (BPCA), contaminants (*), and *n*-alkanes internal standards (IS $_{ALKXX}$).

		Sample id:	**LD23-25300**
		info:	Sector B, grid JA82 Oldest occupation Part of structure E266
		Mineral:	Sandstone
		Dimension:	130, 94, 55 mm 532 g
Morphology:	Tabular	3D:	https://skfb.ly/puzEx
Alteration patterns:	Cracks, sooting		

Lipid analysis

	Lipid yield ($\mu g\ g^{-1}$)	P/S	O/S	$\delta^{13}C_{16:0}$ (‰)	$\delta^{13}C_{18:0}$ (‰)	$\Delta^{13}C$ (‰)	Lipid content
External (e)	135.94	0.93		-30.23	-27.94	2.29	SFA (C12, C14-26, C28), BrFA (C13, C15, C17), UFA (C16:1, C18:1, 22:1), ALK (C24-26, C27, C28, C29), pri (tr), phy (41% SRR), ster (Cholesterol, β-Sitosterol, Stigmastanol, Lanostenol)
Internal (i)	87.19	0.91		-32.46	-28.08	4.38	SFA (C12, C14-20, C22, C24, C26, C28), BrFA (C15, C17), UFA (C18:1), ALK (C25-26, C27, C28, C29), pri (tr), ster (Lanostenol), B3CA (tr)

Molecular signature:	Mixed resources
HAS interpretation:	Culinary feature



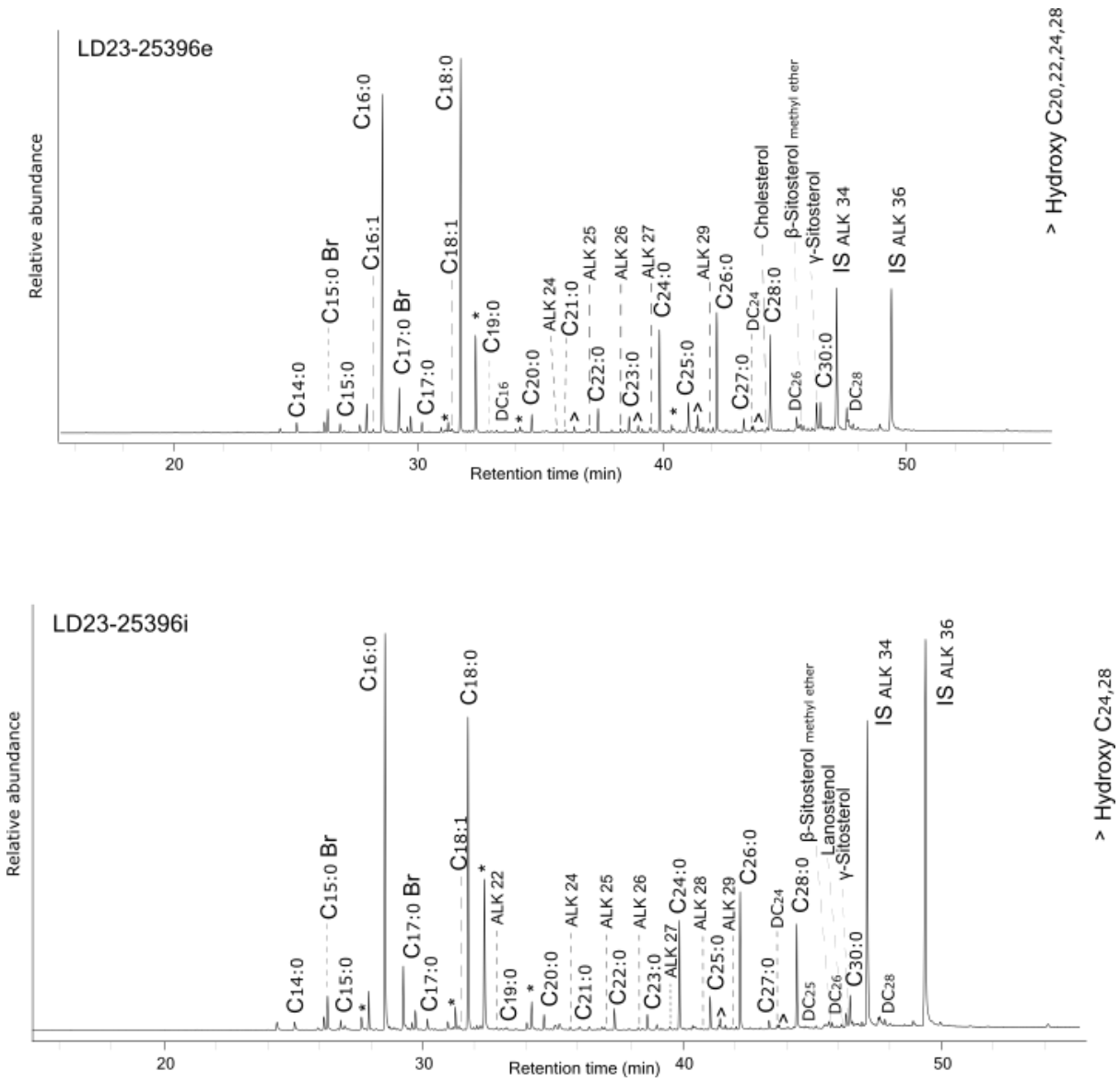
Partial total ion chromatograms (TIC) of acid/methanol extract of sample LD23-25300e/i showing saturated fatty acids ($C_{XX:0}$), branched fatty acids ($C_{XX:0}$ Br), unsaturated fatty acids ($C_{XX:1}$), benzene polycarboxylic acid (BPCA), *n*-alkanes (ALK xx), sterols, contaminants (*), and *n*-alkanes internal standards (IS $_{ALKXX}$).

		Sample id:	**LD23-25396**
		info:	Sector B, level, VII-0, grid JB82 Oldest occupation Part of structure E269
		Mineral:	Volcanic (Scoria)
		Dimension:	88, 73, 67 mm 219 g
Morphology:	Spherical	3D:	https://skfb.ly/puzEx
Alteration patterns:	Sooting		

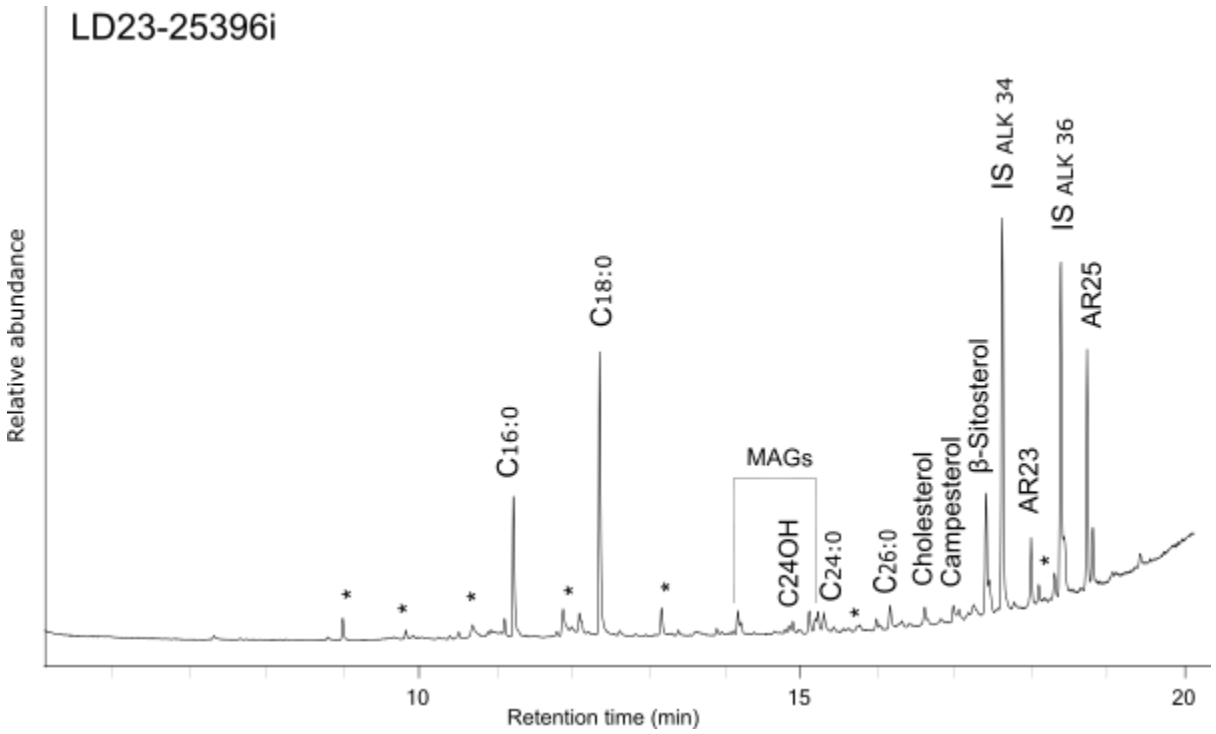
Lipid analysis

	Lipid yield ($\mu g\ g^{-1}$)	P/S	O/S	$\delta^{13}C_{16:0}$ (‰)	$\delta^{13}C_{18:0}$ (‰)	$\Delta^{13}C$ (‰)	Lipid content
External (e)	84.08	0.92	48.14	-31.85	-27.64	4.21	SFA (C14-28, C30), BrFA (C15, C17), UFA (C16:1, C18:1), Hy (C20, C22, C24, C28), DC (C16, C24, C26, C28), ALK (C24-27, C28, C29), OH (C24, C26), pri, phy (37% SRR), ster (Cholesterol, Cholestan-3-ol, β-Sitosterol methyl ether, γ-Sitosterol, β-Sitosterol, Stigmastanol), MAGs, AR (AR23, 25)
Internal (i)	30.72	1.39	13.33	-35.93	-29.59	6.34	SFA (C14-28, C30), BrFA (C15, C17), UFA (C18:1), Hy (C24, C28), DC (C24-26, C28), OH (C24), pri, phy (38% SRR), ster (Cholesterol, β-Sitosterol methyl ether, γ-Sitosterol, Lanostenol, Campesterol, β-Sitosterol, Stigmastanol), MAGs, AR (AR23, 25)

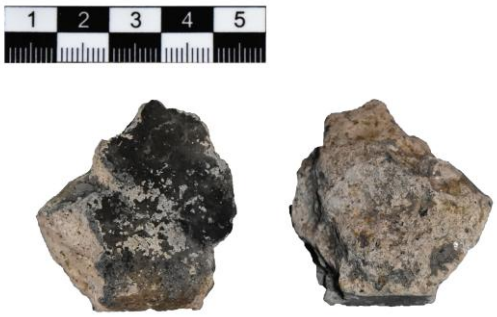
Molecular signature:	Plant resources (cereals)
HAS interpretation:	Grinder and (subsequently) combustion feature



Partial total ion chromatograms (TIC) of acid/methanol extract of sample LD23-25396e/i showing saturated fatty acids ($C_{XX:0}$), branched fatty acids ($C_{XX:0}$ Br), unsaturated fatty acids ($C_{XX:1}$), diacids (DC_{XX}), hydroxy fatty acids (^), *n*-alkanes (ALK xx), sterols, contaminants (*), and *n*-alkanes internal standards (IS_{ALKXX}).



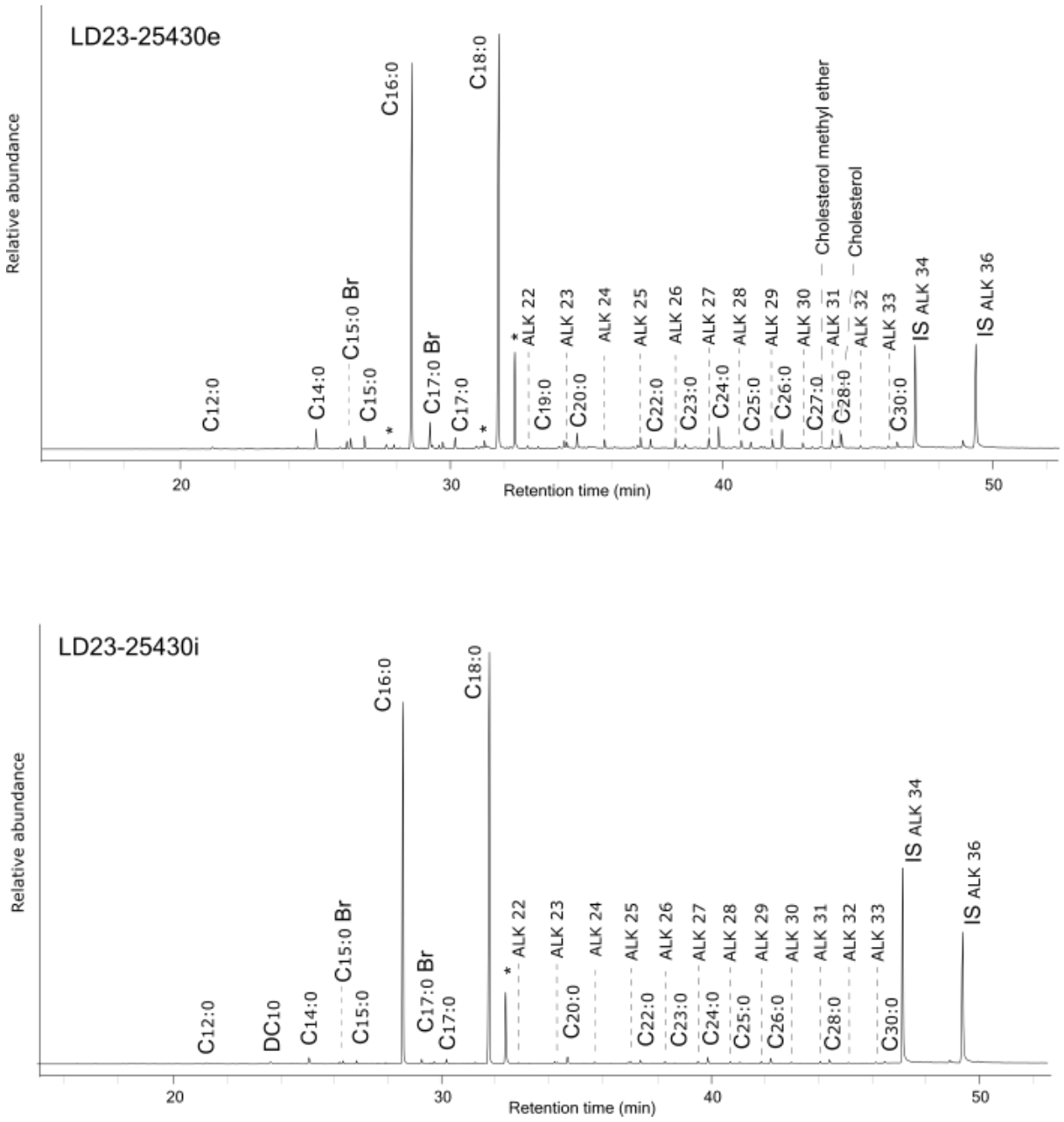
Partial total ion chromatogram (TIC) of solvent extract of sample LD23-25396i showing saturated fatty acids ($C_{XX:0}$), alcohols (CxxOH), monoacylglycerols (MAGs), sterols, alkylresorcinols (ARxx), contaminants (*), and *n*-alkanes internal standards (IS $_{ALKXX}$).

		Sample id:	**LD23-25430**
		info:	Sector B, level, VII-0, grid JB82 Oldest occupation Part of structure E269
		Mineral:	Volcanic
		Dimension:	40, 50, 29 mm 30 g
Morphology:	Tabular	3D:	https://skfb.ly/puzEx
Alteration patterns:	Sooting		

Lipid analysis

	Lipid yield ($\mu g\ g^{-1}$)	P/S	O/S	$\delta^{13}C_{16:0}$ (‰)	$\delta^{13}C_{18:0}$ (‰)	$\Delta^{13}C$ (‰)	Lipid content
External (e)	114.90	0.90		-30.98	-27.84	3.14	SFA (C12, C14-20, C22-28, C30), BrFA (C15, C17), ALK (C22-27, C28, C29, C30, C31, C32, C33), pri, ster (Cholesterol)
Internal (i)	36.36	0.82		-30.50	-28.78	1.72	SFA (C12, C14-18, C20, C22-26, C28, C30), BrFA (C15, C17), DC (C10), ALK (C22-27, C28, C29, C30, C31, C32, C33)

Molecular signature:	Mixed resources
HAS interpretation:	Combustion feature



Partial total ion chromatograms (TIC) of acid/methanol extract of sample LD23-25430e/i showing saturated fatty acids ($C_{XX:0}$), branched fatty acids ($C_{XX:0}$ Br), diacids (DC_{XX}), *n*-alkanes (ALK xx), sterols, contaminants (*), and *n*-alkanes internal standards (IS $_{ALKXX}$).

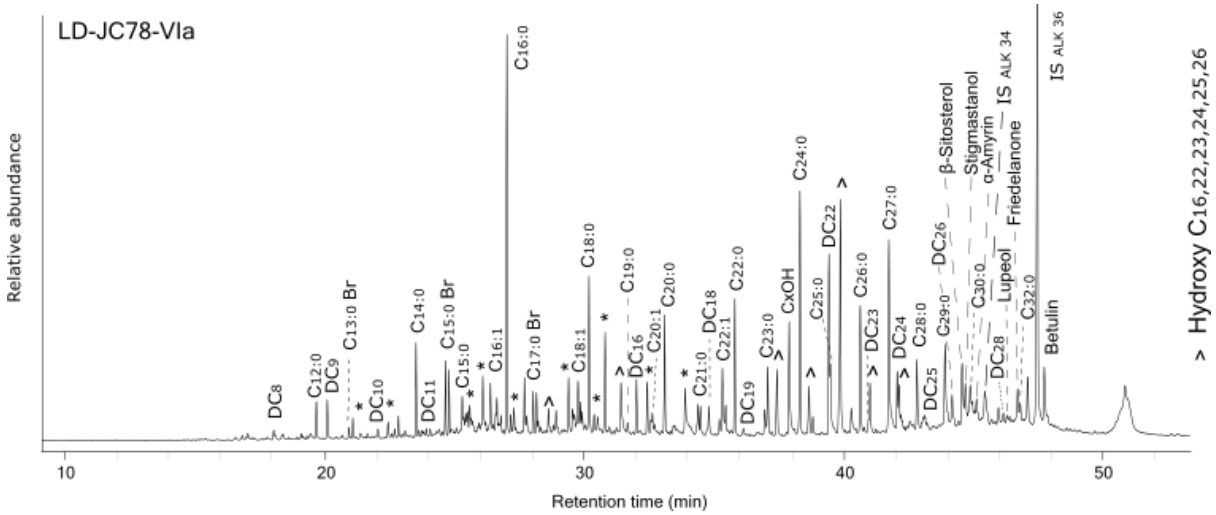
Sediments

Sample id:	**JC78-VIa**
info:	Sector D, level VIa, grid JC78 More recent occupation

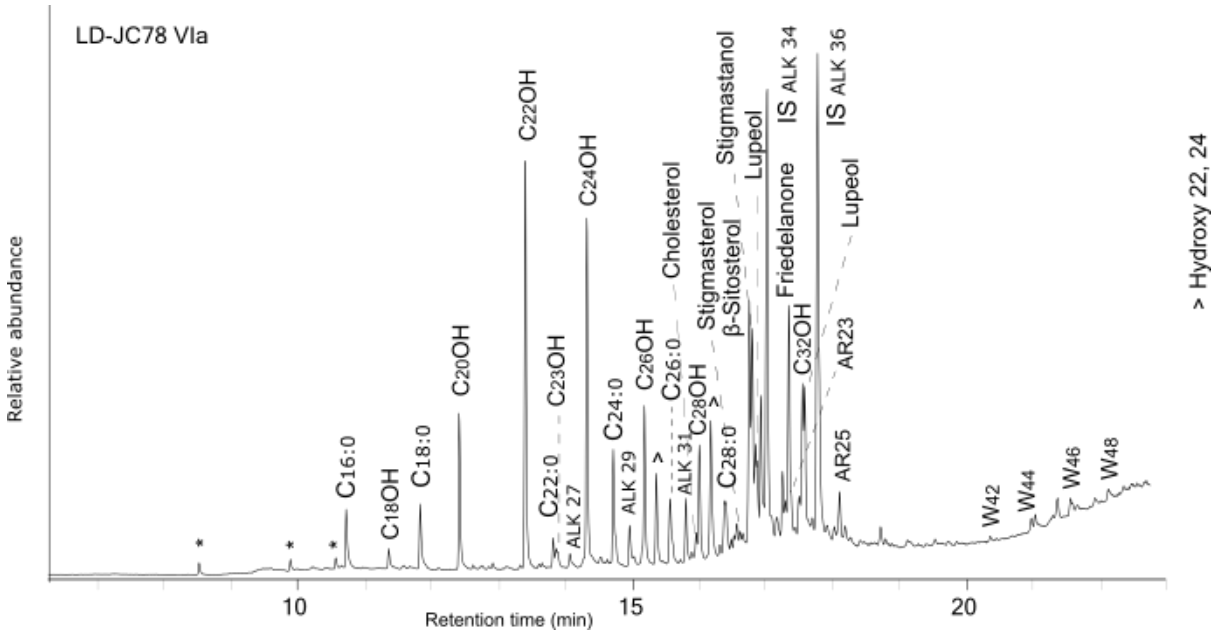
Lipid analysis

Lipid yield (µg g^{-1})	P/S	O/S	$\delta^{13}C_{16:0}$ (‰)	$\delta^{13}C_{18:0}$ (‰)	$\Delta^{13}C$ (‰)	Lipid content
1742.27	2.59	1.47	-30.95	-30.73	0.22	SFA (C12, C14-28, C29, C30, C32), BrFA (C13, C15, C17), UFA (C16:1, C18:1, C20:1, C22:1), Hy (C16, C22, C23, C24, C25, C26), DC (C8, C9-11, C16, C18, C19, C22, C23, C24-26, C28), ALK (C27, C29, C31), OH (C18, C20, C22, C23, C24, C26, C28, C32), terp (Amyrin, Friedelen-3-one, Betulin, Lupeol, Lupeol der), 4,8,12-TMTD, pri, phy (68% SRR), ster (Cholesterol, Stigmasterol, β-Sitosterol, Stigmastanol), WE (C42, 44, 46, 48), AR (AR23, 25)

Molecular signature:	Plant-derived resources
Contextual interpretation:	Site-specific activities



Partial total ion chromatogram (TIC) of acid/methanol extract of sample LD-JC78-VIa showing saturated fatty acids ($C_{XX:0}$), branched fatty acids ($C_{XX:0}$ Br), unsaturated fatty acids ($C_{XX:1}$), diacids (DC_{XX}), hydroxy fatty acids (^), *n*-alkanes (ALK xx), sterols, terpenes, contaminants (*), and *n*-alkanes internal standards (IS $_{ALKXX}$).



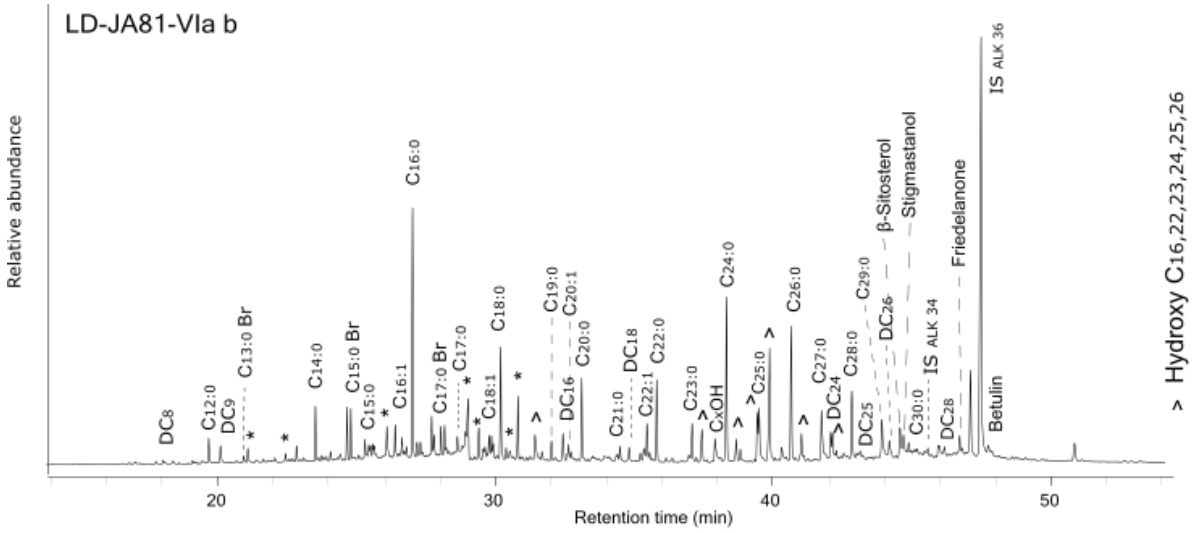
Partial total ion chromatogram (TIC) of solvent extract of sample LD-JC78-VIa showing saturated fatty acids ($C_{XX:0}$), alcohols (CxxOH), *n*-alkanes (ALK xx), sterols, terpenes, alkylresorcinols (ARxx), wax esters (Wxx), contaminants (*), and *n*-alkanes internal standards (IS $_{ALKXX}$).

Sample id:	**JA81-VIa b**
info:	Sector D, level VIa, grid JA81 More recent occupation

Lipid analysis

Lipid yield (µg g^{-1})	P/S	O/S	$\delta^{13}C_{16:0}$ (‰)	$\delta^{13}C_{18:0}$ (‰)	$\Delta^{13}C$ (‰)	Lipid content
1750.49	2.19	2.26	-31.53	-34.70	-3.17	SFA (C12, C14-28, C29, C30), BrFA (C13, C15, C17), UFA (C16:1, C18:1, C20:1, C22:1), Hy (C16, C22, C23, C24, C25, C26), DC (C8, C9, C16, C18, C24-26, C28), terp (Amyrin, Friedelen-3-one, Betulin), 4,8,12-TMTD, pri, phy (69% SRR), ster (β-Sitosterol, Stigmastanol)

Molecular signature:	Plant-derived resources
Contextual interpretation:	Site-specific activities



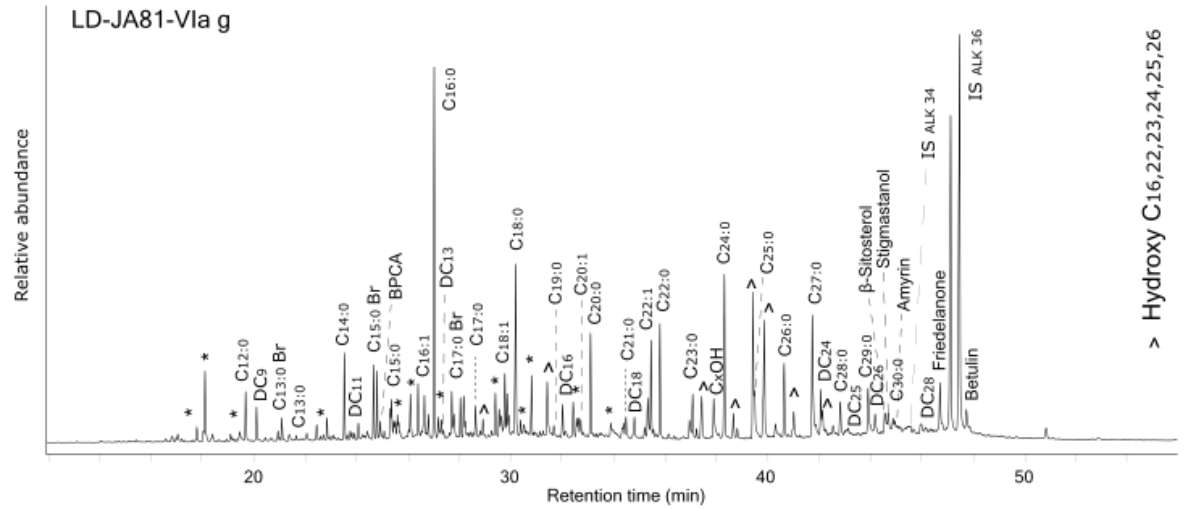
Partial total ion chromatogram (TIC) of acid/methanol extract of sample LD-JA81-VIa b showing saturated fatty acids ($C_{XX:0}$), branched fatty acids ($C_{XX:0}$ Br), unsaturated fatty acids ($C_{XX:1}$), diacids (DC_{XX}), hydroxy fatty acids (^), *n*-alkanes (ALK xx), sterols, terpenes, contaminants (*), and *n*-alkanes internal standards (IS $_{ALKXX}$).

Sample id:	**JA81-VIa g**
info:	Sector D, level VIa, grid JA81 More recent occupation

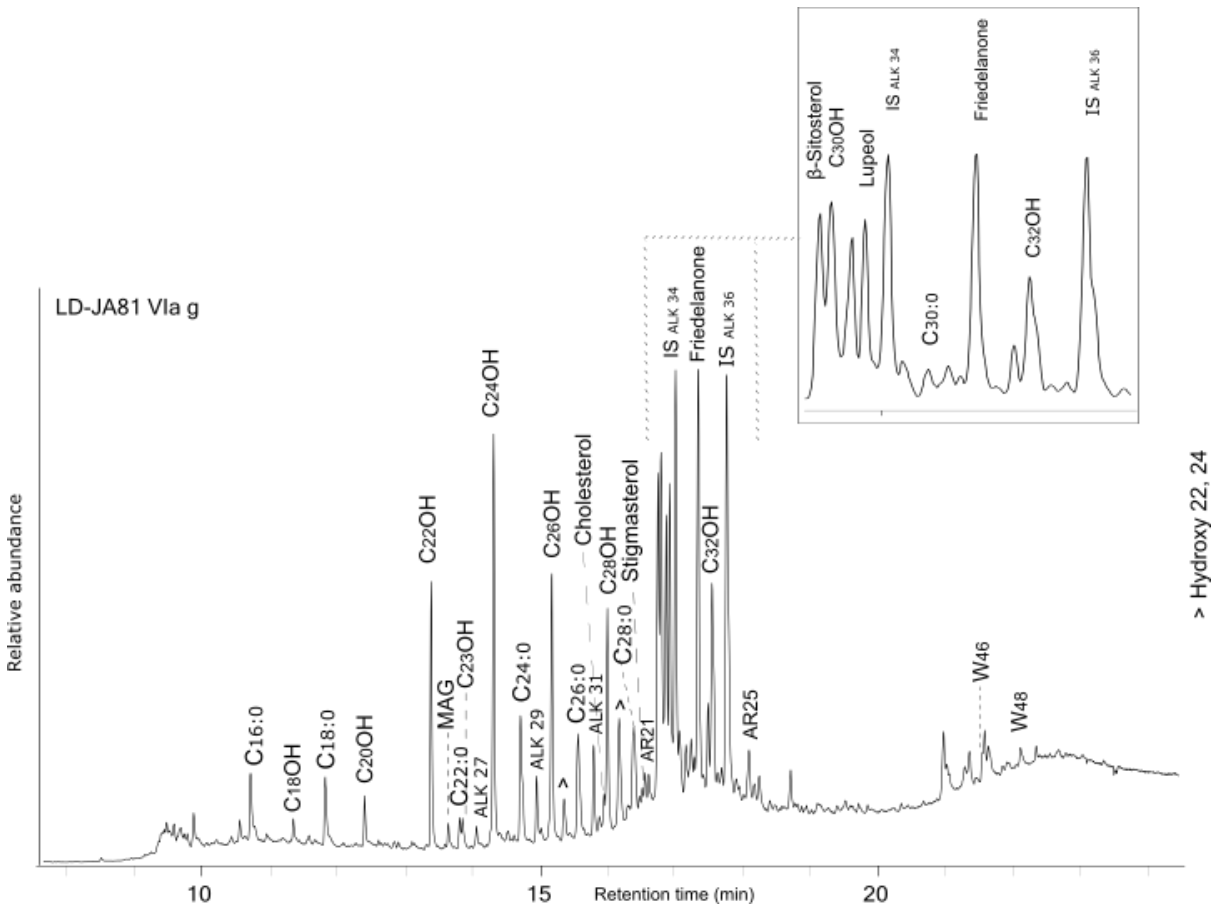
Lipid analysis

Lipid yield (µg g^{-1})	P/S	O/S	$\delta^{13}C_{16:0}$ (‰)	$\delta^{13}C_{18:0}$ (‰)	$\Delta^{13}C$ (‰)	Lipid content
1070.80	2.17	2.12	-30.55	-31.44	-0.89	SFA (C12-28, C29, C30), BrFA (C13, C15, C17), UFA (C16:1, C18:1, C20:1, C22:1), Hy (C16, C22, C23, C24, C25, C26), DC (C9, C11, C13, C16, C18, C24-26, C28), ALK (C27, C29, C31), OH (C18, C20, C22, C23, C24, C26, C28, C32), terp (Amyrin, Friedelen-3-one, Betulin, Lupeol der), 4,8,12-TMTD, pri, phy (75% SRR), ster (Cholesterol, Stigmasterol, β-Sitosterol, Stigmastanol), MAGs, WE (C46, 48), AR (AR21, 25), B3CA

Molecular signature:	Plant-derived resources
Contextual interpretation:	Site-specific activities



Partial total ion chromatogram (TIC) of acid/methanol extract of sample LD-JA81-VIa g showing saturated fatty acids ($C_{XX:0}$), branched fatty acids ($C_{XX:0}$ Br), unsaturated fatty acids ($C_{XX:1}$), benzene polycarboxylic acid (BPCA), diacids (DC_{XX}), hydroxy fatty acids (^), *n*-alkanes (ALK xx), sterols, terpenes, contaminants (*), and *n*-alkanes internal standards (IS_{ALKXX}).



Partial total ion chromatogram (TIC) of solvent extract of sample LD-JA81-VIa g showing saturated fatty acids ($C_{XX:0}$), alcohols (CxxOH), *n*-alkanes (ALK xx), monoacylglycerols (MAGs), sterols,

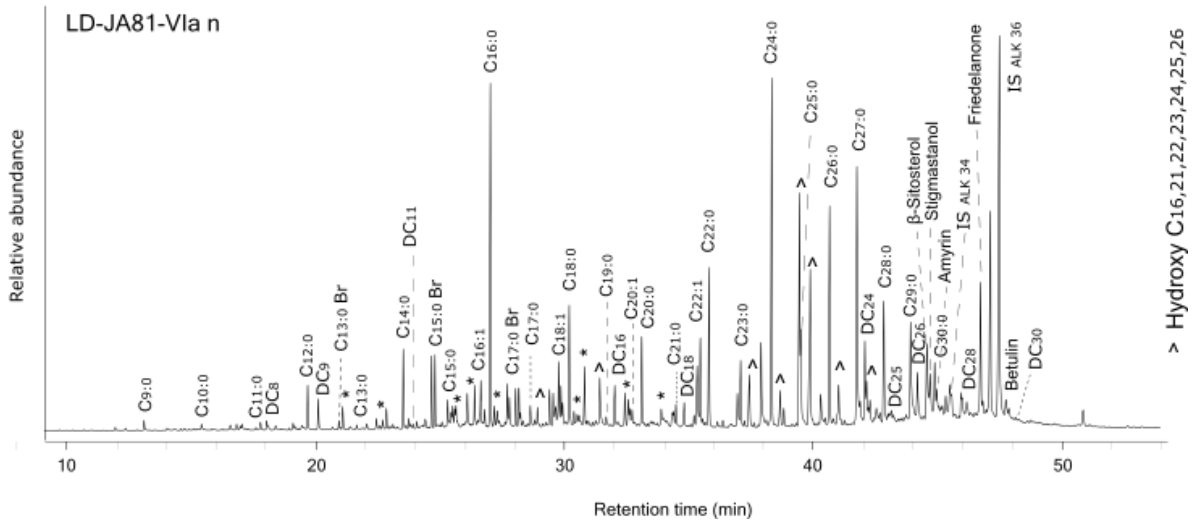
terpenes, alkylresorcinols (ARxx), wax esters (Wxx), contaminants (*), and *n*-alkanes internal standards (IS $_{ALKXX}$).

Sample id:	**JA81-VIa n**
info:	Sector D, level VIa, grid JA81 More recent occupation

Lipid analysis

Lipid yield (µg g^{-1})	P/S	O/S	$\delta^{13}C_{16:0}$ (‰)	$\delta^{13}C_{18:0}$ (‰)	$\Delta^{13}C$ (‰)	Lipid content
399.97	2.79	1.63	-	-	-	SFA (C9-28, C29, C30), BrFA (C13, C15, C17), UFA (C16:1, C18:1, C20:1, C22:1), Hy (C16, C21, C22, C23, C24, C25, C26), DC (C8, C9, C16, C18, C24-26, C28, C30), terp (Amyrin, Friedelen-3-one, Betulin), 4,8,12-TMTD, pri, phy (71% SRR), ster (β-Sitosterol, Stigmastanol)

Molecular signature:	Plant-derived resources
Contextual interpretation:	Site-specific activities



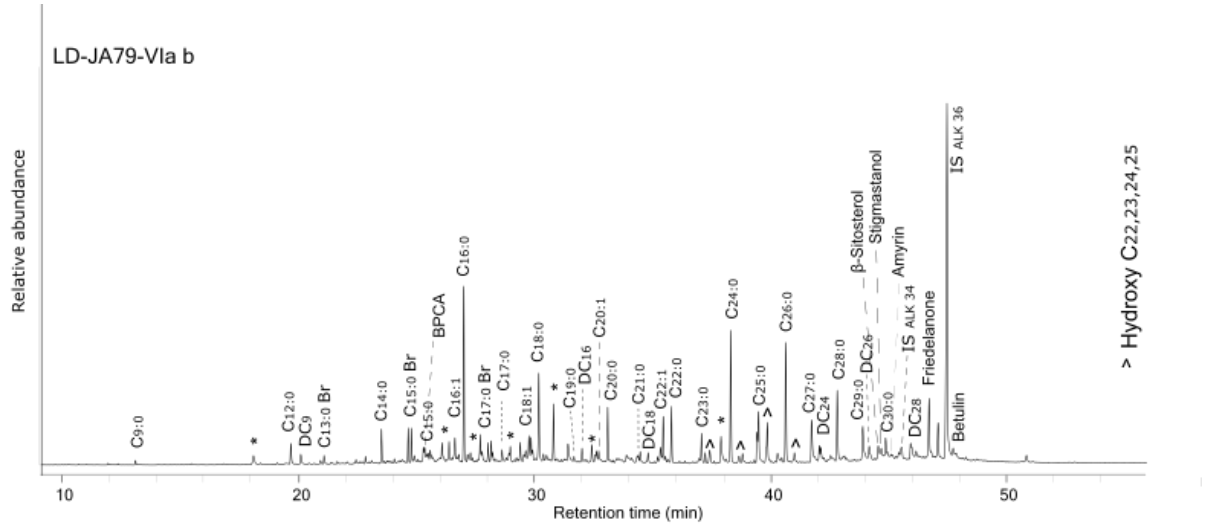
Partial total ion chromatogram (TIC) of acid/methanol extract of sample LD-JA81-VIa n showing saturated fatty acids ($C_{XX:0}$), branched fatty acids ($C_{XX:0}$ Br), unsaturated fatty acids ($C_{XX:1}$), diacids (DC_{XX}), hydroxy fatty acids (^), sterols, terpenes, contaminants (*), and *n*-alkanes internal standards (IS_{ALKXX}).

Sample id:	**JA79-VIa b**
info:	Sector D, level VIa, grid JA79 More recent occupation

Lipid analysis

Lipid yield (µg g^{-1})	P/S	O/S	$\delta^{13}C_{16:0}$ (‰)	$\delta^{13}C_{18:0}$ (‰)	$\Delta^{13}C$ (‰)	Lipid content
348.08	1.97	2.06	-	-	-	SFA (C9, C11-12, C14-28, C29, C30), BrFA (C13, C15, C17), UFA (C16:1, C18:1, C20:1, C22:1), Hy (C22, C23, C24, C25), DC (C9, C16, C18, C24, C26, C28), terp (Amyrin, Friedelen-3-one, Betulin), ster (β-Sitosterol, Stigmastanol), B3CA

Molecular signature:	Plant-derived resources
Contextual interpretation:	Site-specific activities



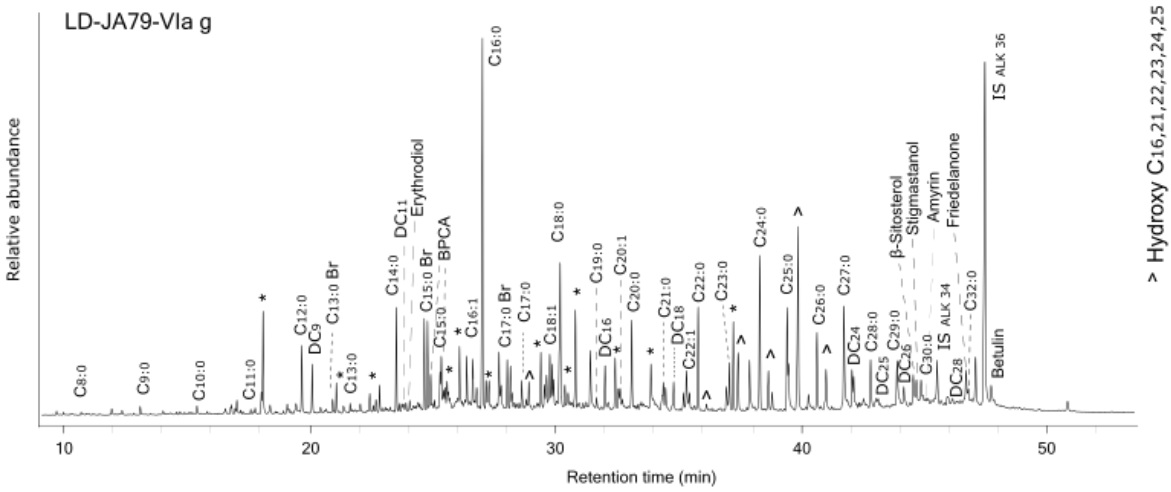
Partial total ion chromatogram (TIC) of acid/methanol extract of sample LD-JA79-VIa b showing saturated fatty acids ($C_{XX:0}$), branched fatty acids ($C_{XX:0}$ Br), unsaturated fatty acids ($C_{XX:1}$), benzene polycarboxylic acid (BPCA), diacids (DC_{XX}), hydroxy fatty acids (^), sterols, terpenes, contaminants (*), and *n*-alkanes internal standards (IS $_{ALKXX}$).

Sample id:	**JA79-VIa g**
info:	Sector D, level VIa, grid JA79 More recent occupation

Lipid analysis

Lipid yield (µg g^{-1})	P/S	O/S	$\delta^{13}C_{16:0}$ (‰)	$\delta^{13}C_{18:0}$ (‰)	$\Delta^{13}C$ (‰)	Lipid content
545.32	2.63	1.70	-	-	-	SFA (C8-28, C29, C30, C32), BrFA (C13, C15, C17), UFA (C16:1, C18:1, C20:1, C22:1), Hy (C16, C21, C22, C23, C24, C25), DC (C9, C11, C16, C18, C24-26, C28), terp (Erythrodiol, Amyrin, Friedelen-3-one, Betulin), 4,8,12-TMTD, pri, phy (62% SRR), ster (β-Sitosterol, Stigmastanol), B3CA

Molecular signature:	Plant-derived resources
Contextual interpretation:	Site-specific activities



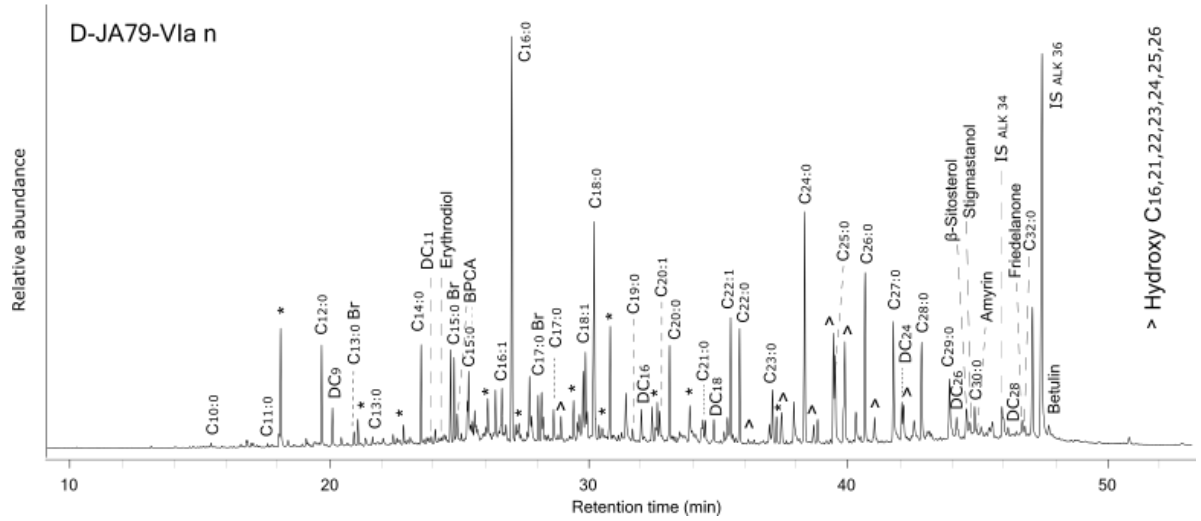
Partial total ion chromatogram (TIC) of acid/methanol extract of sample LD-JA79-VIa g showing saturated fatty acids ($C_{XX:0}$), branched fatty acids ($C_{XX:0}$ Br), unsaturated fatty acids ($C_{XX:1}$), benzene polycarboxylic acid (BPCA), diacids (DC_{XX}), hydroxy fatty acids (^), sterols, terpenes, contaminants (*), and *n*-alkanes internal standards (IS $_{ALKXX}$).

Sample id:	**JA79-VIa n**
info:	Sector D, level VIa, grid JA79 More recent occupation

Lipid analysis

Lipid yield (µg g^{-1})	P/S	O/S	$\delta^{13}C_{16:0}$ (‰)	$\delta^{13}C_{18:0}$ (‰)	$\Delta^{13}C$ (‰)	Lipid content
2658.14	1.83	1.91	-	-	-	SFA (C10-28, C29, C30, C32), BrFA (C13, C15, C17), UFA (C16:1, C18:1, C20:1, C22:1), Hy (C16, C21, C22, C23, C24, C25, C26), DC (C9, C11, C16, C18, C24, C26, C28), terp (Erythrodiol, Amyrin, Friedelen-3-one, Betulin), 4,8,12-TMTD, pri, phy (70% SRR), ster (β-Sitosterol, Stigmastanol), B3CA

Molecular signature:	Plant-derived resources
Contextual interpretation:	Site-specific activities



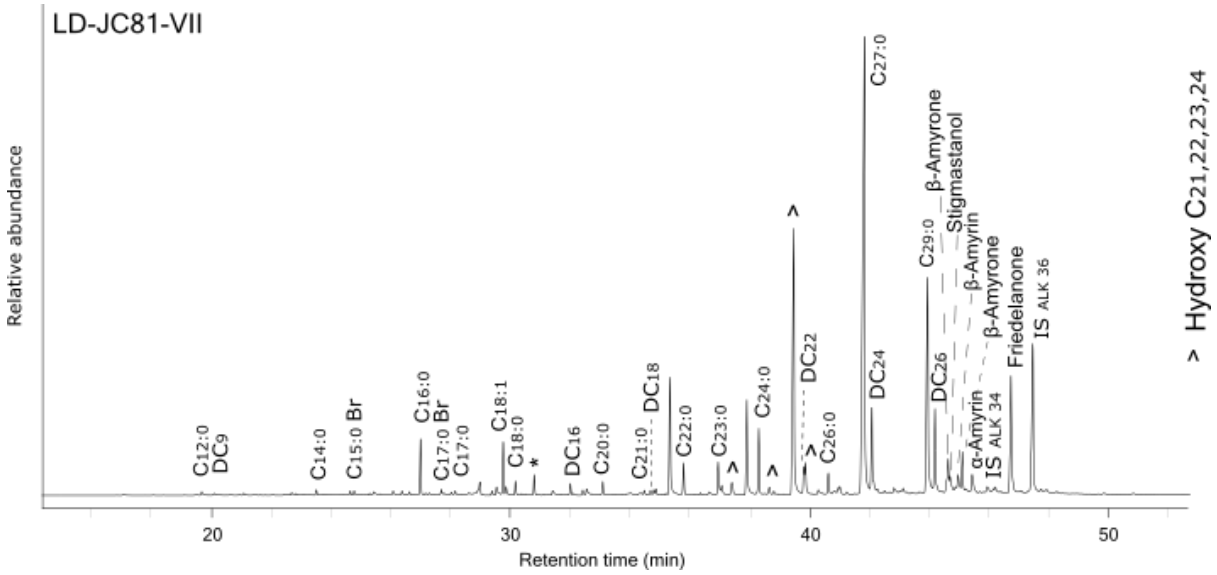
Partial total ion chromatogram (TIC) of acid/methanol extract of sample LD-JA79-VIa n showing saturated fatty acids ($C_{XX:0}$), branched fatty acids ($C_{XX:0}$ Br), unsaturated fatty acids ($C_{XX:1}$), benzene polycarboxylic acid (BPCA), diacids (DC_{XX}), hydroxy fatty acids (^), sterols, terpenes, contaminants (*), and *n*-alkanes internal standards (IS $_{ALKXX}$).

Sample id:	**JC81-VII**
info:	Sector D, level VII, grid JC81 Oldest occupation

Lipid analysis

Lipid yield (µg g^{-1})	P/S	O/S	$\delta^{13}C_{16:0}$ (‰)	$\delta^{13}C_{18:0}$ (‰)	$\Delta^{13}C$ (‰)	Lipid content
290.60	3.75	1.20	-	-	-	SFA (C12, C14, C16-18, C20-28, C29), BrFA (C15, C17), UFA (C18:1), Hy (C21, C22, C23, C24, C25, C26), DC (C9, C16, C18, C22, C24, C26), terp (Amyrin, β-Amyrone, Friedelen-3-one), 4,8,12-TMTD, pri, phy (58% SRR), ster (Stigmastanol)

Molecular signature:	Plant-derived resources
Contextual interpretation:	Site-specific activities



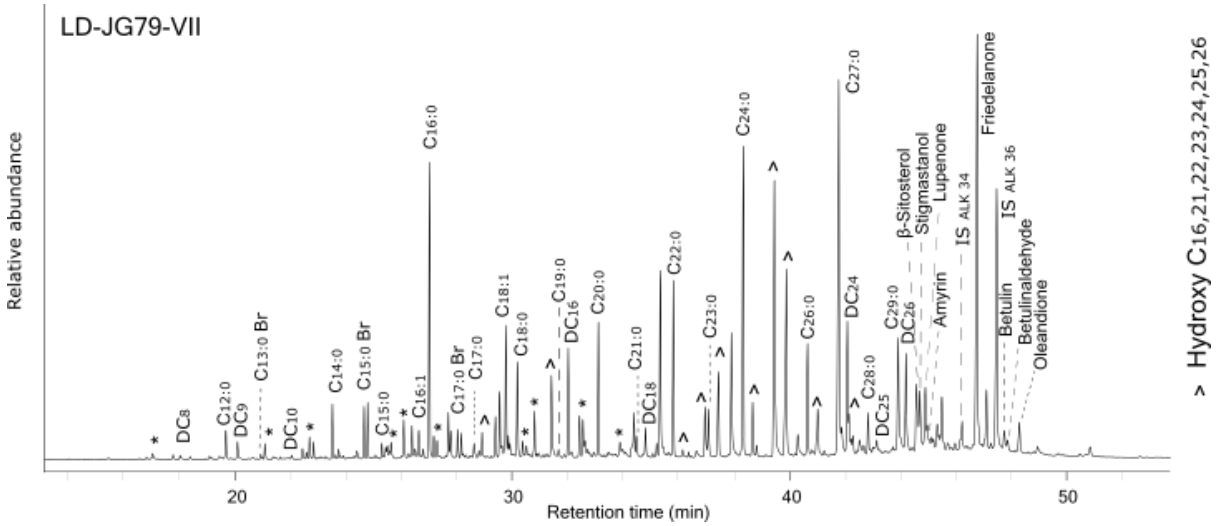
Partial total ion chromatogram (TIC) of acid/methanol extract of sample LD-JC81-VII showing saturated fatty acids ($C_{XX:0}$), branched fatty acids ($C_{XX:0}$ Br), unsaturated fatty acids ($C_{XX:1}$), diacids (DC_{XX}), hydroxy fatty acids (^), sterols, terpenes, contaminants (*), and *n*-alkanes internal standards (IS_{ALKXX}).

Sample id:	**JG79-VII**
info:	Sector D, level VII, grid JG79 Oldest occupation

Lipid analysis

Lipid yield (µg g^{-1})	P/S	O/S	$\delta^{13}C_{16:0}$ (‰)	$\delta^{13}C_{18:0}$ (‰)	$\Delta^{13}C$ (‰)	Lipid content
134.50	2.86	1.67	-29.93	-31.14	-1.21	SFA (C12, C14-24, C26-28, C29), BrFA (C13, C15, C17), UFA (C16:1, C18:1), Hy (C16, C21, C22, C23, C24, C25, C26), DC (C8-C10, C16, C18, C24-26), terp (Lupenone, Amyrin, Friedelen-3-one, Betulin, Betulinaldehyde, Oleandione), 4,8,12-TMTD, pri, phy (65% SRR), ster (β-Sitosterol, Stigmastanol)

Molecular signature:	Plant-derived resources
Contextual interpretation:	Site-specific activities



Partial total ion chromatogram (TIC) of acid/methanol extract of sample LD-JG79-VII showing saturated fatty acids ($C_{XX:0}$), branched fatty acids ($C_{XX:0}$ Br), unsaturated fatty acids ($C_{XX:1}$), diacids (DC_{XX}), hydroxy fatty acids (^), sterols, terpenes, contaminants (*), and *n*-alkanes internal standards (IS_{ALKXX}).

Pendimoun - Datasheet

		Sample id:	**PDM-N04-15250**
		info:	US 14647, grid L20 occupation phase 3
		Mineral:	Limestone
		Dimension:	135 g
Firing structure:	Cooking place	3D:	https://skfb.ly/puzEA
Alteration patterns:	Superficial deposit		

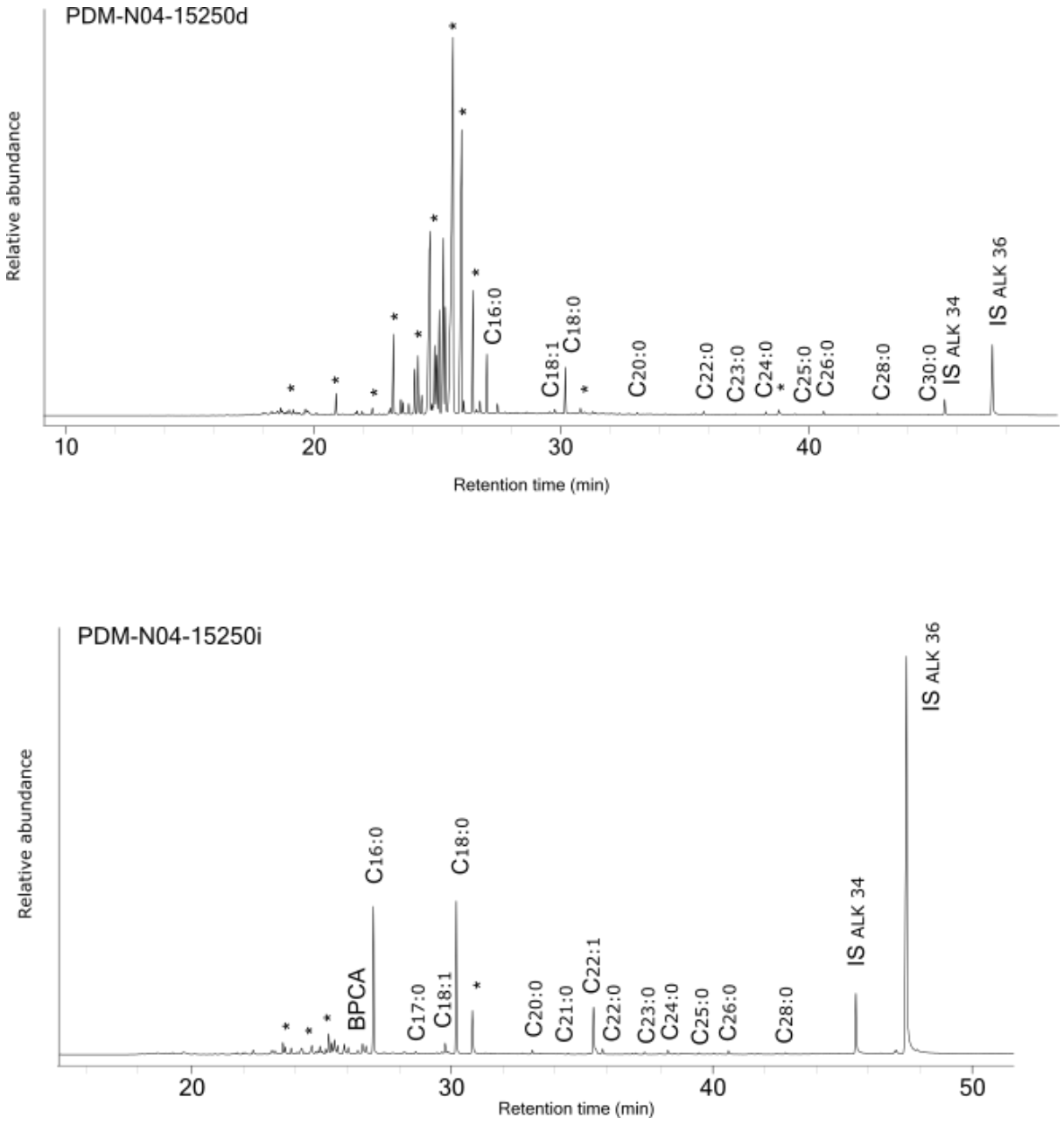
Lipid analysis

	Lipid yield ($\mu g\ g^{-1}$)	P/S	O/S	$\delta^{13}C_{16:0}$ (‰)	$\delta^{13}C_{18:0}$ (‰)	$\Delta^{13}C$ (‰)	Lipid content
Deposit (d)	51.61	1.26	9.12	-	-	-	SFA (C16, C18, C20, C22-26, C28, C30), UFA (C18:1), ALK (C31), OH (C13, C16, C18), 4,8,12-TMTD, pri
Internal (i)	29.32	1.00	14.12	-29.81	-29.53	0.28	SFA (C16-18, C20-26, C28), UFA (C18:1, C22:1), OH (C18), pri, phy (89% SRR), B3CA (tr)

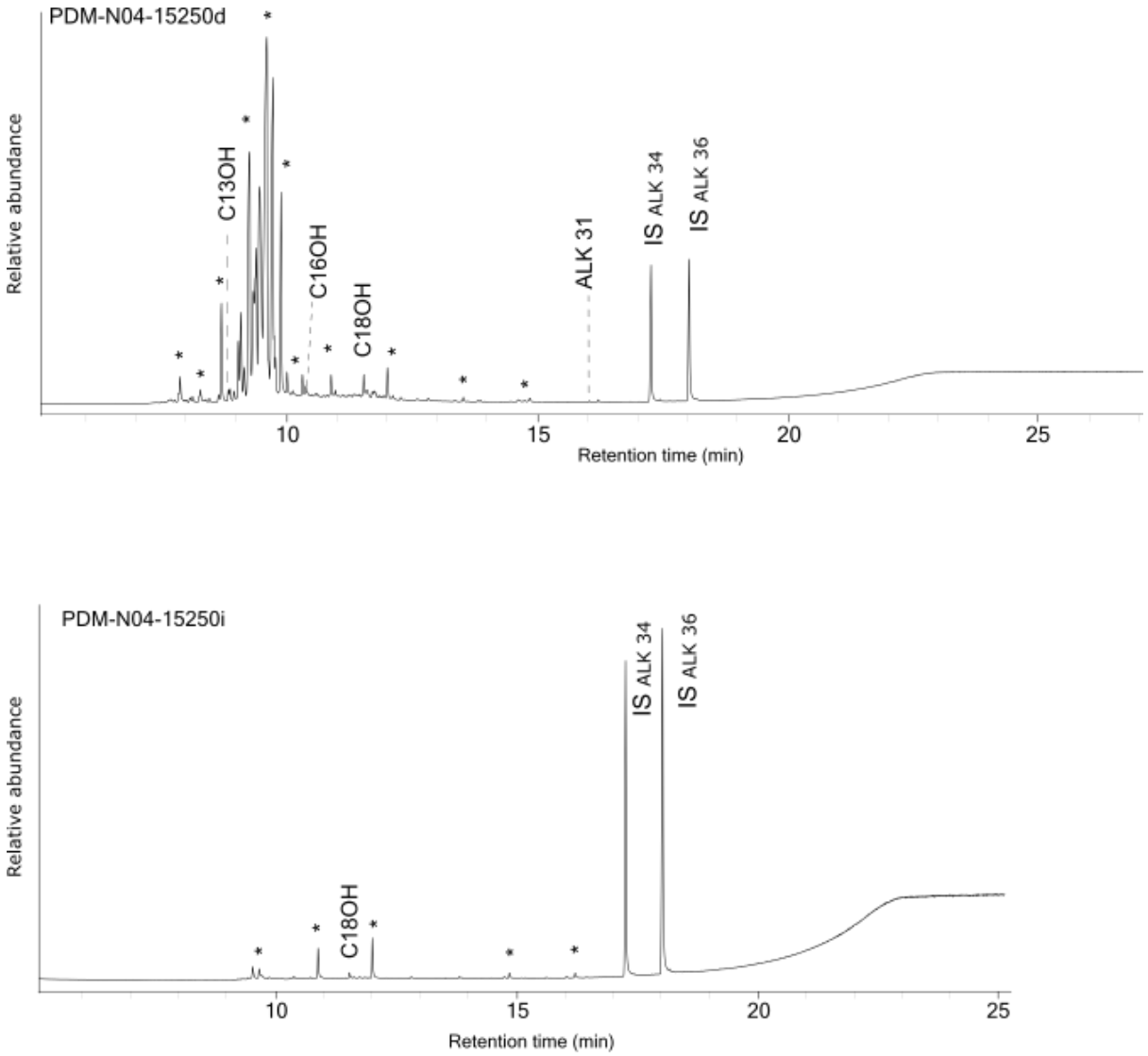
Molecular signature:	-
HAS interpretation:	Culinary feature

Protein analysis

Molecular signature:	-



Partial total ion chromatograms (TIC) of acid/methanol extract of sample PDM-N04-15250d/i showing saturated fatty acids ($C_{XX:0}$), unsaturated fatty acids ($C_{XX:1}$), benzene polycarboxylic acid (BPCA), contaminants (*), and *n*-alkanes internal standards (IS $_{ALKXX}$).



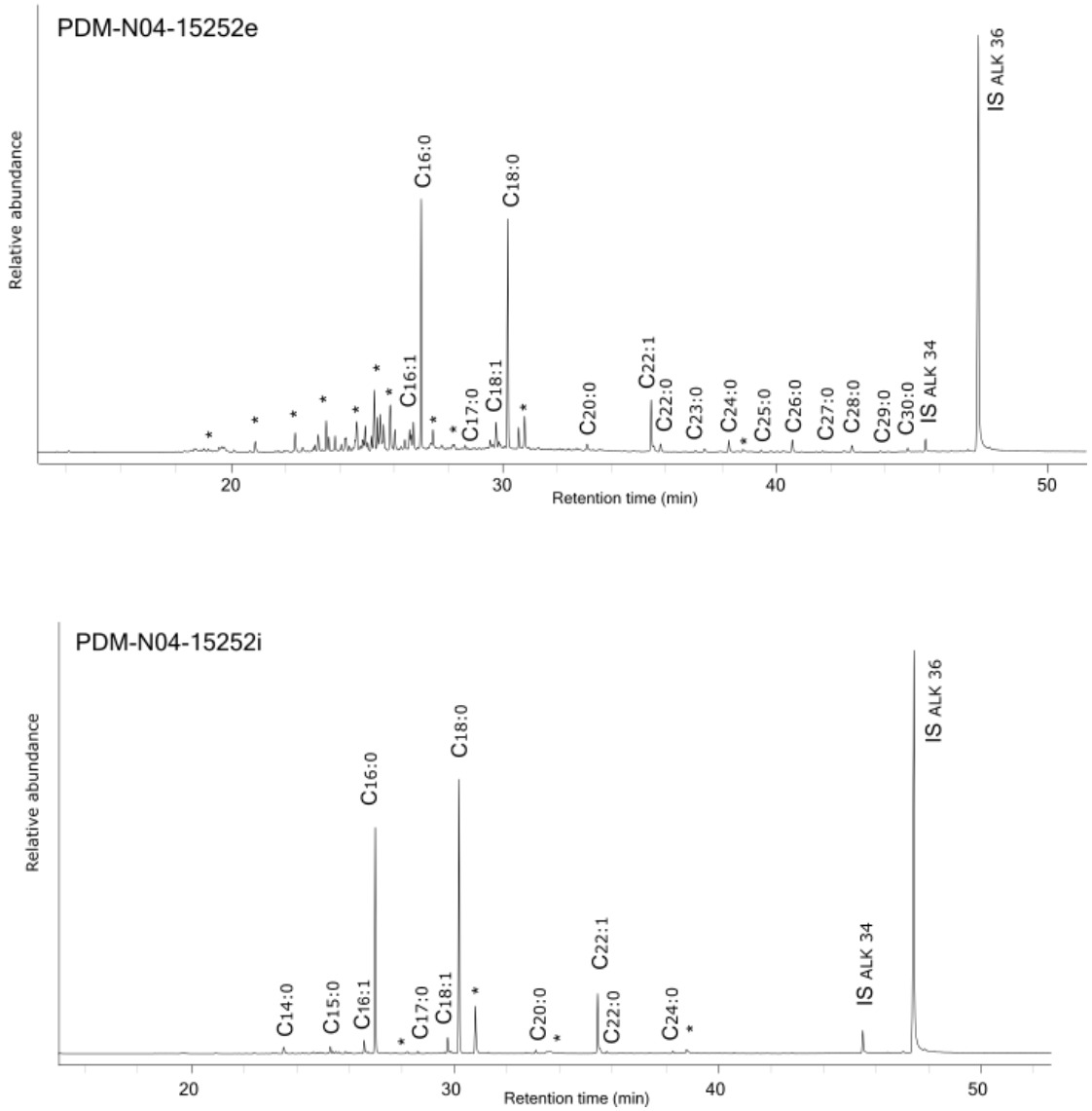
Partial total ion chromatograms (TIC) of solvent extract of sample PDM-N04-15250d/i showing alcohols (CxxOH), *n*-alkanes (ALK xx), contaminants (*), and *n*-alkanes internal standards (IS $_{ALKXX}$).

		Sample id:	**PDM-N04-15252**
		info:	US 14647, grid L20 occupation phase 3
		Mineral:	Limestone
		Dimension:	38 g
Firing structure:	Cooking place	3D:	https://skfb.ly/puzEA
Alteration patterns:	Cracks, sooting		

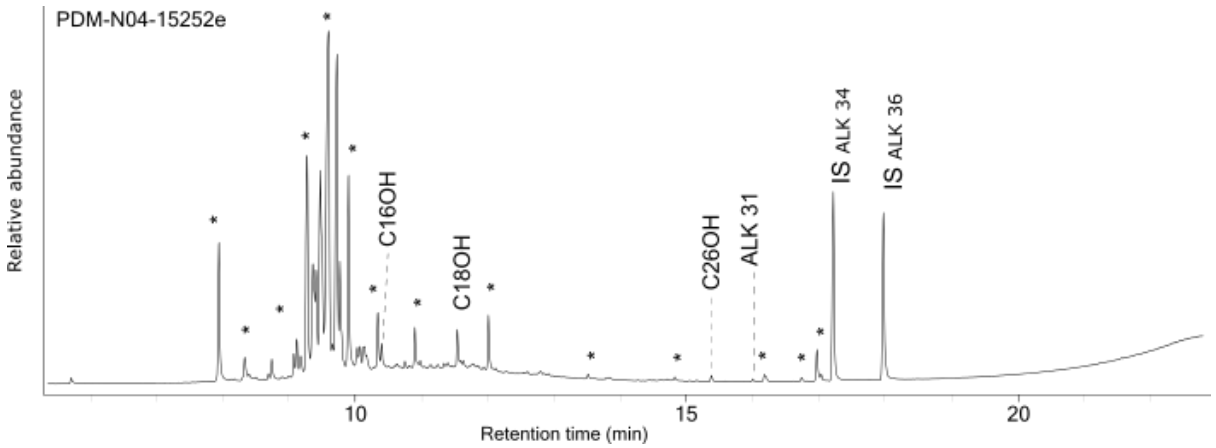
Lipid analysis

	Lipid yield ($\mu g\ g^{-1}$)	P/S	O/S	$\delta^{13}C_{16:0}$ (‰)	$\delta^{13}C_{18:0}$ (‰)	$\Delta^{13}C$ (‰)	Lipid content
External (e)	218.70	1.14	4.30	-29.56	-29.53	0.03	SFA (C16-18, C20, C22-30), UFA (C16:1, C18:1, C22:1), ALK (C31), OH (C16, C18, C26), 4,8,12-TMTD (tr), pri, phy (94% SRR)
Internal (i)	90.93	1.30	7.53	-29.61	-29.32	0.29	SFA (C14-18, C20, C22, C24), UFA (C16:1, C18:1, C22:1), pri

Molecular signature:	-
HAS interpretation:	Culinary feature



Partial total ion chromatograms (TIC) of acid/methanol extract of sample PDM-N04-15252e/i showing saturated fatty acids ($C_{XX:0}$), unsaturated fatty acids ($C_{XX:1}$), contaminants (*), and *n*-alkanes internal standards (IS $_{ALKXX}$).



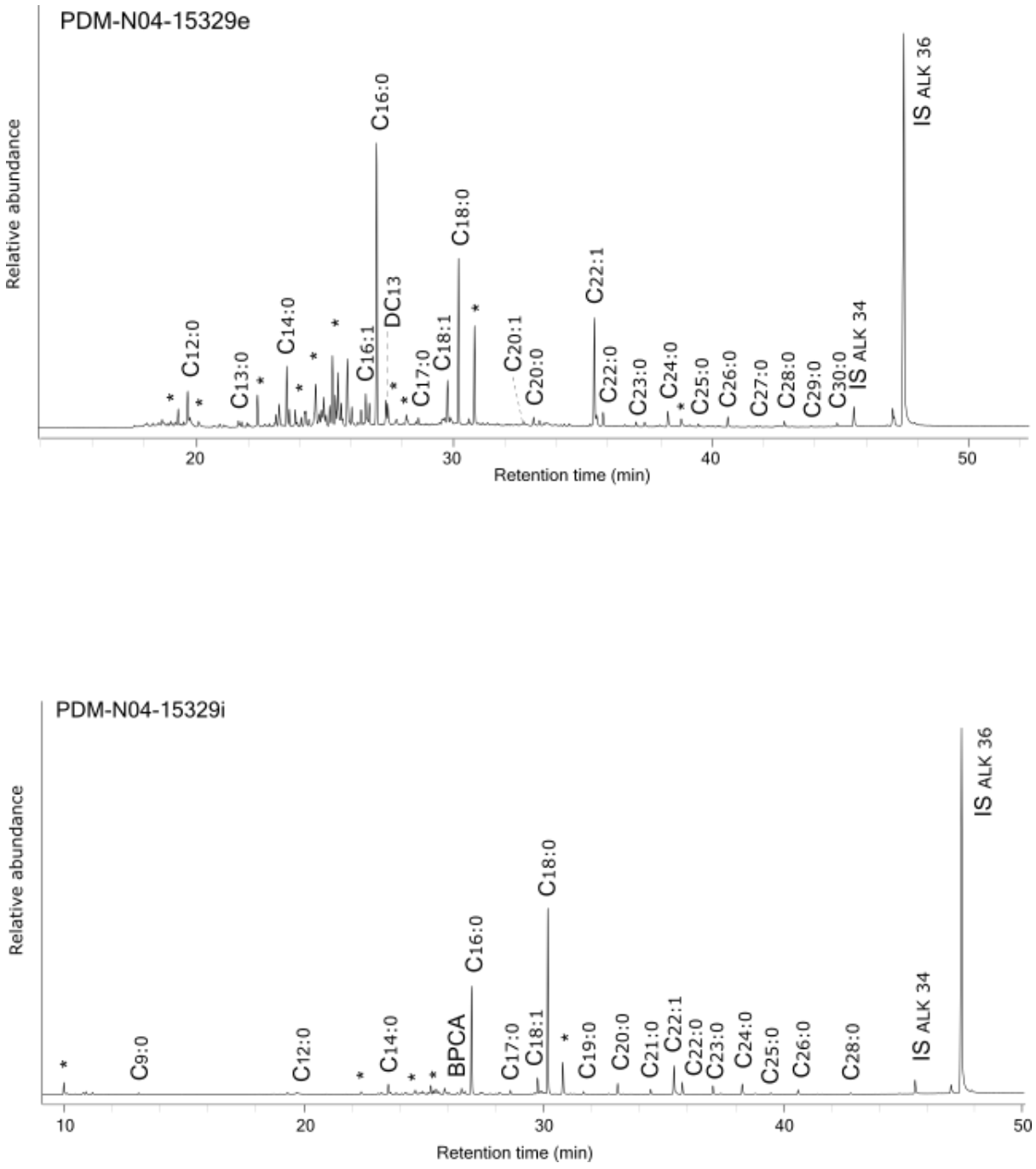
Partial total ion chromatogram (TIC) of solvent extract of sample PDM-N04-15252e showing alcohols (CxxOH), *n*-alkanes (ALK xx), contaminants (*), and *n*-alkanes internal standards (IS $_{ALKXX}$).

		Sample id:	**PDM-N04-15329**
		info:	US 14647, grid L20 occupation phase 3
		Mineral:	Limestone
		Dimension:	92 g
Firing structure:	Cooking place	3D:	https://skfb.ly/puzEA
Alteration patterns:	Sooting		

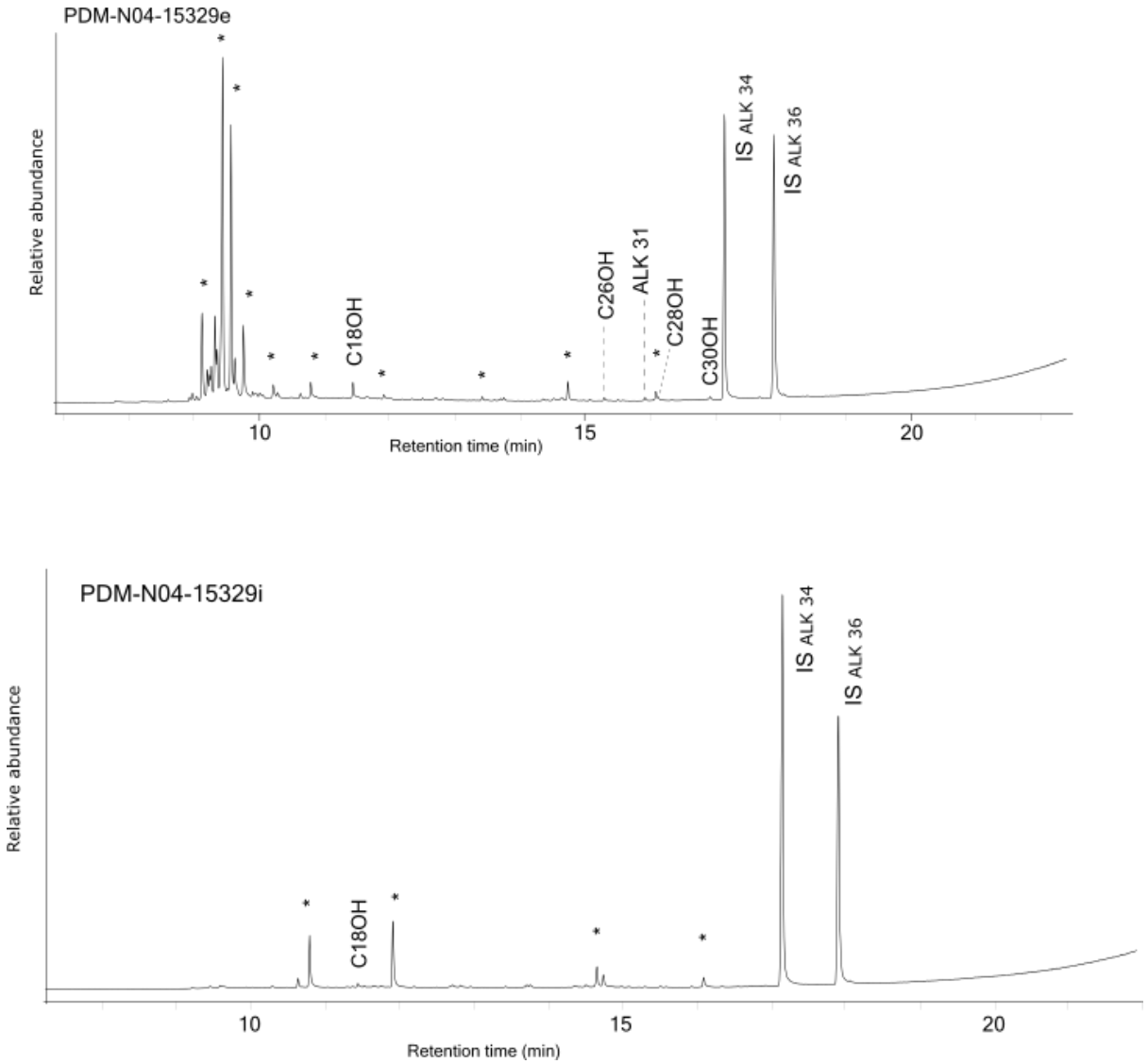
Lipid analysis

	Lipid yield ($\mu g\ g^{-1}$)	P/S	O/S	$\delta^{13}C_{16:0}$ (‰)	$\delta^{13}C_{18:0}$ (‰)	$\Delta^{13}C$ (‰)	Lipid content
External (e)	280.53	1.69	3.28	-28.63	-30.06	-1.43	SFA (C12-14, C16-18, C20, C22-30), UFA (C16:1, C18:1, C20:1, C22:1), DC (C13), ALK (C31), OH (C18, C26, C28, C30), 4,8,12-TMTD, pri, phy (69% SRR)
Internal (i)	125.46	0.64	12.10	-28.73	-31.23	-2.50	SFA (C12, C14, C16-26, C28), UFA (C18:1, C22:1), OH (C18), pri, phy (79% SRR), B3CA (tr)

Molecular signature:	Ruminant resources
HAS interpretation:	Culinary feature



Partial total ion chromatograms (TIC) of acid/methanol extract of sample PDM-N04-15329e/i showing saturated fatty acids ($C_{XX:0}$), unsaturated fatty acids ($C_{XX:1}$), benzene polycarboxylic acid (BPCA), diacids (DC_{xx}), contaminants (*), and *n*-alkanes internal standards (IS $_{ALKXX}$).



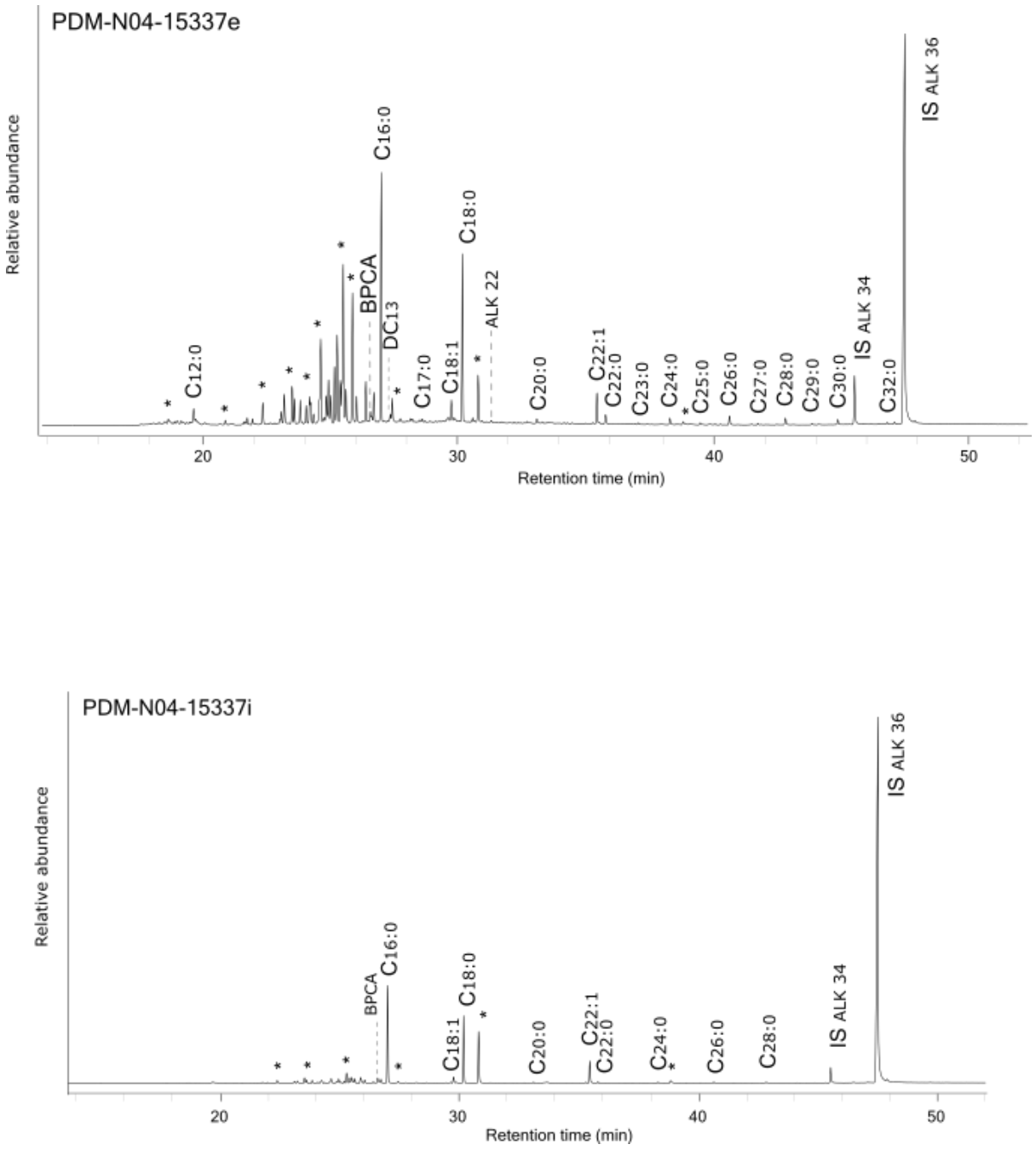
Partial total ion chromatograms (TIC) of solvent extract of sample PDM-N04-15329e/i showing alcohols (CxxOH), contaminants (*), and *n*-alkanes internal standards (IS $_{ALKXX}$).

		Sample id:	**PDM-N04-15337**
		info:	US 14647, grid L20 occupation phase 3
		Mineral:	Limestone
		Dimension:	100 g
Firing structure:	Cooking place	3D:	https://skfb.ly/puzEA
Alteration patterns:	Discoloration		

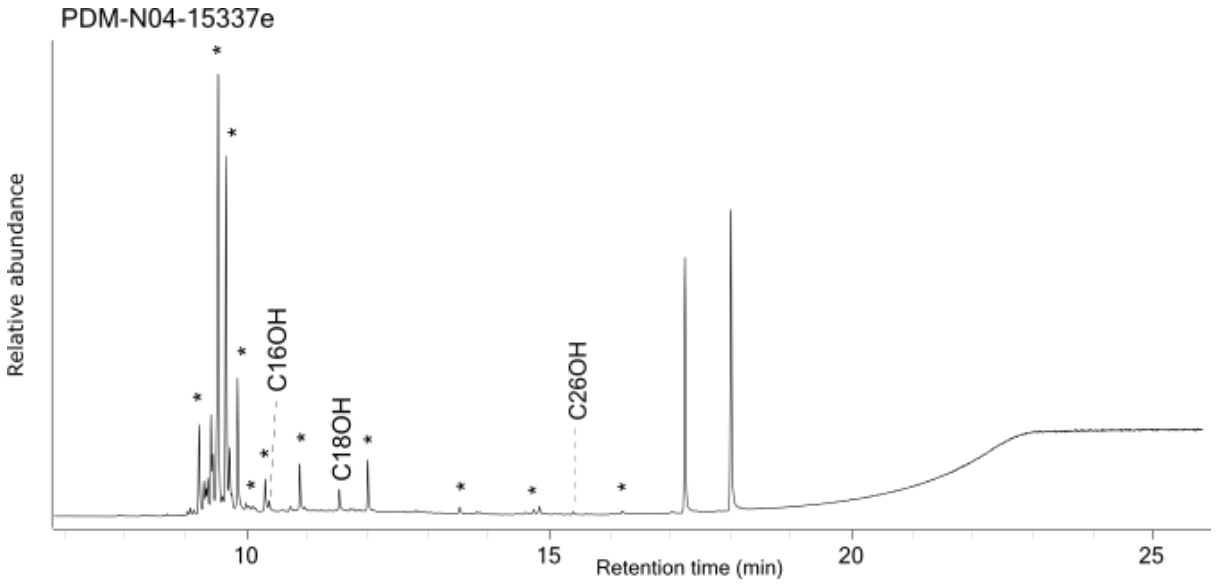
Lipid analysis

	Lipid yield ($\mu g\ g^{-1}$)	P/S	O/S	$\delta^{13}C_{16:0}$ (‰)	$\delta^{13}C_{18:0}$ (‰)	$\Delta^{13}C$ (‰)	Lipid content
External (e)	66.53	1.63	8.99	-	-	-	SFA (C12, C14, C16-18, C20, C22-30, C32), UFA (C18:1, C22:1), DC (C13), ALK (C22), OH (C16, C18, C26), 4,8,12-TMTD, pri, phy (93% SRR), B3CA (tr)
Internal (i)	40.69	2.03		-30.10	-30.04	0.06	SFA (C16, C18, C20, C22, C24, C26, C28), UFA (C18:1, C22:1), pri (tr), B3CA (tr)

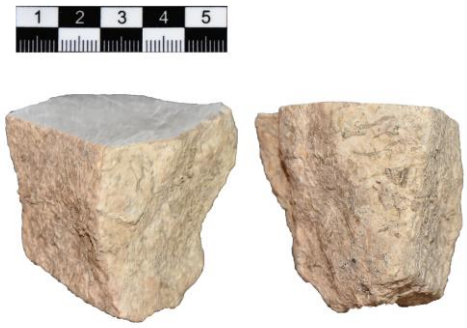
Molecular signature:	-
HAS interpretation:	Culinary feature



Partial total ion chromatograms (TIC) of acid/methanol extract of sample PDM-N04-15337e/i showing saturated fatty acids ($C_{XX:0}$), unsaturated fatty acids ($C_{XX:1}$), benzene polycarboxylic acid (BPCA), diacids (DC_{XX}), *n*-alkanes (ALK xx), contaminants (*), and *n*-alkanes internal standards (IS $_{ALKXX}$).



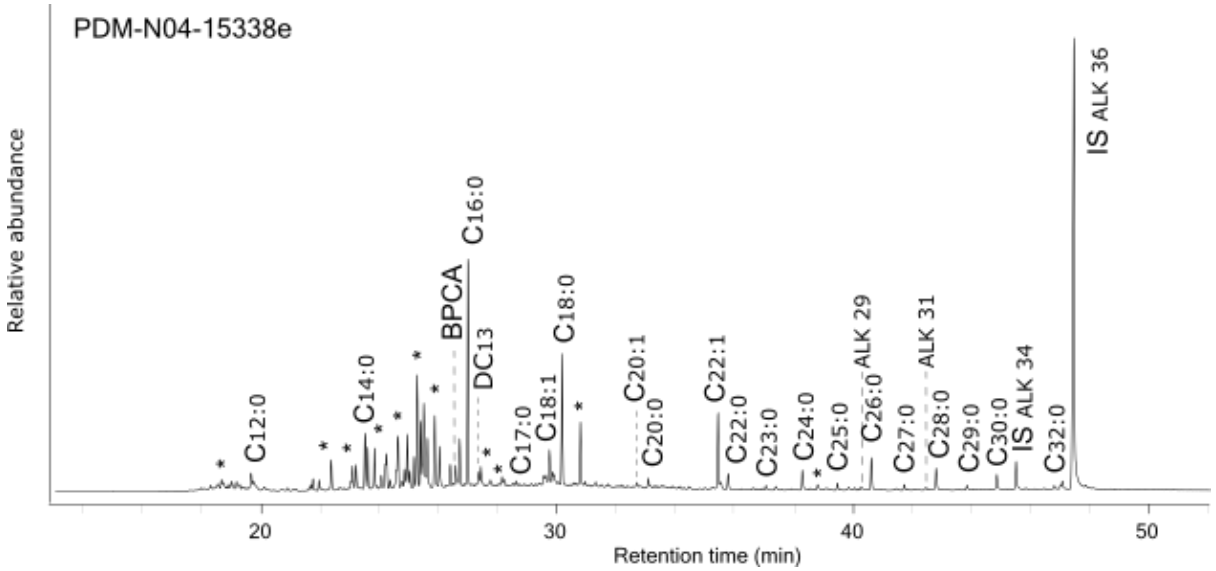
Partial total ion chromatogram (TIC) of solvent extract of sample PDM-N04-15337e showing alcohols (CxxOH), contaminants (*), and *n*-alkanes internal standards (IS $_{ALKXX}$).

		Sample id:	**PDM-N04-15338**
		info:	US 14647, grid L20 occupation phase 3
		Mineral:	Limestone
		Dimension:	118 g
Firing structure:	Cooking place	3D:	https://skfb.ly/puzEA
Alteration patterns:	-		

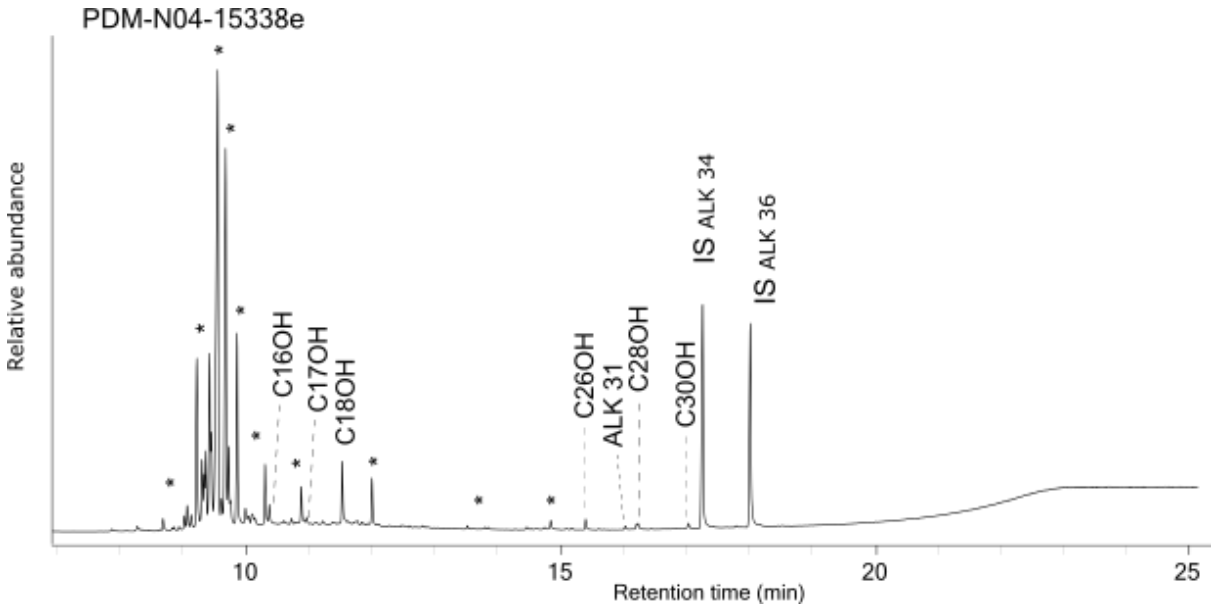
Lipid analysis

	Lipid yield ($\mu g\ g^{-1}$)	P/S	O/S	$\delta^{13}C_{16:0}$ (‰)	$\delta^{13}C_{18:0}$ (‰)	$\Delta^{13}C$ (‰)	Lipid content
External (e)	177.35	1.68	1.81	-29.80	-29.85	-0.05	SFA (C12, C14, C16-18, C20, C22-30, C32), UFA (C18:1, C20:1, C22:1), DC (C13), ALK (C29, C31), OH (C16, C17, C18, C26, C28, C30), 4,8,12-TMTD, pri, phy (95% SRR), B3CA (tr)
Internal (i)	-	-	-	-	-	-	-

Molecular signature:	Plant resources
HAS interpretation:	Culinary feature



Partial total ion chromatograms (TIC) of acid/methanol extract of sample PDM-N04-15338e showing saturated fatty acids ($C_{XX:0}$), unsaturated fatty acids ($C_{XX:1}$), benzene polycarboxylic acid (BPCA), diacids (DC_{XX}), *n*-alkanes (ALK xx), contaminants (*), and *n*-alkanes internal standards (IS $_{ALKXX}$).



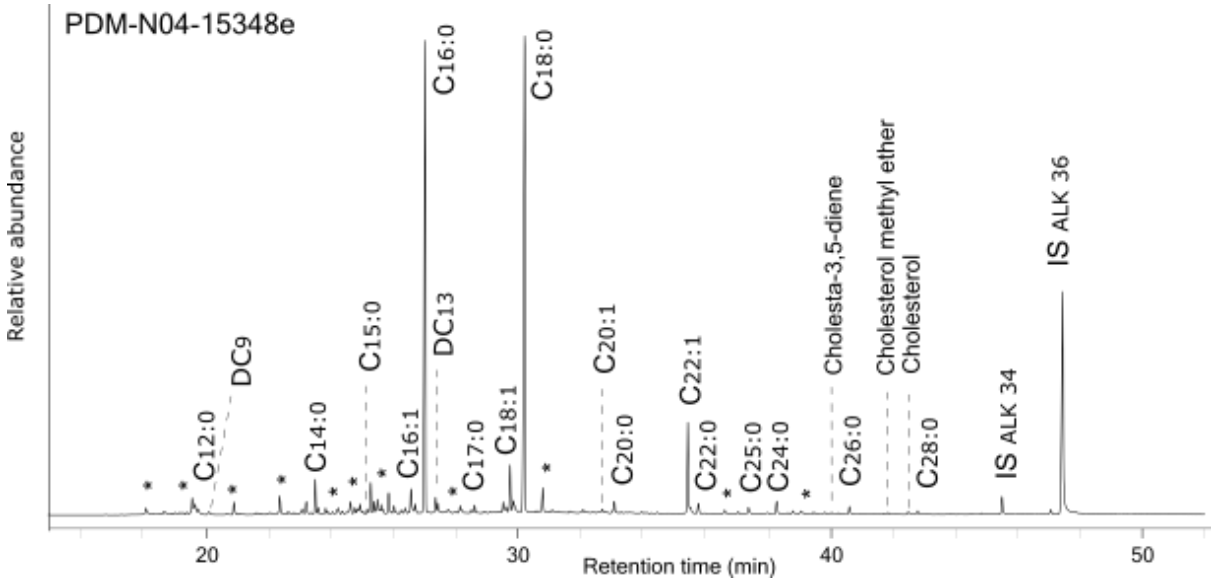
Partial total ion chromatogram (TIC) of solvent extract of sample PDM-N04-15338e showing alcohols (CxxOH), *n*-alkanes (ALK xx), contaminants (*), and *n*-alkanes internal standards (IS $_{ALKXX}$).

		Sample id:	**PDM-N04-15348**
		info:	US 14647, grid L20 occupation phase 3
		Mineral:	Limestone
		Dimension:	42 g
Firing structure:	Cooking place	3D:	https://skfb.ly/puzEA
Alteration patterns:	Cracks		

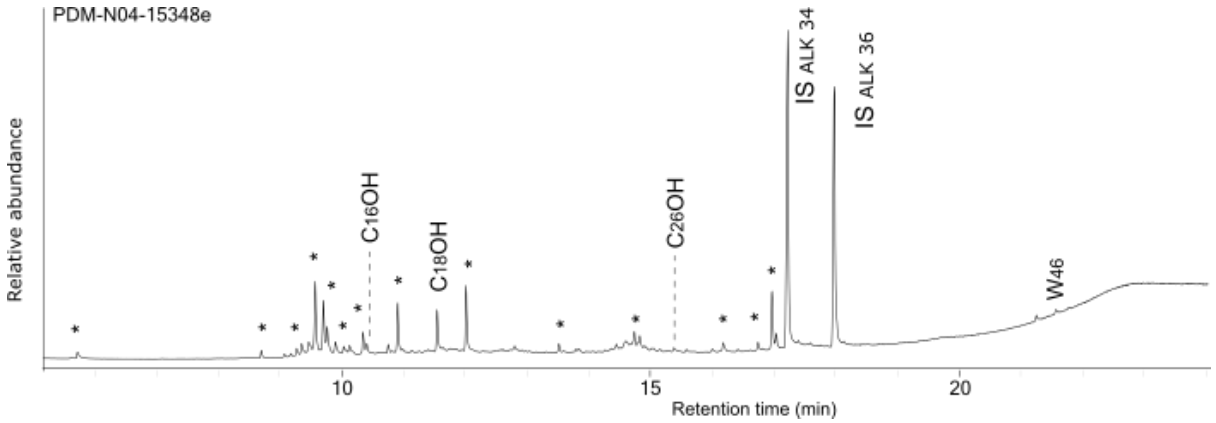
Lipid analysis

	Lipid yield ($\mu g\ g^{-1}$)	P/S	O/S	$\delta^{13}C_{16:0}$ (‰)	$\delta^{13}C_{18:0}$ (‰)	$\Delta^{13}C$ (‰)	Lipid content
External (e)	466.68	1.00	7.25	-29.41	-29.23	0.18	SFA (C12, C14-18, C20, C22, C24-26, C28), UFA (C16:1, C18:1, C20:1, C22:1), DC (C9, 13), OH (C16, C18, C26), pri, phy (91% SRR), ster (Cholesta-3,5-diene, Cholesterol methyl ether, Cholesterol), WE (C46 tr)
Internal (i)	-	-	-	-	-	-	-

Molecular signature:	Mixed resources
HAS interpretation:	Culinary feature



Partial total ion chromatograms (TIC) of acid/methanol extract of sample PDM-N04-15348e showing saturated fatty acids ($C_{XX:0}$), unsaturated fatty acids ($C_{XX:1}$), diacids (DC_{XX}), *n*-alkanes (ALK xx), contaminants (*), and *n*-alkanes internal standards (IS $_{ALKXX}$).



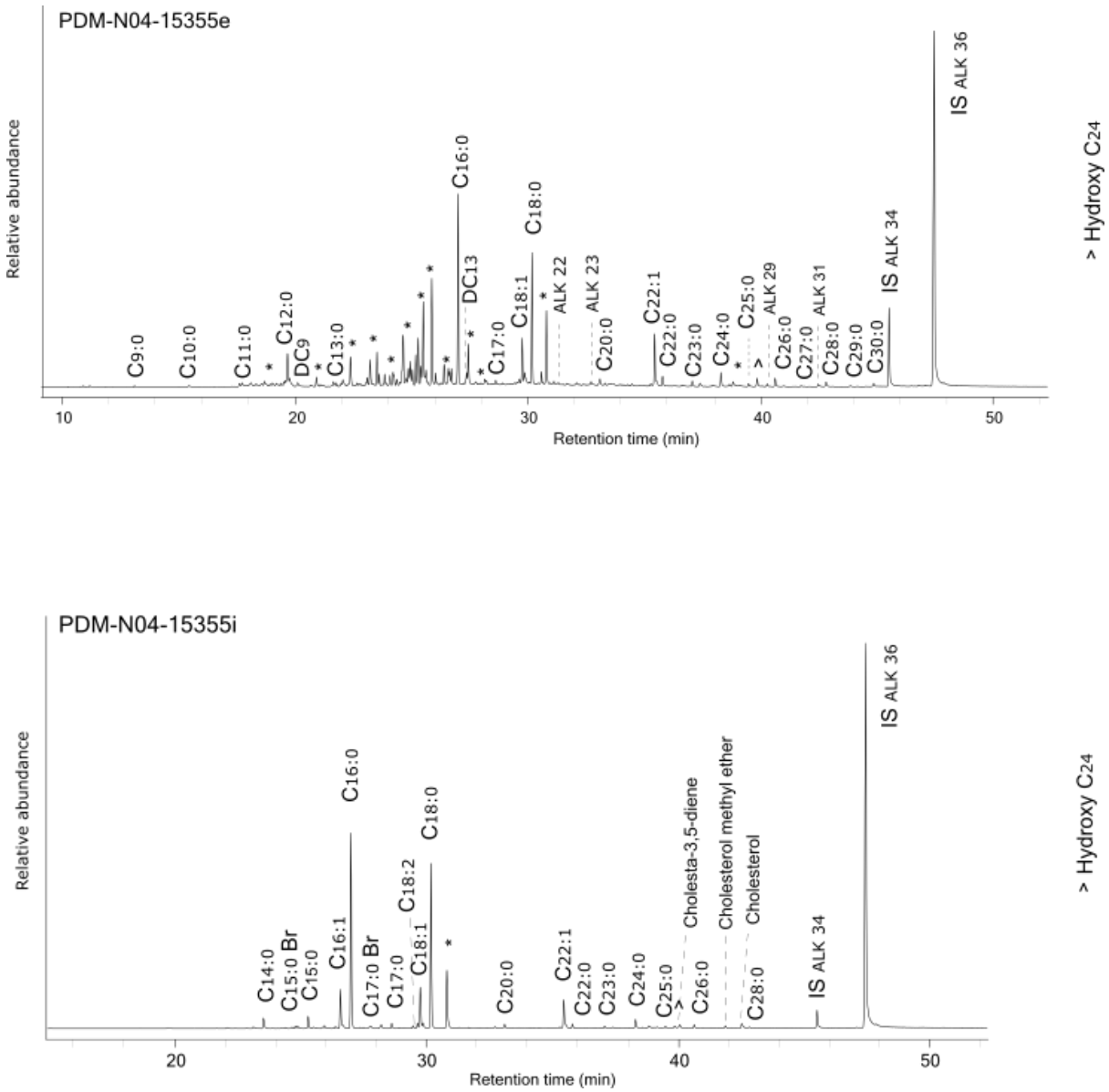
Partial total ion chromatogram (TIC) of solvent extract of sample PDM-N04-15348e showing alcohols (CxxOH), wax esters (Wxx), contaminants (*), and *n*-alkanes internal standards (IS $_{ALKXX}$).

		Sample id:	**PDM-N04-15355**
		info:	US 14647, grid L20 occupation phase 3
		Mineral:	Limestone
		Dimension:	62 g
Firing structure:	Cooking place	3D:	https://skfb.ly/puzEA
Alteration patterns:	-		

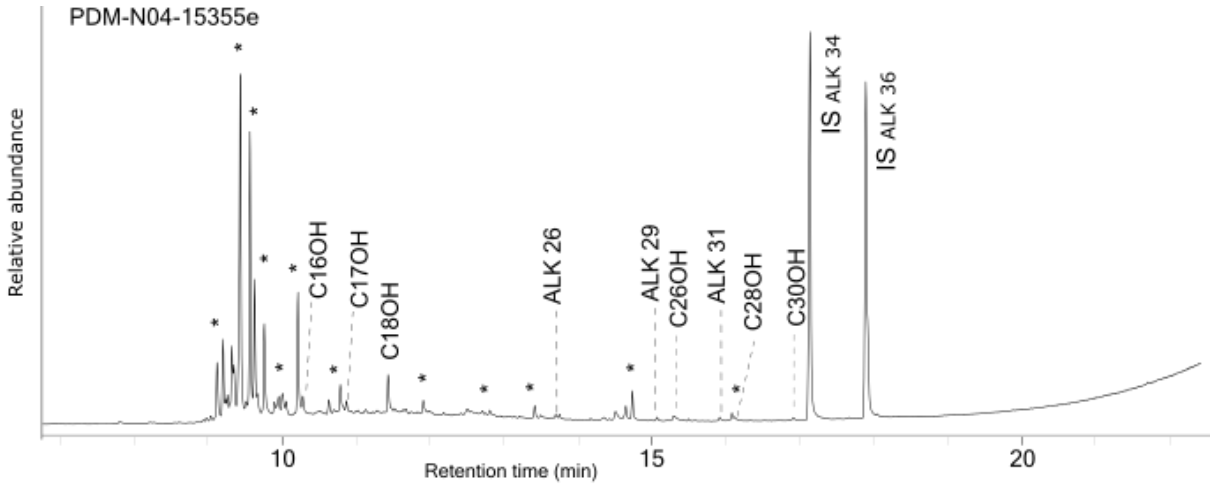
Lipid analysis

	Lipid yield (µg g^{-1})	P/S	O/S	$\delta^{13}C_{16:0}$ (‰)	$\delta^{13}C_{18:0}$ (‰)	$\Delta^{13}C$ (‰)	Lipid content
External (e)	48.04	1.48	1.79	-29.60	-30.38	-0.78	SFA (C9-13, C16-18, C20, C22-30), UFA (C18:1, C22:1), Hy (C24), DC (C9, C13), ALK (C22, C23, C26, C29, C31), OH (C16, C17, C18, C26, C28, C30), 4,8,12-TMTD, pri, phy (90% SRR)
Internal (i)	113.59	1.24	3.90	-28.72	-29.48	-0.76	SFA (C14-18, C20, C22-26, C28), BrFA (C17), UFA (C16:1, C18:1, C18:2, C22:1), Hy (C24), pri, ster (Cholesta-3,5-diene, Cholesterol methyl ether, Cholesterol)

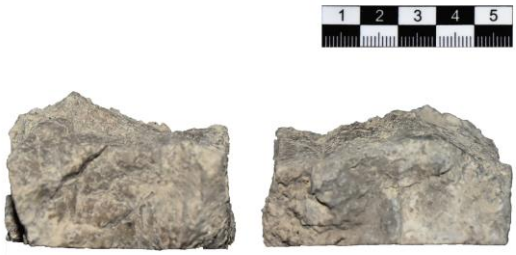
Molecular signature:	Mixed resources
HAS interpretation:	Culinary feature



Partial total ion chromatograms (TIC) of acid/methanol extract of sample PDM-N04-15355e/i showing saturated fatty acids ($C_{XX:0}$), branched fatty acids ($C_{XX:0}$ Br), unsaturated fatty acids ($C_{XX:1}$), diacids (DC_{XX}), hydroxy fatty acids (^), *n*-alkanes (ALK xx), sterols, contaminants (*), and *n*-alkanes internal standards (IS_{ALKXX}).



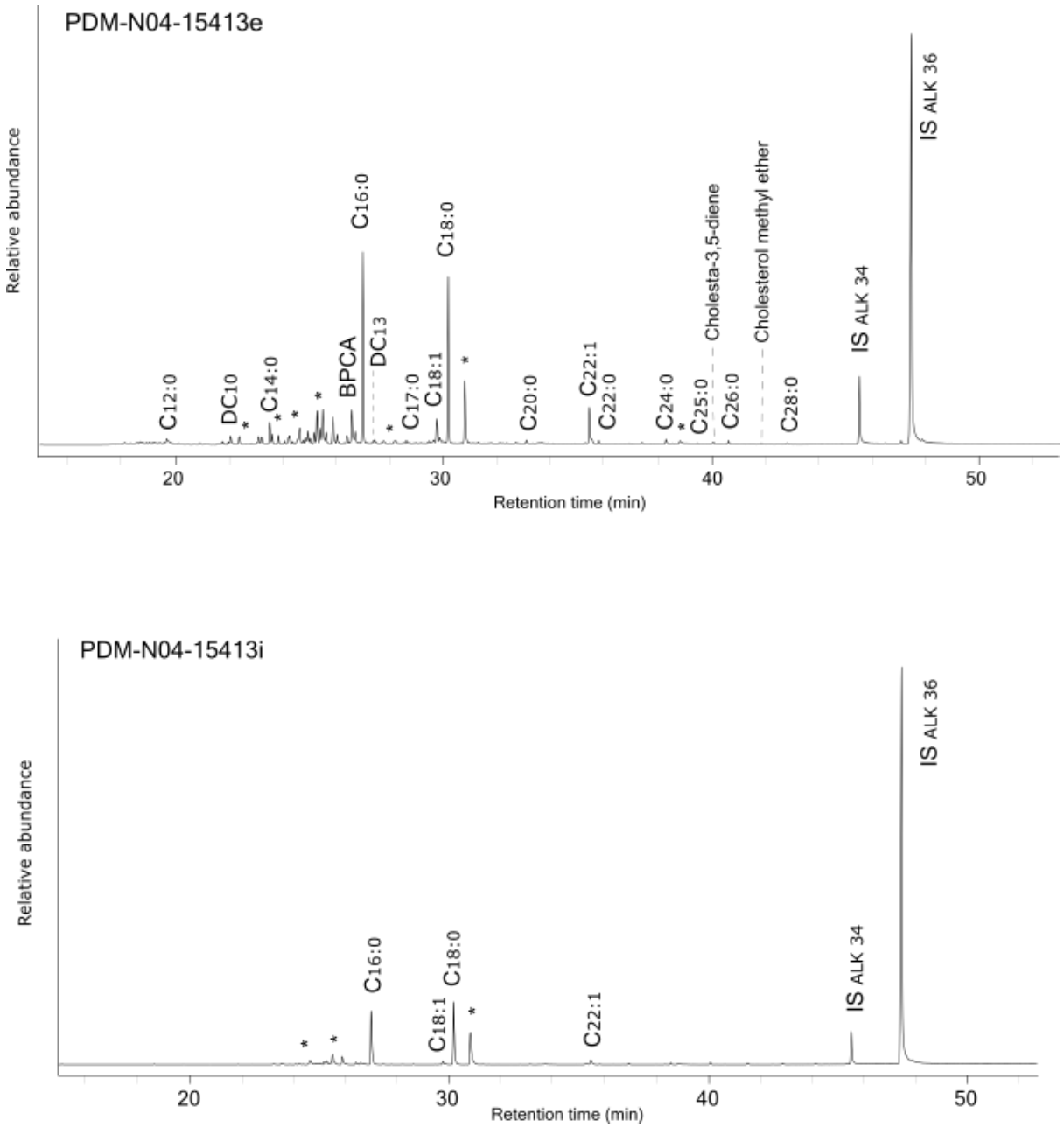
Partial total ion chromatogram (TIC) of solvent extract of sample PDM-N04-15355e showing alcohols (CxxOH), *n*-alkanes (ALK xx), contaminants (*), and *n*-alkanes internal standards (IS $_{ALKXX}$).

		Sample id:	**PDM-N04-15413**
		info:	US 14647, grid L20 occupation phase 3
		Mineral:	Limestone
		Dimension:	174 g
Firing structure:	Cooking place	3D:	https://skfb.ly/puzEA
Alteration patterns:	-		

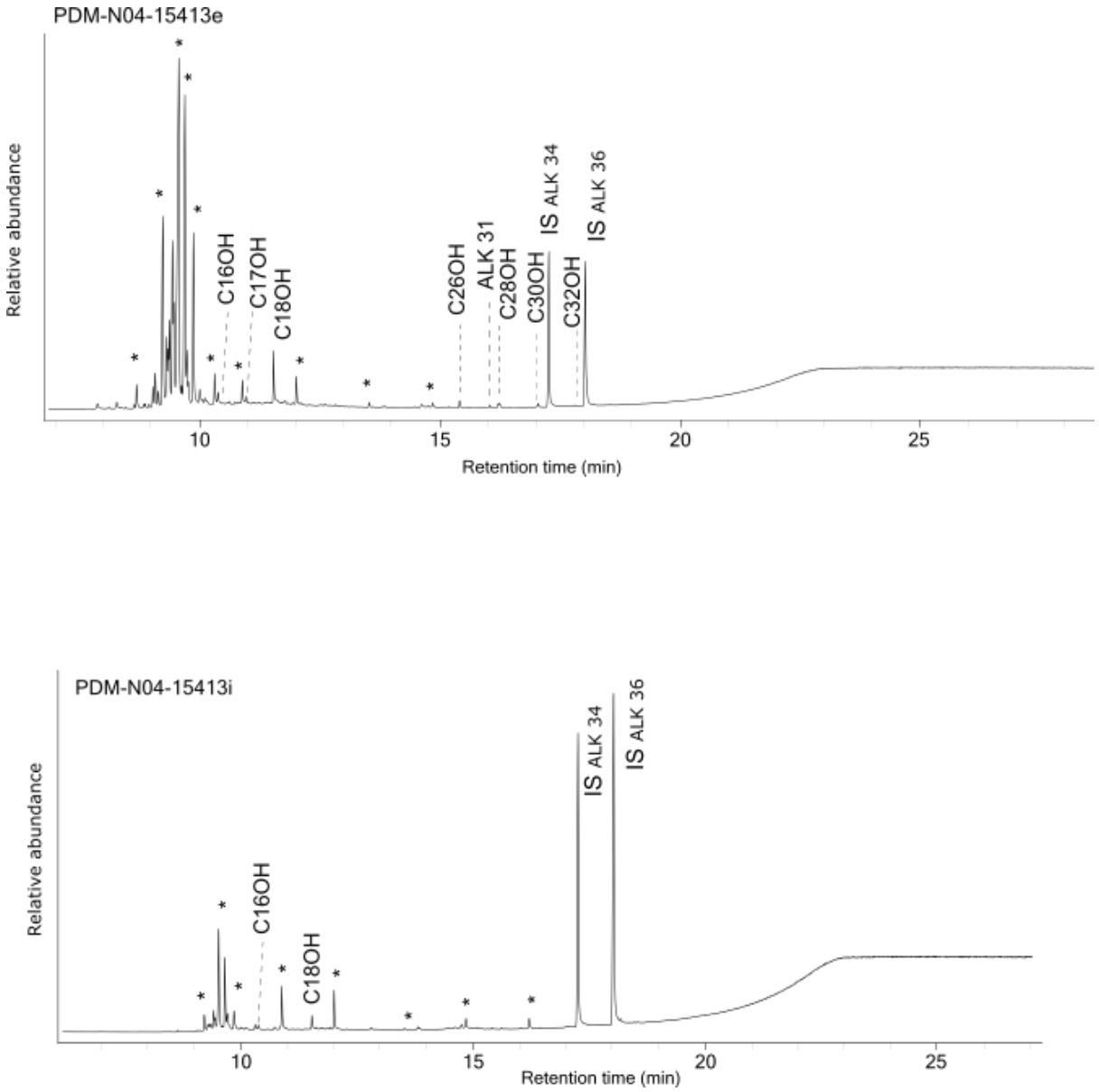
Lipid analysis

	Lipid yield ($\mu g\ g^{-1}$)	P/S	O/S	$\delta^{13}C_{16:0}$ (‰)	$\delta^{13}C_{18:0}$ (‰)	$\Delta^{13}C$ (‰)	Lipid content
External (e)	144.86	1.32	2.35	-30.10	-29.68	0.42	SFA (C12, C14, C16-18, C20, C22, C24-26, C28), UFA (C18:1, C22:1), DC (C10, C13), ALK (C31), OH (C16, C17, C18, C26, C28, C30, C32), pri, phy (89% SRR), ster (Cholesta-3,5-diene, Cholesterol methyl ether), B3CA (tr)
Internal (i)	29.02	1.18	6.22	-29.53	-29.55	-0.02	SFA (C16, C18), UFA (C18:1, C22:1), OH (C16, C18), pri (tr)

Molecular signature:	Mixed resources
HAS interpretation:	Culinary feature



Partial total ion chromatograms (TIC) of acid/methanol extract of sample PDM-N04-15355e/i showing saturated fatty acids ($C_{XX:0}$), unsaturated fatty acids ($C_{XX:1}$), benzene polycarboxylic acid (BPCA), diacids (DC_{XX}), sterols, contaminants (*), and *n*-alkanes internal standards (IS_{ALKXX}).



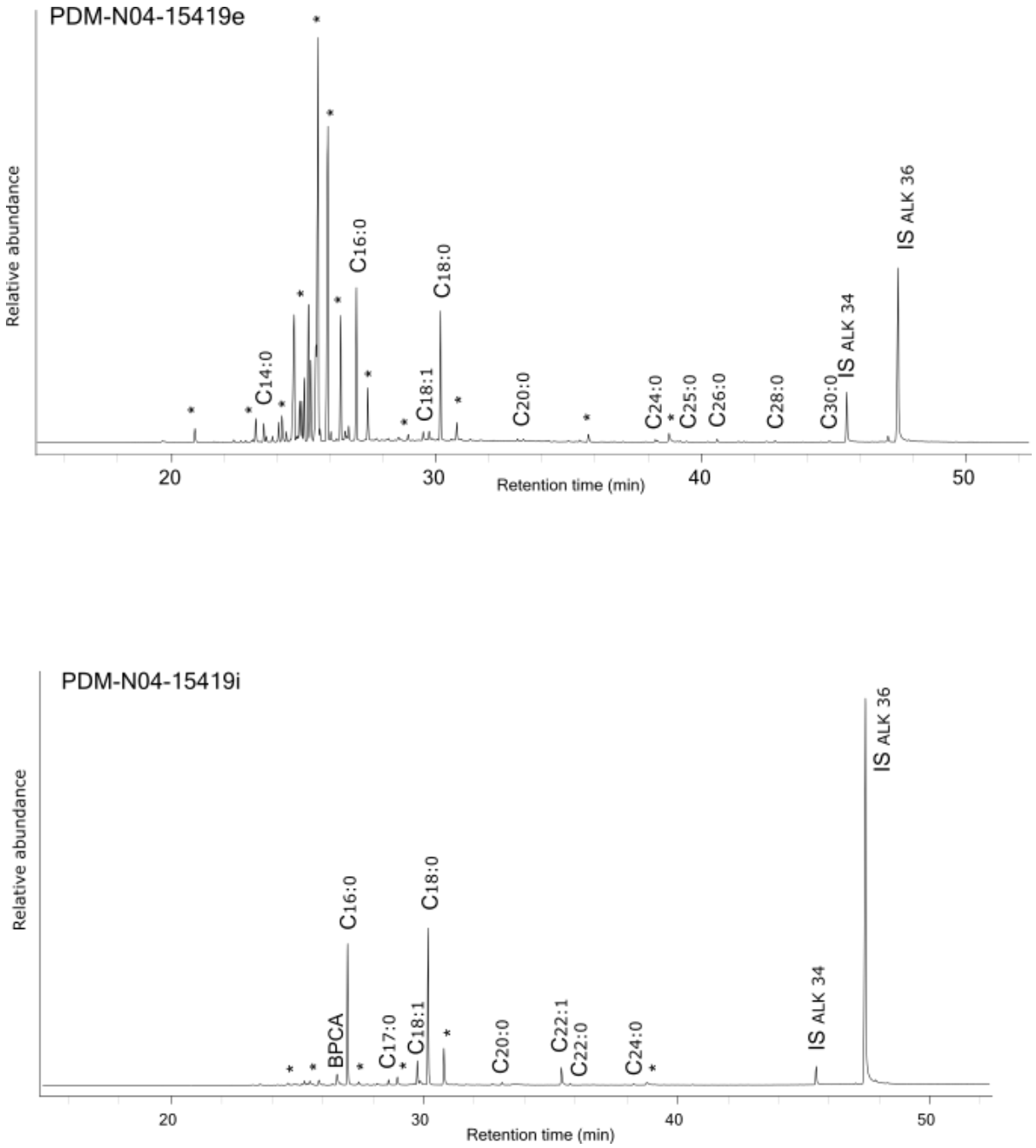
Partial total ion chromatograms (TIC) of solvent extract of sample PDM-N04-15413e/i showing alcohols (CxxOH), *n*-alkanes (ALK xx), contaminants (*), and *n*-alkanes internal standards (IS $_{ALKXX}$).

  		Sample id:	**PDM-N04-15419**
		info:	US 14647, grid L20 occupation phase 3
		Mineral:	Limestone
		Dimension:	30 g
Firing structure:	Cooking place	3D:	https://skfb.ly/puzEA
Alteration patterns:	Discoloration		

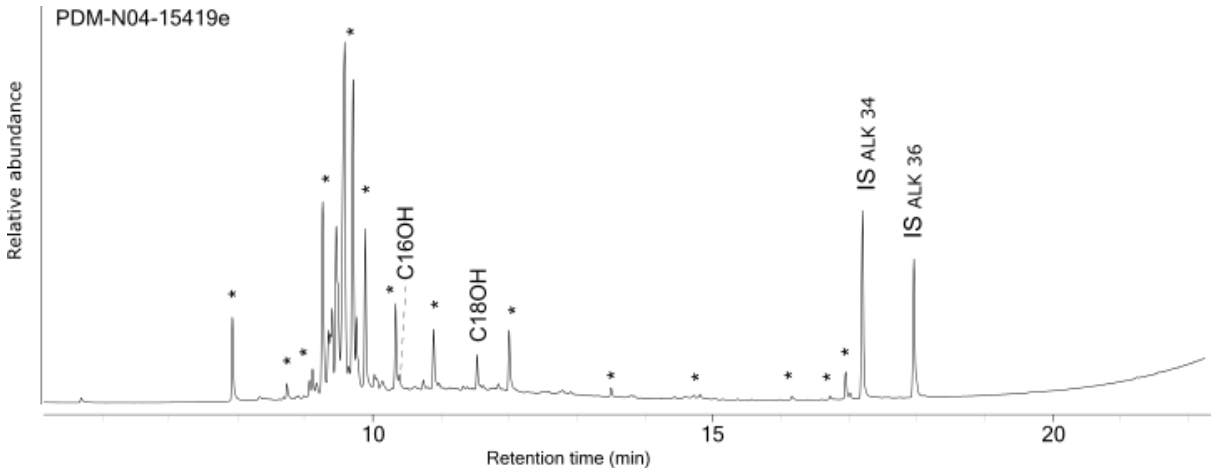
Lipid analysis

	Lipid yield ($\mu g\ g^{-1}$)	P/S	O/S	$\delta^{13}C_{16:0}$ (‰)	$\delta^{13}C_{18:0}$ (‰)	$\Delta^{13}C$ (‰)	Lipid content
External (e)	47.77	1.29	11.95	-30.54	-29.59	0.95	SFA (C14, C16, C18, C20, C24-26, C28, C30), UFA (C18:1), OH (C16, C18), 4,8,12-TMTD (tr), pri (tr)
Internal (i)	39.09	1.42		-28.24	-28.24	0.00	SFA (C16-18, C20, C22, C24), UFA (C18:1, C22:1), B3CA

Molecular signature:	Non-ruminant resources
HAS interpretation:	Culinary feature



Partial total ion chromatograms (TIC) of acid/methanol extract of sample PDM-N04-15419e/i showing saturated fatty acids ($C_{XX:0}$), unsaturated fatty acids ($C_{XX:1}$), benzene polycarboxylic acid (BPCA), contaminants (*), and *n*-alkanes internal standards (IS $_{ALKXX}$).



Partial total ion chromatogram (TIC) of solvent extract of sample PDM-N04-15419e showing alcohols (CxxOH), contaminants (*), and *n*-alkanes internal standards (IS $_{ALKXX}$).

		Sample id:	**PDM-N04-15431**
		info:	US 14647, grid L20 occupation phase 3
		Mineral:	Limestone
		Dimension:	64 g
Firing structure:	Cooking place	3D:	https://skfb.ly/puzEA
Alteration patterns:	-		

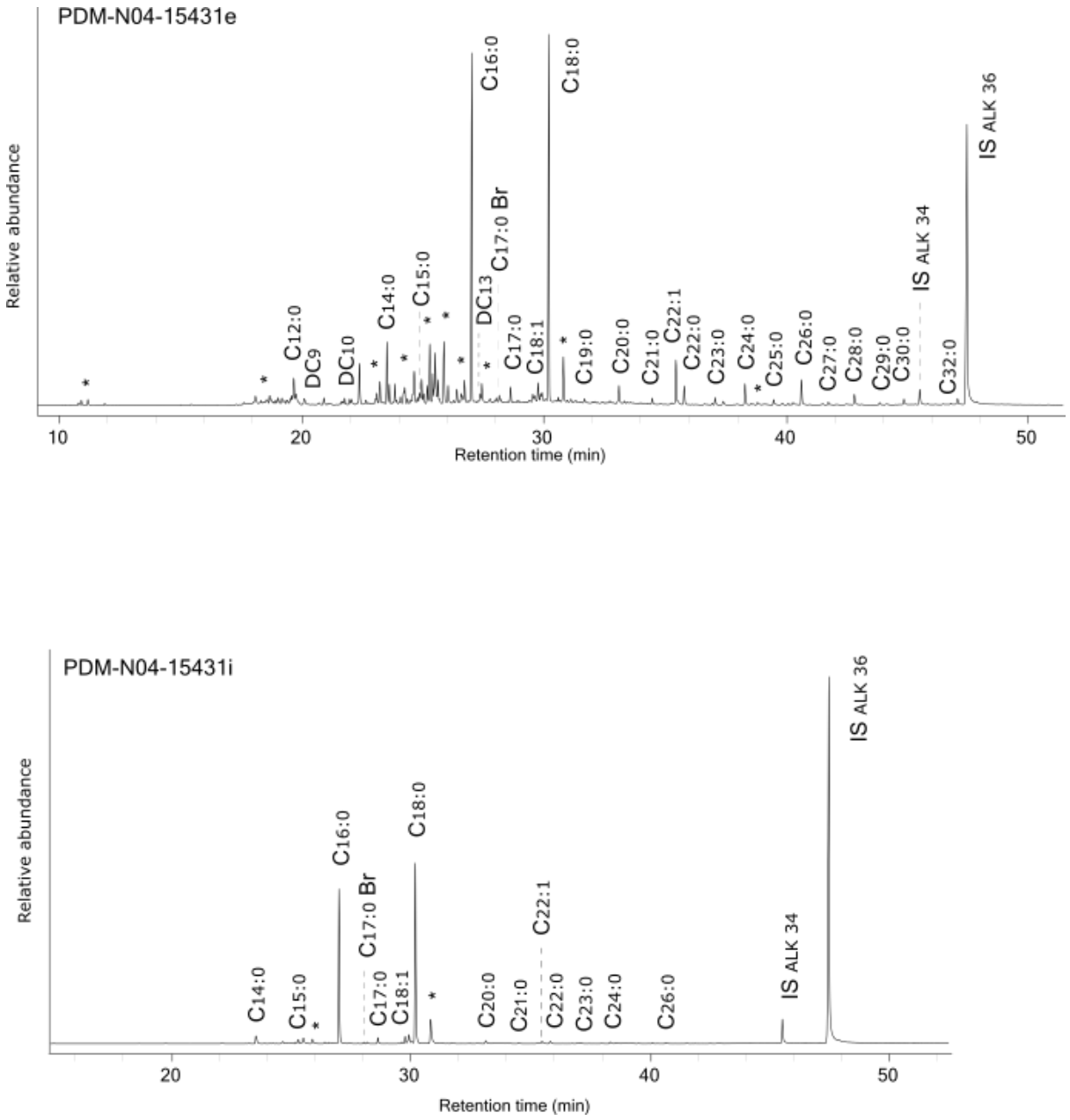
Lipid analysis

	Lipid yield ($\mu g\ g^{-1}$)	P/S	O/S	$\delta^{13}C_{16:0}$ (‰)	$\delta^{13}C_{18:0}$ (‰)	$\Delta^{13}C$ (‰)	Lipid content
External (e)	403.22	0.94	9.64	-28.61	-32.20	-3.59	SFA (C12, C14-30, C32), BrFA (C17), UFA (C18:1, C22:1), DC (C9, C10, C13), ALK (C29, C31), OH (C16, C18, C26, C28), 4,8,12-TMTD, pri, phy (79% SRR)
Internal (i)	59.91	0.93	12.71	-28.82	-32.81	-3.99	SFA (C14-18, C20-24, C26), BrFA (C17), UFA (C18:1, C22:1), phy (62% SRR)

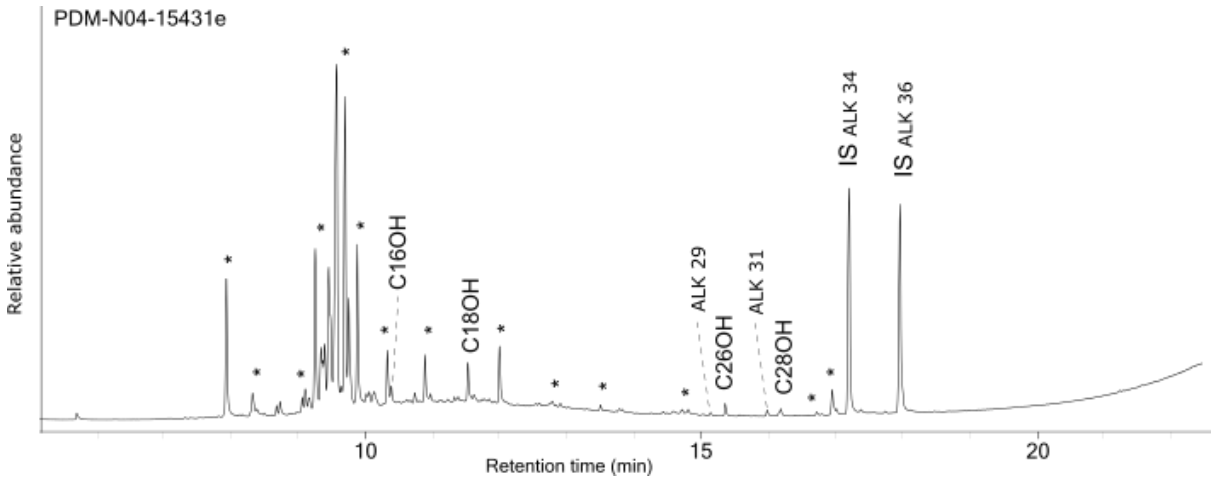
Molecular signature:	Wild ruminant resources (dairy)
HAS interpretation:	Culinary feature

Protein analysis

Molecular signature:	-



Partial total ion chromatograms (TIC) of acid/methanol extract of sample PDM-N04-15431e/i showing saturated fatty acids ($C_{XX:0}$), branched fatty acids ($C_{XX:0}$ Br), unsaturated fatty acids ($C_{XX:1}$), diacids (DC_{XX}), contaminants (*), and *n*-alkanes internal standards (IS $_{ALKXX}$).



Partial total ion chromatogram (TIC) of solvent extract of sample PDM-N04-15431e showing alcohols (CxxOH), *n*-alkanes (ALK xx), contaminants (*), and *n*-alkanes internal standards (IS $_{ALKXX}$).

		Sample id:	**PDM-N04-15433**
		info:	US 14647, grid L20 occupation phase 3
		Mineral:	Limestone
		Dimension:	36 g
Firing structure:	Cooking place	3D:	https://skfb.ly/puzEA
Alteration patterns:	Sooting		

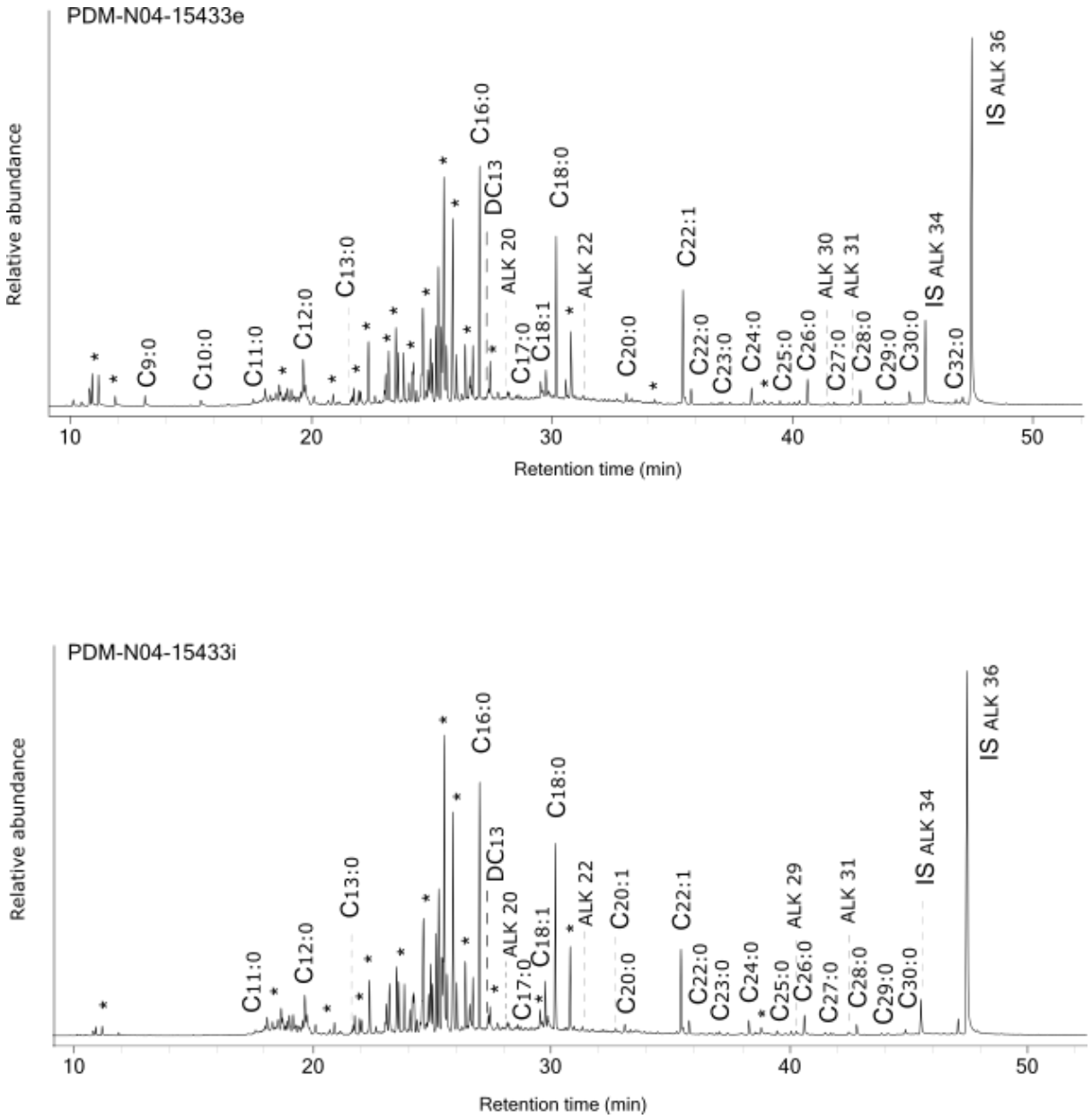
Lipid analysis

	Lipid yield ($\mu g\ g^{-1}$)	P/S	O/S	$\delta^{13}C_{16:0}$ (‰)	$\delta^{13}C_{18:0}$ (‰)	$\Delta^{13}C$ (‰)	Lipid content
External (e)	118.40	1.46	3.69	-	-	-	SFA (C9-13, C16-18, C20, C22-30, C32), UFA (C18:1, C22:1), DC (C13), ALK (C20, C22, C29, C30, C31), OH (C16, C18, C26, C28), phy (96% SRR)
Internal (i)	12.13	1.69		-27.45	-29.63	-2.18	SFA (C11-13, C16-18, C20, C22-30), UFA (C18:1, C22:1), DC (C13), ALK (C20, C22, C29, C30, C31), 4,8,12-TMTD, pri, phy (94% SRR)

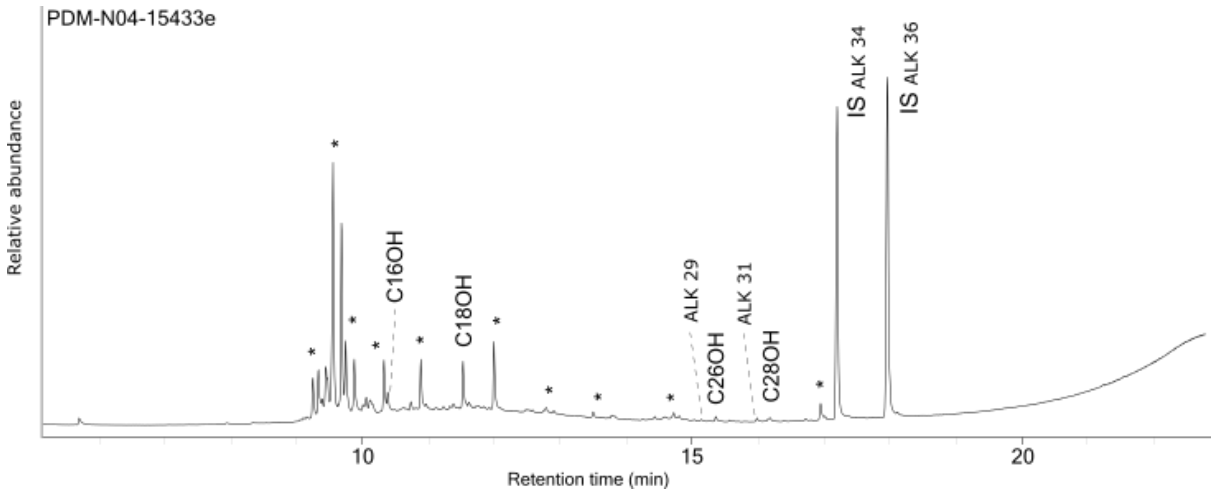
Molecular signature:	Ruminant resources
HAS interpretation:	Culinary feature

Protein analysis

Molecular signature:	-



Partial total ion chromatograms (TIC) of acid/methanol extract of sample PDM-N04-15433e/i showing saturated fatty acids ($C_{XX:0}$), branched fatty acids ($C_{XX:0}$ Br), unsaturated fatty acids ($C_{XX:1}$), diacids (DC_{XX}), *n*-alkanes (ALK xx), contaminants (*), and *n*-alkanes internal standards (IS $_{ALKXX}$).



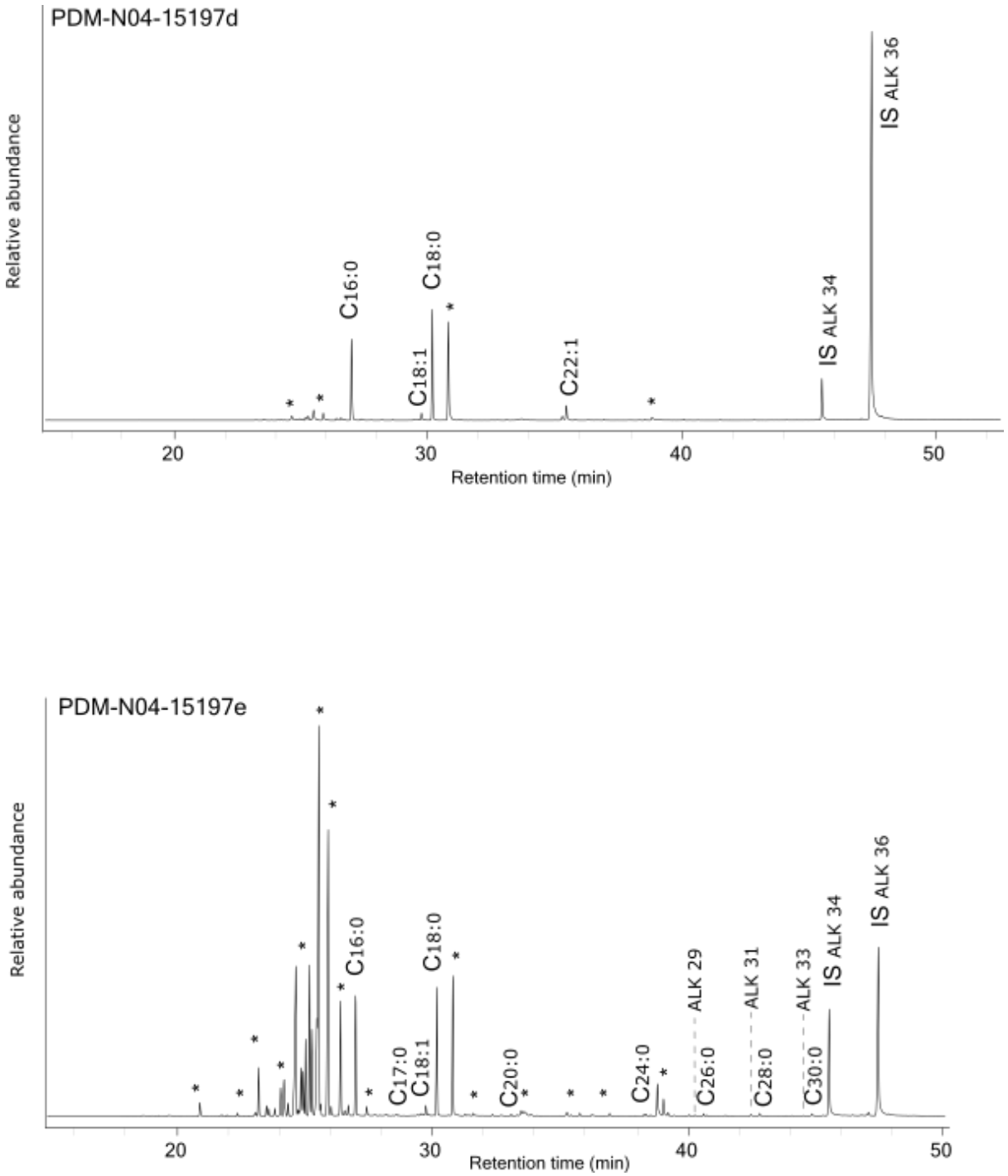
Partial total ion chromatogram (TIC) of solvent extract of sample PDM-N04-15433e showing alcohols (CxxOH), *n*-alkanes (ALK xx), contaminants (*), and *n*-alkanes internal standards (IS $_{ALKXX}$).

		Sample id:	**PDM-N04-15197**
		info:	US 14549, grid L21 occupation phase 3
		Mineral:	Limestone
		Dimension:	154 g
Firing structure:	Fireplace	3D:	https://skfb.ly/puzEA
Alteration patterns:	Sooting, discoloration, superficial deposit		

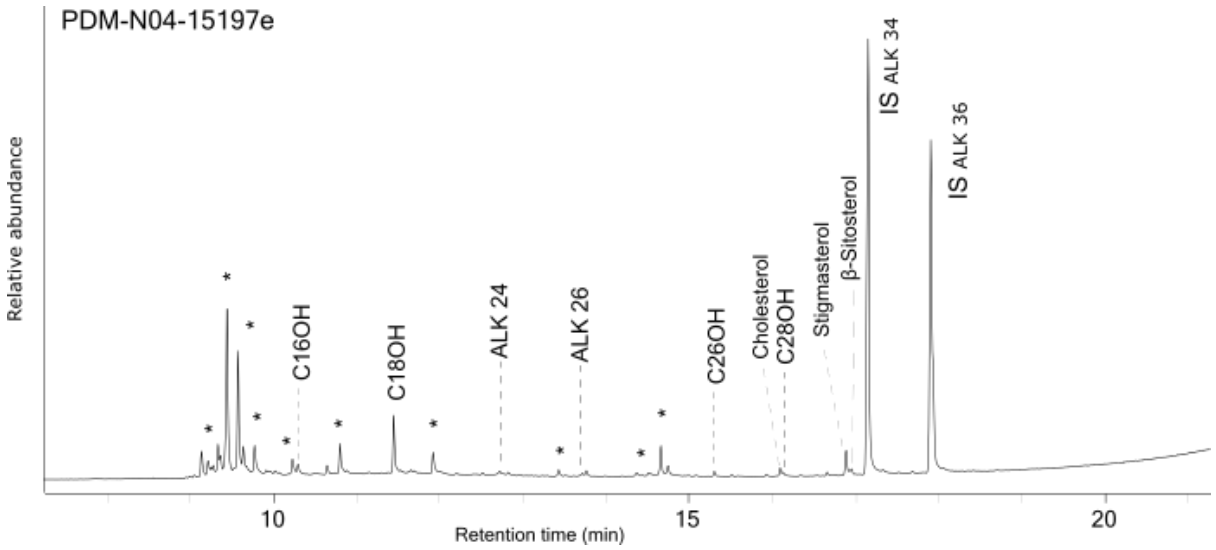
Lipid analysis

	Lipid yield ($\mu g\ g^{-1}$)	P/S	O/S	$\delta^{13}C_{16:0}$ (‰)	$\delta^{13}C_{18:0}$ (‰)	$\Delta^{13}C$ (‰)	Lipid content
Deposit (d)	6.77	-	-	-	-	-	SFA (C16), UFA (C18:1, C22:1), pri (tr)
External (e)	17.68	1.05	12.23	-30.42	-30.07	0.35	SFA (C16-18, C20, C24, C26, C28, C30), UFA (C18:1), ALK (C24, C26, C29, C31, C33), OH (C16, C18, C26, C28), 4,8,12-TMTD (tr), pri (tr), ster (Cholesterol, Stigmasterol, β-Sitosterol)
Internal (i)	-	-	-	-	-	-	-

Molecular signature:	Plant resources
HAS interpretation:	Combustion feature



Partial total ion chromatograms (TIC) of acid/methanol extract of sample PDM-N04-15197d/e showing saturated fatty acids ($C_{XX:0}$), unsaturated fatty acids ($C_{XX:1}$), *n*-alkanes (ALK xx), contaminants (*), and *n*-alkanes internal standards (IS $_{ALKXX}$).



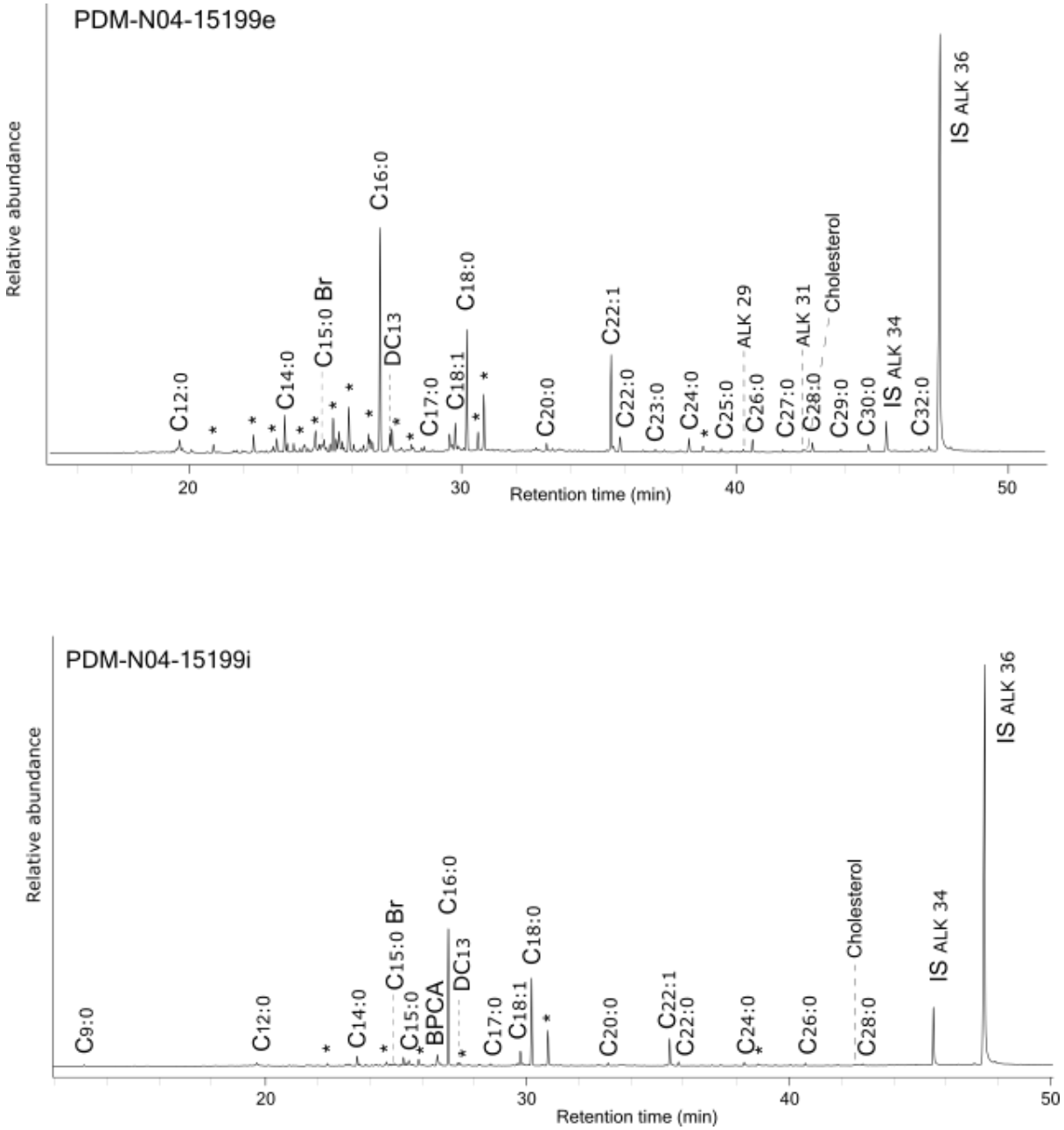
Partial total ion chromatogram (TIC) of solvent extract of sample PDM-N04-15197e showing alcohols (CxxOH), *n*-alkanes (ALK xx), sterols, contaminants (*), and *n*-alkanes internal standards (IS $_{ALKXX}$).

		Sample id:	**PDM-N04-15199**
		info:	US 14549, grid L21 occupation phase 3
		Mineral:	Limestone
		Dimension:	163 g
Firing structure:	Fireplace	3D:	https://skfb.ly/puzEA
Alteration patterns:	-		

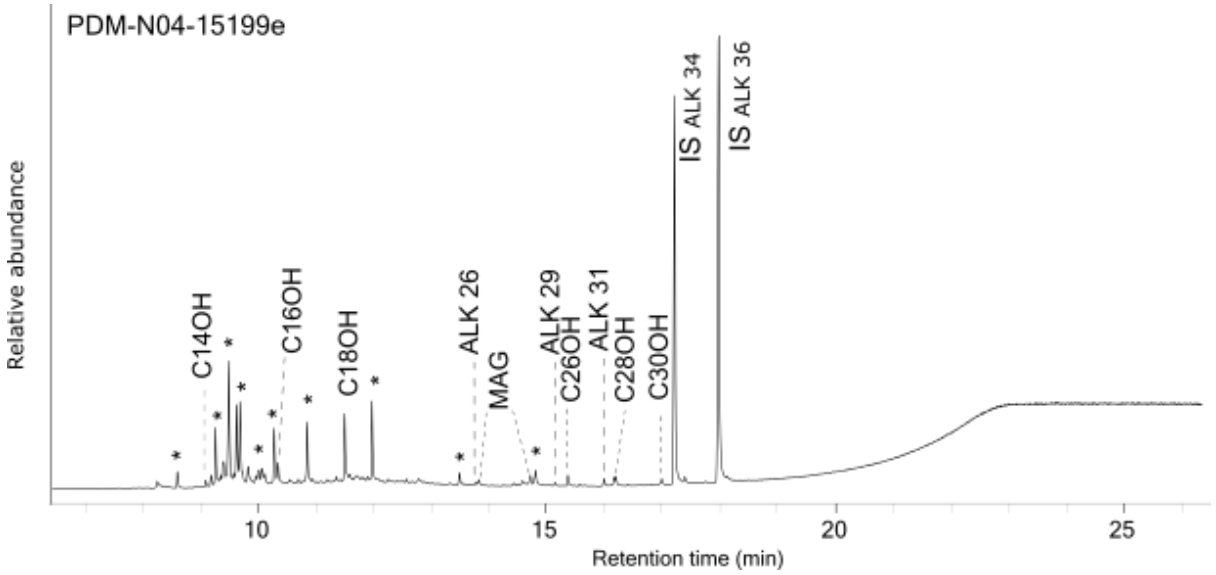
Lipid analysis

	Lipid yield ($\mu g\ g^{-1}$)	P/S	O/S	$\delta^{13}C_{16:0}$ (‰)	$\delta^{13}C_{18:0}$ (‰)	$\Delta^{13}C$ (‰)	Lipid content
External (e)	145.75	1.97	4.03	-29.94	-31.06	-1.12	SFA (C12, C14, C16-18, C20, C22-30, C32), BrFA (C15), UFA (C18:1, C22:1), ALK (C26, C29, C31), DC (C13), OH (C14, C16, C18, C26, C28, C30), 4,8,12-TMTD, pri, phy (87% SRR), MAGs
Internal (i)	24.57	1.79	6.30	-	-	-	SFA (C9, C12, C14-18, C20, C22, C24, C26, C28), BrFA (C15), UFA (C18:1, C22:1), DC (C13), pri (tr), B3CA (tr)

Molecular signature:	Plant resources, thermal alteration
HAS interpretation:	Combustion feature



Partial total ion chromatograms (TIC) of acid/methanol extract of sample PDM-N04-15199e/i showing saturated fatty acids ($C_{XX:0}$), unsaturated fatty acids ($C_{XX:1}$), benzene polycarboxylic acid (BPCA) diacids (DC_{XX}), *n*-alkanes (ALK xx), sterols, contaminants (*), and *n*-alkanes internal standards (IS $_{ALKXX}$).



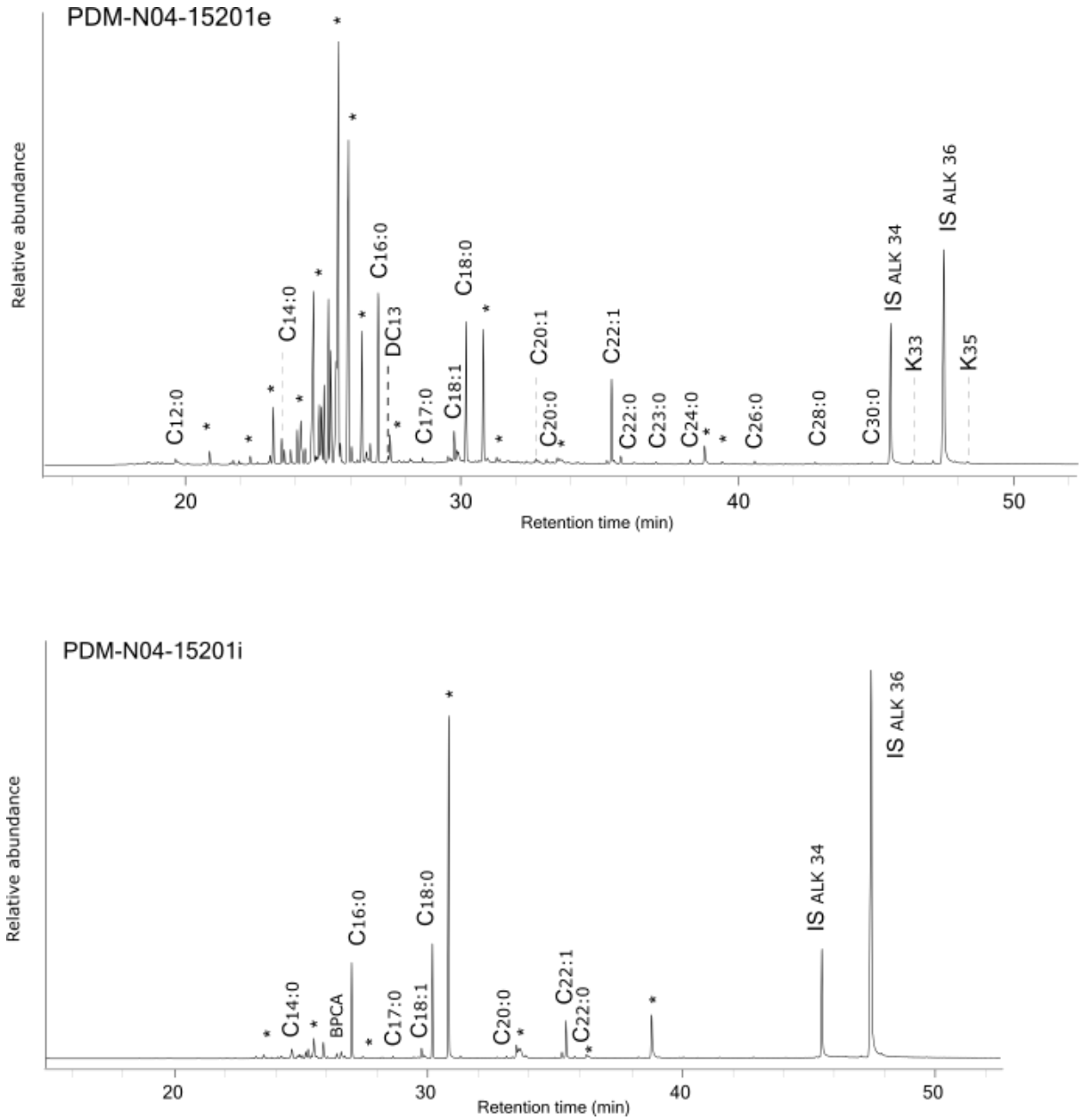
Partial total ion chromatogram (TIC) of solvent extract of sample PDM-N04-15199e showing alcohols (CxxOH), *n*-alkanes (ALK xx), monoacylglycerols (MAGs), contaminants (*), and *n*-alkanes internal standards (IS $_{ALKXX}$).

		Sample id:	**PDM-N04-15201**
		info:	US 14549, grid L21 occupation phase 3
		Mineral:	Limestone
		Dimension:	85 g
Firing structure:	Fireplace	3D:	https://skfb.ly/puzEA
Alteration patterns:	Discoloration		

Lipid analysis

	Lipid yield ($\mu g\ g^{-1}$)	P/S	O/S	$\delta^{13}C_{16:0}$ (‰)	$\delta^{13}C_{18:0}$ (‰)	$\Delta^{13}C$ (‰)	Lipid content
External (e)	19.21	1.24	2.29				SFA (C12, C14, C16-18, C20, C22-24, C26, C28, C30), UFA (C18:1, C20:1, C22:1), DC (C13), OH (C18), K (C33, 35), 4,8,12-TMTD (tr), pri, phy (77% SRR)
Internal (i)	6.84	1.21		-29.77	-29.77	0.00	SFA (C14, C16-18, C20, C22), UFA (C18:1, C22:1), pri (tr), B3CA

Molecular signature:	Plant resources, thermal alteration
HAS interpretation:	Combustion feature



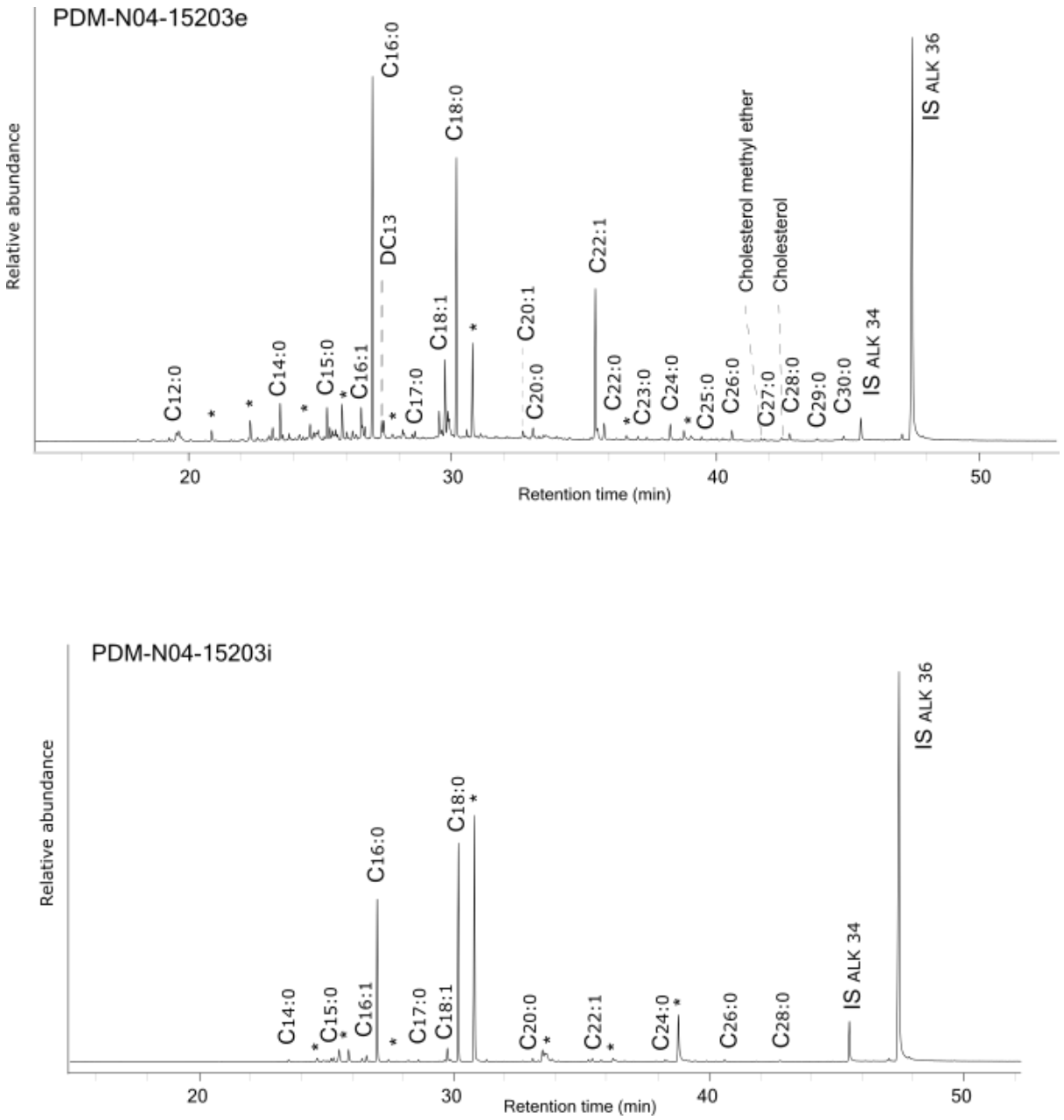
Partial total ion chromatograms (TIC) of acid/methanol extract of sample PDM-N04-15201e/i showing saturated fatty acids ($C_{XX:0}$), unsaturated fatty acids ($C_{XX:1}$), benzene polycarboxylic acid (BPCA), diacids (DC_{XX}), ketones (Kxx), contaminants (*), and *n*-alkanes internal standards (IS $_{ALKXX}$).

		Sample id:	**PDM-N04-15203**
		info:	US 14549, grid L21 occupation phase 3
		Mineral:	Limestone
		Dimension:	52 g
Firing structure:	Fireplace	3D:	https://skfb.ly/puzEA
Alteration patterns:	-		

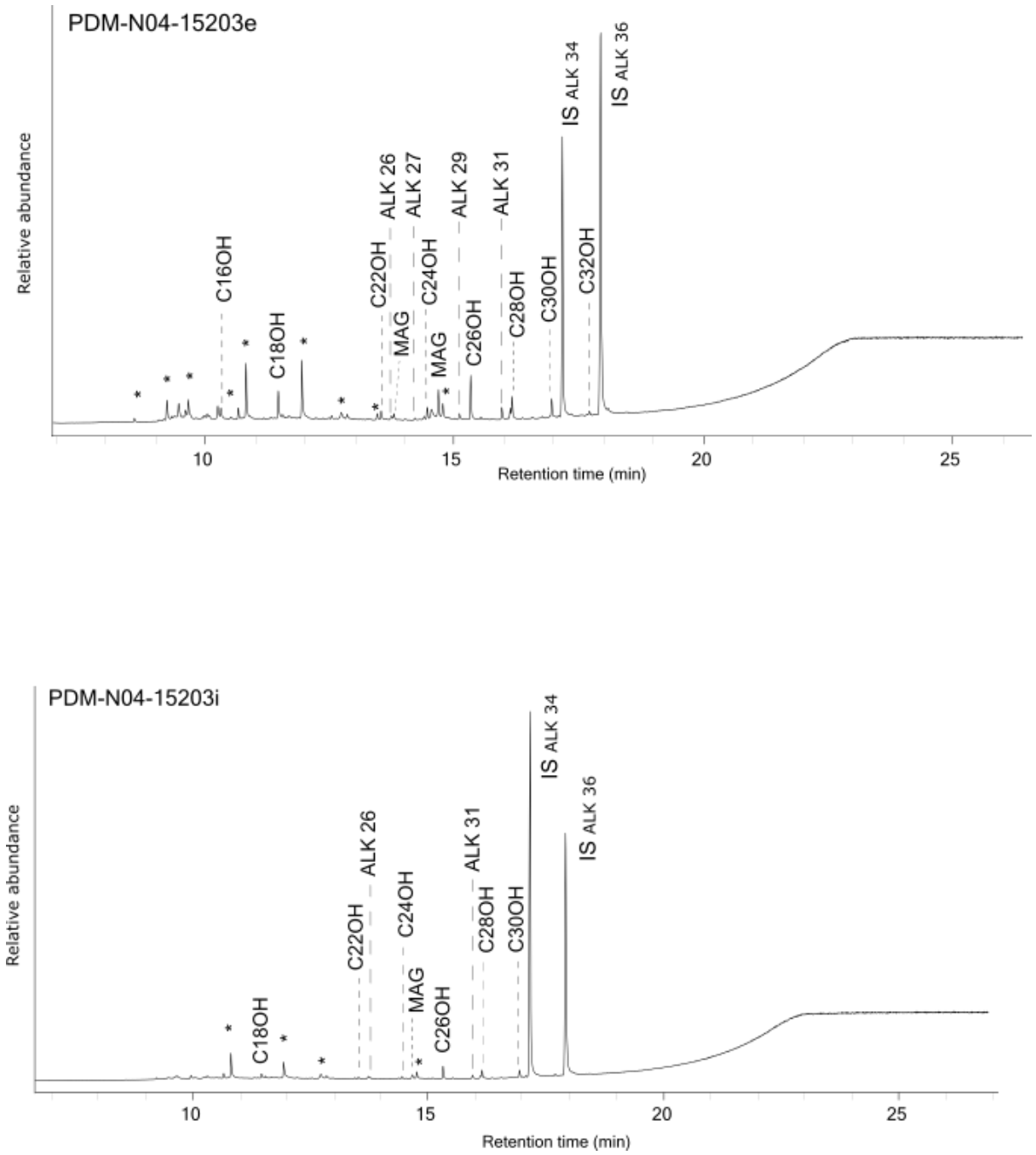
Lipid analysis

	Lipid yield ($\mu g\ g^{-1}$)	P/S	O/S	$\delta^{13}C_{16:0}$ (‰)	$\delta^{13}C_{18:0}$ (‰)	$\Delta^{13}C$ (‰)	Lipid content
External (e)	241.34	1.28	1.99	-28.78	-29.17	-0.39	SFA (C12, C14-18, C20, C22-30), UFA (C16:1, C18:1, C20:1, C22:1), DC (C13), ALK (C26, C27, C29, C31), OH (C16, C18, C22, C24, C26, C28, C30, C32), 4,8,12-TMTD (tr), pri, phy (80% SRR), ster (Cholesterol methyl ether, Cholesterol), MAGs
Internal (i)	33.43	1.32		-29.51	-29.28	0.23	SFA (C14-18, C20, C24, C26, C28), UFA (C18:1, C18:1, C22:1), ALK (C26, C31), OH (C18, C22, C24, C26, C28, C30), MAGs

Molecular signature:	Plant resources
HAS interpretation:	Combustion feature



Partial total ion chromatograms (TIC) of acid/methanol extract of sample PDM-N04-15203e/i showing saturated fatty acids ($C_{XX:0}$), unsaturated fatty acids ($C_{XX:1}$), diacids (DC_{XX}), sterols, contaminants (*), and *n*-alkanes internal standards (IS $_{ALKXX}$).



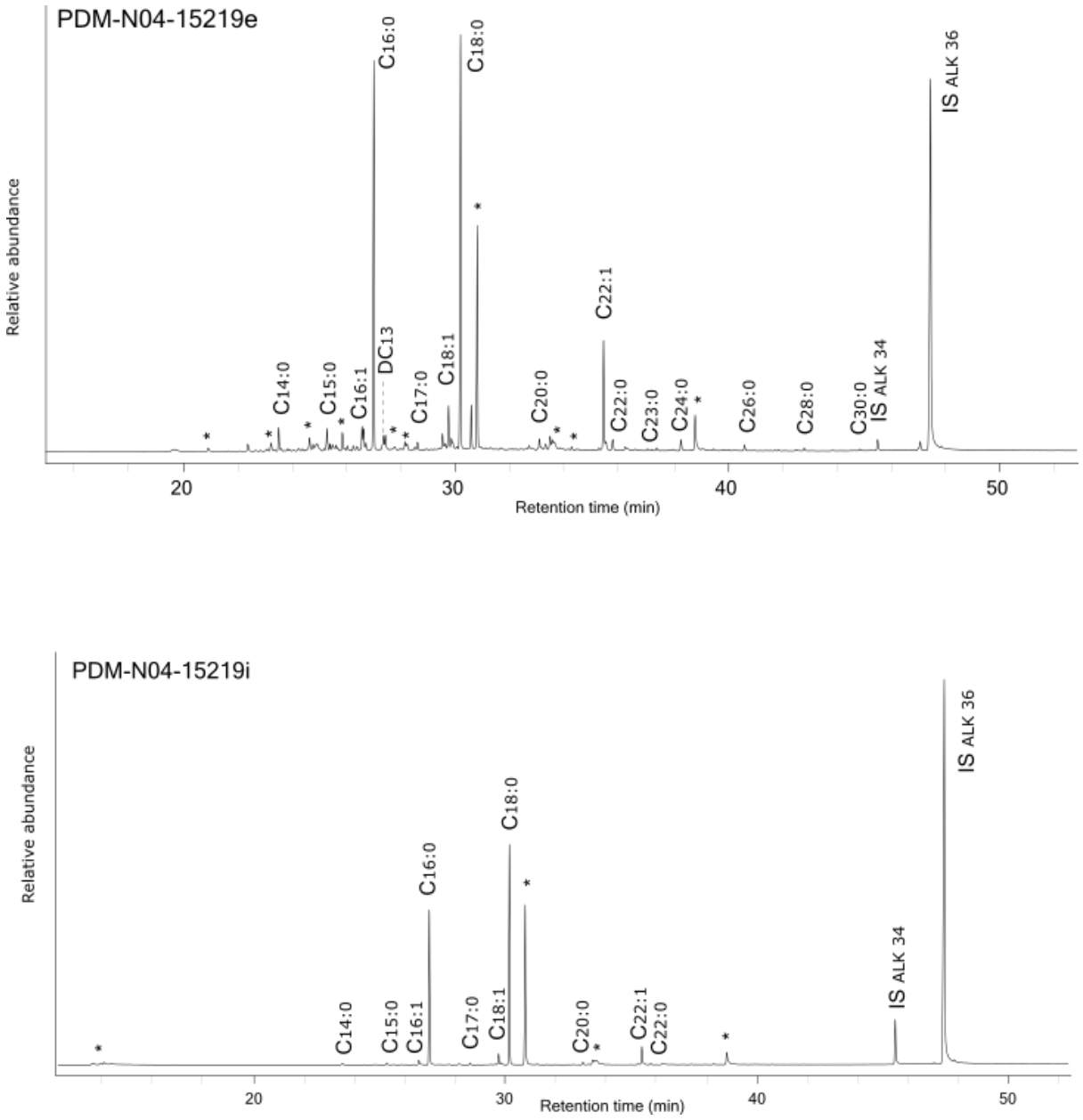
Partial total ion chromatograms (TIC) of solvent extract of sample PDM-N04-15203e/i showing alcohols (CxxOH), *n*-alkanes (ALK xx), monoacylglycerols (MAGs), contaminants (*), and *n*-alkanes internal standards (IS $_{ALKXX}$).

		Sample id:	**PDM-N04-15219**
		info:	US 14549, grid L21 occupation phase 3
		Mineral:	Limestone
		Dimension:	38 g
Firing structure:	Fireplace	3D:	https://skfb.ly/puzEA
Alteration patterns:	Sooting, discoloration, superficial deposit		

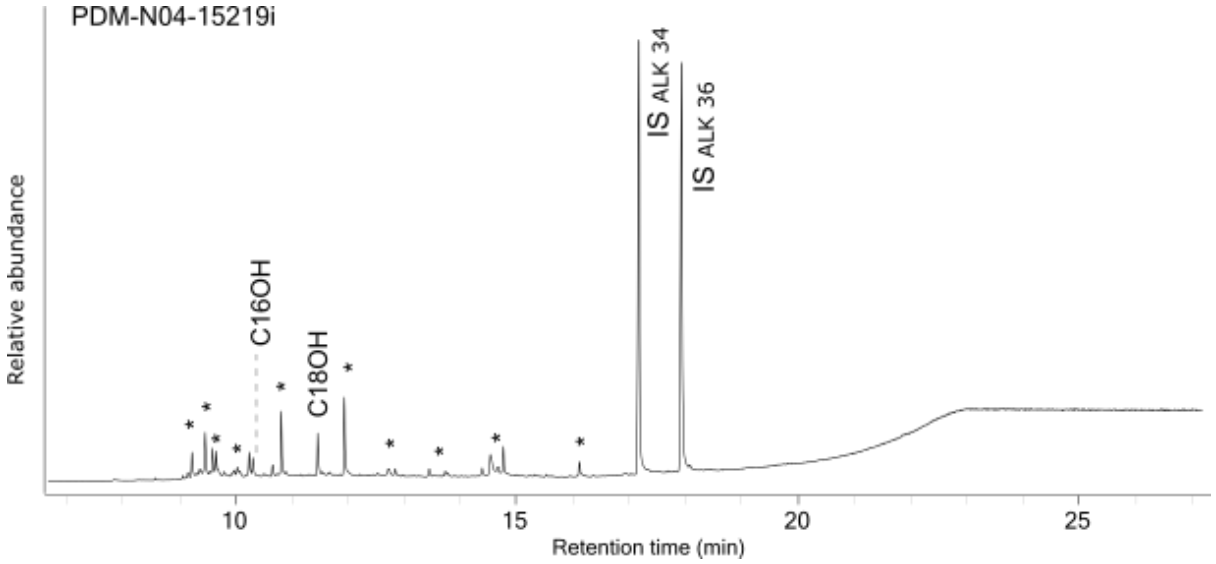
Lipid analysis

	Lipid yield ($\mu g\ g^{-1}$)	P/S	O/S	$\delta^{13}C_{16:0}$ (‰)	$\delta^{13}C_{18:0}$ (‰)	$\Delta^{13}C$ (‰)	Lipid content
External (e)	519.83	0.94	8.14	-29.24	-29.27	-0.03	SFA (C14-18, C20, C22-24, C26, C28, C30), UFA (C16:1, C18:1, C22:1), DC (C13), 4,8,12-TMTD (tr), pri, phy (72% SRR)
Internal (i)	12.63	-	-	-	-	-	SFA (C14-18, C20, C22), UFA (C16:1, C18:1, C22:1), OH (C16, C18), pri (tr)

Molecular signature:	-
HAS interpretation:	Combustion feature



Partial total ion chromatograms (TIC) of acid/methanol extract of sample PDM-N04-15219e/i showing saturated fatty acids ($C_{XX:0}$), unsaturated fatty acids ($C_{XX:1}$), diacids (DC_{XX}), contaminants (*), and *n*-alkanes internal standards (IS $_{ALKXX}$).



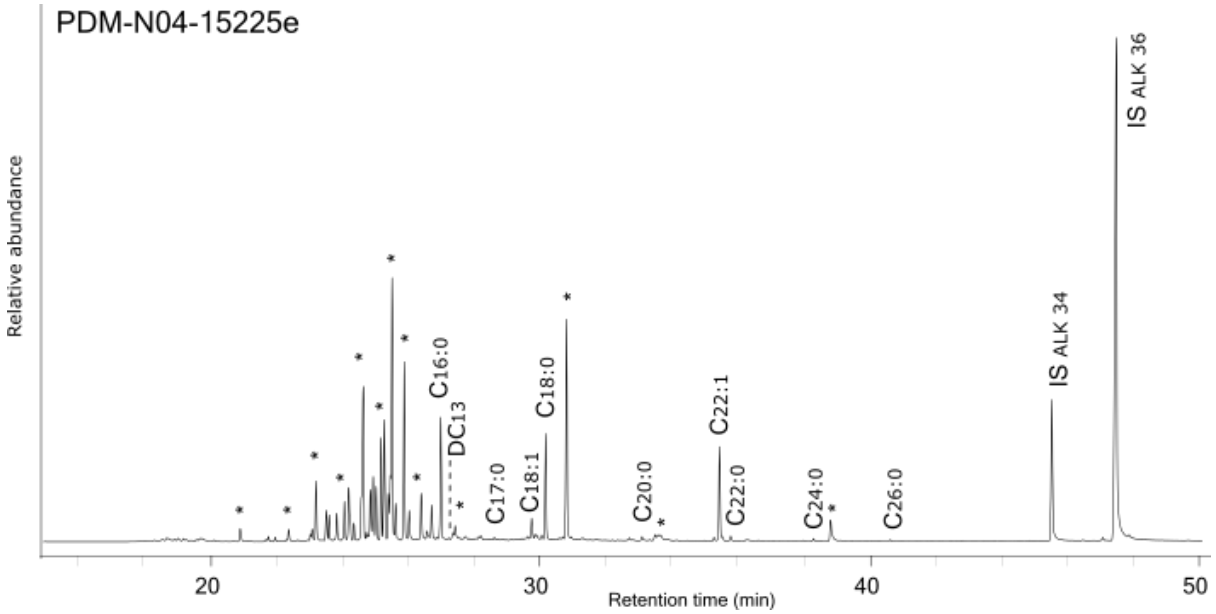
Partial total ion chromatogram (TIC) of solvent extract of sample PDM-N04-15219i showing alcohols (CxxOH), contaminants (*), and *n*-alkanes internal standards (IS $_{ALKXX}$).

		Sample id:	**PDM-N04-15225**
		info:	US 14549, grid L21 occupation phase 3
		Mineral:	Limestone
		Dimension:	90 g
Firing structure:	Fireplace	3D:	https://skfb.ly/puzEA
Alteration patterns:	Sooting		

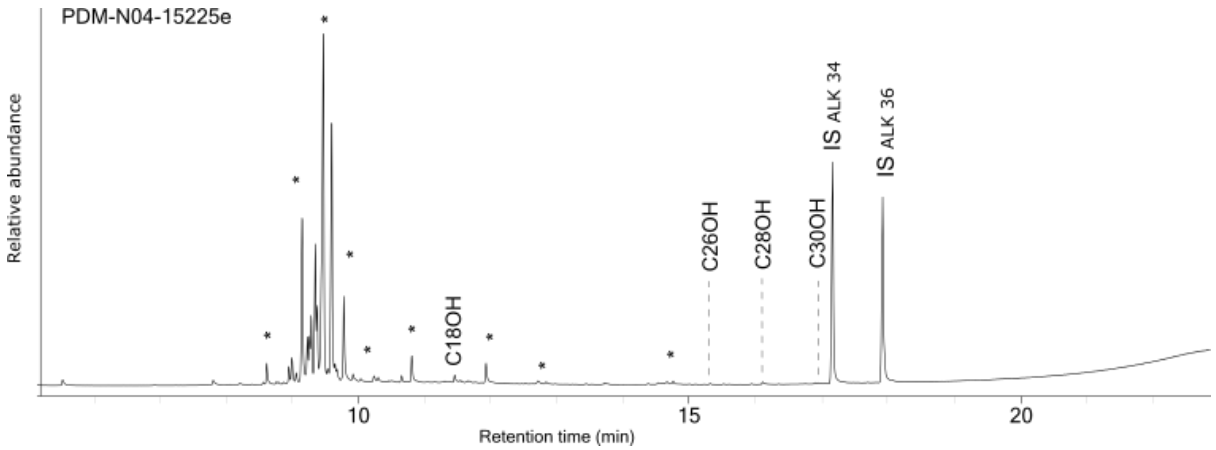
Lipid analysis

	Lipid yield ($\mu g\ g^{-1}$)	P/S	O/S	$\delta^{13}C_{16:0}$ (‰)	$\delta^{13}C_{18:0}$ (‰)	$\Delta^{13}C$ (‰)	Lipid content
External (e)	7.04	1.69	8.78	-30.04	-30.12	-0.08	SFA (C16-18, C20, C22, C24, C26), UFA (C18:1, C22:1), DC (C13), OH (C18, C26, C28, C30), 4,8,12-TMTD (tr), pri
Internal (i)	-	-	-	-	-	-	-

Molecular signature:	-
HAS interpretation:	Combustion feature



Partial total ion chromatogram (TIC) of acid/methanol extract of sample PDM-N04-15225e showing saturated fatty acids ($C_{XX:0}$), unsaturated fatty acids ($C_{XX:1}$), diacids (DC_{XX}), contaminants (*), and *n*-alkanes internal standards (IS $_{ALKXX}$).



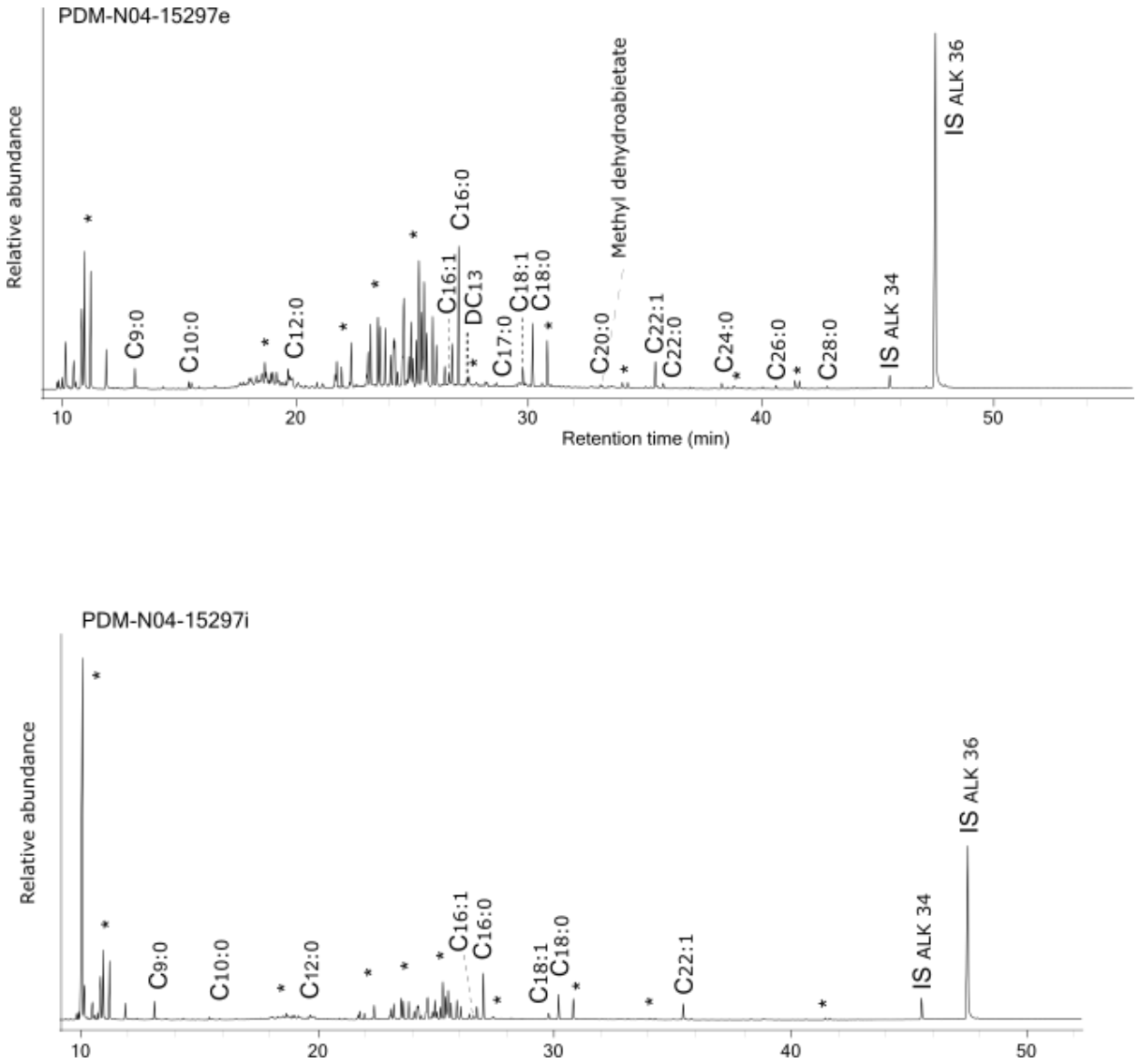
Partial total ion chromatogram (TIC) of solvent extract of sample PDM-N04-15225e showing alcohols (CxxOH), contaminants (*), and *n*-alkanes internal standards (IS $_{ALKXX}$).

		Sample id:	**PDM-N04-15297**
		info:	US 14549, grid L21 occupation phase 3
		Mineral:	Detrital carbonate rock
		Dimension:	243 g
Firing structure:	Fireplace	3D:	https://skfb.ly/puzEA
Alteration patterns:	Discoloration		

Lipid analysis

	Lipid yield ($\mu g\ g^{-1}$)	P/S	O/S	$\delta^{13}C_{16:0}$ (‰)	$\delta^{13}C_{18:0}$ (‰)	$\Delta^{13}C$ (‰)	Lipid content
External (e)	381.78	2.33	3.58	-29.17	-29.12	0.05	SFA (C9, C10, C12, C16-18, C20, C22, C24, C26, C28), UFA (C16:1, C18:1, C22:1), DC (C13), terp (Methyl dehydroabietate), 4,8,12-TMTD, pri, phy (77% SRR)
Internal (i)	48.37	2.17	4.24	-29.85	-29.22	0.63	SFA (C9, C10, C12, C16, C18), UFA (C16:1, C18:1, C22:1), pri

Molecular signature:	Plant resources
HAS interpretation:	Combustion feature



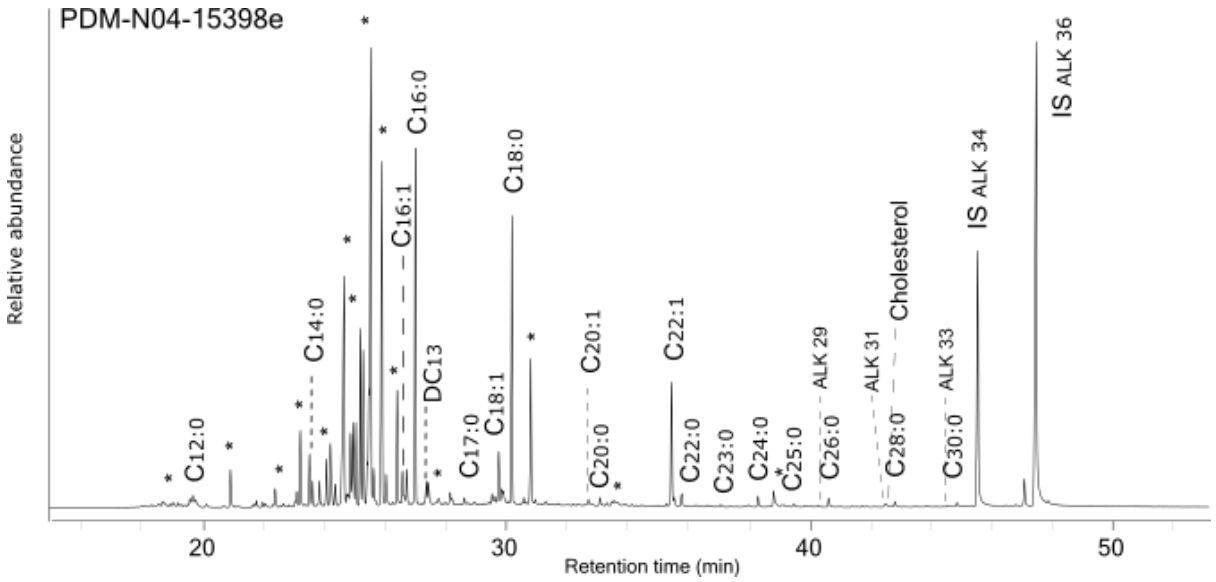
Partial total ion chromatograms (TIC) of acid/methanol extract of sample PDM-N04-15297e/i showing saturated fatty acids ($C_{XX:0}$), unsaturated fatty acids ($C_{XX:1}$), diacids (DC_{XX}), terprenes, contaminants (*), and *n*-alkanes internal standards (IS_{ALKXX}).

		Sample id:	**PDM-N04-15398**
		info:	US 14549, grid L21 occupation phase 3
		Mineral:	Limestone
		Dimension:	197 g
Firing structure:	Fireplace	3D:	https://skfb.ly/puzEA
Alteration patterns:	Discoloration		

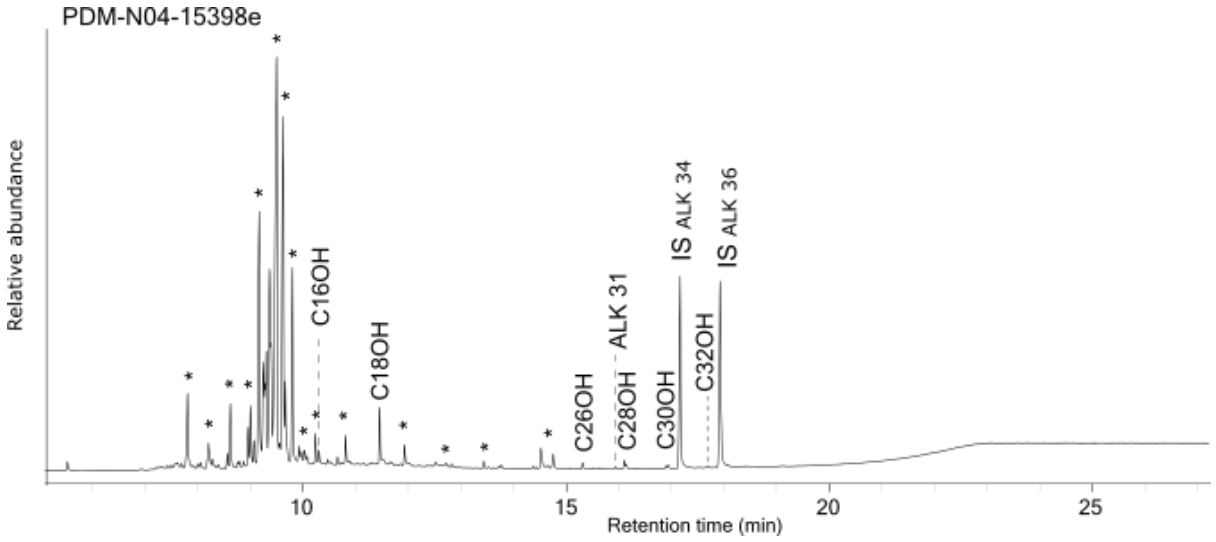
Lipid analysis

	Lipid yield ($\mu g\ g^{-1}$)	P/S	O/S	$\delta^{13}C_{16:0}$ (‰)	$\delta^{13}C_{18:0}$ (‰)	$\Delta^{13}C$ (‰)	Lipid content
External (e)	26.88	1.31	2.60	-29.26	-29.87	-0.61	SFA (C12, C14, C16-18, C20, C22-26, C28, C30), UFA (C16:1, C18:1, C22:1), DC (C13), ALK (C29, C31, C33), OH (C16, C18, C26, C28, C30, C32), 4,8,12-TMTD (tr), pri, phy (85% SRR), ster (Cholesterol)
Internal (i)	-	-	-	-	-	-	-

Molecular signature:	Plant resources
HAS interpretation:	Combustion feature



Partial total ion chromatogram (TIC) of acid/methanol extract of sample PDM-N04-15398e showing saturated fatty acids ($C_{XX:0}$), unsaturated fatty acids ($C_{XX:1}$), diacids (DC_{XX}), *n*-alkanes (ALK xx), sterols, contaminants (*), and *n*-alkanes internal standards (IS $_{ALKXX}$).



Partial total ion chromatogram (TIC) of solvent extract of sample PDM-N04-15398e showing alcohols (CxxOH), *n*-alkanes (ALK xx), contaminants (*), and *n*-alkanes internal standards (IS $_{ALKXX}$).

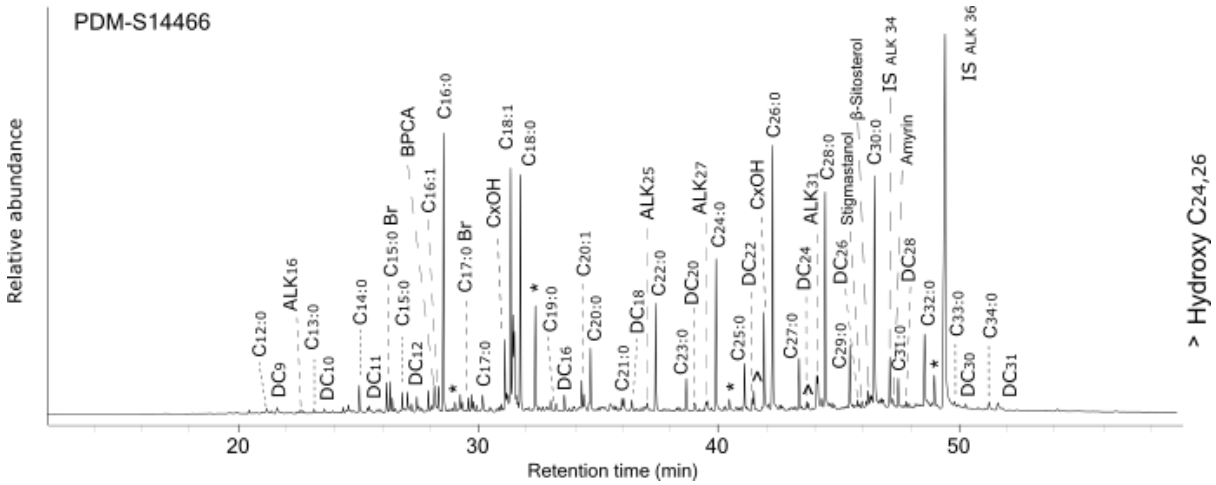
Sediments

Sample id:	**PDM-S14466**
info:	US 14438, grid M21 occupation phase 3
Feature:	White ashes

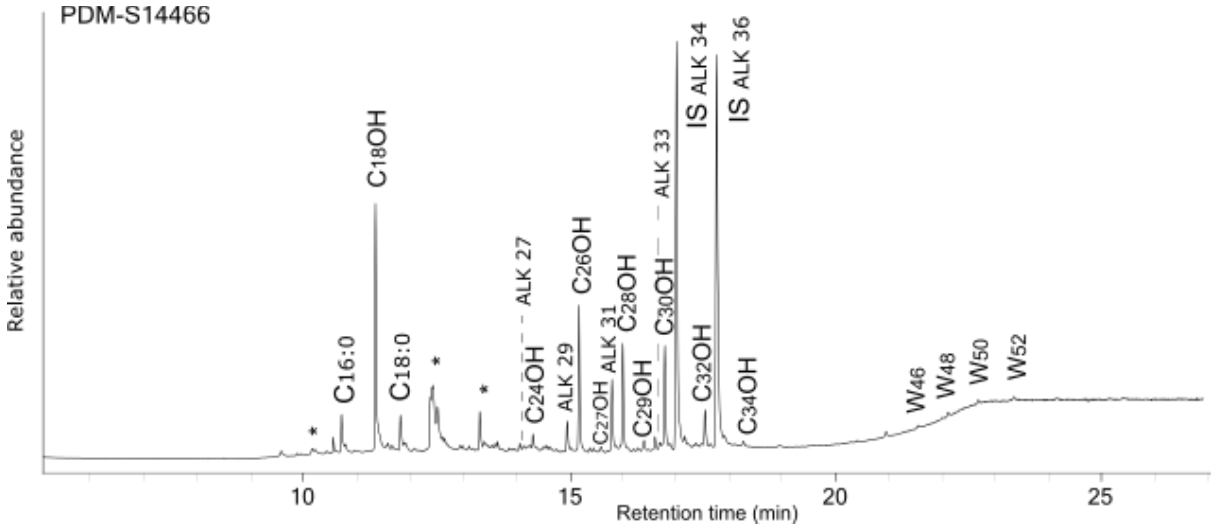
Lipid analysis

Lipid yield (µg g^{-1})	P/S	O/S	$\delta^{13}C_{16:0}$ (‰)	$\delta^{13}C_{18:0}$ (‰)	$\Delta^{13}C$ (‰)	Lipid content
577.68	1.24	0.47	-29.70	-30.14	-0.44	SFA (C12-30, C31, C32, C33, C34), BrFA (C17), UFA (C16:1, C18:1, C20:1), Hy (C24, C26), DC (C9, C10, C11, C12, C16, C18, C20, C22, C24, C26, C28, C30, C31), ALK (C16, 25, 27, 29, 31, 33), OH (C18, C22, C24, C26-30, C32, C34), terp (Amyrin), 4,8,12-TMTD, pri (tr), phy (96% SRR), ster (Stigmastanol, β-Sitosterol), MAG, WE (C46, 48, 50, 52), B3CA

Molecular signature:	Plant-derived resources
Contextual interpretation:	Environmental background



Partial total ion chromatogram (TIC) of acid/methanol extract of sample PDM-S14466 showing saturated fatty acids ($C_{XX:0}$), branched fatty acids ($C_{XX:0}$ Br), unsaturated fatty acids ($C_{XX:1}$), benzene polycarboxylic acid (BPCA), diacids (DC_{XX}), hydroxy fatty acids (^), *n*-alkanes (ALK xx), sterols, terpenes, contaminants (*), and *n*-alkanes internal standards (IS $_{ALKXX}$).



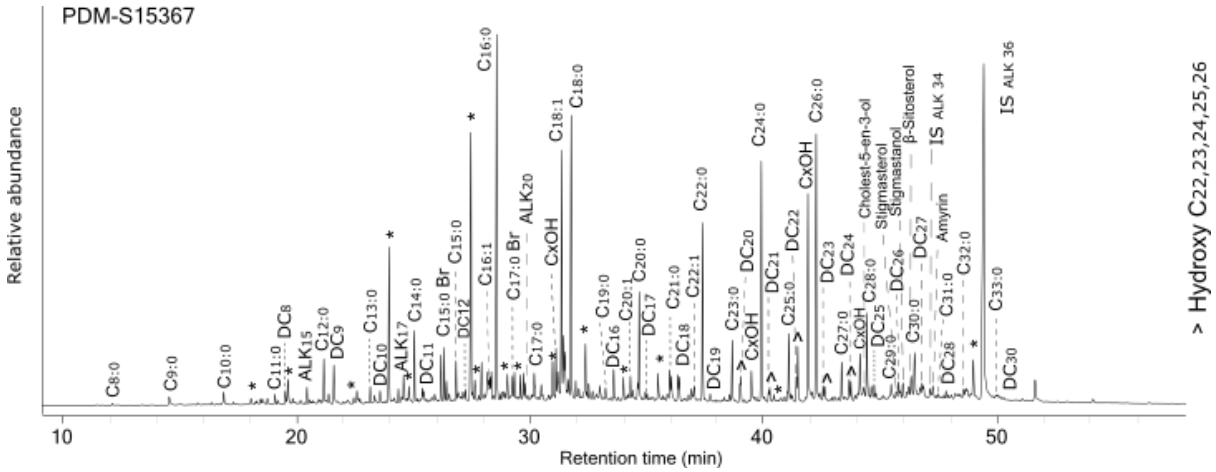
Partial total ion chromatogram (TIC) of solvent extract of sample PDM-S14466 showing saturated fatty acids ($C_{XX:0}$), alcohols (CxxOH), *n*-alkanes (ALK xx), wax esters (Wxx), contaminants (*), and *n*-alkanes internal standards (IS $_{ALKXX}$).

Sample id:	**PDM-S15367**
info:	US 14647, grid L20 occupation phase 3
Firing structure:	Cooking place

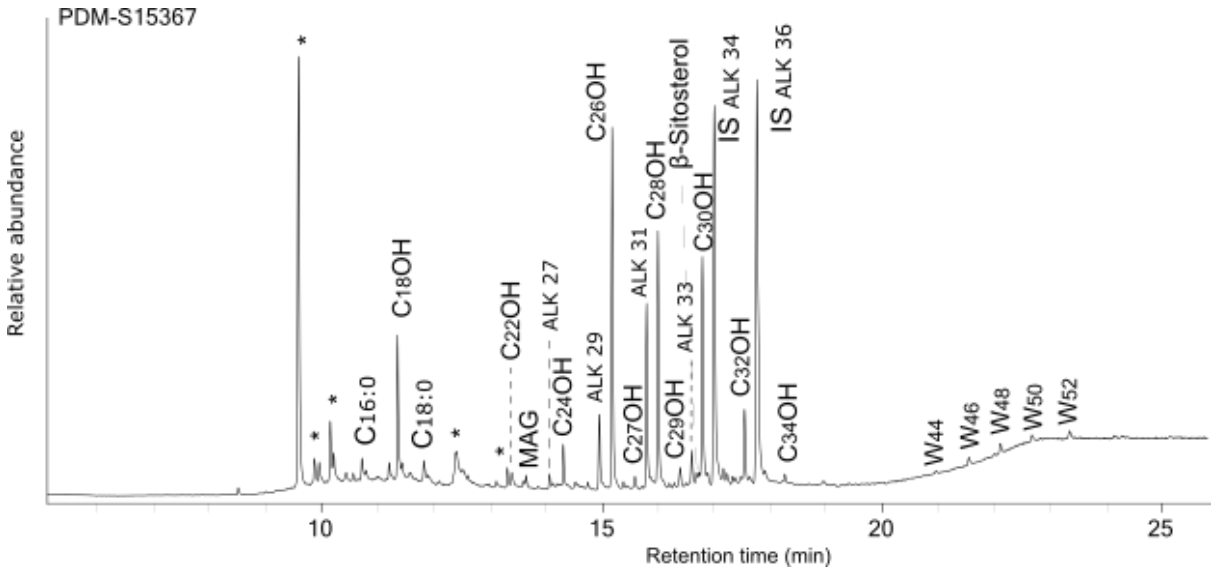
Lipid analysis

Lipid yield (µg g^{-1})	P/S	O/S	$\delta^{13}C_{16:0}$ (‰)	$\delta^{13}C_{18:0}$ (‰)	$\Delta^{13}C$ (‰)	Lipid content
5165.71	1.54	0.65	-30.50	-30.82	-0.32	SFA (C8, C9, C10, C12-30, C31, C32, C33), BrFA (C15, C17), UFA (C16:1, C18:1, C20:1, C22:1), Hy (C22, C23, C24, C25, C26), DC (C8, C9, C10, C11, C12, C16-28, C30), ALK (C15, 17, 20, 27, 29, 31, 33), OH (C18, C22, C24, C26, C27, C28, C29, C30, C32, C34), terp (Amyrin), 4,8,12-TMTD, pri (tr), phy (96% SRR), ster (Cholest-5-en-3-ol, Stigmasterol, Stigmastanol, β-Sitosterol), MAG, WE (C44, 46, 48, 50, 52)

Molecular signature:	Plant-derived resources
Contextual interpretation:	Environmental background



Partial total ion chromatogram (TIC) of acid/methanol extract of sample PDM-S15367 showing saturated fatty acids ($C_{XX:0}$), branched fatty acids ($C_{XX:0}$ Br), unsaturated fatty acids ($C_{XX:1}$), diacids (DC_{XX}), hydroxy fatty acids (^), *n*-alkanes (ALK xx), sterols, contaminants (*), and *n*-alkanes internal standards (IS $_{ALKXX}$).



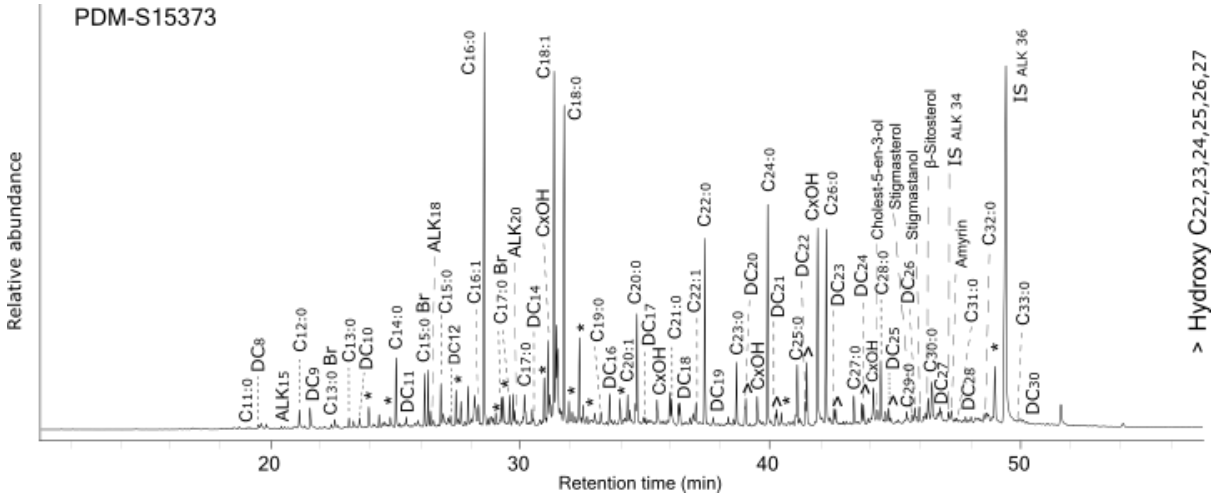
Partial total ion chromatogram (TIC) of solvent extract of sample PDM-S15367 showing saturated fatty acids ($C_{XX:0}$), alcohols (CxxOH), monoacylglycerols (MAGs), *n*-alkanes (ALK xx), sterols, wax esters (Wxx), contaminants (*), and *n*-alkanes internal standards (IS $_{ALKXX}$).

Sample id:	**PDM-S15373**
info:	US 14647, grid L20 occupation phase 3
Firing structure:	Cooking place

Lipid analysis

Lipid yield (µg g^{-1})	P/S	O/S	$\delta^{13}C_{16:0}$ (‰)	$\delta^{13}C_{18:0}$ (‰)	$\Delta^{13}C$ (‰)	Lipid content
4875.11	1.39	0.48	-30.25	-31.00	-0.75	SFA (C11-30, C31, C32, C33), BrFA (C17), UFA (C16:1, C18:1, C20:1, C22:1), Hy (C22, C23, C24, C25-27), DC (C8, C9, C10, C11, C12, C14, C16, C17, C18, C19-21, C22, C23, C24, C25, C26, C27, C28, C30), ALK (C15, 18, 20), OH (?), terp (Amyrin), 4,8,12-TMTD, pri (tr), phy (96% SRR), ster (Cholest-5-en-3-ol, Stigmasterol, Stigmastanol, β-Sitosterol)

Molecular signature:	Plant-derived resources
Contextual interpretation:	Environmental background



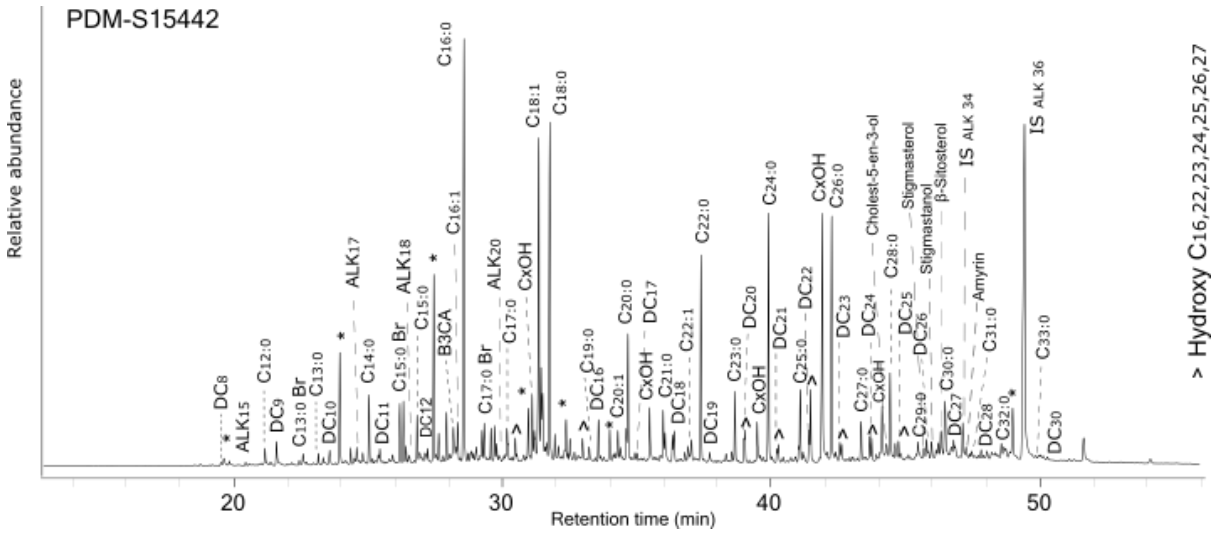
Partial total ion chromatogram (TIC) of acid/methanol extract of sample PDM-S15373 showing saturated fatty acids ($C_{XX:0}$), branched fatty acids ($C_{XX:0}$ Br), unsaturated fatty acids ($C_{XX:1}$), diacids (DC_{XX}), hydroxy fatty acids (^), *n*-alkanes (ALK xx), sterols, terpenes, contaminants (*), and *n*-alkanes internal standards (IS_{ALKXX}).

Sample id:	**PDM-S15442**
info:	US 14647, grid L20 occupation phase 3
Firing structure:	Cooking place

Lipid analysis

Lipid yield (µg g^{-1})	P/S	O/S	$\delta^{13}C_{16:0}$ (‰)	$\delta^{13}C_{18:0}$ (‰)	$\Delta^{13}C$ (‰)	Lipid content
1301.13	1.47	0.59	-30.44	-31.28	-0.84	SFA (C12-30, C31, C32), BrFA (C13, C15, C17), UFA (C16:1, C18:1, C20:1, C22:1), Hy (C22, C23, C24, C25, C26, C27, C28), DC (C9, C10, C11, C12, C15-30), ALK (C15, 17, 18, 20), OH (?), terp (Amyrin), ,8,12-TMTD, pri (tr), phy (96% SRR), ster (Cholest-5-en-3-ol, Stigmasterol, Stigmastanol, β-Sitosterol), B3CA

Molecular signature:	Plant-derived resources
Contextual interpretation:	Environmental background



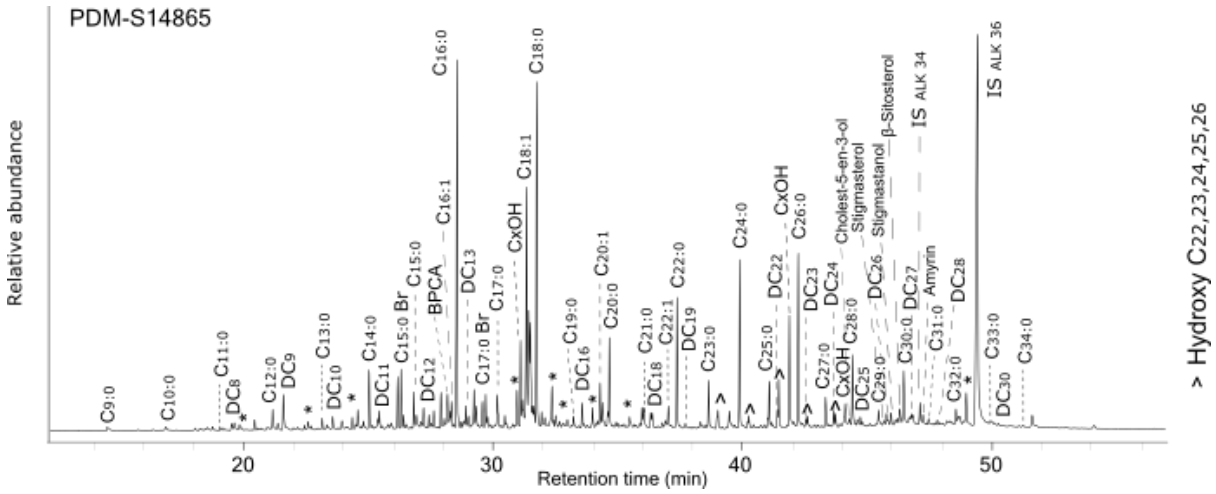
Partial total ion chromatogram (TIC) of acid/methanol extract of sample PDM-S15442 showing saturated fatty acids ($C_{XX:0}$), branched fatty acids ($C_{XX:0}$ Br), unsaturated fatty acids ($C_{XX:1}$), diacids (DC_{XX}), benzene polycarboxylic acid (BPCA), hydroxy fatty acids (^), *n*-alkanes (ALK xx), sterols, terpenes, contaminants (*), and *n*-alkanes internal standards (IS $_{ALKXX}$).

Sample id:	**PDM-S14865**
info:	US 14549, grid L21 occupation phase 3
Firing structure:	Fireplace

Lipid analysis

Lipid yield (µg g^{-1})	P/S	O/S	$\delta^{13}C_{16:0}$ (‰)	$\delta^{13}C_{18:0}$ (‰)	$\Delta^{13}C$ (‰)	Lipid content
1506.23	1.18	0.60	-29.61	-30.23	-0.62	SFA (C9-30, C31, C32, C33, C34), BrFA (C15, C17), UFA (C16:1, C18:1, C20:1, C22:1), Hy (C22, C23, C24, C25, C26), DC (C8, C9, C10, C11, C12, C16, C18, C19, C22-26, C28, C30), OH (?), terp (Amyrin), ,8,12-TMTD, pri (tr), phy (96% SRR), ster (Cholest-5-en-3-ol, Stigmasterol, Stigmastanol, β-Sitosterol), B3CA

Molecular signature:	Plant-derived resources
Contextual interpretation:	Environmental background



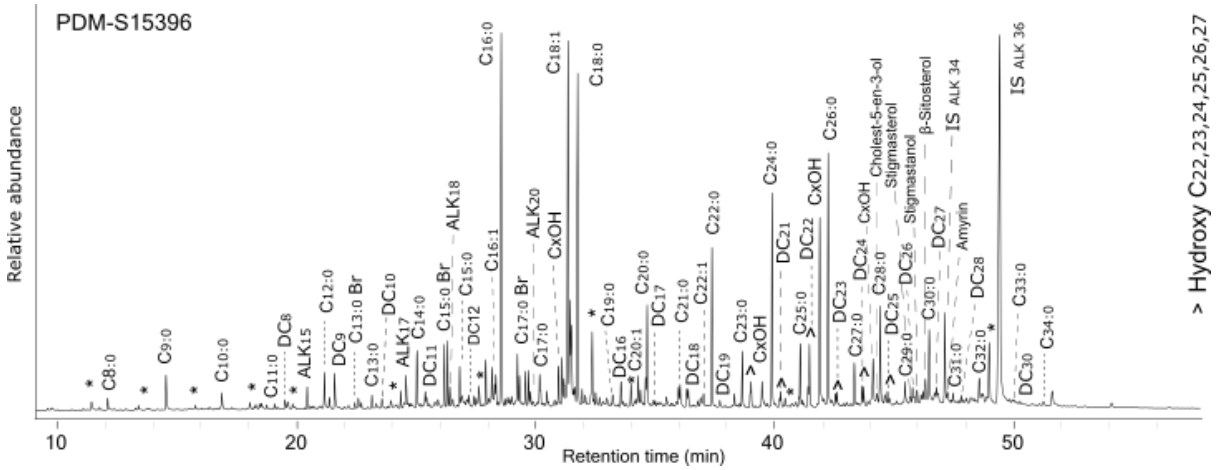
Partial total ion chromatogram (TIC) of acid/methanol extract of sample PDM-S14865 showing saturated fatty acids ($C_{XX:0}$), branched fatty acids ($C_{XX:0}$ Br), unsaturated fatty acids ($C_{XX:1}$), diacids (DC_{XX}), benzene polycarboxylic acid (BPCA), hydroxy fatty acids (^), *n*-alkanes (ALK xx), sterols, terpenes, contaminants (*), and *n*-alkanes internal standards (IS_{ALKXX}).

Sample id:	**PDM-S15396**
info:	US 14549, grid L21 occupation phase 3
Firing structure:	Fireplace

Lipid analysis

Lipid yield (µg g^{-1})	P/S	O/S	$\delta^{13}C_{16:0}$ (‰)	$\delta^{13}C_{18:0}$ (‰)	$\Delta^{13}C$ (‰)	Lipid content
1047.82	1.31	0.47	-30.07	-30.89	-0.82	SFA (C8, C9, C10, C12-30, C31, C32, C33, C34), BrFA (C13, C15, C17), UFA (C16:1, C18:1, C20:1, C22:1), Hy (C22, C23, C24, C25-27), DC (C8, C9, C10, C11, C12, C16-19, C21-28, C30), ALK (C15, 17, 18, 20), OH (?), terp (Amyrin), ,8,12-TMTD, pri (tr), phy (96% SRR), ster (Cholest-5-en-3-ol, Stigmasterol, Stigmastanol, β-Sitosterol)

Molecular signature:	Plant-derived resources
Contextual interpretation:	Environmental background



Partial total ion chromatogram (TIC) of acid/methanol extract of sample PDM-S15396 showing saturated fatty acids ($C_{XX:0}$), branched fatty acids ($C_{XX:0}$ Br), unsaturated fatty acids ($C_{XX:1}$), diacids (DC_{XX}), hydroxy fatty acids (^), *n*-alkanes (ALK xx), sterols, terpenes, contaminants (*), and *n*-alkanes internal standards (IS $_{ALKXX}$).

Annex 5

The mathematical model of mixing is as follows:

$$\delta^{13}C_{(RC1+RC2)} = \delta^{13}C_{(RC1)}\{[RC1(\%\ in\ RC1)]/[RC1(\%\ in\ RC1) + RC2(\%\ in\ RC2)]\} + \delta^{13}C_{(RC2)}\{[RC2(\%\ in\ RC2)]/[RC1(\%\ in\ RC1) + RC2(\%\ in\ RC2)]\}$$

Where RC represents the resource category.

The theoretical mixing curves generated from this model are derived from the percent composition of the individual fatty acids of the pure fats and the individual $\delta^{13}C$ values (Annex 3). The variation in the $\delta^{13}C$ values of the individual fatty acids with mixing are non-linear due to the differences in the relative fatty acid compositions of the various resource categories.

Percent composition of fatty acids ($C_{16:0}$ and $C_{18:0}$) and their corresponding stable carbon isotope values ($\delta^{13}C_{16:0}$ and $\delta^{13}C_{18:0}$) for different resource categories used in the mixing model.

Resource category	*$C_{16:0}$ (%)*	*$C_{18:0}$ (%)*	*Average $\delta^{13}C_{16:0}$*	*Average $\delta^{13}C_{18:0}$*	*Reference*
C3 plant (C3)	13.5	3.1	-32.01	-31.70	Codex alimentarium, CXS 210-1999 (FAO) https://www.fao.org/fao-who-codexalimentarius/sh-proxy/tr/?lnk=1&url=https%253A%252F%252Fworkspace.fao.org%252Fsites%252Fcodex%252FStandards%252FCXS%2B210-1999%252FCXS_210e.pdf
Dairy (D)	30.6	12.2	-25.03	-28.60	https://pmc.ncbi.nlm.nih.gov/articles/PMC2596709/
Domestic ruminant (DR)	27.2	17.1	-26.24	-27.57	https://www.iastatedigitalpress.com/mmb/article/id/12251/
Freshwater (F)	21.2	8.5	-32.21	-31.92	https://www.sciencedirect.com/science/article/pii/S0308814606007862

Porcine adipose (PA)	25.0	12.8	-23.86	-22.46	https://www.iastatedigitalpress.com/mmb/article/id/12251/
Wild non-ruminant (WNR)	21.5	11.2	-26.79	-26.43	https://www.mdpi.com/2076-2615/12/7/810
Wild ruminant (WR)	15.9	14.6	-28.39	-30.75	https://www.mdpi.com/2304-8158/9/7/923

fat portions in mixture		***fatty acid composition %***				***average δ13C***		***average δ13C***		***Modelled mixed values***	
DR	**PA**	**$C_{16:0}$%DR**	**$C_{18:0}$%DR**	**$C_{16:0}$%PA**	**$C_{18:0}$%PA**	**$\delta^{13}C_{16:0}$DR**	**$\delta^{13}C_{18:0}$DR**	**$\delta^{13}C_{16:0}$PA**	**$\delta^{13}C_{18:0}$PA**	**$\delta^{13}C_{16:0}$ (DR+PA)**	**$\delta^{13}C_{18:0}$ (DR+PA)**
100	0	27.2	17.1	25.0	12.8	-26.24	-27.57	-23.86	-22.46	-26.24	-27.57
90	10	27.2	17.1	25.0	12.8	-26.24	-27.57	-23.86	-22.46	-26.0	-27.2
80	20	27.2	17.1	25.0	12.8	-26.24	-27.57	-23.86	-22.46	-25.8	-26.8
70	30	27.2	17.1	25.0	12.8	-26.24	-27.57	-23.86	-22.46	-25.6	-26.3
60	40	27.2	17.1	25.0	12.8	-26.24	-27.57	-23.86	-22.46	-25.3	-25.9
50	50	27.2	17.1	25.0	12.8	-26.24	-27.57	-23.86	-22.46	-25.1	-25.4
40	60	27.2	17.1	25.0	12.8	-26.24	-27.57	-23.86	-22.46	-24.9	-24.9
30	70	27.2	17.1	25.0	12.8	-26.24	-27.57	-23.86	-22.46	-24.6	-24.3
20	80	27.2	17.1	25.0	12.8	-26.24	-27.57	-23.86	-22.46	-24.4	-23.7
10	90	27.2	17.1	25.0	12.8	-26.24	-27.57	-23.86	-22.46	-24.1	-23.1
0	100	27.2	17.1	25.0	12.8	-26.24	-27.57	-23.86	-22.46	-23.86	-22.46

C3	PA	$C_{16:0}$%C3	$C_{18:0}$%C3	$C_{16:0}$%PA	$C_{18:0}$%PA	$\delta^{13}C_{16:0}$C3	$\delta^{13}C_{18:0}$C3	$\delta^{13}C_{16:0}$PA	$\delta^{13}C_{18:0}$PA	$\delta^{13}C_{16:0}$ (C3+PA)	$\delta^{13}C_{18:0}$ (C3+PA)
100	0	13.5	3.1	25.0	12.8	-32.01	-31.70	-23.86	-22.46	-32.01	-31.70
90	10	13.5	3.1	25.0	12.8	-32.01	-31.70	-23.86	-22.46	-30.6	-28.8
80	20	13.5	3.1	25.0	12.8	-32.01	-31.70	-23.86	-22.46	-29.4	-27.0
70	30	13.5	3.1	25.0	12.8	-32.01	-31.70	-23.86	-22.46	-28.4	-25.8
60	40	13.5	3.1	25.0	12.8	-32.01	-31.70	-23.86	-22.46	-27.5	-24.9
50	50	13.5	3.1	25.0	12.8	-32.01	-31.70	-23.86	-22.46	-26.7	-24.3
40	60	13.5	3.1	25.0	12.8	-32.01	-31.70	-23.86	-22.46	-26.0	-23.7
30	70	13.5	3.1	25.0	12.8	-32.01	-31.70	-23.86	-22.46	-25.4	-23.3
20	80	13.5	3.1	25.0	12.8	-32.01	-31.70	-23.86	-22.46	-24.8	-23.0
10	90	13.5	3.1	25.0	12.8	-32.01	-31.70	-23.86	-22.46	-24.3	-22.7

0	100	13.5	3.1	25.0	12.8	-32.01	-31.70	-23.86	-22.46	-23.86	-22.46

WNR	**PA**	**$C_{16:0}$%WNR**	**$C_{18:0}$%WNR**	**$C_{16:0}$%PA**	**$C_{18:0}$%PA**	**$\delta^{13}C_{16:0}$WNR**	**$\delta^{13}C_{18:0}$WNR**	**$\delta^{13}C_{16:0}$PA**	**$\delta^{13}C_{18:0}$PA**	**$\delta^{13}C_{16:0}$ (WNR+PA)**	**$\delta^{13}C_{18:0}$ (WNR+PA)**
100	0	21.5	11.2	25.0	12.8	-26.79	-26.43	-23.86	-22.46	-26.79	-26.43
90	10	21.5	11.2	25.0	12.8	-26.79	-26.43	-23.86	-22.46	-26.5	-26.0
80	20	21.5	11.2	25.0	12.8	-26.79	-26.43	-23.86	-22.46	-26.1	-25.5
70	30	21.5	11.2	25.0	12.8	-26.79	-26.43	-23.86	-22.46	-25.8	-25.1
60	40	21.5	11.2	25.0	12.8	-26.79	-26.43	-23.86	-22.46	-25.5	-24.7
50	50	21.5	11.2	25.0	12.8	-26.79	-26.43	-23.86	-22.46	-25.2	-24.3
40	60	21.5	11.2	25.0	12.8	-26.79	-26.43	-23.86	-22.46	-24.9	-23.9
30	70	21.5	11.2	25.0	12.8	-26.79	-26.43	-23.86	-22.46	-24.6	-23.5
20	80	21.5	11.2	25.0	12.8	-26.79	-26.43	-23.86	-22.46	-24.4	-23.2

10	90	21.5	11.2	25.0	12.8	-26.79	-26.43	-23.86	-22.46	-24.1	-22.8
0	100	21.5	11.2	25.0	12.8	-26.79	-26.43	-23.86	-22.46	-23.86	-22.46

WR	**PA**	**$C_{16:0}$%WR**	**$C_{18:0}$%WR**	**$C_{16:0}$%PA**	**$C_{18:0}$%PA**	**$\delta^{13}C_{16:0}$WR**	**$\delta^{13}C_{18:0}$WR**	**$\delta^{13}C_{16:0}$PA**	**$\delta^{13}C_{18:0}$PA**	**$\delta^{13}C_{16:0}$ (WR+PA)**	**$\delta^{13}C_{18:0}$ (WR+PA)**
100	0	15.9	14.6	25.0	12.8	-28.39	-30.75	-23.86	-22.46	-28.39	-30.75
90	10	15.9	14.6	25.0	12.8	-28.39	-30.75	-23.86	-22.46	-27.7	-30.0
80	20	15.9	14.6	25.0	12.8	-28.39	-30.75	-23.86	-22.46	-27.1	-29.3
70	30	15.9	14.6	25.0	12.8	-28.39	-30.75	-23.86	-22.46	-26.6	-28.5
60	40	15.9	14.6	25.0	12.8	-28.39	-30.75	-23.86	-22.46	-26.1	-27.7
50	50	15.9	14.6	25.0	12.8	-28.39	-30.75	-23.86	-22.46	-25.6	-26.9
40	60	15.9	14.6	25.0	12.8	-28.39	-30.75	-23.86	-22.46	-25.2	-26.0
30	70	15.9	14.6	25.0	12.8	-28.39	-30.75	-23.86	-22.46	-24.8	-25.2

20	80	15.9	14.6	25.0	12.8	-28.39	-30.75	-23.86	-22.46	-24.5	-24.3
10	90	15.9	14.6	25.0	12.8	-28.39	-30.75	-23.86	-22.46	-24.2	-23.4
0	100	15.9	14.6	25.0	12.8	-28.39	-30.75	-23.86	-22.46	-23.86	-22.46

D	**PA**	**$C_{16:0}$%D**	**$C_{18:0}$%D**	**$C_{16:0}$%PA**	**$C_{18:0}$%PA**	**$\delta^{13}C_{16:0}$D**	**$\delta^{13}C_{18:0}$D**	**$\delta^{13}C_{16:0}$PA**	**$\delta^{13}C_{18:0}$PA**	**$\delta^{13}C_{16:0}$ (D+PA)**	**$\delta^{13}C_{18:0}$ (D+PA)**
100	0	30.6	12.2	25.0	12.8	-25.03	-28.60	-23.86	-22.46	-25.03	-28.60
90	10	30.6	12.2	25.0	12.8	-25.03	-28.60	-23.86	-22.46	-24.9	-28.0
80	20	30.6	12.2	25.0	12.8	-25.03	-28.60	-23.86	-22.46	-24.8	-27.3
70	30	30.6	12.2	25.0	12.8	-25.03	-28.60	-23.86	-22.46	-24.7	-26.7
60	40	30.6	12.2	25.0	12.8	-25.03	-28.60	-23.86	-22.46	-24.6	-26.1
50	50	30.6	12.2	25.0	12.8	-25.03	-28.60	-23.86	-22.46	-24.5	-25.5
40	60	30.6	12.2	25.0	12.8	-25.03	-28.60	-23.86	-22.46	-24.4	-24.8

30	70	30.6	12.2	25.0	12.8	-25.03	-28.60	-23.86	-22.46	-24.3	-24.2
20	80	30.6	12.2	25.0	12.8	-25.03	-28.60	-23.86	-22.46	-24.1	-23.6
10	90	30.6	12.2	25.0	12.8	-25.03	-28.60	-23.86	-22.46	-24.0	-23.0
0	100	30.6	12.2	25.0	12.8	-25.03	-28.60	-23.86	-22.46	-23.86	-22.46

F	**PA**	**$C_{16:0}$%F**	**$C_{18:0}$%F**	**$C_{16:0}$%PA**	**$C_{18:0}$%PA**	**$\delta^{13}C_{16:0}$F**	**$\delta^{13}C_{18:0}$F**	**$\delta^{13}C_{16:0}$PA**	**$\delta^{13}C_{18:0}$PA**	**$\delta^{13}C_{16:0}$ (F+PA)**	**$\delta^{13}C_{18:0}$ (F+PA)**
100	0	21.2	8.5	25.0	12.8	-32.21	-31.92	-23.86	-22.46	-32.21	-31.92
90	10	21.2	8.5	25.0	12.8	-32.21	-31.92	-23.86	-22.46	-31.2	-30.6
80	20	21.2	8.5	25.0	12.8	-32.21	-31.92	-23.86	-22.46	-30.3	-29.3
70	30	21.2	8.5	25.0	12.8	-32.21	-31.92	-23.86	-22.46	-29.4	-28.2
60	40	21.2	8.5	25.0	12.8	-32.21	-31.92	-23.86	-22.46	-28.5	-27.2
50	50	21.2	8.5	25.0	12.8	-32.21	-31.92	-23.86	-22.46	-27.7	-26.2

40	60	21.2	8.5	25.0	12.8	-32.21	-31.92	-23.86	-22.46	-26.9	-25.4
30	70	21.2	8.5	25.0	12.8	-32.21	-31.92	-23.86	-22.46	-26.1	-24.6
20	80	21.2	8.5	25.0	12.8	-32.21	-31.92	-23.86	-22.46	-25.3	-23.8
10	90	21.2	8.5	25.0	12.8	-32.21	-31.92	-23.86	-22.46	-24.6	-23.1
0	100	21.2	8.5	25.0	12.8	-32.21	-31.92	-23.86	-22.46	-23.86	-22.46

C3	**DR**	**$C_{16:0}$%C3**	**$C_{18:0}$%C3**	**$C_{16:0}$%DR**	**$C_{18:0}$%DR**	**$\delta^{13}C_{16:0}$C3**	**$\delta^{13}C_{18:0}$C3**	**$\delta^{13}C_{16:0}$DR**	**$\delta^{13}C_{18:0}$DR**	**$\delta^{13}C_{16:0}$ (C3+DR)**	**$\delta^{13}C_{18:0}$ (C3+DR)**
100	0	13.5	3.1	27.2	17.1	-32.01	-31.70	-26.24	-27.57	-32.01	-31.70
90	10	13.5	3.1	27.2	17.1	-32.01	-31.70	-26.24	-27.57	-31.0	-30.1
80	20	13.5	3.1	27.2	17.1	-32.01	-31.70	-26.24	-27.57	-30.1	-29.3
70	30	13.5	3.1	27.2	17.1	-32.01	-31.70	-26.24	-27.57	-29.3	-28.8
60	40	13.5	3.1	27.2	17.1	-32.01	-31.70	-26.24	-27.57	-28.7	-28.5

50	50	13.5	3.1	27.2	17.1	-32.01	-31.70	-26.24	-27.57	-28.2	-28.2
40	60	13.5	3.1	27.2	17.1	-32.01	-31.70	-26.24	-27.57	-27.7	-28.0
30	70	13.5	3.1	27.2	17.1	-32.01	-31.70	-26.24	-27.57	-27.3	-27.9
20	80	13.5	3.1	27.2	17.1	-32.01	-31.70	-26.24	-27.57	-26.9	-27.7
10	90	13.5	3.1	27.2	17.1	-32.01	-31.70	-26.24	-27.57	-26.5	-27.6
0	100	13.5	3.1	27.2	17.1	-32.01	-31.70	-26.24	-27.57	-26.24	-27.57

WNR	**DR**	**$C_{16:0}$%WNR**	**$C_{18:0}$%WNR**	**$C_{16:0}$%DR**	**$C_{18:0}$%DR**	**$\delta^{13}C_{16:0}$WNR**	**$\delta^{13}C_{18:0}$WNR**	**$\delta^{13}C_{16:0}$DR**	**$\delta^{13}C_{18:0}$DR**	**$\delta^{13}C_{16:0}$ (WNR+DR)**	**$\delta^{13}C_{18:0}$ (WNR+DR)**
100	0	21.5	11.2	27.2	17.1	-26.79	-26.43	-26.24	-27.57	-26.79	-26.43
90	10	21.5	11.2	27.2	17.1	-26.79	-26.43	-26.24	-27.57	-26.7	-26.6
80	20	21.5	11.2	27.2	17.1	-26.79	-26.43	-26.24	-27.57	-26.7	-26.7
70	30	21.5	11.2	27.2	17.1	-26.79	-26.43	-26.24	-27.57	-26.6	-26.9

60	40	21.5	11.2	27.2	17.1	-26.79	-26.43	-26.24	-27.57	-26.5	-27.0
50	50	21.5	11.2	27.2	17.1	-26.79	-26.43	-26.24	-27.57	-26.5	-27.1
40	60	21.5	11.2	27.2	17.1	-26.79	-26.43	-26.24	-27.57	-26.4	-27.2
30	70	21.5	11.2	27.2	17.1	-26.79	-26.43	-26.24	-27.57	-26.4	-27.3
20	80	21.5	11.2	27.2	17.1	-26.79	-26.43	-26.24	-27.57	-26.3	-27.4
10	90	21.5	11.2	27.2	17.1	-26.79	-26.43	-26.24	-27.57	-26.3	-27.5
0	100	21.5	11.2	27.2	17.1	-26.79	-26.43	-26.24	-27.57	-26.24	-27.57

WR	**DR**	**$C_{16:0}$%WR**	**$C_{18:0}$%WR**	**$C_{16:0}$%DR**	**$C_{18:0}$%DR**	**$\delta^{13}C_{16:0}$WR**	**$\delta^{13}C_{18:0}$WR**	**$\delta^{13}C_{16:0}$DR**	**$\delta^{13}C_{18:0}$DR**	**$\delta^{13}C_{16:0}$ (WR+DR)**	**$\delta^{13}C_{18:0}$ (WR+DR)**
100	0	15.9	14.6	27.2	17.1	-28.39	-30.75	-26.24	-27.57	-28.39	-30.75
90	10	15.9	14.6	27.2	17.1	-28.39	-30.75	-26.24	-27.57	-28.1	-30.4
80	20	15.9	14.6	27.2	17.1	-28.39	-30.75	-26.24	-27.57	-27.8	-30.0

70	30	15.9	14.6	27.2	17.1	-28.39	-30.75	-26.24	-27.57	-27.5	-29.7
60	40	15.9	14.6	27.2	17.1	-28.39	-30.75	-26.24	-27.57	-27.2	-29.4
50	50	15.9	14.6	27.2	17.1	-28.39	-30.75	-26.24	-27.57	-27.0	-29.0
40	60	15.9	14.6	27.2	17.1	-28.39	-30.75	-26.24	-27.57	-26.8	-28.7
30	70	15.9	14.6	27.2	17.1	-28.39	-30.75	-26.24	-27.57	-26.7	-28.4
20	80	15.9	14.6	27.2	17.1	-28.39	-30.75	-26.24	-27.57	-26.5	-28.1
10	90	15.9	14.6	27.2	17.1	-28.39	-30.75	-26.24	-27.57	-26.4	-27.8
0	100	15.9	14.6	27.2	17.1	-28.39	-30.75	-26.24	-27.57	-26.24	-27.57

D	**DR**	**$C_{16:0}$%D**	**$C_{18:0}$%D**	**$C_{16:0}$%DR**	**$C_{18:0}$%DR**	**$\delta^{13}C_{16:0}$D**	**$\delta^{13}C_{18:0}$D**	**$\delta^{13}C_{16:0}$DR**	**$\delta^{13}C_{18:0}$DR**	**$\delta^{13}C_{16:0}$ (D+DR)**	**$\delta^{13}C_{18:0}$ (D+DR)**
100	0	30.6	12.2	27.2	17.1	-25.03	-28.60	-26.24	-27.57	-25.03	-28.60
90	10	30.6	12.2	27.2	17.1	-25.03	-28.60	-26.24	-27.57	-25.1	-28.5

80	20	30.6	12.2	27.2	17.1	-25.03	-28.60	-26.24	-27.57	-25.3	-28.3
70	30	30.6	12.2	27.2	17.1	-25.03	-28.60	-26.24	-27.57	-25.4	-28.2
60	40	30.6	12.2	27.2	17.1	-25.03	-28.60	-26.24	-27.57	-25.5	-28.1
50	50	30.6	12.2	27.2	17.1	-25.03	-28.60	-26.24	-27.57	-25.6	-28.0
40	60	30.6	12.2	27.2	17.1	-25.03	-28.60	-26.24	-27.57	-25.7	-27.9
30	70	30.6	12.2	27.2	17.1	-25.03	-28.60	-26.24	-27.57	-25.8	-27.8
20	80	30.6	12.2	27.2	17.1	-25.03	-28.60	-26.24	-27.57	-26.0	-27.7
10	90	30.6	12.2	27.2	17.1	-25.03	-28.60	-26.24	-27.57	-26.1	-27.6
0	100	30.6	12.2	27.2	17.1	-25.03	-28.60	-26.24	-27.57	-26.24	-27.57

F	**DR**	**$C_{16:0}$%F**	**$C_{18:0}$%F**	**$C_{16:0}$%DR**	**$C_{18:0}$%DR**	**$\delta^{13}C_{16:0}$F**	**$\delta^{13}C_{18:0}$F**	**$\delta^{13}C_{16:0}$DR**	**$\delta^{13}C_{18:0}$DR**	**$\delta^{13}C_{16:0}$ (F+DR)**	**$\delta^{13}C_{18:0}$ (F+DR)**
100	0	21.2	8.5	27.2	17.1	-32.21	-31.92	-26.24	-27.57	-32.21	-31.92

90	10	21.2	8.5	27.2	17.1	-32.21	-31.92	-26.24	-27.57	-31.5	-31.1
80	20	21.2	8.5	27.2	17.1	-32.21	-31.92	-26.24	-27.57	-30.8	-30.5
70	30	21.2	8.5	27.2	17.1	-32.21	-31.92	-26.24	-27.57	-30.1	-29.9
60	40	21.2	8.5	27.2	17.1	-32.21	-31.92	-26.24	-27.57	-29.5	-29.4
50	50	21.2	8.5	27.2	17.1	-32.21	-31.92	-26.24	-27.57	-28.9	-29.0
40	60	21.2	8.5	27.2	17.1	-32.21	-31.92	-26.24	-27.57	-28.3	-28.7
30	70	21.2	8.5	27.2	17.1	-32.21	-31.92	-26.24	-27.57	-27.7	-28.3
20	80	21.2	8.5	27.2	17.1	-32.21	-31.92	-26.24	-27.57	-27.2	-28.0
10	90	21.2	8.5	27.2	17.1	-32.21	-31.92	-26.24	-27.57	-26.7	-27.8
0	100	21.2	8.5	27.2	17.1	-32.21	-31.92	-26.24	-27.57	-26.24	-27.57

WNR	**C3**	**$C_{16:0}$%WNR**	**$C_{18:0}$%WNR**	**$C_{16:0}$%C3**	**$C_{18:0}$%C3**	**$\delta^{13}C_{16:0}$WNR**	**$\delta^{13}C_{18:0}$WNR**	**$\delta^{13}C_{16:0}$C3**	**$\delta^{13}C_{18:0}$C3**	**$\delta^{13}C_{16:0}$ (WNR+C3)**	**$\delta^{13}C_{18:0}$ (WNR+C3)**

100	0	21.5	11.2	13.5	3.1	-26.79	-26.43	-32.01	-31.70	-26.79	-26.43
90	10	21.5	11.2	13.5	3.1	-26.79	-26.43	-32.01	-31.70	-27.1	-26.6
80	20	21.5	11.2	13.5	3.1	-26.79	-26.43	-32.01	-31.70	-27.5	-26.8
70	30	21.5	11.2	13.5	3.1	-26.79	-26.43	-32.01	-31.70	-27.9	-27.0
60	40	21.5	11.2	13.5	3.1	-26.79	-26.43	-32.01	-31.70	-28.3	-27.2
50	50	21.5	11.2	13.5	3.1	-26.79	-26.43	-32.01	-31.70	-28.8	-27.6
40	60	21.5	11.2	13.5	3.1	-26.79	-26.43	-32.01	-31.70	-29.3	-28.0
30	70	21.5	11.2	13.5	3.1	-26.79	-26.43	-32.01	-31.70	-29.9	-28.5
20	80	21.5	11.2	13.5	3.1	-26.79	-26.43	-32.01	-31.70	-30.5	-29.2
10	90	21.5	11.2	13.5	3.1	-26.79	-26.43	-32.01	-31.70	-31.2	-30.2
0	100	21.5	11.2	13.5	3.1	-26.79	-26.43	-32.01	-31.70	-32.01	-31.70

WR	C3	$C_{16:0}$%WR	$C_{18:0}$%WR	$C_{16:0}$%C3	$C_{18:0}$%C3	$\delta^{13}C_{16:0}$WR	$\delta^{13}C_{18:0}$WR	$\delta^{13}C_{16:0}$C3	$\delta^{13}C_{18:0}$C3	$\delta^{13}C_{16:0}$ (WR+C3)	$\delta^{13}C_{18:0}$ (WR+C3)
100	0	15.9	14.6	13.5	3.1	-28.39	-30.75	-32.01	-31.70	-28.39	-30.75
90	10	15.9	14.6	13.5	3.1	-28.39	-30.75	-32.01	-31.70	-28.7	-30.8
80	20	15.9	14.6	13.5	3.1	-28.39	-30.75	-32.01	-31.70	-29.0	-30.8
70	30	15.9	14.6	13.5	3.1	-28.39	-30.75	-32.01	-31.70	-29.4	-30.8
60	40	15.9	14.6	13.5	3.1	-28.39	-30.75	-32.01	-31.70	-29.7	-30.9
50	50	15.9	14.6	13.5	3.1	-28.39	-30.75	-32.01	-31.70	-30.1	-30.9
40	60	15.9	14.6	13.5	3.1	-28.39	-30.75	-32.01	-31.70	-30.4	-31.0
30	70	15.9	14.6	13.5	3.1	-28.39	-30.75	-32.01	-31.70	-30.8	-31.1
20	80	15.9	14.6	13.5	3.1	-28.39	-30.75	-32.01	-31.70	-31.2	-31.2
10	90	15.9	14.6	13.5	3.1	-28.39	-30.75	-32.01	-31.70	-31.6	-31.4
0	100	15.9	14.6	13.5	3.1	-28.39	-30.75	-32.01	-31.70	-32.01	-31.70

D	C3	$C_{16:0}$%D	$C_{18:0}$%D	$C_{16:0}$%C3	$C_{18:0}$%C3	$\delta^{13}C_{16:0}$D	$\delta^{13}C_{18:0}$D	$\delta^{13}C_{16:0}$C3	$\delta^{13}C_{18:0}$C3	$\delta^{13}C_{16:0}$ (D+C3)	$\delta^{13}C_{18:0}$ (D+C3)
100	0	30.6	12.2	13.5	3.1	-25.03	-28.60	-32.01	-31.70	-25.03	-28.60
90	10	30.6	12.2	13.5	3.1	-25.03	-28.60	-32.01	-31.70	-25.4	-28.7
80	20	30.6	12.2	13.5	3.1	-25.03	-28.60	-32.01	-31.70	-25.7	-28.8
70	30	30.6	12.2	13.5	3.1	-25.03	-28.60	-32.01	-31.70	-26.1	-28.9
60	40	30.6	12.2	13.5	3.1	-25.03	-28.60	-32.01	-31.70	-26.6	-29.0
50	50	30.6	12.2	13.5	3.1	-25.03	-28.60	-32.01	-31.70	-27.2	-29.2
40	60	30.6	12.2	13.5	3.1	-25.03	-28.60	-32.01	-31.70	-27.8	-29.5
30	70	30.6	12.2	13.5	3.1	-25.03	-28.60	-32.01	-31.70	-28.6	-29.8
20	80	30.6	12.2	13.5	3.1	-25.03	-28.60	-32.01	-31.70	-29.5	-30.2
10	90	30.6	12.2	13.5	3.1	-25.03	-28.60	-32.01	-31.70	-30.6	-30.8

0	100	30.6	12.2	13.5	3.1	-25.03	-28.60	-32.01	-31.70	-32.01	-31.70

F	**C3**	**$C_{16:0}$%F**	**$C_{18:0}$%F**	**$C_{16:0}$%C3**	**$C_{18:0}$%C3**	**$\delta^{13}C_{16:0}$F**	**$\delta^{13}C_{18:0}$F**	**$\delta^{13}C_{16:0}$C3**	**$\delta^{13}C_{18:0}$C3**	**$\delta^{13}C_{16:0}$ (F+C3)**	**$\delta^{13}C_{18:0}$ (F+C3)**
100	0	21.2	8.5	13.5	3.1	-32.21	-31.92	-32.01	-31.70	-32.21	-31.92
90	10	21.2	8.5	13.5	3.1	-32.21	-31.92	-32.01	-31.70	-32.2	-31.9
80	20	21.2	8.5	13.5	3.1	-32.21	-31.92	-32.01	-31.70	-32.2	-31.9
70	30	21.2	8.5	13.5	3.1	-32.21	-31.92	-32.01	-31.70	-32.2	-31.9
60	40	21.2	8.5	13.5	3.1	-32.21	-31.92	-32.01	-31.70	-32.2	-31.9
50	50	21.2	8.5	13.5	3.1	-32.21	-31.92	-32.01	-31.70	-32.1	-31.9
40	60	21.2	8.5	13.5	3.1	-32.21	-31.92	-32.01	-31.70	-32.1	-31.8
30	70	21.2	8.5	13.5	3.1	-32.21	-31.92	-32.01	-31.70	-32.1	-31.8
20	80	21.2	8.5	13.5	3.1	-32.21	-31.92	-32.01	-31.70	-32.1	-31.8

10	90	21.2	8.5	13.5	3.1	-32.21	-31.92	-32.01	-31.70	-32.0	-31.8
0	100	21.2	8.5	13.5	3.1	-32.21	-31.92	-32.01	-31.70	-32.01	-31.70

WNR	**WR**	**$C_{16:0}$%WNR**	**$C_{18:0}$%WNR**	**$C_{16:0}$%WR**	**$C_{18:0}$%WR**	**$\delta^{13}C_{16:0}$WNR**	**$\delta^{13}C_{18:0}$WNR**	**$\delta^{13}C_{16:0}$WR**	**$\delta^{13}C_{18:0}$WR**	**$\delta^{13}C_{16:0}$ (WNR+WR)**	**$\delta^{13}C_{18:0}$ (WNR+WR)**
100	0	21.5	11.2	15.9	14.6	-26.79	-26.43	-28.39	-30.75	-26.79	-26.43
90	10	21.5	11.2	15.9	14.6	-26.79	-26.43	-28.39	-30.75	-26.9	-27.0
80	20	21.5	11.2	15.9	14.6	-26.79	-26.43	-28.39	-30.75	-27.0	-27.5
70	30	21.5	11.2	15.9	14.6	-26.79	-26.43	-28.39	-30.75	-27.2	-28.0
60	40	21.5	11.2	15.9	14.6	-26.79	-26.43	-28.39	-30.75	-27.3	-28.4
50	50	21.5	11.2	15.9	14.6	-26.79	-26.43	-28.39	-30.75	-27.5	-28.9
40	60	21.5	11.2	15.9	14.6	-26.79	-26.43	-28.39	-30.75	-27.6	-29.3
30	70	21.5	11.2	15.9	14.6	-26.79	-26.43	-28.39	-30.75	-27.8	-29.7

20	80	21.5	11.2	15.9	14.6	-26.79	-26.43	-28.39	-30.75	-28.0	-30.1
10	90	21.5	11.2	15.9	14.6	-26.79	-26.43	-28.39	-30.75	-28.2	-30.4
0	100	21.5	11.2	15.9	14.6	-26.79	-26.43	-28.39	-30.75	-28.39	-30.75

WNR	**D**	**$C_{16:0}$%WNR**	**$C_{18:0}$%WNR**	**$C_{16:0}$%D**	**$C_{18:0}$%D**	**$\delta^{13}C_{16:0}$WNR**	**$\delta^{13}C_{18:0}$WNR**	**$\delta^{13}C_{16:0}$D**	**$\delta^{13}C_{18:0}$D**	**$\delta^{13}C_{16:0}$ (WNR+D)**	**$\delta^{13}C_{18:0}$ (WNR+D)**
100	0	21.5	11.2	30.6	12.2	-26.79	-26.43	-25.03	-28.60	-26.79	-26.43
90	10	21.5	11.2	30.6	12.2	-26.79	-26.43	-25.03	-28.60	-26.5	-26.7
80	20	21.5	11.2	30.6	12.2	-26.79	-26.43	-25.03	-28.60	-26.3	-26.9
70	30	21.5	11.2	30.6	12.2	-26.79	-26.43	-25.03	-28.60	-26.1	-27.1
60	40	21.5	11.2	30.6	12.2	-26.79	-26.43	-25.03	-28.60	-25.9	-27.3
50	50	21.5	11.2	30.6	12.2	-26.79	-26.43	-25.03	-28.60	-25.8	-27.6
40	60	21.5	11.2	30.6	12.2	-26.79	-26.43	-25.03	-28.60	-25.6	-27.8

30	70	21.5	11.2	30.6	12.2	-26.79	-26.43	-25.03	-28.60	-25.4	-28.0
20	80	21.5	11.2	30.6	12.2	-26.79	-26.43	-25.03	-28.60	-25.3	-28.2
10	90	21.5	11.2	30.6	12.2	-26.79	-26.43	-25.03	-28.60	-25.2	-28.4
0	100	21.5	11.2	30.6	12.2	-26.79	-26.43	-25.03	-28.60	-25.03	-28.60

WNR	**F**	**$C_{16:0}$%WNR**	**$C_{18:0}$%WNR**	**$C_{16:0}$%F**	**$C_{18:0}$%F**	**$\delta^{13}C_{16:0}$WNR**	**$\delta^{13}C_{18:0}$WNR**	**$\delta^{13}C_{16:0}$F**	**$\delta^{13}C_{18:0}$F**	**$\delta^{13}C_{16:0}$ (WNR+F)**	**$\delta^{13}C_{18:0}$ (WNR+F)**
100	0	21.5	11.2	21.2	8.5	-26.79	-26.43	-32.21	-31.92	-26.79	-26.43
90	10	21.5	11.2	21.2	8.5	-26.79	-26.43	-32.21	-31.92	-27.3	-26.9
80	20	21.5	11.2	21.2	8.5	-26.79	-26.43	-32.21	-31.92	-27.9	-27.3
70	30	21.5	11.2	21.2	8.5	-26.79	-26.43	-32.21	-31.92	-28.4	-27.8
60	40	21.5	11.2	21.2	8.5	-26.79	-26.43	-32.21	-31.92	-28.9	-28.3
50	50	21.5	11.2	21.2	8.5	-26.79	-26.43	-32.21	-31.92	-29.5	-28.8

40	60	21.5	11.2	21.2	8.5	-26.79	-26.43	-32.21	-31.92	-30.0	-29.3
30	70	21.5	11.2	21.2	8.5	-26.79	-26.43	-32.21	-31.92	-30.6	-29.9
20	80	21.5	11.2	21.2	8.5	-26.79	-26.43	-32.21	-31.92	-31.1	-30.6
10	90	21.5	11.2	21.2	8.5	-26.79	-26.43	-32.21	-31.92	-31.7	-31.2
0	100	21.5	11.2	21.2	8.5	-26.79	-26.43	-32.21	-31.92	-32.21	-31.92

WR	**D**	**$C_{16:0}$%WR**	**$C_{18:0}$%WR**	**$C_{16:0}$%D**	**$C_{18:0}$%D**	**$\delta^{13}C_{16:0}$WR**	**$\delta^{13}C_{18:0}$WR**	**$\delta^{13}C_{16:0}$D**	**$\delta^{13}C_{18:0}$D**	**$\delta^{13}C_{16:0}$ (WR+D)**	**$\delta^{13}C_{18:0}$ (WR+D)**
100	0	15.9	14.6	30.6	12.2	-28.39	-30.75	-25.03	-28.60	-28.39	-30.75
90	10	15.9	14.6	30.6	12.2	-28.39	-30.75	-25.03	-28.60	-27.8	-30.6
80	20	15.9	14.6	30.6	12.2	-28.39	-30.75	-25.03	-28.60	-27.3	-30.4
70	30	15.9	14.6	30.6	12.2	-28.39	-30.75	-25.03	-28.60	-26.9	-30.2
60	40	15.9	14.6	30.6	12.2	-28.39	-30.75	-25.03	-28.60	-26.5	-30.0

50	50	15.9	14.6	30.6	12.2	-28.39	-30.75	-25.03	-28.60	-26.2	-29.8
40	60	15.9	14.6	30.6	12.2	-28.39	-30.75	-25.03	-28.60	-25.9	-29.6
30	70	15.9	14.6	30.6	12.2	-28.39	-30.75	-25.03	-28.60	-25.6	-29.3
20	80	15.9	14.6	30.6	12.2	-28.39	-30.75	-25.03	-28.60	-25.4	-29.1
10	90	15.9	14.6	30.6	12.2	-28.39	-30.75	-25.03	-28.60	-25.2	-28.9
0	100	15.9	14.6	30.6	12.2	-28.39	-30.75	-25.03	-28.60	-25.03	-28.60

WR	**F**	**$C_{16:0}$%WR**	**$C_{18:0}$%WR**	**$C_{16:0}$%F**	**$C_{18:0}$%F**	**$\delta^{13}C_{16:0}$WR**	**$\delta^{13}C_{18:0}$WR**	**$\delta^{13}C_{16:0}$F**	**$\delta^{13}C_{18:0}$F**	**$\delta^{13}C_{16:0}$ (WR+F)**	**$\delta^{13}C_{18:0}$ (WR+F)**
100	0	15.9	14.6	21.2	8.5	-28.39	-30.75	-32.21	-31.92	-28.39	-30.75
90	10	15.9	14.6	21.2	8.5	-28.39	-30.75	-32.21	-31.92	-28.9	-30.8
80	20	15.9	14.6	21.2	8.5	-28.39	-30.75	-32.21	-31.92	-29.3	-30.9
70	30	15.9	14.6	21.2	8.5	-28.39	-30.75	-32.21	-31.92	-29.8	-31.0

60	40	15.9	14.6	21.2	8.5	-28.39	-30.75	-32.21	-31.92	-30.2	-31.1
50	50	15.9	14.6	21.2	8.5	-28.39	-30.75	-32.21	-31.92	-30.6	-31.2
40	60	15.9	14.6	21.2	8.5	-28.39	-30.75	-32.21	-31.92	-30.9	-31.3
30	70	15.9	14.6	21.2	8.5	-28.39	-30.75	-32.21	-31.92	-31.3	-31.4
20	80	15.9	14.6	21.2	8.5	-28.39	-30.75	-32.21	-31.92	-31.6	-31.6
10	90	15.9	14.6	21.2	8.5	-28.39	-30.75	-32.21	-31.92	-31.9	-31.7
0	100	15.9	14.6	21.2	8.5	-28.39	-30.75	-32.21	-31.92	-32.21	-31.92

D	**F**	**$C_{16:0}$%D**	**$C_{18:0}$%D**	**$C_{16:0}$%F**	**$C_{18:0}$%F**	**$\delta^{13}C_{16:0}$D**	**$\delta^{13}C_{18:0}$D**	**$\delta^{13}C_{16:0}$F**	**$\delta^{13}C_{18:0}$F**	**$\delta^{13}C_{16:0}$ (D+F)**	**$\delta^{13}C_{18:0}$ (D+F)**
100	0	30.6	12.2	21.2	8.5	-25.03	-28.60	-32.21	-31.92	-25.03	-28.60
90	10	30.6	12.2	21.2	8.5	-25.03	-28.60	-32.21	-31.92	-25.5	-28.8
80	20	30.6	12.2	21.2	8.5	-25.03	-28.60	-32.21	-31.92	-26.1	-29.1

70	30	30.6	12.2	21.2	8.5	-25.03	-28.60	-32.21	-31.92	-26.7	-29.4
60	40	30.6	12.2	21.2	8.5	-25.03	-28.60	-32.21	-31.92	-27.3	-29.7
50	50	30.6	12.2	21.2	8.5	-25.03	-28.60	-32.21	-31.92	-28.0	-30.0
40	60	30.6	12.2	21.2	8.5	-25.03	-28.60	-32.21	-31.92	-28.7	-30.3
30	70	30.6	12.2	21.2	8.5	-25.03	-28.60	-32.21	-31.92	-29.5	-30.7
20	80	30.6	12.2	21.2	8.5	-25.03	-28.60	-32.21	-31.92	-30.3	-31.0
10	90	30.6	12.2	21.2	8.5	-25.03	-28.60	-32.21	-31.92	-31.2	-31.5
0	100	30.6	12.2	21.2	8.5	-25.03	-28.60	-32.21	-31.92	-32.21	-31.92

Annex 6

Summary of lipid analyses results and interpretations for ceramic vessels from **La Draga** (Tarifa Mateo, 2019). Lipid yields are presented alongside the principal compounds detected through solvent extraction (SE), including saturated fatty acids (SFA), unsaturated fatty acids (UFA) and triacylglycerols (TAGs). Associated stable carbon isotope data are reported as $\delta^{13}C_{16:0}$ (‰), $\delta^{13}C_{18:0}$ (‰), with the isotopic offset $\Delta^{13}C$ (‰), calculated as $\delta^{13}C_{18:0} - \delta^{13}C_{16:0}$.

Samples ID	*Grid*	*Strat. context*	*Lipid yield (µg/g)*	*P/S*	*Detected compounds*	*$\delta^{13}C_{16:0}$ (‰)*	*$\delta^{13}C_{18:0}$ (‰)*	*$\Delta^{13}C$ (‰) ($\delta^{13}C_{18:0}$ - $\delta^{13}C_{16:0}$)*	*Interpretation*
D1	JA79	VIa	345.4		SFA (C10:0-C26:0), UFA (C16:1, C18:1), TAGs (C44, 46, 48, 50, 52, 54)				Subcutaneous animal fat
D2	JD80	VII	402.5		SFA (C9:0-C26:0), TAGs (C44, 46, 48, 50, 52, 54)	-26,52	-30,45	-3.39	Dairy products
D3	JC79	VII	344.4		SFA (C9:0-C26:0), UFA (C16:1, C18:1), TAGs (C44, 46, 48, 50, 52, 54)				Dairy products
D4	IJ81	VIa	53.4		SFA (C12:0-C26:0) UFA (C16:1, C18:1)				Subcutaneous animal fat
D5	KA79	VII	23.4		SFA (C14:0-C26:0)				Subcutaneous animal fat
D6	JH80	VII	167.7		SFA(C8:0-C24:0), UFA (C16:1, C18:1), TAGs (C46, 48, 50, 52, 54)	-25,87	-26,48	-0.61	Domestic ruminant fat
D7	JD79	VIa	78.9		SFA (C12:0-C26:0) UFA (C16:1, C18:1), TAGs (C46, 48, 50, 52, 54)				Subcutaneous animal fat
D8	JD80	VI	58.8		SFA (C12:0-C18:0), TAGs (C46, 48, 50, 52, 54)				Subcutaneous animal fat
D9	JB78	VIa	176.1		SFA (C10:0-C30:0), UFA (C16:1, C18:1)				Subcutaneous animal fat

Samples ID	Grid	Strat. context	Lipid yield (µg/g)	P/S	Detected compounds	$\delta^{13}C_{16:0}$ (‰)	$\delta^{13}C_{18:0}$ (‰)	$\Delta^{13}C$ (‰) ($\delta^{13}C_{18:0}$ - $\delta^{13}C_{16:0}$)	Interpretation
D10	JA81	VIa	67.7		SFA (C9:0-C28:0), UFA (C16:1, C18:1)				Subcutaneous animal fat
D11	JB78	VII	221.5		SFA (C14:0-C26:0), UFA (C16:1, C18:1), TAGs (C46, 48, 50, 52)				Subcutaneous animal fat
D12	JB78	VIa	220.1		SFA (C10:0-C30:0), UFA (C16:1, C18:1)				Subcutaneous animal fat
D13	JC81	VII	67.8		SFA (C12:0-C28:0), UFA (C16:1, C18:1), TAGs (C46, 48, 50, 52, 54)				Dairy products
D14	JB78	VIa	142.2		SFA (C12:0-C26:0), UFA (C16:1, C18:1), TAGs (C44, 46, 48, 50, 52, 54)				Subcutaneous animal fat
D15	JD79	VII	220.0		SFA (C9:0-C26:0), TAGs (C44, 46, 48, 50, 52, 54)	-25,63	-31,29	-5.66	Dairy products
D16	JD81	III	-		-				-
D17	JD81	VIII	6.5		SFA (C14:0-C24:0)				Subcutaneous animal fat
D18	JG81	VII	134.5		SFA (C14:0-C30:0)				Subcutaneous animal fat
D19	JE79	VII	36.2		SFA (C12:0-C18:0)				Subcutaneous animal fat
D20	IJ79	VIa	54.3		SFA (C12:0-C26:0)				Subcutaneous animal fat
D21	JJ78	VIII	59.9		SFA (C9:0-C18:0), UFA (C16:1, C18:1)				Subcutaneous animal fat
D22	JD78	VII	10.9		SFA (C16:0-C18:0)				Subcutaneous animal fat
D23	JJ79	VII	64.2		SFA (C14:0-C18:0)				Subcutaneous animal fat
D24	JE79	VII	339.9		SFA (C9:0-C30:0)				Subcutaneous animal fat
D25	JG81	VII	329.8		SFA (C16:0-C30:0)				Subcutaneous animal fat

Samples ID	*Grid*	*Strat. context*	*Lipid yield (µg/g)*	*P/S*	*Detected compounds*	*$\delta^{13}C_{16:0}$ (‰)*	*$\delta^{13}C_{18:0}$ (‰)*	*$\Delta^{13}C$ (‰) ($\delta^{13}C_{18:0}$ - $\delta^{13}C_{16:0}$)*	*Interpretation*
D26	JE78	VII	58.3		SFA (C12:0-C26:0)				Subcutaneous animal fat
D27	JB79	VIa	67.8		SFA (C12:0-C26:0)				Subcutaneous animal fat
D28	JE78	VII	125.9		SFA (C9:0-C30:0)				Subcutaneous animal fat

Summary of lipid analysis results and interpretations for ceramic vessels from **Pendimoun**. Data are reproduced from the supplementary material (Table S1) of (Drieu et al., 2021), available online at https://doi.org/10.1016/j.jasrep.2020.102682.

Samples ID	*Period*	*Lipid yield (µg/g)*	*P/S*	*O/S*	*Detected compounds*	*$\delta^{13}C_{16:0}$ (‰)*	*$\delta^{13}C_{18:0}$ (‰)*	*$\Delta^{13}C$ (‰) ($\delta^{13}C_{18:0}$ - $\delta^{13}C_{16:0}$)*	*Interpretation*
AP_0001	Impressa	75.04	0.96	0.18	long chain FA (C20:0-C25:0)	-27.27	-25.94	1.33	Porcine adipose fat
AP_0002	Impressa	36.27	2.12	1.04	long chain FA (C20:0-C26:0), cholesterol	-29.18	-29.46	-0.29	Plant product?
AP_0003	Impressa	10.59	0.94	0.18	long chain FA (C20:0-C26:0)	-30.80	-31.03	-0.23	Undetermine fat (wild non ruminant or cereals). See Discussion part
AP_0004	Impressa	86.77	1.22	0.23	long chain FA (C20:0-C26:0)	-28.90	-30.37	-1.47	Ruminant adipose fat
AP_0007	Impressa	64.26	1.15	0.20	long chain FA (C20:0-C24:0), cholesterol	-29.19	-29.98	-0.78	Undetermine fat (wild non ruminant or cereals). See Discussion part
AP_0008	Impressa	402.12	0.84	0.13	long chain FA (C20:0-C24:0), linear and branched odd-numbered FA (C15:0 and C17:0), C18:0 APAAs, 4,8,12-TMTD, pristanic and phytanic acid (76% SSR)	-28.61	-31.90	-3.29	Ruminant adipose fat
AP_0011	Impressa	59.78	4.51	0.46	long chain FA (C20:0-C32:0), odd-numbered alkanes (C27-C33), linear alcohols (C24OH-C34OH), wax esters (W40-W48)	-26.85	-29.23	-2.38	Beeswax and animal adipose fat
AP_0014	Impressa	5.48	1.73	0.27		n.d.	n.d.	n.d.	Low amount of lipid
AP_0015	Impressa	8.95	2.67	0.37		n.d.	n.d.	n.d.	Plant product?

Samples ID	*Period*	*Lipid yield (µg/g)*	*P/S*	*O/S*	*Detected compounds*	*$\delta^{13}C_{16:0}$ (‰)*	*$\delta^{13}C_{18:0}$ (‰)*	*$\Delta^{13}C$ (‰) ($\delta^{13}C_{18:0}$ - $\delta^{13}C_{16:0}$)*	*Interpretation*
AP_0016	Impressa	17.03	1.13	0.13	long chain FA (C20:0)	-29.84	-29.94	-0.10	Undetermine fat (wild non ruminant or cereals). See Discussion part
AP_0018	Impressa	256.65	0.25	0.09	long chain FA (C20:0-C26:0), linear and branched odd-numbered FA (C15:0 and C17:0)	-28.39	-29.35	-0.96	Undetermine fat (wild non ruminant or cereals). See Discussion part
AP_0019	Impressa	28.15	1.09	0.09	4,8,12-TMTD (tr.)	-30.20	-30.41	-0.21	Undetermine fat (wild non ruminant or cereals). See Discussion part
AP_0020	Impressa	18.94	0.82	0.16	long chain FA (C20:0)	-30.21	-30.41	-0.20	Undetermine fat (wild non ruminant or cereals). See Discussion part
AP_0022	Impressa	87.62	1.10	0.18	long chain FA (C20:0-C24:0)	-27.37	-26.36	1.01	Porcine adipose fat
AP_0027	Impressa	140.14	0.91	0.17	long chain FA (C20:0-C22:0), C18:0 APAAs, 4,8,12-TMTD (tr.) and phytanic acid (tr.)	-27.79	-28.97	-1.18	Ruminant adipose fat
AP_0028	Impressa	546.88	1.25	0.43	long chain FA (C20:0-C26:0)	-26.99	-26.87	0.12	Porcine adipose fat
AP_0029	Impressa	39.22	3.93	2.40	long chain FA (C20:0-C24:0)	-28.41	-30.05	-1.64	Ruminant adipose fat, plant product?
AP_0030	Impressa	31.94	0.59	0.10	long chain FA (C20:0-C28:0), phytanic acid (tr.)	-30.02	-30.57	-0.55	Undetermine fat (wild non ruminant or cereals). See Discussion part
AP_0036	Impressa	50.59	0.99	0.13	long chain FA (C20:0-C26:0), C18:0 APAAs, 4,8,12-TMTD, pristanic and phytanic acid (58% SSR)	-29.08	-31.75	-2.67	Ruminant adipose fat

Samples ID	Period	Lipid yield (µg/g)	P/S	O/S	Detected compounds	$\delta^{13}C_{16:0}$ (‰)	$\delta^{13}C_{18:0}$ (‰)	$\Delta^{13}C$ (‰) ($\delta^{13}C_{18:0}$ - $\delta^{13}C_{16:0}$)	Interpretation
AP_0037	Impressa	32.22	2.06	0.51	long chain FA (C20:0-C24:0), 4,8,12-TMTD (tr.), cholesterol	-27.64	-28.89	-1.25	Ruminant adipose fat, plant product?
AP_0039	Impressa	11.45	2.22	0.44		-28.16	-28.44	-0.29	Plant product?
AP_0042	Impressa	17.38	1.48	0.16	long chain FA (C20:0-C26:0), cholesterol	-30.62	-31.38	-0.76	Undetermine fat (wild non ruminant or cereals). See Discussion part
AP_0045	Impressa	182.17	0.57	0.17	long chain FA (C20:0-C24:0), linear and branched odd-numbered FA (C15:0 and C17:0)	-28.33	-29.61	-1.29	Ruminant adipose fat
AP_0046	Impressa	5.60	1.70	0.26		n.d.	n.d.	n.d.	Low amount of lipid
AP_0052	Impressa	21.57	1.49	0.47	long chain FA (C20:0-C26:0), cholesterol	-30.26	-31.78	-1.52	Ruminant adipose fat
AP_0053	Impressa	11.52	2.40	1.01	long chain FA (C20:0-C30:0), 4,8,12-TMTD (tr.)	-29.69	-30.45	-0.76	Plant product?
AP_0081	Impressa	19.29	1.12	0.26	long chain FA (C20:0), 4,8,12-TMTD	-30.20	-31.05	-0.85	Undetermine fat (wild non ruminant or cereals). See Discussion part
AP_0137	Impressa	80.68	1.37	0.49	long chain FA (C20:0-C26:0), 4,8,12-TMTD	-28.61	-30.15	-1.54	Ruminant adipose fat
AP_0038	Cardial (transition I/C)	80.08	1.19	0.47	long chain FA (C20:0-C26:0), cholesterol	-29.26	-30.17	-0.91	Undetermine fat (wild non ruminant or cereals). See Discussion part
AP_0146	Cardial (transition I/C)	77.82	1.10	0.25	long chain FA (C20:0-C26:0), 4,8,12-TMTD	-30.56	-31.38	-0.82	Undetermine fat (wild non ruminant or cereals). See Discussion part

Samples ID	*Period*	*Lipid yield (µg/g)*	*P/S*	*O/S*	*Detected compounds*	$\delta^{13}C_{16:0}$ (‰)	$\delta^{13}C_{18:0}$ (‰)	$\Delta^{13}C$ (‰) ($\delta^{13}C_{18:0}$ - $\delta^{13}C_{16:0}$)	*Interpretation*
AP_0040	Cardial	5.21	2.79	0.00		n.d.	n.d.	n.d.	Low amount of lipid
AP_0148	Cardial	7.00	1.23	0.11		n.d.	n.d.	n.d.	Low amount of lipid
AP_0152	Cardial	151.70	1.85	0.24	long chain FA (C20:0-C26:0), 4,8,12-TMTD, cholesterol	-28.74	-30.80	-2.06	Ruminant adipose fat
AP_0157	Cardial	104.91	1.03	0.08	long chain FA (C20:0-C26:0), linear and branched odd-numbered FA (C15:0 and C17:0), pristanic and phytanic acid (61% SSR)	-27.91	-33.00	-5.09	Dairy product
AP_0158	Cardial	15.30	1.44	0.39	long chain FA (C20:0-C30:0), 4,8,12-TMTD, odd-numbered alkanes (C27-C33)	-28.64	-29.85	-1.21	Ruminant adipose fat
AP_0163	Cardial	176.17	0.55	0.03	long chain FA (C20:0-C26:0)	-28.07	-29.03	-0.96	Undetermine fat (wild non ruminant or cereals). See Discussion part
AP_0164	Cardial	20.87	3.11	0.21		-27.55	-28.85	-1.30	Ruminant adipose fat, plant product?
AP_0165	Cardial	43.24	1.26	0.19	long chain FA (C20:0-C22:0), 4,8,12-TMTD, cholesterol	-29.39	-30.37	-0.99	Undetermine fat (wild non ruminant or cereals). See Discussion part
AP_0166	Cardial	13.25	1.33	0.29	long chain FA (C20:0-C26:0)	-29.60	-30.10	-0.49	Undetermine fat (wild non ruminant or cereals). See Discussion part
AP_0170	Cardial	43.94	1.09	0.07	long chain FA (C20:0-C25:0)	-29.62	-30.24	-0.63	Undetermine fat (wild non ruminant or cereals). See Discussion part

Samples ID	*Period*	*Lipid yield (µg/g)*	*P/S*	*O/S*	*Detected compounds*	$\delta^{13}C_{16:0}$ (‰)	$\delta^{13}C_{18:0}$ (‰)	$\Delta^{13}C$ (‰) ($\delta^{13}C_{18:0}$ - $\delta^{13}C_{16:0}$)	*Interpretation*
AP_0171	Cardial	9.12	1.58	0.19	long chain FA (C20:0-C26:0), 4,8,12-TMTD	-28.86	-31.11	-2.25	Ruminant adipose fat
AP_0174	Cardial	34.14	1.08	0.03	long chain FA (C20:0-C22:0)	-29.64	-30.18	-0.54	Undetermine fat (wild non ruminant or cereals). See Discussion part
AP_0175	Cardial	358.38	0.45	0.09	long chain FA (C20:0-C28:0), linear and branched odd-numbered FA (C15:0 and C17:0), pristanic and phytanic acid (46% SSR)	-28.07	-30.78	-2.70	Ruminant adipose fat
AP_0176	Cardial	22.41	0.91	0.16	long chain FA (C20:0-C26:0)	-28.83	-28.85	-0.03	Undetermine fat (wild non ruminant or cereals). See Discussion part
AP_0176r	Cardial	58.65	1.10	0.33	long chain FA (C20:0-C28:0), ketones (K31, K33, K35)	-27.51	-29.30	-1.79	Heated ruminant adipose fat
AP_0178	Cardial	6.48	1.42	0.18	long chain FA (C20:0-C28:0)	n.d.	n.d.	n.d.	Low amount of lipid
AP_0180	Cardial	39.57	1.63	0.26	long chain FA (C20:0-C28:0)	-29.83	-31.69	-1.85	Ruminant adipose fat
AP_0181	Cardial	13.86	1.32	0.00		-28.33	-29.32	-0.99	Undetermine fat (wild non ruminant or cereals). See Discussion part
AP_0182	Cardial	103.98	0.47	0.05	long chain FA (C20:0-C24:0)	-28.98	-29.84	-0.85	Undetermine fat (wild non ruminant or cereals). See Discussion part
AP_0187	Cardial	33.75	1.36	0.12	long chain FA (C20:0-C24:6), 4,8,12-TMTD (tr.) and phytanic acid (tr.)	-30.32	-29.93	0.39	Undetermine fat (wild non ruminant or cereals). See Discussion part

Samples ID	*Period*	*Lipid yield (µg/g)*	*P/S*	*O/S*	*Detected compounds*	*$\delta^{13}C_{16:0}$ (‰)*	*$\delta^{13}C_{18:0}$ (‰)*	*$\Delta^{13}C$ (‰) ($\delta^{13}C_{18:0}$ - $\delta^{13}C_{16:0}$)*	*Interpretation*
AP_0206	Cardial	14.90	0.95	0.10	long chain FA (C20:0-C22:0)	-30.51	-30.21	0.30	Undetermine fat (wild non ruminant or cereals). See Discussion part
AP_0207	Cardial	66.23	0.44	0.12	long chain FA (C20:0-C26:0)	-29.99	-31.02	-1.03	Ruminant adipose fat
AP_0212	Cardial	11.37	1.34	0.33	4,8,12-TMTD, cholesterol	-28.90	-30.10	-1.20	Ruminant adipose fat